



International Hydrological Programme

Integrated Basin Management under Changing Climate

The Twenty-seventh IHP Training Course
Winter School for Applying Technology to Climate Change

4th – 15th December, 2017

Kyoto, Japan

Water Resources Research Center, Disaster Prevention Research Institute,
Kyoto University
Institute for Space-Earth Environmental Research, Nagoya University
International Program on Resilient Society Development
under Changing Climate



International Hydrological Programme

Integrated Basin Management under Changing Climate

The Twenty-seventh IHP Training Course Winter School for Applying Technology to Climate Change

Outline

A two-week training course on integrated basin management strategies including aspects of water resources, water related disasters under climate change is programmed for participants from Asia-Pacific regions as a part of Japanese contribution to the International Hydrological Program (IHP). The course composed of a series of lectures, model practices, field exercise and technical visits will be held at Disaster Prevention Research Institute (DPRI), Kyoto University during the two weeks from 4th to 15th December 2017.

Objectives

Development of resilient society has become an inevitable issue under the recent climate change increasing the frequency of extreme phenomena such as unprecedented flood and severe drought. In order to make our society more resilient, social adaptation to the hazards and countermeasure for disasters are required based on technologies for prediction and assessment on the future conditions of water resources.

In light of the Focal Area 1.1 “Risk management as adaptation to global change” and 1.2 “Understanding coupled human and natural processes” under the Theme 1 “Water related disasters under hydrological change” of the IHP-VIII, the 27th IHP training course is focused on following three objectives: 1) to acquire the latest knowledge on climate change impacts on water resources, water related disasters and ecosystem services, 2) to make practice on rainfall-runoff-inundation estimation at river basin scale, and 3) to discuss strategies of integrated basin management to realize resilient society under climate change.

Dates 4th – 15th December, 2017

Venue DPRI, Kyoto University, Uji, Kyoto, Japan

Conveners

Convener: TANAKA, Shigenobu (DPRI, Kyoto University)

Chief assistant: TAKEMON, Yasuhiro (DPRI, Kyoto University)

Secretary: KOZAKI, Sachiko and KAWASAKI, Yuko (DPRI, Kyoto University)

Lecturers

HORI, Tomoharu (DPRI, Kyoto University)
KOBAYASHI Sohei (DPRI, Kyoto University)
NAKAKITA, Eiichi (DPRI, Kyoto University)
NOHARA, Daisuke (DPRI, Kyoto University)
SAYAMA, Takahiro (DPRI, Kyoto University)
SUMI, Tetsuya (DPRI, Kyoto University)
TACHIKAWA, Yasuto (Graduate School of Engineering, Kyoto University)
TAKARA, Kaoru (DPRI, Kyoto University)
TAKEMON, Yasuhiro (DPRI, Kyoto University)
TANAKA, Kenji (DPRI, Kyoto University)
TANAKA, Shigenobu (DPRI, Kyoto University)

Lectures' contents at the Lecture Room (HW401) of DPRI, Kyoto University

Keynote 1	Resilient society development under changing climate	K. Takara
Keynote 2	Climate change impact assessment on disaster environments	E. Nakakita
Lecture 1	Fundamentals of basin-scale hydrological analysis	Y. Tachikawa
Lecture 2	Fundamentals in flood frequency analysis	S. Tanaka
Lecture 3	Fundamentals in rainfall-runoff-inundation modelling	T. Sayama
Lecture 4	Fundamentals in land-surface processes	K. Tanaka
Lecture 5	Fundamentals in optimum operation of reservoir systems	T. Hori
Lecture 6	Optimum operation of reservoir systems	D. Nohara
Lecture 7	Integrated sediment management for reservoir sustainability	T. Sumi
Lecture 8	Sustainable management of river basin ecosystem services	S. Kobayashi

Indoor practices at the Seminar Room (S217D) of DPRI, Kyoto University

Exercise 1 & 4	Rainfall-runoff-inundation modelling	T. Sayama
Exercise 2 & 3	Processing method of geographical and meteorological data	K. Tanaka

Field exercises

Exercise 5	Evaluation procedure of river-bed geomorphology	S. Kobayashi & Y. Takemon
Exercise 6	Riverbed habitat evaluation procedure	Y. Takemon & S. Kobayashi

Model experiment

Exercise 7	Dam operation experiment using a laboratory model	T. Sumi
------------	---	---------

Technical visit Lake Biwa, Seta River Weir, Amagase Dam and Uji River

Schedule (4th to 15th December, 2017)

Date		Time	Program	Venue	Lecturers
4-Dec	Mon	(AM) 9:00 – 9:15 9:15 – 10:00 10:00 – 10:15 10:20 – 12:10	Registration Guidance Opening Ceremony Self-introduction and country report	S217D	Y. Takemon All participants
		(PM) 13:00 – 14:30 14:45 – 16:15	Keynote 1 Keynote 2	HW401	K. Takara E. Nakakita
		16:30 – 18:00	Welcome party	S217D	Y. Takemon
5-Dec	Tue	(AM) 9:00 – 11:30	Lecture 1	HW401	Y. Tachikawa
		(PM) 13:30 – 16:00	Lecture 2		S. Tanaka
6-Dec	Wed	(AM) 9:30 – 12:00	Lecture 3	HW401	T. Sayama
		(PM) 13:30 – 16:30	Exercise 1	S217D	T. Sayama
7-Dec	Thu	(AM) 9:30 – 12:00	Lecture 4	HW401	K. Tanaka
		(PM) 13:30 – 16:30	Exercise 2	S217D	K. Tanaka
8-Dec	Fri	(AM) 9:30 – 12:00	Exercise 3	S217D	K. Tanaka
		(PM) 13:30 – 16:30	Exercise 4		T. Sayama
9-Dec	Sat	9:00 – 17:00	Technical visits to the Lake Biwa and the Uji River	by bus	Y. Takemon
10-Dec	Sun	10:00–17:00	Cultural exchange in Kyoto City	free	All participants
11-Dec	Mon	(AM) 9:30 – 12:00	Lecture 5	HW401	T. Hori
		(PM) 14:00 – 16:30	Lecture 6		D. Nohara
12-Dec	Tue	(AM) 9:30 – 12:00	Lecture 7	HW401	T. Sumi
		(PM) 14:00 – 16:30	Lecture 8		S. Kobayashi
13-Dec	Wed	9:00 – 17:00	Field Exercise 5 & 6 at the Uji River and the Kizu River	by bus	Y. Takemon S. Kobayashi
14-Dec	Thu	(AM) 9:30 – 12:00	Exercise 7	S217D	T. Sumi
		(PM) 13:00 – 16:30	Report preparation	S217D	Y. Takemon
15-Dec	Fri	(AM) 9:30–11:30 11:40–12:00	Report presentation by each participant Completion ceremony	S217D	All participants Y. Takemon
		(PM) 12:00–13:00	Farewell party	S217D	Y. Takemon

Index of Lecture Materials

Keynote 1	Resilient society development under changing climate K. Takara	1
Keynote 2	Climate change impact assessment on disaster environments E. Nakakita	7
Lecture 1	Fundamentals of basin-scale hydrological analysis Y. Tachikawa	23
Lecture 2	Fundamentals in flood frequency analysis S. Tanaka	71
Lecture 3	Fundamentals in rainfall-runoff-inundation modelling T. Sayama	85
Exercise 1 & 4	Rainfall-runoff-inundation modelling T. Sayama	95
Lecture 4	Fundamentals in land-surface processes K. Tanaka	
Exercise 2 & 3	Processing method of geographical and meteorological data K. Tanaka	213
Lecture 5	Fundamentals in optimum operation of reservoir systems T. Hori	225
Lecture 6	Optimum operation of reservoir systems D. Nohara	241
Lecture 7	Integrated sediment management for reservoir sustainability T. Sumi	251
Lecture 8	Sustainable management of river basin ecosystem services S. Kobayashi	271
Exercise 5 & 6	Evaluation procedure of riverbed geomorphology and habitat Y. Takemon & S. Kobayashi	279
Technical visits	A Guide of the Lake Biwa and the Uji River Y. Takemon	281

LECTURE MATERIALS

Keynote 1: Resilient society development under changing climate

Kaoru TAKARA (*Professor, Disaster Prevention Research Institute, Kyoto University; Dean, Graduate School of Advanced Integrated Studies in Human Survivability*)

Abstract:

This keynote presents some aspects of global agendas relating to disaster risk reduction (DRR) and resilient society such as the Sendai Framework for DRR 2015-2030, the Sustainable Development Goals (SDGs) and the Paris Agreement agreed in international conferences in 2015.

It also describes how to recognize disaster risk, interpreting situations in Sendai and Hiroshima, Japan. Disaster risk is composed of three factors: H , E , and V . Hazard (H) is a natural phenomenon causing disasters. Exposure (E) is defined as something (people and properties) to be affected by natural disasters. Vulnerability (V) is defined as a condition resulting from physical, environmental, social or economic factors or processes, which increases the susceptibility of people. There was a tsunami hazard map in Sendai City area, which shows the areas where tsunami waves had been assumed to come up. Caused by the Great East Japan Earthquake on 11 March 2011, actual tsunami waves came up to the areas beyond the border assumed in the tsunami hazard map and killed hundreds of people. Then Sendai City has revised the tsunami hazard map. In this case, H was too big to evacuate and survive. Not only vulnerable areas but also safer places were much damaged; E was increased. Hiroshima City was much damaged by landslides and debris flows on 19-20 August 2014, which killed 74 people and destroyed 133 houses. Geological and meteorological conditions in this area are characterized as: weathered granite that can easily be landslides and flowed down as debris, and more than 200 mm rainfall during three hours. Almost all exposures (people and properties) were living in vulnerable places, which were indicated in the flood hazard map provided by Hiroshima City. In this Hiroshima case, H was big and hit vulnerable places where many exposures (E) were there.

Disaster risk depends on the physiographical conditions: location, geology, meteorology and hydrology, as well as the time of the day or of the week and the season of the year.

The discussion here has denoted vulnerability mainly in terms of vulnerable place; however, vulnerability also can be applied to people and societies. People and societies who are well educated regarding hazards and disasters are less vulnerable and can adapt to emergency situations in their daily life. Climate change impacts certainly affect people with serious losses and damages, which means the importance of efforts for establishment of resilient society.

Resilient society development under changing climate

Kaoru TAKARA

Disaster Prevention Research Institute,
Kyoto University

2017/12/04



Today's talk

Introduces two episodes,

- Sendai earthquake and tsunami in 2011
- Hiroshima storm and landslide in 2014
- Disaster risk interpretation
- Tsunami hazard risk map revised in Sendai
- Flood and landslide hazard map indicated disaster risk in Hiroshima

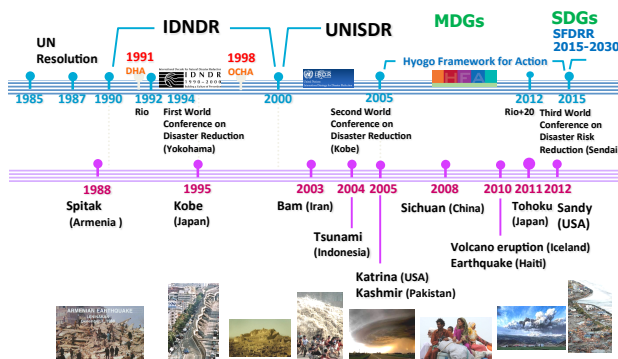
AS well as

- + Global agenda for DRR
- + Sendai Framework for DRR 2015-2030
- + SDGs
- + How to build resilient society



History of global DRR agenda

Courtesy of Badaoui Rouhban (2015)



Sendai Framework for DRR (SFDRR) 2015-2030

The Seven Global Targets

- Substantially **reduce** global disaster **mortality** by 2030, aiming to lower average per 100,000 global mortality rate in the decade 2020-2030 compared to the period 2005-2015.
- Substantially **reduce** the number of **affected people** globally by 2030, aiming to lower average global figure per 100,000 in the decade 2020-2030 compared to the period 2005-2015.
- Reduce** direct disaster **economic loss** in relation to global gross domestic product (GDP) by 2030.
- Substantially **reduce** disaster **damage** to critical infrastructure and disruption of basic services, among them health and educational facilities, including through developing their resilience by 2030.
- Substantially **increase** the **number of countries** with national and local disaster risk reduction strategies by 2020.
- Substantially **enhance international cooperation** to developing countries through adequate and sustainable support to complement their national actions for implementation of this Framework by 2030.
- Substantially **increase** the **availability** of and **access** to multi-hazard early warning systems and disaster risk information and assessments to the people by 2030.

4



Sendai Framework for DRR 2015-2030

Four priorities for Action

1. Understanding disaster risk
2. Strengthening disaster risk governance to manage disaster risk
3. Investing in disaster risk reduction for resilience
4. Enhancing preparedness for effective response, and to “Build back Better” in recovery, rehabilitation and reconstruction

5



Disaster Risk

6

$$DR = [H] \times [E] \times [V] / [C]$$

DR: disaster risk

H: hazard

(magnitude, frequency, severity, ...)

E: exposure

(population, assets, landscape, ...)

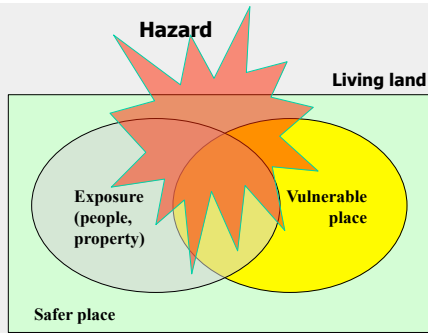
V: vulnerability

(age, gender, health; knowledge, awareness and preparedness; ...)

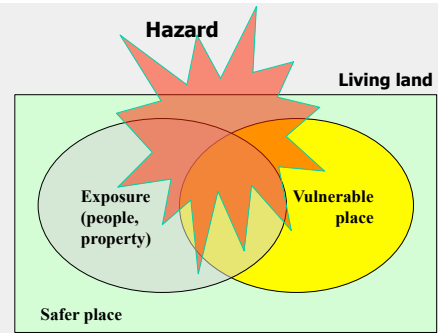
C: countermeasure

(infrastructure, early warning systems, hazard risk maps, ...)

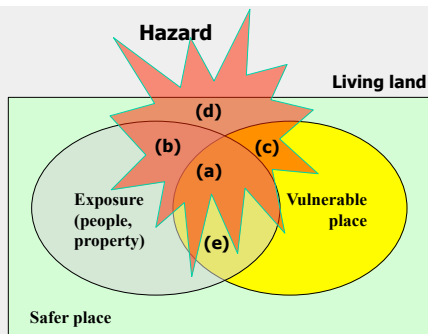




A conceptual explanation about disaster risk, hazard, exposure, and vulnerability.



A conceptual explanation about disaster risk, hazard, exposure, and vulnerability.



A conceptual explanation about disaster risk, hazard, exposure, and vulnerability.

- (a) Serious disaster damage is possible because people and properties are exposed by the hazard in the vulnerable place.
- (b) People and properties are affected by the hazard but there is no damage because they are located in the safer place.
- (c) The hazard hits the vulnerable place but there is no damage because there are no people and properties there.
- (d) No damage because there is no exposures in safer place.
- (e) Risky but no damage; exposures in the vulnerable place are about to be hit by the hazard, but it does not reach them.



Based on Disaster Risk concept

This talk

shows interpretation of two episodes in Japan:

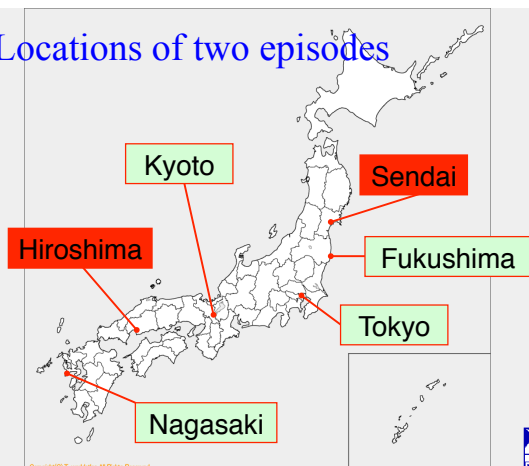
- Earthquake and tsunami in Sendai (11 March 2011)
- Heavy rain and landslides in Hiroshima (20 August 2015)

and

considers how to decrease disaster risk.



Locations of two episodes

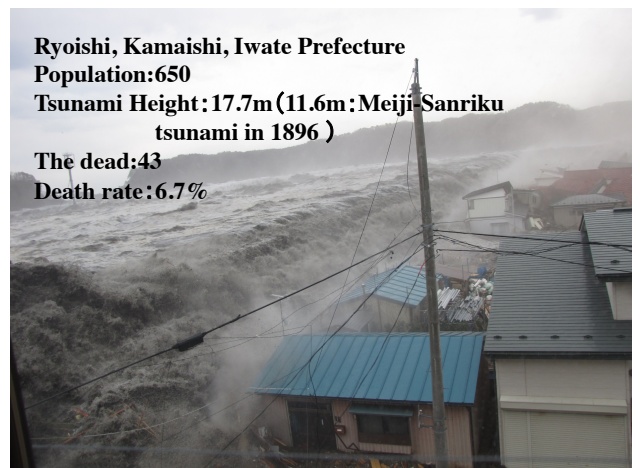


Copyright© T-workshop All Rights Reserved

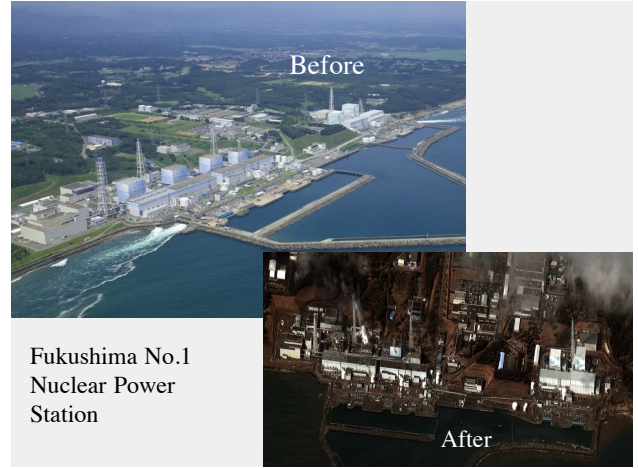


Ryoishi, Kamaishi, Iwate Prefecture
Population: 650
Tsunami Height: 17.7m (11.6m: Meiji-Sanriku tsunami in 1896)

The dead: 43
Death rate: 6.7%



Minami-Sanriku Town



Fukushima No.1
Nuclear Power
Station

Comparison Among 1923 The Great Kanto Earthquake, 1995 Hanshin-Awaji Earthquake, and 2011 Great East Japan Earthquake and Tsunami

	1923 Great Kanto Earthquake	1995 Hanshin-Awaji Earthquake	2011 Great East Japan Earthquake and Tsunami
Occurrence Date	Sept. 1, 1923	Jan. 17, 1995	March 11, 2011
Earthquake Magnitude	7.9	7.3	9.0
Severe Damage Prefecture	Tokyo, Kanagawa, Chiba	Hyogo	Iwate, Miyagi, Fukushima
Dead/Missing	105,385	6,434/3	15,824/3,824
Injured	103,733	43,773	5,942
Evacuee (at peak)	About 1.9 million	About 310,000	400,000 +
Houses Damaged (Fully and Half Destroyed)	More than 210,000	249,180	274,797
Amount of Damage / National Budget	5.5 billion Yen/ 1.5 b.Y.	9.6 trillion Yen/ 70 t.Y.	16.9 trillion Yen/ 85 t.Y.
Family at Temporal Housing Unit	More than 20,000	46,617	52,358
Type of disaster	Densely populated area with wood houses	Urban disaster	Super-Extensive disaster
Description	City fire killed people. 1.95 billion Yen (Reconstruction budget)	Crushed to death under collapsed houses Disaster related death (930)	Compound disaster with earthquake, tsunami and nuclear power plant accident

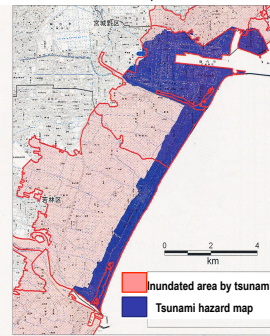
October 18, 2011



Comparison of Inundated Area by Tsunami with Tsunami Hazard Map

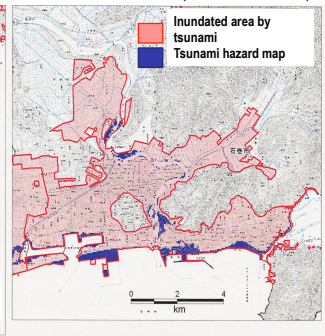
Sendai City:

Comparison of inundated area by the tsunami of the 2011 off the Pacific Coast of Tohoku Earthquake with Tsunami Hazard Map



Ishinomaki City:

Comparison of inundated area by the tsunami of the 2011 off the Pacific Coast of Tohoku Earthquake with Tsunami Hazard Map



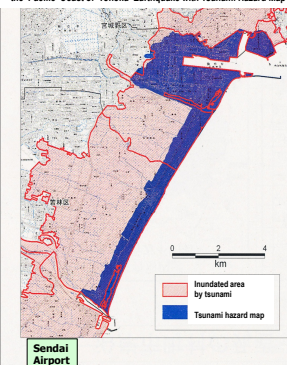
(出典) 東北地方太平洋沖地震津波被害調査報告書(国土院報告書)より中部
ハザードマップ、仙台市「仙台市津波ハザードマップ」、石巻市「石巻市津波ハザードマップ」

18

Comparison of Inundated Area by Tsunami with Tsunami Hazard Map

Sendai City:

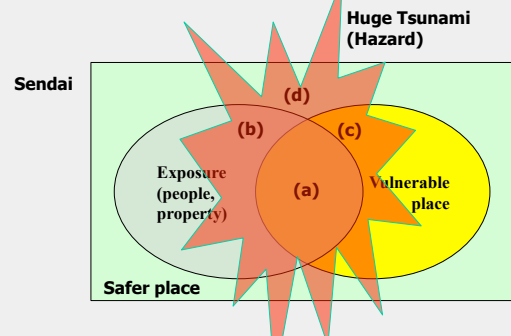
Comparison of inundated area by the tsunami of the 2011 Off the Pacific Coast of Tohoku Earthquake with Tsunami Hazard Map



Tsunami hazard map had shown **vulnerable** place.

But other places that had been assumed as **safer** were also vulnerable to huge tsunami.

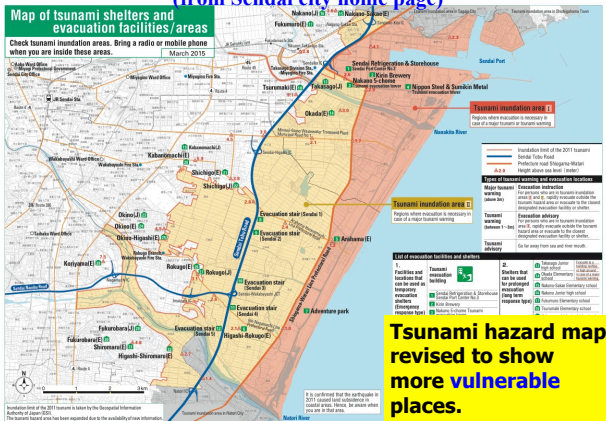
A conceptual explanation about disaster risk, hazard, exposure, and vulnerability (Interpretations for huge tsunami in Sendai).



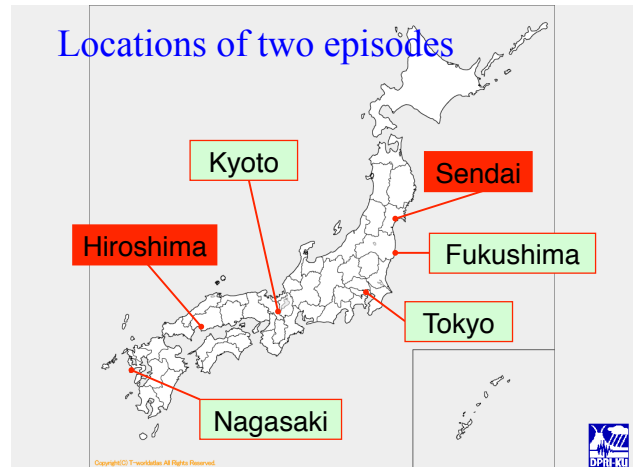
- (a) almost all exposures (people and properties) in vulnerable place were completely damaged;
- (b) exposures were assumed to be safe from the tsunami because they were in safer places;
- (c) vulnerable places were damaged by liquefaction or land subsidence, which affected agricultural lands (mainly rice paddy fields) through salt water from the sea;
- (d) safer places were also damaged because the tsunami run-up height at some locations in the middle and upstream of rivers was 40 m high.



Figure 2: Tsunami hazard map in Sendai after 3.11
(from Sendai city home page)



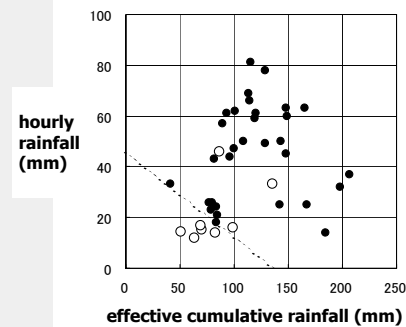
Locations of two episodes



Two landslide and debris flow events in Hiroshima in 1999 and 2014

On 29 June 1999, a severe storm event (50 to 200 mm during five days before the event) caused a landslide and debris flow disaster and **killed 32 people** and **destroyed 101 houses** mainly in Hiroshima Prefecture.

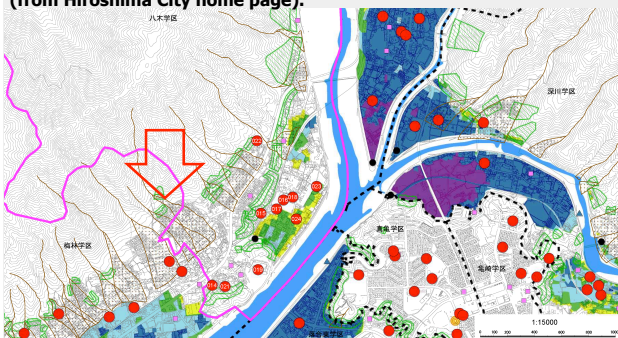
Japanese government established the **Act on Promotion of Sediment Disaster Countermeasures for Sediment Disaster Prone Areas**, which encouraged local governments to disseminate information (hazard maps) about possible sediment disaster caused by heavy rainfall-induced landslides and debris flows.



Critical Line estimated by combination of effective cumulative rainfall (X-axis) and hourly rainfall that triggered landslide (Y-axis) at raingauges around Hiroshima City in June 1999; black circles: landslide occurred, white circles: no landslide (Ushiyama, Ohido and Takara, 2001).



A part of flood hazard map for Yagi District in Asa-Minami-Ku, Hiroshima City; red arrow shows the disaster area given in Photo 3 (from Hiroshima City home page).



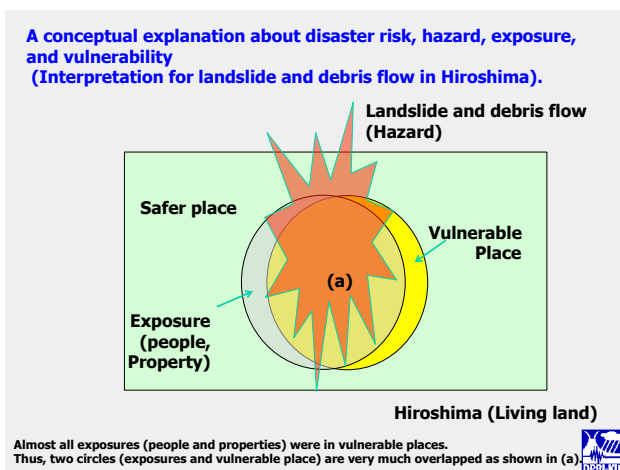
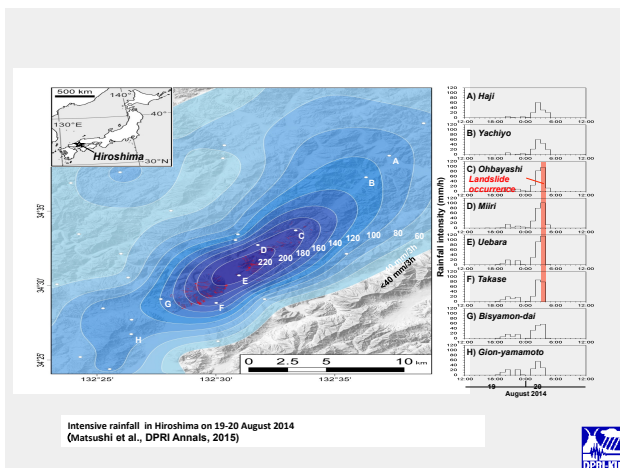
Two landslide and debris flow events in Hiroshima in 1999 and 2014

On 19-20 August 2014, a similar event took place again in Hiroshima, **killing 74 people** and **destroying 133 houses**.

Geological and meteorological conditions in this area are characterized as **weathered granite** that can easily become landslides and flowed down as debris, and **more than 200 mm rainfall during three hours**.

Photos 1 to 3 are typical snapshots of sediment disasters in Asa-Minami-Ku, Hiroshima city. They show that residential areas were still in vulnerable places and many houses were seriously damaged. The flood hazard map indicates the danger of sediment disaster.





SUMMARY

- Two Japanese episodes are interpreted in terms of disaster disk (hazard, exposure, vulnerability).
- Safer places would be vulnerable places if huge hazard comes.
- Hazard maps give us useful information of disaster risk in our society; but we should also be careful of the conditions in which hazard maps are made.
- Exposures should be located in safer places to reduce disaster risk. But such relocation is often very difficult for many reasons.
- Land/city conservation and disaster mitigation can relate infrastructure to hazard risk map information.

CONCLUSIONS

- Disaster risk also depends on the physiographical conditions: location, geology, meteorology and hydrology, as well as the time of the day or of the week and the season of the year.
- The discussion here has denoted vulnerability mainly in terms of vulnerable place; however, vulnerability also can be applied to people and societies. People and societies who are well educated regarding hazards and disasters are less vulnerable and can adapt to emergency situations in their daily life → disaster mitigation.
- Climate change impacts certainly affect people with serious losses and damages, which means the importance of efforts for establishment of resilient society.

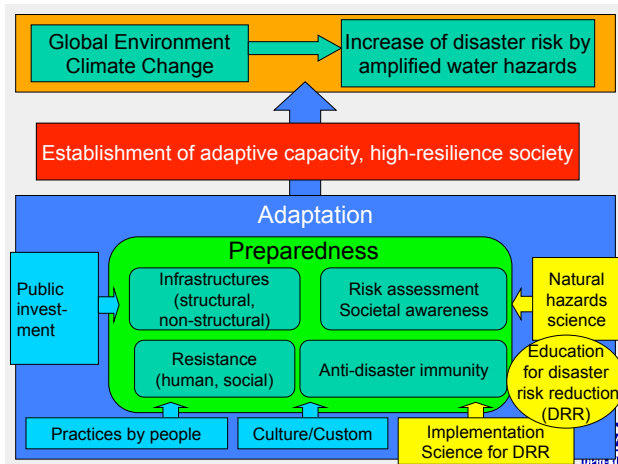


Sustainable Development Goals

Sustainable Development Goals



17 goals and 169 targets
Many of them are related to DRR



Disaster Management Cycle



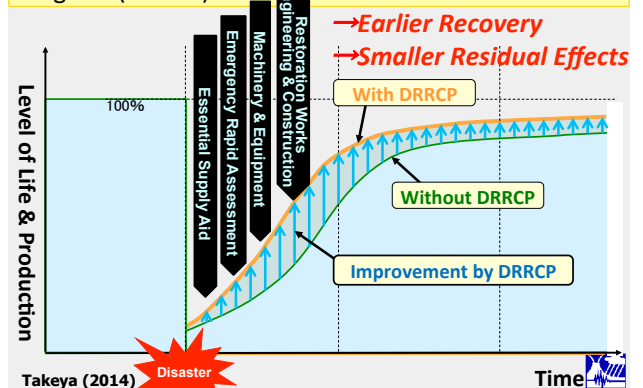
Establishment of Well-Organized Disaster Management System is Important



Takeya (2014)



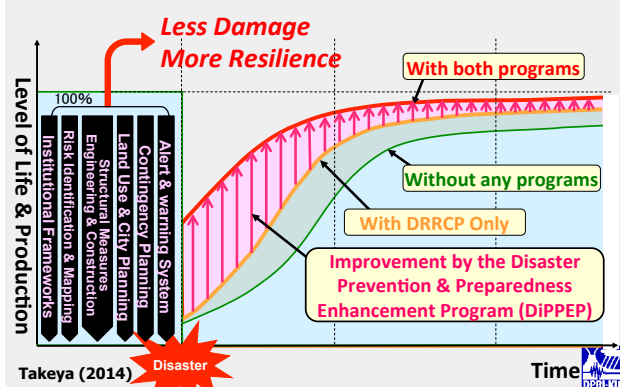
Effect of Disaster Response & Relief Cooperation Program (DRRCP)



Takeya (2014)



Effect of Disaster Prevention & Preparedness Enhancement Program (DiPPEP)



Keynote 2: Climate change impact assessment on disaster environments

First-name EIICHI-NAKAKAIT (*Professor, Disaster Prevention Research Institute, Kyoto University*)

Abstract:

Not long ago, there was a great deal of careful discussion on whether global warming is related to extreme weather phenomena such as the large typhoons and localized heavy rainfall that have been increasing recently. However, Japan experienced any number of close brushes with, and direct hits from, large typhoons and frequent occurrence of strong winds, floods, overflowing rivers, high tides, high waves, and landslides. Concern has spread that these disasters may intensify as global warming progresses.

Theme D, precise impact assessments on climate change, under the program for risk information climate change (SOUSEI program) supported by MEXT, aimed to scientifically demonstrate the connection between the aforementioned increase in natural hazards and global warming and to look 100 years into the future to see how serious it may become. The research results are to be presented as “actual figures” and are expected to be used as data for the government and municipalities to consider how to protect the lives of people in urban and rural areas, coastal areas, and river areas. A “100 year impact assessment” was proposed by this program’s antecedent, KAKUSHIN, but this is the first attempt to produce an actual figure for “the maximum predicted amount of future rainfall.” To generate this kind of specific figure, detailed data with a high degree of precision is required. Even with all the data that we can collect, the sample size and precision are still inadequate. So, in Theme D, we take on the challenge of developing an assessment model that can produce predictions even given the data limitations, and we endeavor to assess extreme phenomena. Broadly speaking, there are three specific research sub-themes. They are “climate change impacts on natural hazards,” “climate change impacts on water resources,” and “climate change impacts on ecosystems and biodiversity.

The first sub-theme, climate change impacts on natural hazards, was handled by DPRI-KU, together with Global Centre of Excellence for Water Hazard and Risk Management (ICHARM/PWRI). We aimed to produce predictions for scenarios including worst-case particularly in the case of typhoons, which cause the most serious weather-related damage in Japan, concerning the frequency, scale, accompanying precipitation, strong winds, high tides, and high waves, including during the Baiu season.

The second sub-theme, climate change impacts on water resources, was handled by DPRI-KU and IIS in the University of Tokyo. When the climate changes due to global warming, the rain amount and rain patterns change significantly. It is also possible that what formerly fell as snow will

change into rain. In Japan which has many mountainous regions, it is anticipated that this would cause a great change in the “pattern of water flowing into rivers.” So, Kyoto University team of this group predicts and assesses the changes in the flow and supply of water in the main rivers in Japan, the impact on rice farming, etc., and the need for flood control such as dams, etc. Similar prediction and assessment are pursued for the world’s major rivers, including in Asia. The University of Tokyo team will predict and assess how the actual water cycle will change on a global scale with the addition of artificial modifications. This team will also study the effectiveness of adaptation strategies.

A new five-years program on “Integrated Research Program for Advancing Climate Models” supported by MEXT started in 2017. In the team D named “Integrated hazard prediction”, “Non-regret adaptation strategies” and “Seamless hazard prediction until the end of the 21st century” will be further focused on.

List of related papers

1) Over all

Kitoh, A., T. Ose, K. Kurihara, S. Kusunoki, M. Sugi, and KAKUSHIN Team-3 Modeling Group, 2009: Projection of changes in future weather extremes using super-high-resolution global and regional atmospheric models in the KAKUSHIN program: Results of preliminary experiments. *Hydro. Res. Lett.*, 3, 49-53.

Mizuta, R., H. Yoshimura, H. Murakami, M. Matsueda, H. Endo, T. Ose, K. Kamiguchi, M. Hosaka, M. Sugi, S. Yukimoto, S. Kusunoki, and A. Kitoh, 2012: Climate simulations using MRI-AGCM3.2 with 20-km grid. *J. Meteor. Soc. Japan*, 90A, 233-258, doi:10.2151/jmsj.2012-A12.

Kitoh, A., and H. Endo, 2016: Changes in precipitation extremes projected by a 20-km mesh global atmospheric model. *Weather and Climate Extremes*. 11, 41-52, doi: 10.1016/j.wace.2015.09.001

Mizuta, R., O. Arakawa, T. Ose, S. Kusunoki, H. Endo and A. Kitoh, 2014: Classification of CMIP5 future climate responses by the tropical sea surface temperature changes. *SOLA*, 10, 167-171, doi:10.2151/sola.2014-035.

2) Natural Hazards

Ito, R., T. Takemi, and O. Arakawa, 2016: A possible reduction in the severity of typhoon wind in the northern part of Japan under global warming: A case study. *SOLA*, 12, 100-105, doi:10.2151/sola.2016-023.

Mori, N., and T. Takemi, 2016: Impact assessment of coastal hazards due to future changes of tropical cyclones in the North Pacific Ocean. *Weather and Climate Extremes*, 11, 53-69, doi:10.1016/j.wace.2015.09.002.

Takayabu, I., K. Hibino, H. Sasaki, H. Shiogama, N. Mori, Y. Shibutani, T. Takemi, 2015: Climate change effects on the worst-case storm surge: a case study of Typhoon Haiyan. *Environ. Res. Lett.*, 10, 064011, doi:10.1088/1748-9326/10/6/064011

Oku, Y., J. Yoshino, T. Takemi, and H. Ishikawa, 2014: Assessment of heavy rainfall-induced disaster potential based on an ensemble simulation of Typhoon Talas (2011) with controlled track and intensity. *Natural Hazards and Earth System Sciences*, 14, 2699-2709, doi:10.5194/nhess-14-2699-2014.

Ishikawa, H., Y. Oku, S. Kim, T. Takemi, and J. Yoshino, 2013: Estimation of a possible maximum flood event in the Tone River basin, Japan caused by a tropical cyclone. *Hydrological Processes*, 27, 3292-3300, doi: 10.1002/hyp.9830.

Sato, Y., Kojiri, T., Michihiro, Y., Suzuki, Y. and Nakakita, E. (2013), Assessment of climate change impacts on river discharge in Japan using the super-high-resolution MRI-AGCM. *Hydrol. Process.*, 27: 3264–3279. doi: 10.1002/hyp.9828

Oku, Y. and Nakakita, E. (2013), Future change of the potential landslide disasters as evaluated from precipitation data simulated by MRI-AGCM3.1. *Hydrol. Process.*, 27: 3332–3340. doi: 10.1002/hyp.9833

Takayabu, I., K. Hibino, H. Sasaki, H. Shiogama, N. Mori, Y. Shibutani and T. Takemi (2015), Climate change effects on the worst-case storm surge: a case study of Typhoon Haiyan, *Environmental Research Letters*, Vol.10, 064011.

Jiang, X, N. Mori, H. Tatano, L. Yang and Y. Shibutani (2015), Estimation of property loss and business interruption loss caused by storm surge inundation due to climate change; A case of Typhoon Vera revisit, *Natural Hazards*, pp.1-15.

Hemer, M.A., Y. Fan, N. Mori, A. Semedo and X.L.Wang (2013) Projected changes in wave climate from a multi-model ensemble, *Nature Climate Change*, 6p., doi:10.1038/nclimate1791.

Climate change impact assessment on disaster environments

Eiichi Nakakita

Professor

Disaster Prevention Research Institute
(DPRI)

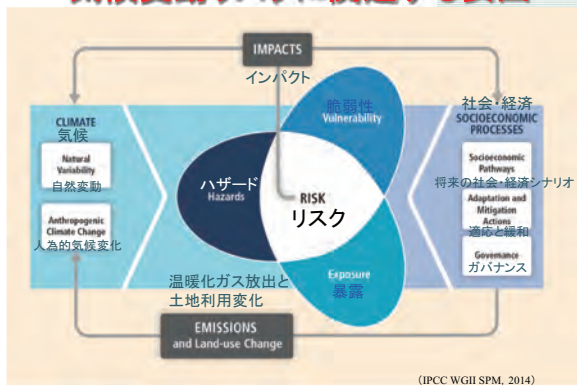
Kyoto University



Contents

- **Back ground**
- **On the SOISEI Program**
- **Some products from direct use of GCM and RCM output**
- **O(5000yrs) Mega Ensemble Experiments "d4PDF"**
- **Worst case class scenarios**
- **Towards building adaptation strategy**

気候変動リスクに関連する要因



Warming of the climate system is unequivocal.

Human influence on the climate system is clear.

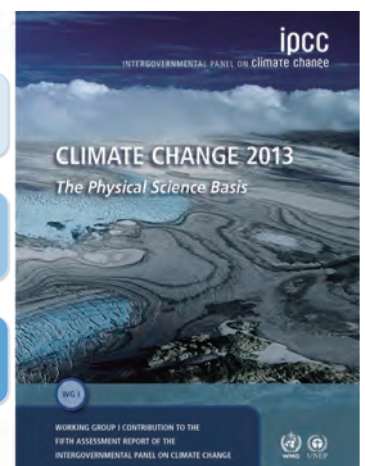
Limiting climate change will require substantial and sustained reductions of greenhouse gas emissions.

(IPCC/AR5)

Observations

Understandings

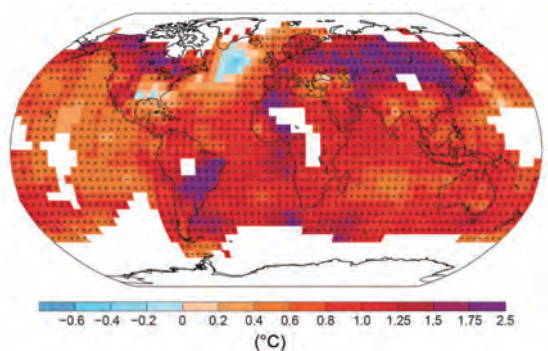
Future



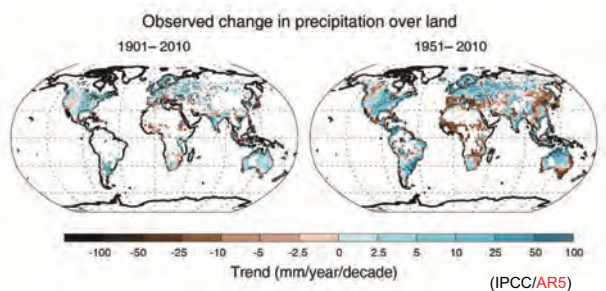
Warming of the climate system is unequivocal. (IPCC/AR5)

Warming of the climate system is unequivocal, and since the 1950s, many of the observed changes are unprecedented over decades to millennia. The atmosphere and ocean have warmed, the amounts of snow and ice have diminished, sea level has risen, and the concentrations of greenhouse gases have increased.

Observed change in surface temperature 1901–2012



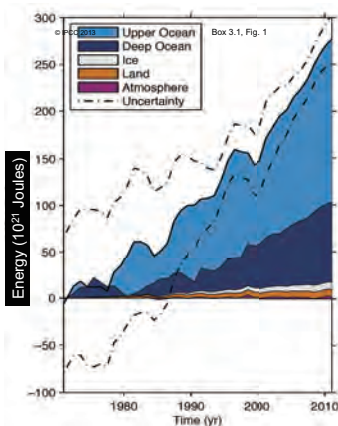
Precipitation



Confidence in precipitation change averaged over global land areas since 1901 is low prior to 1951 and medium afterwards. Averaged over the mid-latitude land areas of the Northern Hemisphere, precipitation has increased since 1901 (medium confidence before and high confidence after 1951).

Extreme events

- Changes in many **extreme weather and climate events** have been observed since about 1950.
- It is very likely that the number of **cold days and nights** has decreased and the number of **warm days and nights** has increased on the global scale.
- It is likely that the frequency of **heat waves** has increased in large parts of Europe, Asia and Australia.
- There are likely more land regions where the number of **heavy precipitation events** has increased than where it has decreased. The frequency or intensity of heavy precipitation events has likely increased in North America and Europe. In other continents, confidence in changes in heavy precipitation events is at most medium.



Ocean warming dominates the increase in energy stored in the climate system, accounting for more than 90% of the energy accumulated between 1971 and 2010 (*high confidence*). It is *virtually certain* that the upper ocean (0–700 m) warmed from 1971 to 2010 (see Figure SPM.3), and it *likely* warmed between the 1870s and 1971.

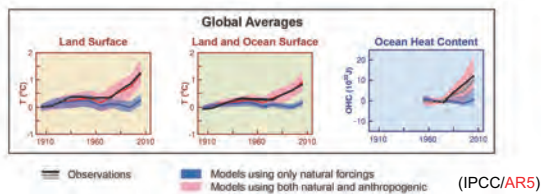
Upper ocean: above 700m
Deep ocean: below 700 m; including below 2000 m estimates starting from 1992

Observations

Understandings

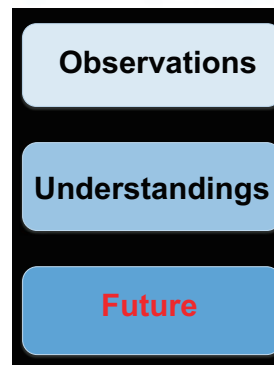
Future



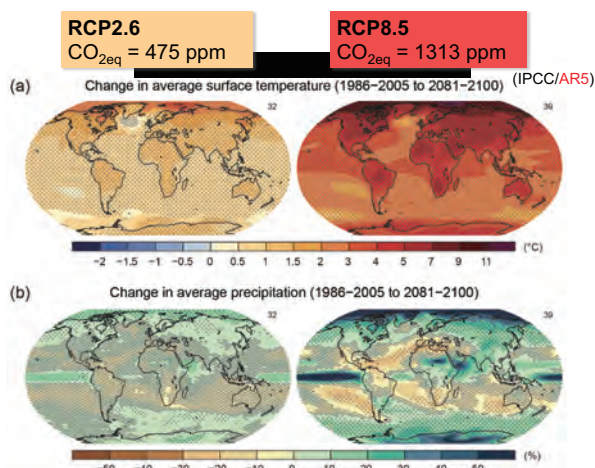
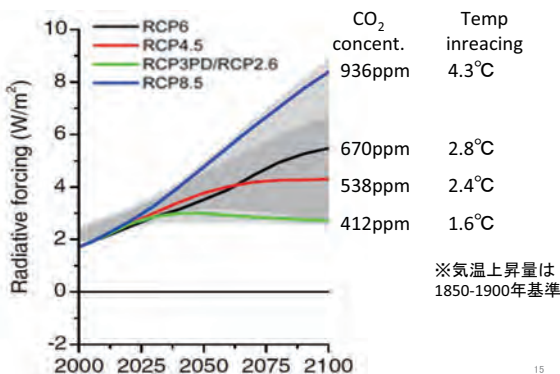


Detection and Attribution of Climate Change

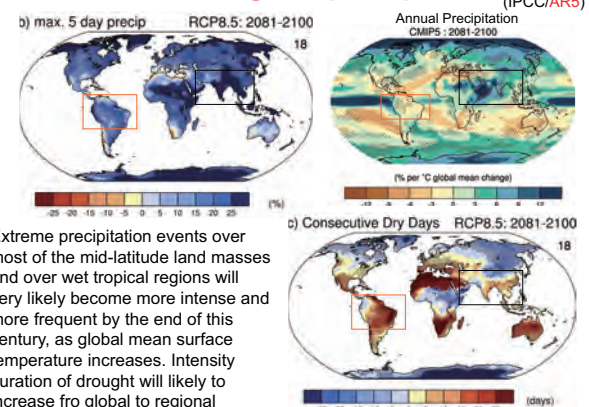
- It is extremely likely that more than half of the observed increase in global average surface temperature from 1951 to 2010 was caused by the anthropogenic increase in greenhouse gas concentrations and other anthropogenic forcings together.
- It is very likely that anthropogenic forcings have made a substantial contribution to increases in global upper ocean heat content (0–700 m) observed since the 1970s.
- It is likely that anthropogenic influences have affected the global water cycle since 1960. Anthropogenic influences have contributed to observed increases in atmospheric moisture content in the atmosphere (medium confidence), to global-scale changes in precipitation patterns over land (medium confidence), to intensification of heavy precipitation over land regions where data are sufficient (medium confidence), and to changes in surface and sub-surface ocean salinity (very likely).



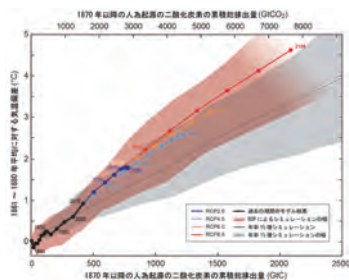
CO₂ scenarios for AR5 (Representative Concentration Pathways: RCP)



Extreme change in precipitation (IPCC/AR5)



Extreme precipitation events over most of the mid-latitude land masses and over wet tropical regions will very likely become more intense and more frequent by the end of this century, as global mean surface temperature increases. Intensity duration of drought will likely to increase from global to regional



Limiting climate change will require substantial and sustained reductions of greenhouse gas emissions.

Budget for the 2°C target: 790 Bill. t C
 CO₂ emitted until 2011: -515 Bill. t C
Remaining emissions: 275 Bill. t C
 CO₂ emissions 2012: 9.7 Bill. t C/yr



Contents

- Back ground
- On the SOUSEI Program
- Some products from direct use of GCM and RCM output
- O(5000yrs) Mega Ensemble Experiments "d4PDF"
- Worst case class scenarios
- Towards building adaptation strategy



SOUSEI Program for Risk Information on Climate Change
 気候変動リスク情報創生プログラム

Supported by MEXT (2012-2017)



Prof. Kimoto

Imminent global climate change (AORI, UT)
 Climate variability and change
 Integrated prediction system

A



Dr. Kawamiya

Stabilization target setting (JAMSTEC)
 Long-term projection
 Large-scale variations

B



Dr. Takayabu

Risk Information (MRI)
 Probabilistic climate projection
 Producing a standard climate scenario

C



Prof. Nakakita

Impact assessments (DPRI, KU)
 Natural Hazards
 Water Resources
 Ec. system

D



Sousei Program, Theme D

Precise impact assessments on climate change
 PI: Prof. E. Nakakita (Kyoto U)
 Secretary: Prof. Mori, Takemi, Tachikawa, Tanaka



7



Sub-groups in Group D

updated 2013/8/1

- **i Climate change impacts on natural hazards (Eiichi Nakakita, Kyoto U)**
 - i-a Meteorological risk (Takemi, Kyoto U) 12
 - i-b River basin risk (Tachikawa, Kyoto U) 25
 - i-c Coastal risk (Mori, Kyoto U) 18
 - i-d Risk management (Tanaka, Kyoto U) 6
 - i-e River risk in global scale (Miyake, PWRI) 15
- **ii Climate change impacts on water resources (Tanaka, Kyoto U)**
 - ii-a Social-economic risk (Tanaka, Kyoto U) 18
 - ii-b Anthropogenic effects (Oki, U Tokyo) 8
- **iii Change impacts on ecosystem and biodiversity (Nakashizuka, Tohoku U)**
 - iii-a Forest and lakes (Nakashizuka, Tohoku U) 4
 - iii-b Social-economic impact (Nakashizuka, Tohoku U) 4
 - iii-c Impact in East and East-South Asia (Kumagai, Nagoya U) 10
 - iii-d Coastal ecosystem (Yamanaka, Hokkaido) 10

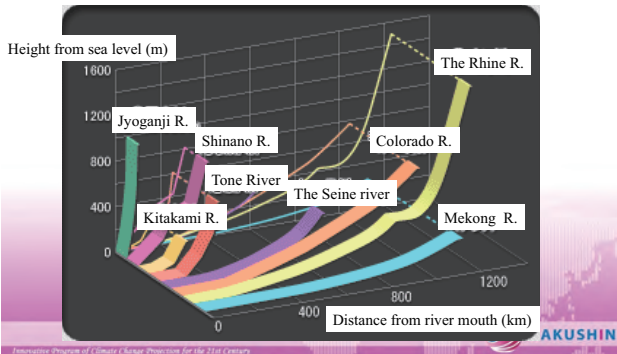


Launching of Sousei Program

- **Kyousei(共生)Program:2002-2007**
 - 20kmRCM (daily rainfall)
- **Kakushin(革新)Program:2007-2012**
 - 20kmGCM, 5,2,1kmRCM (hourly rainfall)
 - Natural hazards (Inc. water resources)
- **Sousei(創生)Program:2012-2017**
 - Impact assessment and producing adaptation methodologies
 - Worst case scenario
 - for Natural Disaster, Water resources, Ecosystem and Eco service
- **Tougou(統合)Program:2017-2022**
 - Non-regret adaptation strategies
 - Seamless hazard prediction until the end of the 21st century

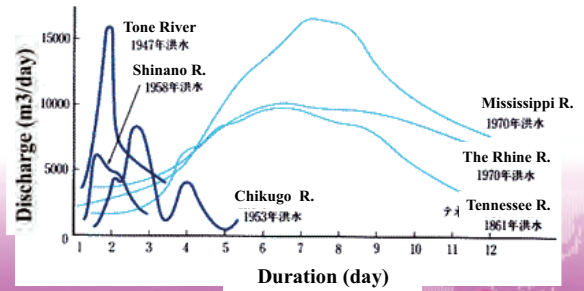
Features of Japanese River(1)

- Short length and steep slope.

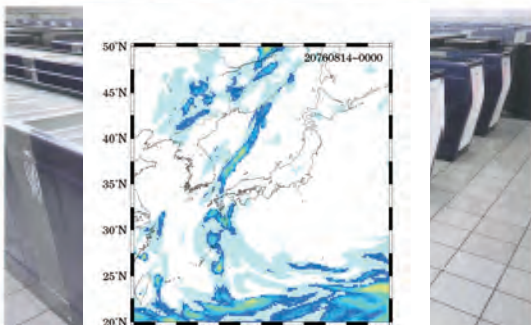


Features of Japanese River(2)

- Large peak discharge, short duration

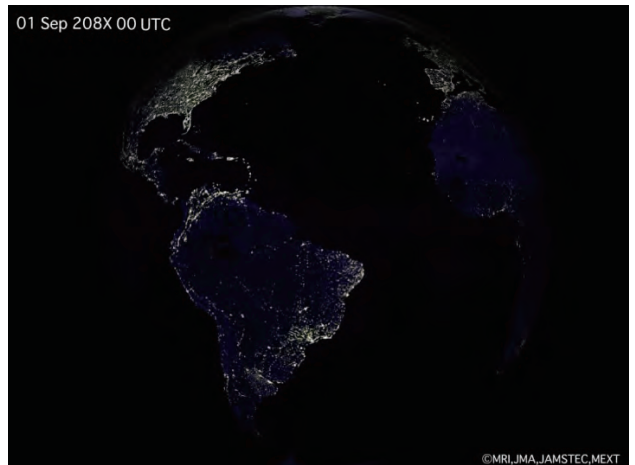
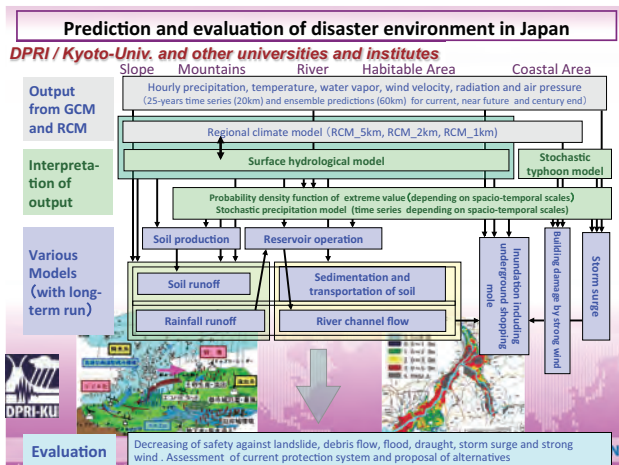
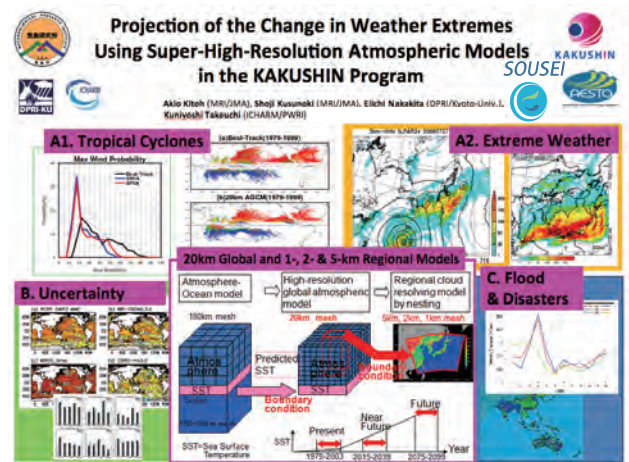


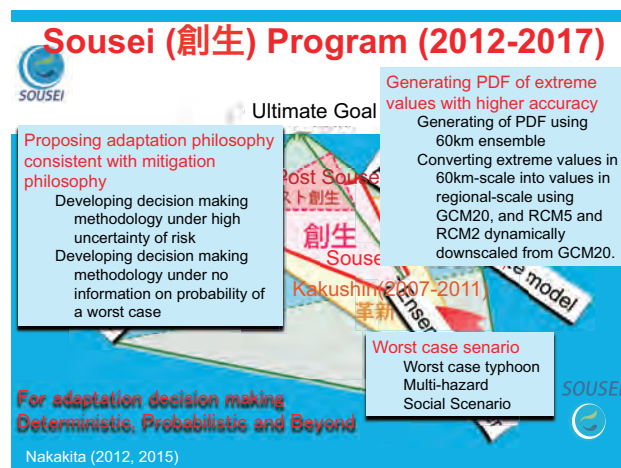
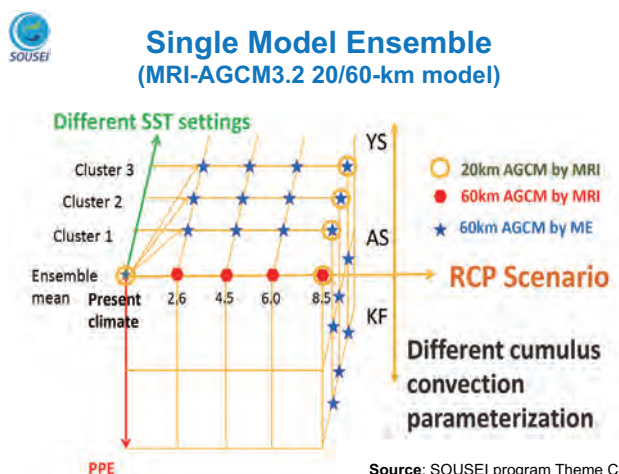
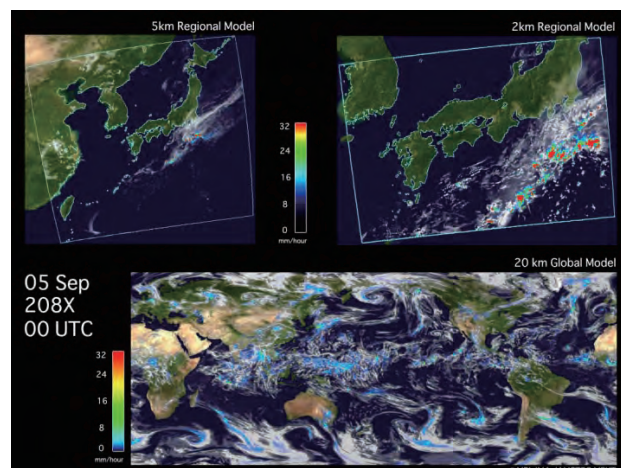
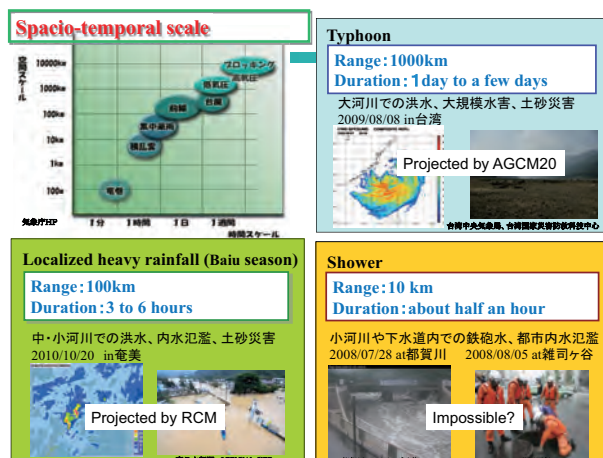
Projected typhoon by GCM20



It is the typhoon resolving output from GCM20 that has realized the impact assessment on Japanese river regime

9





Sub-groups in Group D

updated 2016/4/1
 PI: Eiichi Nakakita

- i Climate change impacts on natural hazards (Eiichi Nakakita, Kyoto U)**
 - i-a Metrological risk (Takemi, Kyoto U) 12
 - i-b River basin risk (Tachikawa, Kyoto U) 25
 - i-c Coastal risk (Mori, Kyoto U) 18
 - i-d Risk management (Tatano, Kyoto U) 6
 - i-e River risk in global scale (Miyake, PWRI) 15
- ii Climate change impacts on water resources (Tanaka, Kyoto U)**
 - ii-a Social-economic risk (Tanaka, Kyoto U) 18
 - ii-b Anthropogenic effects (Oki, U Tokyo) 8
- iii Change impacts on ecosystem and biodiversity (Nakashizuka, Tohoku U)**
 - iii-a Forest and lakes (Nakashizuka, Tohoku U) 4
 - iii-b Social-economic impact (Nakashizuka, Tohoku U) 4
 - iii-c Impact in East and East-South Asia (Kumagai, Nagoya U) 10
 - iii-d Coastal ecosystem (Yamanaka, Hokkaido) 10

Contents

- Back ground**
- On the SOUSEI Program**
- Some products from direct use of GCM and RCM output**
- O(5000yrs) Mega Ensemble Experiments "d4PDF"**
- Worst case class scenarios**
- Towards building adaptation strategy**



Sub-groups in Group D

updated 2016/4/1
Pl: Eiichi Nakakita

- **i Climate change impacts on natural hazards (Eiichi Nakakita, Kyoto U)**
 - i-a Metrological risk (Takemi, Kyoto U) 12
 - i-b River basin risk (Tachikawa, Kyoto U) 25
 - i-c Coastal risk (Mori, Kyoto U) 18
 - i-d Risk management (Tatano, Kyoto U) 6
 - i-e River risk in global scale (Miyake, PWRI) 15
- **ii Climate change impacts on water resources (Tanaka, Kyoto U)**
 - ii-a Social-economic risk (Tanaka, Kyoto U) 18
 - ii-b Anthropogenic effects (Oki, U Tokyo) 8
- **iii Change Impacts on ecosystem and biodiversity (Nakashizuka, Tohoku U)**
 - iii-a Forest and lakes (Nakashizuka, Tohoku U) 4
 - iii-b Social-economic impact (Nakashizuka, Tohoku U) 4
 - iii-c Impact in East and East-South Asia (Kumagai, Nagoya U) 10
 - iii-d Coastal ecosystem (Yamanaka, Hokkaido) 10



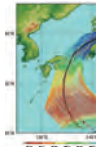
i-a: Metrological Disasters (Takemi, KU)

Downscaling of MRI-GCM/CMIP5 for impact assessment of natural disaster

Dynamic downscaling and perturbation of tracks of historical typhoon to estimate worst class typhoon for natural hazards

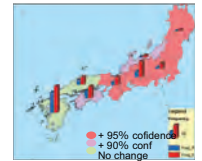
Participation by RCM

Projection of heavy rain falls



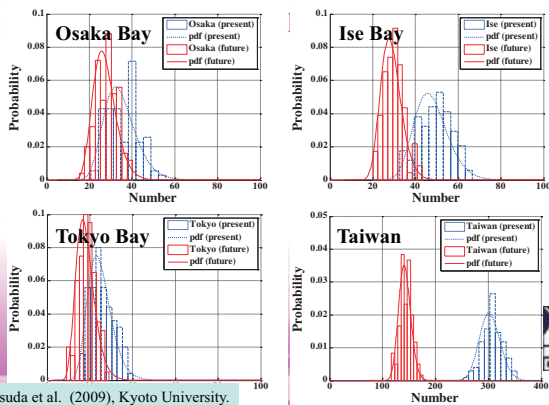
Pseudo-experiments for Ise Bay Typhoon

Statistical downscaling of typhoon



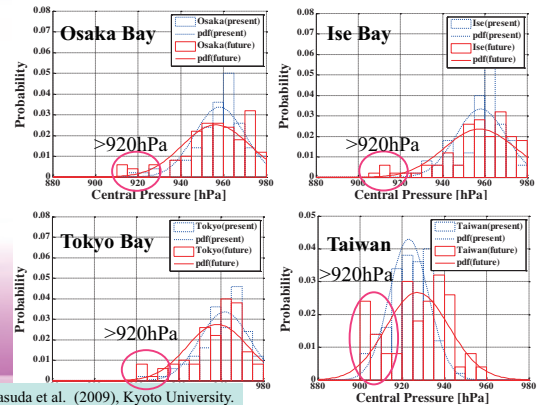
Downscaling of GCM for river discharge, storm surge, waves land side to evaluate regional scale impact

Probability of typhoon attack for 100yrs



Yasuda et al. (2009), Kyoto University.

Probability of center pressure for 100yrs

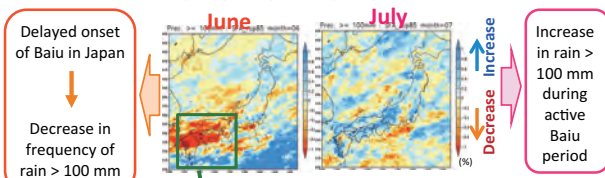


Yasuda et al. (2009), Kyoto University.

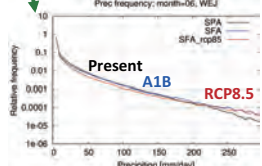


Changes in Baiu rainfall under global warming

Frequency change of daily rainfall > 100 mm



Frequency distribution of daily rainfall in western Japan in June

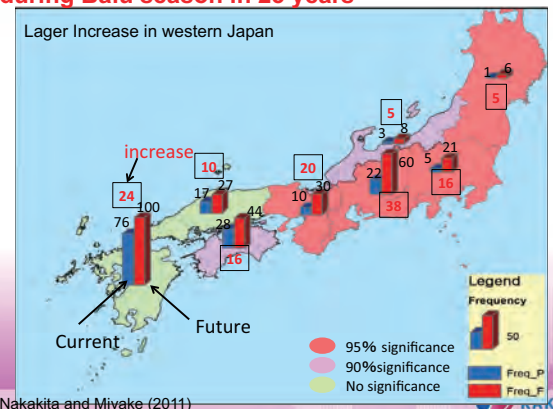


Increase in extreme rain > 200 mm/day

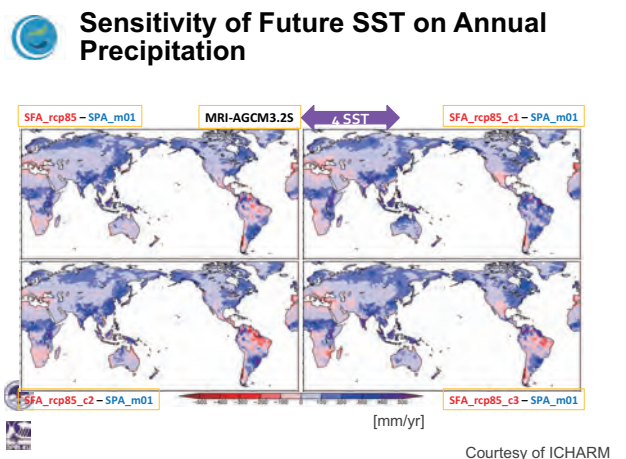
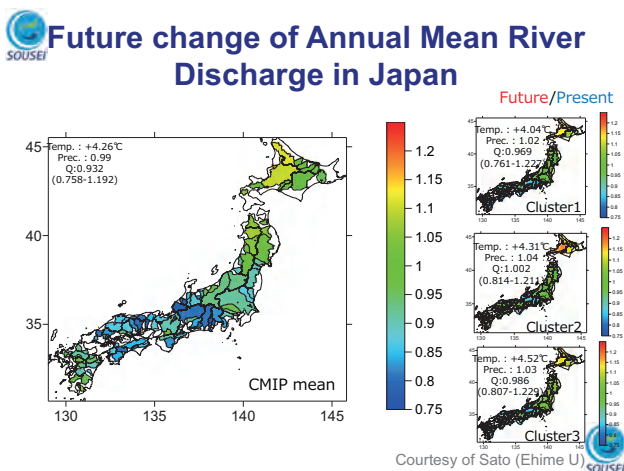
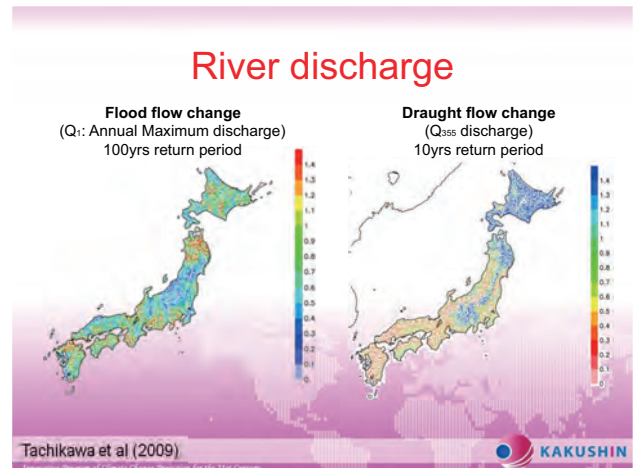
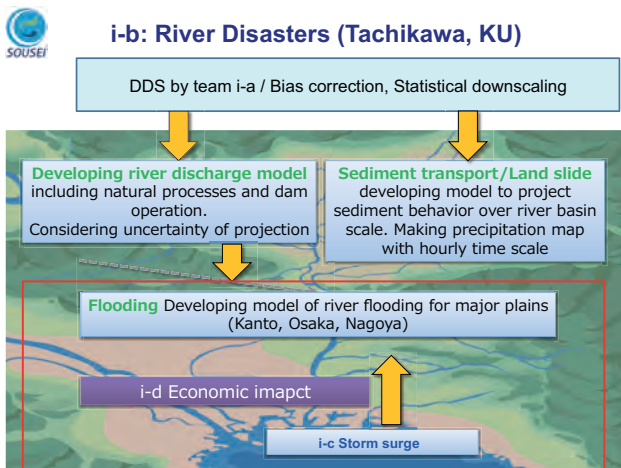
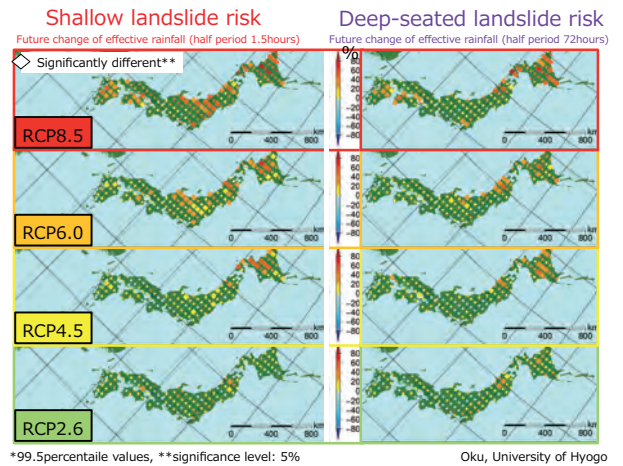
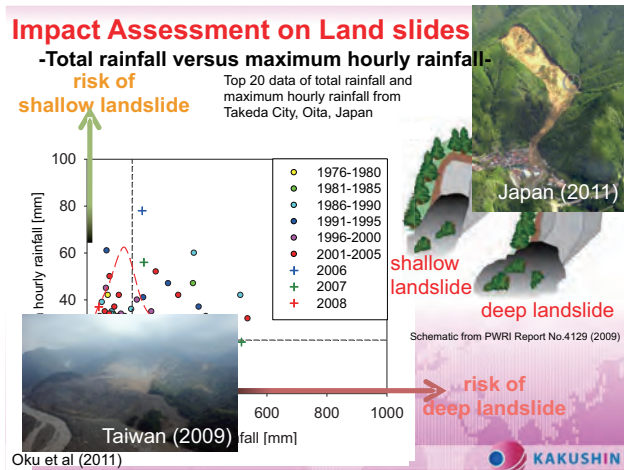
(Okada et al. 2016)

Increase in Number of localized heavy rainfall during Baiu season in 25 years

Larger Increase in western Japan



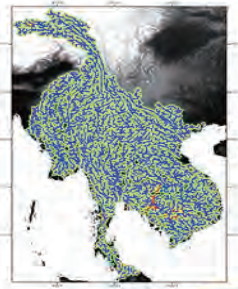
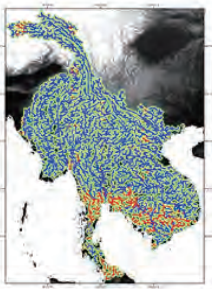
Nakakita and Miyake (2011)



Future change of River Discharge in Mekong Delta

Cloud Convection schemes

SSTs

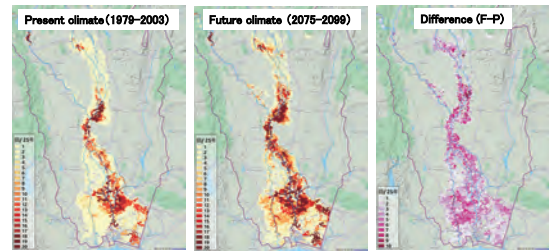


Mean of River Discharge in 25 years

Red: Null hypotheses is rejected.

Courtesy of Tachikawa (Kyoto U)

Frequency of estimated flood inundation in the present and future climate (ICHARM)

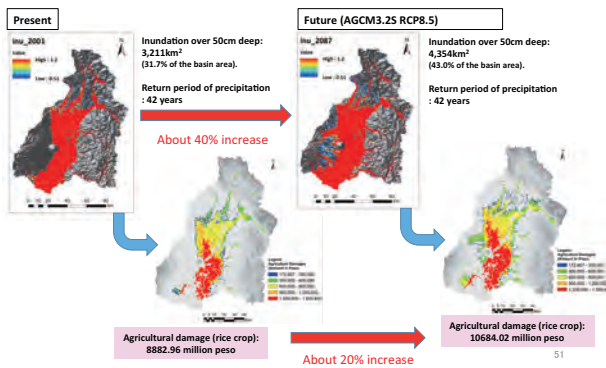


- Annual maximum inundation depths for each year in the present (SPA-m01) and future (RCP8.5, C1-C3) climate conditions are calculated. For each cell, the no. of years that experience peak inundation depth with 0.5m or more is counted.
- There are no visible changes in the maximum flood extent between present and future, however there are significant increases in the flood frequency in the areas along the main channels.

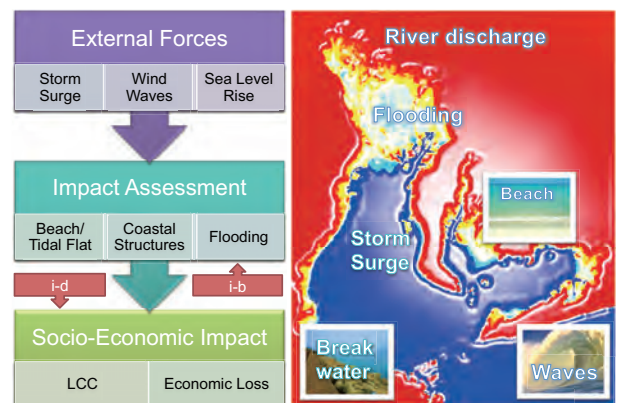
50

Comparison of agricultural damage (rice crop) in the worst cases under present/future climate scenarios (ICHARM)

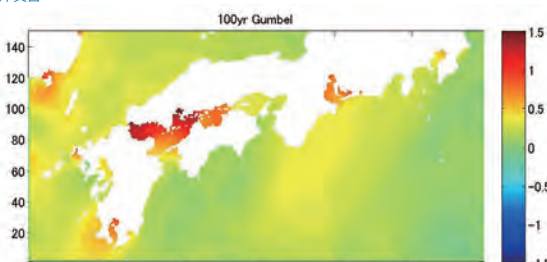
We selected 2001 and 2087 as the worst case years (return period: 42 years) after performing simulations for the largest inundation area under the present and future climate scenarios (25 years). Then we estimated agricultural damage in each case by applying the agricultural damage curve developed by ICHARM. We found that the agricultural damage may increase by 20%, comparing the worst cases.



i-c: Coastal Disasters (Mori, KU)



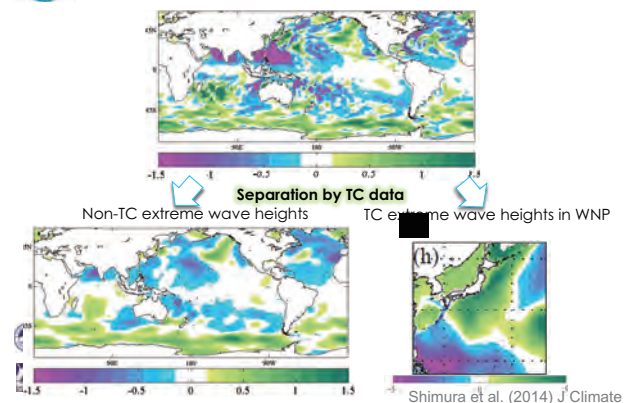
Future Change of Extreme Storm Surge MRI-AGCM3.2S



Future change of 100yrs return value of storm surge height
AGCM20 -> RCM5km -> Storm surge modeling

Yasuda et al. (2014) Coastal Engineering

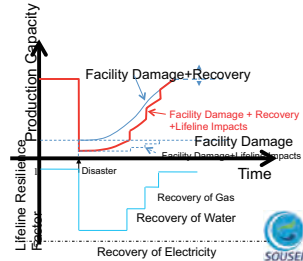
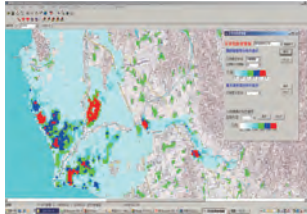
Future Change of Extreme Ocean Waves TC and Non-TC waves



Shimura et al. (2014) J Climate

Measuring socio-economic impacts of climate change and effectiveness of adaptation strategies (Tatano, KyotoU)

1. Developing integrated water hazard risk assessment
2. Socio-economic impact of inundation
3. Cost-benefit of adaptation



Sub-groups in Group D

updated 2013/8/1

- **i Climate change impacts on natural hazards (Eiichi Nakakita, Kyoto U)**
 - i-a Meteorological risk (Takemi, Kyoto U) 12
 - i-b River basin risk (Tachikawa, Kyoto U) 25
 - i-c Coastal risk (Mori, Kyoto U) 18
 - i-d Risk management (Tatano, Kyoto U) 6
 - i-e River risk in global scale (Miyake, PWRI) 15
- **ii Climate change impacts on water resources (Tanaka, Kyoto U)**
 - ii-a Social-economic risk (Tanaka, Kyoto U) 18
 - ii-b Anthropogenic effects (Oki, U Tokyo) 8
- **iii Change impacts on ecosystem and biodiversity (Nakashizuka, Tohoku U)**
 - iii-a Forest and lakes (Nakashizuka, Tohoku U) 4
 - iii-b Social-economic impact (Managi, Tohoku U) 4
 - iii-c Impact in East and East-South Asia (Kumagai, Nagoya U) 10
 - iii-d Coastal ecosystem (Yamanaka, Hokkaido) 10

Theme D-ii Climate change impacts on water resources

- (a) Assessment of socio-economic impacts on water resources and their uncertainties under changing climate
sub-leader: **Kenji Tanaka (Kyoto University, DPRI)**



This team mainly predict and assess the changes in the supply of water in the major rivers in Japan, the impact on rice farming, hydropower, etc.

- (b) Assessment of climate change impacts on the social-ecological systems of water resources and hydrological cycles
sub-leader: **Taikan Oki (University of Tokyo, IIS)**

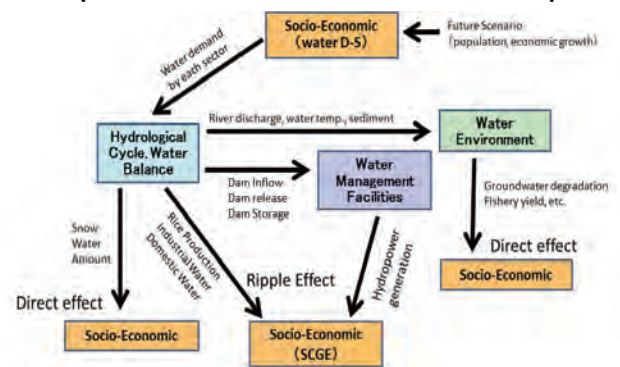


This team predict and assess how the actual water cycle and available water resources will change on a global scale with inclusion of human impact.

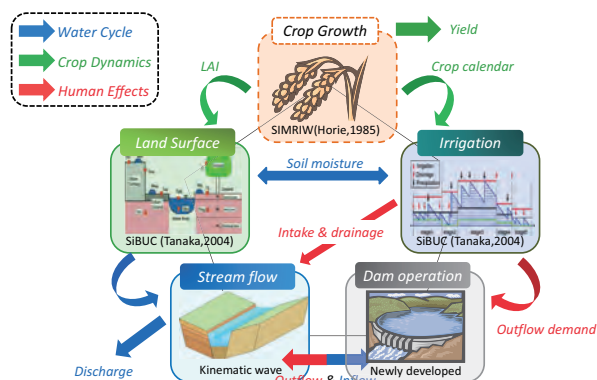
Kyoto University Team



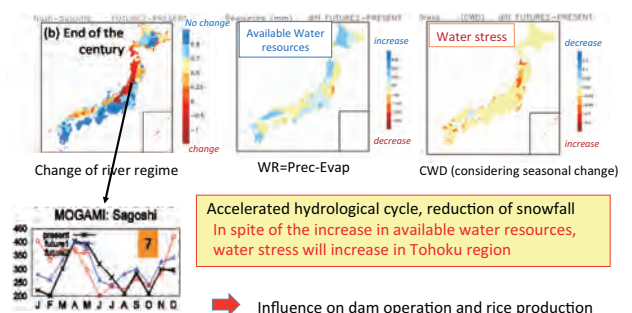
Important Collaboration between sub-Group



Integrated Water Resources Model



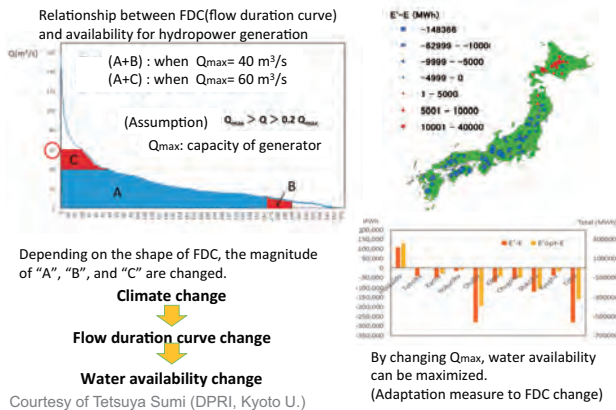
Impact of climate change on water resources in Japan



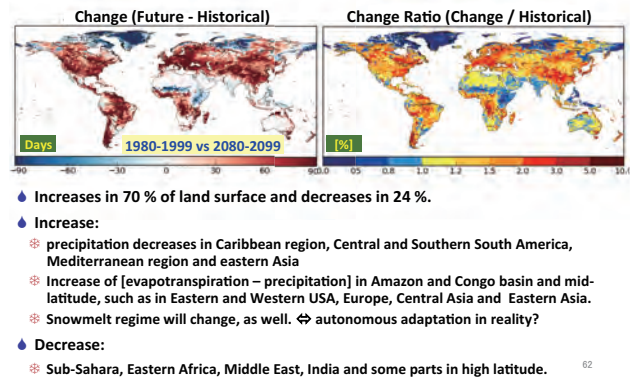
→ Influence on dam operation and rice production

Courtesy of Kenji Tanaka (DPRI, Kyoto U.)

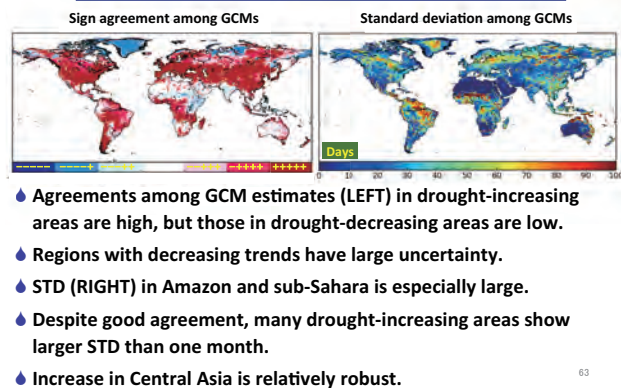
Climate change impact on hydropower generation



Changes of drought days under RCP8.5

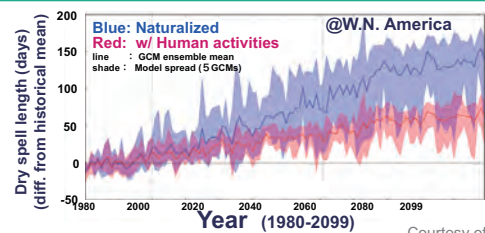


Uncertainty of drought changes



Projection of dry spell length

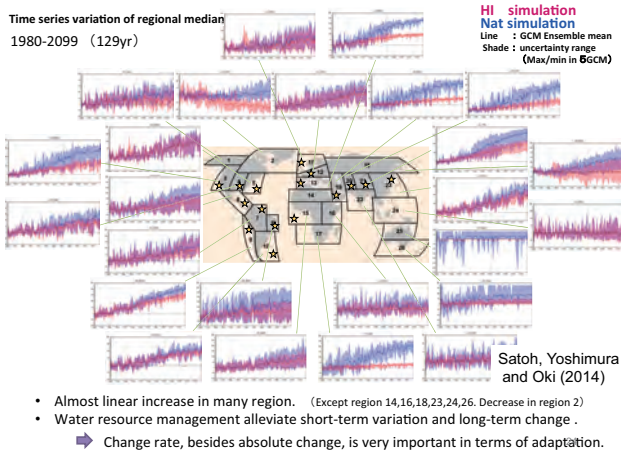
—with and without human activities—



Impacts of human activities

- Smaller inter annual variability → Model spread is also smaller
- Smaller increasing trend → Dry spell length can be overestimated if human activities are not considered

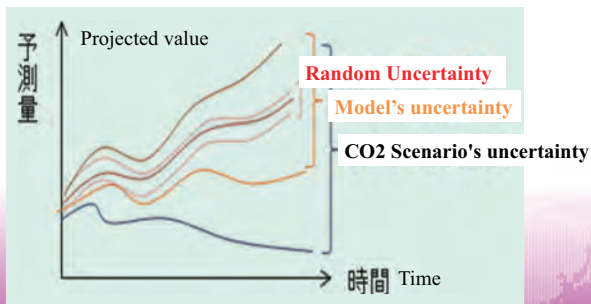
Water resources management reduces the variability and long term changes of dry spell length under climate change



Contents

- Back ground
- On the SOISEI Program
- Some products from direct use of GCM and RCM output
- O(5000yrs) Mega Ensemble Experiments "d4PDF"
- Worst case class scenarios
- Towards building adaptation strategy

Uncertainty inherent to GCM projection



Forecasting Project of Climate Change Projection for the 21st Century

KAKUSHIN

There is high uncertainty in projected design value

- We may be almost sure that average of extreme design value would increase.
- However, projected increase in the design value is merely rough estimation,
- because, for example, the worst case typhoon for a specific river basin may not be realized (computed) in a single projected time series.
- Therefore, it is very important to
 - 1) increase ensemble member
 - 2) estimate river discharge when a worst case typhoon would pass through, even though we cannot estimate return period.

SOUSEI

KAKUSHIN

There is high uncertainty in projected design value

- We may be almost sure that average of extreme design value would increase.
- However, projected increase in the design value is merely rough estimation,
- because, for example, the worst case typhoon for a specific river basin may not be realized (computed) in a single projected time series.
- Therefore, it is very important to
 - 1) increase ensemble member
 - 2) estimate river discharge when a worst case typhoon would pass through, even though we cannot estimate return period.

SOUSEI

KAKUSHIN

Sousei (創生) Program (2012-2017)

SOUSEI

Ultimate Goal

Proposing adaptation philosophy consistent with mitigation philosophy

Developing decision making methodology under high uncertainty of risk
Developing decision making methodology under no information on probability of a worst case

Generating PDF of extreme values with higher accuracy
Generating of PDF using a lot of 60km ensemble
Converting extreme values in 60km-scale into values in regional-scale using RCM5 and RCM2 dynamically downscaled from GCM20.

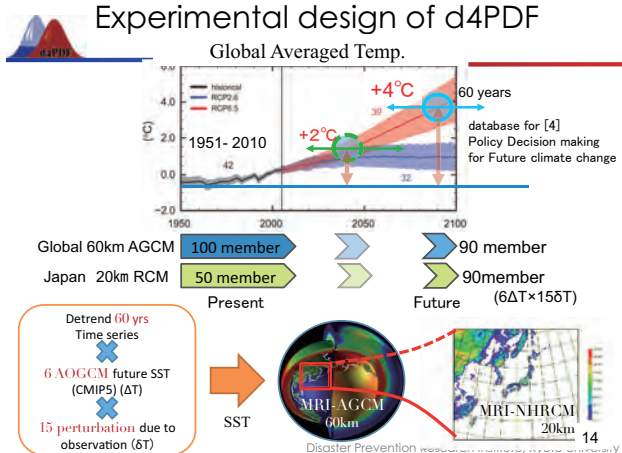
Worst case scenario
Worst case typhoon
Multi-hazard
Social Scenario

For adaptation decision making
Deterministic, Probabilistic and Beyond

Nakakita (2012, 2015)

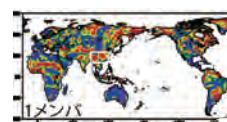
SOUSEI

Experimental design of d4PDF



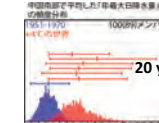
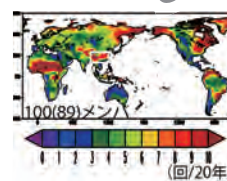
Frequency of annual maximum daily rainfall

Analysis of ES 100x100 experimental analysis



20 years x 1 members

Increase of ensemble member



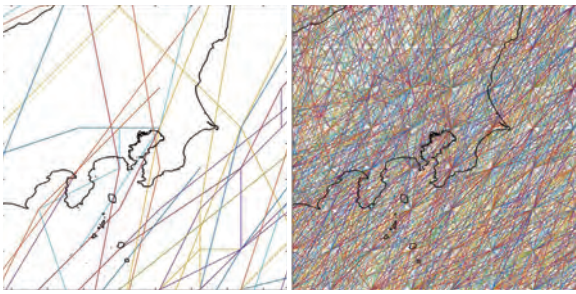
1951~1970 World of +4°C

Shiogama@NIES



Number of TC is insufficient

Mean landfall on Japan: 2.7/yr (MRI)

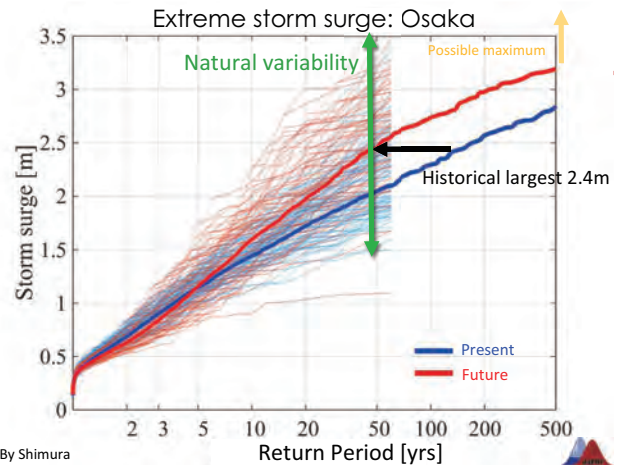


25 years climate run

d4PDF (5400 yrs)

By Shimura

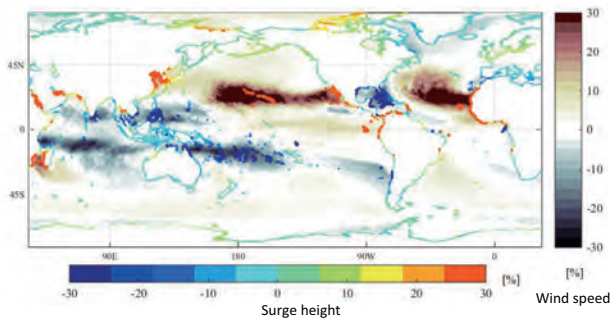
Disaster Prevention Research Institute, Kyoto University



By Shimura

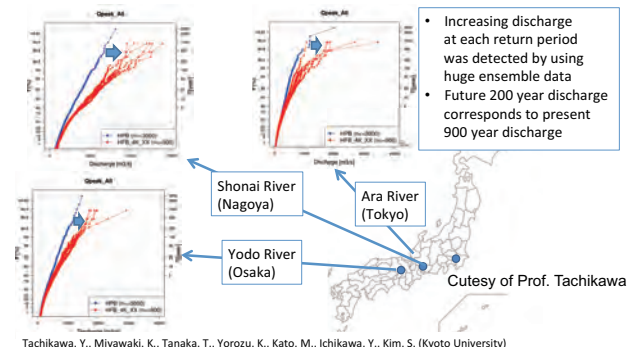


Future change of 100 yrs Storm Surge



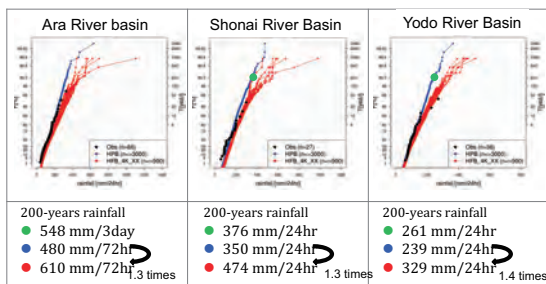
Disaster Prevention Research Institute, Kyoto University

Present(Blue) and Future(red) annual maximum river discharge by d4PDF rainfall data



Tachikawa, Y., Miyawaki, K., Tanaka, T., Yorozu, K., Kato, M., Ichikawa, Y., Kim, S. (Kyoto University)

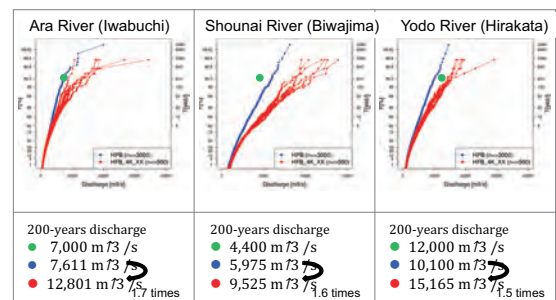
Annual Maximum 24hrs Catchment Average Rainfall



- 200-years rainfall estimated by using observed data, which is used for the river improvement planning at Construction Ministry in Japan.
- 200-year annual maximum rainfall estimated by using d4PDF present simulation data
- 200-year annual maximum rainfall estimated by using d4PDF future simulation data, which is mean of the ones of 6 SSTs.

Cutesy of Prof. Tachikawa

Change of Annual Maximum Hourly Discharge



- 200-years discharge estimated by using observed data, which is used for the river improvement planning at Construction Ministry in Japan.
- 200-year annual maximum discharge estimated by using d4PDF present simulation data
- 200-year annual maximum discharge estimated by using d4PDF future simulation data, which is mean of the ones of 6 SSTs.

Cutesy of Prof. Tachikawa

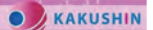


Contents

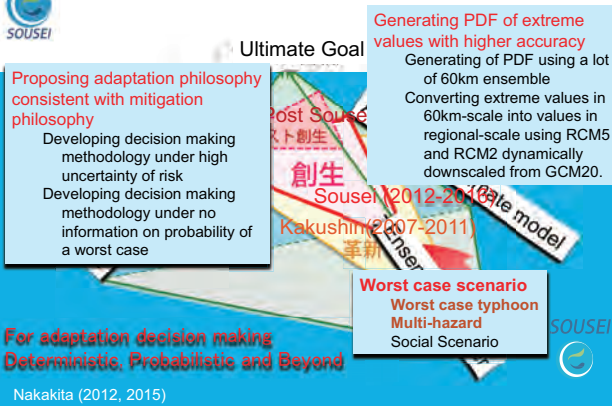
- Back ground
- On the SOISEI Program
- Some products from direct use of GCM and RCM output
- O(5000yrs) Mega Ensemble Experiments "d4PDF"
- Worst case class scenarios
- Towards building adaptation strategy

There is high uncertainty in projected design value

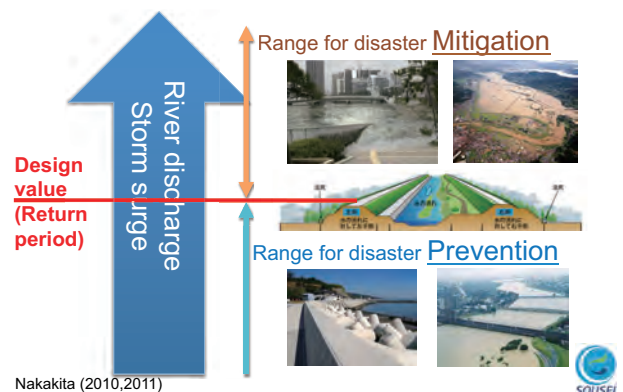
- We may be almost sure that average of extreme design value would increase.
- However, projected increase in the design value is merely rough estimation,
- because, for example, the worst case typhoon for a specific river basin may not be realized (computed) in a single projected time series.
- Therefore, it is very important to
 - 1) increase ensemble member
 - 2) estimate river discharge **when a worst case typhoon would pass through**, even though we cannot estimate return period.



Sousei (創生) Program (2012-2017)

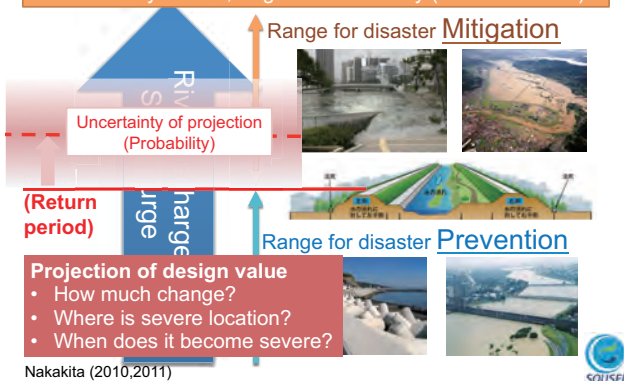


Disasters and Infrastructure Design

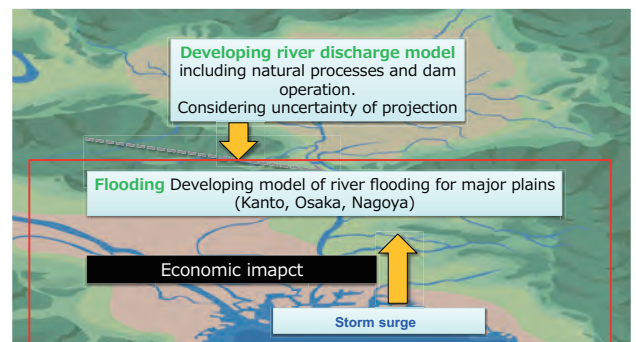


Disasters and Infrastructure Design

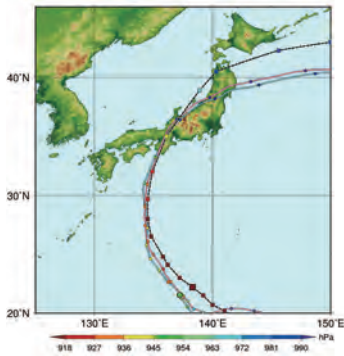
Survivability Critical, Edge of Survivability (The worst case)



Multi-flooding hazards (river and storm surge flooding)



Ise-bay Typhoon **pseudo-global warming** experiment



What is Pseudo-Global Warming (PGM) ?

Re-analyzed past typhoon is numerically simulated by physically based atmospheric model under the GCM projected future SST and ambient atmospheric conditions.

(Nakano, JAMSTEC)



PGW of Ise-bay Typhoon (1959)

『昭和34年9月 伊勢湾台風』

なかでも伊勢湾台風による被害は多大なものでした。



名張市 夏見(赤川橋 夏見橋)



名張市 本町

雨量432ミリ、洪水面積1540ヘクタールを記録し、暴雨により名張川が最大力で決壊しました。橋の流失がいつづ、濁流が市街地の高層を除く全壊に流れ込み、被害額は10億となりました。洪水被害をはじめ、家屋倒壊など、人命財産に多大なる被害をもたらしました。

トモ・サトウ・タナシ



Copyrights © Ministry of Land, Infrastructure and Transport Kizugawa Joryu office All Right Reserved

SOUSEI

Pseudo-global warming (PGW) experiment

PGW = Actual Condition + GW Increment

Actual condition: from analysis fields for a past event

Long-term reanalysis dataset: JRA-55 (available from 1958)

Global warming increment:

Future changes in temperature, pressure, sea surface temperature from GCM climate prediction data

Increment = (GCM future climate) – (GCM present climate)

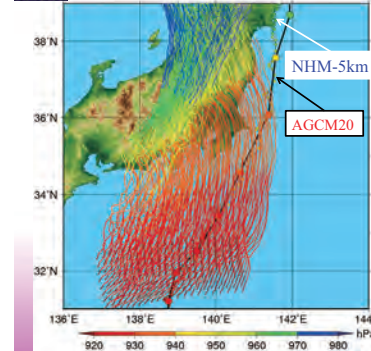
Add global warming increment to past analysis fields

(Pseudo-global warming climate)

= (Reanalysis for actual case) + (Monthly mean GW increment)



Virtual Shifting of typhoon's initial position - for making a worst scenario -



Virtual Shifting of typhoons initial position by keeping potential vorticity same (a vorgas method)

Dynamic downscale by RCM

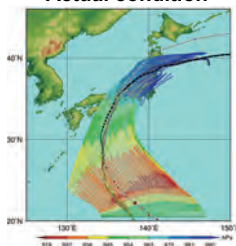
Worst case impact assessment on

- Land: extreme wind and rainfall
- Ocean: storm surge and wave height

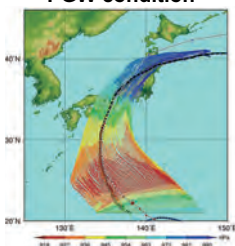
Ishikawa et al (2009)

Virtual Shifting of typhoon's initial position for Ise-bay typhoon (a Worst Case Scenario)

Actual condition



PGW condition



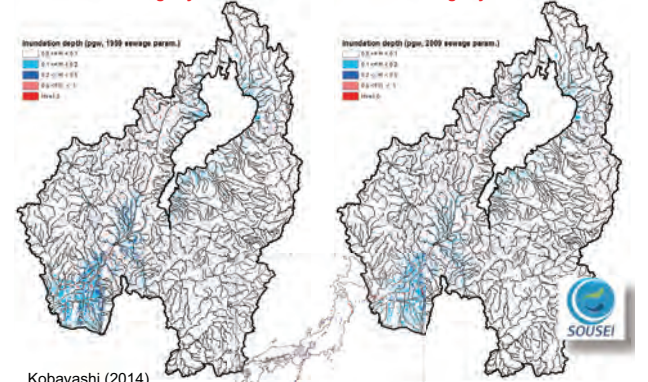
Max. wind	Reproduced	PGW	difference
Ise Bay	35.7(m/s)	41.1(m/s)	+5.4(m/s)
Osaka Bay	32.3	36.3	+4.0

(DPRI : Oku, Takemi, Ishikawa)

Simulated Inundation

PGW with sewage system in 1959

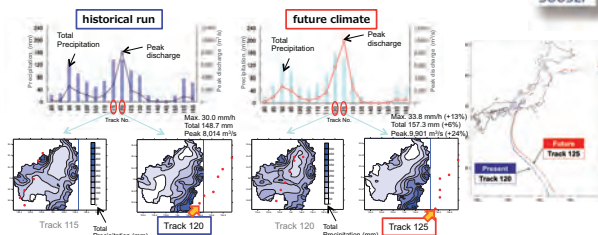
PGW with sewage system in 2009



Kobayashi (2014)



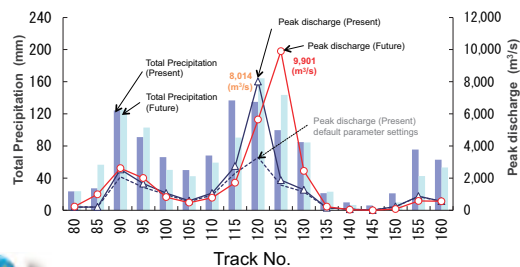
Worst Case Scenario of River Flooding (Yodo River basin)



The worst case flood event (maximum peak discharge) was caused by Track 120 and Track 125 under present and future climate condition respectively.

(Y.Sato, Ehime Univ.)

Total precipitation and peak discharge (Yodo River basin, Hirakata)

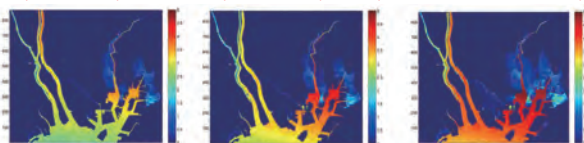


(Y.Sato, Ehime Univ.)

Projected maximum storm surge height with inundation

-typhoon Vera at Ise Bay-

Typhoon Vera (historical run) Extreme typhoon Vera (future climate) Extreme and shifted typhoon Vera (future climate+ worst course)

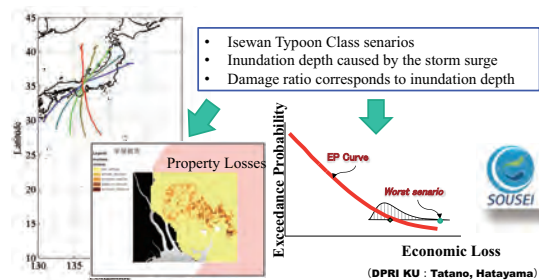


Multiple flooding disaster (river and storm surge flooding)

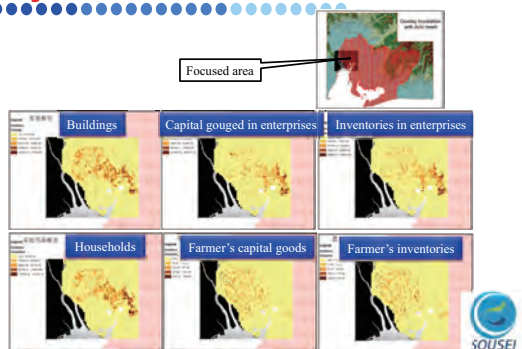
- Worst scenario is different between storm surge and river flooding
- Storm surge
 - Key factors: central pressure and track of the typhoon, astronomical tide
- River flooding
 - Key factors: intensity and duration of precipitation

Shibutani et al, 2014

Toward Economic Impact Assessment (Estimating Property losses)



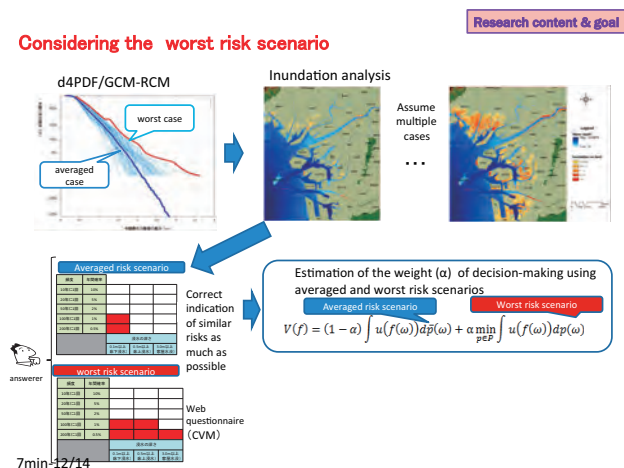
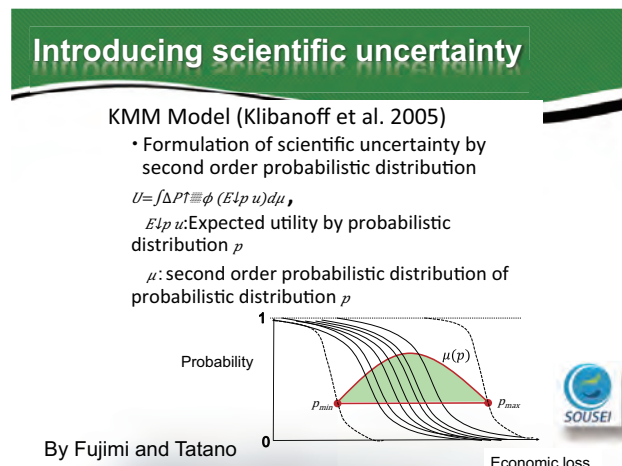
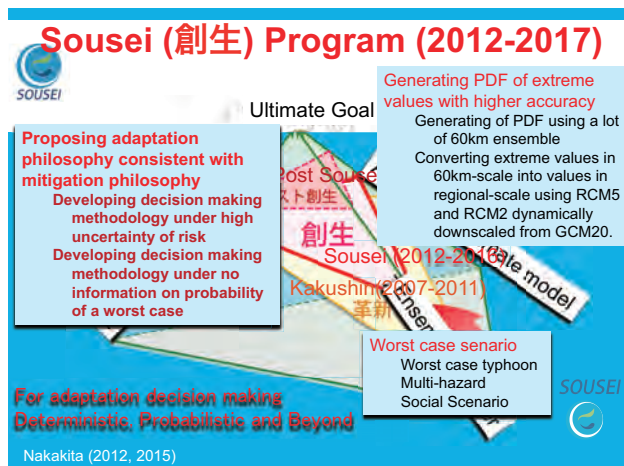
Property Loss Estimation in Ise Bay area



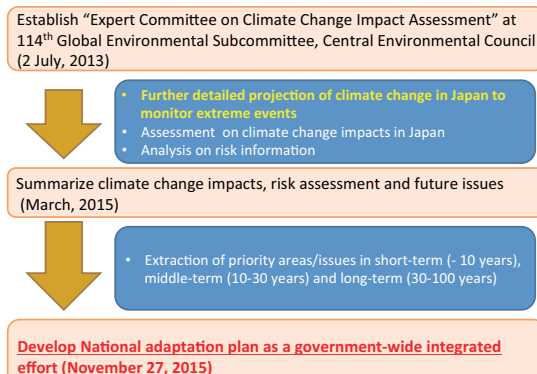
(DPRI, Kyoto Univ. : Tatano, Hatayama, 2014)

Contents

- Back ground
- On the SOISEI Program
- Some products from direct use of GCM and RCM output
- O(5000yrs) Mega Ensemble Experiments "d4PDF"
- Worst case class scenario
- Towards building adaptation strategy

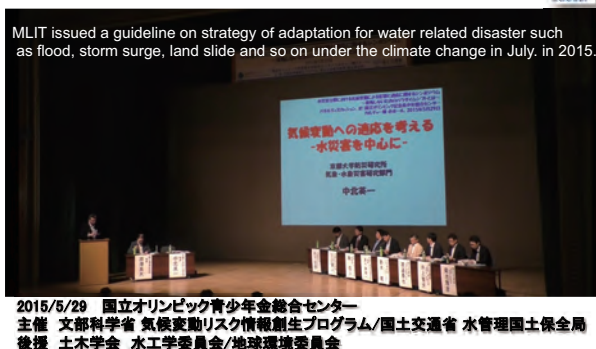


Steps towards National Adaptation Plan



[Slide drawn by MOE modified by Nakakita]

Joint Symposium on Adaptation with Japanese Ministry of Land, Infrastructure and Transport (MLIT)



Summary (1)

- The AGCM and RCM with super-high spatio-temporal resolutions (20 km-1 hour) made it possible to evaluate extreme hazard (ex. Max. discharge) in Japan.
- We can get approximate projection on changes of return values of extreme events.
- However, there is a risk that the return period does not have enough accuracy **because there is no guarantee that quite extreme events could be properly projected within the limited number of ensembles. (Single time series output from the AGCM20 and RCM)**
- In this sense, it may be difficult to project correct design hazard for water management and flood control so on.

Summary (2)

6. On the other hand, the risk management deal with phenomena beyond design hazards. In this sense, it is very important to take into account the result from **a worst class scenarios as one of the forcing hazard for disaster risk management under climate change.**
7. Taking into consideration above items, I think, it is very important for climate change adaptation to **discriminate more between planning with an uncertain design level and risk management with a worst case scenario.**
8. Of cause, **making the number of ensembles increase is essentially important. In this sense, d4PDF is very important and valuable data set.**

Sousei (創生) Program D (2012-2016)

basic consideration

SOUSEI

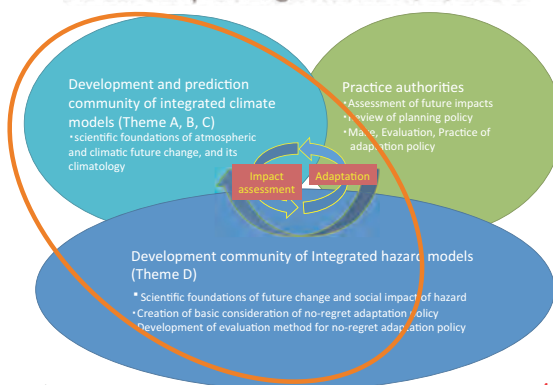
- Targets: natural disasters, water resources, ecology and biodiversity
- Estimation of high accuracy probability (change of design value)
 - Estimation of Probabilistic density distribution using multiple predictions (ensemble simulations) of coarse-resolution models of (Theme C GCM60 (60km-Global climate model) and CMIP5)) => d4PDF
 - Conversion of coarse spatial resolution data into regional scale one using high spatiotemporal resolution models of GCM20(20km-Global climate model) or RCM5, 2 (2km, 5km-Regional climate model) (provided by Theme C)
- Assumption of the greatest external forcing – Survival chance
 - Worst typhoons (Collaborated with Theme C for artificial global warming)
 - Compound disasters
 - Assumptions of social scenarios
- Development of the consideration and philosophy of making adaptation strategy
 - Development of decision-making approach under large uncertainty
 - Development of decision-making approach under the worst scenarios without any probabilistic information
 - Creation of new sense of values, e.g., economic index of ecosystem

Nakakita (2012, 2015)

Summary (3)

9. Ministry of Land, Infrastructure Transportation and Tourism (MLIT), in Japan have decided to introduce the concept of “the risk management with a worst case scenario” into “its official adaptation strategy” partly based on our activity under Kakushin and Sousei programs. The Ministry is waiting for an establishment of methodology of estimating the worst case class scenario, which could be uniformly applied nationwide.

Content of Theme D, Relationship among Themes A, B, and C



4min-1/7

4min/7/4

Other collaborations

Collaboration with academic society 22nd JSCE Earth Environment Symposium

Future perspective of climate change research for adaptation by the viewpoint of civil engineering



SOUSEI-REGGA-DIAS
(MEXT programs)
S-8
(Ministry of the Environment)

4min-11/12

4/7/4min

Other collaborations

Collaborative symposium and research meetings with governmental authorities



National Olympic Memorial Youth Center, May 29, 2015
Organizer SOUSEI Program, MEXT/ Water and Disaster Management Bureau, MLIT
Co-organizer Committee on Hydrosience and Hydraulic Engineering, JSCE
Committee on Earth Environment, JSCE

4min-12/12

4/7/4min

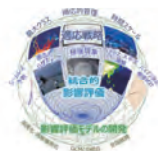
Thank you for your kind attention

Joint Symposium between Sousei themes C and D



Photo: Uji, Kyoto

Integrated Research Program for Advancing Climate Models Theme D: Integrated Hazard Prediction

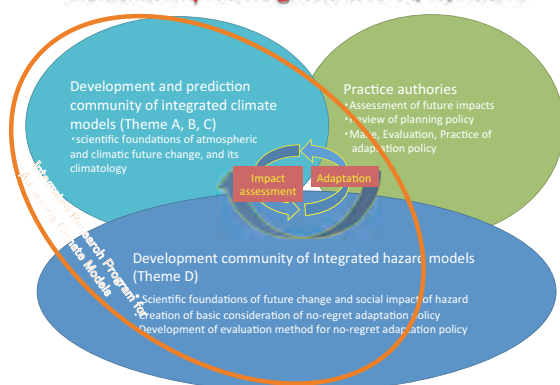


Principal Investigator:
Eiichi NAKAKITA

Atmosphere-Hydrosphere Research Group,
Disaster Prevention Research Institute,
Kyoto University

Content of Theme D, Relationship among Themes A, B, and C

basic consideration



4min-1/7

4min/7/4

Sousei (創生) Program D (2012-2016)

basic consideration



- Targets: natural disasters, water resources, ecology and biodiversity
- Estimation of high accuracy probability (change of design value)
 - Estimation of Probabilistic density distribution using multiple predictions (ensemble simulations) of coarse-resolution models of (Theme C GCM60 (60km-Global climate model) and CMIP5)) => d4PDF
 - Conversion of coarse spatial resolution data into regional scale one using high spatiotemporal resolution models of GCM20 (20km-Global climate model) or RCM5, 2 (2km, 5km-Regional climate model) (provided by Theme C)
- Assumption of the greatest external forcing – Survival chance
 - Worst typhoons (Collaborated with Theme C for artificial global warming)
 - Compound disasters
 - Assumptions of social scenarios
- Development of the consideration and philosophy of making adaptation strategy
 - Development of decision-making approach under large uncertainty
 - Development of decision-making approach under the worst scenarios without any probabilistic information
 - Creation of new sense of values, e.g., economic index of ecosystem

Nakakita (2012, 2015)

Perspectives of post-SOUSEI Program

basic consideration

- Continuous support for the approach and scientific knowledge of “Top-down” adaptation policy
- Requirement of enhancement and refinement of SOUSEI Program for further extension
- Heading towards issues of “evaluation of adaptation strategy” and “no-regret adaptation”
- Further, support of scientific knowledge for making and evaluating adaptation strategy
- Contribution to South-east Asia-Pacific Region

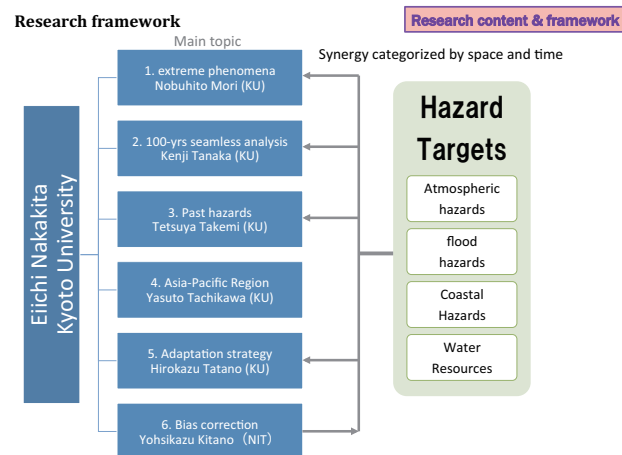
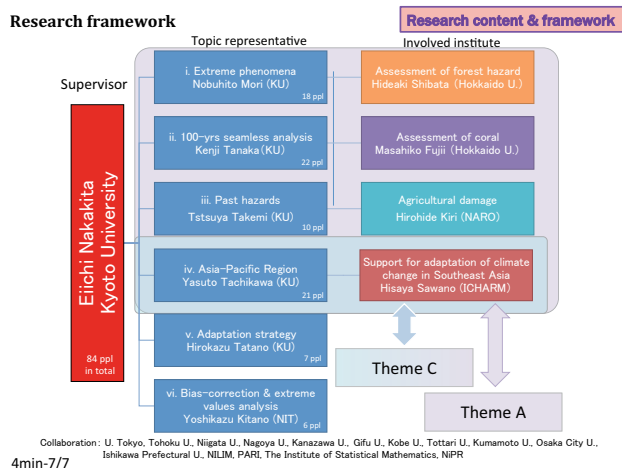
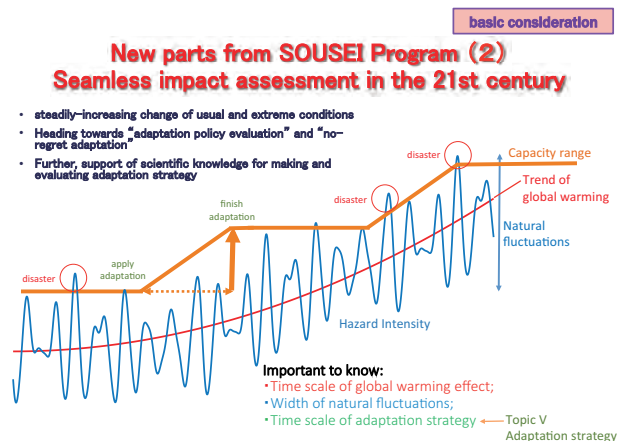
4min-3/7

4min/7/4

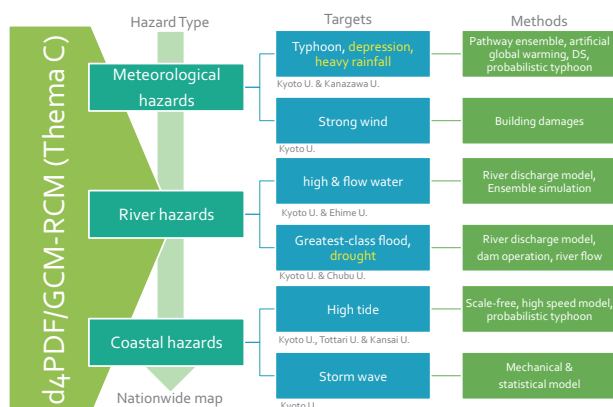
New part form SOUSEI Program (1)

basic consideration

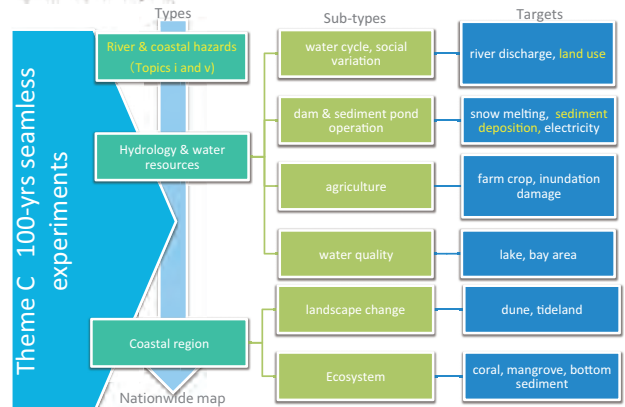
- Requirement of enhancement and refinement for extending SOUSEI program
 - Full application of d4PDF
 - Prediction and uncertainty analysis of extreme events (SOUSEI only had partial analysis.)
 - Probabilistic assessment of the high-end-class disasters



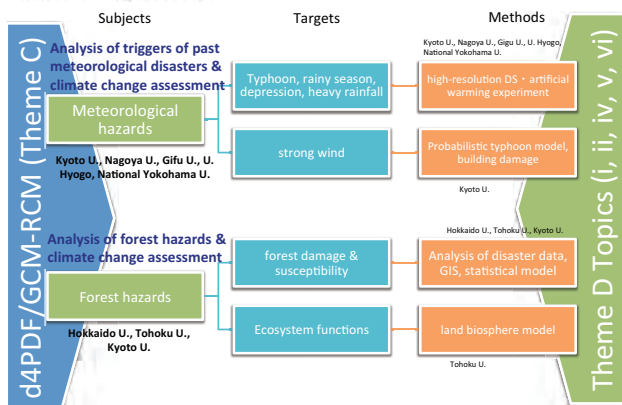
Topic (i): Long-term assessment of intensity and frequency of extreme hazards



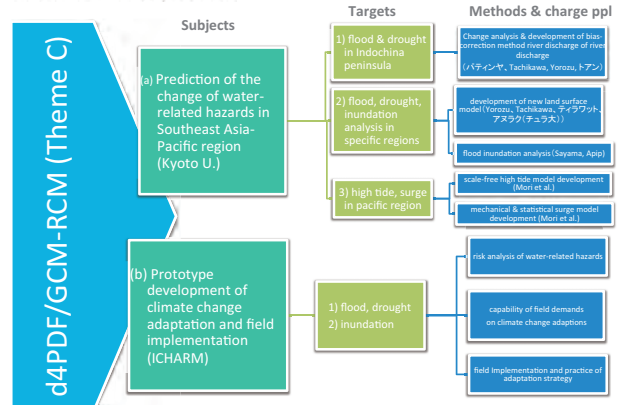
Topic (ii). Seamless hazard prediction until the 21st century (100 years seamless analysis)



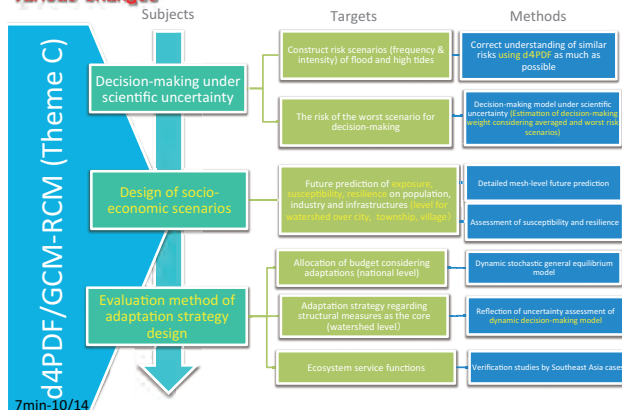
Topic (iii): Hazards analysis of past disasters and assessment of climate change factors



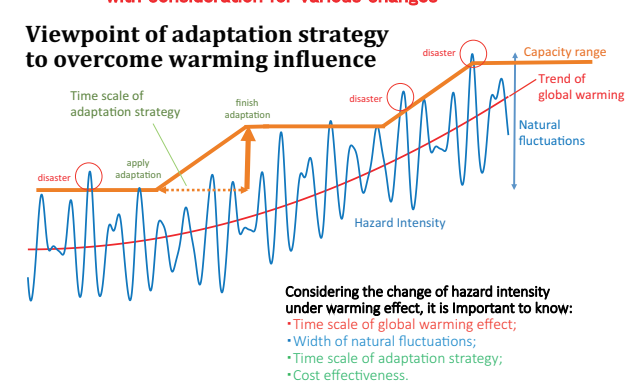
Topic (iv): Hazard assessment in Asia and Pacific countries and international cooperation



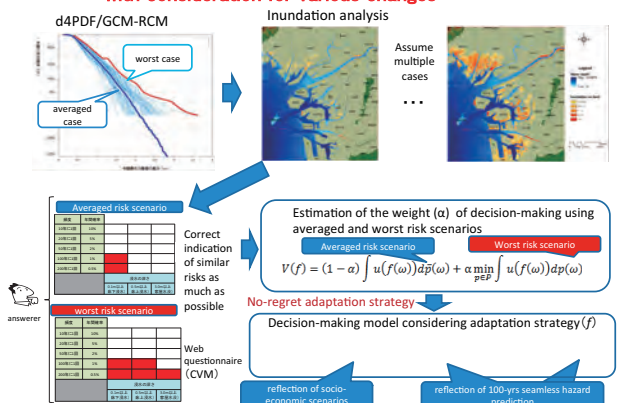
Topic (v): Non-regret adaptation strategies with consideration for various changes



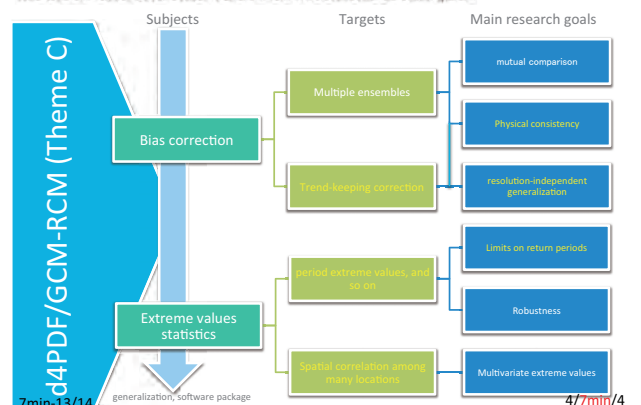
Topic (v): Non-regret adaptation strategies with consideration for various changes



Topic (v): Non-regret adaptation strategies with consideration for various changes



Topic (vi): Development of a bias correction methods and extreme values assessment techniques

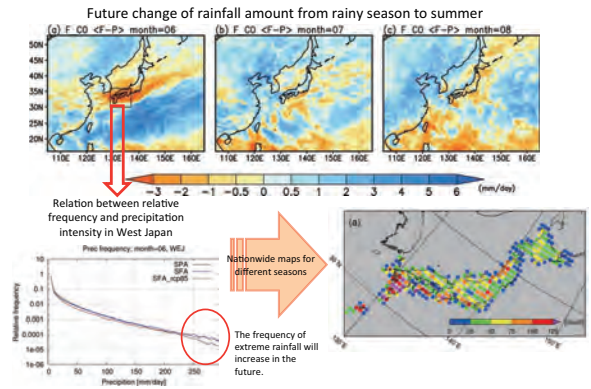


Summary and framework of research content

Research topics	Research subjects				
Topics/Working Group	Meteorology	Water-related disasters	Coastal Region	Water resources & agriculture	Risk assessment
Topic (i) Extreme phenomena	Typhoon, heavy rainfall, depression, strong wind, forest	flood, inundation	High tide, surge, typhoon	Drought, anomaly high temperature	River and coastal inundation
Topic (ii) 100-yr seamless analysis	Heavy rainfall, strong wind, forest	Flood	Sea level rise, dune, water quality, coral, etc.	Water demand, drought, hydropower	River and coastal inundation
Topic (iii) Past hazards	Typhoon, heavy rainfall, strong wind, forest	Flood, inundation	High tide, surge	Water demand, drought	
Topic (iv) Asia-Pacific region	Typhoon	Flood, inundation, drought	High surge, high tide	Water demand, drought, agricultural production	
Topic (v) Adaptation strategy	Typhoon, forest	Inundation	High tide, dune	Farming period shift, land use, ecosystem service	River & coastal inundation, flood countermeasure, disaster prevention investment
Topic (vi) Bias-correction & extreme values statistics	Rainfall amount (heavy rainfall), Wind speed	Rainfall amount, river discharge	Air pressure, wind speed, high tide, high surge	Daily solar radiation, temperature, abnormal little rain, continuously rainless day	

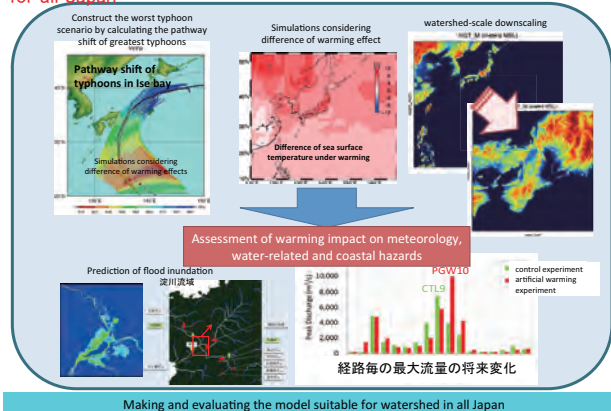
Nationwide map of future change of extreme rainfall

Expected research production



Impact assessment of the greatest typhoon for all Japan

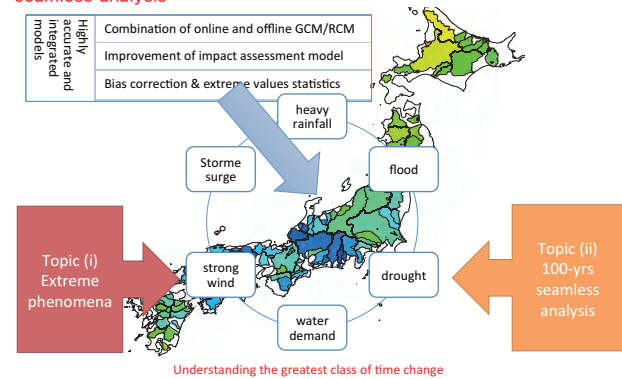
Expected research production



Nationwide mapping

Topics (i): extreme phenomena + (ii): 100-yr seamless analysis

Expected research production



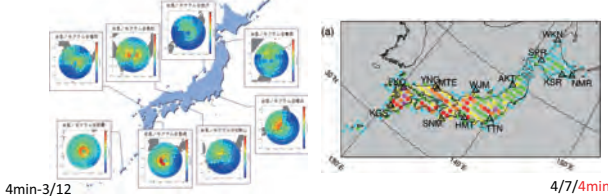
Expected production of Topic (iii): analysis of past hazards

Expected research production

- Analysis of triggering conditions and assessment of climate change impact of notable events from the past to recent years
 - improvement of people's awareness of disasters occurred recently
 - assessment of meteorological hazards considering regional characteristics in all Japan
- Propose a new paradigm for research of ecosystem impact assessment under climate change
 - Conventional nationwide storms, ex: Typhoon 19 in 1991, Typhoon 18 in 2004.
 - New type of disasters (heavy rainfall disaster in Northern Kyushu), ex: Summer typhoon in 2016

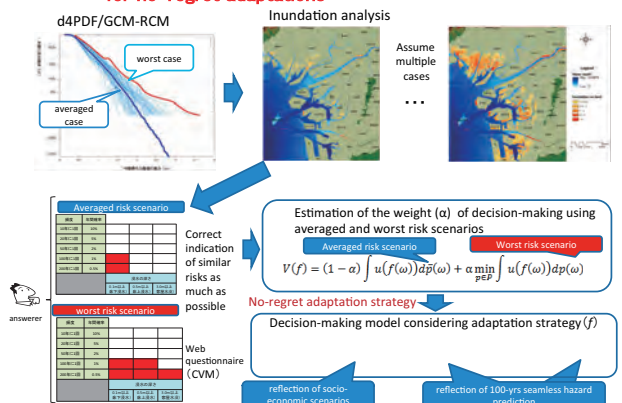
Hazard map of typhoon

Hazard map of squall line



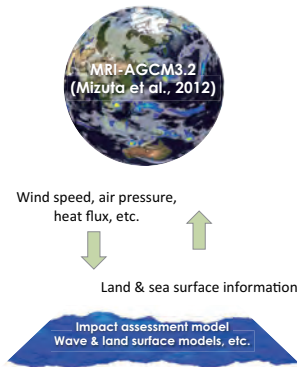
Topic (v): Development of variable strategies for no-regret adaptations

Expected research production



Two-way coupled GCM and Impact assessment model development

Particular part



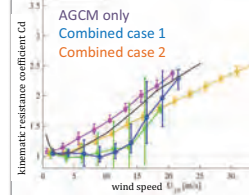
Scientific merits

- Detailed atmospheric feedbacks from land & sea surface processes
- understanding the atmospheric condition during extreme disasters

Impact assessment merits

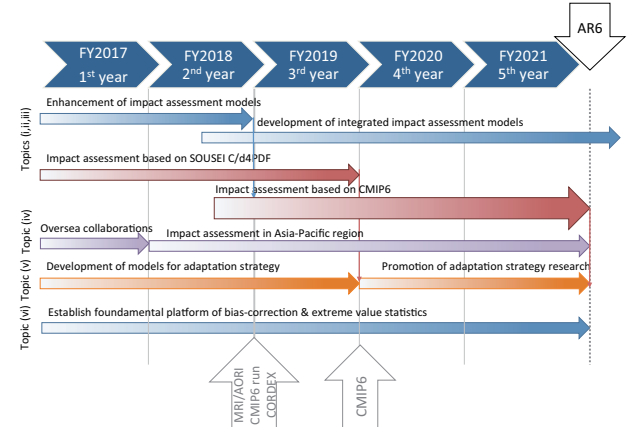
- simultaneously conducting climate model calculation and impact assessment

Test example of AGCM + surge model



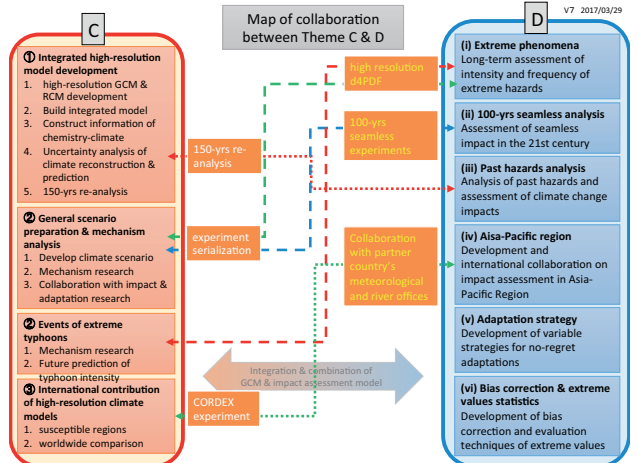
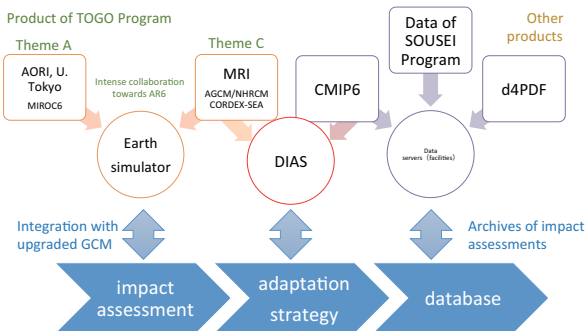
Research Schedule

Research plan



Collaborations with other Themes

Other collaborations

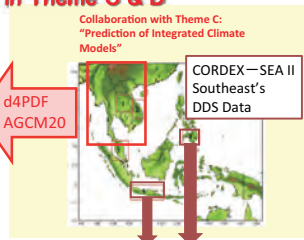


International collaborations in Theme C & D

Other collaborations

iv(a) Change prediction of water-related hazards for Asia-Pacific region (Kyoto U.)

1. Analyze change of flood and drought hazards in Indochina peninsula by developing a river model considering effects of flood plain and water-demand during irrigation, as well as by correcting grid-discharge of land surface model
2. Analyze change of flood and inundation hazards of rivers in Thailand and Indonesia with researchers from Chulalongkorn University and Lembaga Ilmu Pengetahuan Indonesia (LIPI)
3. Conduct long-term change prediction of high-tide and surges in Pacific island nations



iv(b) Development of prototype for field implementation of climate change adaptation strategy (ICHARM)

- Development of prototype for field implementation of climate change adaptation strategy with the help of stakeholder in the field in the watersheds in Philippines and Indonesia
1. Risk analysis of water-related hazards: estimation of flood and drought damages using mechanical-downscaling rainfall and rainfall-runoff & flood model
 2. Understanding the demand and capability of in-situ condition for climate change adaptation
 3. Field implementation of climate change adaptation strategy

Provide assistance foundations for no-regret adaptations in Asian countries

Lecture 1: Fundamentals of basin-scale hydrological analysis

Yasuto TACHIKAWA (*Department of Civil and Earth Resources Engineering, Graduate School of Engineering, Kyoto University*)

Abstract:

"Hydrology is the science which deals with the waters of the Earth, their occurrence, circulation and distribution on the planet, their physical and chemical properties and their interactions with the physical and biological environment, including their responses to human activity. Hydrology is a field which covers the entire history of the cycle of water on the Earth (UNESCO International Hydrological Decade, 1964)". Water is the source of all life on the earth and is indispensable resource for human social and economic activities. The water cycle and its temporal and spatial distribution depend on solar radiation, topography and various conditions of the earth's surface. Hydrology provides understanding of the physical processes of water movement and the foundations for proper use and protection of water resources.

One of the main tasks of hydrologists is to predict river discharge from rainfall, snowmelt and evapotranspiration information under an initial condition (initial soil water) and catchment physical characteristics (topography, soil, vegetation) of a basin. The hydrologic cycle of a river basin can be regarded as a runoff system in which hydrologic processes such as evaporation, transpiration, infiltration, subsurface runoff, and surface runoff interact with each other. A straightforward way to predict river discharge is to represent the runoff system by combining mathematical descriptions of dominant hydrologic processes. This mathematical representation is called a rainfall-runoff model. A rainfall-runoff model is essential for river planning and river basin management. Rainfall-runoff models include conceptual runoff models, spatially distributed models and land surface hydrologic models, which have been developed based on the advancement of observation technology such as precipitation radar, land surface remote sensing, and other geographical information.

Key words: hydrologic cycle, runoff system, rainfall-runoff model, distributed rainfall-runoff model, land surface hydrologic model.

Table of Contents

1. The Science of Hydrology	1
1.1 The Science of Water Cycle: Hydrology	1
1.2 Hydrologic Cycle and Water Balance	3
1.2.1 Water balance equation	3
1.2.2 Global water balance	4
1.2.3 Catchment water balance and water resources	7
1.3 Mean Residence Time	10
References	12
2. Modeling of Rainfall-Runoff System	13
2.1 Rainfall-Runoff System and Rainfall-Runoff Model	13
2.1.1 Rainfall-runoff system	13
2.1.2 Components of rainfall-runoff system and their modeling	15
2.1.3 Applications of rainfall-runoff models	17
2.2 Classification of Rainfall-Runoff Models	19
2.2.1 Short-term and long-term rainfall-runoff models	20
2.2.2 Response, conceptual and physically-based rainfall-runoff models	21
2.2.3 Lumped and distributed rainfall-runoff models	21
2.3 Lumped Rainfall-Runoff Model	22
2.3.1 Rational formula	22
2.3.2 Unit hydrograph method	23
2.3.3 Tank model	24
2.3.4 Storage function method with effective rainfall model	25
2.4 Distributed Rainfall-Runoff Model	27
2.4.1 Open-book type catchment modeling	27
2.4.2 Catchment modeling using digital elevation models	28
2.4.3 Flow modeling in hillslope and channel network	29

2.5	Land Surface Hydrological Model	30
2.5.1	Energy balance equation	31
2.5.2	Water balance equation	32
	References	34

1. The Science of Hydrology

”Hydrology is the science which deals with the waters of the Earth, their occurrence, circulation and distribution on the planet, their physical and chemical properties and their interactions with the physical and biological environment, including their responses to human activity. Hydrology is a field which covers the entire history of the cycle of water on the Earth (UNESCO International Hydrological Decade, 1964)”. Water is the source of all life on the earth and is indispensable resource for human social and economic activities. The water cycle and its temporal and spatial distribution depend on solar radiation, topography and various conditions of the earth’s surface. Hydrology provides understanding of the physical processes of water movement and the foundations for proper use and protection of water resources.

Keywords : hydrology, hydrologic cycle, waters budget, water resources

1.1 The Science of Water Cycle: Hydrology

Water circulates on the earth due to solar and gravitational energy, and changes its phases (ice, liquid, and vapor). **Hydrology** clarifies the movement of water and the distribution of water in time and space on and beneath the earth’s surface, involving transports of sediment, dissolved nutrients, and contaminants. Hydrology provides the basics for applied fields such as engineering and agricultural sciences, which aim for proper development, protection, and management of water resources; mitigation of water-related disasters such as floods and droughts; and agricultural production by drainage and irrigation.

Fig. 1.1 illustrates the major components of the **water cycle**. **Precipitation** falls on the earth’s surface. Trees and vegetation intercept part of this precipitation; it does not reach the ground surface, and is evaporated into the atmosphere. Precipitation that reaches the land surface infiltrates into soil layers and forms **subsurface** and **groundwater flow**, and when it exceeds the soil **infiltration capacity** this forms **surface runoff**.

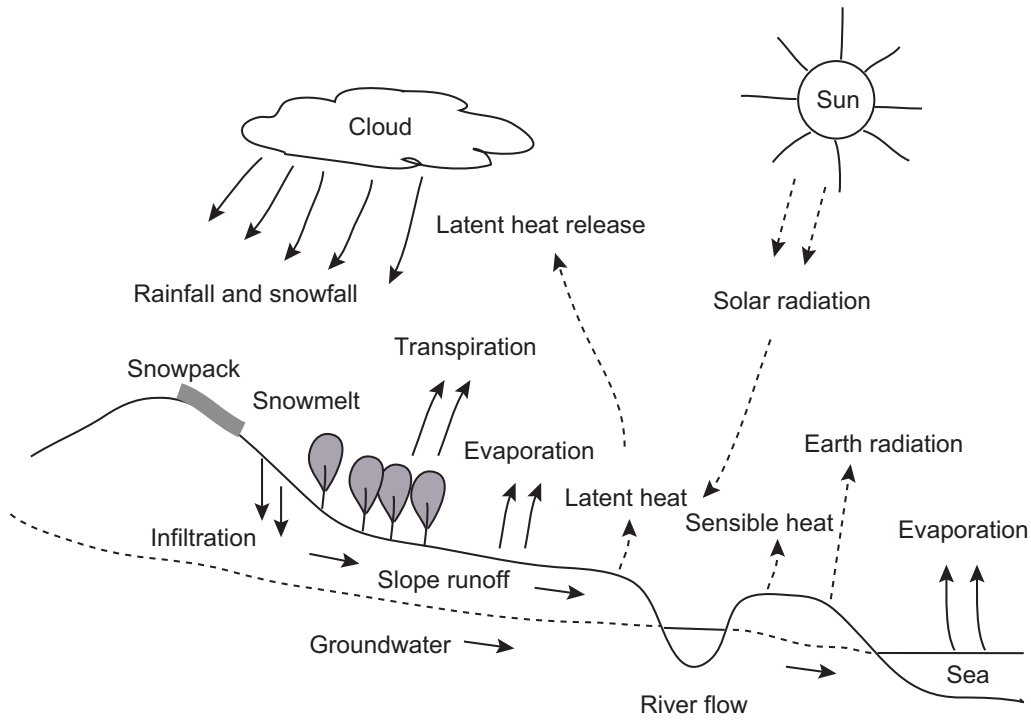


Fig. 1.1: Hydrologic processes and water and energy movement with change of water phase.

Precipitation falling on the ground as snow accumulates as snow cover, which melts and flows through similar routes to runoff from rainfall. The water in the surface soil layer evaporates and returns to the atmosphere. Trees and vegetation absorb soil moisture with their roots and release water vapor through stomata in the process of **transpiration**. The collective term for the combination of **evaporation** with **transpiration** is **evapotranspiration**.

The water cycle is associated with the **energy cycle**. When soil moisture on the ground surface evaporates and changes phase from water to vapor, the **latent heat** moves from the earth's surface to the atmosphere. When the vapor changes to raindrops, the latent heat is released to the atmosphere as **condensation heat**. Thus, the solar energy provided to the earth's surface is transferred to the atmosphere through evaporation and precipitation. The solar energy reaching the earth's surface is spatially and temporary distributed, and determines the climate. The water and energy cycles are closely related to climate and the spatiotemporal distribution of water.

To understand the water and energy cycles, it is necessary to understand the physical mechanism of the water and energy movements by solar radiation as well as the mechanism of water movement governed by the conservation of water mass (continuity equation) and

the moment (momentum conservation). Water movement causes the movement of soils and chemical substances dissolved in water. These movements are closely associated with our lives and the environment. Therefore, the scope of hydrology includes the cycles of water and energy, and the physical, chemical, and biological processes associated with these cycles.

(Note) Hydrology as a science and a profession

Hydrology has both pure and applied aspects. The first aspect relates to questions about how the earth works, and specifically about the role of water in natural processes. The second relates to the use of scientific knowledge to provide a sound basis for proper use and protection of water resources (Hornberger *et al.*, 1998). The second aspect is the main theme of water resources engineering. The research topics include:

- flood and drought
- flood risk management
- water resources management
- climate change and water resources

【Example 1.1】 Topics of hydrologic cycle and water resources

Describe any topics related to the hydrologic cycle and water resources in your countries. For example, flood, drought, water quality, water resources development, and climate change and so on.

1.2 Hydrologic Cycle and Water Balance

1.2.1 Water balance equation

To discuss the spatiotemporal distribution of water, consider a closed compartment (referred to as a control volume) shown in **Fig. 1.2**. M_{in} is the rate of mass flowing into the control volume [M T^{-1}]; M_{out} is the rate of mass flowing out of the control volume [M

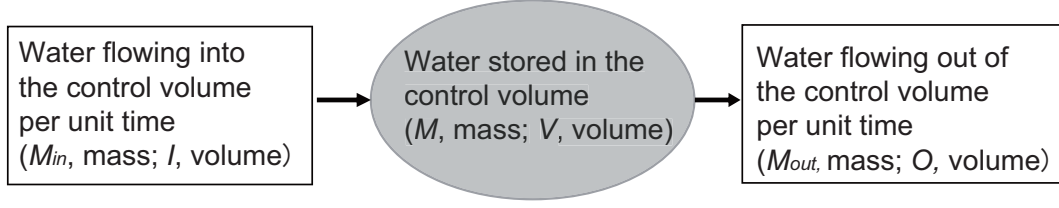


Fig. 1.2: Water balance and continuity relation.

T^{-1}]; and M is the mass stored in the control volume [M]. The equation of **conservation of mass** is given by

$$\Delta M = (M_{\text{in}} - M_{\text{out}})\Delta t \quad (1.1)$$

where ΔM is the change of water mass in the control volume over time Δt . Using the **density** of water ρ , $M = \rho V$, $M_{\text{in}} = \rho I$, and $M_{\text{out}} = \rho O$, where V is the volume of the water stored in the control volume [L^3]; I is the volume inflow rate [$L^3 T^{-1}$]; and O is the volume outflow rate [$L^3 T^{-1}$]. Canceling the the density from both sides of Eq.(1.1) gives

$$\Delta V = (I - O)\Delta t \quad (1.2)$$

By dividing both sides by Δt and taking the limit of Δt , the equation of volume conservation (continuity equation) is given as:

$$\frac{dV}{dt} = I - O \quad (1.3)$$

Generally ρ is regarded as constant and that the continuity equation is expressed as volume, not as mass. The continuity equation is often referred as a **water balance equation** or a **water budget equation**.

1.2.2 Global water balance

We can develop a global water budget equation using Eq.(1.3). For the land, V is the volume of water stored on and in the land, I is precipitation P [$L^3 T^{-1}$], and O consists of evapotranspiration E [$L^3 T^{-1}$] and runoff Q [$L^3 T^{-1}$]. Integrating Eq.(1.3) over a time period τ , the continuity equation becomes

$$\int_{\tau} dV = \int_{\tau} I dt - \int_{\tau} O dt = \int_{\tau} P dt - \int_{\tau} (E + Q) dt \quad (1.4)$$

The integration of dV over a year could be negligibly small. In this case, the continuity equation becomes

$$\int_{\tau} P dt = \int_{\tau} (E + Q) dt \quad (1.5)$$

and evapotranspiration is estimated from observed precipitation and discharge.

【Example 1.2】 Annual precipitation

The water balance is described in terms of reservoirs that store water and the movements between them. **Fig. 1.3** indicates the volume of water stored in the atmosphere, ocean and land on the earth and its annual movement volume. Using the values shown in **Fig. 1.3**, calculate the annual precipitation per unit area on ocean, land, and the surface of the earth. The surface area of the earth is $5.1 \times 10^8 \text{ km}^2$, represented as $4\pi r_e^2$, where r_e is the radius of earth and about 6,371km, There is 71% of earth's surface that is ocean and 29% is land.

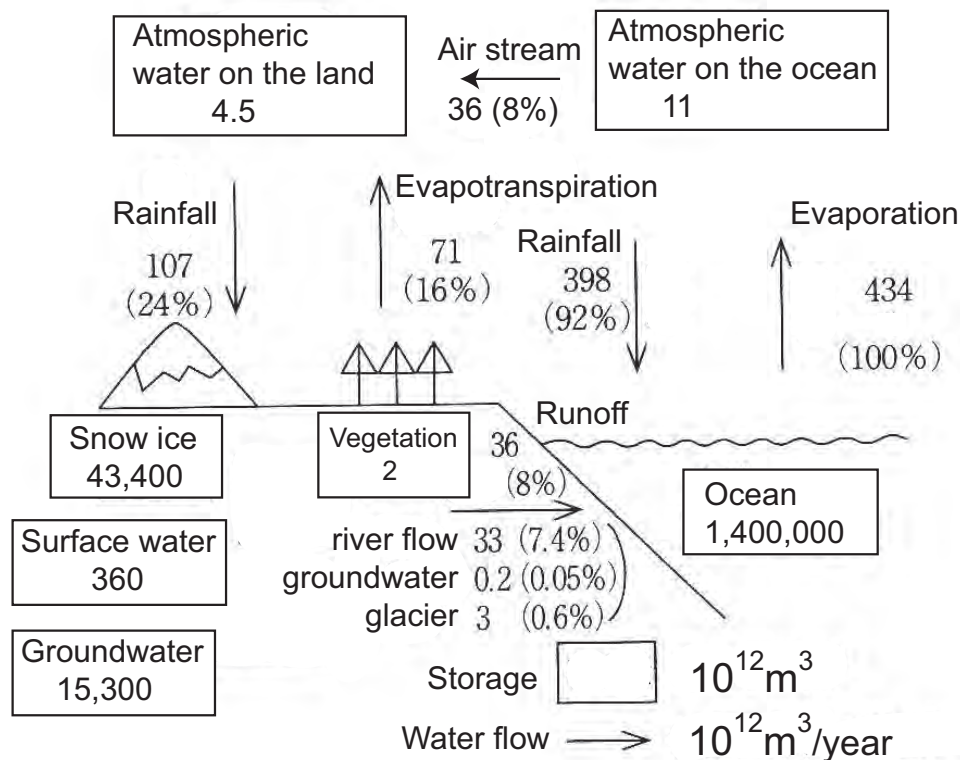


Fig. 1.3: The water stored on the earth and annual movements. The percentages represent the ratio according to annual evaporation from ocean as 100%. (Takeda, T. *et al.*, Meteorology in water environment, University of Tokyo Press, 1992)

(Solution)

The annual precipitation per unit area on ocean is given by dividing the total volume of annual precipitation on ocean by the ocean surface area:

$$\frac{398 \times 10^{12} \text{ m}^3 \text{ yr}^{-1}}{5.1 \times 10^8 \times 0.71 \text{ km}^2} = 1,099 \text{ mm} \cdot \text{yr}^{-1}$$

The annual precipitation per unit area on the land is given by dividing the total volume of annual precipitation on land by the land surface area:

$$\frac{107 \times 10^{12} \text{ m}^3 \text{ yr}^{-1}}{5.1 \times 10^8 \times 0.29 \text{ km}^2} = 723 \text{ mm} \cdot \text{yr}^{-1}$$

The annual precipitation per unit area on the Earth surface is given by dividing the total volume of annual precipitation on the Earth surface by its area:

$$\frac{(398 + 107) \times 10^{12} \text{ m}^3 \text{ yr}^{-1}}{5.1 \times 10^8 \text{ km}^2} = 990 \text{ mm} \cdot \text{yr}^{-1}$$

The annual precipitation amount in Japan is approximately $1,700 \text{ mm} \cdot \text{y}^{-1}$ on average, which is substantially greater than the average annual precipitation on the land. **Fig. 1.3** indicates that approximately $66\%(=71/107)$ of precipitation on the land originates from evapotranspiration from the land. Most precipitation in Japan is brought in the rainy season and typhoons and the rainwater originates from evaporation on the ocean.

【Example 1.3】 Annual evapotranspiration

Using the values shown in **Fig. 1.3**, calculate the annual evapotranspiration per unit area on ocean, land, and the surface of the earth.

(Solution)

The annual evaporation per unit area from the ocean is given by dividing the annual total volume of evaporation from the ocean by the ocean surface area:

$$\frac{434 \times 10^{12} \text{ m}^3 \text{ yr}^{-1}}{5.1 \times 10^8 \times 0.71 \text{ km}^2} = 1,199 \text{ mm} \cdot \text{yr}^{-1}$$

The annual evapotranspiration per unit area from the land is given by dividing the annual total volume of evapotranspiration from the land by the land surface area:

$$\frac{71 \times 10^{12} \text{ m}^3 \text{ yr}^{-1}}{5.1 \times 10^8 \times 0.29 \text{ km}^2} = 480 \text{ mm} \cdot \text{yr}^{-1}$$

The annual evapotranspiration per unit area from the Earth surface is given by dividing the total volume of the annual evapotranspiration from the Earth surface by its area:

$$\frac{(434 + 71) \times 10^{12} \text{ m}^3\text{yr}^{-1}}{5.1 \times 10^8 \text{ km}^2} = 990 \text{ mm}\cdot\text{yr}^{-1}$$

【Example 1.4】 Annual runoff and runoff ratio

Calculate the annual runoff per unit area and runoff ratio on the land using the values in **Fig. 1.3**.

(Solution)

The annual runoff per unit area from the land is given by dividing the total volume of the annual runoff by the land surface area:

$$\frac{36 \times 10^{12} \text{ m}^3\text{yr}^{-1}}{5.1 \times 10^8 \times 0.29 \text{ km}^2} \times 10^3 = 243 \text{ mm}\cdot\text{yr}^{-1}$$

or annual precipitation minus annual evapotranspiration ($723 - 480 = 243 \text{ mm}\cdot\text{yr}^{-1}$).

The runoff ratio is given by dividing the annual runoff by the annual precipitation:

$$\frac{243 \text{ mm}\cdot\text{yr}^{-1}}{723 \text{ mm}\cdot\text{yr}^{-1}} = 0.34$$

1.2.3 Catchment water balance and water resources

A **catchment**, as shown in **Fig. 1.4**, is an area in which rain water drains into a **channel network** (river network) and finally flows to the river mouth. A catchment is separated by a topographically defined watershed boundary. Consider A is the area of a catchment basin [L^2]; r is the precipitation rate [LT^{-1}] (volume of precipitation falling on the catchment basin per unit time per unit area); e is the evapotranspiration rate [LT^{-1}] (the volume of water evaporating per unit time per unit area); and Q is the runoff rate flowing out of the catchment [L^3T^{-1}]. The inflow rate into the catchment I in Eq.(1.3) is

$$I = Ar$$

and the outflow rate is

$$O = Ae + Q$$

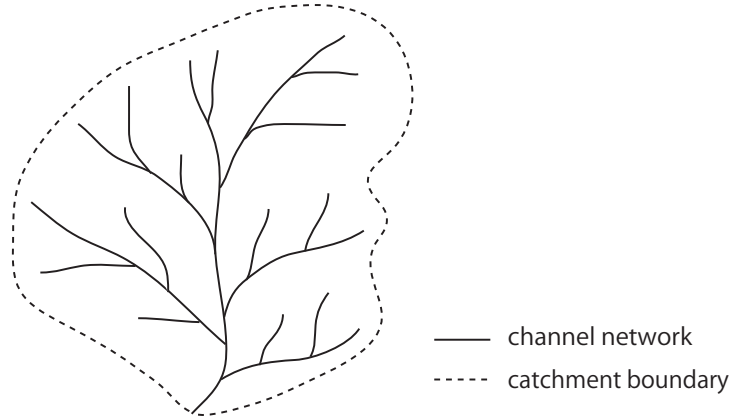


Fig. 1.4: Watershed divide and catchment basin.

Substituting these into Eq.(1.3), the continuity equation in the catchment is defined as

$$\frac{dS}{dt} = A(r - e) - Q \quad (1.6)$$

Integrating Eq.(1.6) from time t_s to t_e , the continuity equation becomes

$$\int_{t_s}^{t_e} dS = S(t_e) - S(t_s) = A \left(\int_{t_s}^{t_e} r dt - \int_{t_s}^{t_e} e dt \right) - \int_{t_s}^{t_e} Q dt$$

Assuming the catchment storatge at t_s and t_e is the same, the continuity equation becomes

$$A \left(\int_{t_s}^{t_e} r dt \right) = A \left(\int_{t_s}^{t_e} e dt \right) + \int_{t_s}^{t_e} Q dt \quad (1.7)$$

For the time period, the total volume of water flowing into the catchment basin is equal to that flowing out of the basin. If we take t_s in the dry season and t_e after one year, the time-integrated value of dS is negligible, and the evapotranspiration value for the time period can be estimated using the observed precipitation and discharge data.

【Example 1.5】 Hydrologic characteristics in Asian regions

Table 1.1 shows the annual precipitation, evapotranspiration, and runoff for the Chao Phraya River basin (CPRB) in Thailand (157,925 km²) and the Katsura River basin in Kyoto, Japan (887 km²). Calculate the values in (1) and (2) in **Table 1.1** and discuss the difference in the catchment hydrologic variables from the view point of water resources.

Table 1.1: Annual catchment hydrologic variables.

Region	Precipitation	Evapotranspiration	Runoff
Chao Phraya River (Thailand)	1,144	962	(1)
Katsura River (Kyoto, Japan)	1,796	708	(2)
World (mean)	723	480	243

*unit is mm/year.

(Solution)

(1) $1,144 - 962 = 182$ mm/yr. (2) $1,796 - 708 = 1,088$ mm/yr.

【Example 1.6】 Annual surface water resources in Thailand and Japan

Table 1.2 shows the estimated mean annual runoff in Thailand, Japan and the world. Calculate the per capita maximum water resources for one year for each area and discuss the difference of the water resources.

Table 1.2: Annual water resources in Thailand and Japan.

Region	Runoff (mm/yr)	Area (km ²)	Population (person)
Chao Phraya River (Thailand)	182	513×10^3	69.5×10^6
Katsura River (Japan)	1,088	378×10^3	126.5×10^6
World (mean)	243	147.9×10^6	$6,968 \times 10^6$

(Solution)

The maximum water resources per capita in the Chao Phraya River basin in Thailand is obtained by dividing the total annual runoff volume by the population, which is

$$\frac{182 \text{ mm/yr} \times 513 \times 10^3 \text{ km}^2}{69.5 \times 10^6 \text{ person}} = \frac{93,366 \times 10^6 \text{ m}^3/\text{yr}}{69.5 \times 10^6 \text{ person}} = 1,343 \text{ m}^3/\text{person/yr}$$

The maximum water resources per capita in the Katsura River basin in Japan and the mean value of the world are

$$\frac{1,088 \text{ mm/yr} \times 378 \times 10^3 \text{ km}^2}{126.5 \times 10^6 \text{ person}} = \frac{411,264 \times 10^6 \text{ m}^3/\text{yr}}{126.5 \times 10^6 \text{ person}} = 3,251 \text{ m}^3/\text{person/yr}$$

$$\frac{243 \text{ mm/yr} \times 147.9 \times 10^6 \text{ km}^2}{6,968 \times 10^6 \text{ person}} = \frac{35,940 \times 10^9 \text{ m}^3/\text{yr}}{6,968 \times 10^6 \text{ person}} = 5,158 \text{ m}^3/\text{person/yr}$$

【Example 1.7】 Surface water resources under a changing climate in Thailand and Japan

Global warming can induce change in the hydrologic cycle. Assuming the amount of annual evapotranspiration increases by 5%, estimate the decrease percentage of river discharge, namely the maximum surface water resources for the Chao Phraya River basin in Thailand and the Katsura River basin in Japan using the values in **Table 1.1**.

(Solution)

In the Chao Phraya River basin, annual runoff is $1,144 - 962 \times 1.05 = 134$ mm/yr. The decrease ratio is

$$\frac{182 - 134}{182} \times 100 = 26\%$$

In the Katsura River basin, annual runoff is $1,796 - 708 \times 1.05 = 1053$ mm/yr. The decrease ratio is

$$\frac{1088 - 1053}{1088} \times 100 = 3.3\%$$

Increased evapotranspiration has a large influence on surface water in Thailand.

1.3 Mean Residence Time

The mean residence time refers to the times that are required for the water in the drainage basin to be completely replaced with new water flowing into the drainage basin. The mean residence time provides a time scale of the movement of water and substances that travel with water in the basin. Assuming the **steady state** condition ($dS/dt = 0$), the mean residence time is easily calculated by dividing the volume of water stored in a control volume by the volume of water that flows into the region per unit time, or by the volume of water that flows out of the region per unit time.

【Example 1.8】 Mean residence time in global water budget

Calculate the mean residence time of water that exists on the land and in the atmosphere, using the values provided in **Fig. 1.3**.

(Solution)

The annual mean precipitation on the lands (sum of annual evapotranspiration and runoff from the land) is $107 \times 10^{12} \text{ m}^3\text{yr}^{-1}$. The total volume of water stored on

and beneath the land is $(43,400 + 360 + 15,300 + 2) \times 10^{12} \text{m}^3$. Therefore, the mean residence time of water on the land is:

$$\frac{(43,400 + 15,300 + 360 + 2) \times 10^{12} \text{ m}^3}{107 \times 10^{12} \text{ m}^3 \text{ yr}^{-1}} = 552 \text{ year}$$

The annual precipitation on the lands and oceans is $(107 + 398) \times 10^{12} \text{m}^3 \text{yr}^{-1}$. The total volume of water stored in the atmosphere is $(4.5 + 11) \times 10^{12} \text{m}^3$. Therefore, the mean residence time of water in the atmosphere is:

$$\frac{(4.5 + 11) \times 10^{12} \text{ m}^3}{(107 + 398) \times 10^{12} \text{ m}^3 \text{ yr}^{-1}} = 11.2 \text{ day}$$

The mean residence time of water in the atmosphere is very short, indicating that water is frequently exchanged with heat energy.

The volume of water in snow ice and groundwater accounts for more than 99% of the water on and beneath the land, and runoff from snow ice and groundwater accounts for less than 10%. Assuming only surface water and water in vegetation move, the mean residence time of the water on the land is

$$\frac{(360 + 2) \times 10^{12} \text{ m}^3}{107 \times 10^{12} \text{ m}^3 \cdot \text{yr}^{-1}} = 3.4 \text{ year}$$

Most of surface water is stored in lakes and soil layers. Movement such water is slower than that of water in rivers. Therefore, the mean residence time of water in rivers is estimated as several ten days.

【Example 1.9】Mean residence time in dam reservoirs

Table 1.3 shows the characteristics of the largest dams in Thailand and Japan. How many years it take to completely replace the water in the full storage capacity at the Bhumibol Dam, the Tokuyama Dam, and the Hiyoshi Dam? Use the annual hydrologic variables in **Table 1.1**.

Table 1.3: Characteristics of the dams in Thailand and Japan.

Dam	Storage capacity($\times 10^6 \text{m}^3$)	Catchment area (km^2)
Bhumibol Dam	13,420	26,400
Tokuyama Dam	660	254.5
Hiyoshi Dam	66	290

(Solution)

The annual inflow to the Bhumibol Dam is $182 \text{ mm/yr} \times 26,400 \text{ km}^2$. The mean residence time of the dam reservoir is given by dividing the storage capacity by the annual inflow:

$$\frac{13,420 \times 10^6 \text{ m}^3}{26,400 \text{ km}^2 \times 182 \text{ mm/yr}} = 2.8 \text{ year}$$

Similarly for the Tokuyama Dam

$$\frac{660 \times 10^6 \text{ m}^3}{254.5 \text{ km}^2 \times 1088 \text{ mm/yr}} = 2.4 \text{ year}$$

and for the Hiyoshi Dam

$$\frac{66 \times 10^6 \text{ m}^3}{290 \text{ km}^2 \times 1088 \text{ mm/yr}} = 0.21 \text{ year}$$

References

- [1] Hornberger, G. M., Raffensperger, J. P., Wiberg, P. L., and Eshleman, K. N: Elements of Physical Hydrology, The Johns Hopkins University Press, pp. 1–15, 1998.
- [2] Maidment, D. R.: Hydrology, in Hydrology Handbook of Hydrology, edited by D. R. Maidment, McGraw-Hill, Chapter 1, pp. 1.1–1.15, 1993.

2. Modeling of Rainfall-Runoff System

One of the main tasks of hydrologists is to predict river discharge from rainfall, snowmelt and evapotranspiration information under an initial condition (initial soil water) and catchment physical characteristics (topography, soil, vegetation) of a basin. The hydrologic cycle of a river basin can be regarded as a runoff system in which hydrologic processes such as evaporation, transpiration, infiltration, subsurface runoff, and surface runoff interact with each other. A straightforward way to predict river discharge is to represent the runoff system by combining mathematical descriptions of dominant hydrologic processes. This mathematical representation is called a **rainfall-runoff model**. A rainfall-runoff model is essential for river planning and river basin management. Rainfall-runoff models include conceptual runoff models, spatially distributed models and land surface hydrologic models, which have been developed based on the advancement of observation technology such as precipitation radar, land surface remote sensing, and other geographical information.

Keywords : runoff system, rainfall-runoff model, distributed rainfall-runoff model, land surface hydrologic model

2.1 Rainfall-Runoff System and Rainfall-Runoff Model

2.1.1 Rainfall-runoff system

Rainfall on a catchment moves through various pathways and flows into a river channel. This process can be regarded as a **runoff system** that consists of various interrelated subsystems transforming inputs to outputs. The purposes of the **Runoff analysis** are to characterize governing physical and statistical principles, to elucidate the interrelationship among the subsystems, to create a mathematical model that represents a behavior of a

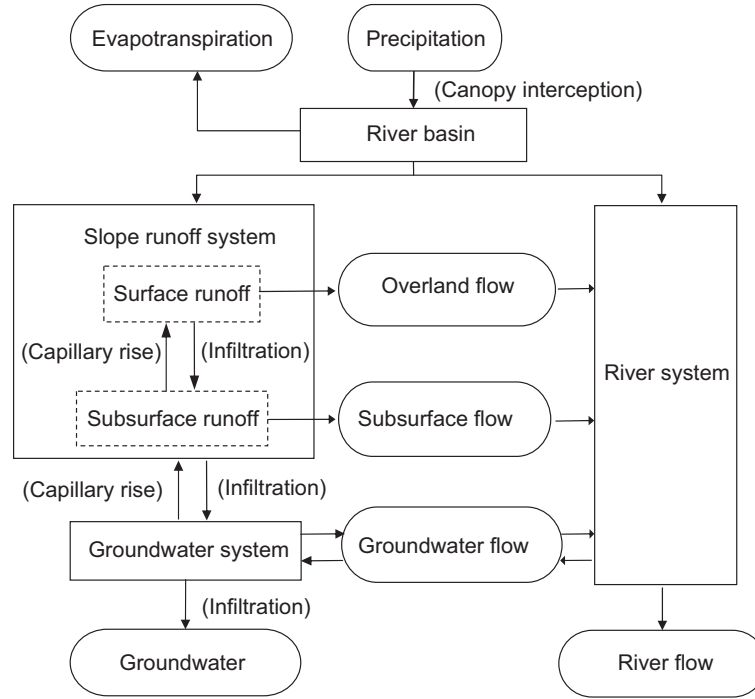


Fig. 2.1: Rainfall-runoff system (Takasao, 1967, 1975).

subsystem and an interrelationship of subsystems, and to predict rainfall-runoff phenomena. Takasao defined the runoff system and indicated the research direction to understand the runoff system as described below (Takasao, 1967, 1975):

A runoff system refers to an ordered set of homogeneous subsystems that are governed by a physical or statistical principle. To understand the characteristics of a runoff system consistently and quantitatively, it is necessary to clarify the mechanism of subsystems and the interrelationship among the subsystems, and to describe the entire system systematically.

Fig. 2.1 shows a block diagram of a runoff system, which represents the flow path of precipitated water on a catchment and the interrelationship of the hydrologic subsystems. A rectangular block stands for a subsystem; a circular block for an input or output; and an arrow for the direction of the input and the output. Three items that characterize a runoff system are:

Input which is external forcing variables to drive the system, for example, rainfall;

Output which is the resultant variables by the system, for example, slope runoff; and **System parameter** which that control the dynamic behaviors of the system, for example, topography gradient, runoff recession constant.

An output of a subsystem may serve as an input to other subsystems as the arrow indicates.

To clarify the runoff system needs extensive researches, which include (1) observation of runoff phenomena and (2) development of a mathematical model that expresses the behaviors of the runoff system. These studies are closely related with each other. Hydrologic variables to be observed and their observation criteria depend on structures and descriptions of hydrologic models, and a representation of a mathematical model is definitely based on the observation of runoff phenomena. To recognize the interaction of hydrologic observation and the model development is the only way to understand a runoff system properly.

A runoff system consists of the natural processes shown in **Fig. 2.1**. Human activities affect the natural system such as water intake from river and groundwater, dam reservoir operations. The transport processes of sediment, water quality and temperature diffusion also interact with the hydrologic cycle. To predict the runoff phenomena, understanding of the subsystems and the interrelation among subsystems are fundamental. The entire system model is developed by combining the mathematical subsystem models which represent the hydrologic behaviors of subsystems.

2.1.2 Components of rainfall-runoff system and their modeling

Fig. 2.2 shows an example of a spatial division of a catchment to identify the sub-basin that connect to each channel segment. A runoff system of each sub-basin as shown in **Fig. 2.1** is modeled as a sub-basin rainfall-runoff model and the sub-basin models are connected to develop the entire runoff system model. Major subsystem components in a runoff system are as follows:

Hillslope runoff system that receives precipitation and transforms it into surface runoff and subsurface runoff.

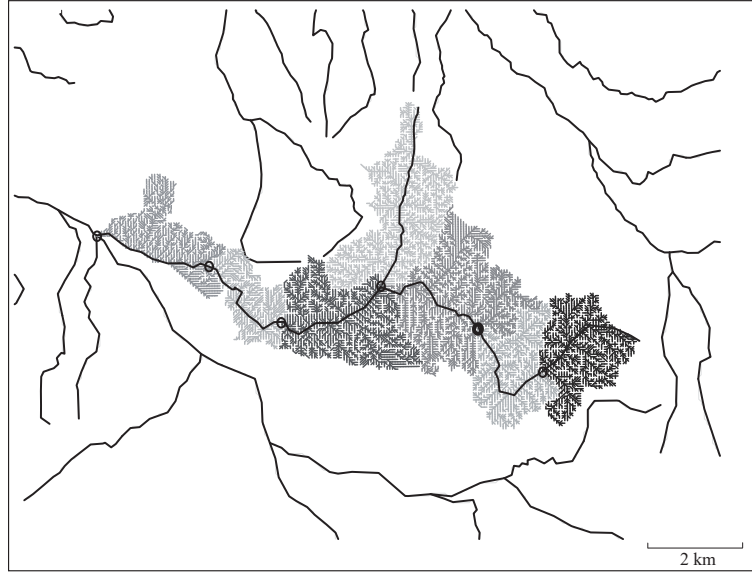


Fig. 2.2: Sub-catchment that forms a part of the entire hydrologic system.

River flow system that receives hillslope discharge and groundwater discharge, and routes them to downstream.

Groundwater system that receives infiltration from the hillslope system and provides groundwater discharge to the river system. The groundwater system and the river system interactively exchange water. In an alluvial fan and its downstream area, the river water may be supplied from the river system to the groundwater system.

Inundation system that receives precipitation and flood water from the river system and distributes flood water to a flood plain or urban district.

Human system that gives an impact on the natural hydrologic cycle such as dam reservoir control for flood disaster mitigation/prevention, water supply for agricultural, industrial and urban use; water intake from the river system and the groundwater system for agricultural, industrial and urban use.

Various subsystems in association with the hydrologic cycle such as sediment runoff, substances movement, water quality and water temperature change, vegetation growth.

A runoff model refers to a mathematical system model that expresses the hydrologic behaviors of a subsystem using governing equations, which enables to predict runoff phe-

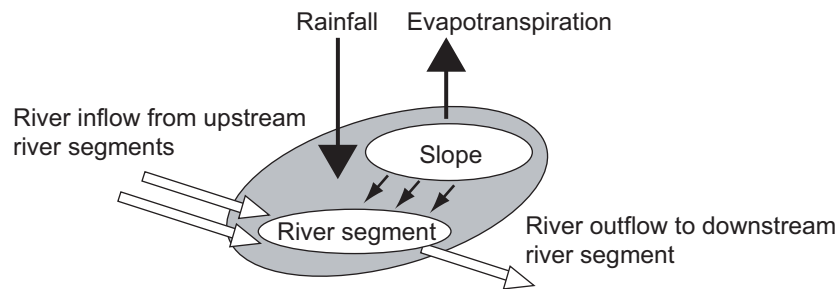


Fig. 2.3: Water movement in a sub-basins.

nomena. Adding components of a runoff system described above, a rainfall system and an evaporation system also play an important role of subsystems. **Fig. 2.3** illustrates the flow of water in a sub-basin, where hillslope flow and river flow routing are dominant hydrological processes. Runoff and flood routing of an entire basin are modeled by spatially combining sub-basin models representing hillslope flow and river flow processes.

In the hydrologic cycle, people use the water and modify the natural hydrologic cycle. Irrigation and drainage projects for agriculture, water supply and sewage system development, reservoir operations for flood control and various water use are major human intervention for the natural hydrologic cycle. These processes influence each other and constitute an actual runoff system. River flow is no longer a natural process, which receives impact of human activities. For river planning and river basin management, a hydrologic simulation model that explicitly includes the effect of human activities on the hydrologic cycle can reproduce actual runoff behaviors and predict future runoff phenomena.

2.1.3 Applications of rainfall-runoff models

One of the applications of a rainfall-runoff model is to understand a runoff system and clarify the interrelationship of subsystems. Engineering applications include to design hydraulic structures for flood control and water resources, to predict river flow for mitigation of flood and drought disasters, and to assess the impact of environment and climate changes on hydrology. The applications are summarized as:

1. understanding of the hydrologic cycle
2. river flow prediction for river planning
3. realtime river flow forecasting

4. long-term river flow predictions for water resources
5. prediction of the hydrologic cycle due to environmental change
6. predictions in ungauged basins

The appropriate structure of a runoff model can be different depending on the objectives.

(1) Understanding of the hydrologic cycle

Hydrological observation cannot provide all aspects the hydrologic cycle. To deepen the understanding of a runoff system, not only to observe the runoff system, but also to develop the theory that explains the runoff system in the river basin is important. A rainfall-runoff model is a mathematical representation that expresses the theory. **Runoff Analysis** includes observation of the hydrologic cycle, development of a theory that explains it, and understanding it through the observations and the theory. A rainfall-runoff model that provides a spatiotemporal distribution of hydrological variables inside the river basin helps the understanding of the runoff system. A framework that enables to simulate the spatiotemporal distribution of hydrologic variables is indispensable to link the observation and the theory.

(2) River flow prediction for river planning

To prevent and mitigate flood disasters, construction of hydraulic structures such as levees, flood control basins, and dam reservoirs are effective. For effective designs of the sizes and locations, to predict a flood hydrograph (design flood) using a rainfall-runoff model is essential.

(3) Real-time river flow forecasting

For issuing flood alert and efficient operation of hydraulic facilities, real-time river flow forecasting is effective. A rainfall-runoff model and rainfall forecasts with several hour lead time are helpful to forecast river flows.

(4) Prediction of the hydrologic cycle under environmental change

The hydrologic cycle may change significantly due to the changes of river basin environment, social conditions, and climate. To predict the hydrologic cycle under environmental change is one of the main tasks of a rainfall-runoff model. A runoff model for this purpose should allow proper model parameter setting due to the environmental changes. A conceptual model whose model parameters are determined only by observation data may not be reliable for this purpose. Because it is impossible to determine the model parameters under the environmental change. A physically-based rainfall-runoff model may be useful with physically reasonable model parameters under the change conditions.

(5) Predictions in ungauged basins

Hydrological observation is the basis of hydrologic predictions for flood prevention and water resources. However, there are some regions that hydrological observation is insufficient regardless the social needs of hydrologic predictions. A physically-based rainfall-runoff model and a meteorological/climate model are effective tools to realize the prediction in ungauged basins.

2.2 Classification of Rainfall-Runoff Models

A rainfall-runoff model is expressed as follows in general:

$$Q(x, t) = f(R(x, t), \text{catchment characteristics, initial condition})$$

where $Q(x, t)$ is the river flow rate at a spatial point x at time t ; $R(x, t)$ is the precipitation intensity associated with the river flow at x and t ; and f is a rainfall-runoff model that represents the runoff process for transforming rainfall intensity to the river flow rate. The catchment characteristics include topography, land use, geology of the river basin and these characteristics are introduced as model parameters of the rainfall-runoff model. The initial condition means the initial values of state variables in the rainfall-runoff model such as soil moisture which represents the wet and dry condition of the river basin.

A rainfall-runoff model is constructed by combining the hydrologic processes, such as evapotranspiration, interception, infiltration, hillslope runoff, and channel routing. Consider a rainfall-runoff model that aims for flood prediction in small river basin (several

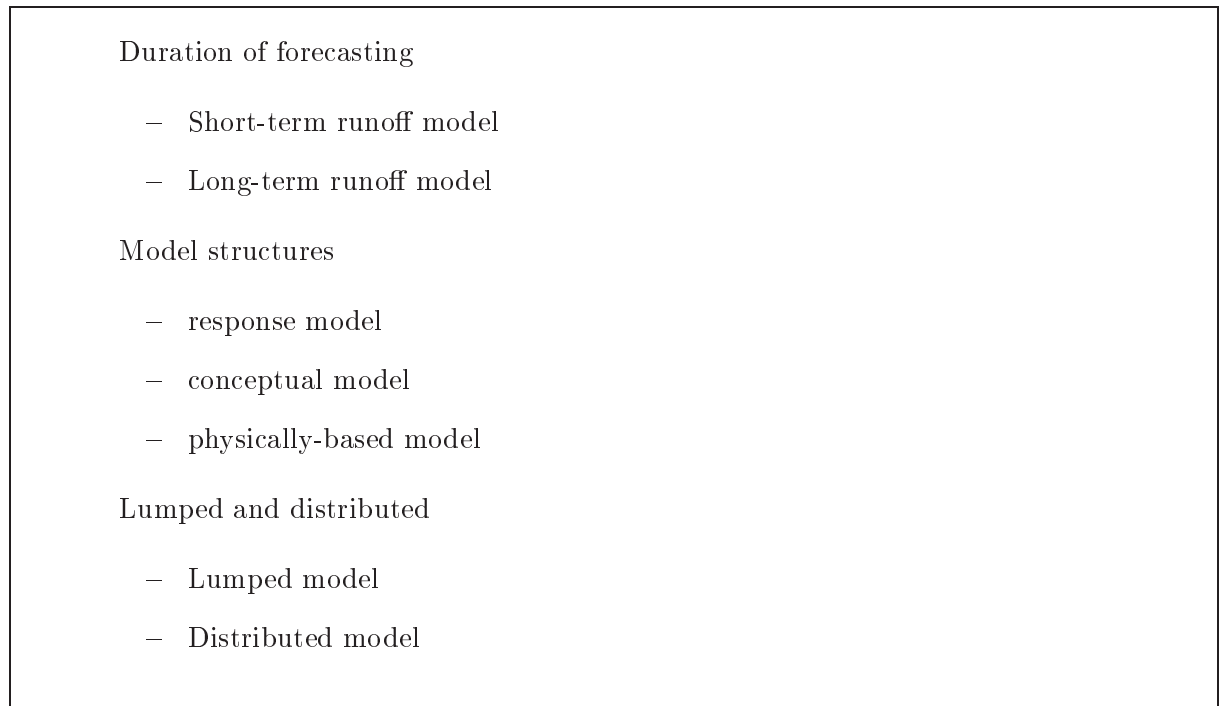


Fig. 2.4: Classification of rainfall-runoff models.

thousand km²). Rainfall amount which causes a flood disaster reaches 100 mm or greater per day. Meanwhile, the amount of evapotranspiration is as small as 6 mm per day even under the conditions in summer sunny day. Therefore, the important hydrologic processes in the rainfall-runoff model is the hillslope runoff and the channel routing. Meanwhile, taking into account the long-term river flow prediction, evapotranspiration plays a major role to determine the river flow rate. In such a case, a rainfall-runoff model needs to include the process of evapotranspiration.

As described above, hydrological processes and data required for a rainfall-runoff model vary depending on the purpose. The type of a rainfall-runoff model is also different depending on whether the runoff model is aimed at forecasting the river flow rate only at the outlet of the river basin or spatiotemporal changes of hydrologic variables. **Fig. 2.4** shows the classification of rainfall-runoff models.

2.2.1 Short-term and long-term rainfall-runoff models

In terms of the duration of forecasting, runoff models are categorized into the short-term and long-term runoff models. A **short-term rainfall-runoff model** is used for

reproducing/forecasting runoff with the duration of several hours to several days. A short-term runoff model is often called a **flood runoff model**. A **long-term runoff model** is used for predicting water resources conditions. The model is requested to reproduce/forecast for long-term flow conditions over several months to years.

2.2.2 Response, conceptual and physically-based rainfall-runoff models

In terms of model construction, runoff models are categorized into a **response model**, a **conceptual model**, and a **physically-based model**. Taking a short-term runoff model as an example, the input to the model is rainfall intensity, and the output from the model is flow rate. Only realizing the input and output as a time series data, a **response model** aims to determine the relationship between input and output just systematically. A response model is sometimes called a **black box model**, because it does not explicitly treat the physical processes in the runoff system.

A **conceptual model** expresses rainfall-runoff system conceptually. The Tank model (Sugawara, 1972), the storage function method (Kimura, 1962), the TOPMODEL (Beven and Kirkby, 1979) are the examples of conceptual models. The Tank model treats catchment storage as combinations of several tanks.

A **physically-based model** consists of the physical equations of the continuity and momentum conservation. The kinematic wave model is one of physically-based rainfall-runoff models.

2.2.3 Lumped and distributed rainfall-runoff models

In terms of the spatial structure of a rainfall-runoff model, it is classified into a **lumped model** and a **distributed model**. When the priority is placed on forecasting at a specific point and the spatial distributions of rainfall and other geographical conditions within a basin can be assumed to be uniform, a lumped rainfall-runoff model may be selected. The input data to a lumped runoff model is a spatial average of rainfall and evapotranspiration intensity in the basin. A lumped model does not include the space dimensions in the governing equations, which are generally formed as ordinary differential equations with time as an independent variable.

On the other hand, sometimes predictions of spatial distribution of soil moisture and flow movement is requested. For the purpose, a rainfall-runoff model that predicts a spatiotemporal distribution of hydrological variables is required. A runoff model of this type is called a **distributed runoff model**. The input of a distributed rainfall-runoff is the spatiotemporal rainfall observation such as radar observed rainfall, the spatial distribution of topography, land use, geological condition of the river basin. A rainfall-runoff model that takes into account spatial hydrological variables can also be realized by spatially combining several lumped models for sub-basins. Including these hydrologic models, a hydrologic model that can consider spatial distributions of hydrologic variables is called a distributed runoff model.

2.3 Lumped Rainfall-Runoff Model

2.3.1 Rational formula

A relational formula is used for estimating the maximum flow rate from a drainage basin during a rainstorm. Suppose that spatial mean rainfall intensity in the study basin is R [$\text{mm}\cdot\text{h}^{-1}$]; the area is A [km^2]. Then the maximum flow rate Q [m^3s^{-1}] from the outlet is expressed as

$$Q = f \times r \text{ [mm}\cdot\text{h}^{-1}] \times A \text{ [km}^2] = \frac{1}{3.6} f R A \text{ [m}^3\text{s}^{-1}]$$

where f is a non-dimensional coefficient having a value of 1 or less, called the **runoff coefficient**, considering rainwater that does not contribute to the flood runoff by interception and infiltration etc. The constant $1/3.6$ is a coefficient required to transform the unit.

The rational formula expresses the relationship between the rainfall intensity and the flow rate at the time at which the flow rate reaches its maximum when the rainfall continues at a constant intensity. Theoretically, as explained by the kinematic wave model, this formula assumes the steady state condition, meaning that the characteristic curve departing from the upper end of the hillslope has reached the lower end when the rainfall continues at a constant intensity. The rational formula is used for the design of hydraulic facilities for small-scale basins (10km^2 or smaller).

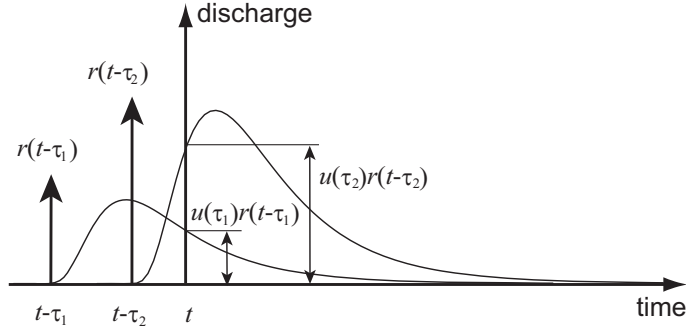


Fig. 2.5: Concept of unit hydrograph method

2.3.2 Unit hydrograph method

Suppose that in the case where rainfall whose size is 1 at time $t - \tau$, $\tau \geq 0$ is applied. Then, the runoff intensity at time t is expressed as $u(\tau)$, and the runoff intensity at time t due to the rainfall intensity $r(t - \tau)$ at time $t - \tau$ is expressed as $u(\tau)r(t - \tau)$. This $u(\tau)$ is the **unit hydrograph method** and is known as the unit impulse response function. The unit hydrograph method is a way of modeling the process of transformation of rainfall to runoff by overlapping the runoff intensities.

When the rainfall intensity is expressed as $r_e(t)$, the runoff intensity (height of runoff) is expressed as $q(t)$, the runoff intensity at time t due to the rainfall intensity $r_e(t - \tau_1)$ at time $t - \tau_1$ is expressed as $u(\tau_1)r(t - \tau_1)$, and the runoff intensity at time t due to the rainfall intensity $r_e(t - \tau_2)$ at time $t - \tau_2$ is expressed as $u(\tau_2)r_e(t - \tau_2)$. Add them together, and we find the runoff intensity at time t , as shown in **Fig. 2.5**, as follows:

$$q(t) = u(\tau_1)r_e(t - \tau_1) + u(\tau_2)r_e(t - \tau_2)$$

Therefore, the runoff intensity due to the continuous rainfall intensity $r_e(t)$ is given by integrating the runoff intensity due to the rainfall before time t :

$$q(t) = \int_0^\infty u(\tau)r_e(t - \tau)d\tau, \quad \int_0^\infty u(\tau)d\tau = 1 \quad (2.1)$$

Here, we derive an equation using the unit hydrographs of discrete time. Consider specific time T , and suppose that when $\tau > T$, $u(\tau) = 0$, and that

$$\int_0^T u(\tau)d\tau = 1$$

We set $\Delta t = T/N$, where N is a positive integer. Suppose that an amount of rainfall is obtained at an interval of this time, and the amount of rainfall $P_{t-k\Delta t}$ between time

$t - (k + 1)\Delta t$ to $t - k\Delta t$ is

$$P_{t-k\Delta t} = \int_{k\Delta t}^{(k+1)\Delta t} r_e(t - \tau) d\tau$$

Suppose also that the rainfall intensity is constant at an interval of time divided by Δt and that the amount of rainfall between time $t - (k + 1)\Delta t$ to $t - k\Delta t$ is $P_{t-k\Delta t}/\Delta t$. Here, on the basis of Eq.(2.1), $q(t)$ is expressed as

$$\begin{aligned} q(t) &= \int_0^\infty u(\tau) r_e(t - \tau) d\tau = \int_0^T u(\tau) r_e(t - \tau) d\tau \\ &= \frac{P_t}{\Delta t} \int_0^{\Delta t} u(\tau) d\tau + \frac{P_{t-\Delta t}}{\Delta t} \int_{\Delta t}^{2\Delta t} u(\tau) d\tau + \cdots \\ &\quad + \frac{P_{t-k\Delta t}}{\Delta t} \int_{k\Delta t}^{(k+1)\Delta t} u(\tau) d\tau + \cdots + \frac{P_{t-(N-1)\Delta t}}{\Delta t} \int_{(N-1)\Delta t}^{N\Delta t} u(\tau) d\tau \end{aligned}$$

Here, suppose that

$$U_k = \frac{1}{\Delta t} \int_{(k-1)\Delta t}^{k\Delta t} u(\tau) d\tau, \quad k = 1, 2, \dots, N \quad (2.2)$$

U_k is the offset of the hydrograph of the discrete time. Using Equation (7.7), we can express the height of runoff $q(t)$ of time t as

$$\begin{aligned} q(t) &= P_t U_1 + P_{t-\Delta t} U_2 + \cdots + P_{t-(k-1)\Delta t} U_k + \cdots + P_{t-(N-1)\Delta t} U_N \\ &= \sum_{k=1}^N P_{t-(k-1)\Delta t} U_k \end{aligned} \quad (2.3)$$

and the amount of runoff from the drainage basin is given by multiplying $q(t)$ by the area of the drainage basin. As shown in **Fig. 2.6**, a flow rate hydrograph represents the addition of unit hydrographs multiplied by the amount of rainfall per unit time for every specific period of time.

2.3.3 Tank model

Tank models express the runoff from a basin conceptually by combining several tanks with outlets at their side and bottom. While there are various combinations of tanks with different outlet settings, a four-layer tank model as shown in **Fig. 2.7** is often used in Japan. Conceptually, runoff from the upper tank is considered surface runoff, from the upper to lower tank as infiltration, and the runoff from the lower tank as groundwater discharge.

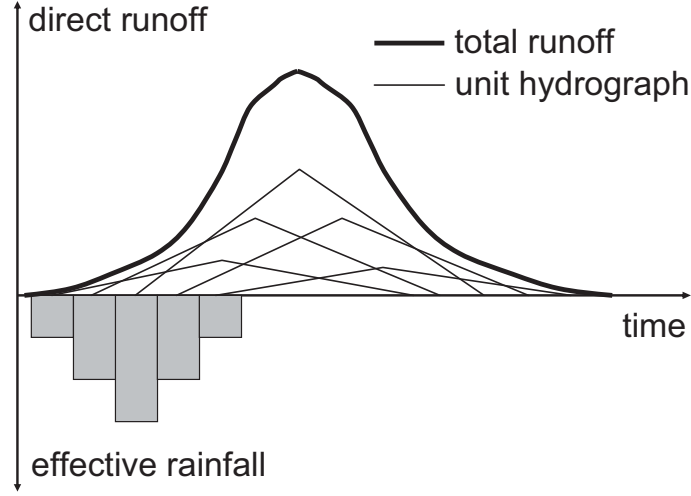


Fig. 2.6: Estimation of runoff by overlapping unit hydrographs

In **Fig. 2.7**, r is the rainfall intensity; e is the evapotranspiration intensity; s_1 is the height of storage for the first tank; q_1 , q_2 and q_3 are overland flow, subsurface flow, and infiltration to the lower tank for the first tank. Suppose that h_1 and h_2 are the heights of the outlets of overland and subsurface flow; a_1 , a_2 and a_3 are the parameters of the runoff to these outlets and the bottom of the tank. Then, the continuity equation of the first tank is given by

$$\frac{ds_1}{dt} = r - e - q_1 - q_2 - q_3$$

The amounts of runoff of the side flow and the downward flow are

$$q_1 = \begin{cases} a_1(s_1 - h_1), & \text{if } s_1 > h_1 \\ 0, & \text{if } s_1 \leq h_1 \end{cases} \quad q_2 = \begin{cases} a_2(s_1 - h_2), & \text{if } s_1 > h_2 \\ 0, & \text{if } s_1 \leq h_2 \end{cases} \quad q_3 = a_3 s_1$$

2.3.4 Storage function method with effective rainfall model

A storage function method with an effective rainfall input is often used for flood simulation for Japanese catchments. Suppose that the height of storage is s ; the direct runoff height is q ; the effective rainfall intensity is r_e ; and model parameters as k , p and T_L . The storage function method consists of the continuity equation and the relation between the storage and runoff as:

$$\frac{ds}{dt} = r_e(t - T_L) - q, \quad s = kq^p \quad (2.4)$$

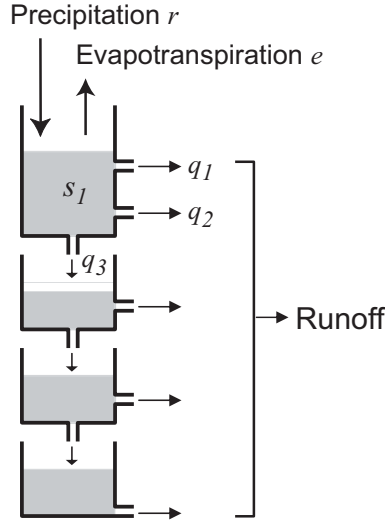


Fig. 2.7: Structure of the tank model.

Suppose that $r(t)$ and t_0 denote the catchment average rainfall intensity and the initial time of calculation, respectively. The effective rainfall intensity $r_e(t)$ is given by

$$r_e(t) = \begin{cases} f_1 r(t), & \text{when } 0 \leq \int_{t_0}^t r(\tau) d\tau < R_{sa} \\ r(t), & \text{when } \int_{t_0}^t r(\tau) d\tau \geq R_{sa} \end{cases} \quad (2.5)$$

where f_1 ($0 < f_1 < 1$) is the parameter relating to effective rainfall. The value of f_1 is usually determined by the relationship between the total amount of rainfall observed in the basin and the direct runoff height. The total amount of runoff $Q(t)$ is expressed as the sum of direct runoff $q(t)$ multiplied by the area of the basin A and the base flow rate Q_b as

$$Q(t) = Aq(t) + Q_b(t)$$

Note that this storage function method is different from Kimura's storage function method in terms of the model structure. Kimura's storage function method deals with two types of storage amount: the amount of storage in the runoff region and that in the infiltration region. f_1 means the ratio of the area of the runoff region to the area of the entire drainage basin. Effective rainfall is considered a part of the model of flow. On the other hand, this storage function method deals with one type of storage amount. f_1 and R_{sa} are used as parameters of the effective rainfall model that is separated from the model of flow. Several effective rainfall models were adopted to calculate direct runoff for the storage function method.

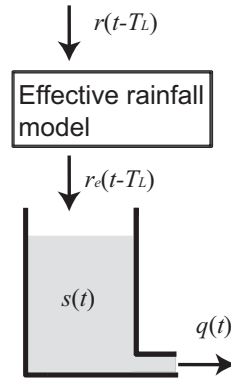


Fig. 2.8: Storage function method with effective rainfall model.

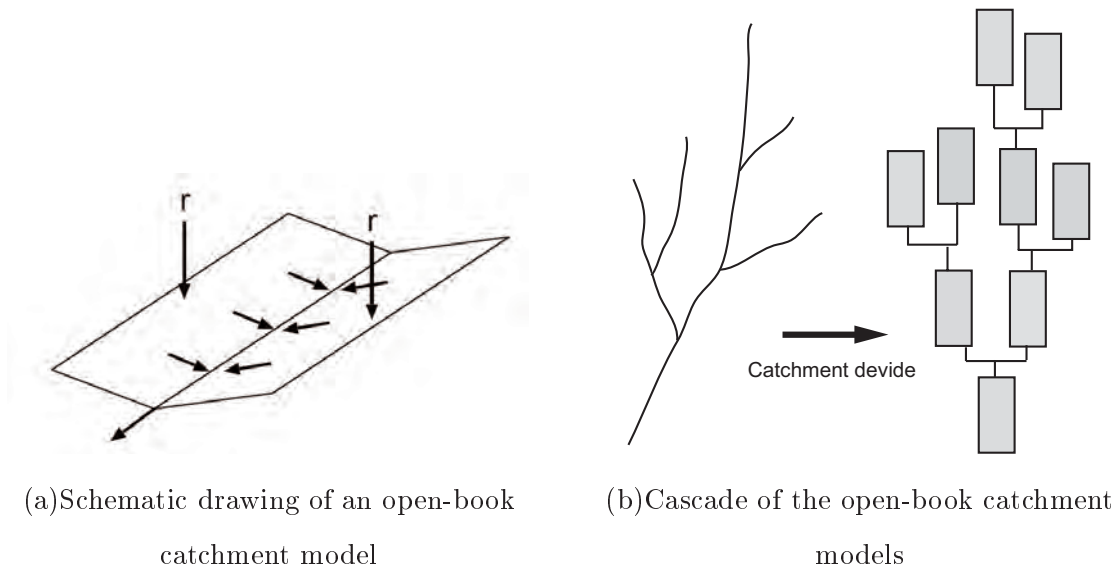


Fig. 2.9: Catchment modeling.

2.4 Distributed Rainfall-Runoff Model

2.4.1 Open-book type catchment modeling

A simple representation of basin topography is provided by an open-book catchment model as shown in **Fig. 2.9(a)**. As its name implies, an open-book catchment model consists of two rectangular planes and a stream. Rain water flows on the planes and flows into the stream, and then the stream flow is routed to the basin outlet. The flows on the rectangular plane and the stream are routed using a flow model such as the kinematic wave model. This forms a simple approximation of catchment hydrology. The entire system model is constructed by a cascade of the open-book element models as shown

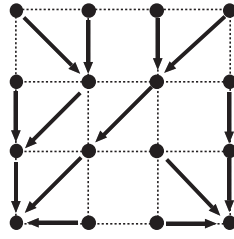


Fig. 2.10: Flow direction information generated from a digital elevation model.

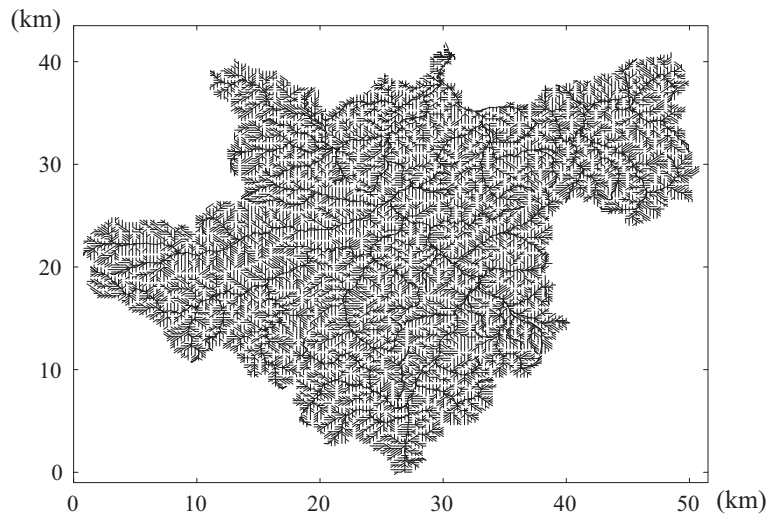


Fig. 2.11: Flow direction map for the Maruyama River basin.

in **Fig. 2.9(b)**. Spatial distribution information of topography, soil characteristics, land cover and rainfall intensity are used for each modeling of sub-catchment.

2.4.2 Catchment modeling using digital elevation models

Digital elevation models (DEMs) are available at any catchments with a high spatial resolution enough to describe local catchment topography. For example, HydroSHED (Hydrological data and maps based on SHuttle Elevation Derivatives at multiple Scales, <http://hydrosheds.cr.usgs.gov/index.php>) provides hydrographic information for regional and global-scale, which includes digital elevations, flow directions determined by the steepest gradient with the eight direction method (**Fig. 2.10**), and flow accumulation with the spatial resolutions of 3 arc-second (about 100m), 15 arc-second (about 500m) and 30 arc-second (about 1km).

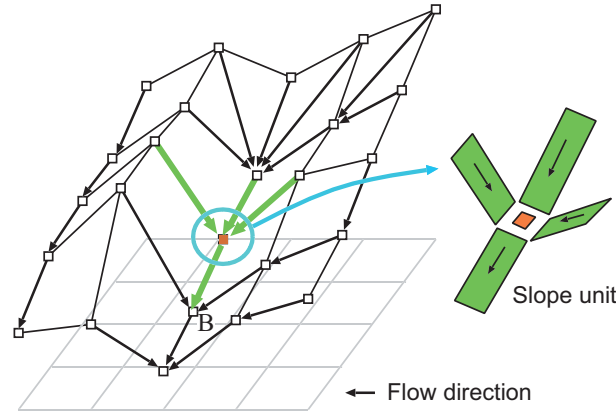


Fig. 2.12: Slope element based on flow information.

After deriving the flow direction information, it is easy to define a river basin to contribute the outlet of a basin as shown in **Fig. 2.11**, which is formed a set of slope units connected according to the flow direction using a 250m resolution DEM. **Fig. 2.12** is a schematic drawing of distributed flow modeling on the derived flow direction information. For each slope unit, its area, length and gradient used for a flow model are easily calculated using DEMs. A rainfall-runoff is applied to slope units and generated runoff is routed according to the flow direction information. Not only water movements, sediment and substance movements are also calculated based on the spatial distribution of rainfall intensity, topography, geography, and land use. One of typical distributed models is the 1K-FRM <http://hywr.kuciv.kyoto-u.ac.jp/products/1K-DHM/1K-DHM.html>.

2.4.3 Flow modeling in hillslope and channel network

To represent flows in a hillslope and a channel network, various numerical models are used. To calculate runoff from a hillslope, rainfall-runoff models such as Tank Model, TOPMODEL, the kinematic wave model are used. To calculate river flow, a flow routing model such as Muskingum method, kinematic wave model, dynamic wave method is used. Model selection is due to the purpose of hydrologic and hydraulic analysis.

A physically-based flow model for hillslope flow is the kinematic wave model. Assuming a rectangular slope as shown in **Fig. 2.13**, x is the distance measured perpendicularly from the upper end of the hillslope t is time; $r(x, t)$ is rainfall intensity; $e(x, t)$ is evapotranspiration rate; $p(x, t)$ is infiltration rate; $q(x, t)$ is unit width flow rate from of the

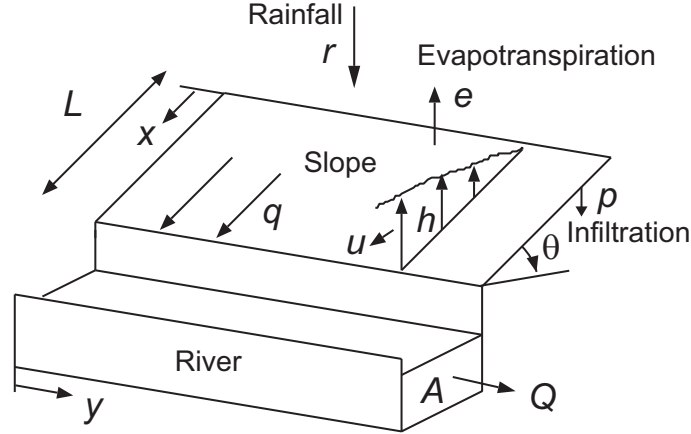


Fig. 2.13: Flow modeling using the kinematic wave model.

hillslope; $h(x, t)$ is water depth measured perpendicularly from the hillslope; and L is the hillslope length. Subtraction of evaporation and infiltration intensity from rainfall intensity forms the effective rainfall intensity r_e , and suppose that it is supplied to the hillslope. The equation of continuity and the equation of motion of the hillslope flow are

$$\frac{\partial h}{\partial t} + \frac{\partial q}{\partial x} = r_e(x, t) = \{r(x, t) - p(x, t) - e(x, t)\} \cos \theta$$

$$q = f(x, h)$$

The unit width flow rate at the lower end of the hillslope is given as $q(L, t)$.

The hillslope runoff is the input to the river routing model. The continuity and momentum equations of the channel flow routing are expressed as

$$\frac{\partial A}{\partial t} + \frac{\partial Q}{\partial y} = q_L(y, t)$$

$$Q = g(y, A)$$

where $q_L(y, t)$ is the slope runoff at distance y along the river channel, $Q(y, t)$ is the flow rate of the river channel, $A(y, t)$ is the flow area. By connecting flow routing model spatially, an entire distributed rainfall-runoff model is constructed.

2.5 Land Surface Hydrological Model

Land surface hydrological models have been introduced as the bottom layer of atmospheric general circulation models (AGCMs) and meso-scale atmospheric models (MSMs).

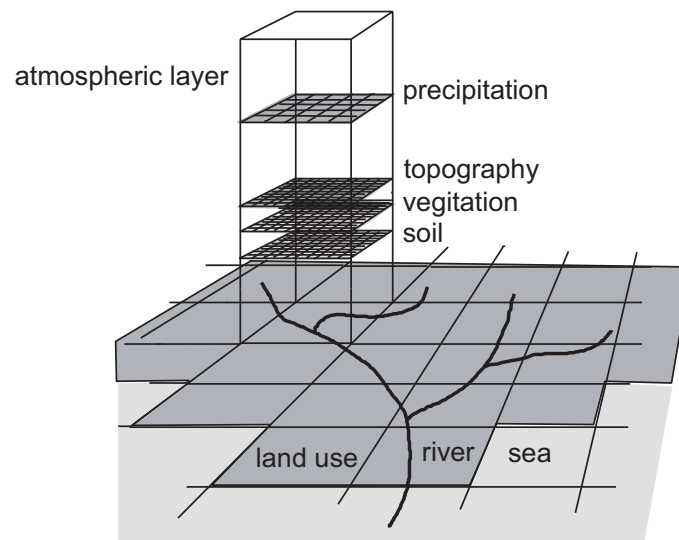


Fig. 2.14: Coupling of atmospheric model, land surface model and river routing model.

These models, known as **soil-vegetation-atmosphere schemes (SVATs)**, describe transfer of water and thermal energy among the atmosphere, vegetation, and soil, as shown in **Fig. 2.14**. A typical land surface hydrological model is the simple biosphere (SiB) model.

This model supposes that vegetation consists of two layers: the vegetation layer (the upper layer) represents the canopy of trees and shrubs and the land surface (the lower layer) represents the grass land and the bare soil. The soil underneath the land surface is considered to consist of three layers: the first layer undergoes significant daily changes in soil moisture and is several centimeters thick; in the second layer soil moisture changes due to transpiration from trees, shrubs, and grasses; and in the third layer soil moisture changes due to transpiration from trees and shrubs. The latent heat transport, the sensible heat transport, the soil moisture content, the canopy temperature, the land surface temperature, and the soil temperature are given by a system of the **energy balance equation** and the **water balance equation** with the temperature and the moisture quantity in each layer as unknown variables.

2.5.1 Energy balance equation

Fig. 2.15 shows hydrological quantities relating to energy balance, except snow cover and snowmelt, among the variables used in the SiB model. The energy balance equation

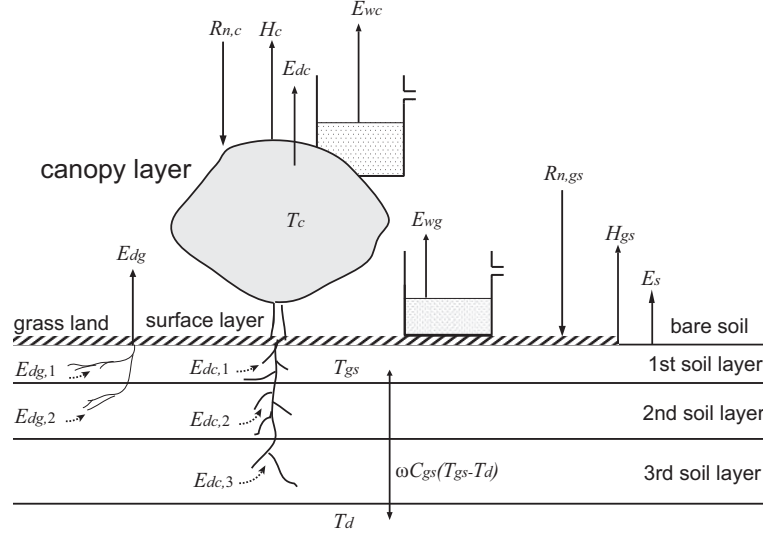


Fig. 2.15: Energy balance of land surface model SiB (Simple Biosphere Model) (excluding snowfall and snowmelting).

of the canopy layer at temperature T_c is expressed as

$$C_c \frac{dT_c}{dt} = R_{n,c} - H_c - \lambda(E_{wc} + E_{dc}) \quad (2.6)$$

where C_c represents the heat capacity of the canopy layer; $R_{n,c}$ represents the net radiation supplied to the canopy layer; H_c represents the sensible heat flux from the canopy layer; and E_{wc} and E_{dc} represent the interception evaporation and the evapotranspiration from the canopy layer.

The energy balance equation of the land surface that combines the grass land and the bare soil land, at the land surface temperature T_{gs} , is expressed as

$$C_{gs} \frac{dT_{gs}}{dt} = R_{n,gs} - H_{gs} - \lambda(E_{wg} + E_{dg} + E_s) - G$$

where C_{gs} is the heat capacity of the land surface that combines the land cover and the bare soil base; $R_{n,gs}$ is the net radiation supplied to the land surface; H_{gs} is the sensible heat flux from the land surface; E_{wg} and E_{dg} are the interception evaporation and the evapotranspiration from the land surface; and E_s is the evaporation from the bare soil.

2.5.2 Water balance equation

Fig. 2.16 shows hydrological variables relating to the water balance, except snow cover and snowmelting, among the variables used in the SiB model. When the interception

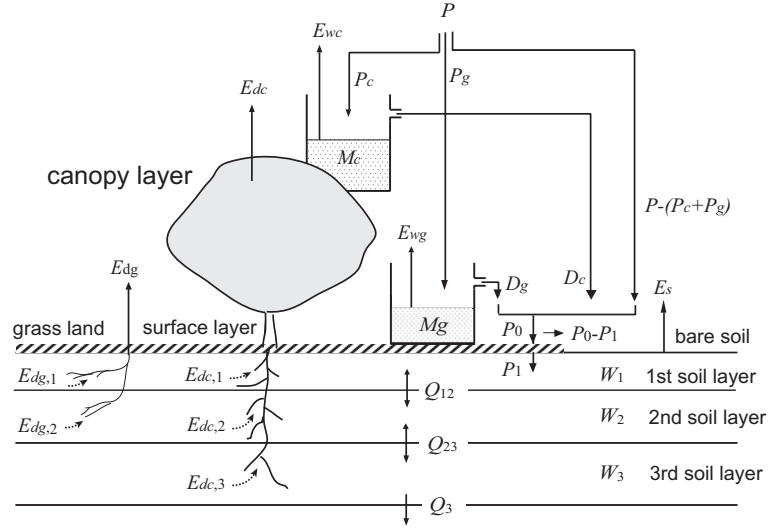


Fig. 2.16: Water balance of land surface model SiB (Simple Biosphere Model) (excluding snowfall and snowmelting).

precipitation amounts of the canopy layer and the grass land are represented by M_c and M_g , respectively, the water balance equations are expressed as follows:

$$\frac{dM_c}{dt} = P_c - D_c - \frac{1}{\rho_w} E_{wc} \quad (2.7)$$

$$\frac{dM_g}{dt} = P_g - D_g - \frac{1}{\rho_w} E_{wg} \quad (2.8)$$

where P_c and P_g represent the precipitation amounts to the canopy layer and the grass land; D_c and D_g are the water drainage from the rainfall storage intercepted by the canopy layer and the grass land; and ρ_w is the density of water. P_c and P_g are determined by factors including the fractional areas covered by the canopy layer and the grass land cover.

When the saturated ratio (=volumetric soil moisture content/porosity) of each of the three soil layers is represented by W_1 , W_2 and W_3 , the time variation of saturated ratio is expressed as follows:

$$\frac{dW_1}{dt} = \frac{1}{\theta_s D_1} \left\{ P_1 - Q_{1,2} - \frac{1}{\rho_w} (E_s + E_{dc,1} + E_{dg,1}) \right\} \quad (2.9)$$

$$\frac{dW_2}{dt} = \frac{1}{\theta_s D_2} \left\{ Q_{1,2} - Q_{2,3} - \frac{1}{\rho_w} (E_{dc,2} + E_{dg,2}) \right\} \quad (2.10)$$

$$\frac{dW_3}{dt} = \frac{1}{\theta_s D_3} \left\{ Q_{2,3} - Q_3 - \frac{1}{\rho_w} E_{dc,3} \right\} \quad (2.11)$$

where θ_s is the soil porosity; D_1 , D_2 and D_3 are the soil depth of each layer of the soil; P_1 is the infiltration of rainfall into the first layer; $Q_{1,2}$ and $Q_{2,3}$ are the soil moisture

transfers from an upper layer to a lower layer; $P_0 - P_1$ is the precipitation excess to the outside of the region; and Q_3 is the gravitational outflow to the outside of the region. $E_{dc,1,2,3}$ represents the transpiration absorbed by the root system spreading each layer of the soil, and $E_{dg,1,2}$ is the transpiration absorbed by the root system of the grass land spreading in the first and second soil layers.

When P represents the precipitation intensity on the canopy layer and P_0 represents the precipitation intensity supplied to the soil, P_0 and P_1 are expressed as

$$P_0 = P - (P_c + P_g) + (D_c + D_g)$$

$$P_1 = \min(P_0, k_1)$$

where k_1 is the hydraulic conductivity at the land surface. This expression indicates that the precipitation intensity less than the hydraulic conductivity at the land surface infiltrates into the soil layer, and that the precipitation amount exceeding the hydraulic conductivity outflows to the outside of the region. Therefore, the runoff Q_{out} flowing out of the region is given by

$$Q_{out} = P_0 - P_1 + Q_3$$

Here, eight equations, Eq.(2.6) – Eq.(2.11), and eight variables, T_c , T_{gs} , T_d , M_c , M_g , W_1 , W_2 and W_3 need to be solved. The right-hand side of each of Eq.(2.6) – Eq.(2.11) is expressed as functions of these eight variables. By solving this system of ordinary differential equations, the land surface temperatures and the moisture contents are obtained. The runoff flowing out of the region Q_{out} is routed through river channels using a slope runoff model and a river routing model.

References

- [1] Bras, R. L.: Hydrology: An Introduction to Hydrologic Science, Addison-Wesley, 1989.
- [2] Brutsaert, W.: Hydrology: An Indroduction, Cambridge Unversity Press, 2005.
- [3] Chow, V. T., D. R. Maidment and L. W. Mays: Applied Hydrology, McGraw-Hill, 1988.
- [4] Eagleson, P. S.: Dynamic Hydrology, McGraw-Hill, 1970.

Lecture 2: Fundamentals in Flood Frequency Analysis

Shigenobu TANAKA (Professor, WRRC, DPRI, Kyoto University)

In the risk management or the risk assessment of water-related disasters, the relationship between the frequency of hazard and its consequence is indispensable. The probability of rare events is important. The aim of this lecture is to introduce fundamental knowledge of flood frequency analysis. There are, in general, two ways of preparing sample for flood frequency analysis based on Extreme Value Theory, that is, Annual Maximum Series(AMS) and Peaks Over Threshold(POT). The method using AMS is popular for flood frequency analysis. Generalized Extreme Value distribution(GEV) including Gumbel distribution as its special case is used corresponding to the analysis of AMS. It is easy to understand that larger hazards cause disasters. Since AMS consists of larger events in the regions where many independent flood events occur in a year, AMS is useful. But there are different regions where very small floods or no flood occur in some years such as semi-arid area. In this case, AMS is no longer applicable and POT is useful. Generalized Pareto distribution(GP or GPD) including Exponential distribution as its special case is corresponding to POT. Further, when both AMS and POT extracted from a time series are available, it is interesting whether the result of each analysis almost coincides or not.

This lecture provides sampling method and corresponding analyses for both sampling method, AMS and POT. When we use POT, we have to extract independent peaks and then there is an issue of selecting threshold. A selection method of threshold based on Exponential distribution is introduced.

Through this lecture, it is introduced that AMS, POT, probability density function(PDF), cumulative distribution function(CDF), return period, return level, Gumbel distribution, Generalized Extreme Value distribution(GEV), Exponential distribution, Generalized Pareto distribution(GP), method of moment, L-moment, probability paper, plotting positions.



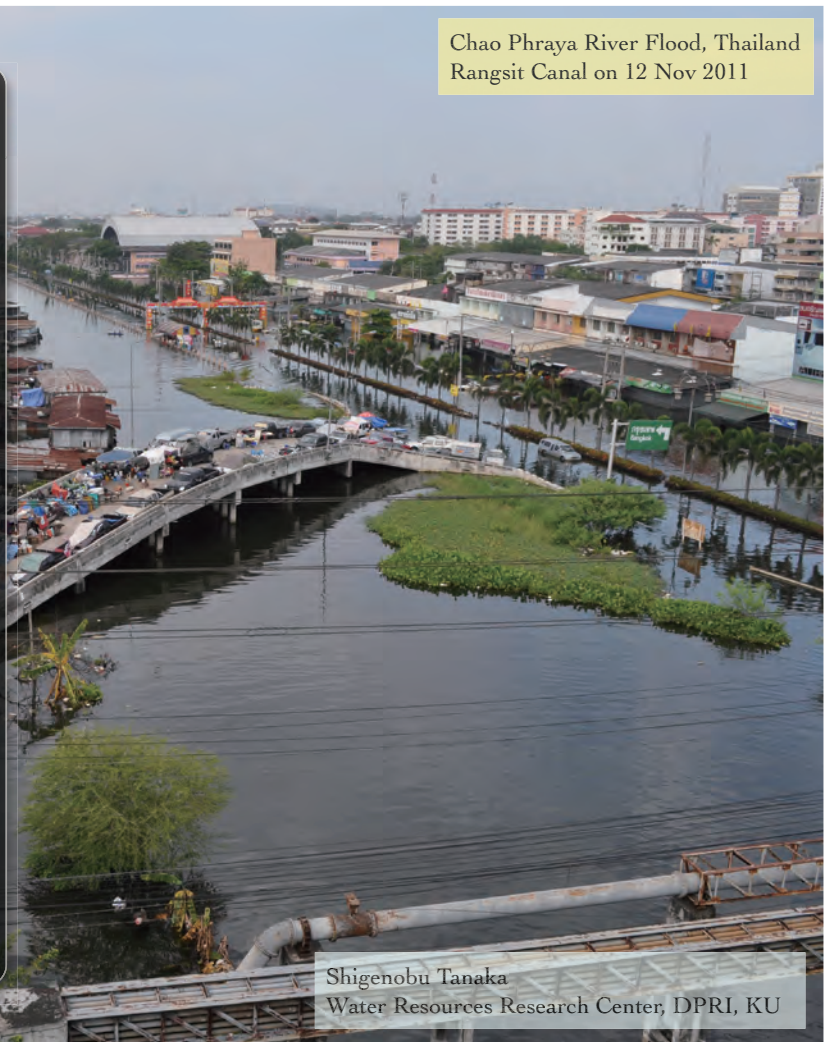
FLOOD FREQUENCY ANALYSIS

Shigenobu Tanaka

CHAPTER 1

FREQUENCY ANALYSIS OF EXTREMES

In order to plan or design the disaster countermeasures, future extreme is one of the important issues. When the maximum record or smaller event is used for design, we don't need frequency analysis. However, if we use extrapolated extreme for design of infrastructure, we need frequency analysis of extremes. Generally, when the asset in the flood prone area become large, we need more insurance or safety. Countermeasures against such extreme event should be implemented before the occurrence.



Shigenobu Tanaka
Water Resources Research Center, DPRI, KU

SECTION 1

Explanatory Hazard Variable for Flood Damages

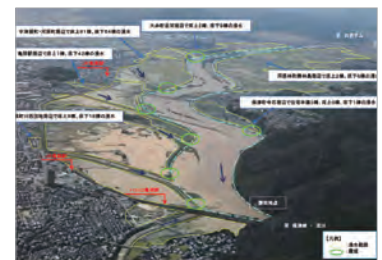
What is the key variable for representing flood magnitude?

REPRESENTATIVE HAZARD

- With what kind of variable can we express flood frequency or flood magnitude?
- In Japan, since one of the most probable cause of dike breach is overtopping of flood water, peak water level is important but the level is easily affected by river morphological change. Peak discharge is an alternative but the observation period is rather short. Then, rainfall during design rainfall duration is used as the variable for flood frequency analysis.
- In the earlier stage of modernization of Japan, the floods once in several years or ten years were used for design of flood control facilities such as embankments.
- Later, the maximum flood record was used for the design.
- After the World War II, the method using historical maximum flood has been replaced by probabilistic flood. Further, not only flood control but also water resources development by reservoir have become popular, which needs hydrograph of discharge.
- Nowadays, assessment of flood risk through planning of flood control facilities have been carried out with rainfall data.
- Because rivers without sufficient embankment such as the Chao Phraya will cause inundation with moderate flood, inundation volume is appropriate to the representative hazard variable for flood damages. It is found that the inundation volume of the Chao Phraya can be estimated by 5-month rainfall depth of the basin.

Flood frequency shows relationship between the magnitude of flood and how often the flood occurs. The magnitude of flood generally depends on rainfall characteristics. In a steep river basin, peak discharge is the most important. On the contrary, in a very flat flood plain, flood inundation water volume is the most important.

The former depends on mostly rainfall intensity and its pattern in time and space but the latter on total rainfall in some period. Further, like in Japan, most rivers are installed with continuous embankments on both sides. Once embankment breach occurs, flood water spreads to the flood plain. Because soil embankment is very vulnerable for over topping, whether overtopping occur or not is critical. Water level can be determined by the peak discharge. Then, peak discharge can be one of the most important factors. So, the peak discharge is used for assessing flood magnitude in practice. However, discharge observation period is usually not so long and discharge and/or water level at a station has been influenced by upstream flooding condition. On the other hand, rainfall observation has been carried out for rather long period compared to discharge observation and not affected by alteration of upstream basin and river channel. Furthermore, the conventional hydrological frequency analysis is based on stationary condition.

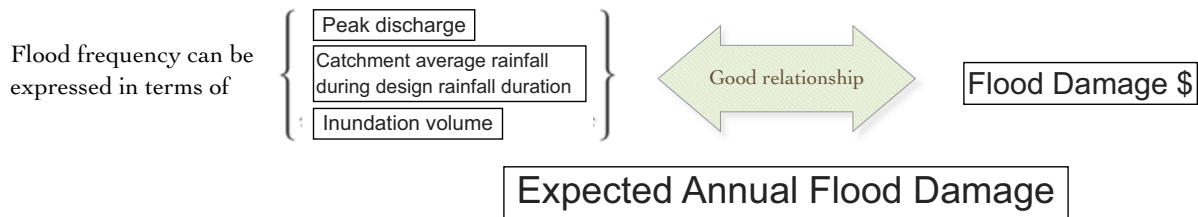


Flooding at midstream attenuate downstream flood. (photo from Kyoto Pref.)



Even attenuated flood water overtopped embankment. Flood fighters are building up sand bags (photo from Kinki R.B., MLIT)

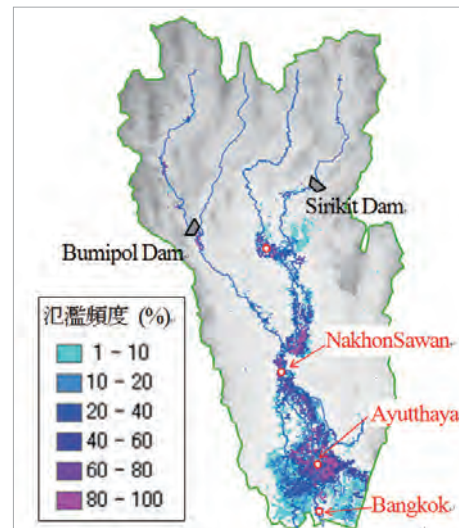
Concurrently with the application of probabilistic



flood and quick development of urbanization, water resources in many river basins had become short and flood control by dam had become necessary to protect existing urbanized area in flood plain. In this context, the peak discharge of hydrograph and catchment averaged rainfall during design rainfall duration have been key variables for the flood risk assessment in Japan.

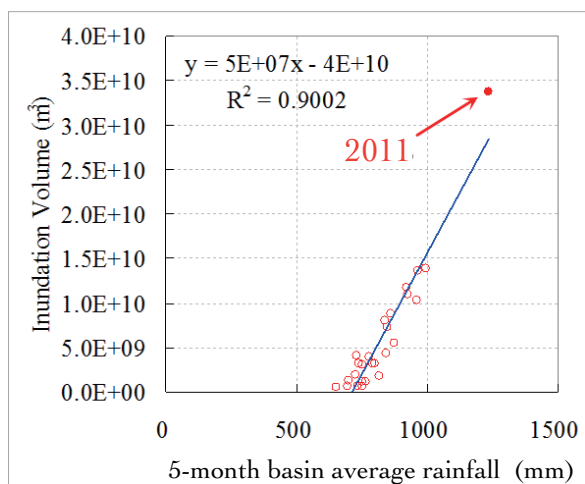
If there exists no sufficient embankment along the river channel such as Chao Phraya river in Thailand, even moderate floods cause inundation and then flood damage. Generally, flood damage depends on water depth and inundation extent. The water depth and inundation extent can be explained by the inundation volume. In such case, the inundation volume should be used for assessing flood frequency. It is investigated that the total amount of five month rainfall explains the inundation volume in the Chao Phraya river basin well.

Explanatory hazard variable depends on dominant factors of flood damage in considering flood plain. Once we know the relationship between frequency of explanatory hazard and flood damage in money, we can know expected annual flood damage.

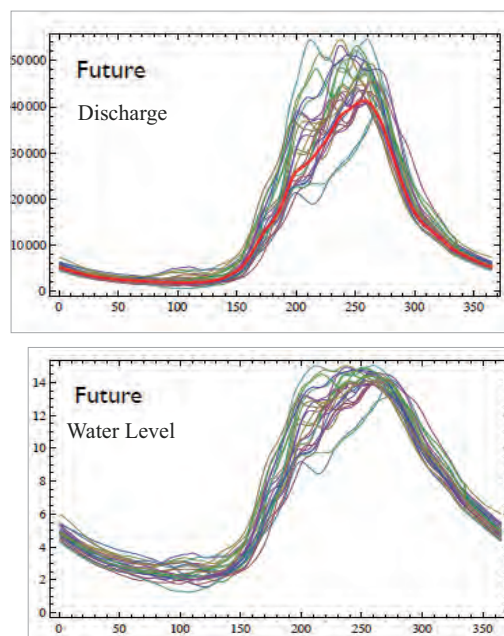


Inundation frequency in Chao Phraya basin

3



Relationship between Annual Maximum 5-month rainfall and calculated Inundation volume in the Chao Phraya basin



Discharge and water level of the Mekong River in Campong Cham, in Cambodia.

4

SECTION 2

Relationship between how much rainfall and how often

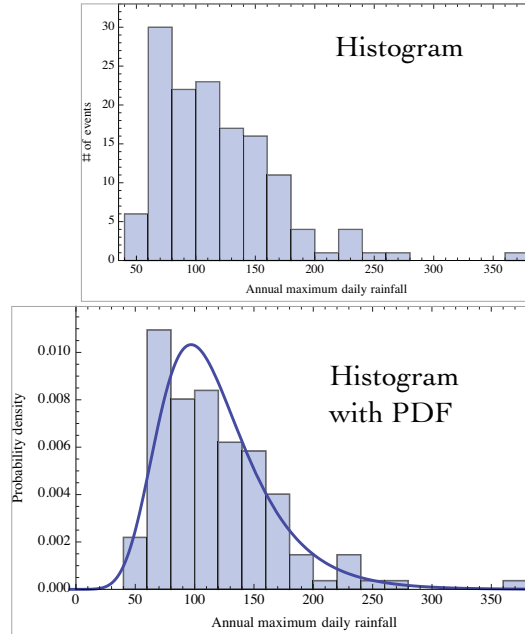
TERMINOLOGY

- Histogram
- Random variable : usually expressed by X , lower case x a possible value of X
- PDF : Probability Density Function, usually expressed $f(x)$
- CDF : Cumulative Distribution Function, usually expressed by $F(x)$
- Non-exceedance probability : usually expressed by F or p
- Exceedance probability : $1-F$ or q
- Quantile : x_p is expressed inverse form of $F(x_p)=p$
- Return period :

$$T = \frac{1}{1-p}$$

•

When you have a set of observations $(X_1, X_2, \dots, X_p, \dots, X_n)$, select arbitrary bin width, for example, 20 mm in the following example and count the number of X_i which falls in each bin such as 6 for from 40 to 60 mm and 30 for 60-80 mm. Histogram plots these numbers against bin specifications. Histogram plots these numbers against bin specifications. Histogram shows relative frequencies of variables. Total of the number of each bin is equal to sample size n . It is seen that the frequency of big rainfall becomes small, that is, extreme event occurs seldom.



Next, if we consider total area of the histogram as 1, the height of each bin will be relative frequency (height of each bin divided by sample size) divided by bin width. So, the dimension of y axes will be $1/(\text{dimension of variables})$. In this sample, there are no data between 280-360 mm. It is expected when the sample size becomes very big and the width of bin becomes very small, the envelope will be rather smooth.

Fig. 2.1 Histogram and PDF fitting

5

- Mean of a random variable X

$$\mu_x = E[X]$$

- Variance : $\text{Var}(X)$ or σ_x^2
 $\sigma_x^2 = \text{Var}(X) = E[(X - \mu_x)^2]$

- Sample : a set of observations $(X_1, X_2, \dots, X_p, \dots, X_n)$

- Sample size : n

- Sample estimators $\hat{\mu}_x = \bar{X} = \frac{1}{n} \sum_{i=1}^n X_i$

$$\hat{\sigma}_x^2 = S^2 = \frac{1}{n-1} \sum_{i=1}^n (X_i - \bar{X})^2$$

(unbiased estimator)

Here, we'd like to see several important definitions. PDF (probability density function) is defined as derivative of CDF (cumulative distribution function).

When we take annual maximum series as variate, **Return Period T** is defined as $1/(1-p)$, the reciprocal of the **exceedance probability**. When $p=0.95$, $1-p=0.05$, for example, then $T=20$. Confirm the relationship between PDF and CDF in the pictures below.

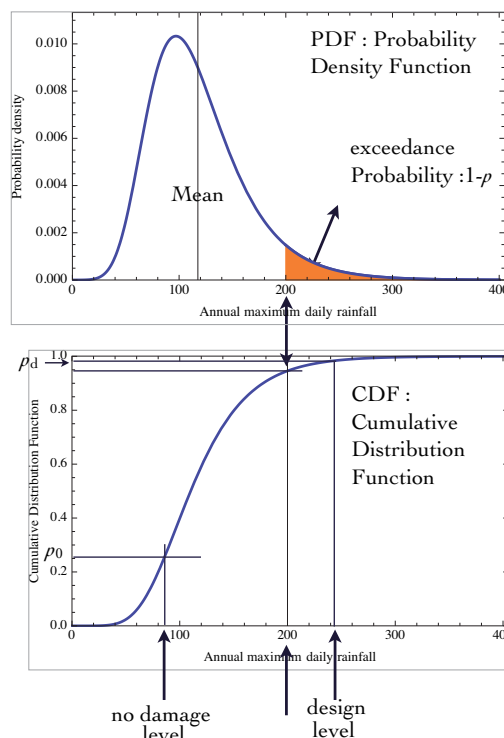


Fig. 2.2 PDF and CDF

6

EXTREME VALUE THEORY

- Block Maximum : Annual Maximum Series(AMS)

Generalized Extreme Value(GEV) distribution

$$F(x) = \exp \left[- \left(1 - k \frac{x - \xi}{\alpha} \right)^{1/k} \right]$$

Gumbel distribution

$$F[x] = \exp \left\{ - \exp \left\{ - \frac{x - \xi}{\alpha} \right\} \right\}$$

We know from experience that the severer natural hazard is, the more infrequent. And also, larger hazard causes extensive damage. Since usual hazard event does not cause significant disaster, our concern is that how large (or small) event will occur how frequent, that is, probability of such unusual event. The extreme value theory deal with this problem.

AMS(Annual Maximum Series) and POT(Peaks Over Threshold)

In this process, mean value such as the mean of the daily precipitations in a year is not useful. Such rainfall does not cause disaster. Our concern is big events which cause disaster. There are several definition of “big events”. The “**block maximum**” is usually used to investigate the behavior of extreme value. Annual maximum daily precipitation, annual maximum temperature, annual maximum peak discharge, annual maximum inundation area and so on are the examples of block maxima. In this theory, the probability distribution of block maxima is discussed not probability of whole data. This means you don’t need to collect whole data but just annual maximum series(AMS). The other popular definition of “big events” is peaks over threshold(POT). In this course, distributions for analyzing AMS and POT will be explained, respectively.

Generalized Extreme Value Distribution(GEV)

It has been proved that there are just three types of extreme value distribution, that is, Gumbel-type distribution, Fréchet-type distribution and Weibull-type distribution. These three types of extreme value distribution can be combined into a single form

7

POT

- Peaks Over Threshold
- Generalized Pareto (GP) distribution

$$G(x) = 1 - \left(1 - k \frac{x - \xi}{\alpha} \right)^{1/k}$$

Exponential distribution

$$G(x) = 1 - \exp \left\{ - \frac{x - \xi}{\alpha} \right\}$$

Threshold Selection : SMEF(Sample Mean Excess Function)

Relationship between AMS and POT

$$F(x) = \exp \left\{ - \lambda (1 - G(x)) \right\}$$

$$F(x) = \exp \left[- \left(1 - k \frac{x - \xi}{\alpha} \right)^{1/k} \right] \quad (3-1)$$

which is called Generalized Extreme Value(GEV) distribution, and where ξ :location parameter, α : scale parameter, k : shape parameter. When $k < 0$, GEV is Fréchet-type distribution and has a finite lower bound $x > \xi + \alpha/k$, on the other hand, when $k > 0$, GEV is Weibull-type distribution and has a finite upper bound $x < \xi + \alpha/k$. Please note there are two forms of definition of GEV with **different sign** of shape parameter. *Handbook of Hydrology* uses the form of Eq.(3-1).

In the special case $k=0$, this equation becomes Gumbel distribution.

$$F(x) = \exp \left\{ - \exp \left(- \frac{x - \xi}{\alpha} \right) \right\} \quad (3-2)$$

where $-\infty < x < \infty$.

In order to estimate the risk of large disaster, the probability $F(x)$ is indispensable. The risk is generally defined as expected annual flood damage and in order to estimate it, we need the probability distribution function $F(x)$ of concerning hazard and damages as its consequence.

Generalized Pareto distribution(GP)

In hydrological frequency analysis, AMS is widely used. However, there are cases that they don’t record every year’s maximum event but all events that they operate their barrages for the flood mitigation and no record in dry years. Every flood with barrage operation is significantly large and usually independent and we can regard them as **POT**. In this case, we cannot apply GEV distribution including Gumbel distribution any more. Generalized Pareto distribution(GP or GPD) including Exponential distribution is used for denoting probability of **POT**.

Eq.(3-3) shows the CDF of GP.

$$G(x) = 1 - \left(1 - k \frac{x - \xi}{\alpha} \right)^{1/k} \quad (3-3)$$

8

where ξ :location parameter, α : scale parameter, k : shape parameter. Please note there are two forms of definition of GP with **different sign** of shape parameter. *Handbook of Hydrology* uses the form of Eq.(3-3).

In the special case $k = 0$, this equation becomes **Exponential** distribution. The CDF and PDF of Exponential distribution(Exp) are shown by Eq.(3-4) and (3-5).

$$G(x) = 1 - \exp\left\{-\frac{x - \xi}{\alpha}\right\} \quad (3-4)$$

$$g(x) = \frac{\exp\left\{-\frac{x - \xi}{\alpha}\right\}}{\alpha} \quad (3-5)$$

The mean of the PDF of Exp becomes α in case of $\xi=0$. Using this characteristics, we can select effective threshold(see sample mean excess function(SMEF)).

Figure 3.1 shows an example of time series of two day rainfall in 62 years and includes AMS and POT. Red points connected with red lines are AMS and blue points with vertical fine lines are POT. The threshold of POT is 85mm in the top figure and 105mm in the bottom

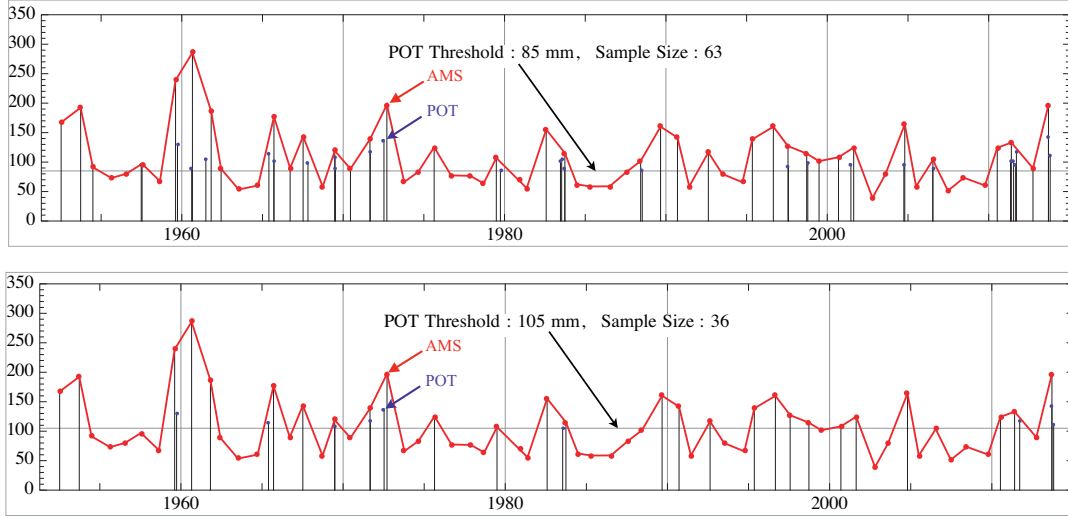


Fig. 3.1 Example of AMS and POT

one. Histograms of AMS and POT are shown in Fig. 3.2 with fitting curves. AMS is fitted with Gumbel distribution and POT with Exponential distribution.

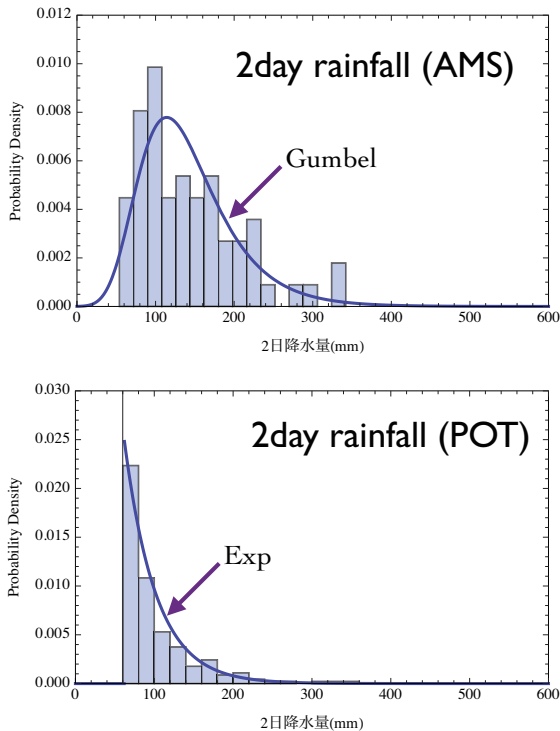


Fig. 3.2 Histogram of AMS and POT

There is an equation (3-6) which connects AMS and POT.

$$F(x) = \exp\left\{-\lambda(1 - G(x))\right\} \quad (3-6)$$

where $F(x)$:distribution function corresponding AMS which shows the probability that the annual maximum in a year will not exceed x , $G(x)$:distribution function of POT which shows the probability of less than x , λ :arrival rate of POT. Eq.(3-6) can be also useful in probability plot of AMS samples with POT's.

Selection of Threshold

As mentioned previously, an interesting characteristics of Exp is used in selecting threshold. Sample mean excess function(SMEF) shown Eq.(3-7) calculate the mean of variable x more than u .

$$e_n(u) = \frac{\sum_{i=1}^n (x_i - u)I(u < x_i)}{\sum_{i=1}^n I(u < x_i)} \quad (3-7)$$

where, $I(u < x) : 1$, if $u < x$ and 0 otherwise. When x more than c are data from Exponential distribution, then Eq.(3-7) is constant in the range $u > c$. See *Statistical Analysis of Extreme Values* (Reiss and Thomas, 1997). An example of SMEF is shown in Fig. 3.3(bottom right). In this example, it seems that candidate thresholds are 108 and 98 mm.

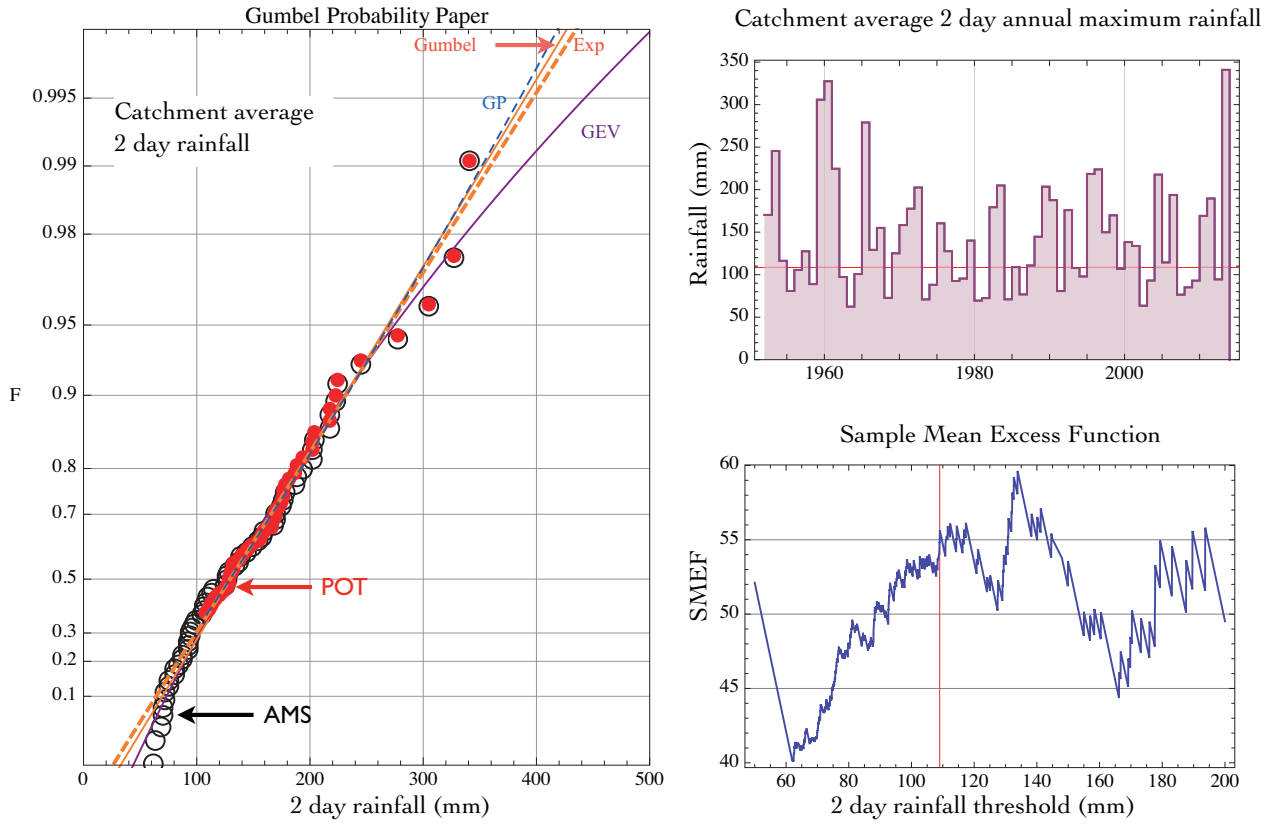


Fig. 3.3 Example of AMS and POT comparison with time series and SMEF

11

SECTION 4

Product Moment and L-Moment

PRODUCT MOMENT

• Mean μ

$$\mu = \int_{-\infty}^{\infty} xf(x) dx$$

• Variance σ^2

$$\sigma^2 = \int_{-\infty}^{\infty} (x - \mu)^2 f(x) dx$$

• Gumbel Distribution's mean μ and variance σ^2

$$\mu = 0.5772 \alpha + \xi$$

$$\sigma^2 = \frac{\pi^2 \alpha^2}{6}$$

Product Moment

When PDF of variable x is denoted as $f(x)$, Mean μ and Variance σ^2 of x are expressed as,

$$\mu = \int_{-\infty}^{\infty} xf(x) dx \quad (4-1)$$

$$\sigma^2 = \int_{-\infty}^{\infty} (x - \mu)^2 f(x) dx \quad (4-2)$$

These values are called Product Moments. $f(x)$ of two parameter distribution includes parameters such as location and scale parameter. GEV is a three parameter distribution and has additional parameter, shape parameter.

In practice, nobody knows the population characteristics such as the parameters of $f(x)$. In order to fit a distribution to given sample, theoretical moments should be same as unbiased sample moments. From this relation, parameters are determined. For example, in Gumbel distribution's case, $f(x)$ is expressed as follows.

$$f(x) = \frac{\exp\left\{-\frac{x-\xi}{\alpha}\right\}}{\alpha} \exp\left[-\exp\left\{-\frac{x-\xi}{\alpha}\right\}\right] \quad (4-3)$$

Then, by substituting Eq.(4-3) into Eq.(4-1) and (4-2) and conducting integration, we can obtain μ and σ^2 for Gumbel distribution as follows.

$$\mu = 0.5772 \alpha + \xi \quad (4-4)$$

$$\sigma^2 = \frac{\pi^2 \alpha^2}{6} \quad (4-5)$$

12

PWM & L-MOMENT

- Basic idea is integration in probability space.

$$E(X) = \int_0^1 x(u) du$$

- Order Statistics

$$X = \{X_{(1)} \geq \dots \geq X_{(n)}\}$$

L-MOMENT

- L-Moment (4-11)

$$\lambda_1 = \beta_0$$

$$\lambda_2 = 2\beta_1 - \beta_0$$

$$\lambda_3 = 6\beta_2 - 6\beta_1 + \beta_0$$

$$\lambda_4 = 20\beta_3 - 30\beta_2 + 12\beta_1 - \beta_0$$

$$\text{L-skewness } \tau_3 = \lambda_3/\lambda_2$$

$$\text{L-kurtosis } \tau_4 = \lambda_4/\lambda_2$$

When we replace product moments μ and σ^2 with sample mean and variance, respectively, we get the simultaneous equations for two parameters, α and ξ .

$$\frac{\sum_{i=1}^n X_i}{n} = 0.5772 \alpha + \xi \quad (4-6)$$

$$\frac{\sum_{i=1}^n (X_i - \bar{X})^2}{n-1} = \frac{\pi^2 \alpha^2}{6} \quad (4-7)$$

For the other distributions, the solutions are shown in Table 18.2.1 of *Handbook of Hydrology* (David Maidment, 1993).

PWM and L-Moment

There may be cases that a sample includes outliers. The product moment method is known to be affected by the outliers excessively since r -th order **product moment** includes x^r . In order to improve this situation, PWM (Probability Weighted Moment) or L-moment method were developed.

The *expectation* of the random variable X is defined as follows.

$$E(X) = \int_{-\infty}^{\infty} x dF(x) = \int_{-\infty}^{\infty} xf(x) dx \quad (4-8)$$

With the transformation of $u = F(x)$, then, $du/dx = f(x)$, we can write as follows.

$$E(X) = \int_0^1 x(u) du \quad (4-9)$$

For higher r -th order moment,

$$b_r = \int_0^1 x(u) u^r du \quad (4-10)$$

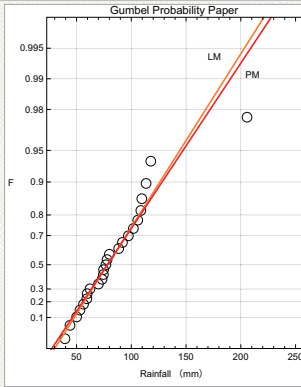


Fig. Outlier and its effect

- Unbiased PWM Estimators (4-12)

$$b_0 = \bar{X}$$

$$b_1 = \sum_{j=1}^{n-1} \frac{(n-j)X_{(j)}}{n(n-1)}$$

$$b_2 = \sum_{j=1}^{n-2} \frac{(n-j)(n-j-1)X_{(j)}}{n(n-1)(n-2)}$$

$$b_3 = \sum_{j=1}^{n-3} \frac{(n-j)(n-j-1)(n-j-2)X_{(j)}}{n(n-1)(n-2)(n-3)}$$

general formula (4-13)

$$b_r = \frac{1}{n} \sum_{j=1}^{n-r} \frac{\binom{n-j}{r} X_{(j)}}{\binom{n-1}{r}}$$

and it includes just first order x . This difference is the advantage of PWM or **L-Moment** against Product Moment. The r -th order L-moments are easily calculated using PWM. The solution of L-moment is shown in Table 18.1.2 in *Handbook of Hydrology*. For more detailed information of L-moments, see *Regional Frequency Analysis* (Hosking and Wallis, 1997)

$$\lambda_1 = \beta_0$$

$$\lambda_2 = 2\beta_1 - \beta_0$$

$$\lambda_3 = 6\beta_2 - 6\beta_1 + \beta_0$$

$$\lambda_4 = 20\beta_3 - 30\beta_2 + 12\beta_1 - \beta_0$$

$$\tau_3 = \lambda_3/\lambda_2, \quad \tau_4 = \lambda_4/\lambda_2$$

(4-11)

The r -th order unbiased PWM estimators are shown in Eq.(4-12).

$$b_0 = \bar{X}$$

$$b_1 = \sum_{j=1}^{n-1} \frac{(n-j)X_{(j)}}{n(n-1)}$$

$$b_2 = \sum_{j=1}^{n-2} \frac{(n-j)(n-j-1)X_{(j)}}{n(n-1)(n-2)} \quad (4-12)$$

$$b_3 = \sum_{j=1}^{n-3} \frac{(n-j)(n-j-1)(n-j-2)X_{(j)}}{n(n-1)(n-2)(n-3)}$$

And Eq.(4-13) is the general formula of Eq.(4-12).

$$b_r = \frac{1}{n} \sum_{j=1}^{n-r} \frac{\binom{n-j}{r} X_{(j)}}{\binom{n-1}{r}} \quad (4-13)$$

Sample estimators λ_i are obtained by replacing β_r by sample estimators b_r from Eq.(4-12).

PARAMETER ESTIMATION BY L-MOMENT FOR AMS

- Gumbel Distribution

$$\lambda_1 = 0.5772 \alpha + \xi$$

$$\lambda_2 = \alpha \ln 2$$

- GEV Distribution

$$c = \frac{2}{3 + \tau_3} - \frac{\ln 2}{\ln 3} = \frac{2\lambda_2}{3\lambda_2 + \lambda_3} - \frac{\ln 2}{\ln 3}$$

$$k \approx 7.859c + 2.9554c^2$$

$$\xi = \lambda_1 - \alpha \left\{ 1 - \Gamma(1+k) \right\} / k$$

$$\alpha = \frac{\lambda_2 k}{(1 - 2^{-k}) \Gamma(1+k)}$$

- Quantile Estimator

- Gumbel Distribution

$$x = \xi - \alpha \ln(-\ln F)$$

- GEV Distribution

$$x = \xi + \frac{\alpha}{k} \left\{ 1 - (-\ln F)^k \right\} \quad (k \neq 0)$$

Parameter Estimation by L-Moment for AMS

For **Gumbel** distribution, the parameters can be given by the combination of L-moment as shown below.

$$\begin{cases} \lambda_1 = 0.5772 \alpha + \xi \\ \lambda_2 = \alpha \ln 2 \end{cases} \quad (4-14)$$

The quantile x of Gumbel distribution is obtained by following equation,

$$x = \xi - \alpha \ln(-\ln F) \quad (4-15)$$

where F is non-exceedance probability.

For GEV distribution, the relationship between three parameters and L-moment estimators is expressed as below.

$$\begin{cases} \lambda_1 = \xi + \alpha \left\{ 1 - \Gamma(1+k) \right\} / k \\ \lambda_2 = \alpha (1 - 2^{-k}) \Gamma(1+k) / k \\ \tau_3 = 2(1 - 3^{-k}) / (1 - 2^{-k}) - 3 \end{cases} \quad (4-16)$$

The relationship between τ_3 and k is not easy to solve but is in simple decreasing function as Fig. 4.1. By defining c with τ_3 as Eq.(4-17), we can get the approximation of shape parameter k .

$$c = \frac{2}{3 + \tau_3} - \frac{\ln 2}{\ln 3} = \frac{2\lambda_2}{3\lambda_2 + \lambda_3} - \frac{\ln 2}{\ln 3}, \quad k \approx 7.859c + 2.9554c^2 \quad (4-17)$$

After obtaining k , we can easily get scale and location parameters α and ξ by Eq.(4-16).

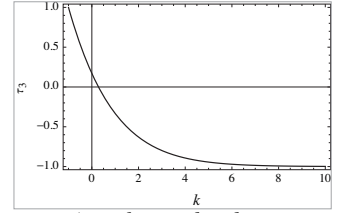


Fig. 4.1 relationship between k and τ_3

PARAMETER ESTIMATION BY L-MOMENT FOR POT(1)

- Exponential Distribution

$$\lambda_1 = \xi + \alpha, \quad \lambda_2 = \frac{1}{2}\alpha$$

- GP Distribution

when ξ is known

$$k = \frac{(\lambda_1 - \xi)}{\lambda_2} - 2$$

$$\alpha = (1+k)(\lambda_1 - \xi)$$

when ξ is unknown

$$k = \frac{1 - 3\tau_3}{1 + \tau_3}$$

$$\alpha = (1+k)(2+k)\lambda_2$$

$$\xi = \lambda_1 - (2+k)\lambda_2$$

$$\alpha = \frac{\lambda_2 k}{(1 - 2^{-k}) \Gamma(1+k)}, \quad \xi = \lambda_1 - \alpha \left\{ 1 - \Gamma(1+k) \right\} / k \quad (4-18)$$

Note that Eq.18.2.22c in Handbook of Hydrology is not correct and above Eq.(4-18) is correct.

The quantile x of GEV distribution is obtained by following equation,

$$x = \xi + \frac{\alpha}{k} \left\{ 1 - (-\ln F)^k \right\} \quad (k \neq 0) \quad (4-19)$$

where F is non-exceedance probability.

[Note]:approximation of gamma function

$$\Gamma(w+1) = w\Gamma(w)$$

$$\Gamma(1+\delta) = 1 + \sum_{i=1}^5 a_i \delta^i + \epsilon$$

where $a_1 = -0.5748646$
 $a_2 = 0.9512363$
 $a_3 = -0.6998588$
 $a_4 = 0.4245549$
 $a_5 = -0.1010678$

Parameter Estimation by L-Moment for POT

In the process of POT, we must realize that $G(x)$ is different from $F(x)$. After parameter estimation of $G(x)$, in order to know annual exceedance probability, it is necessary to transform $G(x)$ to $F(x)$ by Eq.(3-6) with arrival rate λ which is equal to number of events per observation period. Exponential distribution and Generalized Pareto(GP) distribution are generally used for $G(x)$, and parameter estimation by L-Moment is as follows. For **Exponential** distribution,

$$\lambda_1 = \xi + \alpha \quad (4-20)$$

$$\lambda_2 = \frac{1}{2}\alpha \quad (4-21)$$

and for **GP** distribution, we need following three equations,

PARAMETER ESTIMATION BY L-MOMENT FOR POT(2)

- Quantile Estimator
- GP Distribution

$$x = \xi + \alpha \left\{ 1 - (1 - G)^k \right\} / k$$

- Exponential Distribution

$$x = \xi - \alpha \ln(1 - G)$$

- POT to AMS transformation

$$F(x) = \exp \left\{ -\lambda (1 - G(x)) \right\}$$

- AMS to POT transformation

$$G(x) = 1 + \frac{\ln F(x)}{\lambda}$$

$$\lambda_1 = \xi + \alpha / (1 + k) \quad (4-22)$$

$$\lambda_2 = \frac{\alpha}{(1 + k)(2 + k)} \quad (4-23)$$

$$\tau_3 = \frac{1 - k}{3 + k} \quad (4-24)$$

The solution of L-Moment for k is, when ξ is known,

$$k = \frac{(\lambda_1 - \xi)}{\lambda_2} - 2, \quad \alpha = (1 + k)(\lambda_1 - \xi) \quad (4-25)$$

when ξ is unknown,

$$k = \frac{1 - 3\tau_3}{1 + \tau_3}, \quad \alpha = (1 + k)(2 + k)\lambda_2, \quad \xi = \lambda_1 - (2 + k)\lambda_2 \quad (4-26)$$

Quantile estimator for GP and Exponential distribution are as Eq.(4-17) and (4-18), respectively;

GP

$$x = \xi + \alpha \left\{ 1 - (1 - G)^k \right\} / k \quad (4-27)$$

Exponential Distribution

$$x = \xi - \alpha \ln(1 - G) \quad (4-28)$$

In order to obtain return level, it is necessary to get G corresponding F using inverse form of Eq. (3-6).

$$G = 1 + \frac{\ln F}{\lambda} \quad (4-29)$$

SECTION 5

How to use a probability paper

PROBABILITY PAPER & PLOTTING POSITION

- AMS :Gumbel probability paper

$$y_i = -\ln \left[-\ln(1 - q_i) \right]$$

- Plotting Position (exceedance probability)

$$q_i = \frac{i - \alpha}{n + 1 - 2\alpha}$$

where n : sample size, i : order of the order statistics, α : plotting-position parameter

- Cunnane Plot : $\alpha=0.40$
- Weibull Plot : $\alpha=0$
- Gringorten Plot : $\alpha=0.44$
- Hazen Plot : $\alpha=0.50$

In practice, there used to be a probability paper. Normal Probability Paper and Log-Normal Probability Paper are popular. Concerning to annual extreme value, i.e. AMS, **Gumbel probability paper** is recommendable. On Gumbel probability paper, the data of exceedance probability q_i is plotted at y_i in probability axis. And also Gumbel distribution function $F(x)$ is expressed in a straight line.

$$y_i = -\ln \left[-\ln(1 - q_i) \right] \quad (5-1)$$

In Japan, generally, probability paper has variable on horizontal axis and cumulative probability

Table 5.1 Plotting Positions

Name	Formula	α	T_1	Motivation
Weibull	$i/(n+1)$	0	$n+1$	Unbiased exceedance probabilities for all distributions
Median	$(i-0.3175)/(n+0.365)$	0.3175	$1.47n+0.5$	Median exceedance probabilities for all distributions
APL	$(i-0.35)/n$	~ 0.35	$1.54n$	Used with PWMs
Blom	$(i-3/8)/(n+1/4)$	0.375	$1.60n+0.4$	Unbiased normal quantiles
Cunnane	$(i-0.40)/(n+0.2)$	0.40	$1.67n+0.3$	Approximately quantile-unbiased
Gringorten	$(i-0.44)/(n+0.12)$	0.44	$1.79n+0.2$	Optimized for Gumbel Distribution
Hazen	$(i-0.5)/n$	0.5	$2n$	A traditional choice

T_1 is the return period each plotting position assigns to the largest observation in a sample of size n .

on vertical axis(Fig. 5.1). In U.S., probability lies on horizontal axis.

When you plot a sample on a probability paper, you have to know the exceedance or non-exceedance probability for each data of the sample. Plotting position shows them. Several plotting position formulas(Table 5.1) have been proposed to show exceedance probability q_i and they are expressed in an equation with different α .

$$q_i = \frac{i - a}{n + 1 - 2a} \quad (5-2)$$

You have to decide which plotting position you use. **Cunnane plotting position** is recommended for wide range of distribution. After plotting your sample data, you can overlay fitted probability distribution function on it. If you do so, you can easily find any return level corresponding return period and vice versa. And you can also check the goodness of fit and reason of less performance(Fig. 5.1).

Table 5.2 shows plotting positions for sample size 30 with Cunnane plot($\alpha:0.40$). Figure 5.2 shows example plots of sample size 30 using Cunnane plot. It is seen the maximum data is plotted about return period 50 years. Generally, a sample including outliers is fitted by GEV with negative shape parameter k in case of the definition as Eq.(3-1).

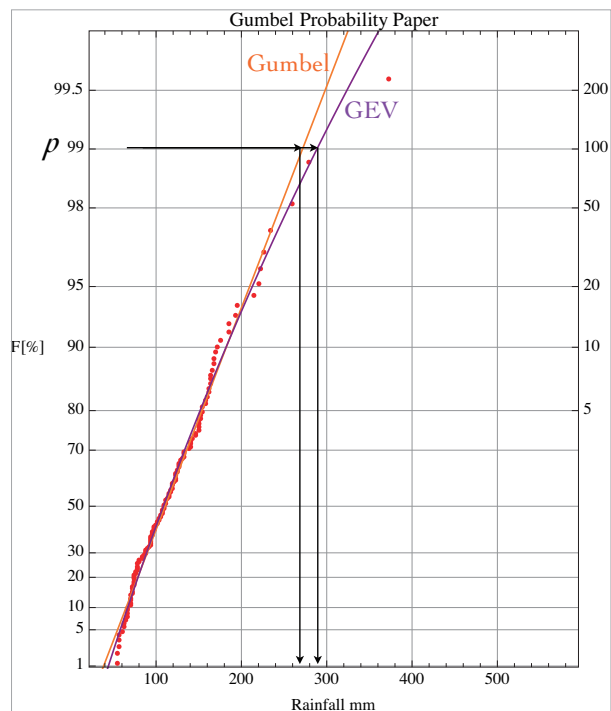


Fig. 5.1 Probability Paper in Japan

19

Table 5.2 Plotting Positions
for sample size 30
(Cunnane plot)

order	q	F
1	0.02	0.98
2	0.053	0.947
3	0.086	0.914
4	0.119	0.881
5	0.152	0.848
6	0.185	0.815
7	0.219	0.781
8	0.252	0.748
9	0.285	0.715
10	0.318	0.682
11	0.351	0.649
12	0.384	0.616
13	0.417	0.583
14	0.45	0.55
15	0.483	0.517
16	0.517	0.483
17	0.55	0.45
18	0.583	0.417
19	0.616	0.384
20	0.649	0.351
21	0.682	0.318
22	0.715	0.285
23	0.748	0.252
24	0.781	0.219
25	0.815	0.185
26	0.848	0.152
27	0.881	0.119
28	0.914	0.086
29	0.947	0.053
30	0.98	0.02

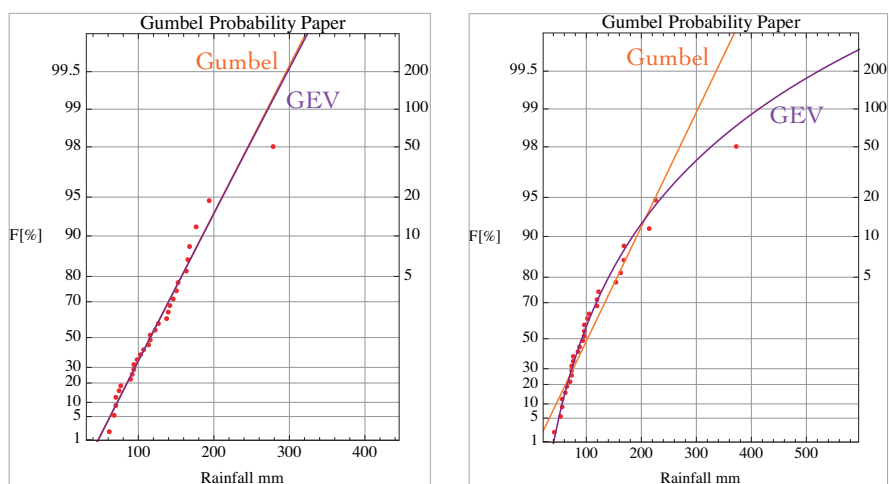


Fig. 5.2 Examples of Probability Plot and Gumbel/GEV fitting
on Gumbel Probability Paper

20

SECTION 6

Frequency Analysis Procedure of a Time Series

TIPS FOR FREQ. ANAL.

- Examine extremes in both AMS and POT
- While similar results are expected, different results come out in general.
- Let's have an experience
- Probability paper is useful for checking the goodness of fit of distributions
- Do not directly compare AMS and POT, use Eq.(3-6)
- The maximum of AMS and that of POT from a time series should show almost identical exceedance probabilities.
- GEV is apt to have long tail than GP in hydrological frequency analysis.

The followings are general procedure of frequency analysis for a time series.

- 1) Checking trend
- 2) Pick up extremes AMS and POT
- 3) assess with AMS
 - 1) probability plot on a Gumbel probability paper using plotting position
 - 2) estimate parameters of distributions
 - 3) plot the distributions onto 1)
 - 4) estimate quantile
- 4) assess with POT
 - 1) probability plot on a Gumbel probability paper
 - 2) plot sample mean excess function and determine the suitable threshold
 - 3) re-select POT more than the threshold
 - 4) estimate parameters of distributions, if necessary, probability plot
 - 5) plot the distributions onto 4-1)
 - 6) estimate quantile
- 5) compare results of AMS with that of POT
- 6) judge

SECTION 6

Exercise

EXERCISE (AMS)

- Draw Histogram
- Draw Probability Plot
 - Obtain Plotting Position q_i
- Fit Gumbel and GEV to the sample
 - Obtain L-moments estimator
 - Obtain Gumbel & GEV distribution parameters
 - Draw both lines onto the Probability Plot
- Obtain 1/30, 1/50 and 1/100 Quantiles by Gumbel and GEV, respectively
- Obtain return periods for the record maximum, 1.1 and 2.0 times of it.

	Group1	Group2	Group3	Group4	Group5	Group6
1	56.3	56.9	62.3	55.3	43.	54.
2	56.9	62.3	67.	60.	54.	56.
3	64.5	66.3	69.9	61.9	55.3	65.5
4	66.3	69.9	70.5	70.1	56.	66.
5	72.2	73.2	74.8	70.6	61.9	70.
6	73.2	74.	77.6	71.5	65.5	73.
7	74.	74.1	88.8	74.8	70.1	74.5
8	76.2	80.5	92.9	77.2	73.	93.5
9	77.8	88.8	93.6	77.6	73.	94.
10	78.9	89.2	94.2	83.9	74.5	96.
11	79.9	96.	97.9	92.2	75.5	97.5
12	80.5	97.9	101.7	93.6	77.2	98.5
13	84.5	106.8	107.6	103.5	83.9	104.5
14	86.4	107.6	113.8	106.2	87.5	107.5
15	99.8	110.1	115.7	116.1	93.	115.
16	106.8	111.7	116.1	118.	96.	119.
17	109.	113.8	122.2	118.5	96.5	122.5
18	109.7	115.7	126.2	119.	97.5	123.5
19	110.1	126.1	138.2	126.2	103.	130.5
20	116.7	129.2	139.7	139.7	104.5	141.
21	123.8	133.5	141.5	141.	118.	151.
22	125.6	138.2	147.	147.	119.	167.5
23	126.1	141.5	150.4	151.3	122.5	185.
24	132.8	146.6	152.8	152.8	154.5	186.
25	133.	158.7	163.6	154.5	161.2	195.
26	149.5	159.4	164.7	157.5	167.5	215.
27	150.9	164.8	168.5	161.2	169.5	220.5
28	159.4	165.9	175.9	164.7	215.	222.5
29	162.	171.5	193.7	278.3	225.5	234.5
30	164.8	193.7	278.3	371.9	371.9	259.5

L-moments estimators

	Group1	Group2	Group3	Group4	Group5	Group6
λ_1	103.587	114.13	123.57	123.87	112.183	131.283
λ_2	19.1547	21.6617	25.3174	32.0489	32.8746	33.573
λ_3	2.31475	1.66655	4.3902	9.74123	12.9197	6.14245
λ_4	0.153344	0.723629	3.436	7.59988	8.65103	1.68383
λ_2 / λ_1	0.184915	0.189799	0.204883	0.25873	0.293044	0.255729
λ_3 / λ_2	0.120845	0.0769353	0.173407	0.303949	0.393001	0.182958
λ_4 / λ_2	0.00800556	0.0334059	0.135717	0.237134	0.263153	0.0501542

Gumbel distribution

	Group1	Group2	Group3	Group4	Group5	Group6
parameters: α	27.6344	31.2513	36.5252	46.2367	47.428	48.4356
ξ	87.6361	96.0918	102.488	97.1822	84.8079	103.326

	Group1	Group2	Group3	Group4	Group5	Group6
quantiles: 1/30	181	202	226	254	245	267
1/50	195	218	245	278	270	292
1/100	215	240	271	310	303	326

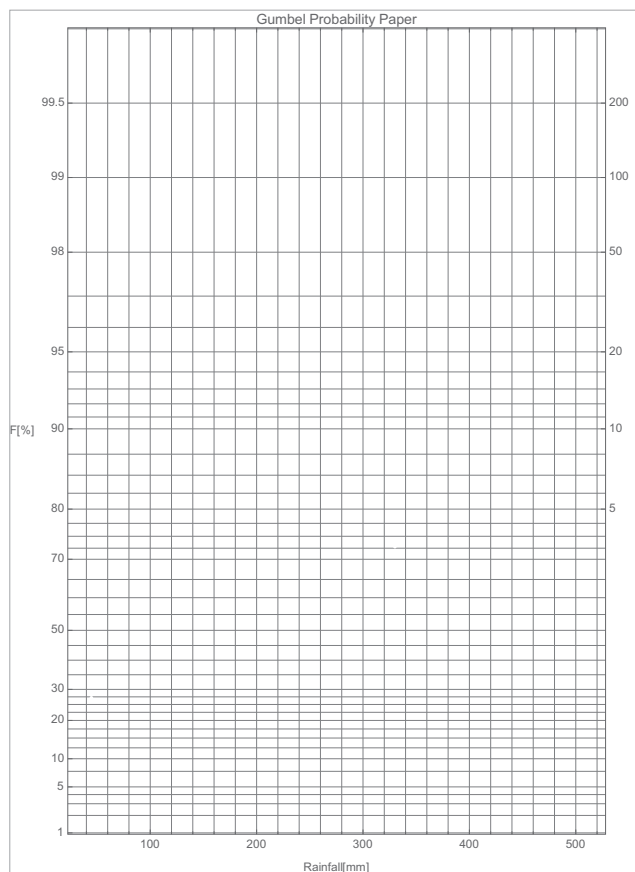
GEV distribution

	Group1	Group2	Group3	Group4	Group5	Group6
parameters: α	29.559	35.2881	36.3413	37.0641	31.7826	47.5198
κ	0.078271	0.150927	-0.00543864	-0.199204	-0.320914	-0.0202833
ξ	88.6616	98.4029	102.397	93.4794	79.2591	102.883

	Group1	Group2	Group3	Group4	Group5	Group6
quantiles: 1/30	177	192	227	273	274	269
1/50	188	202	246	312	327	296
1/100	203	215	272	373	414	332

REFERENCES

- Hosking, J.R.M. and J.R. Wallis : *Regional Frequency Analysis –An Approach Based on L-Moments–*, Cambridge Univ. Press., p.207, 1997.
- Reiss, R.-D. and M. Thomas: *Statistical Analysis of Extreme Values*, Birkhäuser, p.316, 1997.
- Stedinger, J.R., R.M. Vogel, and E. Foufoula-Georgiou: *Frequency Analysis of Extreme Events*, Chap. 18, *Handbook of Hydrology*, (Ed.) D. R. Maidment, McGraw-Hill, New York, pp.18.1-18.66, 1993.



Lecture 3: Fundamentals in rainfall-runoff-inundation modelling

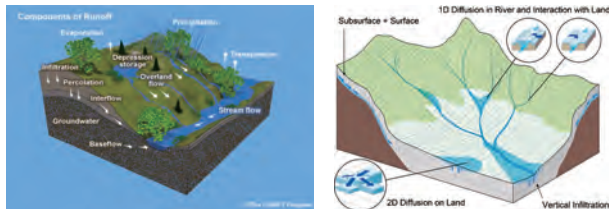
Takahiro SAYAMA (*Associate Professor, Disaster Prevention Research Institute, Kyoto University*)

Abstract:

Flood hazard modelling is an essential process for flood predictions and risk assessment. The goal of this lecture is to provide fundamental knowledge on the flood modeling. The lecture starts with why real-time flood forecasting requires such modeling technique in some situations, followed by the explanation of Japanese flood warning system. Four kinds of models related to flood forecasting will be introduced; namely numerical weather prediction models, rainfall-runoff models, river routing models and flood inundation models. This lecture particularly focuses on rainfall-runoff models and their background concepts in represented hydrologic processes by the model. Among various modeling steps in hydrology, the importance of “perceptual modeling” will be highlighted for adequate representations of the natural processes by models. In addition, we discuss the difference between lumped and distributed rainfall-runoff models as well as their pros and cons of them.

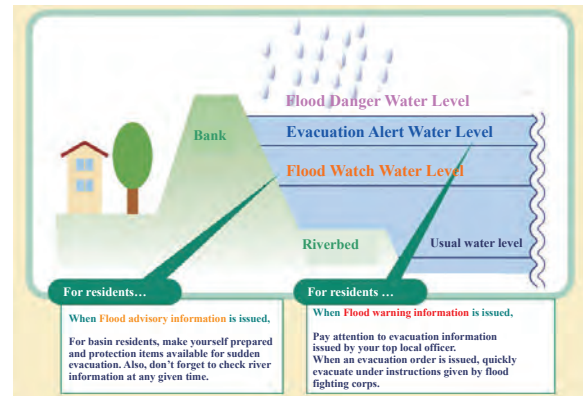
Based upon the above understandings, this lecture will further introduce the concept of the Rainfall-Runoff-Inundation (RRI) model. The model is a two-dimensional model capable of simulating rainfall-runoff and flood inundation simultaneously. The trainees will learn in what circumstances; typical distributed rainfall-runoff models may fail in simulating actual flooding situations and how the RRI model may overcome the issue. By showing some recent applications including the one in Northern Kyushu flooding in July 2017, the lecture will provide basic knowledge on the application of the RRI model also.

Fundamentals in Rainfall-Runoff-Inundation Modelling

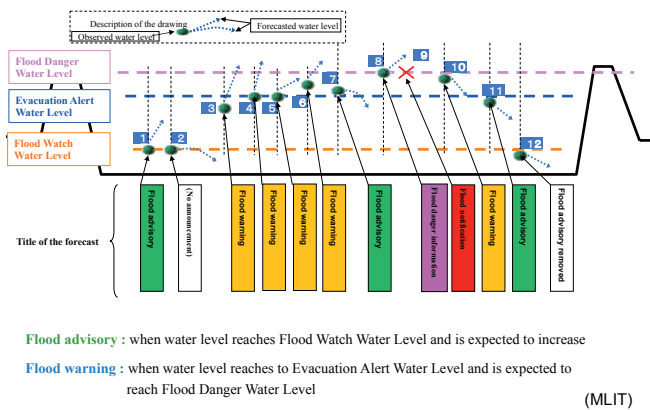


Disaster Prevention Research Institute, Kyoto University
Takahiro Sayama

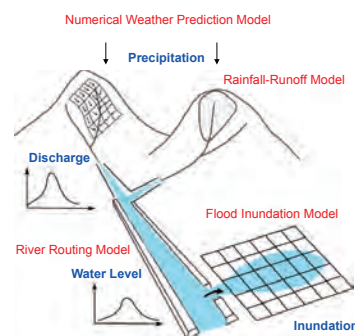
Water Level Criteria for Flood Warning (Japan)



Water Level Criteria for Flood Warning (Japan)



Flood Forecasting



- **Numerical Weather Prediction Model:** Quantitative Precipitation Forecasting (QPF).
- **Rainfall-Runoff Model:** simulating streamflow discharge with rainfall input.
- **River Routing Model:** tracking flood wave movement along a open channel with upstream hydrograph.
- **Flood Inundation Model:** simulating flooded water spreading on floodplains with inflow discharge.

MIKE

Danish Hydraulic Institute (DHI)
<http://mikebydhi.com/>

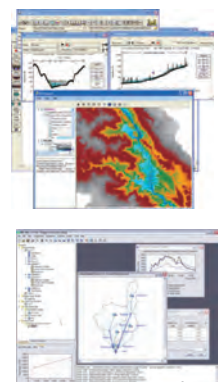
- **MIKE11**
 - One-dimensional river routing model
 - **NAM**: A lumped, conceptual rainfall-runoff model simulating overland flow, interflow and baseflow as a function of the water storage in each of four mutually interrelated storages representing the storage capacity of the catchment.
 - **SHE**: Complex fully distributed process-based oriented modeling
- **MIKE21**
 - Flows, waves, sediments and ecology in rivers, lakes, estuaries, bays, coastal areas and seas in **two dimensions**



HEC

US Army Corps of Engineers
Hydrologic Engineering Centers (HEC)
<http://www.hec.usace.army.mil/>

- **HEC-RAS (River Analysis System)**
 - (1) steady flow water surface profile computations
 - (2) unsteady flow simulation
 - (3) movable boundary sediment transport
 - (4) water quality analysis
- **HEC-HMS (Hydrologic Modeling System)**
 - Elements: subbasin, reach, junction, reservoir, diversion, source, and sink
 - SCS curve number, Green Ampt
 - linear quasi-distributed unit hydrograph method
 - kinematic wave or Muskingum-Cunge
 - Priestley-Taylor method (PET)
 - Snow melt



Steps in the Modeling Process

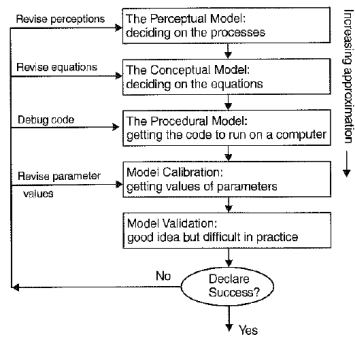
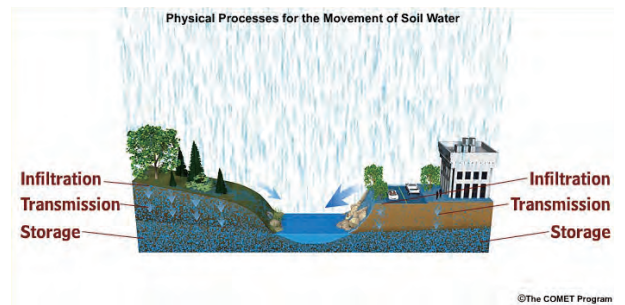


Figure 1.2 A schematic outline of the different steps in the modelling process

"Rainfall-Runoff Modelling, The Primer", by Keith Beven

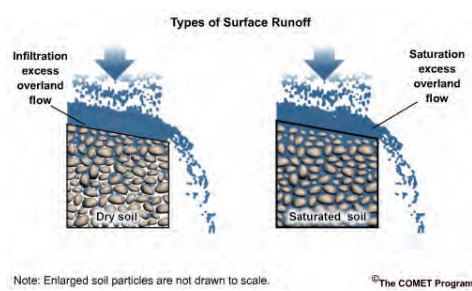
7

Importance of Perceptual Modeling



8

Surface Runoff Generation



9



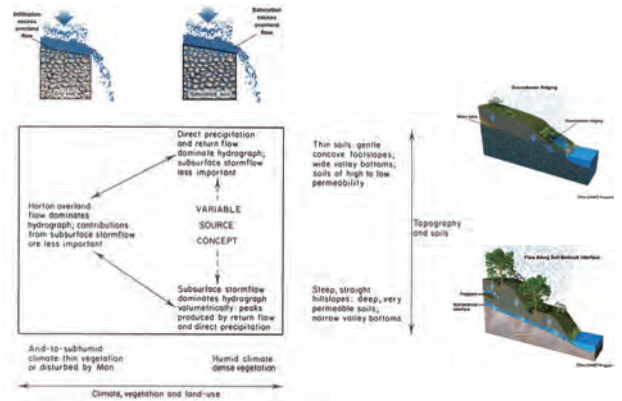
10



11



Runoff Generation Mechanisms



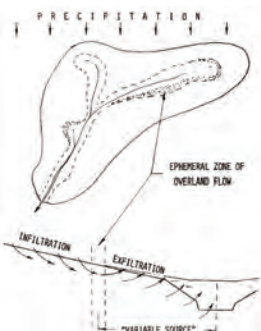
Blochl et al., Runoff Prediction in Ungauged Basins, Cambridge Press

Variable Source Area (VSA) Concept



Petra Fackel, ETH Zurich

Courtesy J.J. McDonnell



Hewlett and Hilbert (1967)
Hewlett and Troendle (1975)

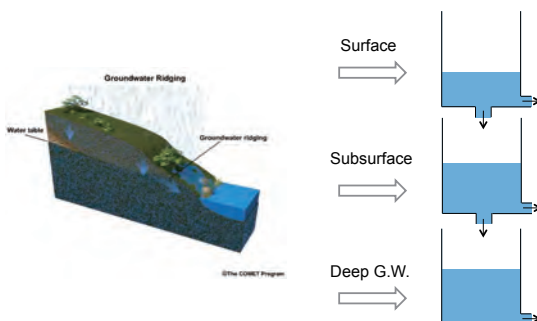
15



Chris Graham PhD thesis

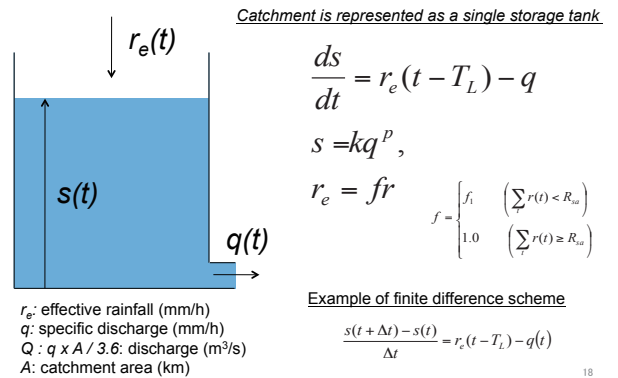
16

Tank Model



17

Storage Function Model



18

Kinematic Wave Rainfall-Runoff Model

Continuous Equation

$$\frac{\partial h}{\partial t} + \frac{\partial q}{\partial x} = r$$

Kinematic wave model

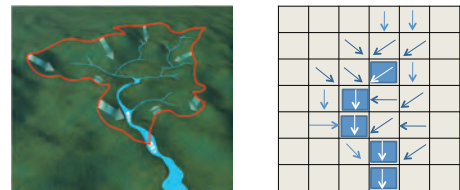
$$q = \frac{\sqrt{i}}{n} h^{5/3}$$

q : discharge
 h : water depth
 r : rainfall
 i : slope
 n : Manning's roughness



KINEROS
14

Grid-cell based Kinematic Wave Rainfall-Runoff Model



20

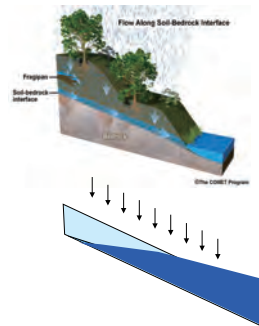
Kinematic Wave Rainfall-Runoff Model for subsurface and surface flow

Continuous Equation

$$\frac{\partial h}{\partial t} + \frac{\partial q}{\partial x} = r$$

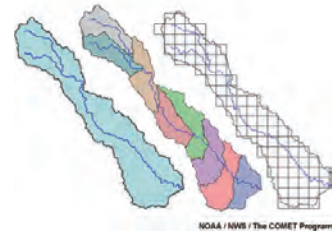
Kinematic wave model for saturated subsurface and surface flow

$$q = \begin{cases} kih & (h < d) \\ \frac{\sqrt{i}}{n} (h-d)^{5/3} + kih & (h > d) \end{cases}$$



21

Lumped Model vs. Distributed Model

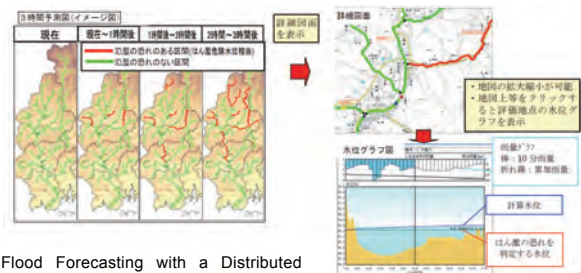


What are the limitation of lumped models?

- cannot reflect the spatial distributions of
- rainfall, topography, state variables
- cannot obtain stream flow at various points in a basin

22

Distributed Flood Forecasting System

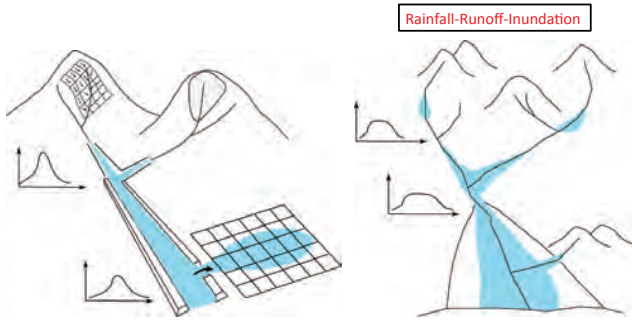


Flood Forecasting with a Distributed Model using Quantitative Precipitation Forecasting: 3 hours read-time, every 10 minutes, at every a few kilometer

(Hyogo Prefecture)

23

Introduction to Rainfall-Runoff-Inundation (RRI) Model

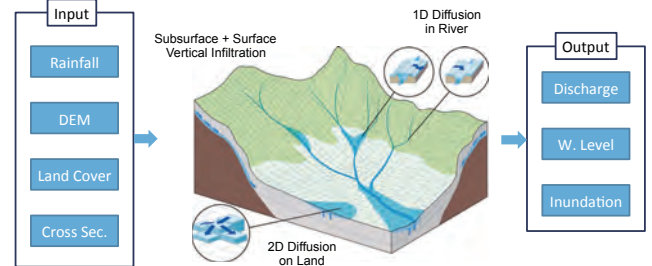


Motivations of using Rainfall-Runoff-Inundation Model

1. Rainfall-runoff and inundation cannot be separated with large inundation
2. Kinematic wave is not suitable for flat topography
3. Important for representing inundation process for better river predictions
4. Inundation itself may be of interest in **lood forecasting** or **risk assessment**

25

Rainfall-Runoff-Inundation Model



- Two-dimensional model capable of simulating **rainfall-runoff and flood inundation simultaneously**
- The model deals with slopes and river channels separately
- At a grid cell in which a river channel is located, the model assumes that both slope and river are positioned within the same grid cell

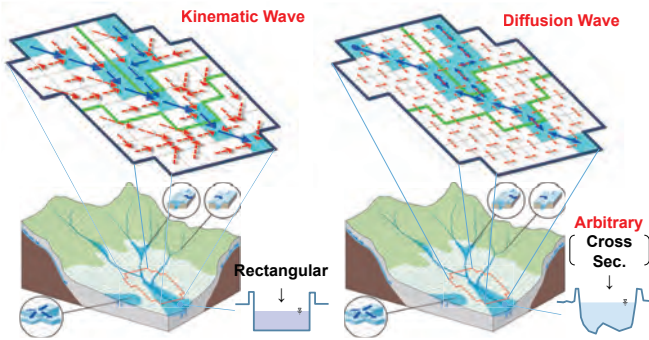
Sayama, T. et al.: Rainfall-Runoff-Inundation Analysis of Pakistan Flood 2010 at the Kabul River Basin, *Hydrological Sciences Journal*, 57(2), pp. 298-312, 2012.

20

Kinematic wave RR model vs RRI model

[Distributed RR Model]

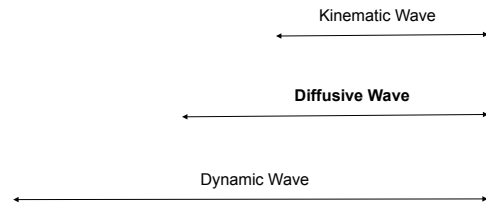
[RRI Model]



Courtesy by Nakamura at ICHARM and MCC

One-dimensional Saint-Venant Equation

$$\frac{\partial q}{\partial t} + \frac{\partial uq}{\partial x} + gh \frac{\partial h}{\partial x} - ghi_0 + \frac{gn^2 q^2}{h^{7/3}} = 0$$



28

Basic Equations

Shallow water equations for typical 2D inundation

Mass balance equation

$$\frac{\partial h}{\partial t} + \frac{\partial q_x}{\partial x} + \frac{\partial q_y}{\partial y} = r$$

Momentum equations

$$\frac{\partial q_x}{\partial t} + \frac{\partial uq_x}{\partial x} + \frac{\partial vq_x}{\partial y} = -gh \frac{\partial H}{\partial x} - \frac{\tau_x}{\rho_w}$$

$$\frac{\partial q_y}{\partial t} + \frac{\partial uq_y}{\partial x} + \frac{\partial vq_y}{\partial y} = -gh \frac{\partial H}{\partial y} - \frac{\tau_y}{\rho_w}$$

Cell storage based model with diffusion wave approx. (e.g. Hunter et al. 2007.)

Mass balance equation

$$\frac{dh^{i,j}}{dt} = \frac{q_x^{i-1,j} - q_x^{i,j}}{\Delta x} + \frac{q_y^{i,j-1} - q_y^{i,j}}{\Delta y} + r^{i,j}$$

Momentum equations

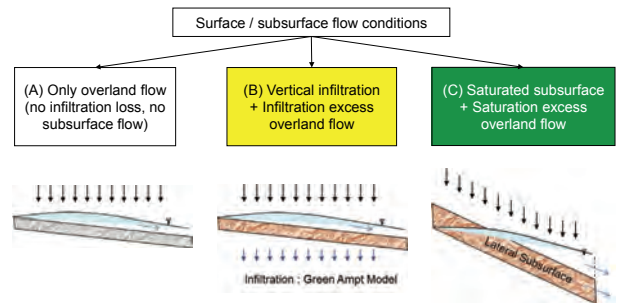
$$q_x = -\frac{1}{n} h^{5/3} \sqrt{\left| \frac{\partial H}{\partial x} \right|} \text{sgn} \left[\frac{\partial H}{\partial x} \right]$$

$$q_y = -\frac{1}{n} h^{5/3} \sqrt{\left| \frac{\partial H}{\partial y} \right|} \text{sgn} \left[\frac{\partial H}{\partial y} \right]$$

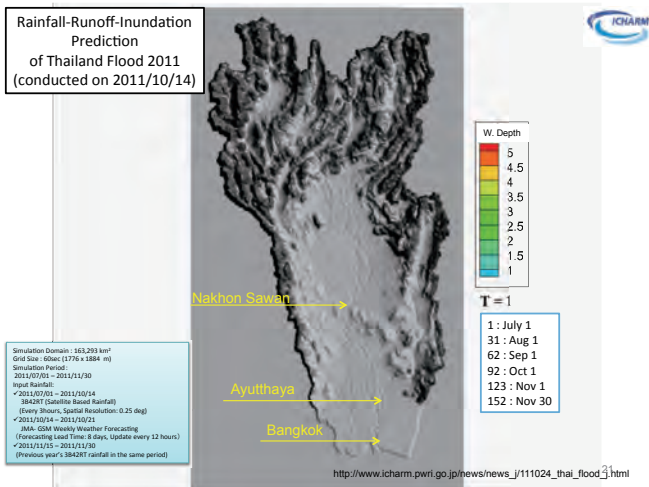
$r^{i,j}$: Rainfall, $h^{i,j}$: Water depth, $q_{x,y}^{i,j}$: Discharge between grid-cells

23

Three Conditions of Surface / Subsurface Flow



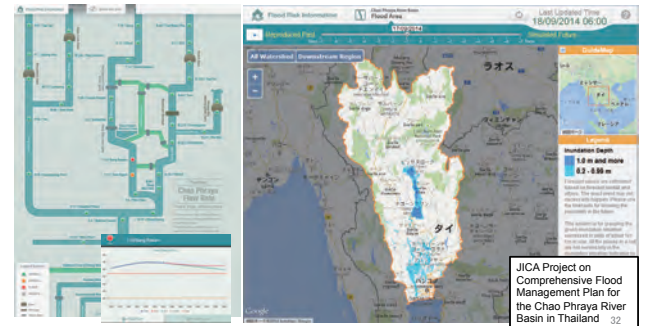
30



Example of RRI Model Application (1)

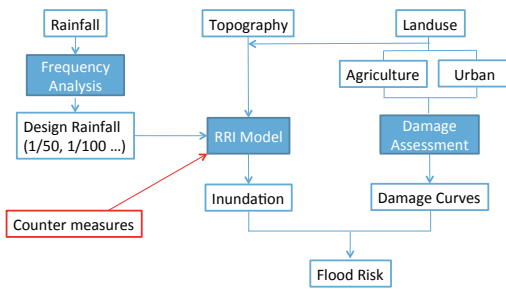
Real-time flood runoff and inundation forecasting system for the Chao Phraya River Basin based on RRI Model (developed by JICA/FRICS and operated under RID, Thailand)

http://floodinfo.rid.go.th/index_en.html



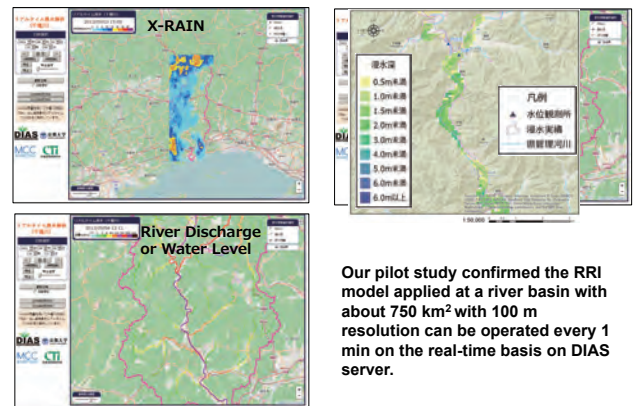
Example of RRI Model Application (2)

1. Flood Risk Assessment with RRI

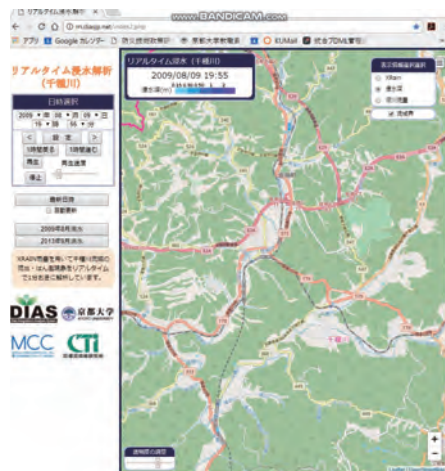


32

Example of the RRI Model Application



34



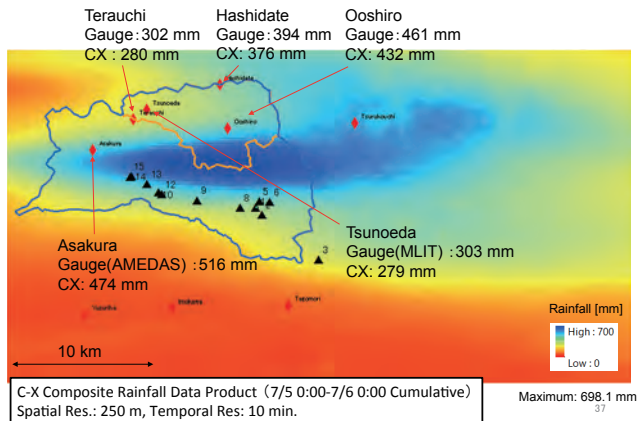
35

Northern-Kyushu Severe Storm Disaster 2017.07

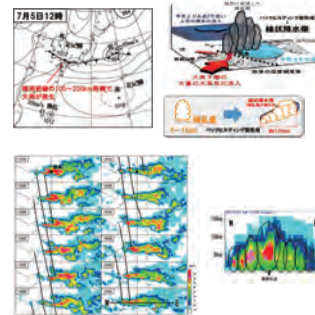


36

One day cumulative rainfall distributions



Meteorological Conditions

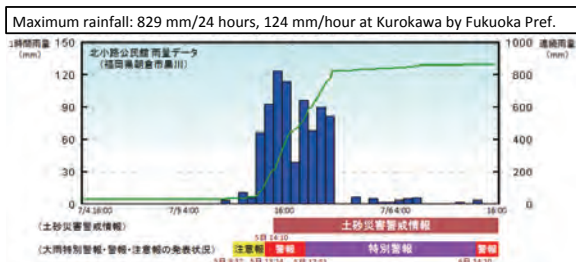


- Due to the Baiu-front, hot and humid air mass was blown into 100-200 km south of the front.
- Upper atmosphere (at the level of 5,500 m), air temperature was about 3 deg colder than average, causing unstable.
- Cumulonimbus clouds were continuously generated and produce back-building type rain band.

Meteorological Research Institute, July 14, 2017.

38

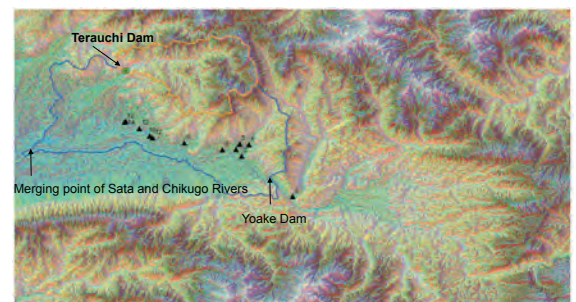
Gauged Rainfall Record



国土交通省九州地方整備局：平成29年7月九州北部豪雨による土砂災害の概要<速報版> Vo. 6より

39

Our Target Area: Tributaries of the Chikugo River

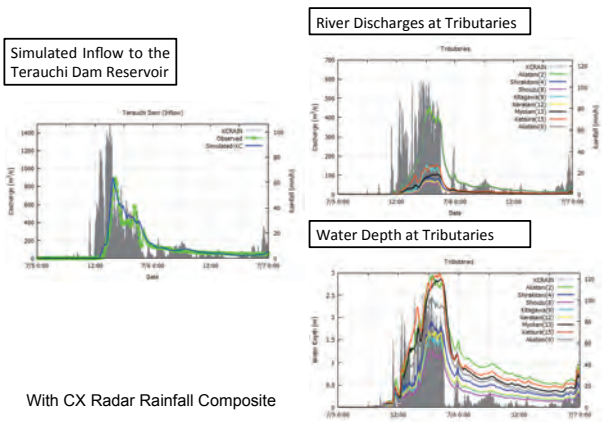


10 km
190.4 km² (incl. Terauchi Dam: 51 km²)
Input Rainfall: CX composite, RRI model (50 m resolution)

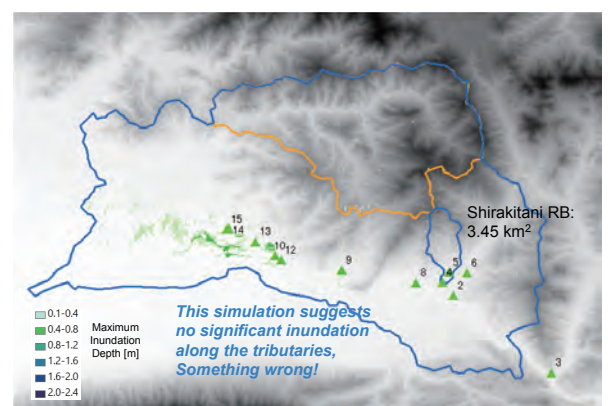
▲ 7/15 GPS observation point
River width, depth and max. inundation level were measured

40

Application to the Kyushu area

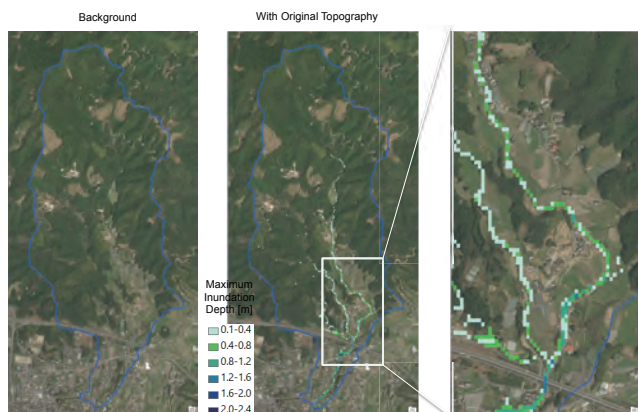


Simulated inundation depths

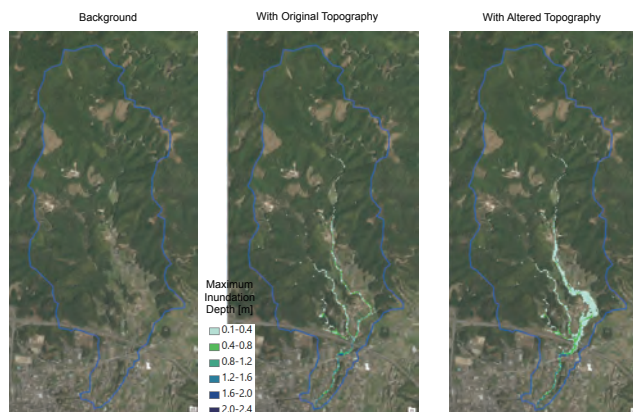


42

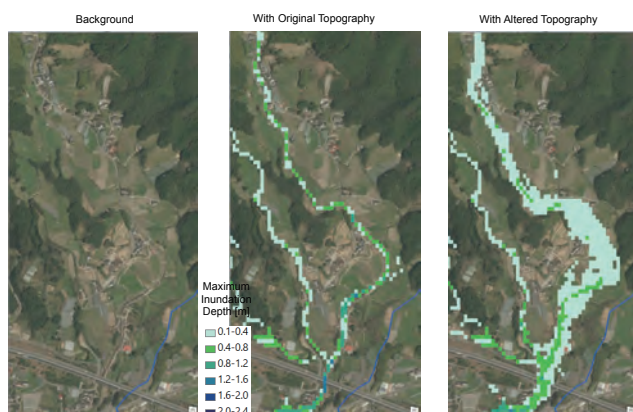
Simulated inundation depths with altered topography



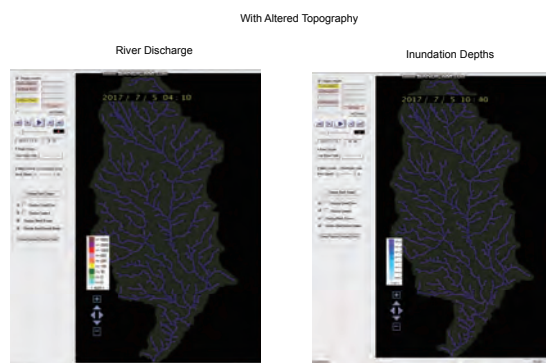
Simulated inundation depths with altered topography



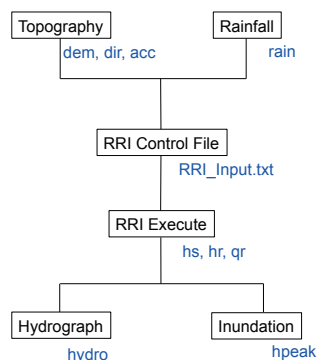
Simulated inundation depths with altered topography



RRI_VIEWER



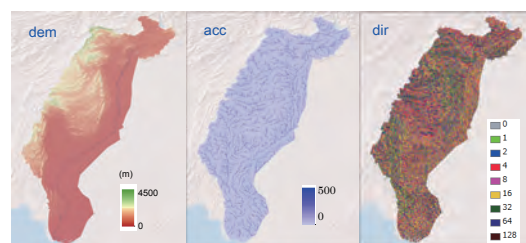
Key Steps in RRI Modeling



25

1. Input Topography

Digital Elevation Model Flow Accumulation Flow Direction

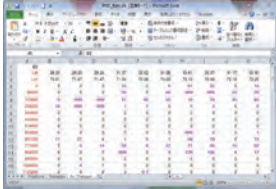


These three datasets can be obtained from HydroSHEDS (SRTM based topography and flow direction dataset)

48

2. Input Rainfall

Rainfall Data
(input)



Thiessen polygon
(output)



Prepare rainfall data with time and location information (e.g. above excel file) and execute rainThiessen.exe program to create rainfall input file

49

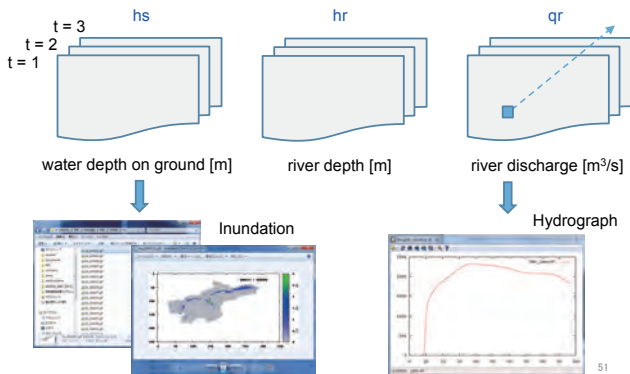
3. RRI Control File (RRI_Input.txt)

```
RRI_Input_Format_Ver1_4_1
/rain.txt
/adem.txt
/acc.txt
/adir.txt
0          # utm(1) or latlon(0)
1          # 4-direction (0), 8-direction(1)
2568      # lasth
600       # dt
60        # dt_riv
104       # outnum
66.0d0    # xllcorner_rain
23.0d0    # yllcorner_rain
0.1 0.1   # cellsize_rain
...
...
(continue)
```

Prepare RRI control file (RRI_Input.txt), which includes parameter settings, and execute 0_rri_1_4_1.exe to run RRI model

50

4. Visualizing Results



51

Key Terms

- **State Variables**
 - A variable in the model that is part of the solution of the model equations and which varies with time during a simulation but which is not a flux or exchange of mass.
- **Boundary conditions**
 - Constraints and values of variables required to run a model for a particular flow domain and time period. May include input variables.
- **Initial conditions**
 - Values of storage or pressure variables to initialize a model at the start of a simulation period.
- **Calibration**
 - The process of adjusting parameter values of a model to obtain a better fit between observed and predicted variables.
- **Validation**
 - A process of evaluation of models to confirm that they are acceptable representations of a system.

From "Rainfall-Runoff-Modelling, The Primer" by Keith Beven 52



Exercise 1 & 4: Rainfall-runoff-inundation modelling

Takahiro SAYAMA (*Associate Professor, Disaster Prevention Research Institute, Kyoto University*)

Abstract:

This is a hand-on exercise of the Rainfall-Runoff-Inundation (RRI) modeling. Based upon the basic understandings of the general concept of distributed rainfall-runoff models and the RRI model, introduced in Lecture 3, this exercise will provide step-by-step model application. The RRI model can be freely downloaded from the webpage of ICHARM, and the package includes Graphical User Interface (GUI) and the original Fortran source codes as well as related tools for supporting the model applications (http://www.icharm.pwri.go.jp/research/rri/rri_top.html). During the seminar, the trainees will learn how to operate the GUI for delineating a catchment, and more importantly you will learn how data from digital elevation model (DEM) is processed to be used in such distributed rainfall-runoff modeling. Furthermore, by introducing the meanings of model equations and their parameters, the trainees will learn the behavior of the model by different settings. The trainees are expected to learn not only the operations of the model but understand the characteristics of flooding at the basin scale during flooding. Hence the exercise provides essential knowledge and techniques for the application of the RRI model and eventually the trainee's will be able to apply the model for any interested catchment in flood predictions and risk assessment.

Rainfall-Runoff-Inundation (RRI) Model

ver. 1.4.2

International Center for Water Hazard and Risk Management (ICHARM)
Public Works Research Institute (PWRI)

^{*)}Disaster Prevention Research Institute (DPRI), Kyoto University

Takahiro SAYAMA^{*)}

Rainfall-Runoff-Inundation Model User's Manual

Table of Contents

1. Outline of Rainfall-Runoff-Inundation (RRI) Model	1-1
1.1 Model Structure Overview	1-1
1.2 Governing Equations of RRI Model	1-2
1.3 One-dimensional River Routing Model	1-5
1.4 River and Slope Water Exchange	1-5
1.5 Numerical Scheme	1-6
2. Getting Started	2-1
2.1 Preparation	2-1
2.2 Run RRI Model	2-2
2.3 Post Analysis	2-3
3. Preparing Input Topography Data	3-1
3.1 Downloading HydroSHEDS Data	3-2
3.2 Delineating HydroSHEDS Data using ArcGIS	3-3
3.3 Delineating HydroSHEDS Data using GLASS GIS (optional)	3-12
3.4 Upscaling the spatial resolutions of DEM, DIR and ACC (optional)	3-23
3.5 DEM Data Adjustment	3-23
4. Preparing Input Rainfall Data	4-1
4.1 Prepare Input Rainfall Data from Gauged Rainfall Records	4-1
4.2 Prepare Input Rainfall Data from GSMaP	4-2
4.3 Prepare Input Rainfall Data from 3B42RT	4-4
4.4 Format of Input Rainfall Data for RRI Model	4-5
4.5 Calculation of Catchment Average Rainfall	4-6
5. Conditions Setting for RRI Simulation	5-1
5.1 Folder Configuration	5-1
5.2 RRI Model Control File (RRI_Input.txt)	5-2
6. Running RRI Model	6-1
7. Visualize Output Data	7-1
7.1 Format of the Output Files	7-1

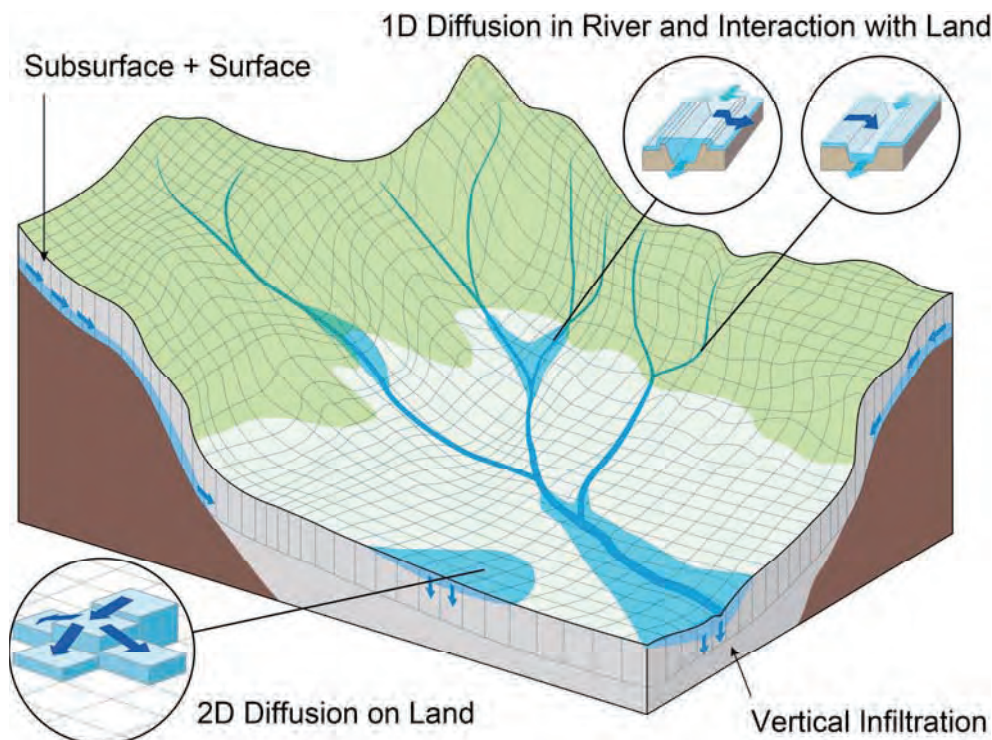
7.2 Visualize Inundation Depth with GNUPLOT	7-1
7.3 Hydrographs at Specific Locations	7-3
7.4 Visualize Peak Inundation Depths.....	7-5
7.5 Visualize Inundation Depths with Google Earth (Optional).....	7-6
7.6 Visualize Results with Tecplot (Optional).....	7-10
 8. Application Example	 8-1
8.1 On Input Topography.....	8-1
8.2 On Input Rainfall	8-2
8.3 On Input Evapotranspiration	8-4
8.4 On River Channel Geometry Setting.....	8-5
8.5 On Embankment Setting	8-7
8.6 On Land Class Setting	8-9
8.7 On Parameter Setting	8-10
8.8 On Boundary Condition.....	8-13
8.9 On Initial Condition.....	8-16
8.10 Diversion option (for advanced users).....	8-16
8.11 Dam option (for advanced users)	8-17
 9. Use of RRI Graphical User Interface (GUI).....	 9-1
9.1 Pre-setting.....	9-1
9.2 Model setup and running with RRI_BUILDER.....	9-2
9.3 Visualizing results with RRI_VIEWER.....	9-11

Last updated on Nov 1, 2015

1. Outline of Rainfall-Runoff-Inundation (RRI) Model

1.1 Model Structure Overview

Rainfall-Runoff-Inundation (RRI) model is a two-dimensional model capable of simulating rainfall-runoff and flood inundation simultaneously (Sayama et al., 2012, Sayama et al., 2015a, Sayama et al., 2015b). The model deals with slopes and river channels separately. At a grid cell in which a river channel is located, the model assumes that both slope and river are positioned within the same grid cell. The channel is discretized as a single line along its centerline of the overlying slope grid cell. The flow on the slope grid cells is calculated with the 2D diffusive wave model, while the channel flow is calculated with the 1D diffusive wave model. For better representations of rainfall-runoff-inundation processes, the RRI model simulates also lateral subsurface flow, vertical infiltration flow and surface flow. The lateral subsurface flow, which is typically more important in mountainous regions, is treated in terms of the discharge-hydraulic gradient relationship, which takes into account both saturated subsurface and surface flows. On the other hand, the vertical infiltration flow is estimated by using the Green-Ampt model. The flow interaction between the river channel and slope is estimated based on different overflowing formulae, depending on water-level and levee-height conditions.



Schematic diagram of Rainfall-Runoff-Inundation (RRI) Model

Model Features

- 1) RRI is a 2D model simulating for rainfall-runoff and flood inundation simultaneously.
- 2) It simulates flows on land and in river and their interactions at a river basin scale.
- 3) It simulates lateral subsurface flow in mountainous areas and infiltration in flat areas.

1.2 Governing Equations of RRI Model

A method to calculate lateral flows on slope grid-cells is characterized as “a storage cell-based inundation model” (e.g. Hunter et al. 2007). The model equations are derived based on the following mass balance equation (1) and momentum equation (2) for gradually varied unsteady flow.

$$\frac{\partial h}{\partial t} + \frac{\partial q_x}{\partial x} + \frac{\partial q_y}{\partial y} = r - f \quad (1)$$

$$\frac{\partial q_x}{\partial t} + \frac{\partial u q_x}{\partial x} + \frac{\partial v q_x}{\partial y} = -gh \frac{\partial H}{\partial x} - \frac{\tau_x}{\rho_w} \quad (2)$$

$$\frac{\partial q_y}{\partial t} + \frac{\partial u q_y}{\partial x} + \frac{\partial v q_y}{\partial y} = -gh \frac{\partial H}{\partial y} - \frac{\tau_y}{\rho_w} \quad (3)$$

where h is the height of water from the local surface, q_x and q_y are the unit width discharges in x and y directions, u and v are the flow velocities in x and y directions, r is the rainfall intensity, f is the infiltration rate, H is the height of water from the datum, ρ_w is the density of water, g is the gravitational acceleration, and τ_x and τ_y are the shear stresses in x and y directions. The second terms of the right side of (2) and (3) are calculated with the Manning’s equation.

$$\frac{\tau_x}{\rho_w} = \frac{gn^2 u \sqrt{u^2 + v^2}}{h^{1/3}} \quad (4)$$

$$\frac{\tau_y}{\rho_w} = \frac{gn^2 v \sqrt{u^2 + v^2}}{h^{1/3}} \quad (5)$$

where n is the Manning’s roughness parameter.

Under the diffusion wave approximation, inertia terms (the left side terms of (2) and (3)) are neglected. Moreover, by separating x and y directions (i.e. ignoring v and u terms in equations (2) and (3) respectively), the following equations are derived:

$$q_x = -\frac{1}{n} h^{5/3} \sqrt{\left| \frac{\partial H}{\partial x} \right|} \operatorname{sgn} \left(\frac{\partial H}{\partial x} \right) \quad (6)$$

$$q_y = -\frac{1}{n} h^{5/3} \sqrt{\left| \frac{\partial H}{\partial y} \right|} \operatorname{sgn} \left(\frac{\partial H}{\partial y} \right) \quad (7)$$

where sgn is the signum function.

The RRI model spatially discretizes mass balance equation (1) as follows:

$$\frac{dh^{i,j}}{dt} + \frac{q_x^{i,j-1} - q_x^{i,j}}{\Delta x} + \frac{q_y^{i-1,j} - q_y^{i,j}}{\Delta y} = r^{i,j} - f^{i,j} \quad (8)$$

where $q_x^{i,j}$, $q_y^{i,j}$ are x and y direction discharges from a grid cell at (i, j) .

By combining the equations of (6), (7) and (8), water depths and discharges are calculated at each grid cell for each time step. One important difference between the RRI model and other inundation models is that the former uses different forms of the discharge-hydraulic gradient relationship, so that it can simulate both surface and subsurface flows with the same algorithm. The RRI model replaces the equations (6) and (7) with the following equations of (9) and (10), which were originally conceptualized by Ishihara and Takasao (1962) and formulated with a single variable by Takasao and Shiiba (1976, 1988) based on kinematic wave approximations. The first equations in (9) and (10) ($h \leq d_a$) describe the saturated subsurface flow based on the Darcy law, while the second equations ($d_a \leq h$) describe the combination of the saturated subsurface flow and the surface flow. Note that for the kinematic wave model, the hydraulic gradient is assumed to be equal to the topographic slope, whereas the RRI model assumes the water surface slope as the hydraulic gradient.

$$q_x = \begin{cases} -k_a h \frac{\partial H}{\partial x}, & (h \leq d_a) \\ -\frac{1}{n} (h - d_a)^{5/3} \sqrt{\left| \frac{\partial H}{\partial x} \right|} \operatorname{sgn} \left(\frac{\partial H}{\partial x} \right) - k_a h \frac{\partial H}{\partial x}, & (d_a < h) \end{cases} \quad (9)$$

$$q_y = \begin{cases} -k_a h \frac{\partial H}{\partial y}, & (h \leq d_a) \\ -\frac{1}{n} (h - d_a)^{5/3} \sqrt{\left| \frac{\partial H}{\partial y} \right|} \operatorname{sgn} \left(\frac{\partial H}{\partial y} \right) - k_a h \frac{\partial H}{\partial y}, & (d_a < h) \end{cases} \quad (10)$$

where k_a is the lateral saturated hydraulic conductivity and d_a is the soil depth times the effective porosity.

Equations (11) and (12) can be also used to simulate the effect of unsaturated, saturated subsurface flow and surface flow with the single variable of h (Tachikawa et al. 2004, Sayama and McDonnell 2009 for English).

$$q_x = \begin{cases} -k_m d_m \left(\frac{h}{d_m} \right)^\beta \frac{\partial H}{\partial x}, & (h \leq d_m) \\ -k_a (h - d_m) \frac{\partial H}{\partial x} - k_m d_m \frac{\partial H}{\partial x}, & (d_m < h \leq d_a) \\ -\frac{1}{n} (h - d_a)^{5/3} \sqrt{\left| \frac{\partial H}{\partial x} \right|} \operatorname{sgn} \left(\frac{\partial H}{\partial x} \right) - k_a (h - d_m) \frac{\partial H}{\partial x} - k_m d_m \frac{\partial H}{\partial x}, & (d_a < h) \end{cases} \quad (11)$$

$$q_y = \begin{cases} -k_m d_m \left(\frac{h}{d_m} \right)^\beta \frac{\partial H}{\partial y}, & (h \leq d_m) \\ -k_a (h - d_m) \frac{\partial H}{\partial y} - k_m d_m \frac{\partial H}{\partial y}, & (d_m < h \leq d_a) \\ -\frac{1}{n} (h - d_a)^{5/3} \sqrt{\left| \frac{\partial H}{\partial y} \right|} \operatorname{sgn} \left(\frac{\partial H}{\partial y} \right) - k_a (h - d_m) \frac{\partial H}{\partial y} - k_m d_m \frac{\partial H}{\partial y}, & (d_a < h) \end{cases} \quad (12)$$

Note that to assure the continuity of the discharge change when $h = d_m$, the lateral hydraulic conductivity in unsaturated zone (k_m) can be computed by $k_m = k_a / \beta$, so that k_m is no longer the model parameter.

These stage-discharge relationship equations were originally developed to be applied to humid forest areas with a high permeable soil layer, where a lateral subsurface flow is the dominant runoff generation mechanism. On the other hand, for relatively flat areas, the vertical infiltration process during the first period of rainfall has more impact on large-scale flooding; therefore, the vertical infiltration can be treated as loss for event-based simulation. Here we calculate infiltration loss f with the Green-Ampt infiltration model (Raws et al., 1992).

$$f = k_v \left[1 + \frac{(\phi - \theta_i) S_f}{F} \right] \quad (13)$$

where k_v is the vertical saturated hydraulic conductivity, ϕ is the soil porosity, θ_i is the initial water volume content, S_f is the suction at the vertical wetting front and F is the cumulative infiltration depth.

Typically for mountainous areas where lateral subsurface flow and saturated excess overland flow dominate, the equations (9) and (10) (or (11) and (12)) can be used with setting f equals to be zero. (Note that the equations (9) and (10) (or (11) and (12)) implicitly assume that the vertical infiltration rate within the soil is infinity.) On the other hand, for plain areas where infiltration excess overland flow dominates, the surface flow equations (6) and (7) can be used with the consideration of vertical infiltration by equation (13). If the vertical

infiltration f is set to be non-zero and the lateral subsurface equations are used instead of the surface flow equation, the lateral subsurface water is infiltrated to bedrock by the rate of f .

As one can see from the equations, the parameter values of k_a , k_m and k_v decide which equations to be used; i.e. (6) and (7) are used when k_a and k_m are zero, (9) and (10) are used when k_m is zero, and (13) is inactivated when k_v is zero.

1.3 One-dimensional River Routing Model

A one-dimensional diffusive wave model is applied to river grid cells. The geometry is assumed to be rectangle, whose shapes are defined by width W , depth D and embankment height H_e . When detailed geometry information is not available, the width and depth are approximated by the following function of upstream contributing area A [km²].

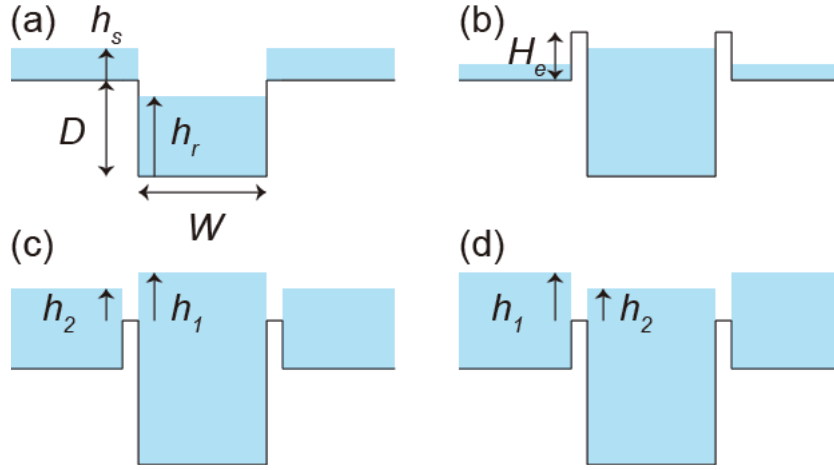
$$W = C_W A^{S_W} \quad (14)$$

$$D = C_D A^{S_D} \quad (15)$$

where C_W , S_W , C_D and S_D are geometry parameters. Here the units of W and D are meters.

1.4 River and Slope Water Exchange

Water exchange between a slope grid cell and an overlying river grid cell is calculated at each time step depending on the relationship among the levels of slope water, river water, levee crown and ground. The figure below shows four different conditions. For each condition, different overtopping formulae are applied to calculate the unit length discharge from slope to river (q_{sr}) or from river to slope (q_{rs}), which are then multiplied by the length of the river vector at each grid cell to calculate the total exchange flow rate (Iwasa and Inoue, 1982).



(a) When the river water level is lower than the ground level, q_{sr} is calculated by the following step fall formula.

$$q_{sr} = \mu_1 h_s \sqrt{gh_s} \quad (16)$$

where μ_1 is the constant coefficient ($= (2/3)^{3/2}$), and h_s is the water depth on a slope cell. As far as the river water level is lower than the ground level, the same equation is used even for the case with levees so that the slope water can flow into the river.

(b) When the river water level is higher than the ground level and both the river and slope water levels are lower than the levee height, no water exchange is assumed between the slope and river.

(c) When the river water level is higher than the levee crown and the slope water level, the following formula is used to calculate overtopping flow q_{rs} from river to slope.

$$q_{rs} = \begin{cases} \mu_2 h_1 \sqrt{2gh_1} & h_2 / h_1 \leq 2/3 \\ \mu_3 h_2 \sqrt{2g(h_1 - h_2)} & h_2 / h_1 > 2/3 \end{cases} \quad (17)$$

where μ_2 and μ_3 are the constant coefficients ($= 0.35, 0.91$), and h_1 is the difference between the river water level and the levee crown.

(d) When the slope water level is higher than the levee height and the river water level, the same formula as (17) is used to calculate overtopping flow q_{sr} from slope to river. In this case, h_1 is the elevation difference between the slope and the river, and h_2 is the elevation difference between the river and the levee crown.

1.5 Numerical Scheme

To solve equations (8), (9) and (10), the fifth-order Runge-Kutta method with adaptive

time-step control is applied. This method solves an ordinary differential equation by the general fifth-order Runge-Kutta formula and estimates its error by an embedded forth-order formula to control the time-step (Cash and Karp 1990, Press et al. 1992).

The general form of the fifth-order Runge-Kutta formula is

$$\begin{aligned}
k_1 &= \Delta t f(t, h_t) \\
k_2 &= \Delta t f(t + a_2 \Delta t, h_t + b_{21} k_1) \\
&\dots \\
k_6 &= \Delta t f(t + a_6 \Delta t, h_t + b_{61} k_1 + \dots b_{65} k_5) \\
h_{t+1} &= h_t + c_1 k_1 + c_2 k_2 + c_3 k_3 + c_4 k_4 + c_5 k_5 + c_6 k_6 + O(\Delta t^6)
\end{aligned} \tag{18}$$

while the embedded forth-order formula (Cash and Karp 1990) is

$$h_{t+1}^* = h_t + c_1^* k_1 + c_2^* k_2 + c_3^* k_3 + c_4^* k_4 + c_5^* k_5 + c_6^* k_6 + O(\Delta t^5) \tag{19}$$

By subtracting h_{t+1} minus h_{t+1}^* , the error can be estimated by using k_1 to k_6 as follows,

$$\delta \equiv h_{t+1} - h_{t+1}^* = \sum_{i=1}^6 (c_i - c_i^*) k_i \tag{20}$$

The constant values (a_i , b_{ij} , c_i , c_i^*) used in this study are the ones introduced by Cash and Karp (1990). If δ exceeds a desired accuracy δ_d , h_{t+1} is recalculated with a smaller time step (Δt_{post}).

$$\Delta t_{post} = \max \left(0.9 \Delta t \left| \frac{\delta_d}{\delta} \right|^{0.25}, 0.5 \Delta t \right) \tag{21}$$

As described above, the RRI model calculates slopes, rivers and slope-river interactions. Model users specify the time step for slope-river interaction Δt , which is also used as an initial time step for slope calculations. Since river calculations usually require smaller time steps because of higher water velocities and depths, the model allows river calculations to proceed independently with different time steps until the next river-slope calculation time step. The initial time step for river calculation (Δt_r) can be also specified by model users as the common divisor of Δt . In this study, $\delta_d = 0.01$, $\Delta t = 600$ sec. and $\Delta t_r = 60$ sec. were used.

References

- Sayama, T., Ozawa, G., Kawakami, T., Nabesaka, S., Fukami, K. (2012) Rainfall-Runoff-Inundation analysis of the 2010 Pakistan flood in the Kabul River basin, *Hydrological Science Journal*, 57(2), 298-312.
- Sayama, T., Tatebe, Y., Tanaka, S. (2015a) An emergency response-type rainfall-runoff-inundation simulation for 2011 Thailand floods, *Journal of Flood Risk Management*, doi:10.1111/jfr3.12147 (in print).

-
- Sayama, T., Tatebe, Y., Iwami, Y., Tanaka, S. (2015b) Hydrologic sensitivity of flood runoff and inundation: 2011 Thailand floods in the Chao Phraya River basin, *Nat. Hazards Earth Syst. Sci.*, 15, pp. 1617-1630, doi:10.5194/nhess-15-1617-2015.
 - Hunter, N.M., Bates, P.D., Horritt, M.S., Wilson, M.D. (2007) Simple spatially-distributed models for predicting flood inundation: A review. *Geomorphology*, 90, 208-225.
 - Takasao, T., Shiiba, M. (1976), A study on the runoff system model based on the topographical framework of river basin, *Proceedings of the Japan Society of Civil Engineers*, 248, 69-82, (in Japanese with English abstract).
 - Takasao, T., Shiiba, M. (1988) Incorporation of the effect of concentration of flow into the kinematic wave equations and its applications to runoff system lumping. *Journal of Hydrology*, 102, 301– 322.
 - Ishihara, T., Takasao T. (1962) A study on the subsurface runoff and its effects on runoff process, *Transactions of the Japan Society of Civil Engineers*, 79, 15-23, (in Japanese with English abstract).
 - Tachikawa, Y., G. Nagatani, K. Takara (2004), Development of stage discharge relationship equation incorporating saturated-unsaturated flow mechanism (in Japanese), *JSCE Annual Hydraulic Engineering*, 48, 7 – 12, (in Japanese with English Abstract).
 - Sayama, T., McDonnell, J. J. (2009) A new time-space accounting scheme to predict stream water residence time and hydrograph source components at the watershed scale, *Water Resour. Res.*, 45, W07401.
 - Raws, W.J., Ahuja, L.R., Brakensiek, D.L. & Shirmohammadi, A. (1992) Infiltration and soil water movement. Handbook of Hydrology, McGraw-Hill Inc., New York, 5.1-5.51.
 - Iwasa, Y., Inoue, K. (1982) Mathematical simulation of channel and overland flood flows in view of flood disaster engineering, *Journal of Natural Disaster Science*, 4(1), 1-30.
 - Cash, J.R. & Karp, A.H. (1990) A variable order Runge-Kutta method for initial value problems with rapidly varying right-hand sides. *ACM Trans. on Math. Software*, 16(3), 201-222.
 - Press, W.H., Teukolsky, S.A., Vetterling, W.T. & Flannery, B.P. (1992) Adaptive stepsize control for Runge-Kuta. Numerical Recipes in Fortran 77, The Art of Scientific Computing Second Edition, Cambridge University Press, 708-716.
-

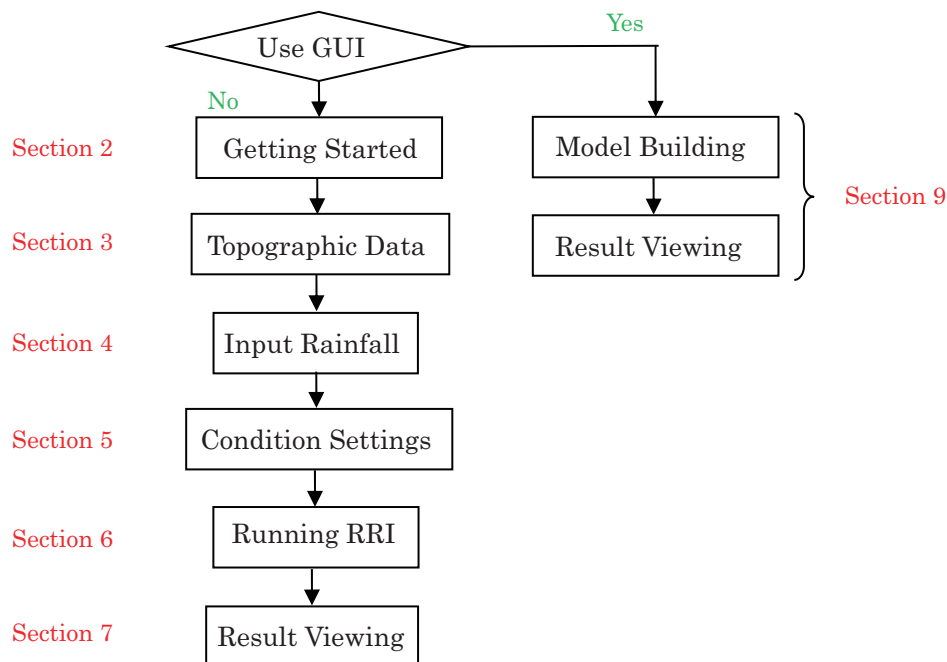
2. Getting Started

RRI model and related tools were originally developed with **Fortran 90** computer language. The model has been operated on **Command User Interface (CUI)** such as Command Prompt on Windows. Since 2014, **RRI-Graphical User Interface (GUI)** has been also developed to support users for efficient model building and result visualization.

For non-experts in hydrologic modeling, it is recommended to use RRI-GUI to begin with by referring to **Section 9** to learn the basic steps with **RRI-GUI**.

Refer to Section 2 (i.e. this following chapter) on the tutorial of RRI-CUI, followed by more detail descriptions in Sections 3 to 7. Section 8 shows an application example including some advanced model settings.

If you use RRI-GUI not RRI-CUI, you can skip the following steps. Go directly to Section 9.



There are essentially five steps to conduct RRI Model simulation.

1. Preparing topography data (Section 3)
2. Preparing input rainfall data (Section 4)
3. Preparing model condition files with parameter settings (Section 5)
4. Executing RRI Model. (Section 6)
5. Plotting output data (Section 7)

Among the five steps, only the essence of step 4 and 5 are described here with sample data of the Solo River Basin (in 30 sec resolution) in Indonesia.

2.1 Preparation for the use of RRI-CUI

- 1) Unzip “**RRI_1.4.2.zip**” and move it under a working directory (e.g. **C:**).
- 2) Add a path to RRI-CUI folder with the following steps (e.g. for Windows 7)
 1. Select Computer from the Start menu
 2. Choose System Properties from the context menu
 3. Click Advanced system settings → Advanced tab
 4. Click on Environment Variables, under User’s Variables, find **PATH**, and click to edit it. If you do not have the item PATH, you may select to add a new variable and add PATH as the name.
 5. In the Edit windows, modify **PATH** by adding “**;C:/RRI/RRI-CUI/bin/**” (for 64 bit) or “**;C:/RRI/RRI-CUI/bin32/**” (for 32 bit) at the end of line.
Note: do not delete existing PATH settings. Only add the above item to the existing line. Also do not forget to add “**;**” to separate it from the existing path folders.
 6. Click OK and close Command Prompt windows if opened.
- 3) If your computer has no Intel Fortran installed, run
RRI/RRI-CUI/etc/w-fcompse/**w_fcompse_redist_intel64_2013.5.198.msi** (for 64 bit) or
RRI/RRI-CUI/etc/w-fcompse/w_fcompse_redist_ia32_2013.5.198.msi (for 32 bit),
which installs necessary library files to execute RRI programs compiled by Intel Fortran.
- 4) Open Command Prompt by Start → All Programs → Accessories → Command Prompt
(If your computer has Intel Fortran installed, you may also operate it from
Start → All Programs → Intel(R) Software Development Tools → Intel(R) Fortran
Compiler ** → Fortran Build Environment for Applications running on ...)

2.2 Run RRI Model

Open “**RRI_Input.txt**” under “RRI-CUI/Project/solo30s” with a text editor and look inside the file. This is a control file used by RRI Model. By editing the RRI_Input.txt file, you change the simulation settings.

```

RRI_Input_Format_Ver1_4_2

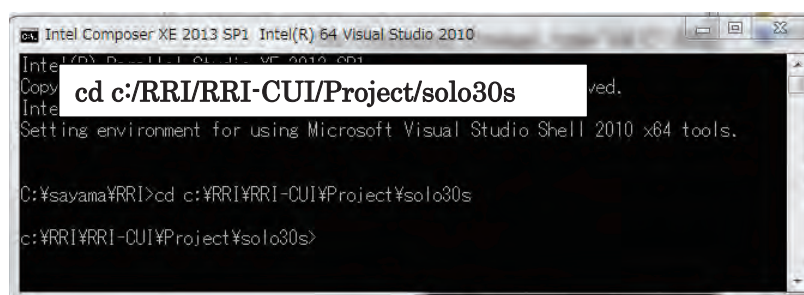
./rain/rain.dat
./topo/adem.txt
./topo/acc.txt
./topo/adir.txt

0          # utm(1) or latlon(0)
1          # 4-direction (0), 8-direction(1)
360        # lasth [hour]
600        # dt [sec]

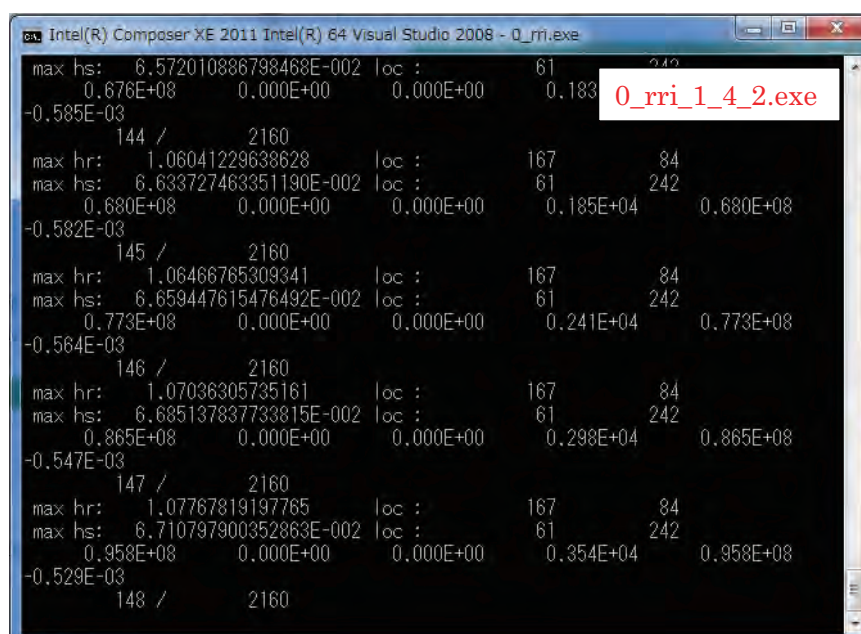
```

For example, L3 specifies the path to an input rainfall file and L4 – L6 specify the paths to input topography files (adem, acc, and adir).

Open Command Prompt and type in “cd C:/RRI/RRI-GUI/Project/solo30s/” to change the current directly.



Type in “0_rri_1_4_2.exe” and enter to execute RRI Model with RRI_Input.txt.



Confirm the output files are successfully created inside the directory of “RRI/RRI-CUI/Project/solo30s/out/”. Note that “**hr_000001.out**” represents the spatial distribution of **river water depths [m]** at the output time step 1. “**hs_000001.out**” and “**qr_000001.out**” represent those of **slope water depths [m]** and **river discharge [m³/s]**, respectively.

2.3 Post Analysis

2.3.1 Visualize Inundation Depth (./out/hs_***.out) with GNUPLOT

Run a GNUPLOT installation program “RRI-CUI/etc/gp466-win32-setup.exe” and install it onto your PC. If the installation is successful, “gnuplot” folder is appeared under All Programs of windows. Choose “gnuplot 4.6” to run GNUPLOT.

Open “[RRI-CUI/Model/hs.plt](#)” with a text editor. It is a GNUPLOT script file to convert from the simulation outputs (e.g. ./out/hs_***.out) to gif files to visualize inundation depth distributions.

```
reset

set terminal gif medium size 672, 408 crop

set pm3d map
set palette defined (0.0 "gray", 1.5 "blue", 3 "green")

set xrange [0:]
set yrange [:] reverse
set zrange [0:] reverse

#set xrange [180:200]
#set yrange [435:455] reverse

set cbrange[0.:3]
set zrange[0.0:]

set output "./hs/hs_000001.gif"
splot "./out/hs_000001.out" matrix t "000001 / 000096"

set output "./hs/hs_000002.gif"
splot "./out/hs_000002.out" matrix t "000002 / 000096"

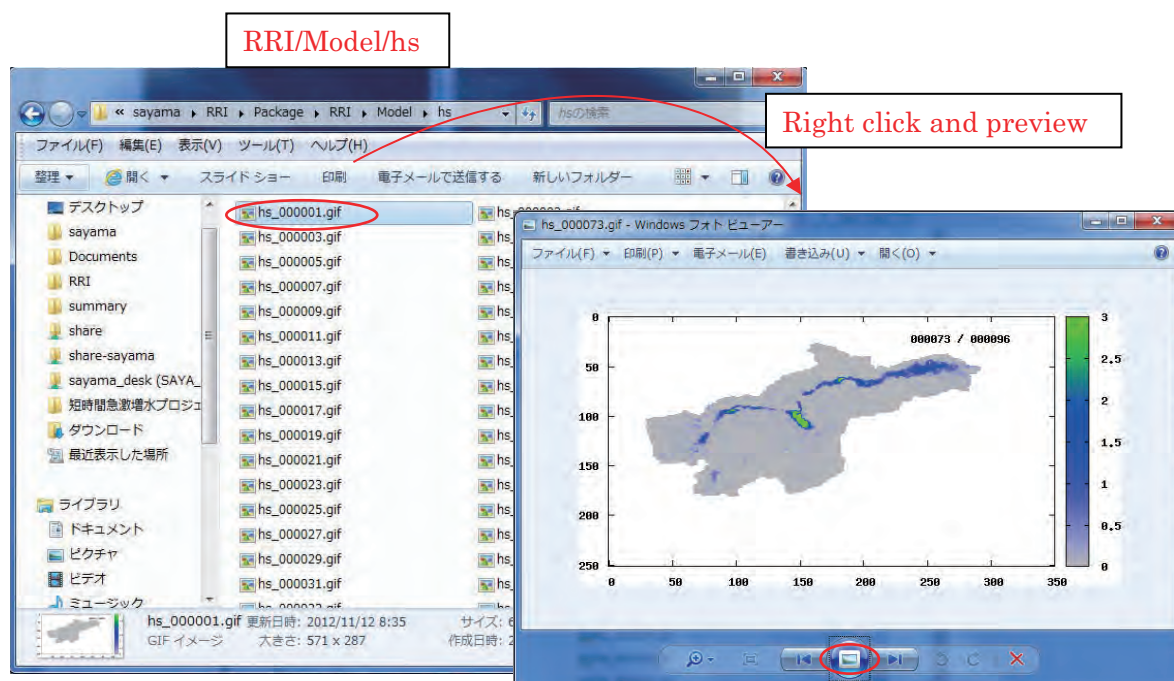
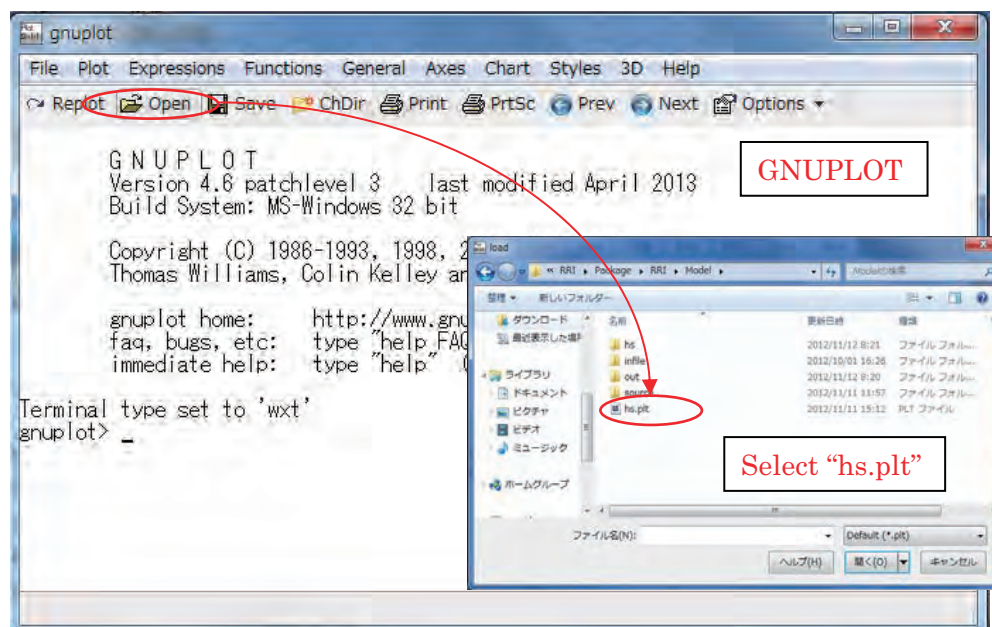
set output "./hs/hs_000003.gif"
splot "./out/hs_000003.out" matrix t "000003 / 000096"
```

hs_plt.txt

From RRI output (hs_***.out) to gif

Select “Open” on GNUPLOT Toolbar and open “RRI-CUI/Project/solo30s/hs.plt”, which is a script file to create gif files from the RRI output (see above figure).

Look at “RRI-CUI/Project/solo30s/hs” directory, where gif files are newly created. Check the created gif files by preview.



2.3.2 Compute hydrograph

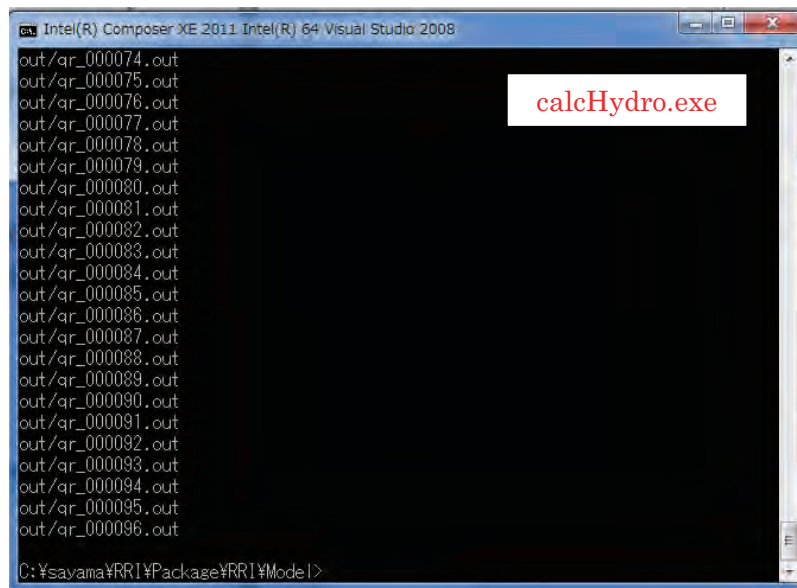
Look at “[RRI/RRI-CUI/Project/solo30s/calcHydro.txt](#)” (see “[./etc/calcHydro/00_readme.txt](#)” for more details)

L1 : [In] location file (e.g. `./location.txt`)

L2 : [In] RRI output file (e.g. `./out/qr_***.txt`)

L3 : [Out] hydrograph file (e.g. `./disc_Cepu.txt`)

On Command Prompt with current folder at “`./Project/solo30s`”, type in “`calcHydro.exe`” to compute time series data from RRI output files.

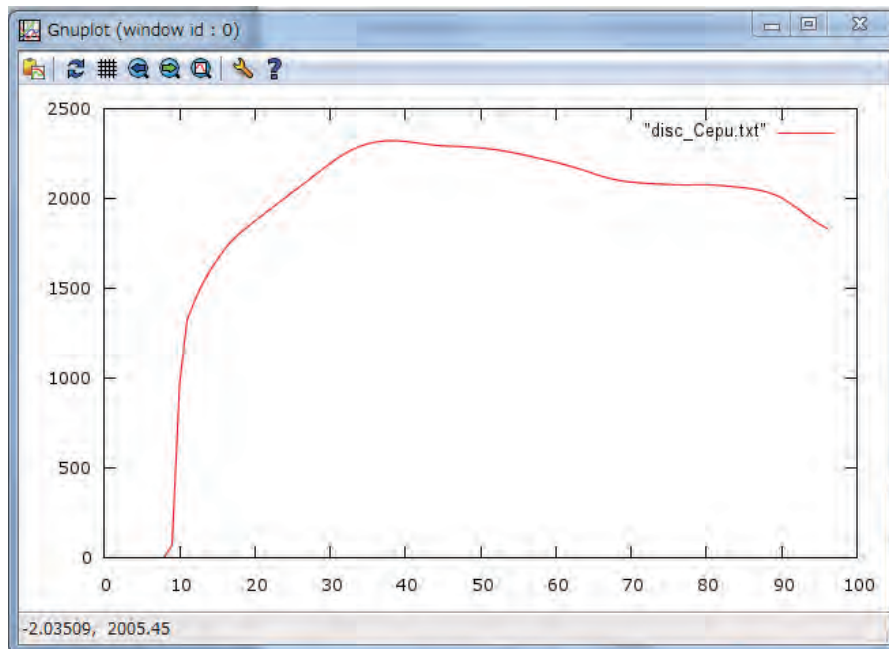


Confirm that a hydrograph file named “`disc_Cepu.txt`” is created.

1	0.00789
2	0.04591
3	0.08256
4	0.10557
5	0.12529
6	0.14543
7	0.24838
8	0.56375
9	69.88281
10	967.36834
11	1322.37727
12	1429.53330
13	1518.85970
.....

Visualize the created hydrograph file (e.g. “./infile/solo30s/disc_Cepu.txt”) by GNUPLOT.

From GNUPLOT screen, open and select “**hydro.plt**”, which is a GNUPLOT script file to plot hydrograph from the “disc_Cepu.txt”.



2.3.3 Compute and visualize peak inundation depths

Look at “./Project/solo30s/calcPeak.txt” (see “./etc/calcPeak/00_readme.txt” for more details) and edit the file if necessary.

- L1 : [in] dem file (e.g. ./topo/adem.txt)
- L2 : [in] output file without numbers or extension (e.g. ./out/hs_)
- L3 : [in] the number of output files (e.g. 96)
- L4 : [out] output peak inundation depth file (e.g. ./hpeak.txt)

On Command Prompt with current folder at “RRI/Project/solo30s/”, type in “**calcPeak.exe**” to compute peak inundation depth.

```

ncols      336
nrows      204
xllcorner  110.2
yllcorner  -8.3
cellsize   0.0083333333333333
NODATA_value -9999
-9999 -9999 -9999 -9999 -9999 -9999 -9999 -9999 -9999 -9999 -9999 -9999
-9999 -9999 -9999 -9999 -9999 -9999 -9999 -9999 -9999 -9999 -9999 -9999
-9999 -9999 -9999 -9999 -9999 -9999 -9999 -9999 -9999 -9999 -9999 -9999
-9999 -9999 -9999 -9999 -9999 -9999 -9999 -9999 -9999 -9999 -9999 -9999

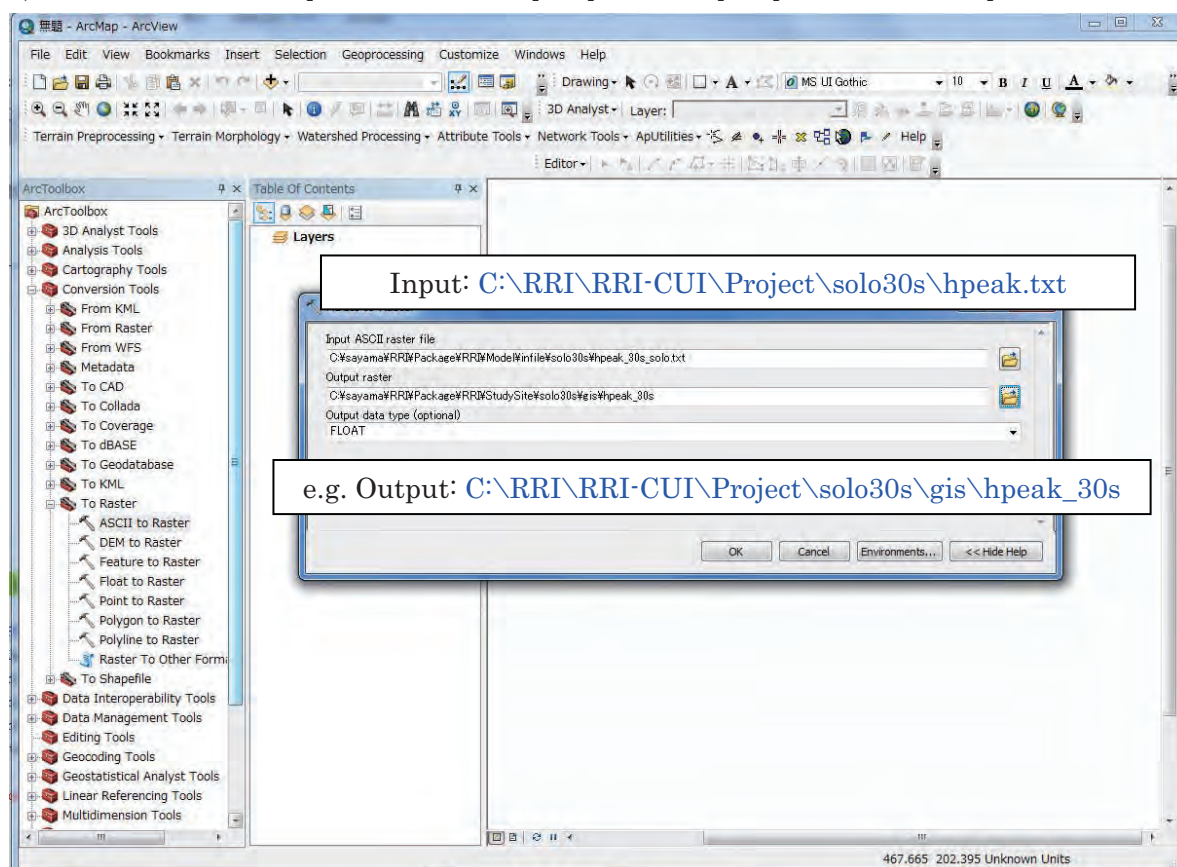
```

hpeak.txt

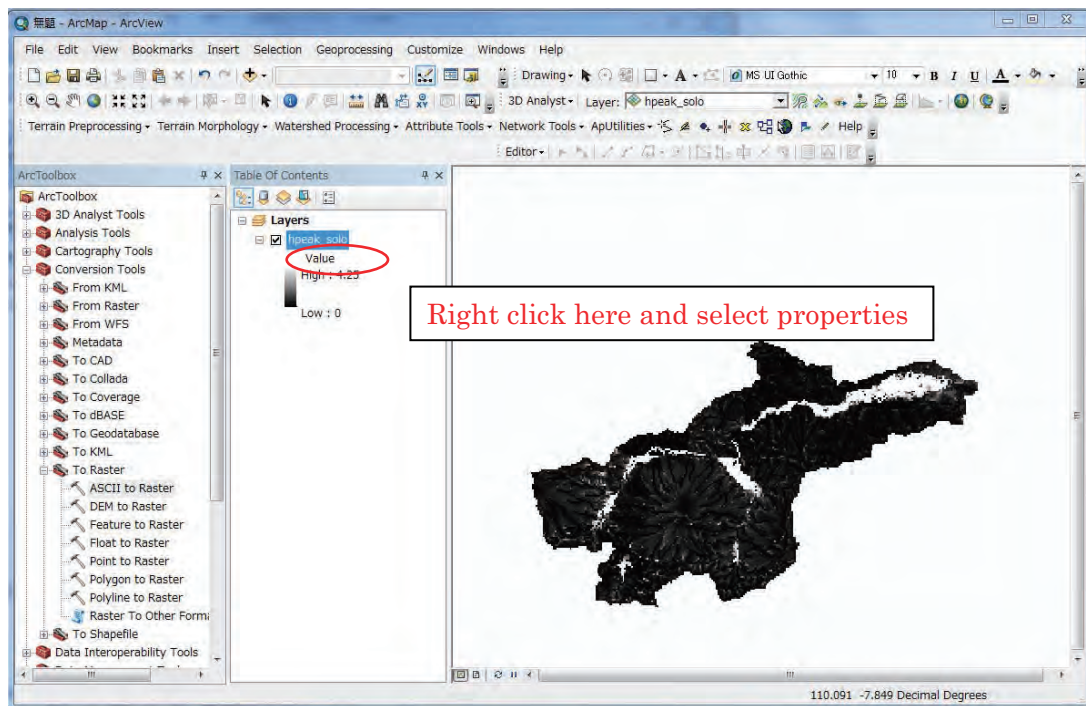
Visualize created “hpeak.txt” on ArcGIS by converting it from ASCII to Raster.

1) Start ArcGIS (Skip the following procedure if ArcGIS software is inaccessible. Consider the use of GRASS GIS by following the instruction in 3.3)

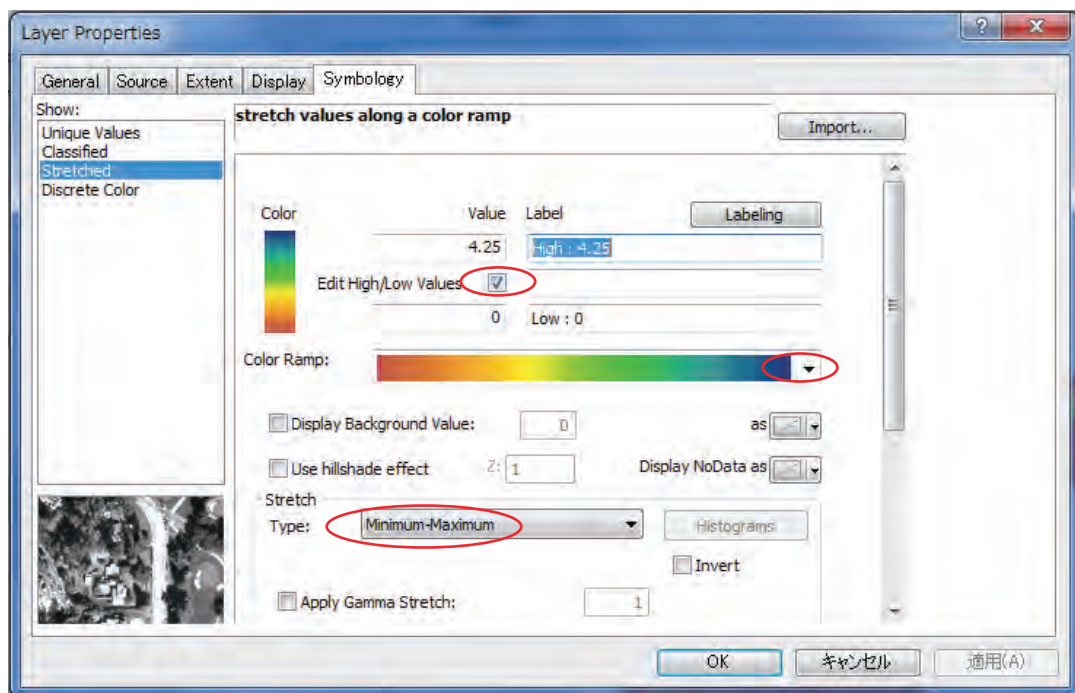
2) From ArcToolbox → [Conversion Tools] → [To Raster] → [ASCII to Raster]



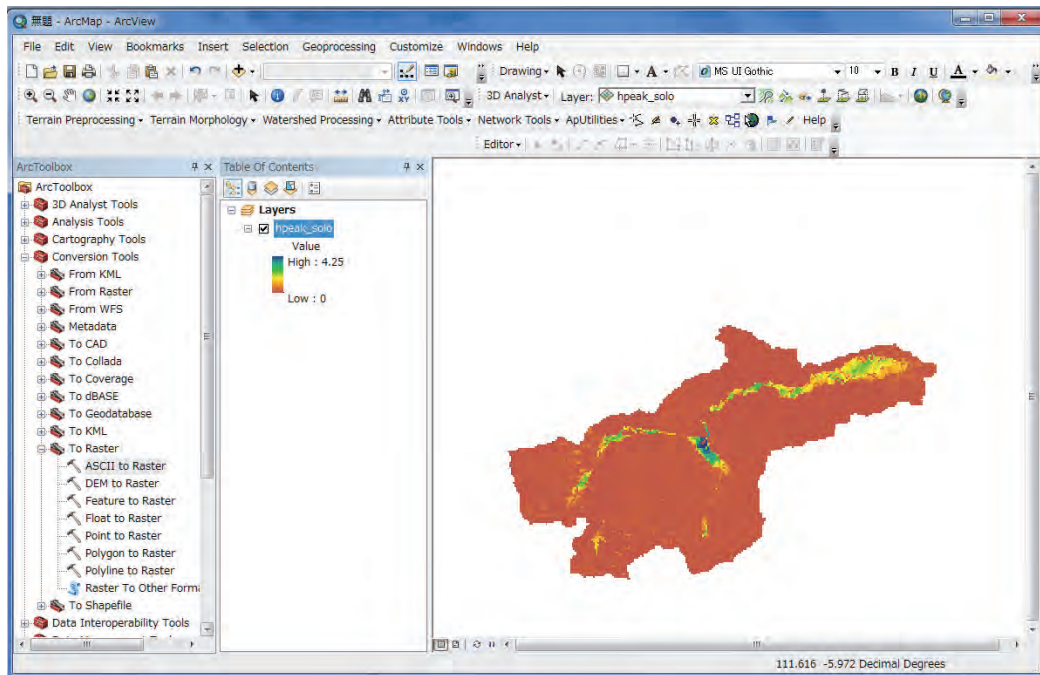
3) For the input data, select “hpeak.txt”. For the output raster, a user may use “RRI/StudySite/solo30s/gis/hpeak_30s”.



4) Right click “hpeak_30s” and select **properties** to change the layer color setting.



5) On the layer property, change the stretch type to **“Minimum-Maximum”** and change Color Ramp if necessary. By checking “Edit High/Low Values”, you can change the max and min value range of the stretching.



3. Preparing Input Topography Data

This section shows the method to prepare topography data input to the RRI Model. The topography data can be prepared by a user or downloaded from the website of USGS HydroSHEDS, which is a global scale dataset offered by the United States Geological Survey (USGS). The dataset includes elevation, flow direction and flow accumulation.

From the downloaded topographic dataset, a user must clip out the target river basin and save them as ESRI/ASCII format files. Then using a program included in RRI Model package, one adjusts the original DEM and flow direction data to be suitable for the RRI simulation. The following chart shows the procedure described in this section. In the previous section, the 30 second resolution of the Solo River Basin data was used, whereas this section presents how to prepare the topographic data in 15 second.

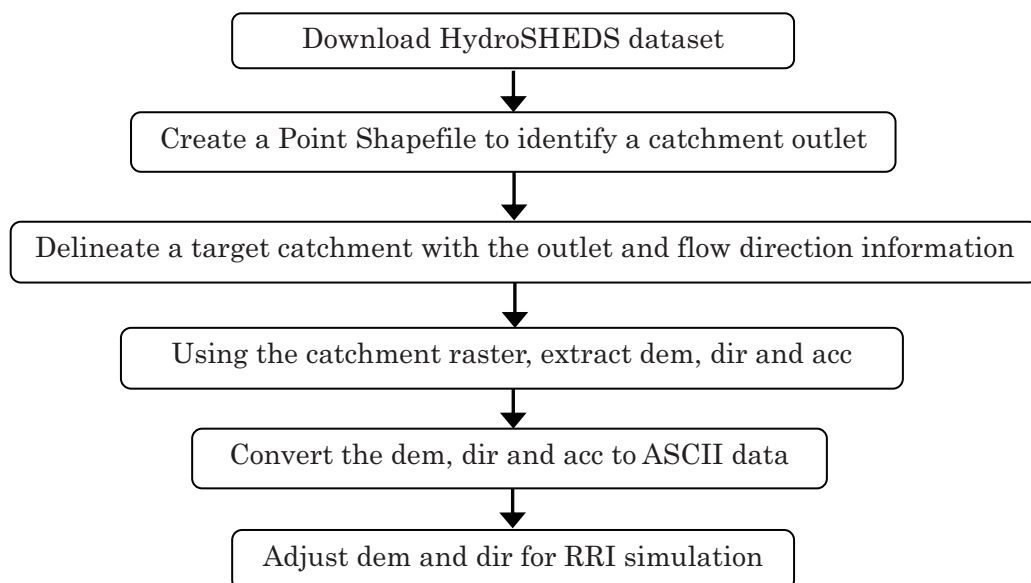
Create a New Project Folder

When you prepare a new input topographic data, create a new project folder:

Copy “[newProject](#)” folder including all the files and folders inside and save it with a new project name under “[RRI-CUI/Project](#)”.

Note: In the package, “[RRI-CUI /Project/solo15s](#)” is prepared in advance for the tutorial.

The flow of the procedure is as follows.



3.1 Downloading HydroSHEDS Data

The following three types of topography data must be downloaded from HydroSHEDS website for RRI simulation.

1) Elevation data

3 arc-second (about 90 m), 15 arc-second (about 500 m), and 30 arc-second (about 1,000 m) are available.

2) Flow direction data

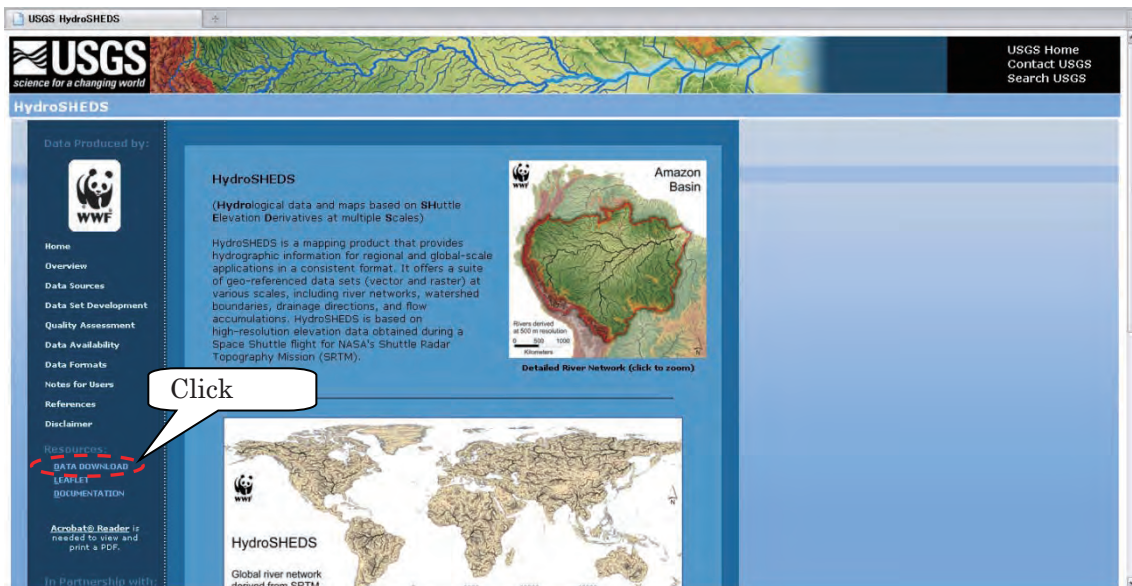
3 arc-second, 15 arc-second, and 30 arc-second are available.

3) Flow accumulation data

Only 15 arc-second and 30 arc-second are available. For 3 arc-second resolution, a user must prepare a flow accumulation by using a GIS function [Spatial Analyst] → [Hydrology] → [Flow Accumulation].

※ For detailed specifications of HydroSHEDS, refer to HydroSHEDS Technical Documentation packaged with the downloaded data.

- ① Access USGS HydroSHEDS website (<http://hydrosheds.cr.usgs.gov/index.php>) from a web browser and then select and click the DATADOWNLOAD button on the lower left.



- ② Select “15sec GRID: Conditioned DEM” and download “as_dem_15s_grid.zip” (207 MB) for Asian region with 15 sec grid-size. **NOTE** that for 3 sec, choose “Void-filled DEM”. For 15 sec and 30 sec, only “Conditioned DEM” is available, but in fact they are the same as previously named as “Void-filled DEM” (i.e. DEM along rivers are **not** deepened).

- ③ Select also “15 sec GRID: Flow Accumulation” and “15 sec Flow Direction” to download “as_acc_15s_grid.zip” (132 MB) and “as_dir_15s_grid.zip” (64 MB) as well.

- ④ Unzip the three types of topography data downloaded.

※Folder naming rule

“Continental range” _ “Data type” _ “resolution”

e.g.) as_acc_15s → Asia catchment area data 15 sec

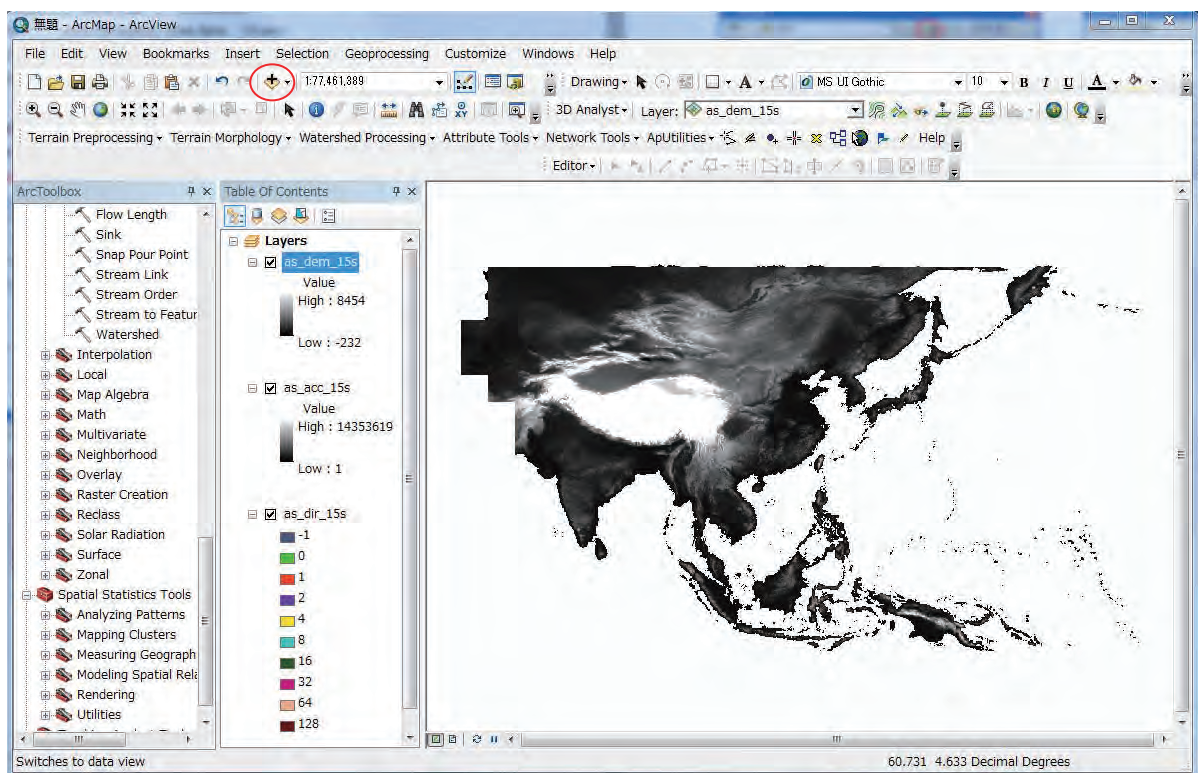
as_dem_15s → Asia digital elevation data 15 sec

as_dir_15s → Asia flow direction data 15 sec

3.2 Delineating HydroSHEDS Data using ArcGIS

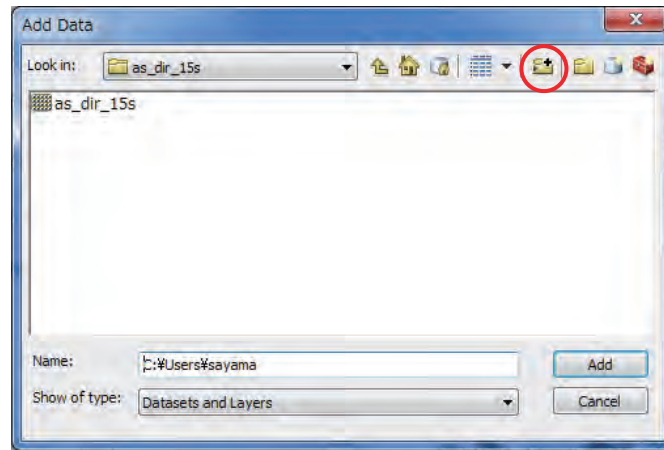
(If ArcGIS is inaccessible, skip this section and go to 3.3 to use free GLASS GIS)

- ① Start ArcMap, and read in the unzipped files by selecting [File]>[Add Data]. (Or use icon of “Add Data” on the standard tool bar). Perform the same operation for all **the three types (dem, dir, acc)** of topography data.

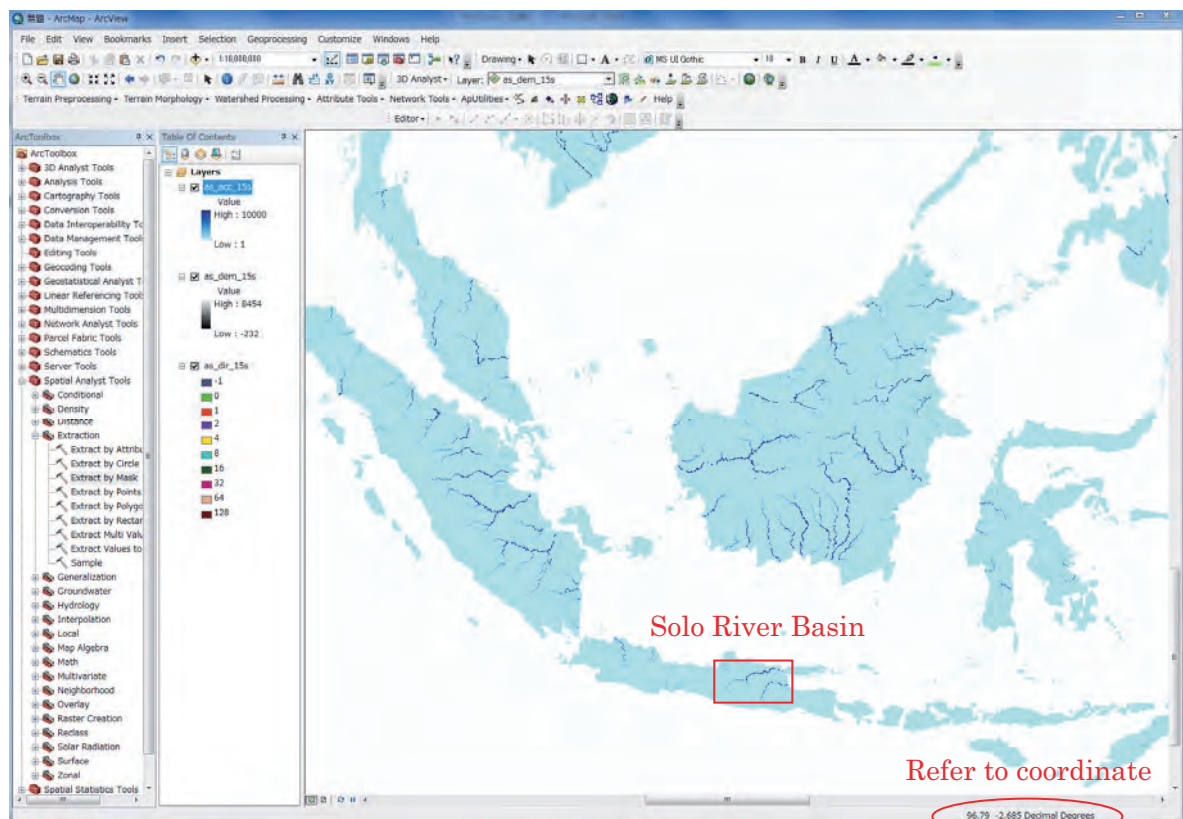


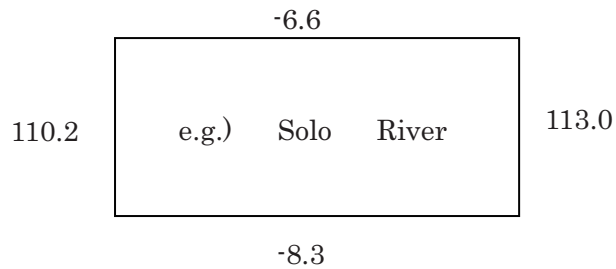
※Selecting the folder to connect

If the folder you need to connect is not displayed in the window, click “Connect to Folder” to connect to the working folder.



- ③ Display the flow accumulation data (i.e. as_acc_15s) on top screen (change the color range to show river network clearly). Then find your target river and decide the rectangular range, which covers all upstream contributing area. (At this stage, the following rectangle range should be just written down on your notebook and no operation is necessary with GIS.)

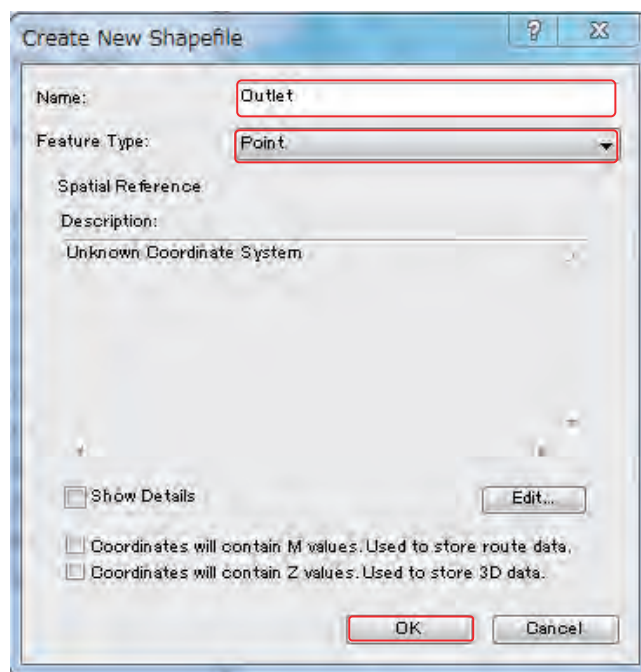




(The range should be written down on your notebook.)

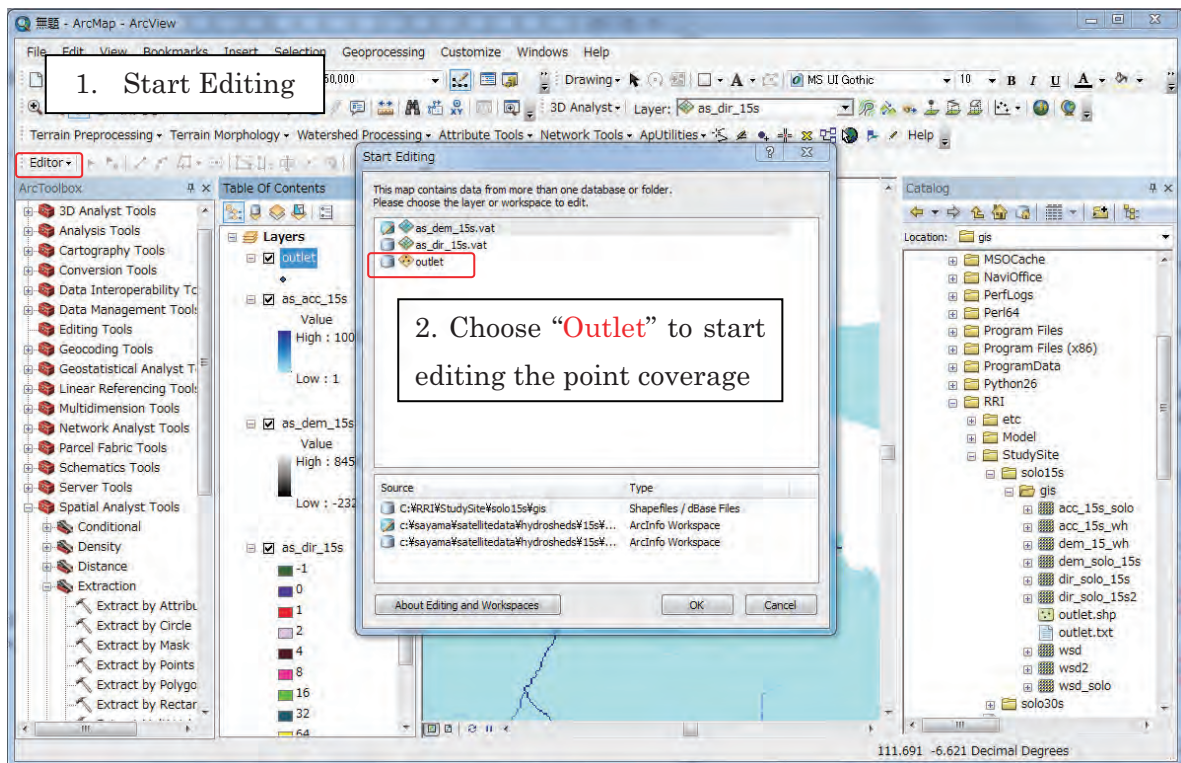
- ④ Show arc catalog (from the main menu, [Windows] → [Catalog]).

On the arc catalog, “Folder Connections” to a working folder (e.g. RRI/Project/solo15s/gis/) and right click to choose New → Shapefile to create a point Shapefile (e.g. Outlet).



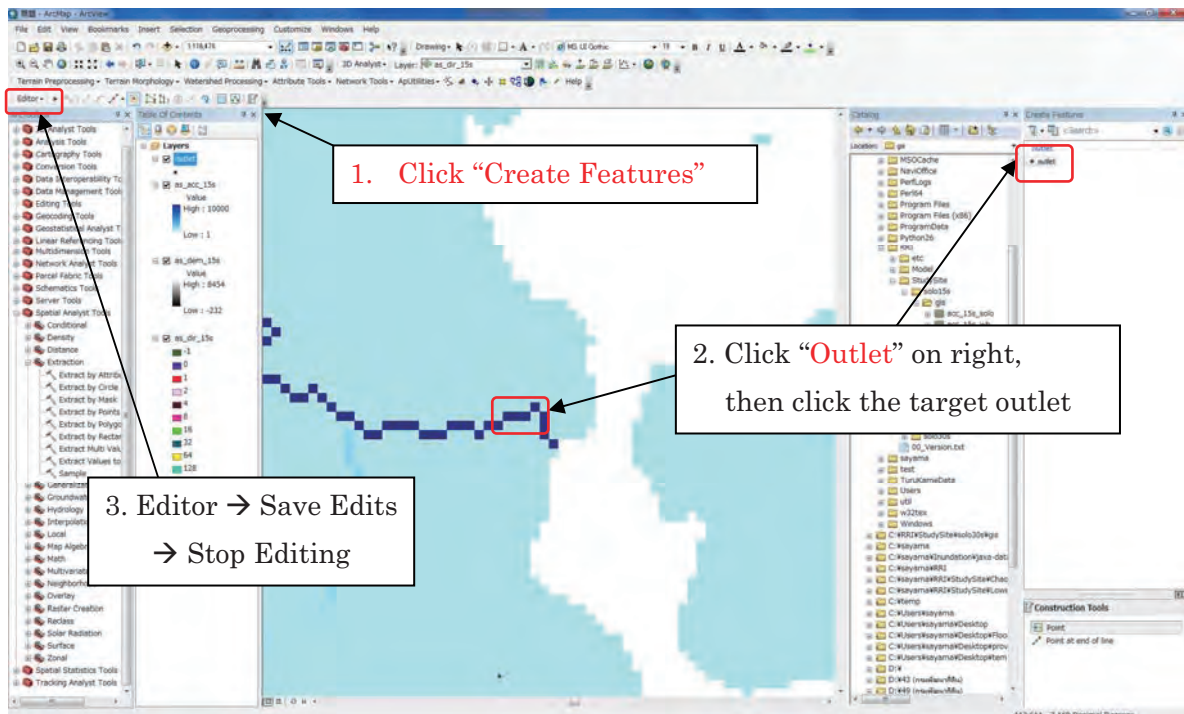
- ⑤ From the main menu [Customize] → [Toolbars] → [Editor]

On the Editor, choose [Start Editing], then Choose “Outlet” (the new Shapefile) to start editing.



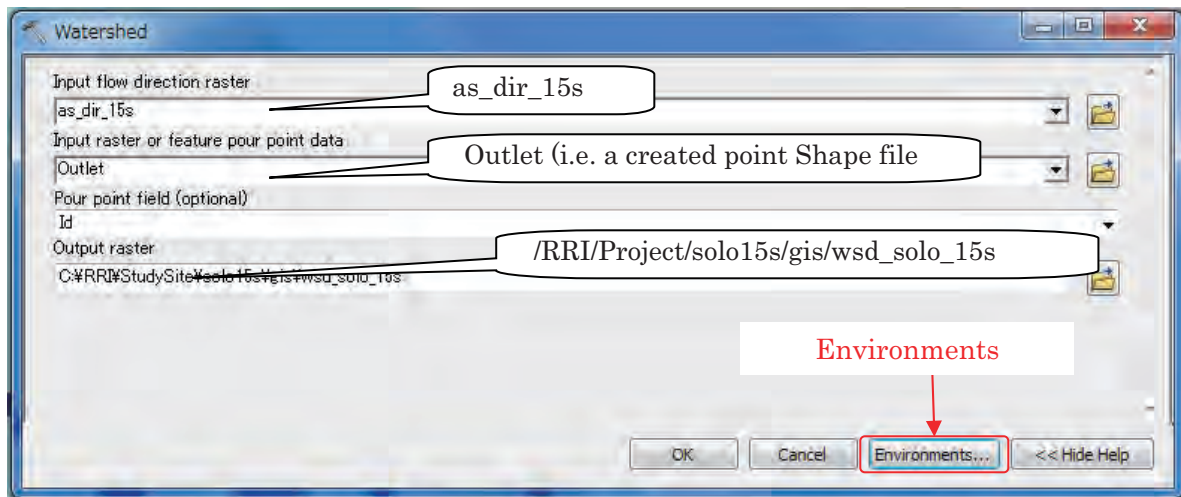
Clicking "Outlet", so that you can bring a point to indicate the target outlet.

After editing the outlet point, go to the editor menu to **save** and **stop** editing.

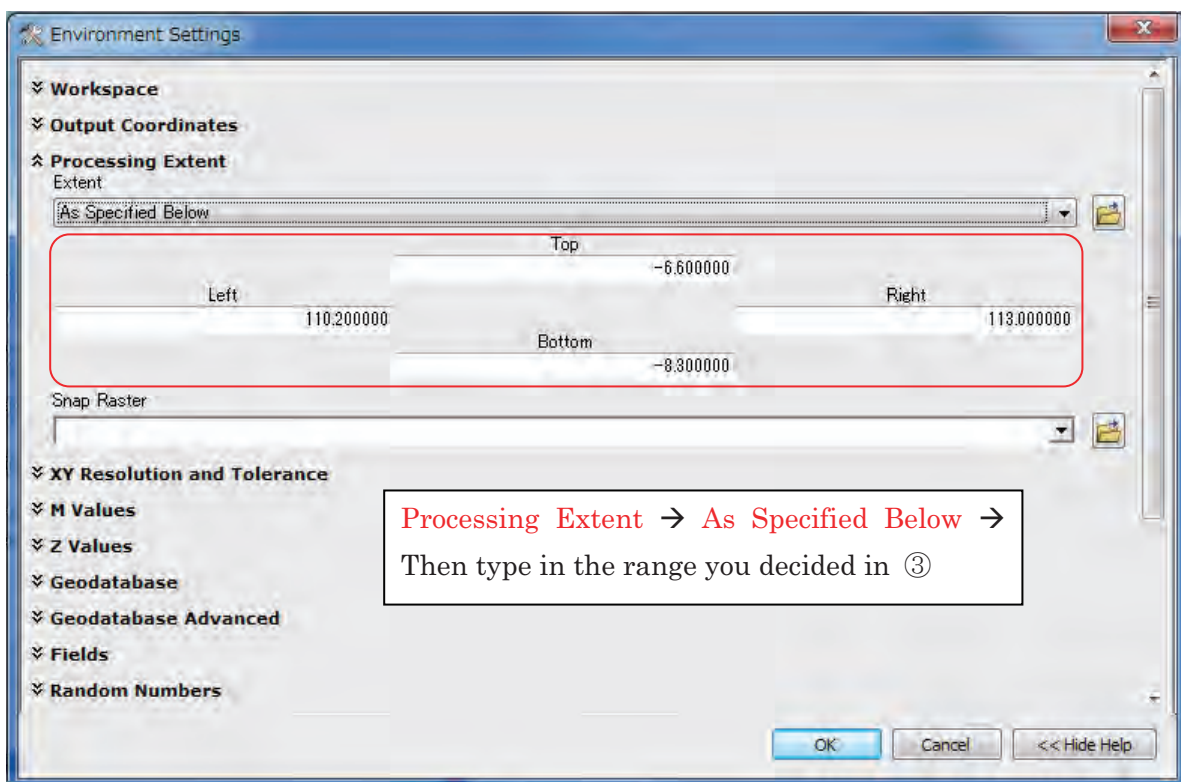


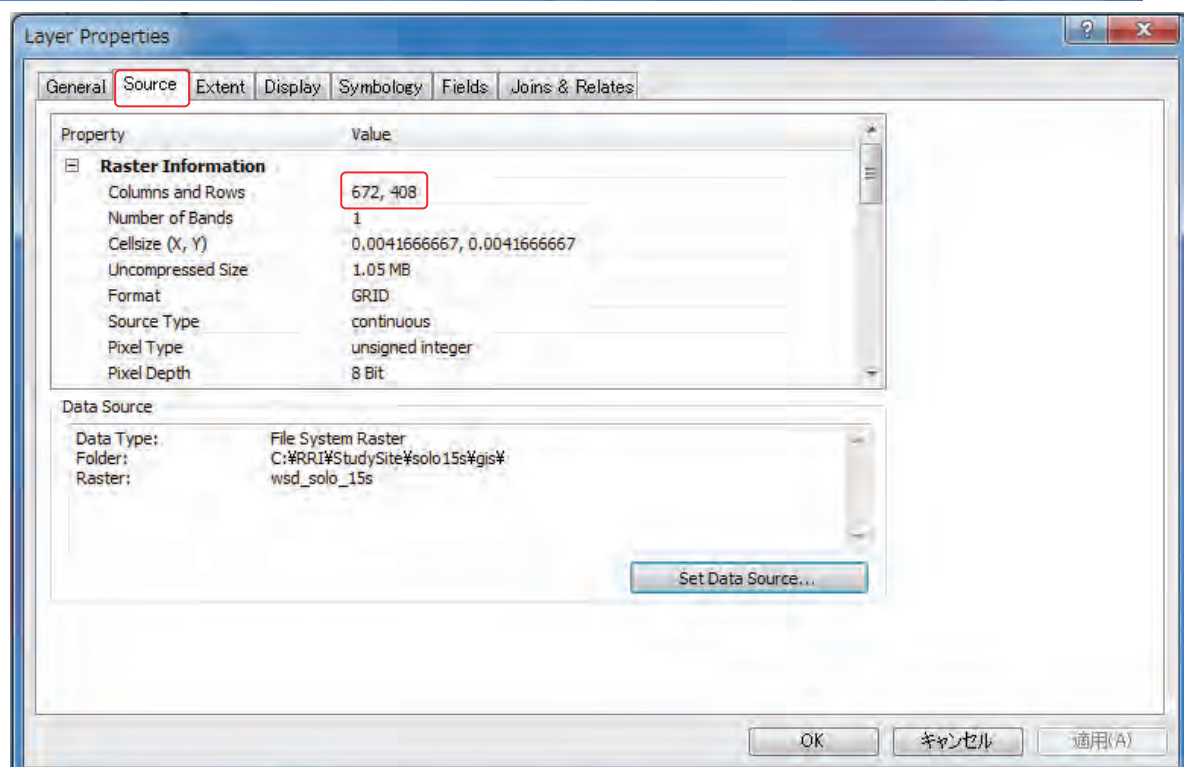
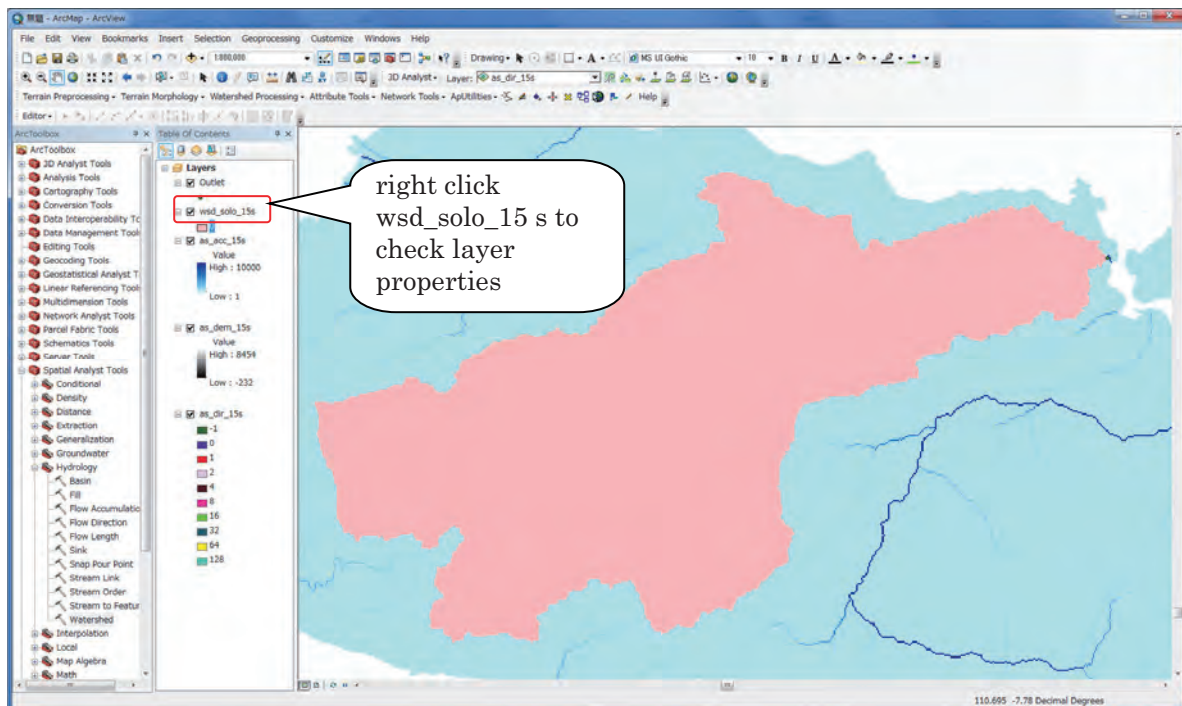
⑥ Using [ArcToolbox] -> [Spatial Analyst Tools] -> [Hydrology] -> [Watershed], delineate a watershed with the defined outlet.

(IMPORTANT) To use [Spatial Analyst Tools] on ArcGIS, you must have the extension and activate it by choosing [Cusomize] → [Extentions] → add a check for [Spatial Analyst].

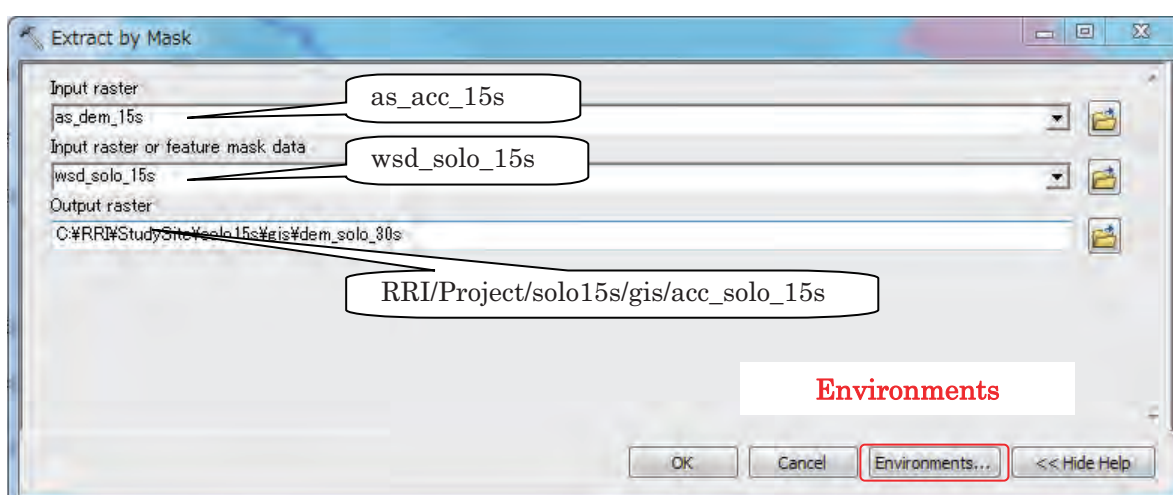
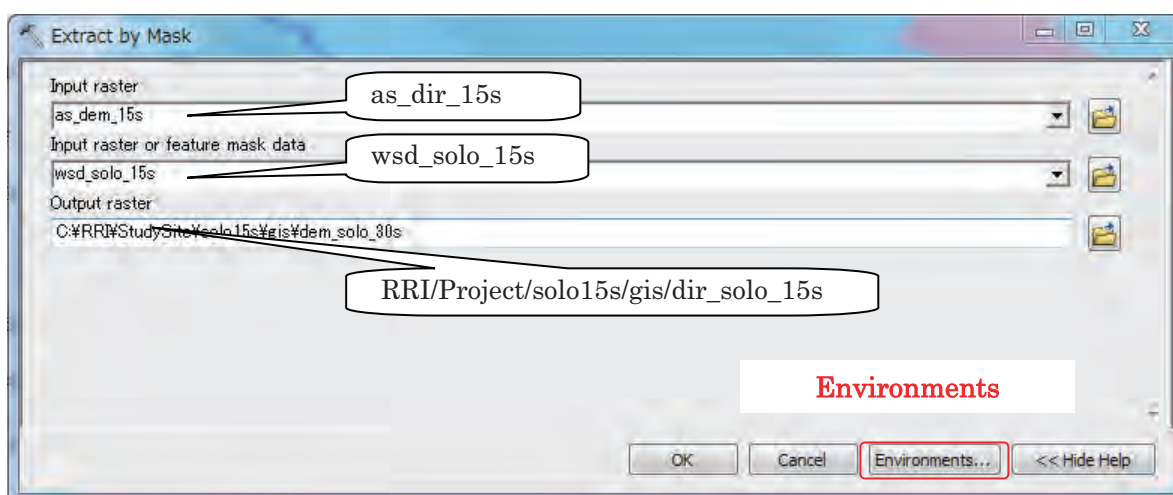
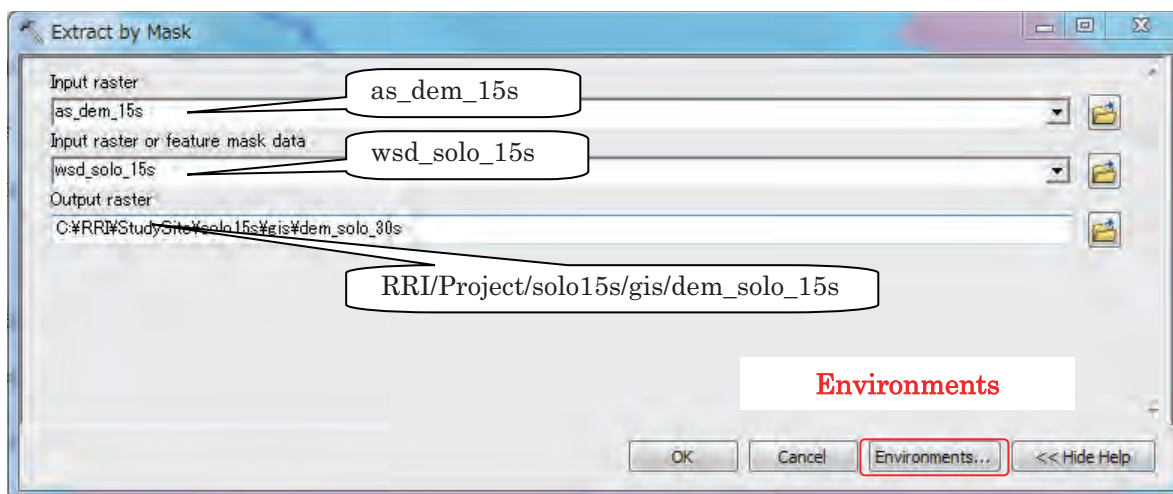


(IMPORTANT) Analysis range must be specified from the “environment” as below;

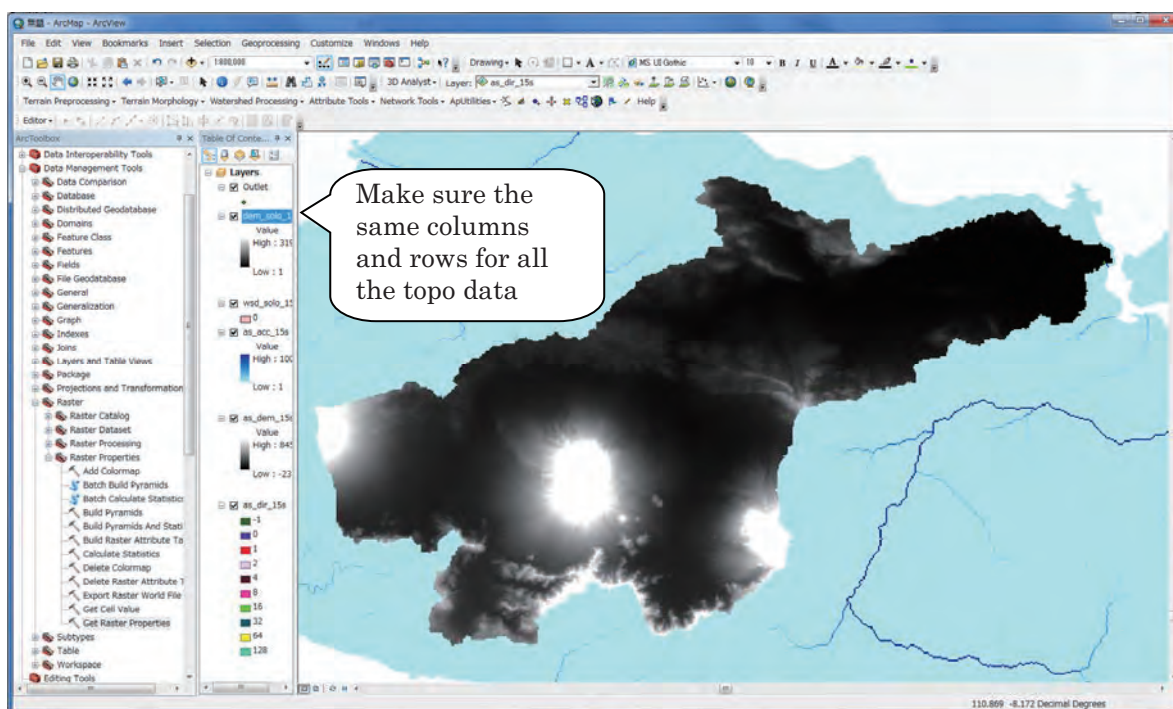




- ⑦ Right click the created watershed raster (e.g. wsd_solo_15s) and check layer properties. Under the “Source” tab, you can check “Columns and Rows”. This will be the number of columns and rows for the topographic data used by RRI Model. If it exceeds more than 1000, using coarser resolution data is recommended to use.
- ⑧ [Spatial Analyst Tools] → [Extraction] → [Extract by Mask], prepare dem (elevation), acc (flow accumulation) and dir (flow direction) masked by the delineated watershed.



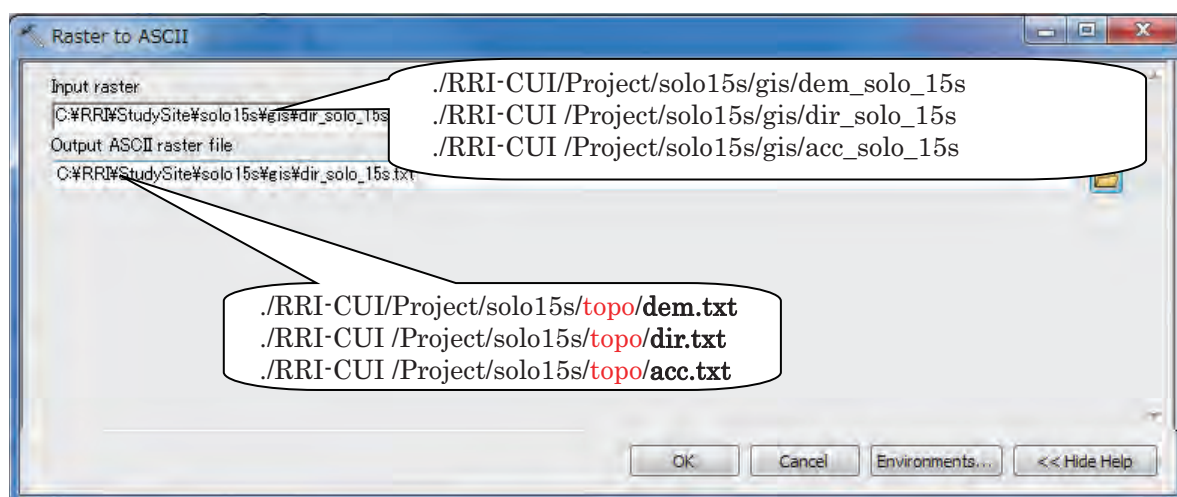
(IMPORTANT) Analysis range must be specified from the “environment” the same as above.



The above figure is the example of **dem**. The **dir** and **acc** must be also extracted in a same way.

- ⑨ Convert all the processed data (i.e. dem, dir, and acc) from ArcGIS Raster to ASCII, which are input data files for RRI Model. Using [Conversion tool] → [Conversion from Raster] → [Raster to ASCII], perform conversion from raster to ASCII for all the three types of topography data.

The output files should be named as “**dem.txt**”, “**dir.txt**” and “**acc.txt**” to be saved under “**topo**” folder in your project folder (e.g. “**./RRI-CUI/Project/solo15s/topo/**”).



The created ASCII data have the following format. Make sure once again all the three datasets have the same numbers in “ncols” and “nrows”.

```

ncols      673
nrows      409
xllcorner  110.2
yllcorner  -8.3
cellsize   0.004166666667
NODATA_value -9999
-9999 -9999 -9999 -9999 -9999 -9999 -9999 -9999 -9999 -9999 -9999 -9999
-9999 -9999 -9999 -9999 -9999 -9999 -9999 -9999 -9999 -9999 -9999 -9999
-9999 -9999 -9999 -9999 -9999 -9999 -9999 -9999 -9999 -9999 -9999 -9999
-9999 -9999 -9999 -9999 -9999 -9999 -9999 -9999 -9999 -9999 -9999 -9999

```

dir.txt

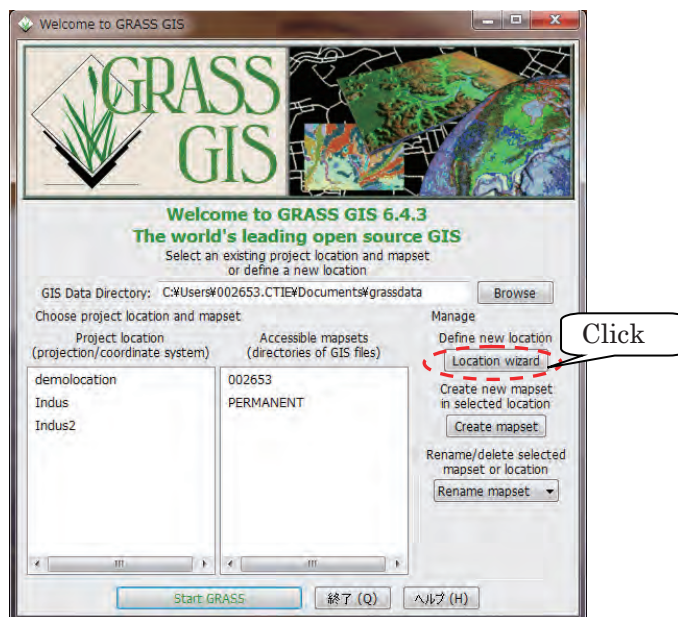
In the RRI model, the following three data must be prepared on the ASCII data format.

- DEM data (dem)
- Flow accumulation data (acc)
- Flow direction data (dir)

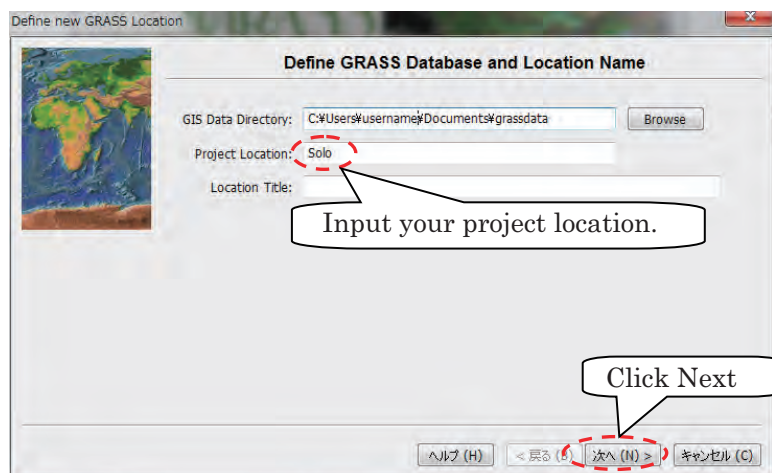
3.3 Delineating HydroSHEDS Data using GLASS GIS (optional)

(If the HydroSHEDS data delineation is completed with ArcGIS, skip this section.)

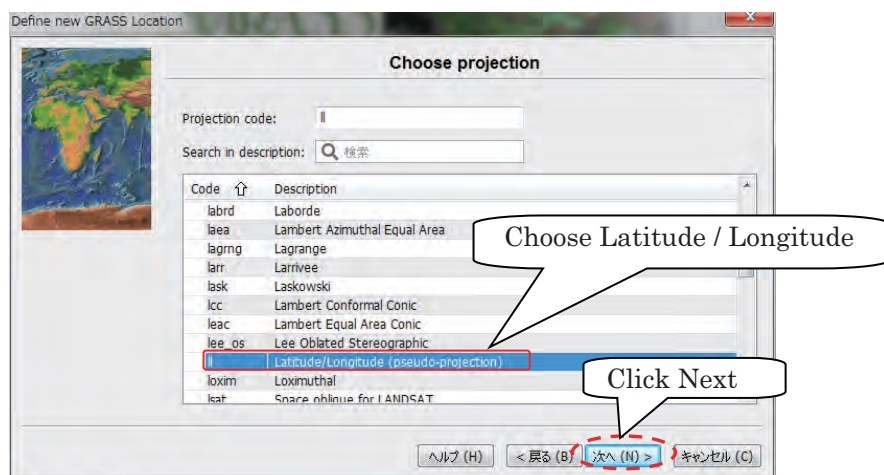
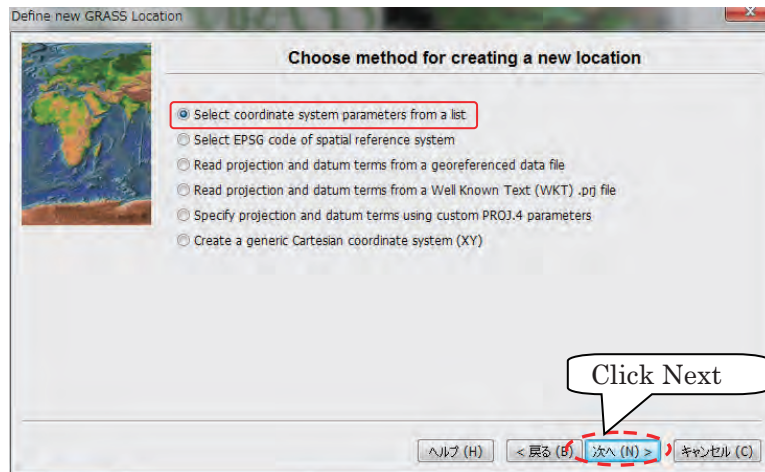
- ① Install the latest GRASS GIS (Latest GRASS in December 2013 is ver 6.4.3.)
(GRASS website: <http://grass.osgeo.org/>).
- ② Start GRASS GIS GUI, and click “Location wizard”.



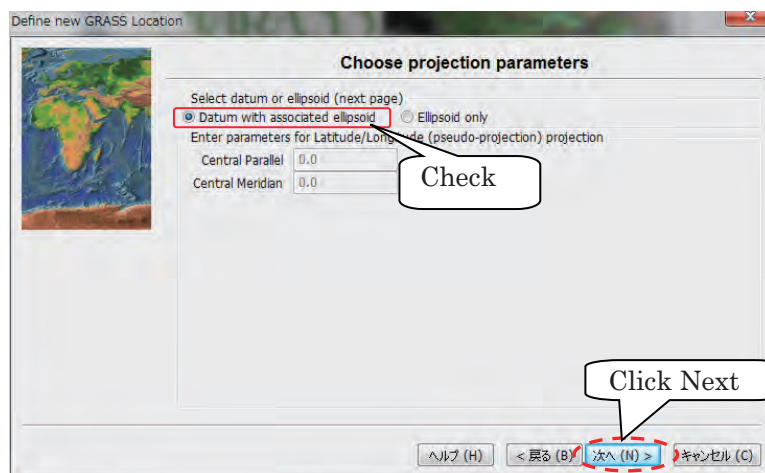
- ③ Input your location name (e.g. Solo) and Click next.



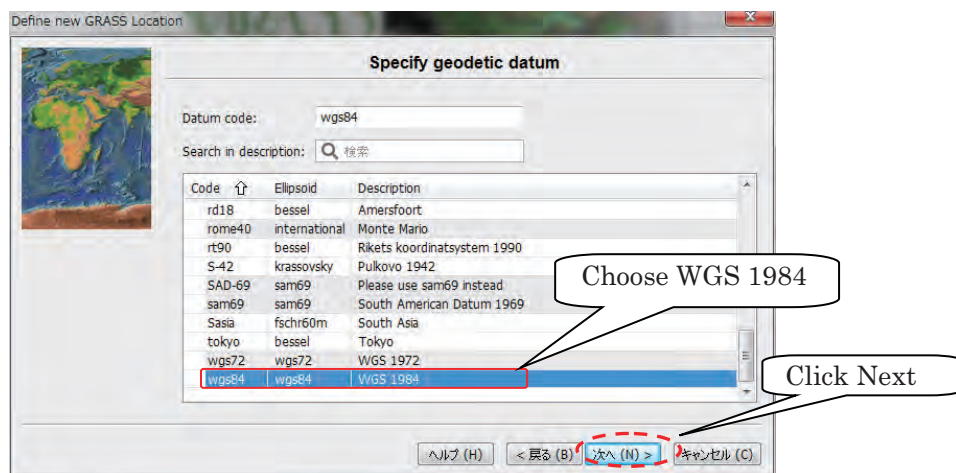
- ④ Select “Select coordinate system parameters from a list” and “Latitude/longitude (Pseudo-projection)” as a projection.



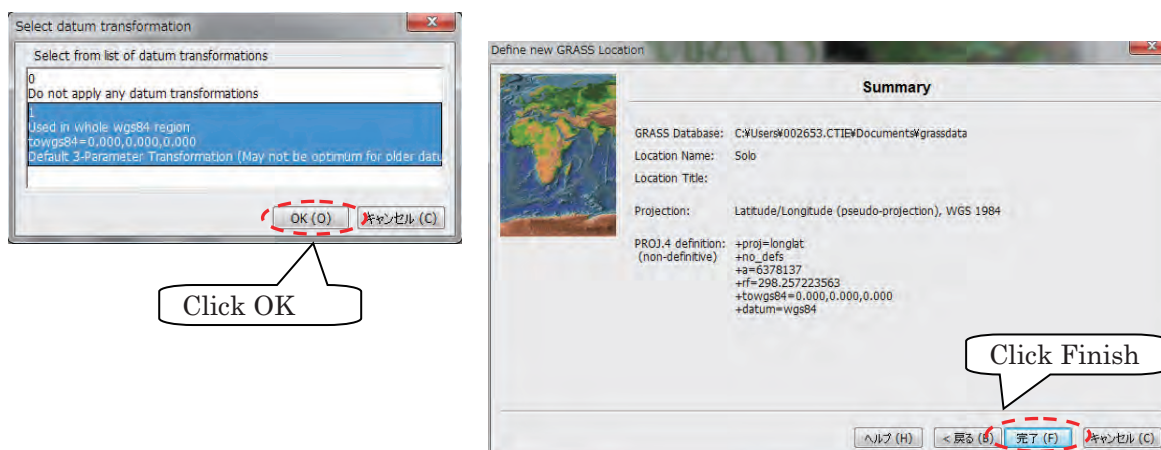
- ⑤ Check “Datum with associated ellipsoid” and click “NEXT”.



- ⑥ Select “WGS 1984” and as a geodetic datum and click “NEXT”.



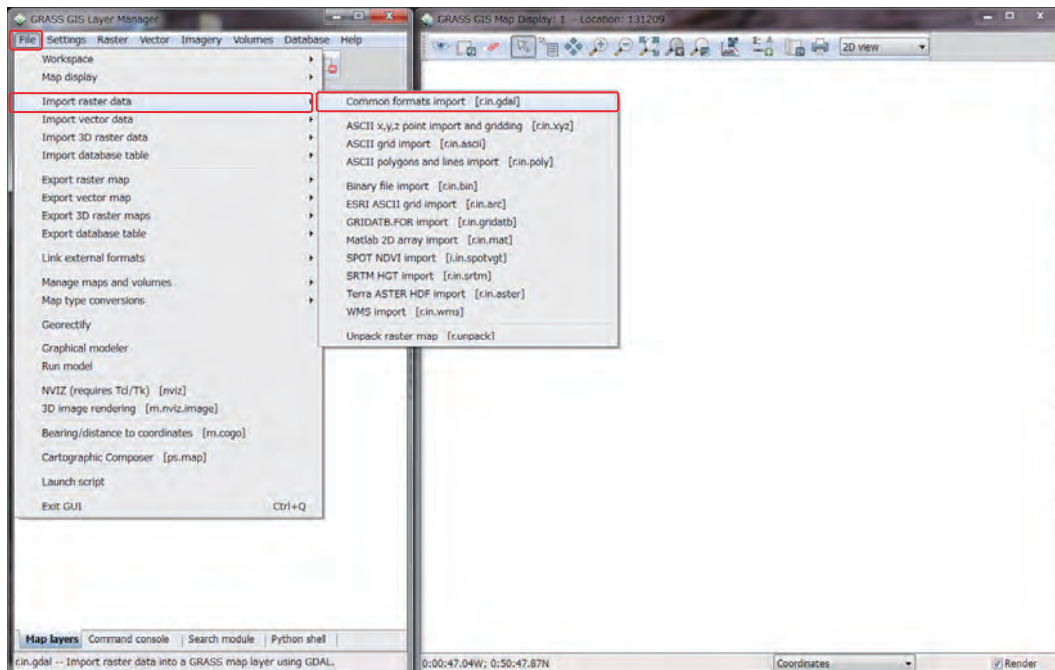
- ⑦ Click “OK” on “Select datum transformation” window and click “FINISH” on Summary window. (Select “Cancel” for default resolution setting).



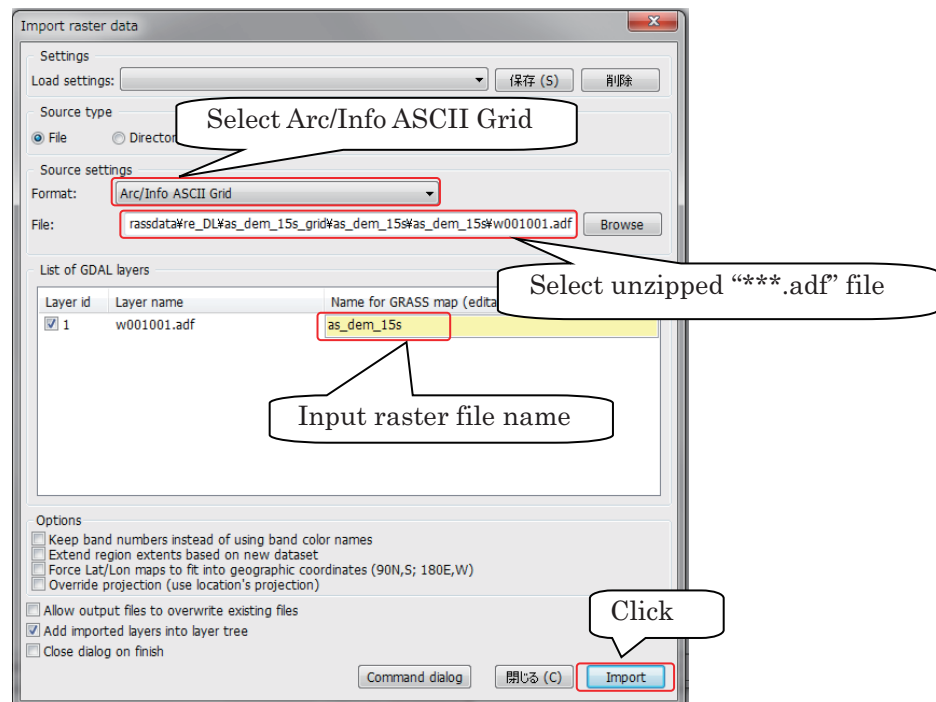
- ⑧ Click “Start GRASS” to start GRASS GIS.



- ⑨ Read in the unzipped files by selecting [File]>[Import raster data] >[Common formats import].

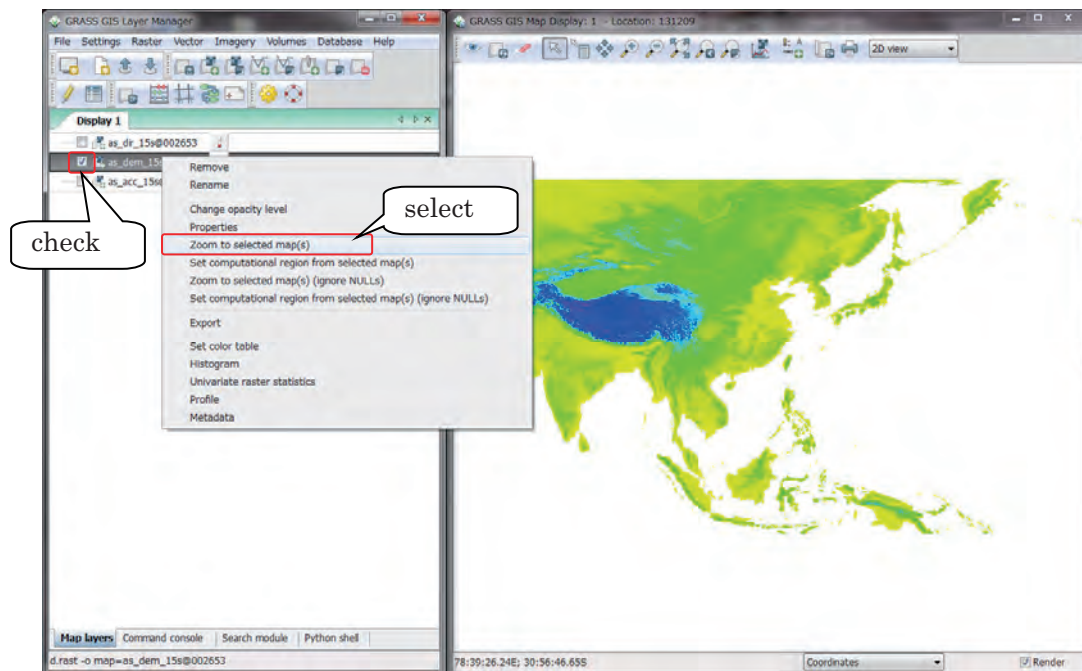


- ⑩ Select “Arc/Info ASCII Grid” from the “Format” list and select unzipped HydroSHEDS raster file name (e.g. w001001.adf for dem). Input “Name for GRASS map (editable)” as “as_dem_15s” for example and click Import.

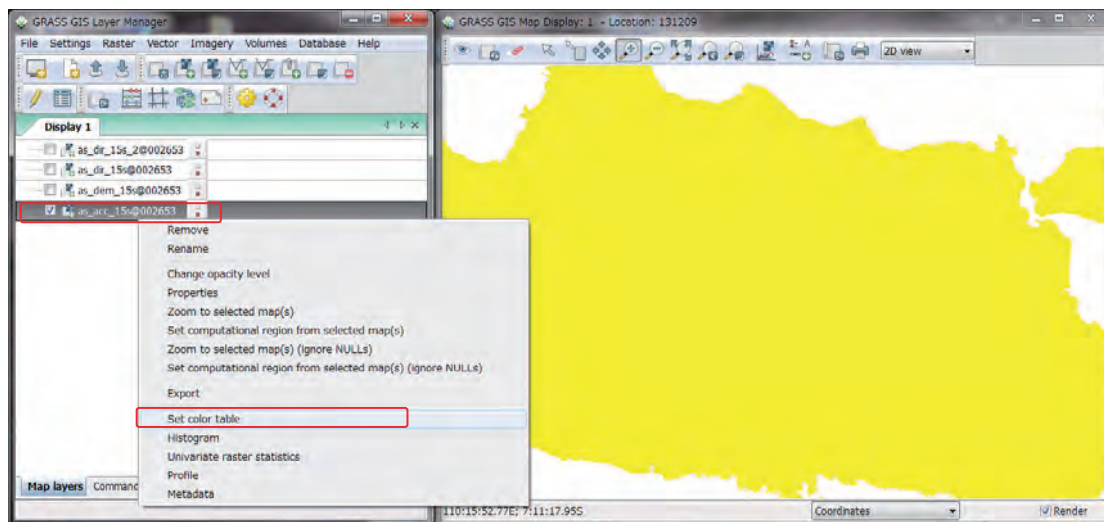


- ⑪ Perform the same operation for all the three types (dem, dir, acc) of topography data.

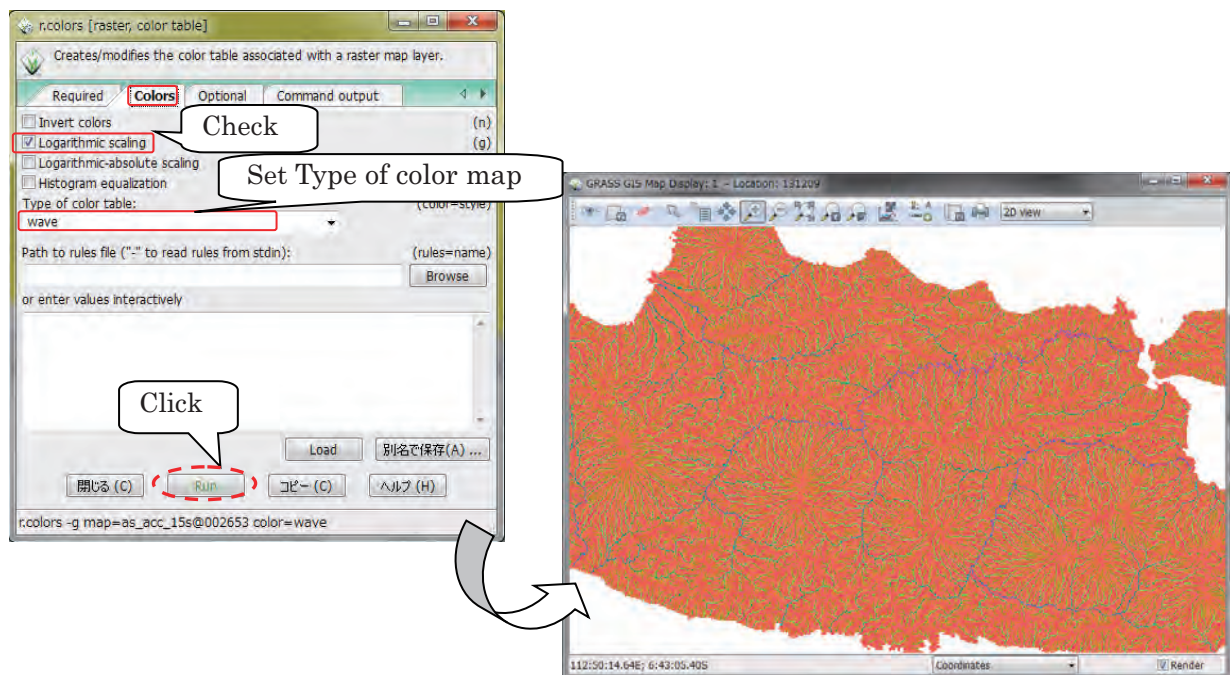
- ⑫ After importing three types of topography data, check the layer and right click on it and “select zoom to selected map(s)”, then the raster file will be displayed in the window. (the following figure shows the example of “dem” display)



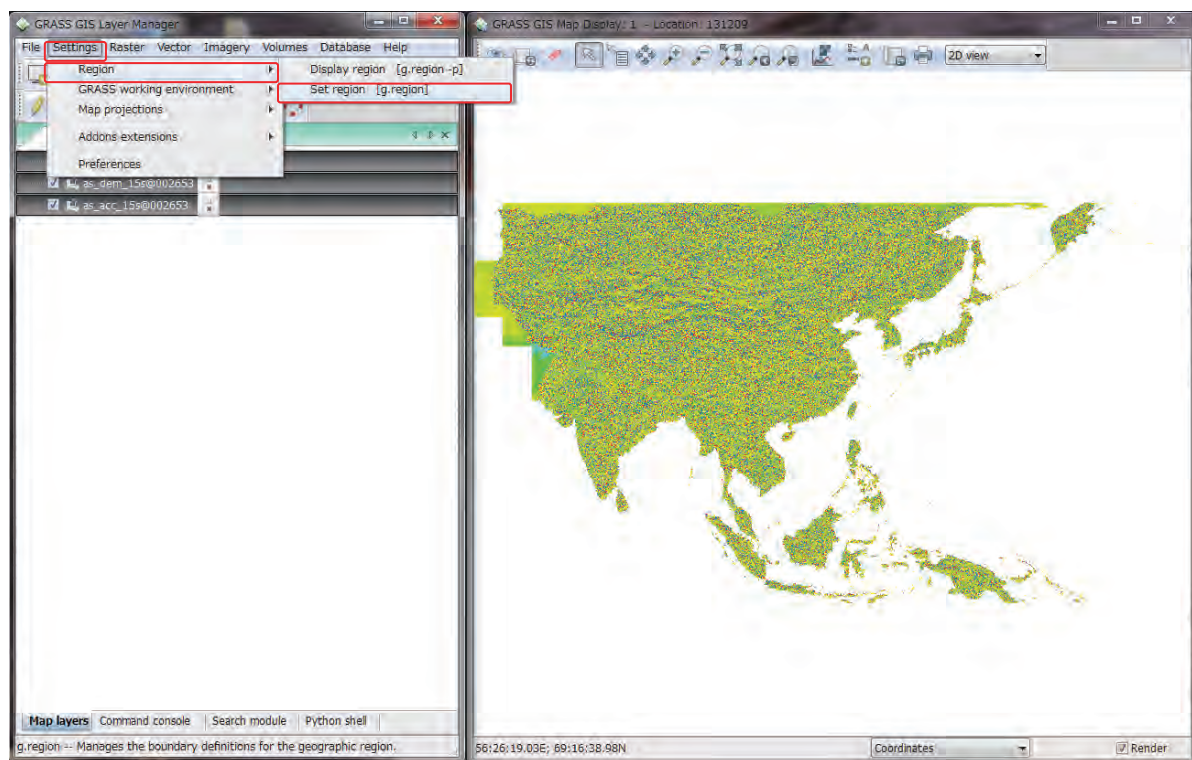
To show the flow accumulation (acc) clearly, right-click the filename of “acc” and select “Set color table”.



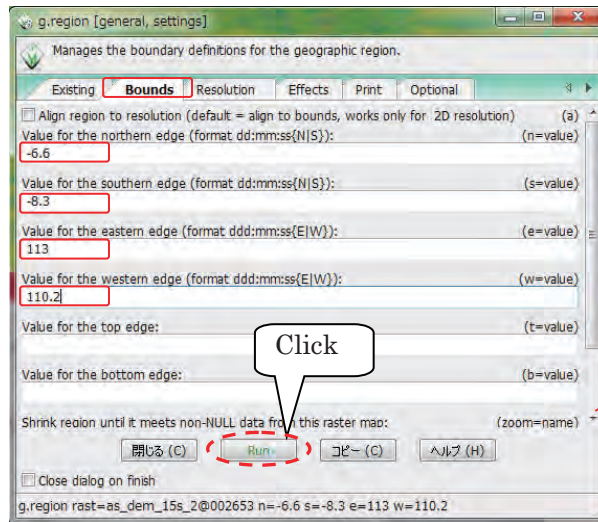
- ⑬ Check “Logarithmic scaling” on “Colors” tab and select “Type of color map”. User can select color table from several color tables. Following figure shows the example selecting “wave” as “Type of color table”.



- ⑭ To set the delineation range, select [Settings] > [Region] > [Set Region].

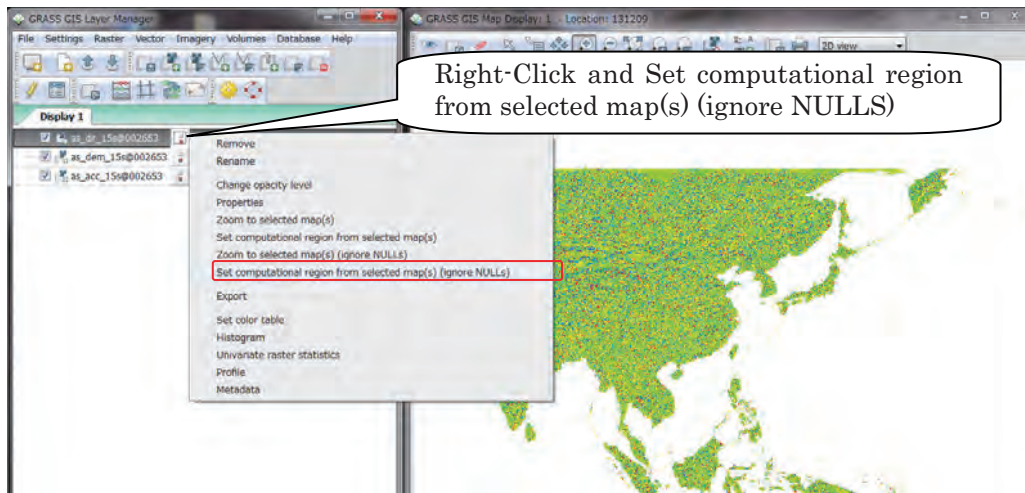


- ⑮ Input values for edges of the target area (coordinates) and set a file for adjusting region cells to cleanly align with a raster map, then click “Run”.
- (To decide your target area, display the flow accumulation data (i.e. as_acc_15s) on top screen to find your target river. The set rectangle range must cover all upstream contributing area.)

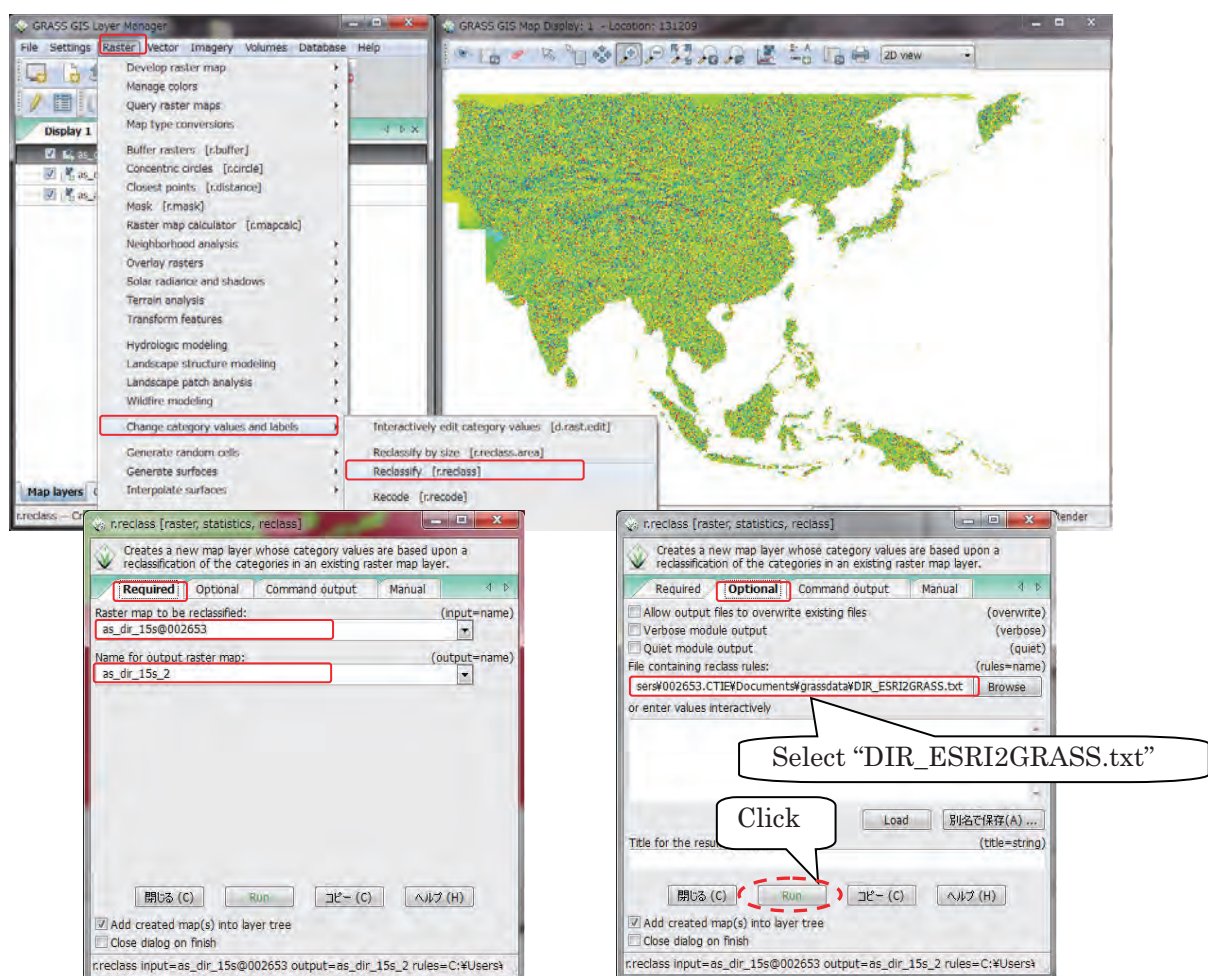


Adjust region cells to
cleanly align with this
raster map → choose
one of the files

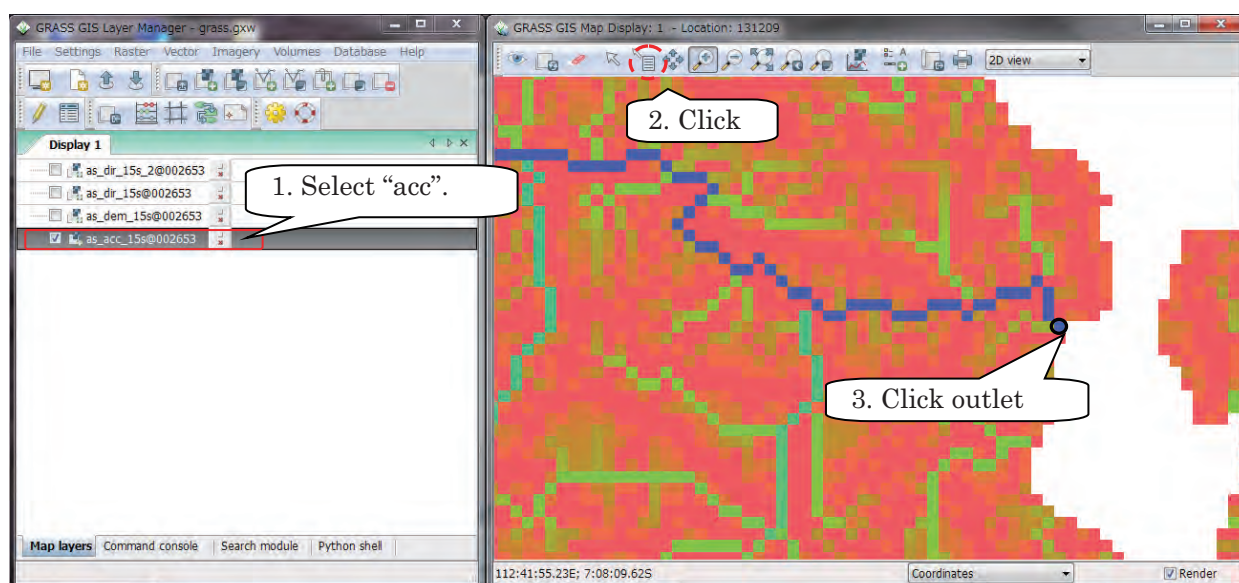
- ⑩ Right-click the filename of “dir” file and select “Set computational region from selected map(s) (ignore NULLS)”. Perform the same operation for all the three types (dem, acc and dir) of topography data.

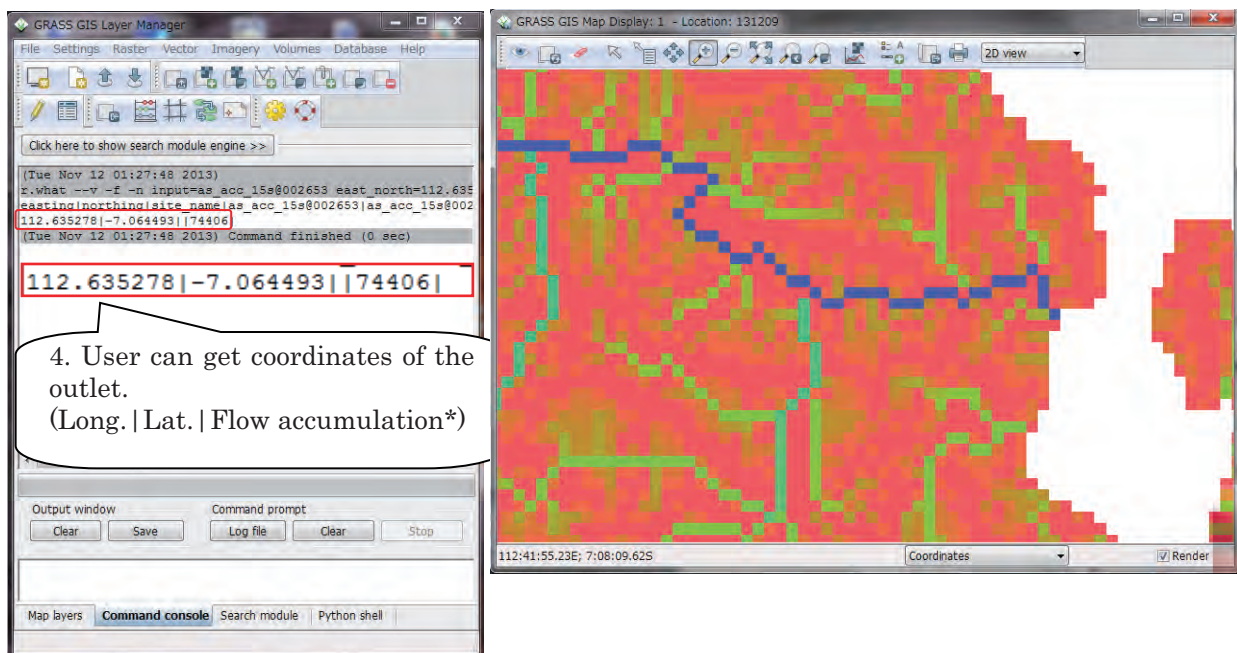


- ⑪ Only for flow direction, change category values (definition of river flow direction in DIR file), from ESRI type (1, 2, 4, 8, 16, 32, 64, 128) to GRASS type (1, 2, 3, 4, 5, 6, 7, 8).
Select [Raster] > [Change category values and labels] > [reclassify]: Select “DIR_ESRI2GRASS.txt”, prepared in package (/RRI/etc), as “File containing reclass rules”

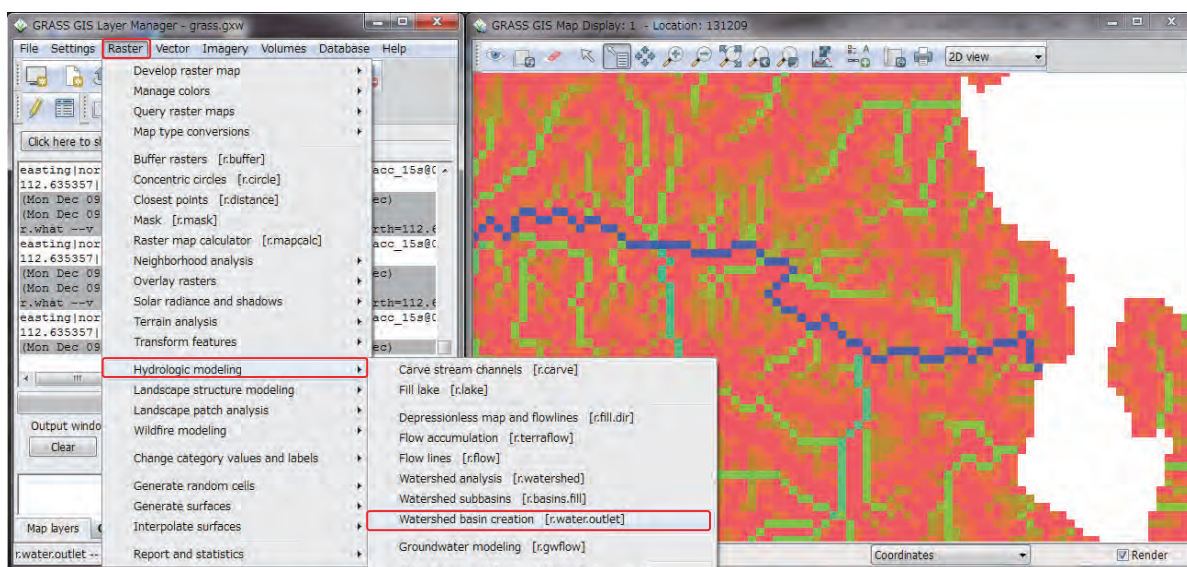


- ⑮ User needs to know the coordinates of the outlet (long./lat.) of target river basin to clip.
Select "acc" file and perform 1, 2, 3 and 4 as shown in following figures.

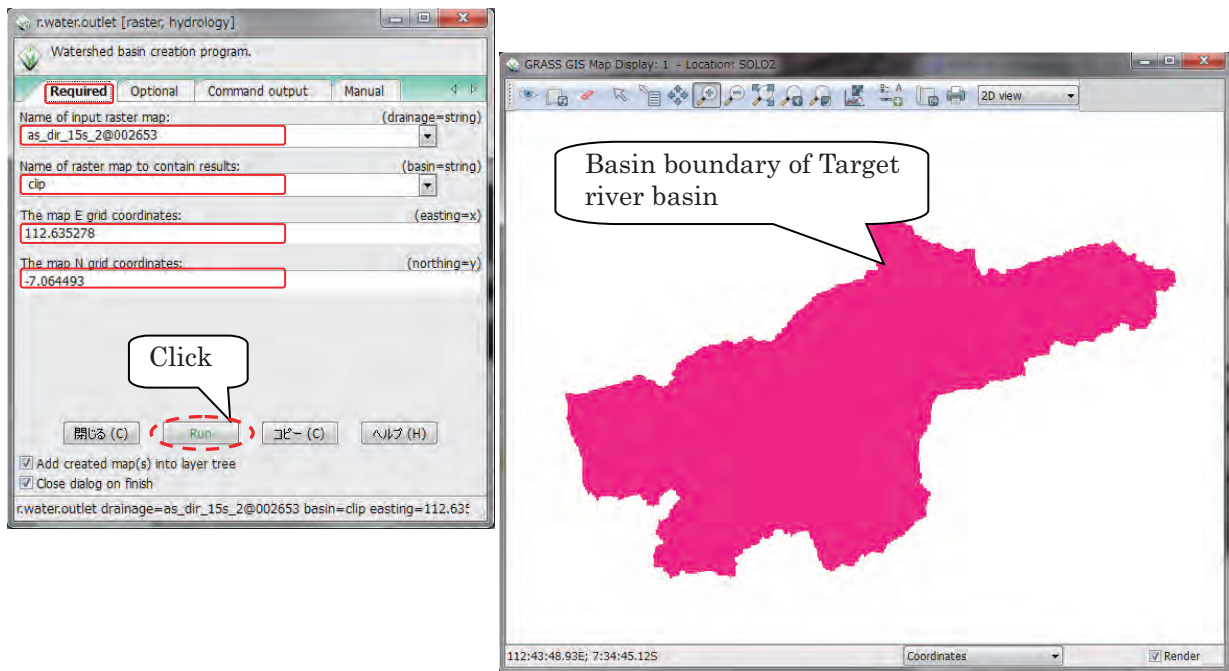




- ①9 To create basin boundary, select the outlet of target river basin.
[Raster]>[Hydrologic modeling]>[Watershed basin creation (r.water.outlet)]

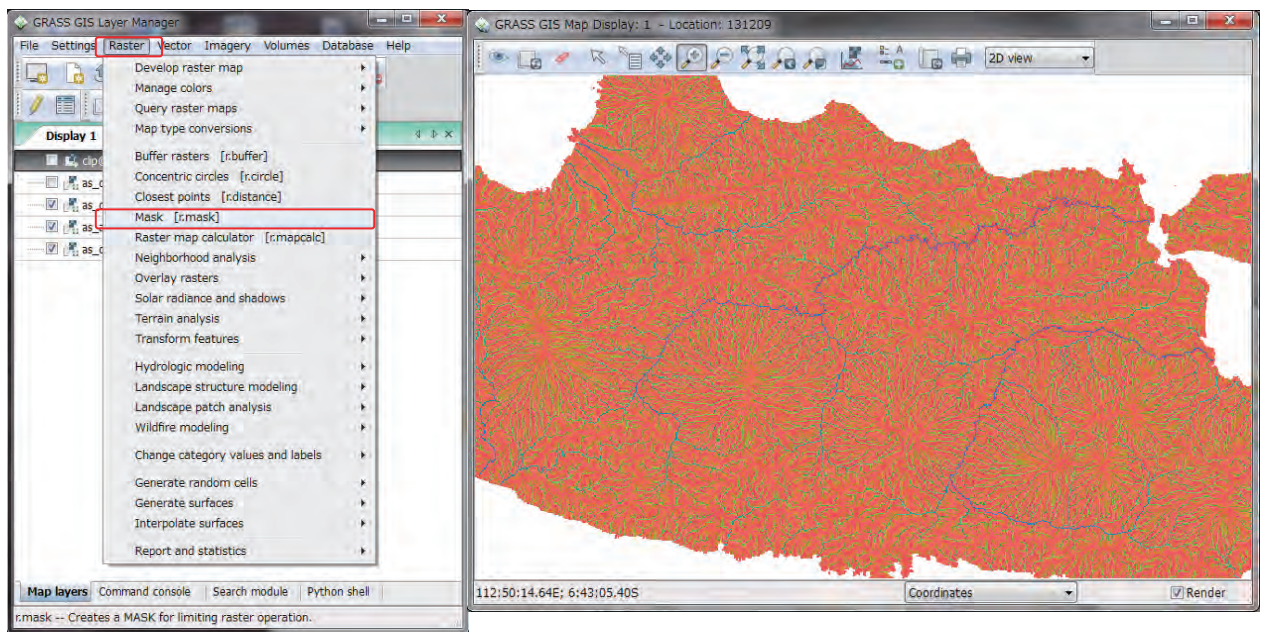


- ②0 Select layer of “dir” file as “Name of input raster map” and input layer name of basin boundary data in “Name of raster map to contain results”.
- ②1 Input x-coordinate(long.) of the outlet in “The map E grid coordinates” and input y-coordinate(lat.) of the outlet in “The map N grid coordinates” and click “Run”. Then, basin boundary layer of target river basin will be shown.

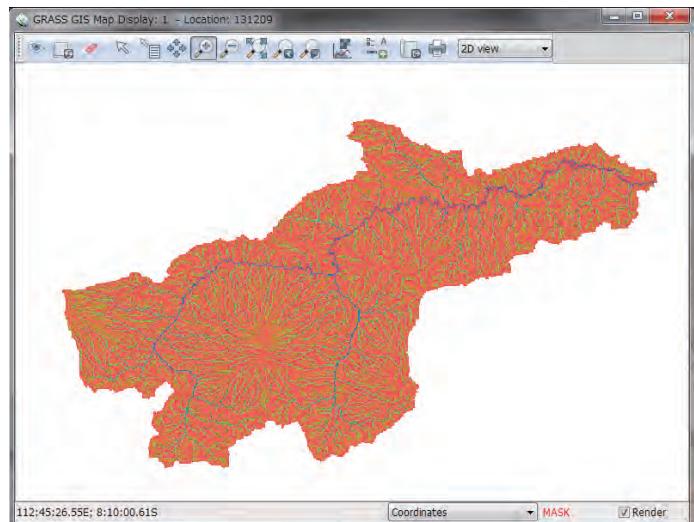
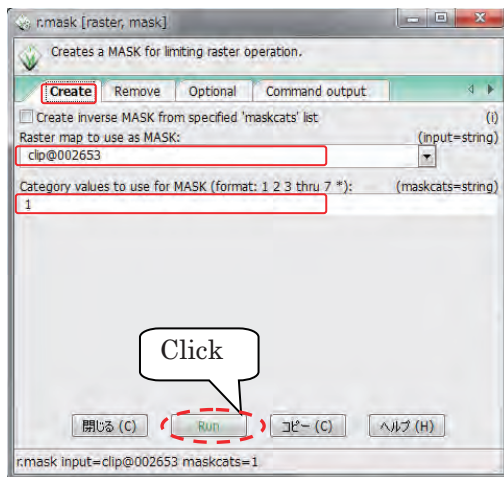


② Clip target river basin by using basin boundary layer.

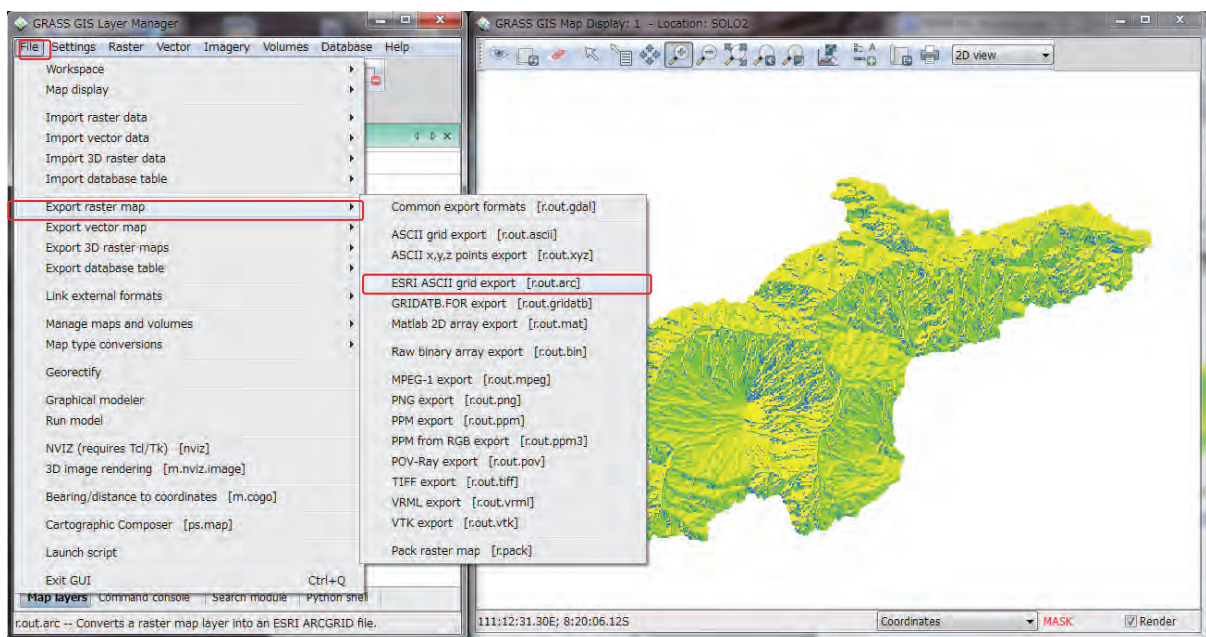
[Raster]>[Mask(r.mask)]



③ Select basin boundary layer as “Raster map to use as MASK” and input “1” in “Category values to use for MASK” on “Create” tab and click “Run”. Then, clipped target river basin will be shown.



- ② Export the three layer data (dem, dir, acc).
 [File]>[Export raster map]>>[ESRI ASCII grid export]

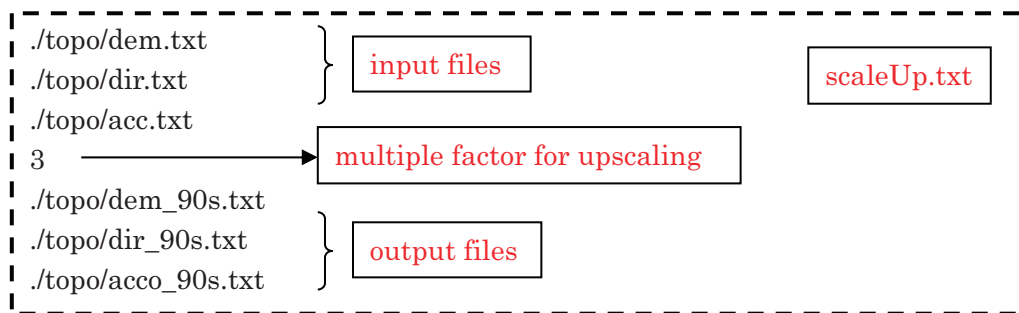


- ③ Select three layer data (dem, dir, acc) and input output file name in “Name for output ARC-GRID map” and click “Run”.
- ④ Perform the same operation for all the three layers (dem, dir, acc).

3.4 Upscaling the spatial resolutions of DEM, DIR and ACC (optional)

If a user needs to upscale the resolutions of the topography files (dem, dir and acc), one can use a program called “**scaleUp.exe**”. By specifying a multiple factor for upscaling the resolution, the program outputs new dem, dir and acc based on the original topography files. For example, if the spatial resolutions of the topography files are 30 sec and the specified multiple factor is 3, the program creates the topography files having 90 sec (30s x 3). The following shows the procedure to use the program.

- ① Copy “scaleUp.txt” file from “RRI-CUI/etc/scaleUp/” and save it under your project folder (e.g. RRI-CUI/Project/solo30s/)



- ② Type in “**scaleUp.exe**” and return to execute **scaleUp.exe** program and find the created three sets of the topographic data indicated in L5, L6 and L7 in **scaleUp.txt**

3.5 DEM Data Adjustment

There are some hollows in the original HydroSHEDS elevation data. Some of them represent actual topographic features, while some of them are caused due to the intrinsic characteristics of DEM. For example, deep and narrow valley, in which a river flows, may be blocked by surrounding topography because of the DEM resolution. In that case, the simulated water depths and river discharges with the original DEM are unrealistic.

Therefore, the following DEM adjustment is always recommended to avoid the unrealistic hollows in the original DEM. The provided program called **demAdjust2** (**demAdjust2.exe**) follows the flow direction of HydroSHEDS and remove all the negative slope along the flow direction by carving and lifting the original DEM.

The algorithm of **demAdjust2** is as follows;

-
1. Based on the flow direction, demAdjust2 finds upstream cells (i.e. cells with no inflow).
 2. Among the detected upstream cells, searching order is determined from the total length of the flow paths from each upstream cell to its most downstream cell.
 3. Following the above decided order, demAdjust2 adjusts elevations based on the following procedures.

- 1) The negative elevation is set to be zero.

- 2) Lifting: If a single cell is extremely low (likely as a noise error) compared to its upstream and downstream cells, the cell's elevation will be replaced by the same elevation as the upstream cell. The parameter "lift" is used as the threshold to detect sudden drop and its default value is set to be 500 m.

- 3) Carving: If the elevation suddenly increases along the flow direction, the cell's elevation will be replaced by the same elevation as the upstream cell. The parameter "carve" is used as the threshold to detect the sudden increase and its default value is 5 m.

- 4) Lifting and Carving: By searching from the most upstream, it finds a cell whose downstream elevation is higher than that cell (point L). By searching from point L toward downstream, it finds a cell whose downstream is lower than that cell (point H). The point L is lifted and point H is carved by the parameter "increment", whose default is 0.01 m.

The demAdjust2 program conducts each of the above procedure repeatedly for each flow path ways from all the detected upstream cells until all negative slopes are removed. Note that the above procedure does not change flow direction.

Edit demAdjust2.txt if necessary and run demAdjustment2 program by typing in "demAdjustment2.exe" on Command Prompt under the project folder (e.g. solo15s or solo30s).

The process is necessary even if a user would like to use original dem data. "demAdjust2" program modifies not only "dem" data but also flow direction data "dir". The modified "dir" (named as "adir") has flow direction equals to zero at outlet cells. This operation must be done and "adir" always must be used for RRI simulation. Also note that there is no correction for "acc", so use the original "acc" regardless the demAdjust2 procedure.

Read the adjusted dem and dir data to ArcGIS to visualize the data.

Select [ArcToolBox] > [Conversion tool] > [Conversion from raster] > [ASCII→Raster].

"adem", "adir", "acc" are the three important topography data for the RRI simulation.

4. Preparing Input Rainfall Data

This section explains the method to prepare rainfall data for RRI Model. A user can prepare the data by any method as far as it follows a specified data format. Currently three program sets are prepared for processing:

- 1) gauged rainfall with Thiessen polygon interpolation (/etc/rainThiessen),
- 2) GSMaP satellite based rainfall (/etc/GSMaP) and
- 3) 3B42RT (/etc/3B42RT) satellite based rainfall.

4.1 Prepare Input Rainfall Data from Gauged Rainfall Records

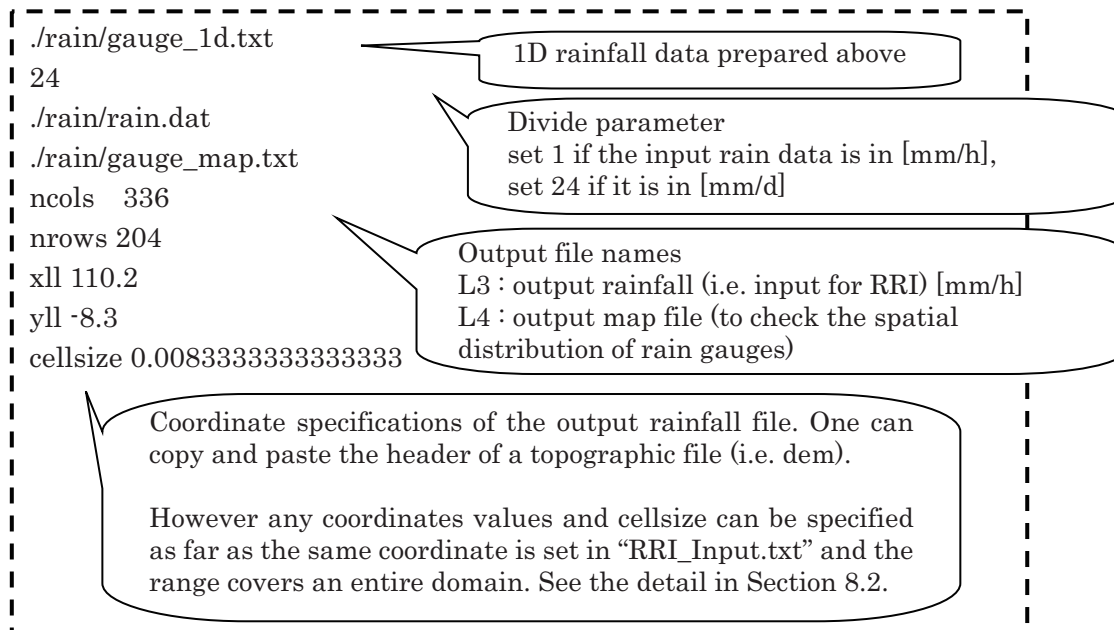
To use ground gauged data for creating input rainfall for the RRI simulation, one can use **rainThiessen.exe** (/RRI-CUI/etc/rainThiessen/rainThiessen.f90) program.

- ① First, prepare rain gauge data in Excel (e.g. /solo30s/rain/gauge_solo_1d.xlsx).

	A3	B3	C3	D3	E3	F3	G3	H3	I3	J3	K3	L3	M3	N3
1	125													
2	lat	-7.1945	-7.12661	-7.08353	-7.22057	-7.2496	-9999	-7.23782	-7.24462	-7.19858	-7.19815	-7.25191	-9999	-7.17517
3	lon	111.954	112.1118	111.5484	111.1092	111.8431	-9999	111.5085	111.8725	112.0301	111.9285	111.4876	-9999	112.0516
4		0	0	0	0	0	0	0	0	0	0	0	0	0
5	86400	15	5	14	0	2	2	6	0	0	0	0	2	3
6	172800	40	52	42	85	61	30	65	68	59	70	48	4	4
7	259200	0	0	0	0	0	0	0	0	0	0	16	0	0
8	345600	14	0	0	0	5	8	0	3	0	0	11	5	0
9	432000	0	0	0	0	0	0	0	0	0	0	0	0	0
10	518400	9	0	0	0	0	0	0	0	0	0	0	0	0
11	604800	16	0	0	0	0	0	0	0	0	0	0	0	0
12	691200	0	0	0	0	0	0	0	0	0	0	0	0	0
13	777600	4	0	0	0	0	0	0	0	0	0	0	0	0
14	864000	6	0	0	0	0	0	0	0	0	0	0	0	0
15	950400	8	0	0	0	0	0	0	0	0	0	0	0	0
16	1036800	9	0	0	0	0	0	0	0	0	0	0	0	0
17	1123200	0	0	0	0	0	0	0	0	0	0	0	0	0
18	1209600	42	0	2	0	0	0	10	0	0	0	0	0	0
19	1296000	8	8	37	3	5	22	0	6	12	30	0	40	7.5
20														

Set any negative value (e.g. -999) for missing data, not to be used for the interpolation.

- ② Select all cells having values, and copy and paste on a text editor. Then save it as txt file (e.g. gauge_1d.txt)
- ③ Edit the input file "rainThiessen.txt" as follows.



- ④ On command prompt under the project file (e.g. RRI/Project/solo30s/), type in "rainThiessen.exe" to execute the program.
- ⑤ Confirm an input rainfall file for RRI Model (e.g. "rain.dat") is newly created.

4.2 Prepare Input Rainfall Data from GSMaP

GSMaP products were updated on September 2014. Now the products include GSMaP_NRT (realtime), GSMaP_MVK (standard ver.5 or ver.6) and GSMaP_Gauge (gauge composite). Refer to the following website for the latest information and the registration to download the data. (<http://sharaku.eorc.jaxa.jp/GSMaP/index.htm>)

4.2.1 Download GSMaP Data

- ① First, create "gsmmap" folder under your project folder (e.g. solo30s).
- ② Under "gsmmap" folder, create "infile" and "cutfile" folders.
- ③ Download all GSMaP rainfall data you would like to proceed and save them in "infile".

4.2.2 Calculate Rainfall Data Range for a Target Catchment

To calculate the range for the data delineation, `calc_area_gsmmap.exe` can be used. Before executing `calc_area_gsmmap.exe`, copy `/etc/GSMaP/calc_area_gsmmap.txt` and paste it under the created "gsmmap" folder.

In the copied “calc_area.txt”, specify “horizontal_resolution [d]” and “temporal_resolution [h]” of original GSMap product you will use. Also specify “ncols” to “cellsize” based on the target catchment, whose parameters can be obtained from the headers of topographic files of “dem”, “acc” or “dir”.

Note: The horizontal resolution of GSMap product is either 0.1 [deg] or 0.25 [deg], and the temporal resolution is either 1 [h] or 24 [h].

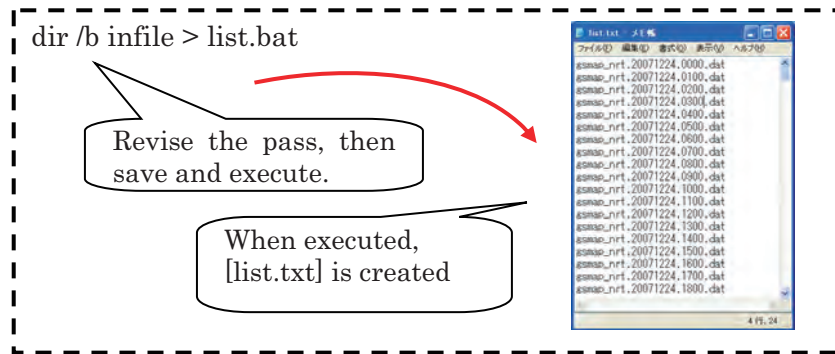
(In case of 0.1 deg → xul = 0.05, yul = 59.95; 0.25 → xul = 0.125, yul = 59.875).

Running calc_area_gsmmap.exe creates a file named “out_by_calc_area_gsmmap.txt”.

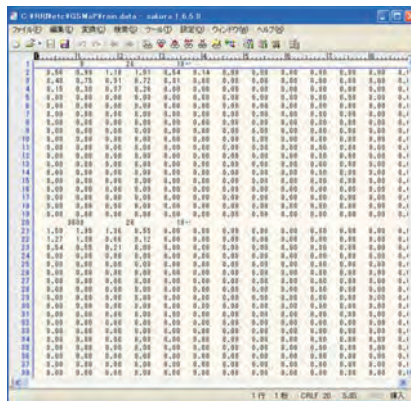
horizontal_resolution [d] :	0.1000000	out_by_calc_area_by_gsmmap.txt
temporal_resolution [h] :	1	
xll :	110.2000	
yll :	-8.300000	
xur :	113.0000	
yur :	-6.600000	
xll_rain :	110.1250	Information that is necessary to delineate GSMap (jleft, ibottom, irlight, itop)
yll_rain :	-8.375000	
xur_rain :	113.1250	
yur_rain :	-6.375000	
jleft :	440	
ibottom :	273	
jright :	452	
itop :	265	Rainfall location information to be specified in the RRI_Input.txt (xllcorner, yllcorner, cellsize)
xllcorner_rain (raster) :	110.0000	
yllcorner_rain (raster) :	-8.500000	
cellsize_rain :	0.2500000	

4.2.3 Delineating GSMap Data for Target Area

- ④ Unzip all the downloaded files (a linux user may use “gunzip *”, otherwise please find an appropriate program to unzip “.dat.gz” files)
- ⑤ Copy “/etc/GSMap/makeList.bat” under “gsmmap” folder and execute it to list up all the unzipped files as “list.txt”



- ⑥ Type in “read_gsmmap.exe” on command prompt at “gsmmap”.



Running the program creates “rain.data”, which is rainfall input file for RRI simulation

4.3 Prepare Input Rainfall Data from 3B42RT

4.3.1 Download 3B42RT Data

- ① Access the following FTP site for downloading 3B42RT data
ftp://trmmopen.gsfc.nasa.gov/pub/merged
- ② Download "3B42RT.20****.7R2.bin.gz" files from the FTP site and save them under ./etc/3B42RT/read/infile/

4.3.2 Calculate Rainfall Data Range for a Target Catchment

To calculate the suitable range for the delineation, ./etc/3B42RT/calc_area.f90 program can be used. See details in 4.2.2, the same process is used for GSMaP data extraction.

4.3.3 Delineating 3B42RT Data for Target Area

- ① The following process uses “bash script”. Windows users may install “clink” program to run bash scripts (*.sh) on windows command prompt. The “clink” program can be downloaded from: <http://code.google.com/p/clink/>
- ② To calculate the suitable range for the delineation, ./etc/3B42RT/calc_area.f90 program

can be used. See details in 4.2.2 because the same process is applied also to GSMap data extraction.

- ③ Execute "**bash unzip.sh**" in /etc/3B42RT/read/ to unzip the downloaded files under ./etc/3B42RT/read/infile.
- ④ Edit "**read_rt_file.sh**" file to set extraction range in L4 to L7 (jleft, ibottom, jright, itop) suggested by calc_area.f90.
- ⑤ Execute "**bash read_rt_file.sh**" to extract data
Note: the extract does not run if the same output files already exist
- ⑥ Edit "**combine.sh**" by setting the extraction range in L4 to L7 (jleft, ibottom, jright, itop) suggested by "out_by_calc_area.txt", and set output file name on L9. Also edit L14, L17 and L20 to indicate which year, month and day of the data should be processed.
- ⑦ Execute "**bash ./combine.sh**" to combine all rainfall files to create the RRI input, so that the rainfall file, which can be read by the RRI program, will be created.

4.4 Format of Input Rainfall Data for RRI Model

Here is the format of the input rainfall data used for RRI Model. By specifying the cell size, xll_corner and yll_corner of the rainfall data into a control file of RRI model (i.e. "RRI_Input.txt"), the model can overlay the rainfall distribution even if the ranges and the resolutions are different from topographic data as far as the rainfall data covers all the simulation extent.

The screenshot shows a spreadsheet with the following structure:

- Columns:** The first column contains time stamps (e.g., 0, 1, 2, 3, 4, 5, 6, 7, 8, 9, 10, 11, 12, 13, 14, 15, 16). The subsequent columns contain numerical values representing rainfall data.
- Annotations:**
 - A red box labeled "Number of X, Y grids" points to the first column.
 - A red box labeled "Number of X grids" points to the first row.
 - A red box labeled "time stamp" points to the first cell of the first column.
 - A red box labeled "time stamp" points to the first cell of the first column.

- ※ The input unit of rainfall must be always **mm/hr** regardless the data interval.
- ※ The time interval is not necessary to be constant.
- ※ Rainfall between 3600 and 7200 is written under the time stamp of 7200 (just like rain gauge data).

【RRI_Input.txt】 · · · Control file of the RRI Model

```

RRI_Input_Format_Ver1_4_2

./rain/rain.dat
./topo/adem.txt
./topo/acc.txt
./topo/adir.txt

0          # utm(1) or latlon(0)
1          # 4-direction (0), 8-direction(1)
360        # lasth
600        # dt
60         # dt_riv
96         # outnum
110.2d0    # xllcorner_rain
-8.3d0     # yllcorner_rain
0.00833333d0 0.00833333d0 # cellsize_rain

```

RRI_Input.txt

Coordinates and grid size of the south-west end of the rainfall data range

4.5 Calculation of Catchment Average Rainfall

To calculate catchment average rainfall from the input rainfall data, a user can use “**rainBasin.exe**” program. To run the program, “**rainBasin.txt**” must be prepared in the following way.

```

./rain/rain.dat
./topo/adem.txt
110.2d0
-8.3d0
0.00833333d0 0.00833333d0
./rain/rain_hyeto.txt
./rain/rain_dist.txt
./rain/rain_cum.txt

```

rainBasin.txt

L1 : [in] rainfall file (RRI format) [mm/h]

L2 : [in] catchment mask file (e.g. dem file)
L3 : [in] rainfall xll corner
L4 : [in] rainfall yll corner
L5 : [in] rainfall cellsize (x, y)
L6 : [out] hyetograph [mm/h]
L7 : [out] total rainfall distribution map [mm]
L8 : [out] cumulative rainfall [mm]

On command prompt, type in “rainBasin.exe” to create three output files identified in L6, L7 and L8 to show hyetograph, total rainfall distribution map and cumulative rainfall, respectively.

Note: To calculate average rainfall over a sub-catchment, one can replace the file indicated in L2. First, one can use GIS to delineate the sub-catchment and convert the mask into ASCII GIS format. For areas having pixel values greater than -10 will be considered as a sub-catchment area.

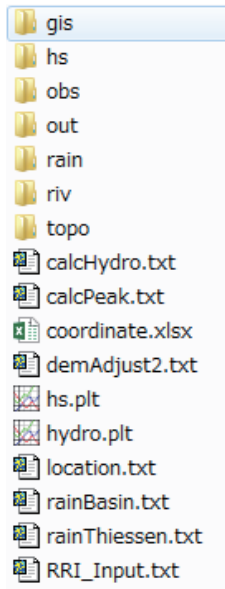
5. Conditions Setting for RRI Simulation

5.1 Folder Configuration

The following shows the folder configuration inside `./RRI-CUI/Project/solo30s`

`[/RRI-CUI/Project/solo30s]`

Folders-



topo : Stores following sets of topographic data

- Digital elevation model (dem.txt)
- **Adjusted** digital elevation model (adem.txt)
- Flow accumulation (acc.txt)
- Flow direction (dir.txt)
- **Adjusted** flow direction (adir.txt)
- (optional) Land use data (landuse.txt)

rain : Stores following sets of input rainfall data

- Rainfall data (rain.dat)
- (optional) Evapotranspiration data (PET.txt)

out : Stores simulation results for each output time step

- *hr_* : River water depth [m]
- *hs_* : Slope water depth [m]
- *qr_* : River discharge [m³/s]
- *qu_* : Slope discharge for x direction [m³/s]
- *qv_* : Slope discharge for y direction [m³/s]
- *gampt_ff* : Green-Ampt cumulative water depth [m]
- *storage.dat* : water balance checking file

hs : Stores figures of inundation depths (hs) by gnuplot

gis : Stores GIS related data

obs : Stores observation related data

riv : Stores river section related data

【Control files】

- **RRI_Input.txt** : RRI model control file for `0_rri_1_4_2.exe`
- **demAdjust2.txt** : demAdjustment program (`demAdjust2.exe`) [pre-processing]
- **rainThiessen.txt** : Rainfall processing program (`rainThiessen.exe`) [pre-processing]
- **calcHydro.txt** : Hydrograph calculation program (`calcHydro.exe`) [post-processing]
- **calcPeak.txt** : Peak inundation depth calculation program (`calcPeak.exe`) [post-processing]
- **rainBasin.txt** : Rainfall analysis program (`rainBasin.exe`) [post-processing]

【Input Files Other Programs and Files】

- *hydro.plt* : gnuplot script to draw hydrograph
- *hs.plt* : gnuplot script to create inundation depths figures (prepared by `/etc/prepHsPlt`)
- *ciirdubate.xlsx* : excel file to covert from (i, j) to (x, y) or (x, y) to (i, j)
- *location.txt* : Location list to draw hydrographs

5.2 RRI Model Control File (RRI_Input.txt)

L1	RRI_Input_Format_Ver1_4_2	
L2		
L3	./rain/rain.dat	
L4	./topo/adem.txt	
L5	./topo/acc.txt	
L6	./topo/adir.txt	
L7		
L8	0	# utm(1) or latlon(0)
L9	1	# 4-direction (0), 8-direction(1)
L10	360	# lasth [hour]
L11	600	# dt [sec]
L12	60	# dt_riv [sec]
L13	96	# outnum [-]
L14	110.2d0	# xllcorner_rain
L15	-8.3d0	# yllcorner_rain
L16	0.00833333d0 0.00833333d0	# cellsize_rain
L17		

Note that #comment is allowed only for lines with numbers like L8 to L16, but it is not allowed for lines with characters like L3 to L6.

L1 : Version of the control file format.

This version has to be compatible with the RRI program version. When RRI Model version is updated, user may be requested to modify this control file to be suitable for the updated version.

L3 – L6 : Paths of the input files (rainfall, dem, acc, dir)

Note that adjusted direction file having zero at the outlet must be read in the flow direction column. This adjustment (for dem and dir) can be implemented through the process of demAdjust2.

L8 : Topographic and rainfall data coordinate system (UTM (1) or Lat Lon(0))

L9 : Simulating with 4- (0) or 8-direction (1) by the two dimensional model [default : 1]

L10 : Simulation period [hour]

L11 : Simulation time step [sec], [default : 600 sec]

L12 : Simulation time step for river [sec], [default : 60 sec]

The above time steps are just initial setting. The adaptive Runge-Kutta algorithm used for RRI simulation may shorten the time steps if necessary.

L13 : Number of output files

Simulation period specified above is equally divided for simulation output.

L14 – L16 : South west coordinate and resolution of rainfall data

Number of col and row are written in the rainfall data.

L18	0.03d0	# ns_river	RRI_Input.txt
L19	1	# num_of_landuse	
L20	1	# diffusion(1) or kinematic(0)	
L21	0.4d0	# ns_slope	
L22	1.0d0	# soildepth	
L23	0.475d0	# gammaa	
L24			
L25	0.d0	# kv (m/s)	
L26	0.3163d0	# Sf (m)	
L27			
L28	0.0d0	# ka (m/s)	
L29	0.0d0	# gammam (-)	
L30	0.0d0	# beta (-)	
L31			

L18 : Manning’s roughness in river channel

L19 : Number of landuse

Parameter sets specified below should correspond to the number of landuse specified here. For example, if there are three landuse types in a catchment, write three different parameter sets. Prepare also the landuse map which has numbers from one to three, so that the parameter sets described below will be assigned to each landuse grid cell. First column parameters are assigned to landuse type “1” in the landuse map.

L20 : diffusion (1) or kinematic (0) [default : 1]

The default mode of RRI model uses diffusion wave equations. However, by setting zero here, RRI model can use kinematic wave approximation.

L21 : Manning’s roughness on slope cells

L22 : Soil depths [m]

L23 : Effective porosity [-]

L25, L26 : Green-Ampt infiltration model parameters

Set ksv = 0 for inactivating Green-Ampt infiltration model.

“ksv” : vertical saturated hydraulic conductivity [m/s], “faif” is the suction at the wetting front defined by S_r

Note: In the previous versions of RRI Model, “delta” and “infiltr_limit” parameters were used. The parameter “delta” is now replaced by “gamma” to represent soil porosity minus initial water volume content ($\phi - \theta_i$). The “infiltr_limit” parameter is computed within the RRI program by multiplying “soildepth” and “gamma” to estimate the maximum cumulative infiltration depths in meter. Once the cumulative infiltration depths reaches to this maximum depths, no more infiltration happens at the grid-cells.

L28 – L30 : lateral subsurface and surface model parameters

L28 and L30 are options to consider unsaturated and saturated subsurface flow and surface flow in lateral direction. “kv” is lateral saturated hydraulic conductivity (which is typically two or three orders high compared with the vertical hydraulic conductivity set for Green-Ampt model. To start with, set zero for “dm” to inactivate the option to consider unsaturated subsurface flow. Setting zero makes no saturated subsurface flow consideration. See 8.7 for the details of the parameter settings.

Note: In the previous version of RRI Model, a parameter “da” was used to represent maximum water depth in saturated subsurface flow. Now this is calculated as “soil depth” times “gammaa” within the program.

L32 – L36

Set “ksg = 0.d0” to avoid deep groundwater component, whose algorithm is under development and not completed at RRI ver1.4.2. L33-L36 become inactive with ksg = 0.d0.

L38 – L44 : River channel geometry setting by equations

$$\begin{aligned} width &= c_w A^{s_w} \\ depth &= c_d A^{s_d} \end{aligned}$$

The above equations are used as default settings for river channel widths and depths.

Note that A in the equations is the upstream catchment area [km²] for each river grid-cell.

L46 – L49 : River channel geometry setting by files (optional)

If one would like to set width, depth and embankment height from files instead of the above equations, set 1 in L46 and prepare the files in ESRI/ASCII format.

L38	100	# riv_thresh	RRI_Input.txt
L39	5.0d0	# width_param_c	
L40	0.35d0	# width_param_s	
L41	0.95d0	# depth_param_c	
L42	0.20d0	# depth_param_s	
L43	0.d0	# height_param	
L44	20	# height_limit_param	
L45			
L46	0		
L47	./riv/width.txt		
L48	./riv/depth.txt		
L49	./riv/height.txt		
L50			

L51 – L55 : Initial water depth on slope, river, groundwater and GA Model cumulative by files (optional)

If one would like to set initial water depths on slope and river for each grid cell, set 1 in L51 and prepare the initial condition distribution files specified in L52, L53, L54 and L55. Note that the format of the files is the same as RRI model output.

L51	0 0 0 0	RRI_Input.txt
L52	./init/hs_init_dummy.out	
L53	./init/hr_init_dummy.out	
L54	./init/hg_init_dummy.out	
L55	./init/gamptff_init_dummy.out	
L56		
L57	0 0	
L58	./bound/hs_bound.txt	
L59	./bound/hr_bound.txt	
L60		
L61	0 0	
L62	./bound/qs_bound.txt	
L63	./bound/qr_bound.txt	
L64		

L57 – L59 : Water depths boundary conditions (optional)

L57 : Slope water depths boundary conditions, L58 : River water depths boundary conditions
See Section 8 for the format of the boundary condition files. Use flag 1 for one-dimensional data format (i.e. time series data at specific boundary condition locations). Use flag 2 in case the boundary condition files are prepared in two-dimensional data format, whose number of grid-cells must be the same as the topographic data including dem, dir, and acc. In both cases,

time stamps in the boundary condition can vary within the file.

L61 – L63 : Water discharge boundary conditions (optional)

(Same as L57 – L59)

L65	0	
L66	./topo/landuse.txt	RRI_Input.txt
L67		
L68	0	
L69	./dam.txt	
L70		
L71	0	
L72	./div.txt	
L73		
L74	0	
L75	./infile/PET.txt	
L76	110.2d0	# xllcorner_evp
L77	-8.3d0	# yllcorner_evp
L78	0.00833333d0 0.00833333d0	# cellsize_rain
L79		
L80	0	
L81	./riv/length.txt	
L82		
L83	0	
L84	./riv/sec_map.txt	
L85	./riv/section/sec_	
L86		

L65 – L66 : Landuse setting (optional)

If one would like to use multiple parameter sets for different grid-cells, set 1 in L65 and read landuse file specified in L66.

L68 – L69 : Dam condition setting (optional)

RRI model simulates the effect of dam reservoir operations based on simple rule. Refer to the source code “RRI_Dam.f90” for details. (See also 8.11)

L71 – L72 : River diversion setting (optional)

River channel diversion setting (See also 8.10)

L74 – L78 : Evapotranspiration setting (optional)

Prepare ET file and specify the path on L75. The format of ET file is the same as rainfall. The resolution and xll and yll corners can be different from the rainfall file as far as it covers all the simulation domain.

L80 – L81 : River length setting (**optional**) : newly added option to set arbitrary the length of river channel for each river grid cell (under preparation for more detail on this option).

L83 – L85 : River cross section settings (**optional**) : newly added option to set arbitrary cross section information for each river grid cell (under preparation for more detail on this option).

L87	1 1 0 1 0 0 0 0 1	RRI_Input.txt
L88	./out/hs_	
L89	./out/hr_	
L90	./out/hg_	
L91	./out/qr_	
L92	./out/qu_	
L93	./out/qv_	
L94	./out/gu_	
L95	./out/gv_	
L96	./out/gampt_ff_	
L97	./out/storage.dat	
L98		
L99	1	
L100	./location.txt	

L87 – L97 : Output file settings

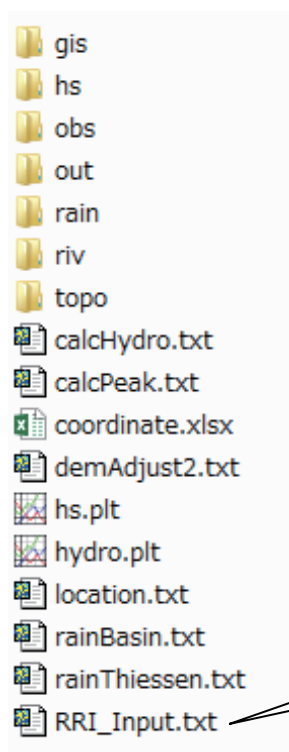
Change the settings of L87 to “1” to output different sets of simulation results listed in the same order between L88 and L97

L99 – L100 : Output hydrographs at specified locations (**Optional**)

Set 1 in L99 to read the location file and output hydrographs at the specified locations.

6. Running RRI Model

- ① Prepare “RRI_Input.txt” under your project folder (e.g. “./RRI-CUI/Project/solo30s”)
- ② Move current folder to your project folder and type in “0_rri_1_4_2.exe” and return.



Prepare “RRI_Input.txt” before
executing **0_rri_1_4_2.exe**

```

C:\YRRIModel\Rri.exe
rainfile : ./infile/rain_2d_solo.data
demfile : ./infile/adem_solo.txt
accfile : ./infile/acc_solo.txt
dirfile : ./infile/dir_solo.txt

utm : 0
eight_dir : 1
lasth : 360
dt : 600
dt_riv : 60
outnum : 96
xllcorner_rain : 110.30000
yllcorner_rain : -8.30000
cellsize_rain_x : 0.10000 cellsize_rain_y : 0.10000

num_of_landuse : 3
dm : 0.000 0.000 0.000
da : 0.000 0.000 0.000
ka : 0.000 0.000 0.000
beta : 0.000 0.000 0.000
soildepth : 0.000 0.000 0.000 0.000
ns_slope : 2.000 0.600 0.400
ns_river : 0.040
  
```

Calculation status is
displayed

```

C:\YRRIModel\Rri.exe
1 / 2160
max hr: 0.000000000000000E+000 loc : 1 1
max hs: 0.000000000000000E+000 loc : 1 1
0.000 0.000 0.000 0.000 0.000

2 / 2160
max hr: 0.000000000000000E+000 loc : 1 1
max hs: 0.000000000000000E+000 loc : 1 1
0.000 0.000 0.000 0.000 0.000

3 / 2160
max hr: 0.000000000000000E+000 loc : 1 1
max hs: 0.000000000000000E+000 loc : 1 1
0.000 0.000 0.000 0.000 0.000

4 / 2160
max hr: 0.000000000000000E+000 loc : 1 1
max hs: 0.000000000000000E+000 loc : 1 1
0.000 0.000 0.000 0.000 0.000

5 / 2160
max hr: 0.000000000000000E+000 loc : 1 1
max hs: 0.000000000000000E+000 loc : 1 1
0.000 0.000 0.000 0.000 0.000

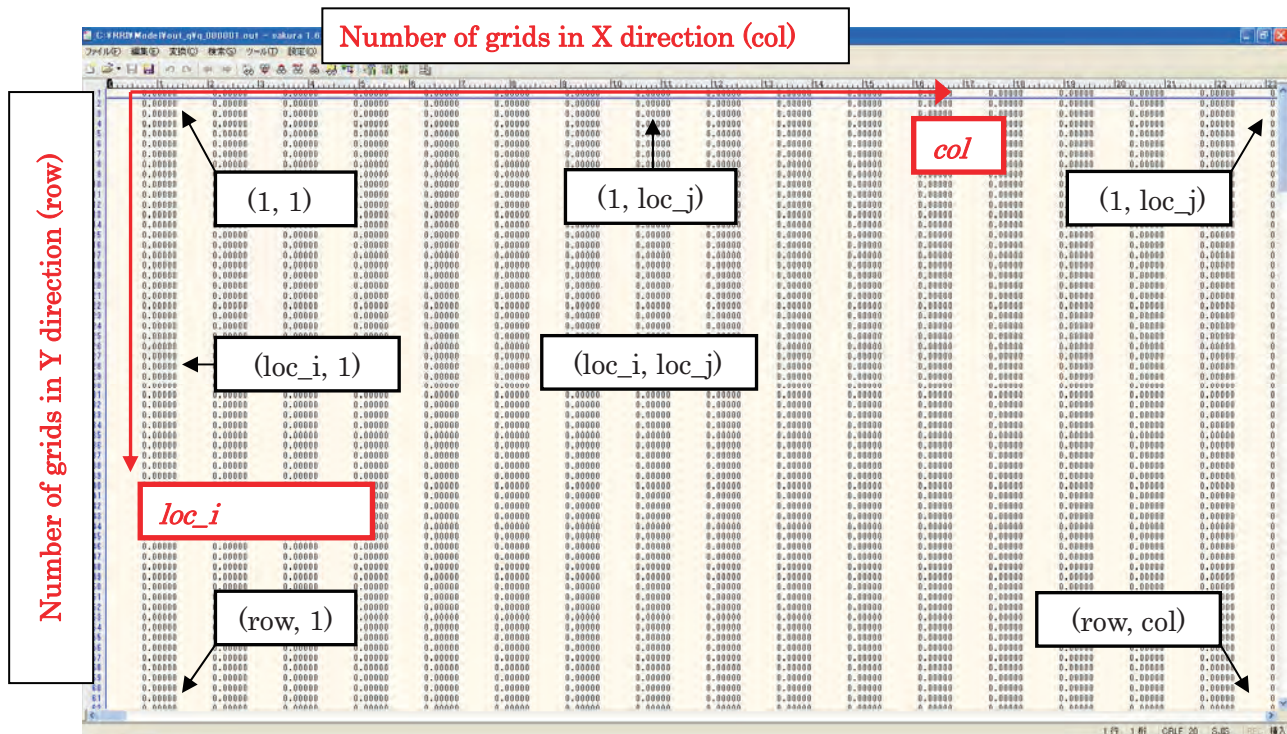
6 / 2160
  
```

7. Visualize Output Data

This section explains how to visualize RRI Model output.

7.1 Format of the Output Files

Each output file contains water depths on slope (hs_) and on river (hr_) and river discharges (qr_) on river at a particular time step. The units of the output are [m] for water depths and [m³/s] for discharge.



※The numbers of rows and columns are the same as those of the topographic data.

Note that for each type of model output, the number of the files is defined in RRI_Input.txt (L13 : outnum). The simulation period is equally divided by “outnum” and the number assigned to each output file represents the output time stamp.

7.2 Visualize Inundation Depth with GNUPLOT

GNUPLOT can be used to illustrate flood inundation depth distributions. Inside the project folder, the GNUPLOT script named “hs.plt” is included. To change the settings, one can edit “hs.plt” directly or create another “hs.plt” by using a Fortran program named “prepHsPlt.f90” saved in “RRI/etc/prepHsPlt”.

- ① Edit “hs.plt” file to change the configurations.

```

reset

set terminal gif medium size 672, 408 crop

set pm3d map
set palette defined (0.0 "gray", 1.5 "blue", 3 "green")

set xrange [0:]
set yrange [:] reverse
set zrange [0:] reverse

#set xrange [180:200]
#set yrange [435:455] reverse

set cbrange[0.:3]
set zrange[0.0:]

set output "/hs/hs_000001.gif"
splot "/out/hs_000001.out" matrix t "000001 / 000096"

set output "/hs/hs_000002.gif"
splot "/out/hs_000002.out" matrix t "000002 / 000096"

set output "/hs/hs_000003.gif"
splot "/out/hs_000003.out" matrix t "000003 / 000096"

```

hs_plt.txt

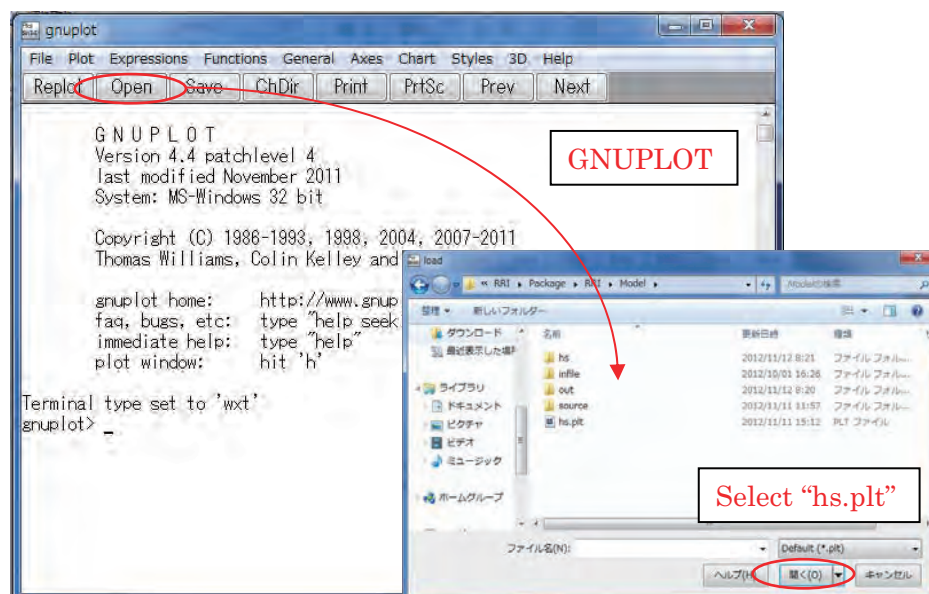
The size of output GIF file, X and Y direction. Use the same X and Y ratio as DEM's col and row.

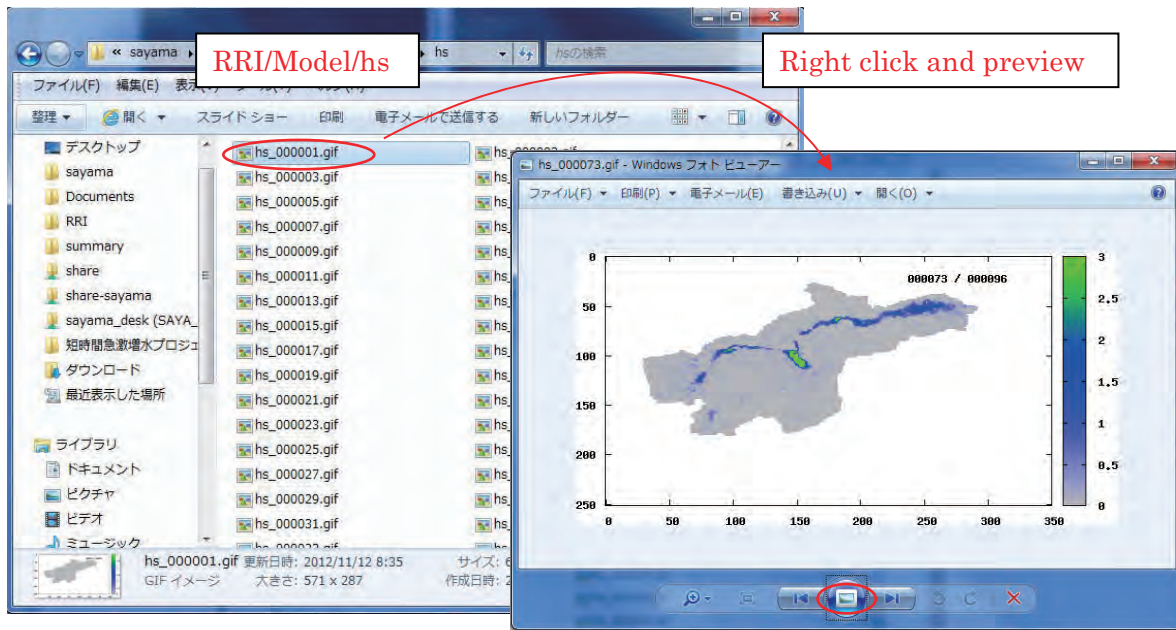
Color pattern settings

Color range

From RRI output (hs_***.out) to gif

- ② Start GNUPLOT program by clicking “/RRI-CUI/etc/gnuplot/binary/wgnuplot.exe”
Then open and select “hs.plt” script file.





7.3 Hydrographs at Specific Locations

A Fortran program named “**calcHydro.exe**” can be used to generate hydrographs by picking up values from “out/qr_***.txt” at specified locations.

- ① Edit “**RRI/Model/calcHydro.txt**” (see more details “RRI-CUI/etc/calcHydro/00_readme.txt”)
 - L1 : [In] location file (e.g. ./infile/solo30s/location_solo_30s.txt)
 - L2 : [In] RRI output file (e.g. ./out/qr_)
 - L3 : [Out] hydrograph file (e.g. ./infile/solo30s/disc_)

./infile/solo30s/location_solo_30s.txt out/qr_ ./infile/solo30s/disc_	calcHydro.txt
Cepu 68 167 (list all target locations)	location_30s_solo.txt

- ② Run “calcHydro.exe”. (Execute “makePostProcess.bat” in advance to compile.)
- ③ Check the created files specified in L3 of “calcHydro.txt”. (e.g. ./infile/solo30s/disc_)
- ④ From GNUPLT screen, open and select “hydrograph.plt”, which is a GNUPLT script file to plot hydrographs. Any other plotting software, such as Excel, can be also used to

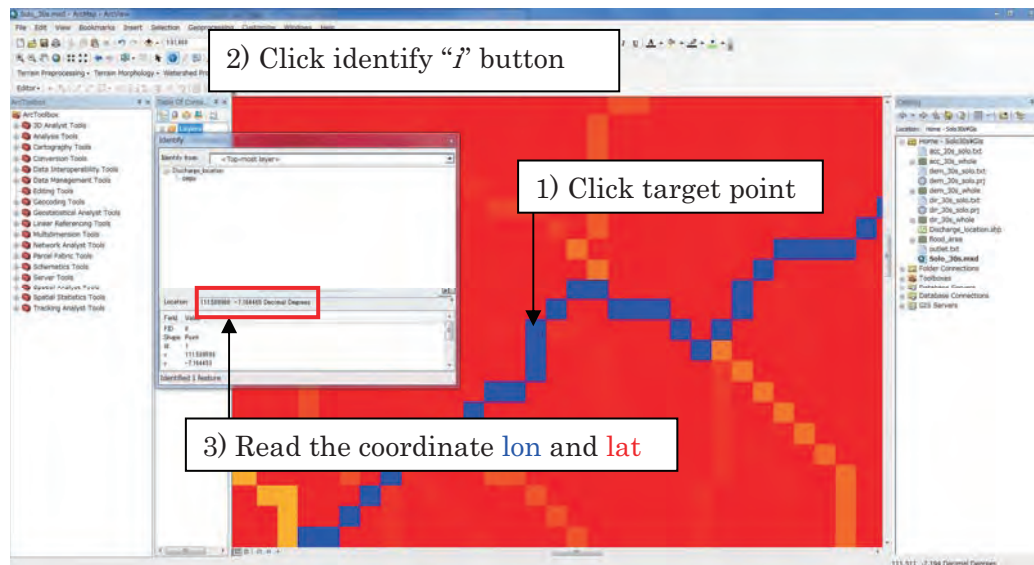
draw hydrographs from created files (e.g. ./infile/solo30s/disc_Cepu.txt).

In the location file (e.g. ./infile/solo30s/location_solo_30s.txt), one can list all target points, which you want to calculate hydrographs. Write the “*name of location*” and “**loc_i**” (**y-direction**) and “**loc_j**” (**x-direction**)

Note that “loc_i” is the **row** (**y-direction from top**) and “loc_j” is the **col** (**x-direction from left**).

To identify the observation points in mesh coordinate (**loc_i**, **loc_j**), one can use “/RRI/etc/coordinate.xlsx” to calculate based on the coordinate in **latitude(y)** and **longitude(x)**.

- ① Find the **latitude (y)** and **longitude (x)** of the observation point using ArcGIS.



(Displaying “acc” on top to make sure the selected point is on a river grid cell.)

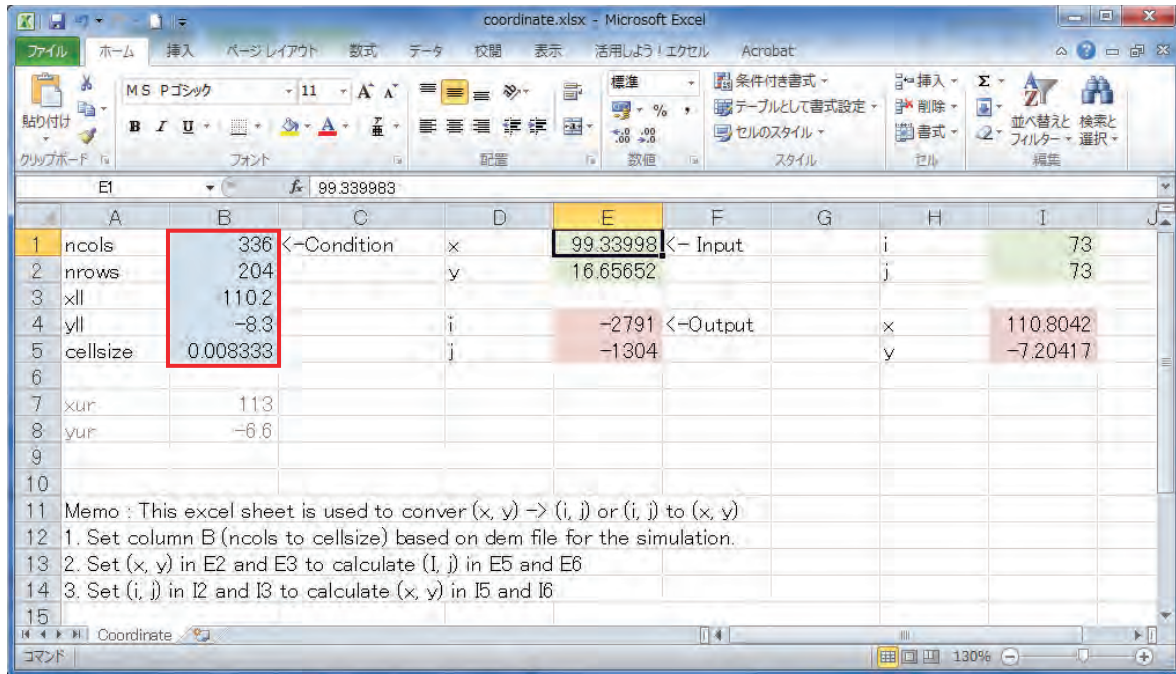
- ② Open one of the topographic data (i.e. dem, dir, or acc)

```
ncols      336
nrows      204
xllcorner  110.2
yllcorner  -8.3
cellsize   0.0083333333333333
NODATA_value -9999
```

acc_solo_30s.txt

```
-9999 -9999 -9999 -9999 -9999 -9999 -9999 -9999 -9999 -9999 -9999
-9999 -9999 -9999 -9999 -9999 -9999 -9999 -9999 -9999 -9999 -9999
-9999 -9999 -9999 -9999 -9999 -9999 -9999 -9999 -9999 -9999 -9999
-9999 -9999 -9999 -9999 -9999 -9999 -9999 -9999 -9999 -9999 -9999
```

- ③ Read the header part (red box in the above figure) of the topographic data and copy the same information in the Excel file (i.e. [/RRI-CUI/etc/coordinate.xlsx](#)).



- ④ Type x and y (or **lon** and **lat**) coordinate of the target point, then the calculated mesh coordinate (**loc_i**, **loc_j**) appears in (E4, E5).

“coordinate.xlsx” can be used also to convert from (loc_i, loc_j) to (lon, lat).

7.4 Visualize Peak Inundation Depths

Fortran program named “calcPeak.exe” can be used to compute the maximum flood depths based on RRI Model output (“out/hs_*.out”). See 2.2.3 the procedure more in detail.

- ① Edit “RRI/Model/calcPeak.txt” file after RRI model execution.
In “calcPeak.txt”, L1 sets the path of dem file, L2 sets the RRI model output file to calculate the peak, and L3 sets the number of output files. L4 defines the output file of calcPeak program. See details the readme file of “/etc/calcPeak”.
- ② Execute “calcPeak.exe”. (Execute “makePostProcess.bat” if the executable file does not exist.)
- ③ Check the created files specified in L4 of “calcPeak.txt”.
- ④ The obtained peak water data follows ESRI/ASCII format that can be visualized with ArcGIS.

7.5 Visualize Inundation Depths with Google Earth (Optional)

7.5.1 Preparing KML File

By using “RRI/etc/makeKML.f90”, a kml file (e.g. “runoff.kml”) can be prepared.

User needs to edit “RRI/etc/Kml_input.txt”.

2007 12 24 0 0	: Start time (Year Month Day Hour Min (UTC))
96	: Number of gif files(= "outnum" of RRI_Input.txt)
3.75	: Timestep (hourly) (\div "lasth / outnum" of RRI_Input.txt)
./infile/solo/adem_30s_solo.txt	: Dem file name (for lat,lon)
./runoff.kml	: Output file name

Kml_input.txt

“Time step” needs to be input as “hourly” data.
This “Time step” should be “lasth” / “outnum” input
in “RRI_Input.dat”.

When it is executed,
“runoff.kml” is output.

```
<Folder>
  <GroundOverlay>
    <TimeSpan>
      <begin>2007-12-24T00:00Z</begin>
      <end>2007-12-24T03:45Z</end>
    </TimeSpan>
    <Icon>
      <href>hs_kml/hs_000001.gif</href>
    </Icon>
    <LatLonBox>
      <north> -6.60000</north>
      <south> -8.30000</south>
      <east> 113.00000</east>
      <west> 110.20000</west>
    </LatLonBox>
  </GroundOverlay>
  ...
```

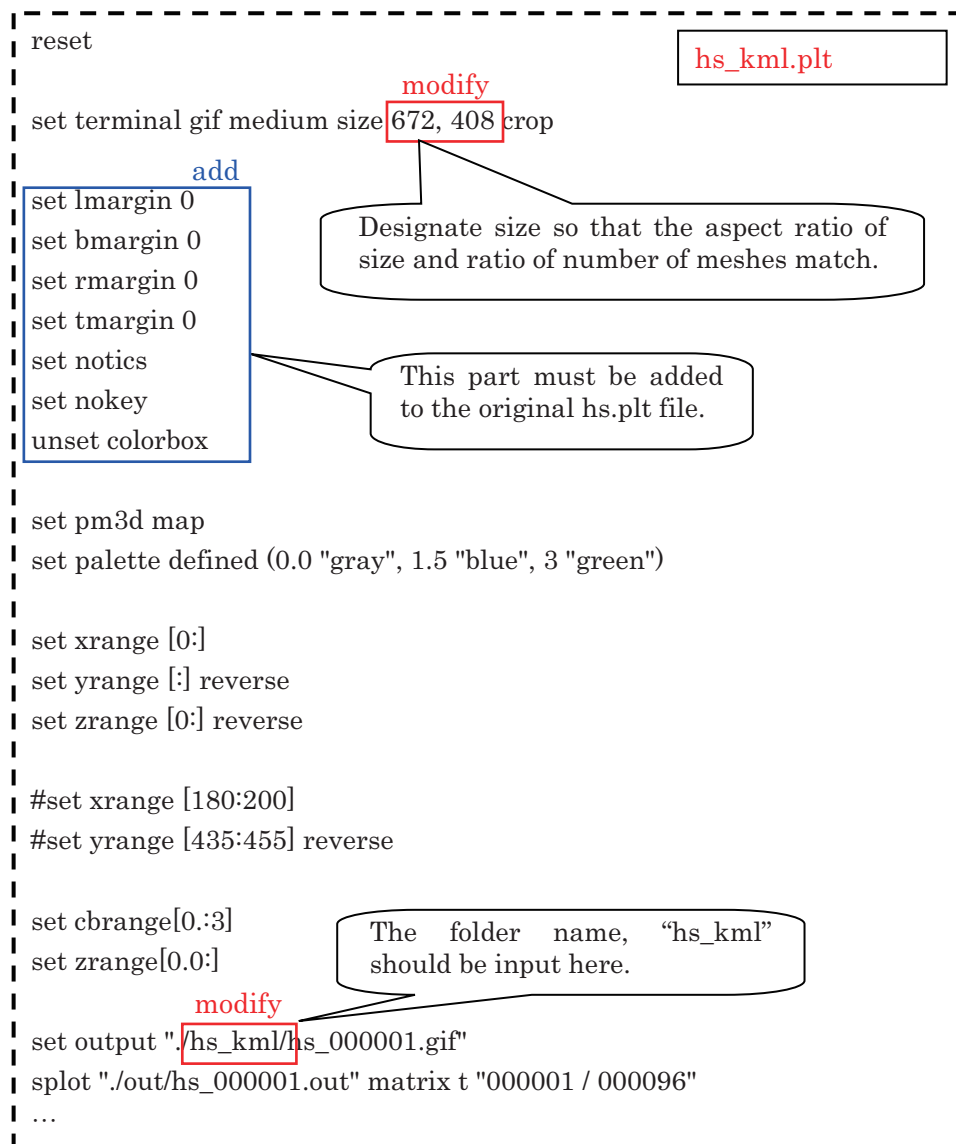
runoff.kml

※ The output of “runoff.kml” reads gif files created in the folder of “hs_kml”.

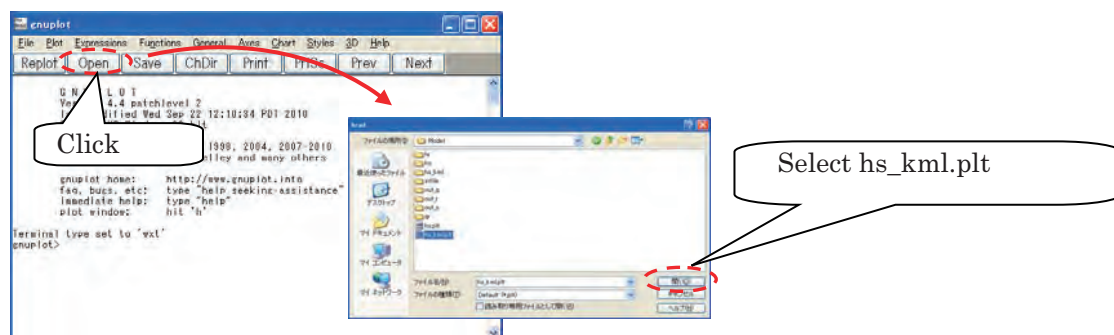
7.5.2 Preparing GIF Files with GNUPLOT

The method of plotting “hs_kml.plt” using “gnuplot” is shown below.

- ① Prepare a gnuplot file (e.g. “RRI/Model/hs_kml.plt”), which can be essentially the same as hs.plt explained above. However, the gnuplot script file used here (i.e. hs_kml.plt) must have some additional statements in the blue box in the following figure. The statements delete unnecessary axis and legends to be appropriately overlay on Google Earth.



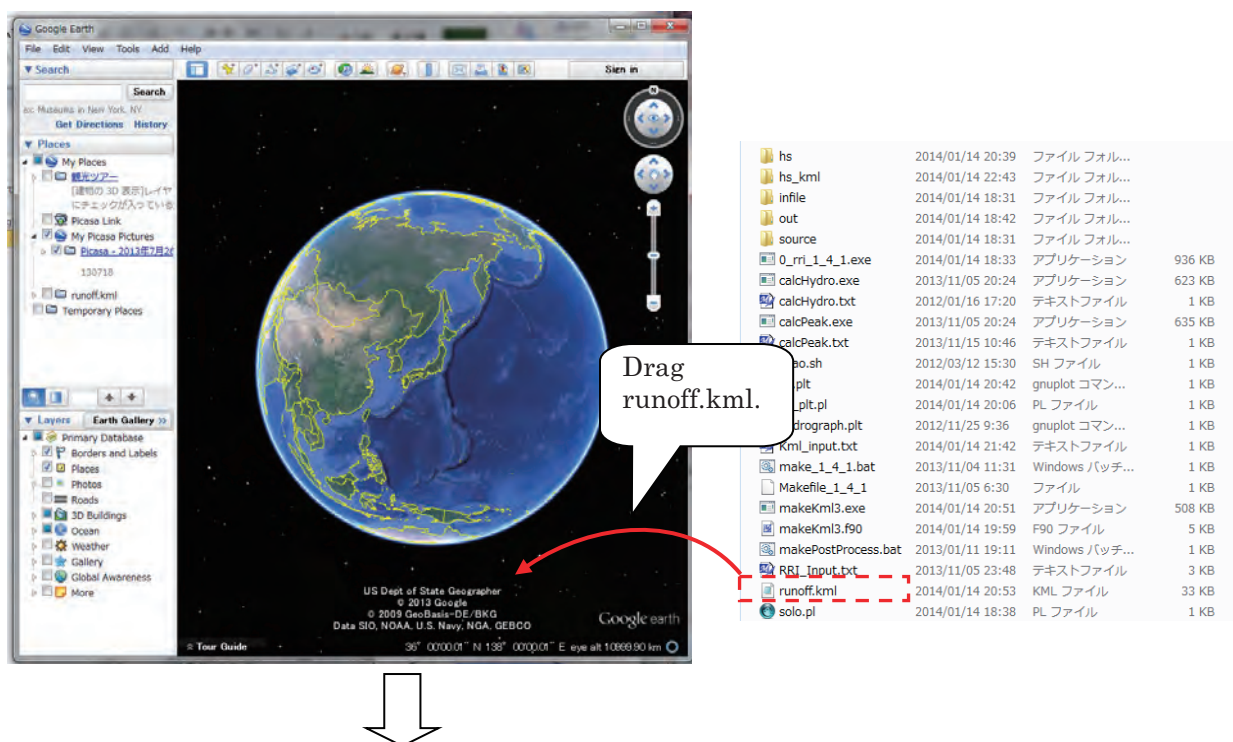
- ② Start “GNU PLOT” and run “RRI/Model/ hs_kml.plt”.

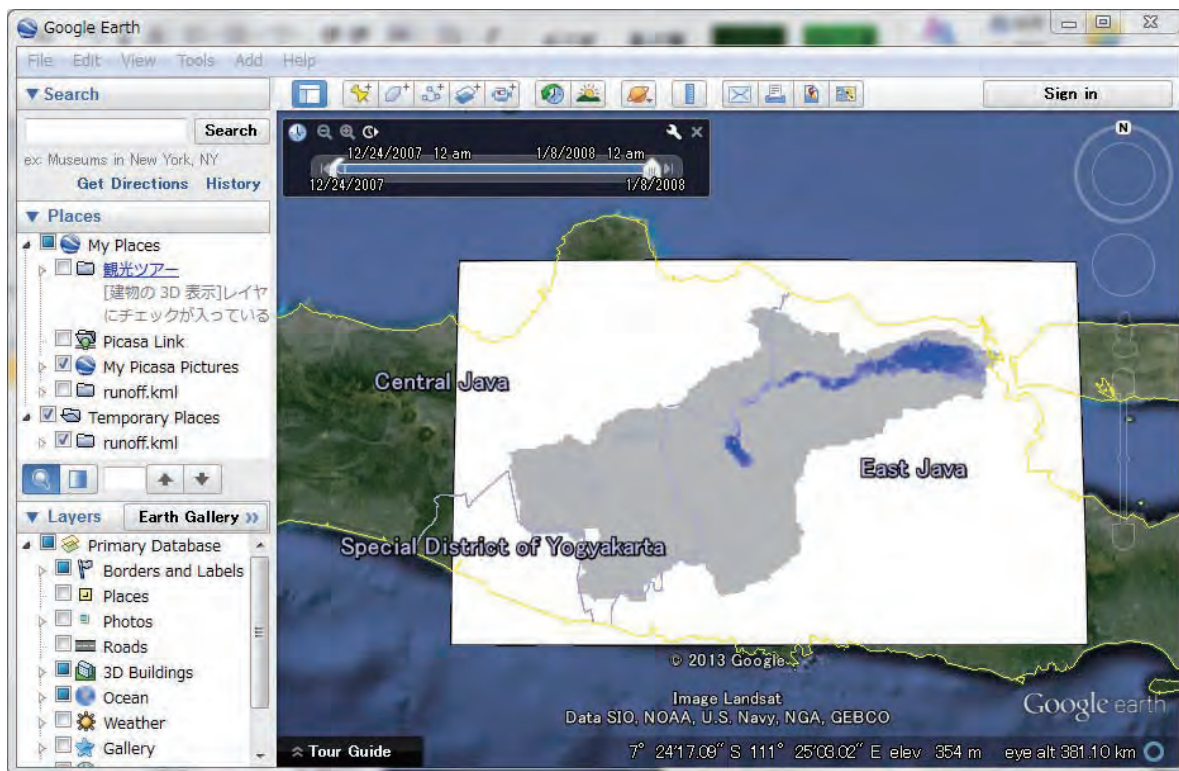


- ③ An image file is prepared in the “RRI/Model/hs_kml” folder. (Note that a new folder hs_kml must be created in advance.)

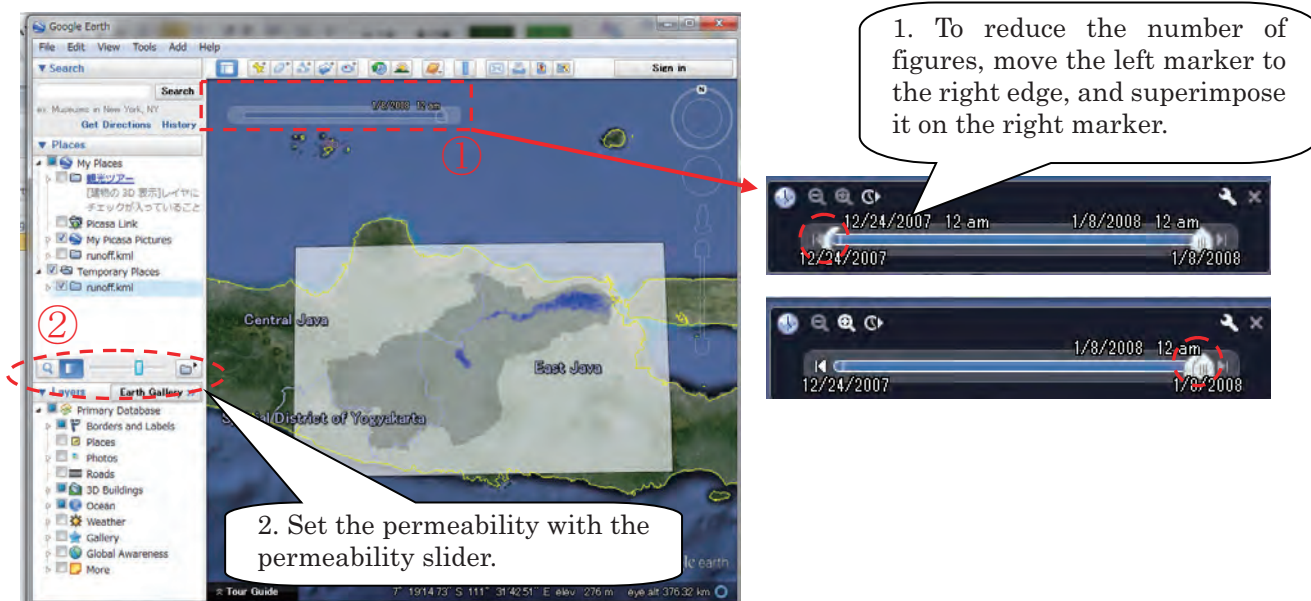
7.5.3 Visualize GIF files with Google Earth

- ① Start Google Earth and drag “/RRI/Model/runoff.kml”.





② Designate the number of figures to display at once and their transparency.



※ On time slider: The right marker represents the present time, while the left marker is used for the number of figures to overlay. Figures in the period between two markers are displayed.

③ Execute animation.

1. Drag the right marker, and move it to the start time.

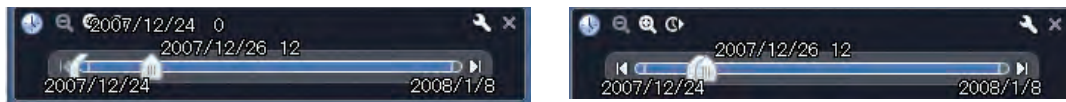
2. Clicking starts animation display.

3. If user wants to change the speed of animation, click option button.

Set the animation speed by this slider.

The first screenshot shows a timeline with markers for 12/24/2007 and 1/8/2008. A red circle highlights the right marker. The second screenshot shows the same timeline with a play button highlighted by a red circle. The third screenshot shows the 'Options' dialog box with a red dashed circle around the 'Animation speed' slider and the 'Loop animation' checkbox.

※ <note>. During the animation, two markers should be moved at the same time.
If user can't move the left marker, stop the animation and fit the left marker to the position of right marker and restart the animation.



④ Save the results with kmz file, so that it can be distributed to other users without gif files.

Select "kmz" from types of file, designate the file name as "runoff.kmz", and click the save button.

Select "Save Place as ..." from the right click menu.

The first screenshot shows the Google Earth interface with a right-click menu open over a map. A red dashed circle highlights the 'Save Place as ...' option. The second screenshot shows the 'Save file' dialog box with 'runoff.kmz' entered in the file name field and 'kmz' selected in the file type dropdown. A red dashed circle highlights the 'Save' button.

7.6 Visualize Results with Tecplot (Optional)

7.6.1 Preparing input File of Tecplot

```

2007 12 24 00      # start time
360                # lasth [hour]
96                # outnum [-]

./Model/infile/solo30s/rain_solo_30s_gauge.dat
./Model/infile/solo30s/adem_30s_solo.txt

110.2d0           # xllcorner_rain
-8.3d0            # yllcorner_rain
0.00833333d0 0.00833333d0 # cellsize_rain

1 1 0 1 1 1 0 0 0 1
./Model/out/hs_
./Model/out/hr_
./Model/out/hg_
./Model/out/qr_
./Model/out/qu_
./Model/out/qv_
./Model/out/gu_
./Model/out/gv_
./Model/out/gampt_ff_

./calcTecplot_out.dat

```

: Year, Month, Day, Hour
: calculation time (1.10)
: output file number (1.13)

: Rainfall file (1.3)
: Dem file (1.4)

grid data of Rainfall
(from 1.14 to 1.16)

Output file from RRI
(from 1.87 to 1.96)

User needs to edit these lines in "calcTecplot.txt".
All the lines except for the first line (start time)
can be copied from "RRI_Input.txt" to be
compatible with simulation setting.

Output file name for Tecplot
(use "dat" for the extension)

```

TITLE      = "Internally created data set"
VARIABLES = "X"
"Y"
"DEM (m)"
"Rainfall (mm/h)"
"Water depth hs (m)"
"Water depth hr (m)"
"Water depth hg (m)"
"River discharge qr (m3/s)"
"Slope discharge qu (m3/s)"
"Slope discharge qv (m3/s)"
"Ground discharge gu (m3/s) "
"Ground discharge gv (m3/s)"
"g-ampt (m)"

```

All data outside the red border are
header information, which is not
necessary to be modified.

"VARIABLES =" ... shows the variables to
be displayed on Tecplot. Edit this if
necessary.

```

ZONE T="Contour T ="
STRANDID=1, SOLUTIONTIME=
I=336, J=204, K=1, ZONETYPE=Ordered
DATAPACKING=POINT
DT=(SINGLE SINGLE SINGLE SINGLE SINGLE SINGLE SINGLE SINGLE SINGLE SINGLE
SINGLE SINGLE SINGLE SINGLE)

```

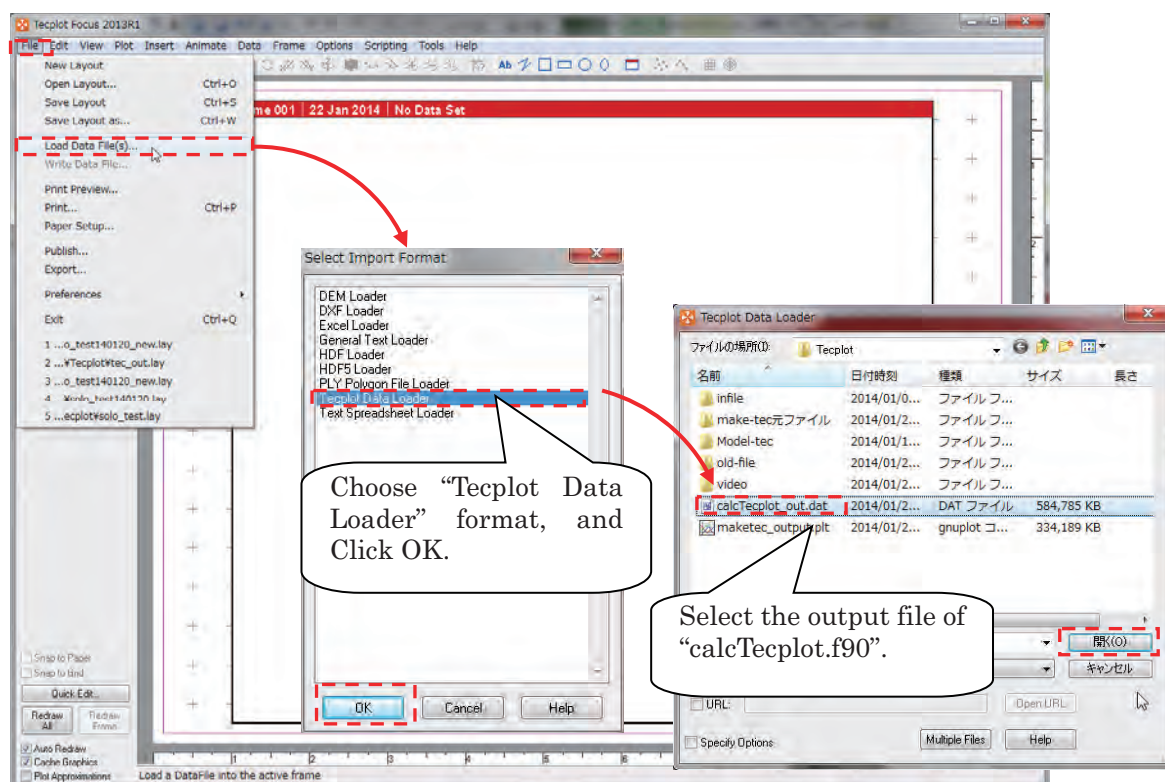
Use “RRI/etc/calcTecplot.f90” to prepare an input file for Tecplot (e.g. “calcTecplot_out.dat”). Prior to running calcTecplot.exe, edit “RRI/etc/calcTecplot.txt”, which sets the condition for generating the input file.

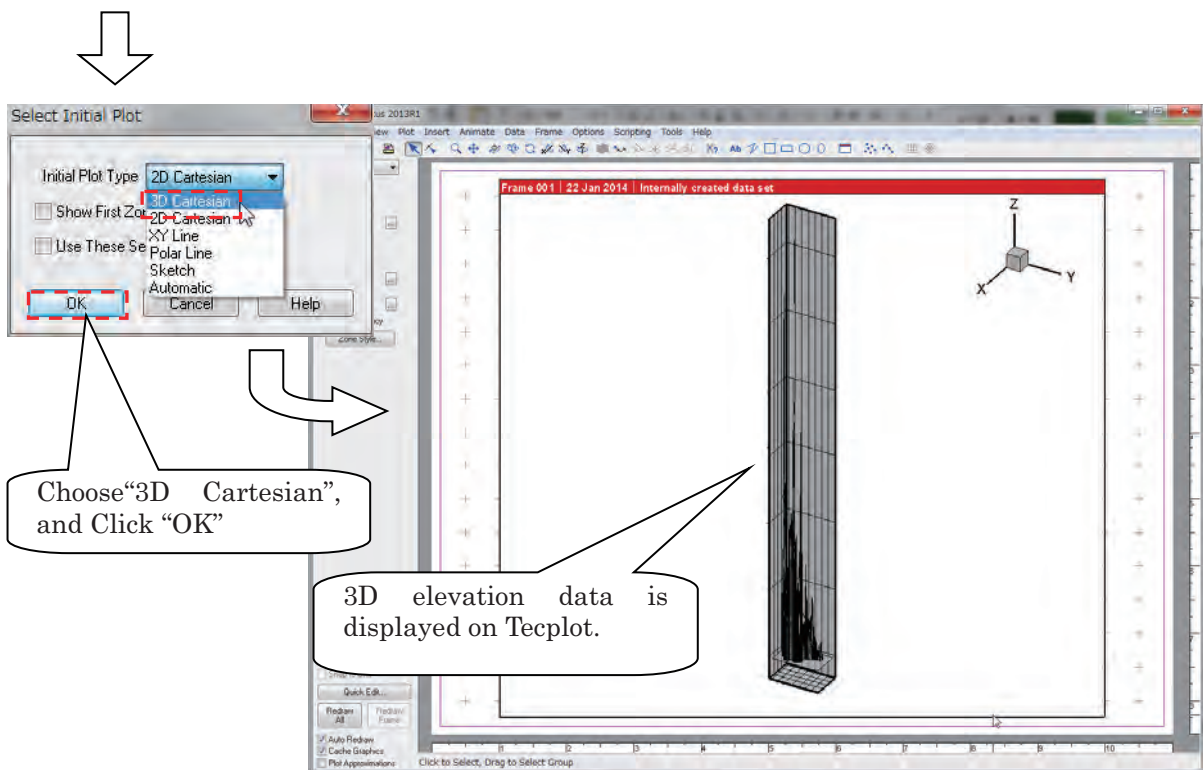
7.6.2 Displaying on Tecplot

- ① Start Tecplot, and load data file.

[File] > [Load Data file(s)] > [Tecplot Data Loader] > [calcTecplot_out.dat]

It takes several minutes to load the data file.



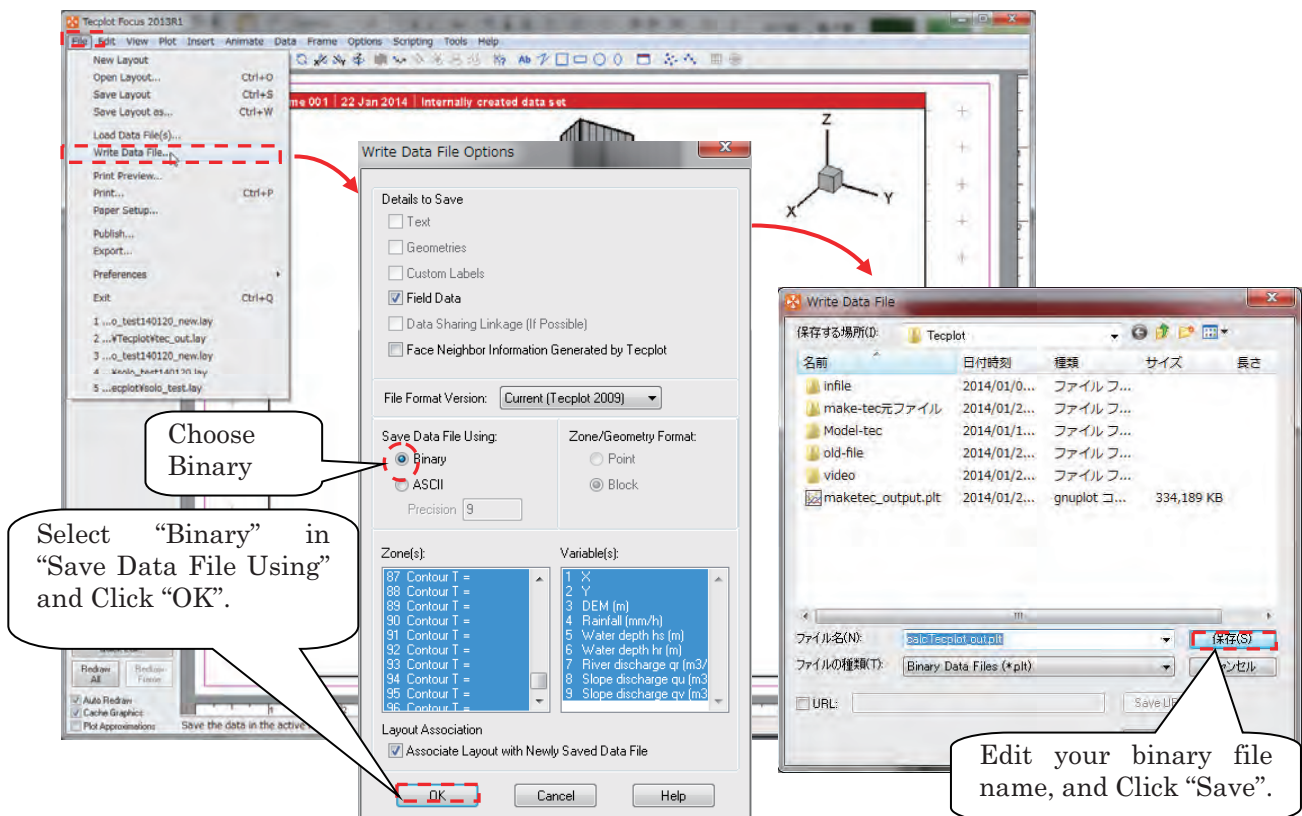


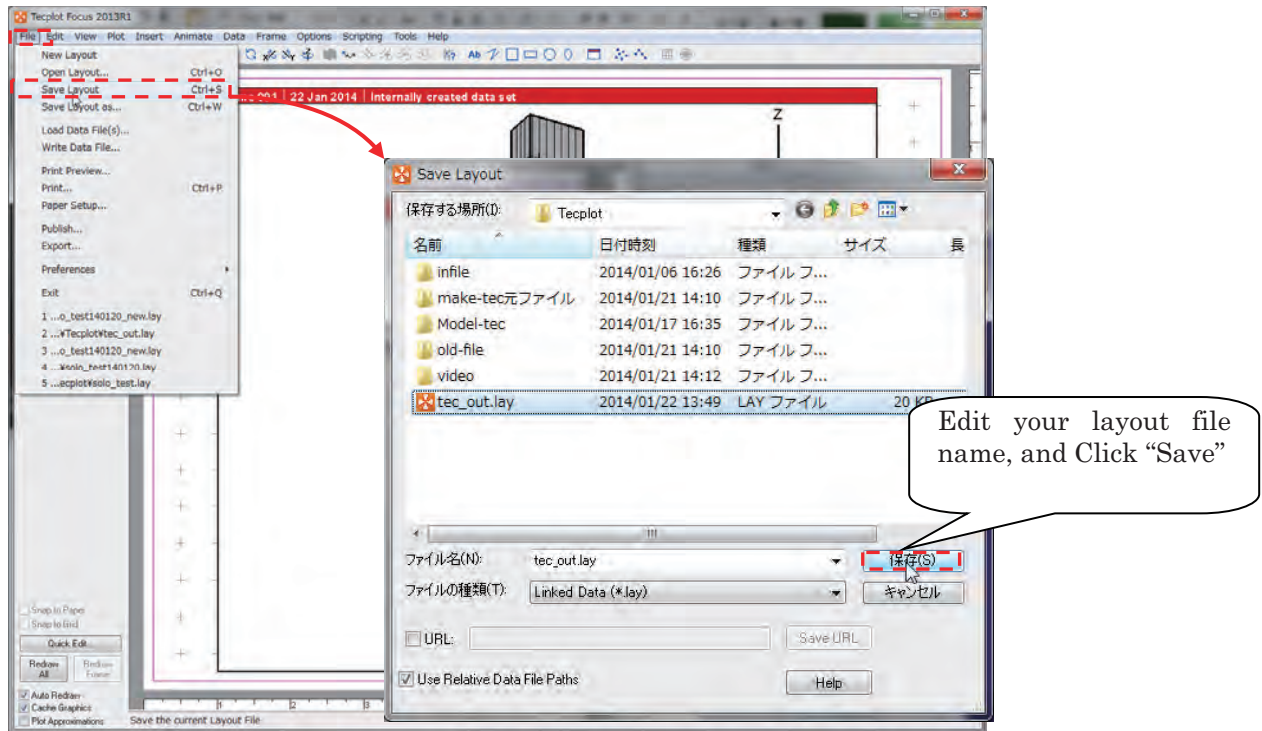
② Write data file (changing input data to binary data), and also save as layout file.

[File] > [Write Data file...]

[File] > [Save Layout] ..

By Making the binary data (*.plt), user can reduce the amount of time to reload layout file. User needs longer time to reload without the binary file.

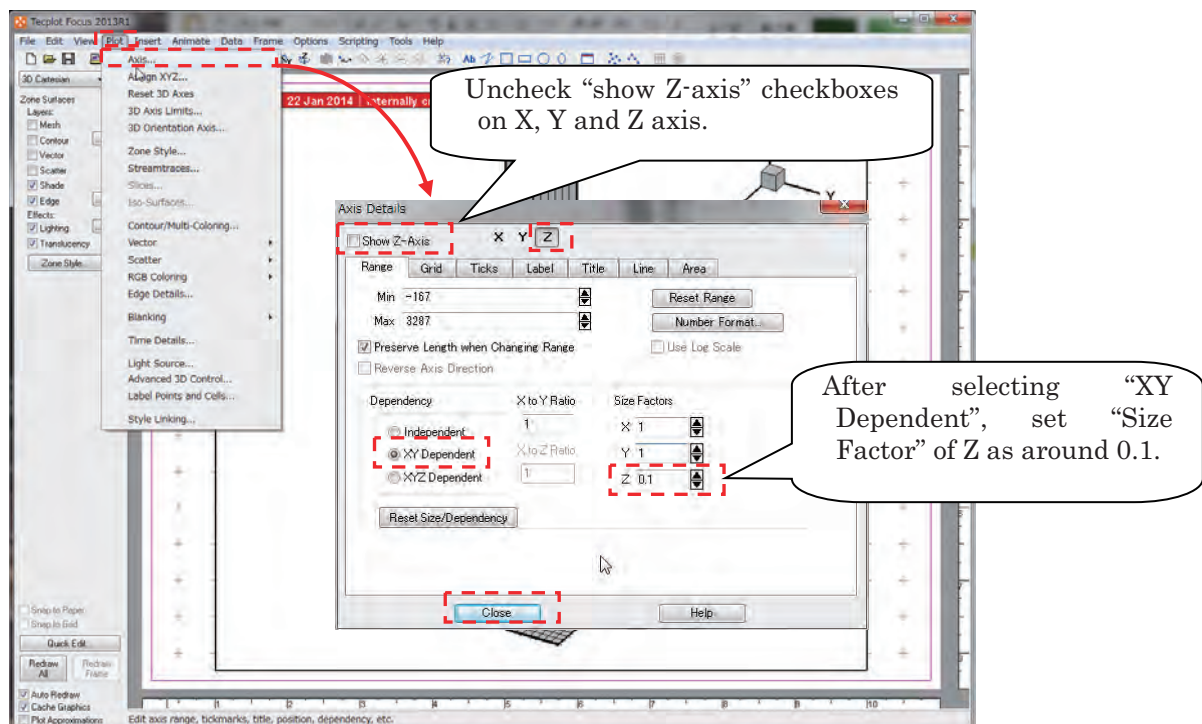




7.6.3 Edit display options on Tecplot

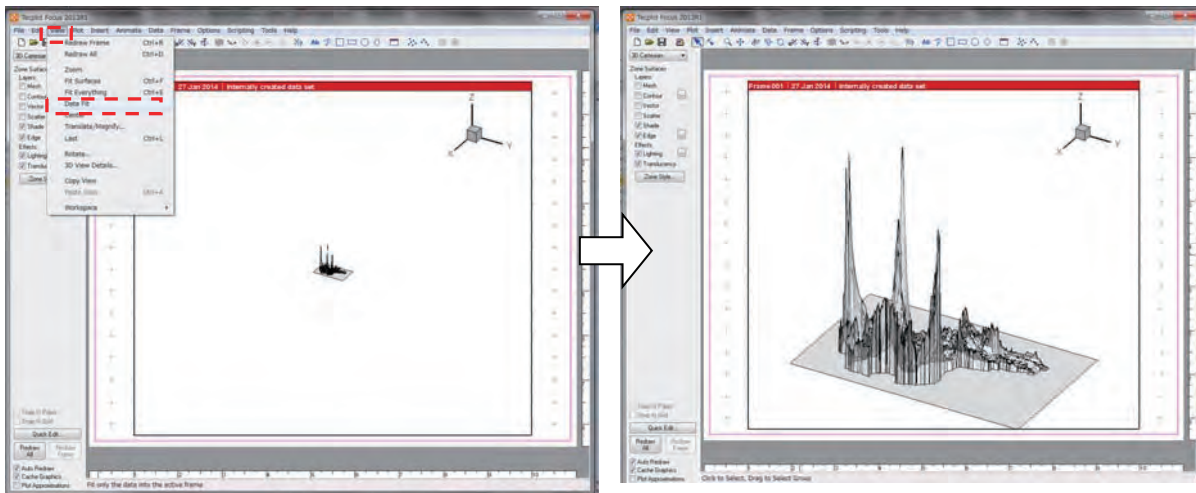
- ① Edit the ratio of XYZ and hide the axes.

[Plot] > [Axis ...] Select "XY Dependent" in Dependency on "Z" tab and input Size Factors in Z (following example shows the Size Factors Z is set to 0.1). Uncheck "Show X(Y,orZ)-axis" on X, Y and Z tab to hide the axis.



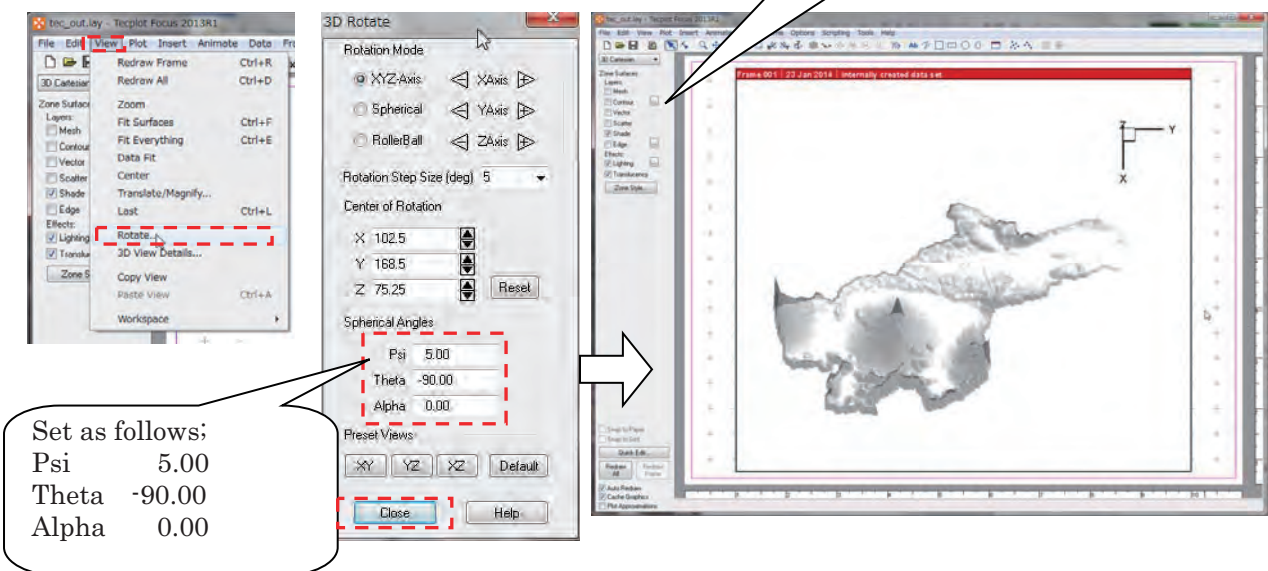
- ② Fit the data display range to the target range.

[View] > [Data fit]



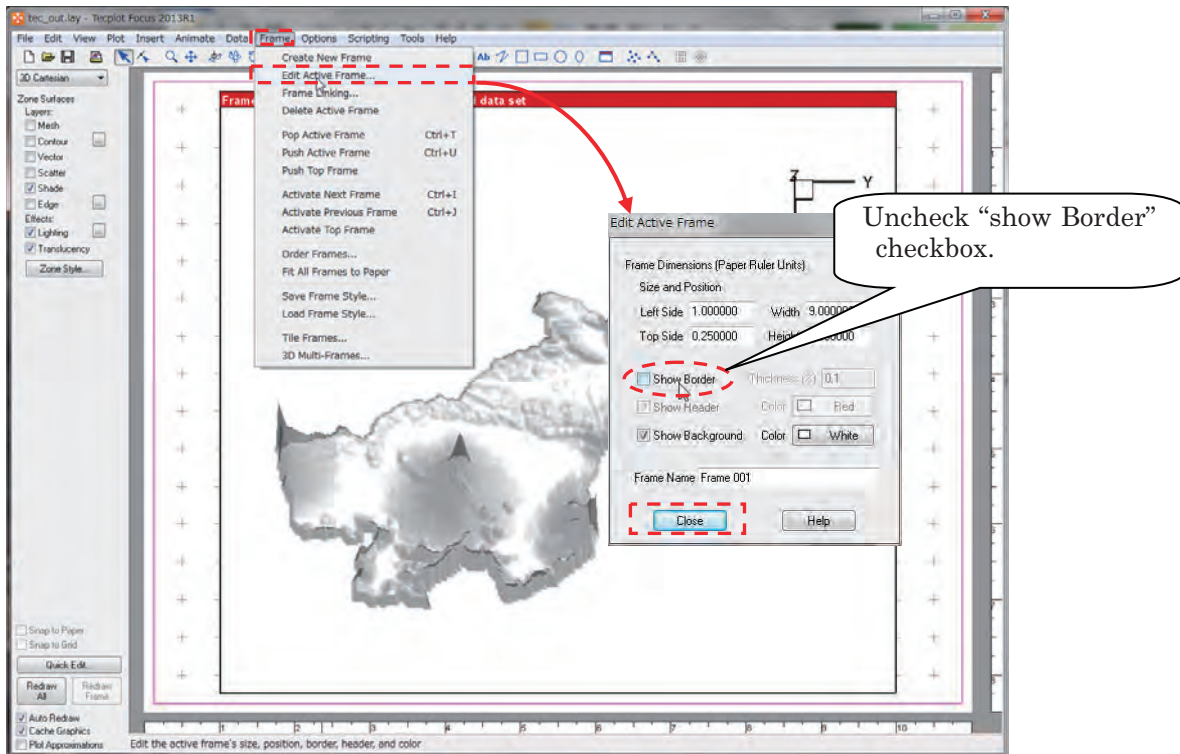
- ③ Edit point of sight angle.

[View] > [Rotate...]



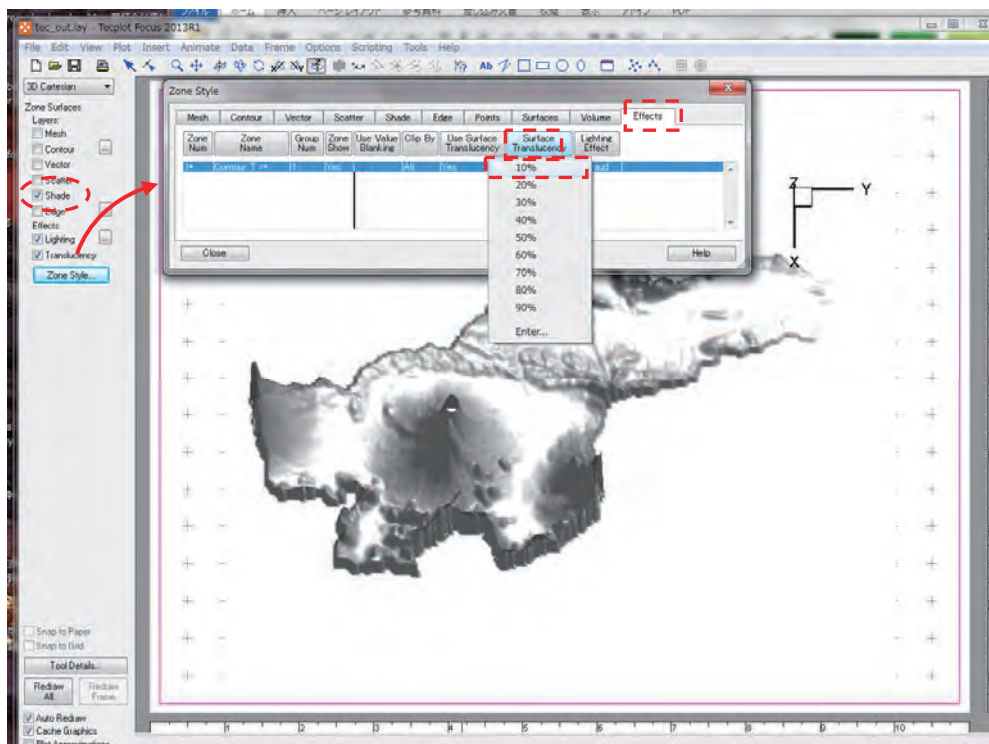
④ Delete unnecessary frame

[Frame] > [Edit Active Frame...]



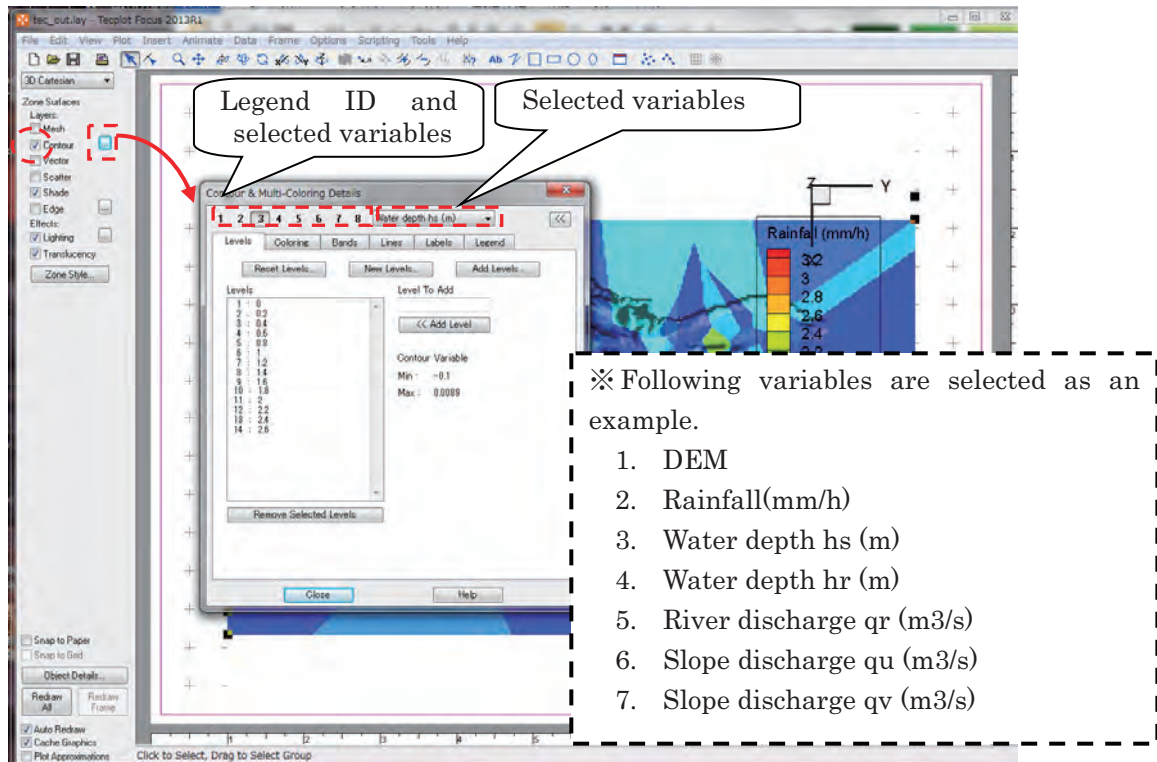
⑤ Edit translucency of shade

Click "Zone Style" and edit the value of "Surface Translucency" on "Effects Tab" to change the translucency of shade (e.g. 10%).

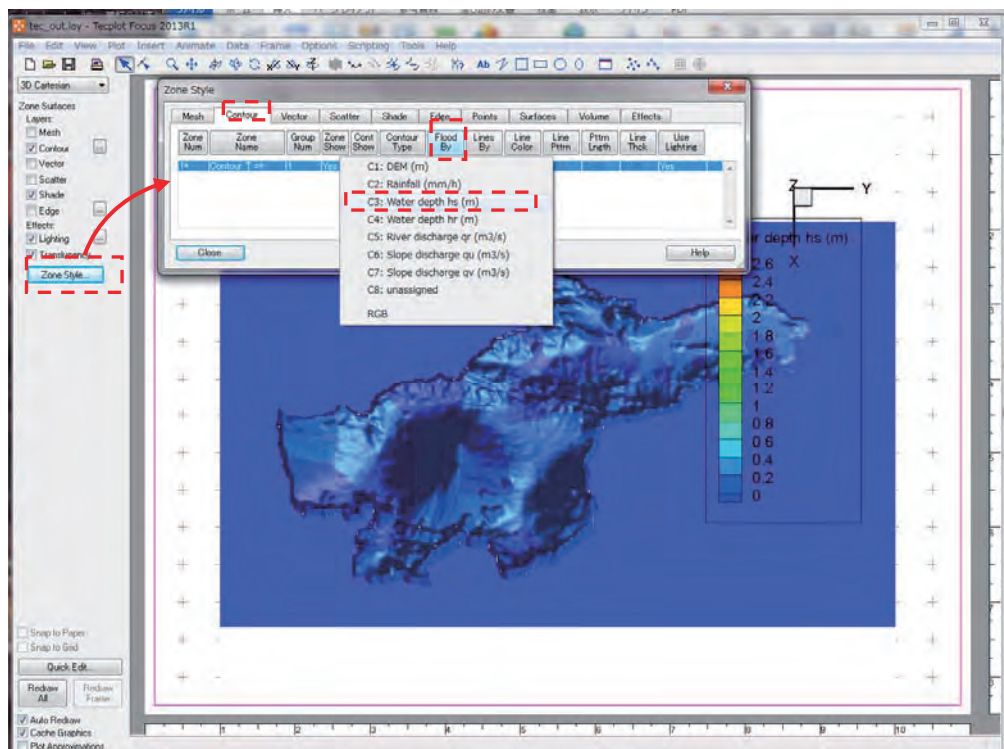


7.6.4 Draw contour figure on Tecplot

- ① Select variables to draw contour. User can select variables up to eight variables. The legends of variables are automatically set. The method to edit them is described in ③.

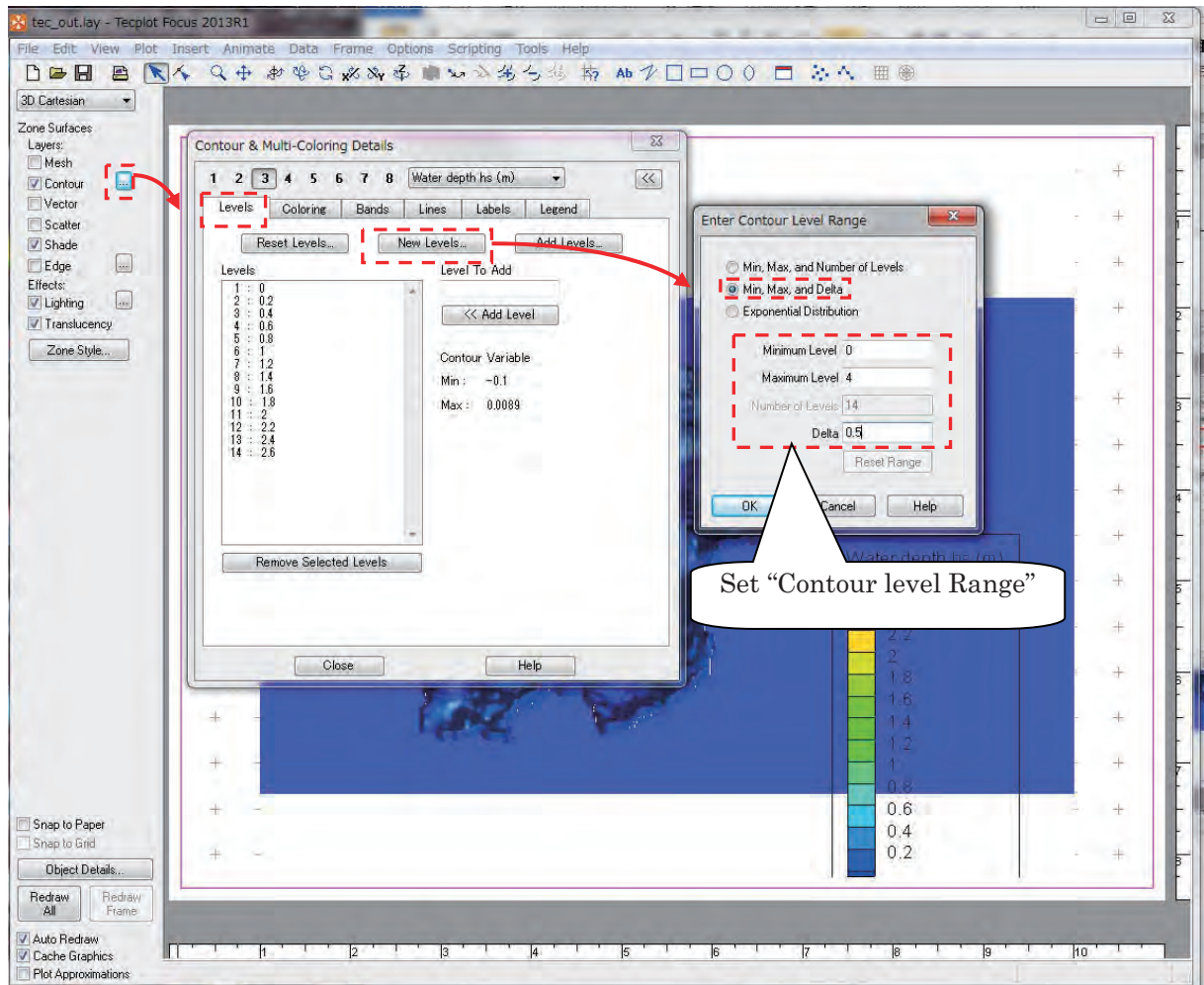


- ② Select variable to display. User can select variable from variables identified in ①. Click “Zone Style” and edit “Flood By” on “Contour” tab to edit target variable and its legend. “Water depth hs (m)” is selected in the following figure as an example.

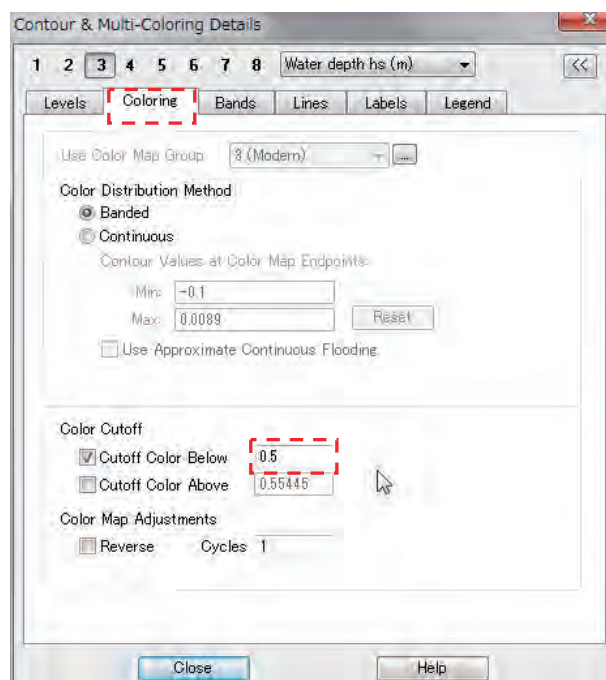


③ Edit legend.

User can edit color legend of contour as follows;

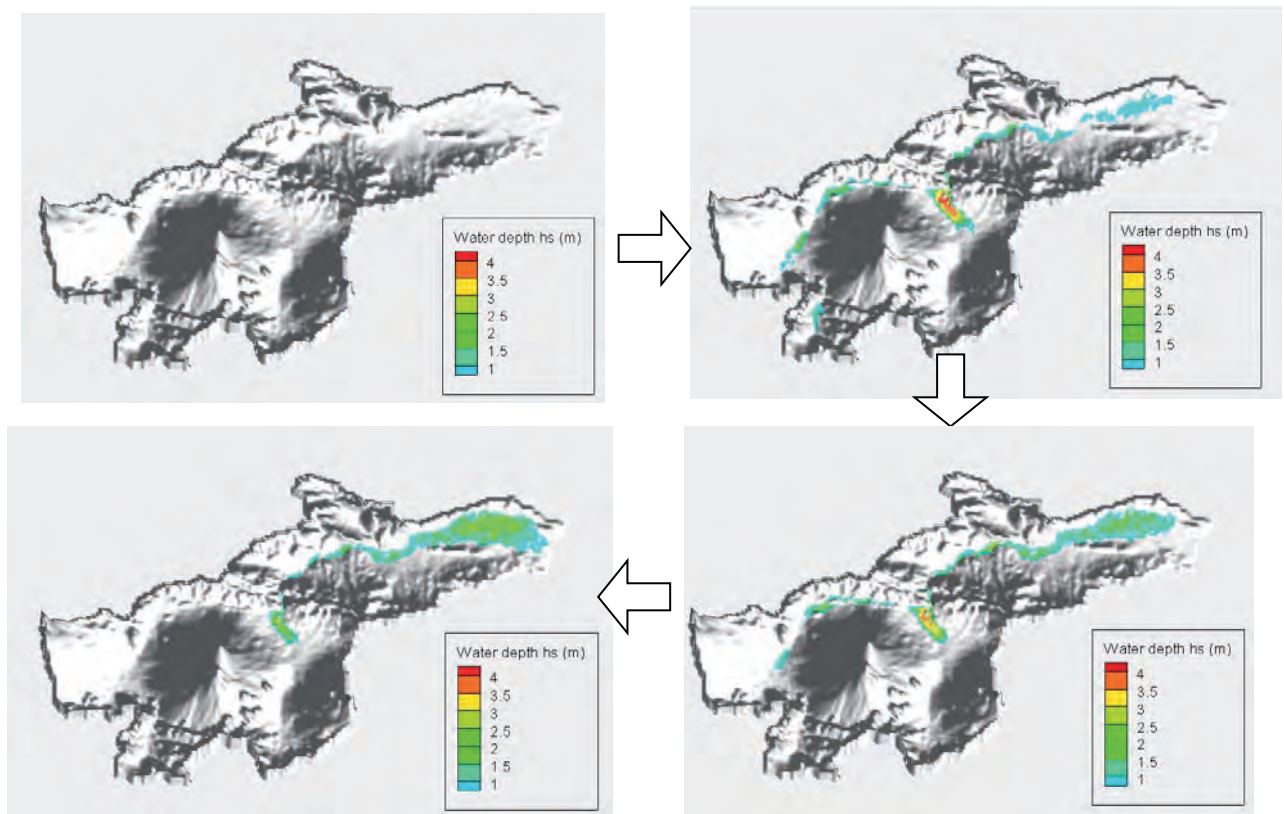
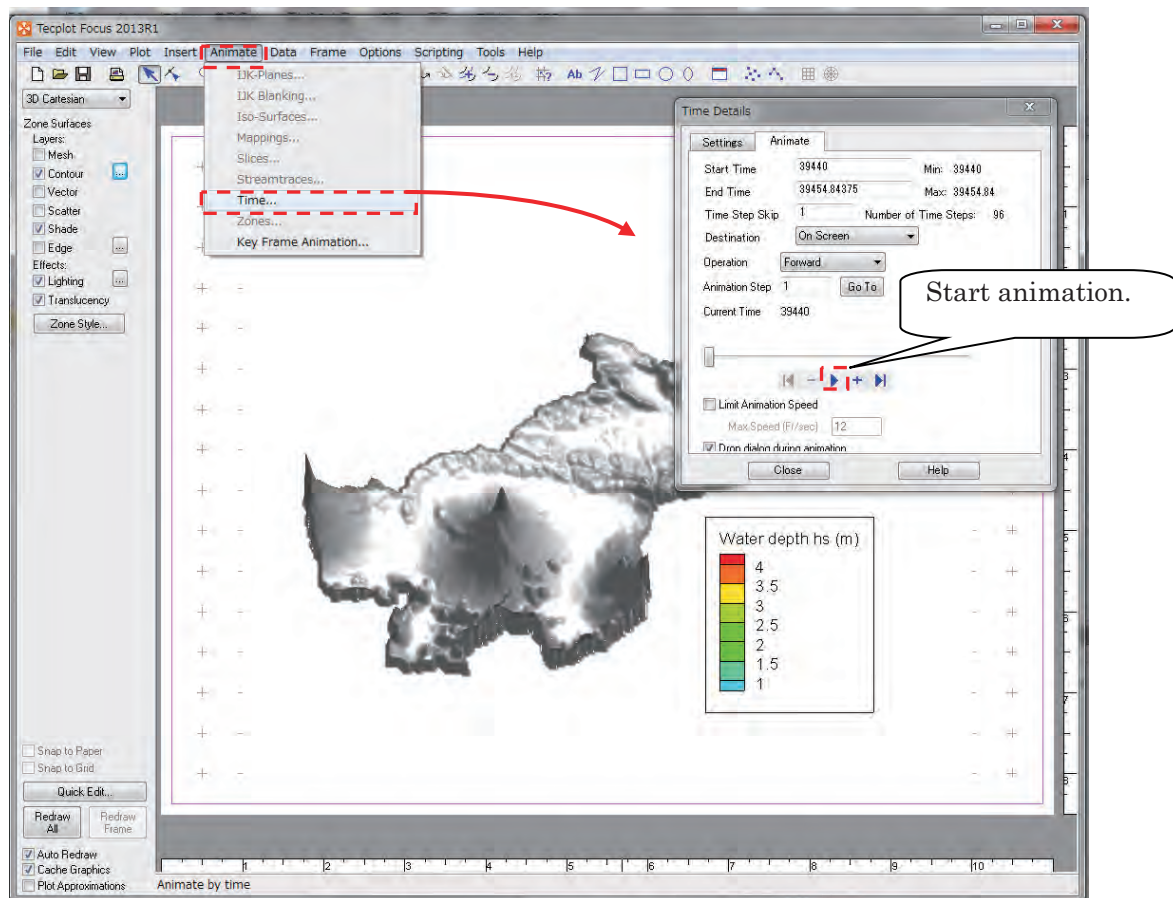


④ User also can edit “cut off” to display upper and lower color limits. Color up to 0.5m is cut in the following figure as an example.



- ⑤ User can check the time series of the contour figure.

[Animate] > [Time...]

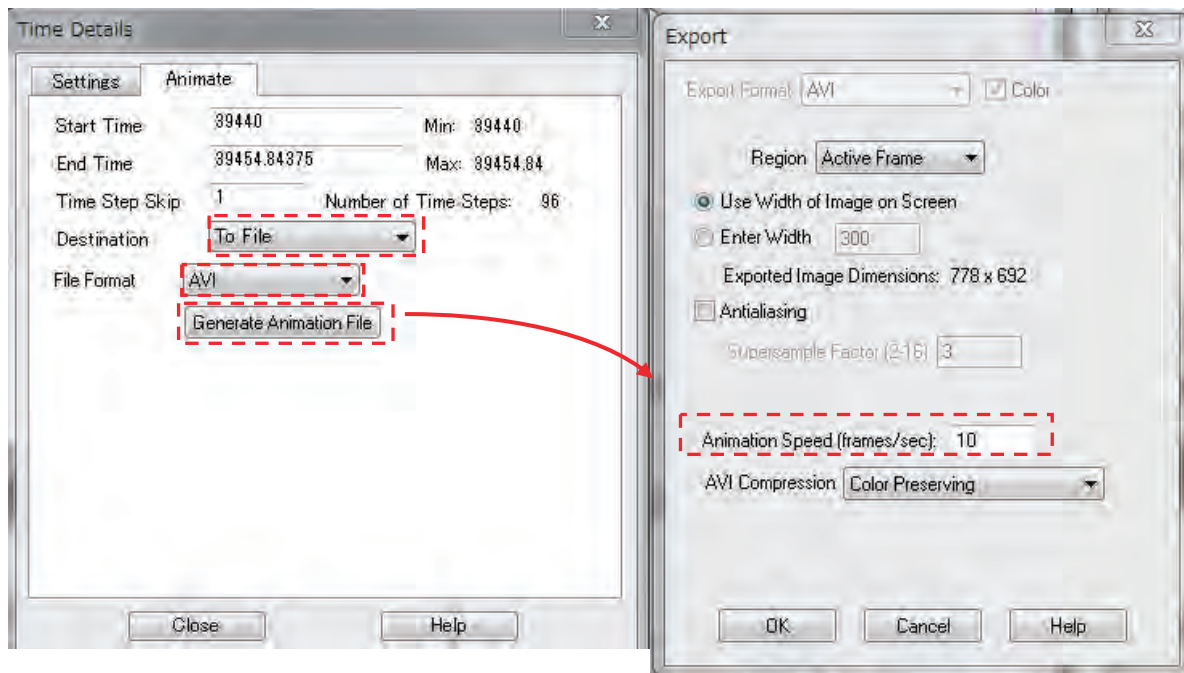


⑥ Export animation file

User can export animation file.

[Animate] > [Time...]

Select “To File” in “Destination” and “AVI” in “File Format” on “Animates” tab in “Time Details”. If user needs to edit animation speed, click “Generate Animation File” and edit “Animation Speed” if necessary.



7.6.5 Supplement of display

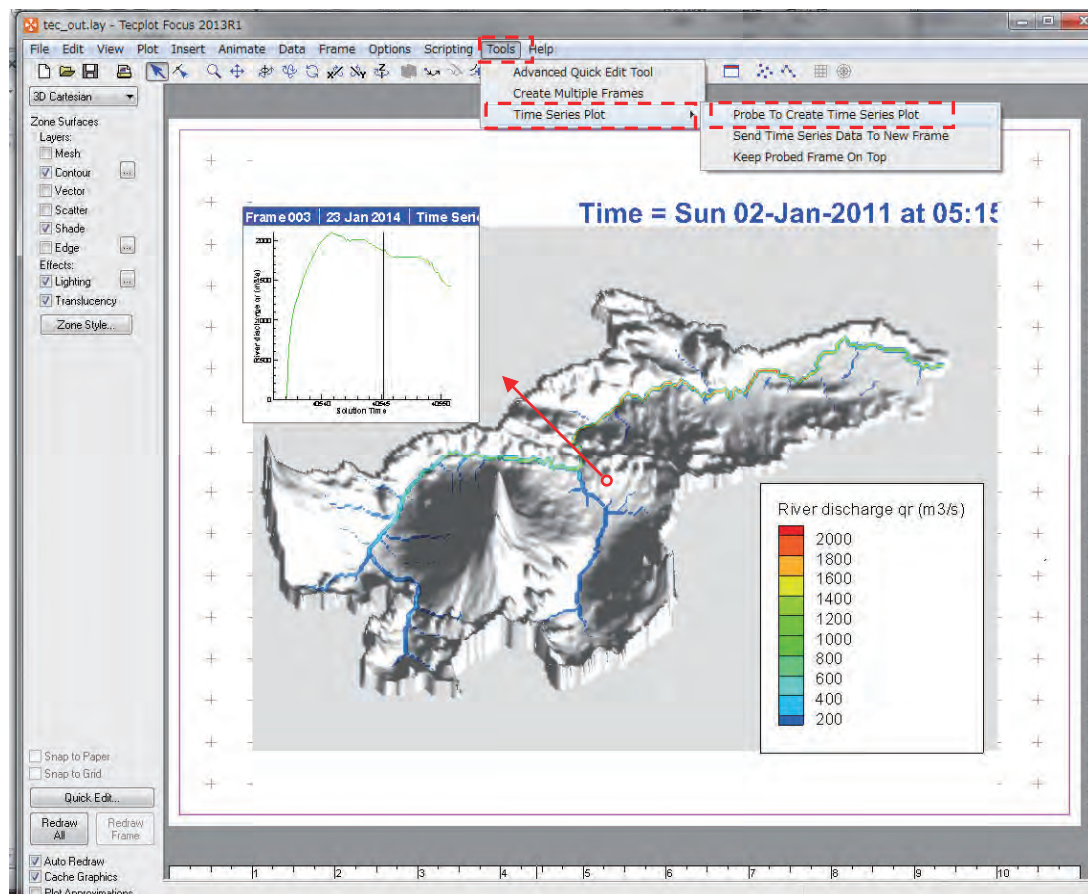
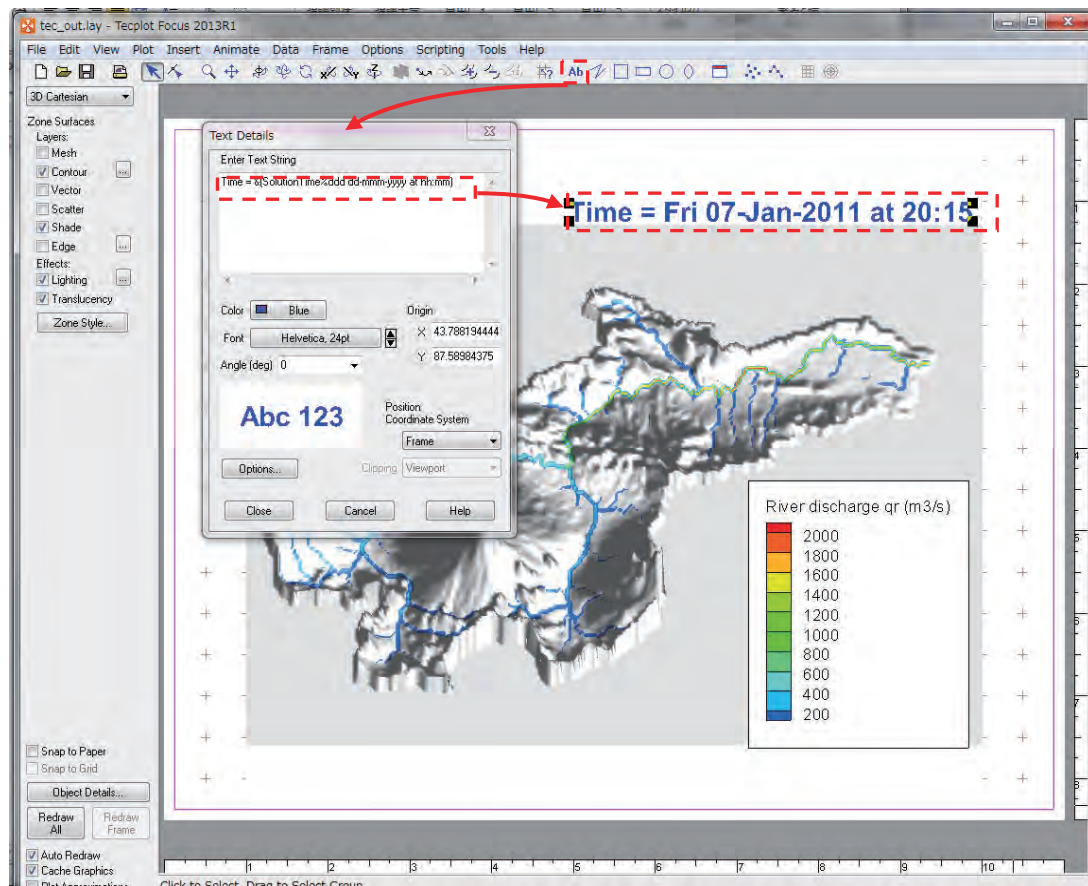
① Display timestamp information on animation

If user needs to display timestamp information on the contour figure, add textbox and input as follows:

Time = &(SolutionTime%ddd dd-mmm-yyyy at hh:mm)

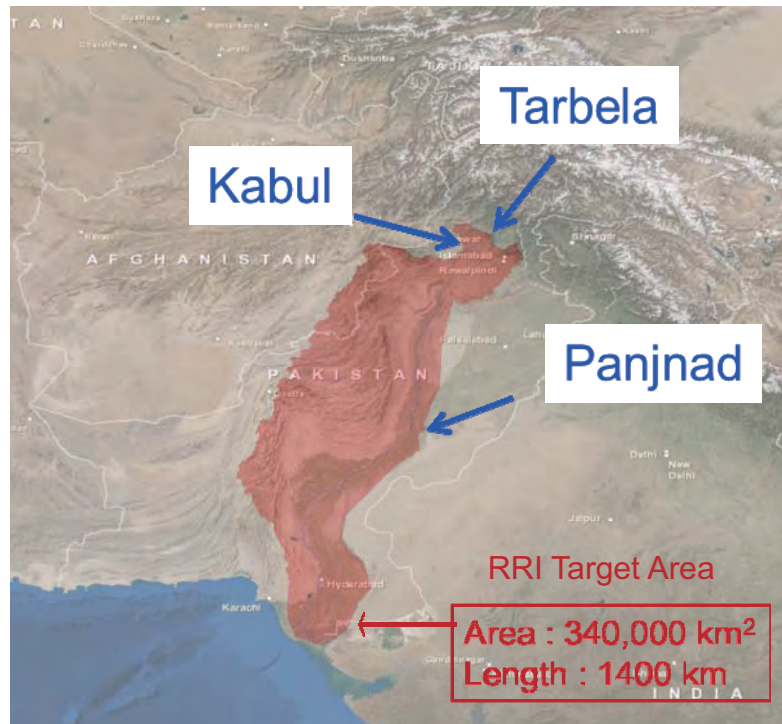
② Display time series graph on plane view.

Select [Tools] > [Time Series Plot] > [Probe To Create Time Series Plot] and identify the position by left click with the pointer “+” to display the time-series. Note that the variable selected as “Flood By” will be shown on the time series graph. Hence user needs to change the setting of Zone Style and “Flood By” to display different time-series (e.g. qr).



8. Application Example

This section presents the application of RRI Model to the lower Indus River basin. The target area is below Tarbela dam, Kabul and Panjnad points as indicated below. The simulation domain is about 340,000 km² and the river length is about 1,400 km. In this example, the river discharge boundary conditions are prepared based on observed discharge records during 2010 floods to force the model with rainfall records.

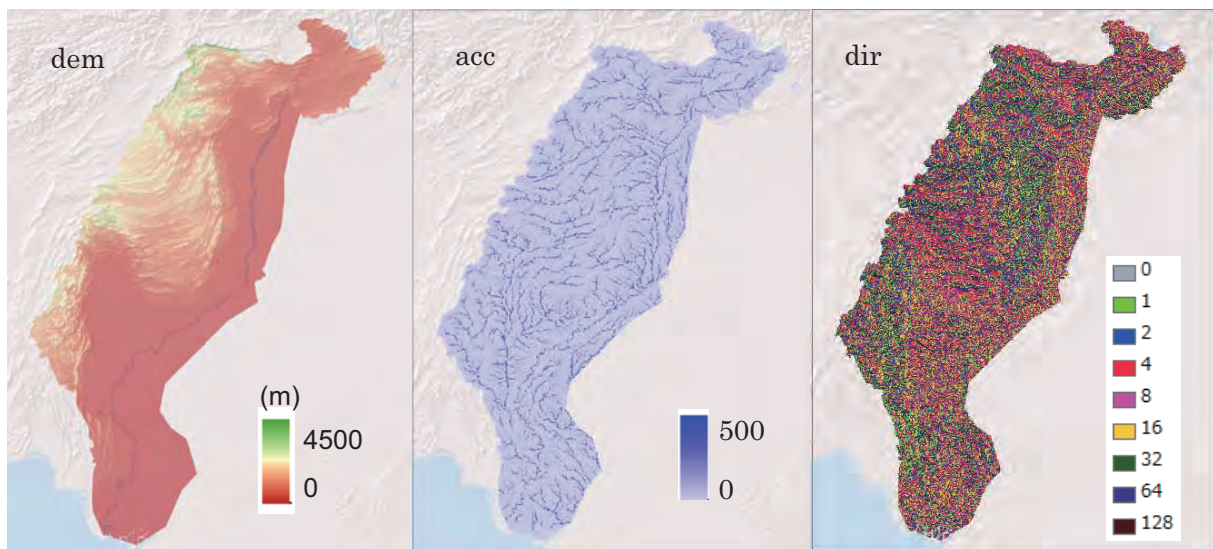


A polygon covering the simulation target (the red mask in the above figure) was prepared first. The flow direction data in HydroSHEDS (30sec) was used to identify the entire Indus River basin. Then the upstream areas above Tarbela, Kabul and Panjnad were removed from the entire Indus River basin.

The background image of the above figure can be obtained from the following site (http://goto.arcgisonline.com/maps/World_Imagery) and used in ArcGIS.

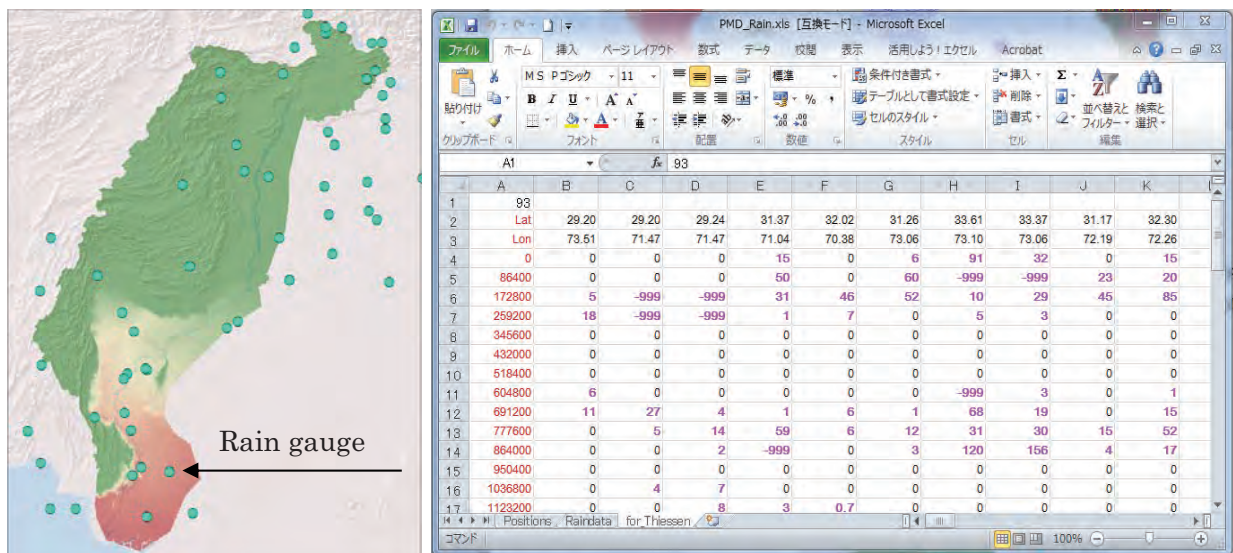
8.1 On Input Topography

By using the catchment polygon, **dem**, **acc** and **dir** datasets were clipped for the catchment area. The function embedded in ArcGIS ([Spatial Analyst Tools] → [Conditional] → [Con]) was used to mask the target area out of the regional datasets of HydroSHEDS (30 second resolution). Then “demAdjust2” program was used to adjust **dem** and **dir** to create **adem** and **adir**.



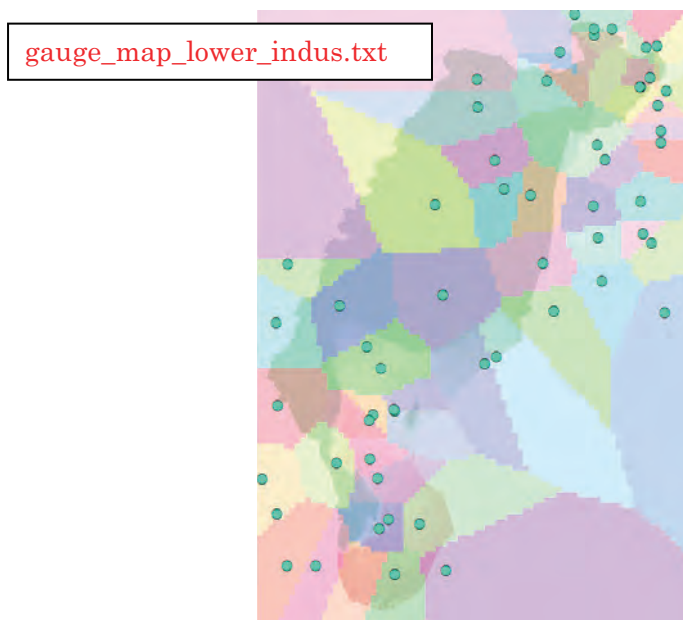
8.2 On Input Rainfall

Ground gauged rainfall records provided by Pakistan Meteorological Department (PMD) were used for the simulation. The green dots in the left figure below show their spatial distribution. The below right figure is the formatted ground gauged rainfall data with the latitude and longitude information. Total 93 data was used to create spatially distributed rainfall data.



Note that the first column of the excel sheet represents the time stamp of the rainfall data in second. For example, at the row of 172800 sec, the daily rainfall [mm/d] between time 86400 and 172800 sec was stored. Then all the data was copied to a text editor and save it as ASCII.

The ASCII file is the input data of `/etc/rainThiessen` program that generates the spatially distributed rainfall data. Note that the “`gauge_map_lower_indus.txt`” is also created after running `/etc/rainThiessen` program, so that one can check the spatial representation of each rain gauge (see the figure below after converting from the ASCII to Raster with ArcGIS).



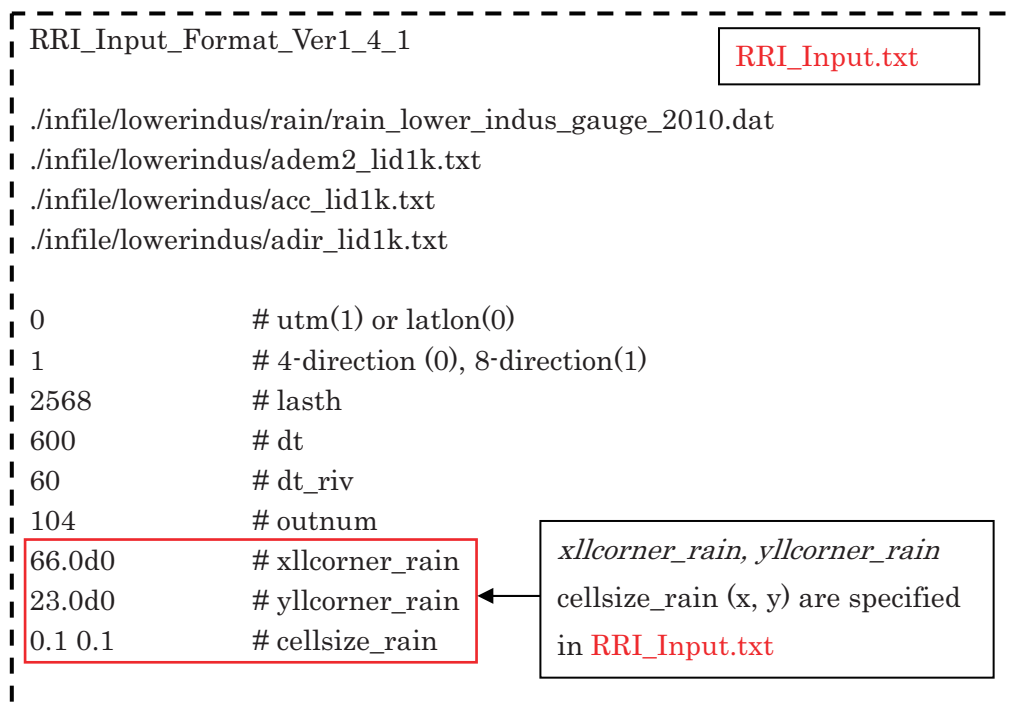
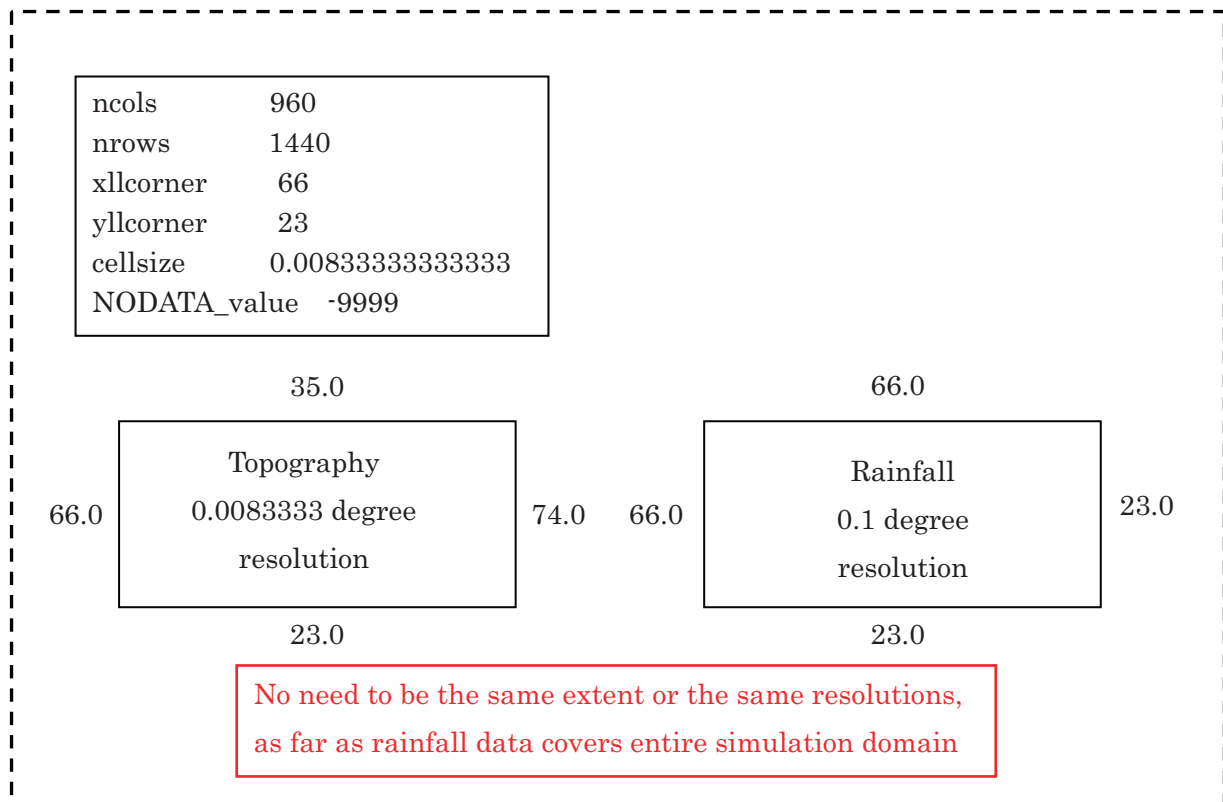
Here is the sample of the rainThiessen program input file (`rainThiessen.txt`).

```

./indus/gauge_1d_2010.txt
24
./indus/rain_lower_indus_gauge_2010.dat
./indus/gauge_map_lower_indus.txt
ncols 80
nrows 120
xll 66.0
yll 23.0
cellsize 0.1 → in degree

```

The rainfall data must cover all the simulation domain. However, it is not necessary to have the same resolution or the same coverage area. For example, 0.1 degree (approx. 10 km) may be fine enough to distribute the ground gauged rainfall for this case. Thus above `rainThiessen.txt` read by the `rainThiessen` program specifies the output resolution of 0.1 degree.



8.3 On Input Evapotranspiration

Current version of RRI Model does not have a function to estimate evapotranspiration from climate variables. However, by giving evapotranspiration rate as one of the input files, the model takes the equivalent amount of water from surface and subsurface storages.

The format of the evapotranspiration input is the same as rainfall. Hence the grid cell size and time step of evapotranspiration file can be arbitrary set. For example, to set the constant rate of evapotranspiration, one can prepare the following input file (e.g. evp_4mm.txt), in which the value of 0.166667 mm/h corresponds to 4 mm/d of evapotranspiration.

0 1 1	evp_4mm.txt
0.166667	
10000000 1 1	
0.166667	

To read the evapotranspiration input file, set flag 1 on the L71 and specify the input file name. The coordinate of south west corner (xllcorner and yllcorner) as well as the cellsize (x and y direction) must be also set in L73-L75.

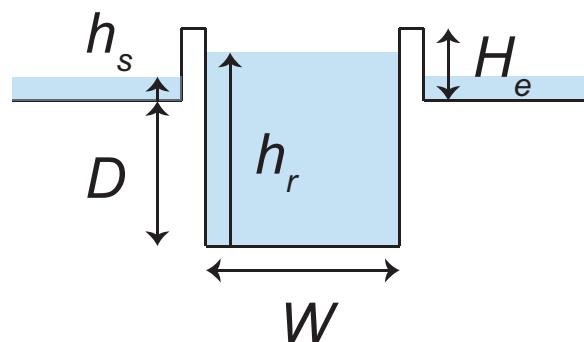
L71	1	RRI_Input.txt
L72	./infile/lowerindus/evp_4mm.txt	
L73	66.0d0 # xllcorner_evp	
L74	23.0d0 # yllcorner_evp	
L75	1000.d0 1000.d0 # cellsize_rain	

← xllcorner_evp, yllcorner_evp
cellsize_rain (x, y) are specified
in RRI_Input.txt

Note that if sufficient water exists on a slope grid cell, and if the grid cell store water in the Green Ampt-Model, the model takes water from the cumulative water in GA model. If a user wants to avoid the evapotranspiration from the GA model, use flag “2” instead of “1” on L71.

8.4 On River Channel Geometry Setting

RRI Model assumes the rectangle shape for all river cross sections. To determine river cross sections (incl. width W , depth D and levee height H_e), the following two options are available.



-
- { A) Use empirical equations with parameters defined in RRI_Input.txt
 B) Read the values from files and specify the files in RRI_Input.txt

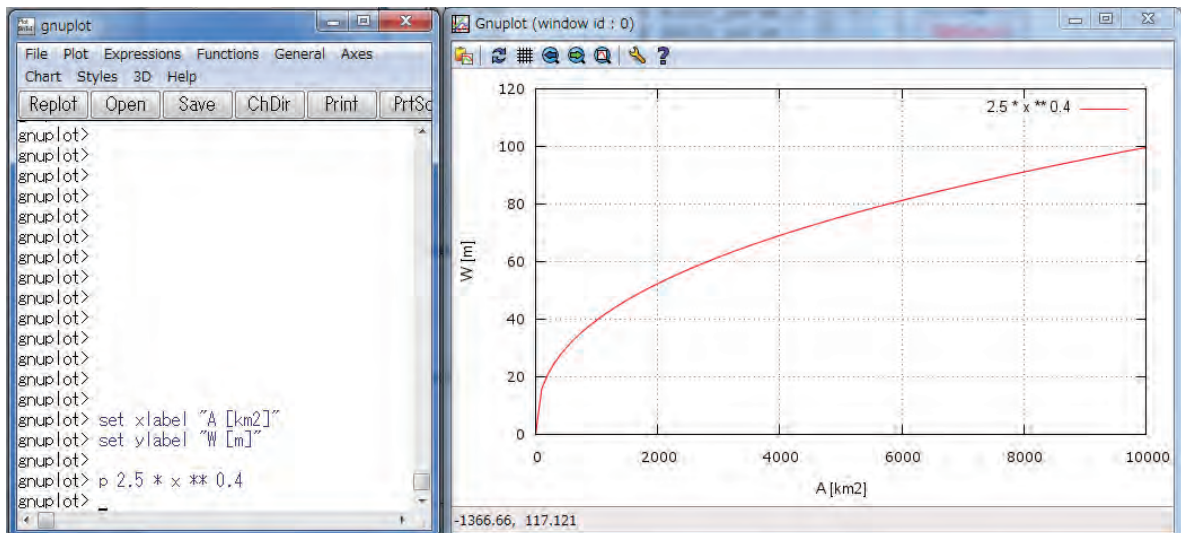
L38	100	# riv_thresh	}	RRI_Input.txt	
L39	2.5d0	# width_param_c			
L40	0.4d0	# width_param_s			
L41	0.1d0	# depth_param_c			
L42	0.4d0	# depth_param_s			
L43	0.d0	# height_param			
L44	20	# height_limit_param	}	Option A	
L45					
L46	1	← 0 : Option A / 1 : Option B (Read from files)		}	Option B
L47	./infile/lowerindus/width_lid1k.txt				
L48	./infile/ lowerindus /depth_lid1k.txt				
L49	./infile/ lowerindus /height_lid1k.txt				
L50					

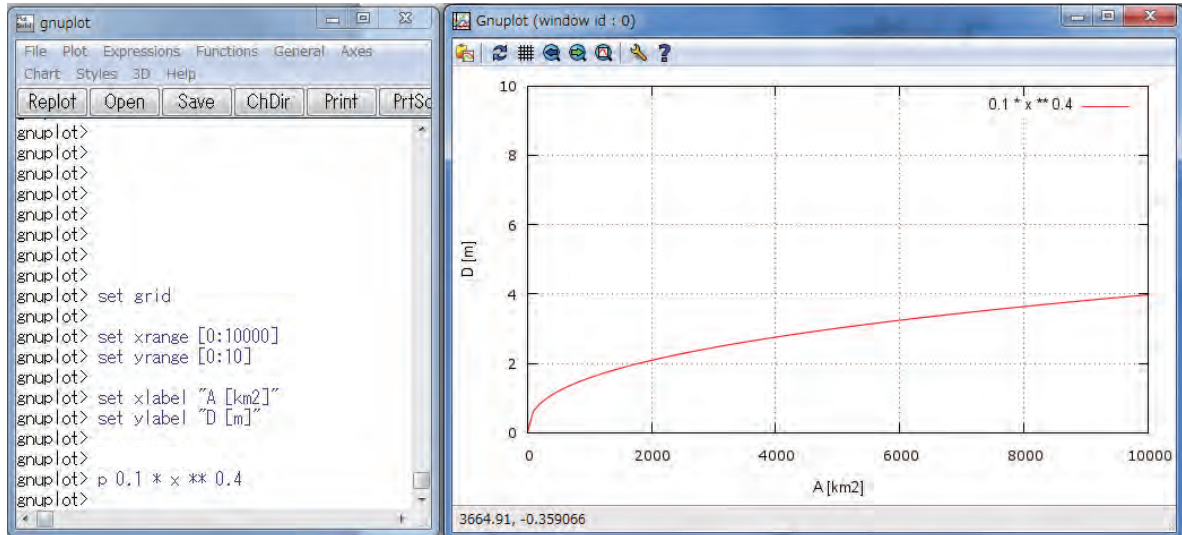
A) For the first option, the parameters of the following empirical equations must be appropriately set to represent target catchment condition (L38 – L44 of RRI_Input.txt).

$$width = c_w A^{s_w}$$

$$depth = c_d A^{s_d}$$

where A in the equations is the upstream catchment area [km²] for each river grid-cell. The unit of width and depth are [m]. The parameter “riv_thresh” defines the threshold of flow accumulation (i.e. number of upstream cells) to distinguish river grid cells or slope grid cells. Recall that for RRI model, slope exists even on a river grid cell.





B) For the second option, a user can prepare three files separately to represent width, depth, and height distributions. All those files must have the same number of row, column and resolution as the topography data (i.e. adem, acc and adir). The format of these data is ArcGIS ASCII format (i.e. the same as the topography data).

Note that the width file (e.g. `./infile/lowerindus/width_lid1k.txt`) is used to decide whether each grid-cell has river or not ($width > 0$ is treated as a river grid cell). The values of depths and heights must be appropriately defined on a cell where the $width > 0$.

To support for creating the width, depth and height files, a Fortran program called `/etc/makeRiver2/` can be used. The program reads “acc” file to calculate the upstream catchment area A [km²] for each grid cell and a user can define different equations or fixed values within the program to create the three river cross section files.

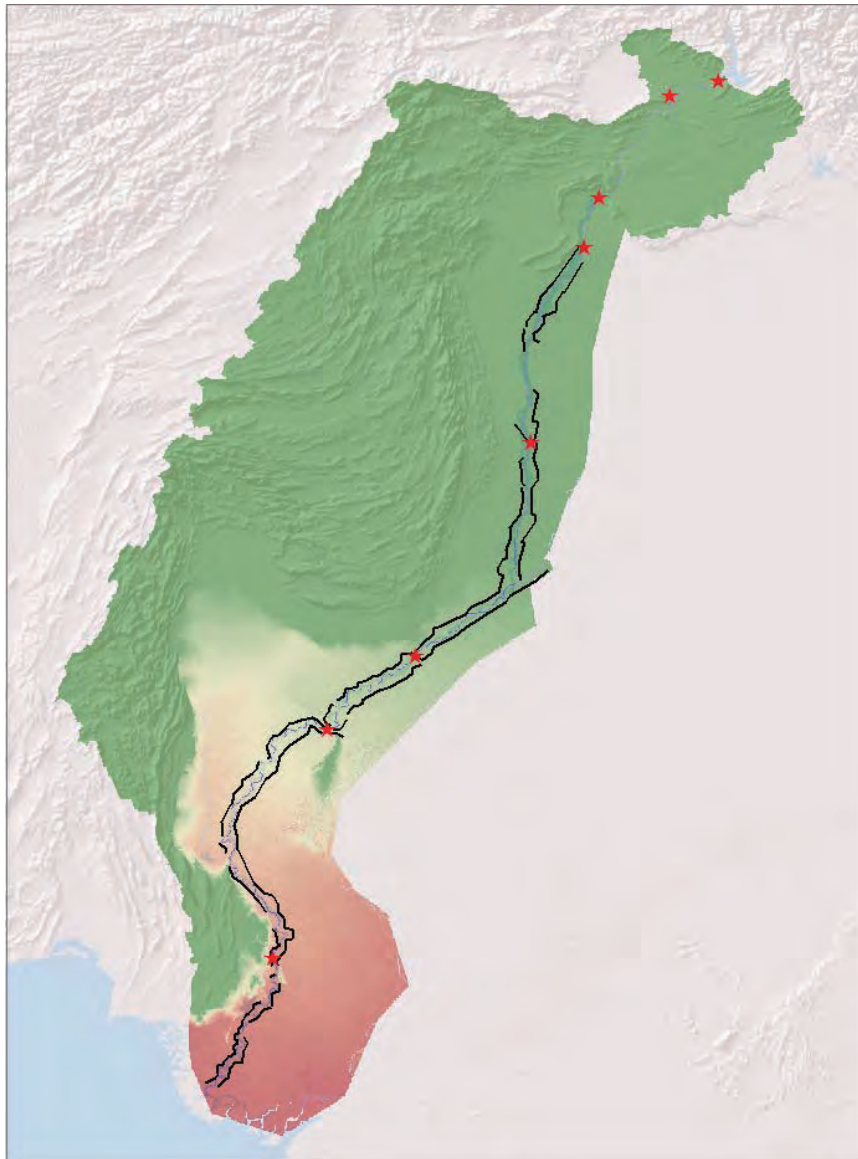
8.5 On Embankment Setting

There are two kinds of embankment settings in RRI simulation.

- A) Embankment along rivers
- B) Embankment on slope grid cells

A) The first type of embankment is illustrated in the figure of a river cross section. The effect of embankment is considered during the interaction of water between river and slope. To include the first type of embankment, the height value ($height > 0$) must be set on river grid cells ($width > 0$). Because of the RRI Model basic structure, a river is set as a centerline of a

slope grid, it is not possible to apply different embankment height for different side of the river for this option.



B) The second type of embankment represents roads, railways or other structures that prevent water to across. Since the embankment along the main Indus River is located a few kilometers apart from the main channel (see above figure), this second type suits better. The location information of the embankment was converted to raster data having the same resolution with topographic data on ArcGIS. The above mentioned “*height*” file specified in RRI_Input.txt can contain the height information (and therefore the embankment location information) on slope grid cells.

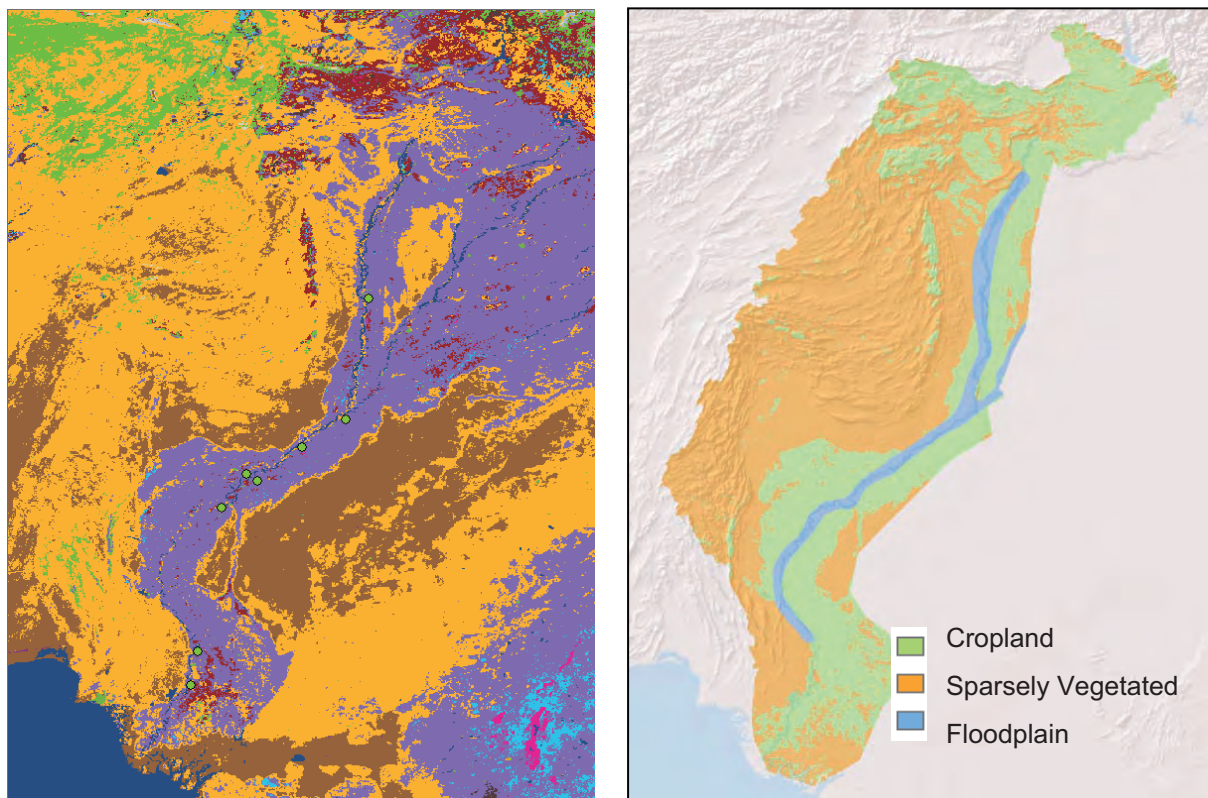
Note that even if a user intends to set a continuous embankment apart from a main river, if a tributary joins into the river and if the “*height*” value is set on a river grid cell where *width* >

0, the embankment would be regarded as the embankment of Type A. As a result, the set embankment will be discontinuous at the location.

To avoid the situation and elevate DEM even on the tributary (or river grid cells), one can use the flag of “2” on L46.

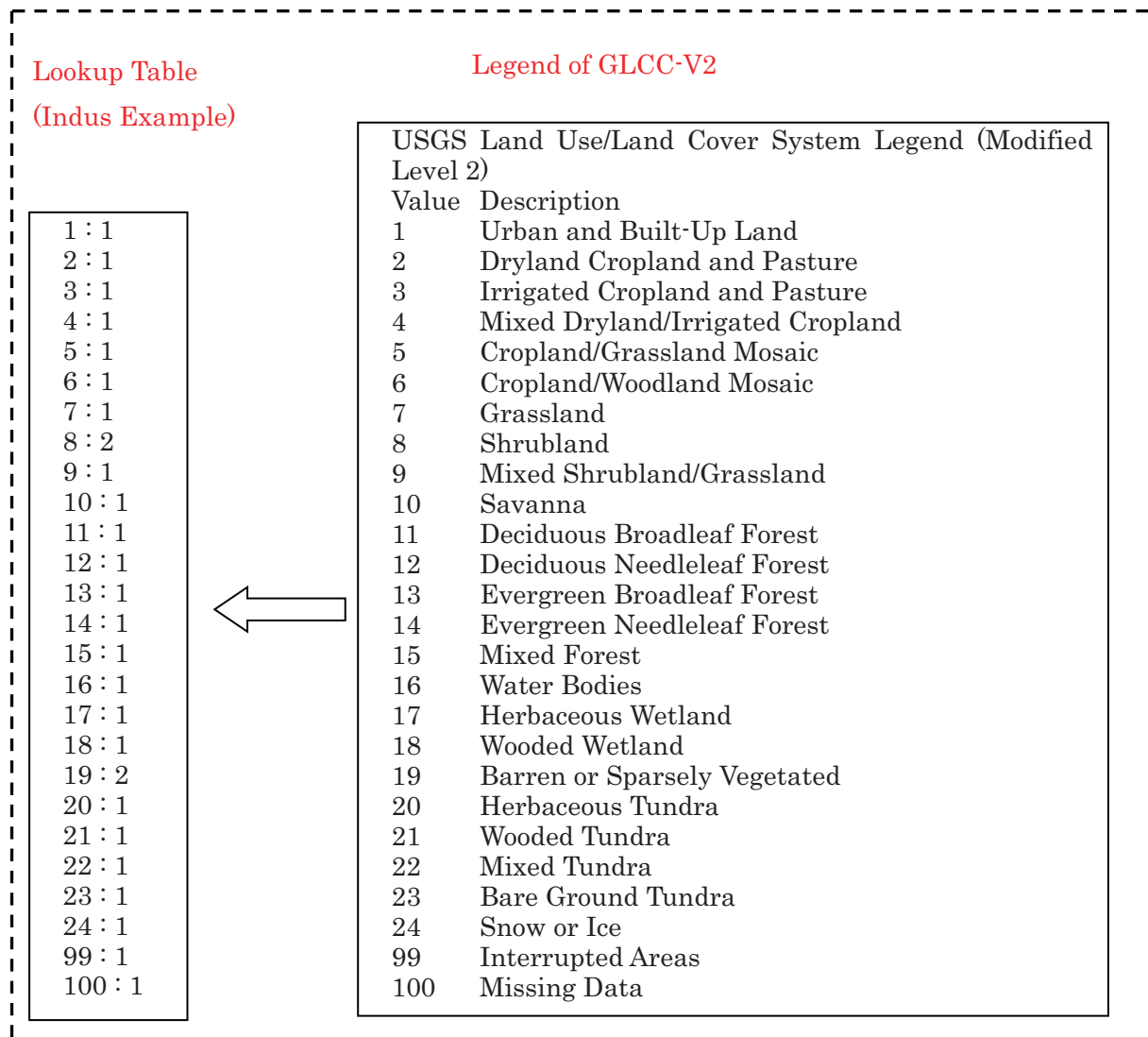
8.6 On Land Class Setting

The effects of land cover (or soil type) can be reflected by assigning different model parameters. In this example, GLCC-V2 (Global Land Cover Characterization) provided by USGS was used. The original land cover data (left) is too detail to assign all different parameters; therefore, similar land cover types were merged into two categories: **Cropland** and **Sparsely Vegetated**, and also overlaid additional **Floodplain** polygon.



For re-classing the original land cover data, ArcGIS function [Spatial Analyst Tools] → [Reclass] → [Reclass by ASCII File] was used. The following lookup table was prepared by a text editor to define the re-class. Different lookup tables may be defined for different projects. Note that the number of the raster data (in this case 1, 2 and 3) corresponds to the column of parameter sets in **RRI_Input.txt**. Thus provide sequential numbers starting from 1 for representing different land covers.

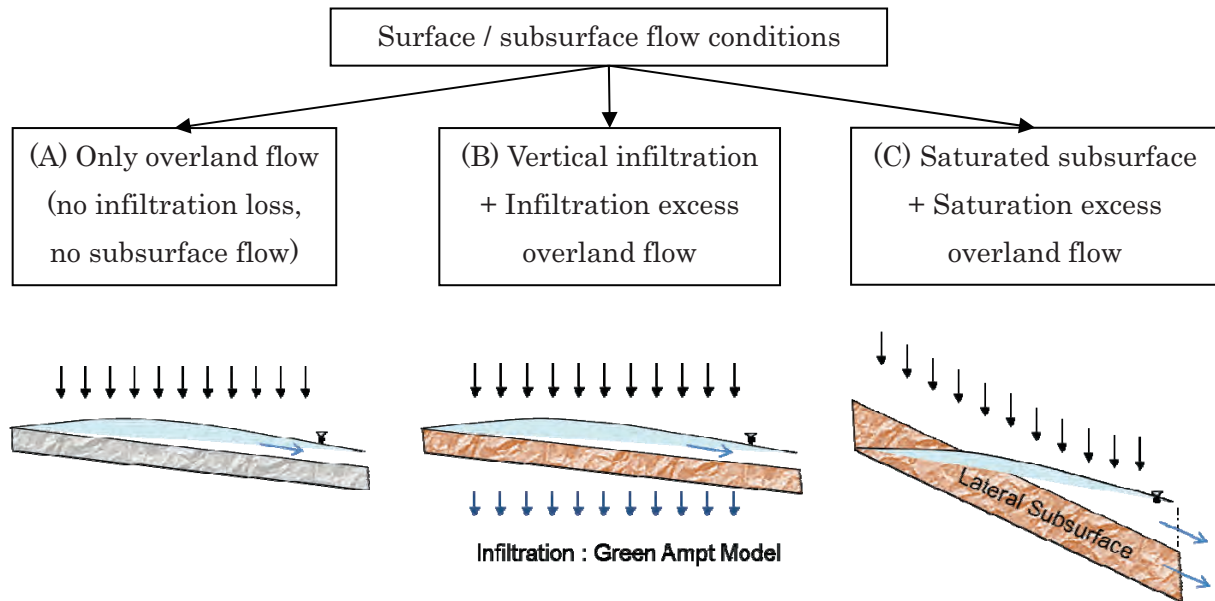
Finally the re-classed land cover was converted to the ArcGIS/ASCII format and saved it as “lu_lid1k.txt”. Note that the file can be read by RRI Model by indicating the file link in “RRI_Input.txt”.



8.7 On Parameter Setting

Model parameter values are defined in RRI_Input.txt. In this section, the general idea to decide model parameters are described first, then a calibrated model parameter set for the Indus River basin will be shown as an example.

For each land cover class, decide (A), (B) or (C) in the following figure depending on infiltration and subsurface processes, so that the number of calibration parameters will be limited.



Example of parameter values (their recommended ranges)

Parameters	Notation	(A)	(B)	(C)
n (River) ($\text{m}^{-1/3}\text{s}$)	ns_river		0.03d0 (0.015 ~ 0.04)	
n (Land) ($\text{m}^{-1/3}\text{s}$)	ns_slope		0.3 d0 (0.15 ~ 1.0)	
Soil depth (m)	soildepth		1.0 d0 (0.5 ~ 2.0)	
Porosity (-)	gammaa		0.471d0 (0.3 ~ 0.5)	
k_v (m/s)	kv	0.d0	5.56d-7	0.d0
S_f	Sf	inactive	0.273d0	inactive
k_a (m/s)	ka	0.d0	0.d0	0.1d0 (0.01-0.3)
Unsat. porosity (-)	gammam		Inactive	0.d0
β	beta	inactive	Inactive	inactive

Note: 0.d0 is used in RRI_Input.txt to represent double precision of 0.0.

For case (A), where only overland flow without infiltration or subsurface flow process are considered, **set both kv and ka equal to 0**.

For case (B), where vertical infiltration + infiltration excess overland flow are considered, **set ka = 0**, and the parameter “da” is equal to “soil depth” times “porosity”.

For case (c), where saturated subsurface + saturation excess overland flow are considered, **set kv = 0**, and the infiltration limit (defined as a parameter in the previous versions of the RRI model) equals to “soil depth” times “porosity”.

Note that the parameter values in the above table are just one example values (approximate ranges).

Note that even though the values in `inactive` part do not affect the simulation result, a double precision value like 0.0d0 must be filled in `RRI_Input.txt` (see the sample below).

* Set “`ksg = 0.d0`” to avoid groundwater computation, whose algorithm is under development and not completed at `RRI ver1.4.2`.

** If both `ka` and `kv` are set to be non-zero, `RRI` will stop with an error message.

The following figure shows an example of parameter settings

L18	0.03d0	# ns_river	RRI_Input.txt
L19	3	# num_of_landuse	
L20	1 1 1	# diffusion(1) or kinematic(0)	
L21	0.15d0 0.15d0 0.15d0	# ns_slope	
L22	1.0d0 1.0d0 1.0d0	# soildepth	
L23	0.4d0 0.4d0 0.4d0	# gammaa	
L24			
L25	5.556d-7 6.056d-7 0.d0	# kv	
L26	0.273d0 0.1101d0 0.d0	# Sf	
L27			
L28	0.1d0 0.1d0 0.1d0	# ka	
L29	0.0d0 0.0d0 0.0d0	# gammam	
L29	8.0d0 8.0d0 8.0d0	# beta	
L31			
L32	0.d0 0.d0 0.d0	# ksg	
L33	L36 are inactive under ksg = 0.d0		

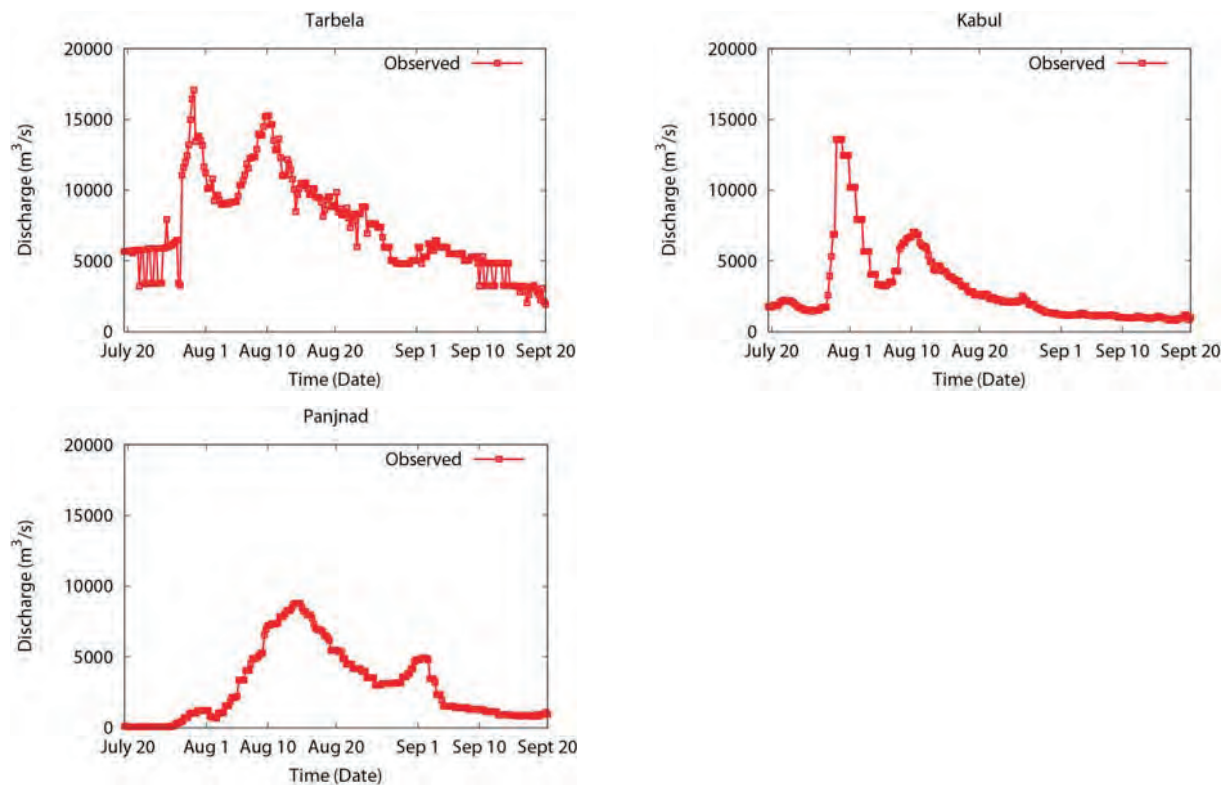
Reference Table : Green-Ampt Infiltration Parameters for different soil texture

Soil texture class	k_v (m/s)	ϕ [gammaa]	S_f (m)
Sand	6.54E-05	0.437	0.0495
Loamy sand	1.66E-05	0.437	0.0613
Sandy loam	6.06E-06	0.453	0.1101
Loam	3.67E-06	0.463	0.0889
Silt loam	1.89E-06	0.501	0.1668
Sandy clay loam	8.33E-07	0.398	0.2185
Clay loam	5.56E-07	0.464	0.2088
Silty clay loam	5.56E-07	0.471	0.273
Sandy clay	3.33E-07	0.43	0.239
Silty clay	2.78E-07	0.479	0.2922
Clay	1.67E-07	0.475	0.3163

From Rawls, W.J. et al., 1992. Infiltration and soil water movement. In: Handbook of hydrology. New York: McGraw-Hill Inc., 5.1–5.51. (Units are converted for RRI Model)

8.8 On Boundary Condition

The following river boundary conditions were set based on the observed discharges at the three locations during the 2010 flood.

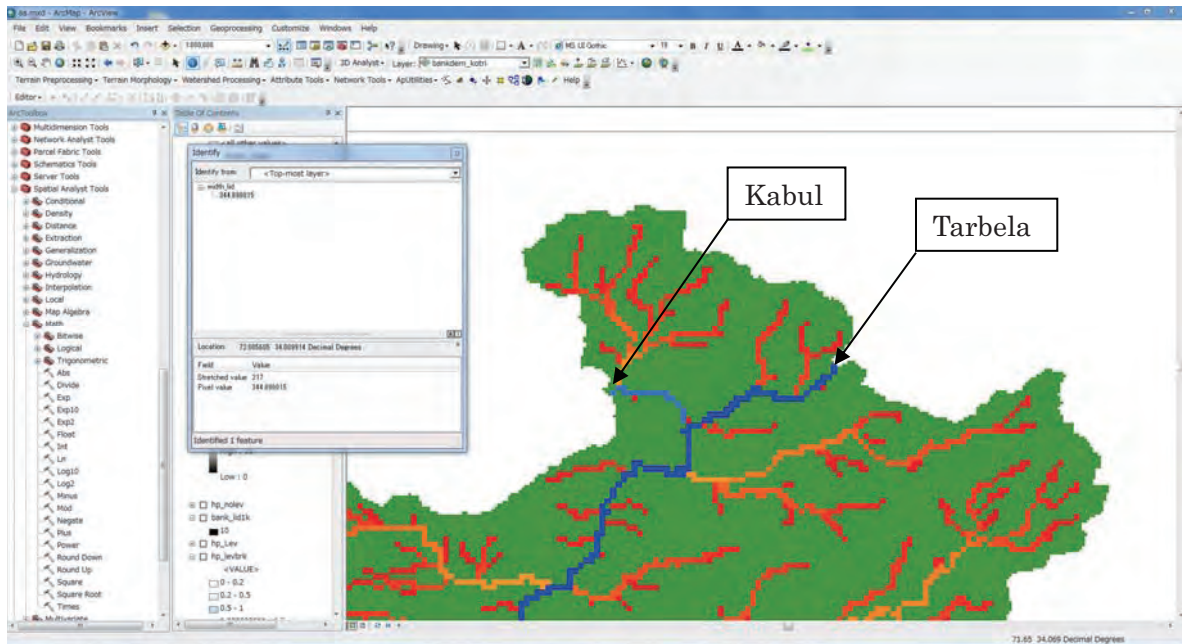


The steps to set river discharge boundary conditions are described below.

- ① Find locations to provide the boundary conditions.

Viewing **acc** values on ArcGIS can help you to identify appropriate position with lat lon information along a river channel. Use i (identify) icon to find out the coordinate.

Then use the “**/etc/coordinate.xls**” to convert from the lat lon coordinate to loc_i and loc_j. See Section 7.3 on the conversion in detail.



- ② Prepare a 1D boundary condition file with the following format.

The number of boundary condition setting points

③

The loc_i and loc_j of all points to give boundary conditions

loc_i	110	119	680	
loc_j	803	719	602	
0	3936.041733	3007.249151	917.4658428	
21600	3936.041733	3007.249151	917.4658428	
43200	3936.041733	3007.249151	917.4658428	
64800	3879.408039	3044.061053	917.4658428	
86400	4813.86399	3015.744206	917.4658428	
108000	4700.596602	2944.952088	917.4658428	
129600	4842.180837	2899.645133	917.4658428	
151200	4672.279755	2922.29861	1093.030294	
....	

Time series of the boundary condition data (units: [m³/s] for river discharge, and [m] for water depth)

- ③ Settings in RRI_Input.txt

After preparing the boundary condition file (e.g. **disc_lid1k_2010.txt**) and move the file in the appropriate folder (e.g. ./infile/lowerindus/), edit the RRI_Input.txt file as follows.

L51 0 0 0 0 L52 ./infile/lowerindus/hs_init_dummy.out L53 ./infile/lowerindus/hr_init_lid1k.txt L54 ./infile/lowerindus/hg_init_sample.out L55 ./infile/lowerindus/gampt_ff_init_dummy.out L56 L57 0 0 L58 ./infile/wlev_bound_dummy.txt L59 ./infile/hr_bound_dummy.txt L60 L61 0 1 L62 ./infile/as_bound_dummy.txt L63 ./infile/lowerindus/bounds/bound_lid_2010.txt L64	<div style="border: 1px solid black; padding: 5px; width: fit-content; margin-bottom: 10px; color: red;">RRI_Input.txt</div> <div style="border: 1px solid black; padding: 5px; width: fit-content; margin-bottom: 10px;">Write the file name of river discharge boundary</div> <div style="border: 2px solid red; padding: 2px; display: inline-block; color: red;">./infile/lowerindus/bounds/bound_lid_2010.txt</div>
---	--

Another option is to use two-dimension format for setting boundary conditions. In that case, prepare the following “**setBound.txt**” first as the input file to “/RRI/etc/setBound” program, which creates the input boundary condition file (e.g. **disc_lid1k_2010.txt**) on two dimensional basis. The two-dimensional boundary condition files can be read with flag 2 on L61.

../Model/infile/lowerindus/adem_lid1k.txt ../Model/infile/lowerindus/acc_lid1k.txt ../Model/infile/lowerindus/adir_lid1k.txt ./infile/lowerindus/disc_Constant.txt ../Model/infile/lowerindus/disc_lid1k_Constant.txt 3 119 719 110 803 680 602	<div style="border: 1px solid black; padding: 5px; width: fit-content; color: red;">setBound.txt</div>
---	--

In the above example of “**setBound.txt**”, L1 to L3 are the paths to the topography files (dem, acc and dir). L4 is the 1D discharge file (input) prepared above and the L5 is the output of the setBound program. L6 indicates the number of points to give the boundary conditions, followed by the positions in loc_i and loc_j.

The created boundary condition files have the same format as the rainfall file. However, unlike rainfall files, the number of columns and rows must be exactly the same as the topography data, so that RRI Model knows where to give the boundary.

Note that discharge boundary conditions including along river and on slope must have the information of the directions. In other words, they should be vector values rather than the scalar values. To decide the direction of the discharge boundary conditions, RRI Model refers to the flow direction in “dir” file.

Water level boundary conditions on slope and/or river can be also set by changing the value on L57 to 1 and specifying the boundary condition file name. The file format is the same as the river discharge boundary condition.

8.9 On Initial Condition

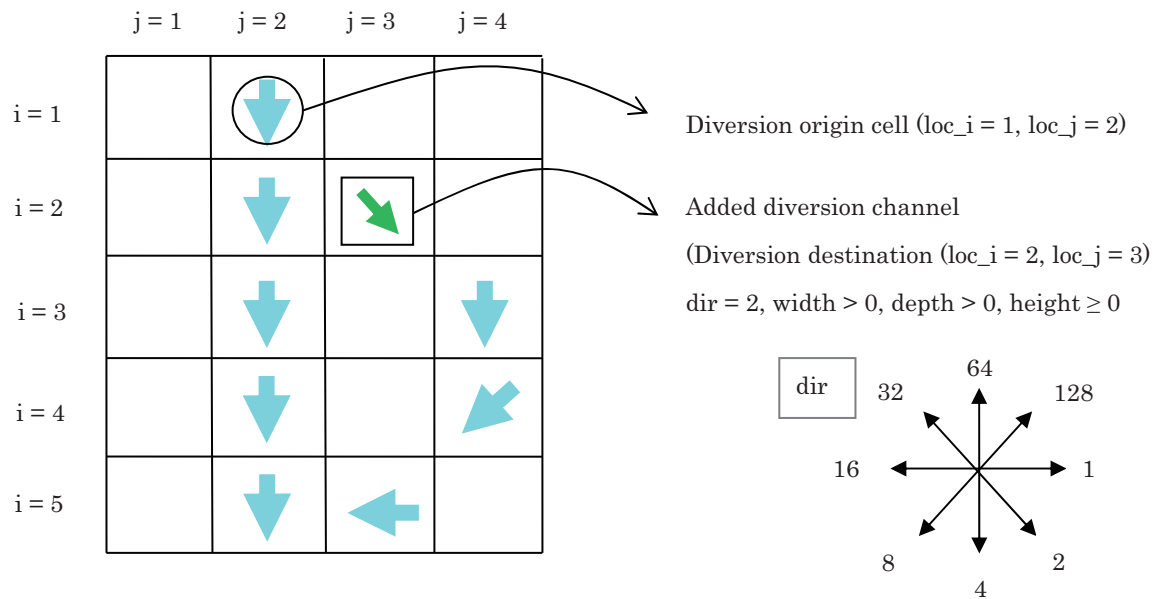
RRI Model can take initial conditions for water depths on slope and river as well as the cumulative water depth in the Green-Ampt model. The format of the files is the same as the output of those variables, so that one can use the output of the RRI as the input for the next simulation.

This feature enables the continuous long-term simulation. In order to read the initial conditions, L49 to L52 in the RRI_Input.txt must be edited in a same manner as the example of the boundary condition setting.

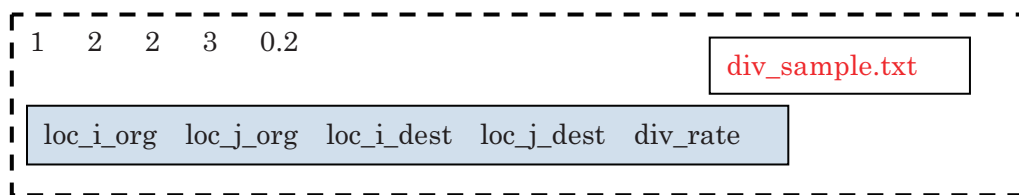
8.10 Diversion option (for advanced users)

RRI model can simulate the effect of diversion in a simple way. The portion of the diversion from a main channel to a diversion channel must be pre-defined by a model user and described in RRI_Div.f90 program. The followings are the basic steps to activate the option.

- ① Edit input river cross section files (i.e. width, depth, height) and flow direction files to add necessary diversion channels (e.g. green arrow for the below figure).
- ② Check a origin cell (loc_i_org, loc_j_org) and a destination cell (loc_i_dest, loc_j_dest).
Both the origin and destination cells must be specified on river grid-cells. Typically these two are adjacent, but not necessary (i.e. diverted water can jump into an apart cell).



- ③ Prepare a file to specify the origin and destination cells based on the following format. One can list up multiple lines if more than one diversion should be considered. “div_rate” specifies the ratio of discharge diverted from the main river to the diversion..



- ④ Activate this option by setting flag 1 on L70 and specify the diversion file name (e.g. div_sample.txt) on L71 in RRI_Input.txt.

8.11 Dam option (for advanced users)

RRI model can simulate the effect of dam reservoirs in a simple way. The dam model has two parameters: outflow discharge and maximum storage volume. The model takes storage volume as a state variable, which continues being updated based on simulated inflow and outflow. The outflow is maintained at a certain discharge rate that is lower than the inflow rate until the storage volume reaches the dam’s maximum storage level. After the storage volume exceeds the maximum level, the model is designed to release the water at the same rate as the inflow rate. The parameters must be determined based on dam operation records. The followings are the basic steps to activate the dam model.

- ① Prepare a dam parameter file by the following format.

2					
Bhumibol	166	71	5800000000	150	dam_sample.txt
Sirikit	135	166	3510000000	500	
dam names, loc_i_dam, loc_j_dam, storage volume [m ³], constant discharge [m ³ /s]					

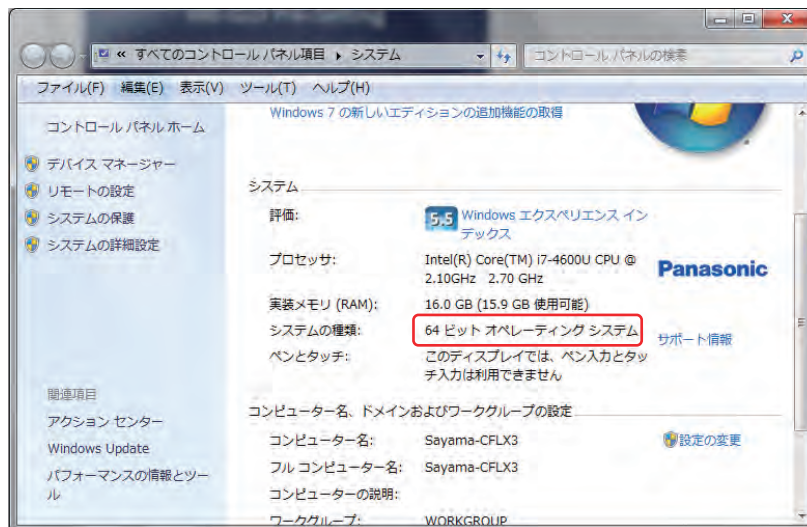
- ② Activate the dam model by setting flag 1 on L65 and specify the dam file name on L66 in RRI_Input.txt.

9. Use of RRI Graphical User Interface (GUI)

This section explains how to use RRI-GUI to apply the model at a basin and visualize the simulation results.

9.1 Pre-setting

- 1) Unzip “RRI_1_4_2.zip” and save it under a working folder (e.g. C:\).
- 3) Check your PC is 32 or 64 bit. (My Computer → Property)



- 4) Install two programs saved in “RRI-GUI/Pre-setting”

- ① `w_fcompxe_redist_intel64.msi`
- ② `vcredist_x64.exe`

(for 32 bit, install `vcredist_x86.exe` and `w_fcompxe_redist_ia32.msi`)

For “`vcredist_x64.exe`”, you may encounter an error message suggesting you have already the newer version of “Microsoft Visual C++ 2010 Redistributable”. In that case, you can just close the error message and cancel to install “`vcredist_x64.exe`”.

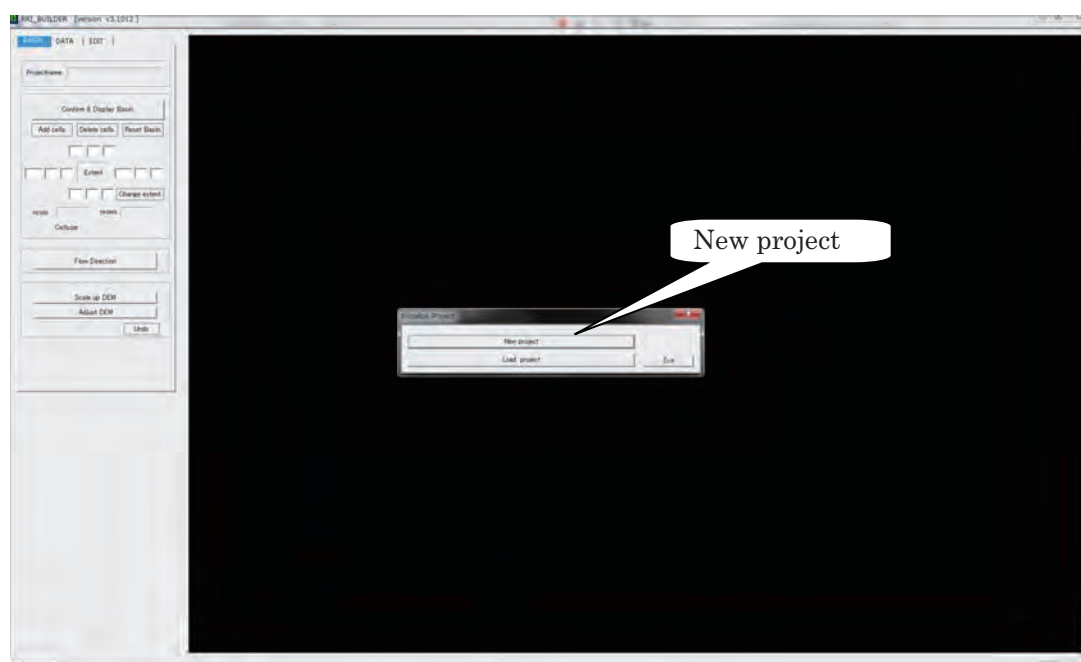
- 5) Execute `RRI_BUILDER_64.exe`

(for 32 bit machine, execute `RRI_BUILDER_32.exe`)

9.2 Model application and running with RRI_BUILDER

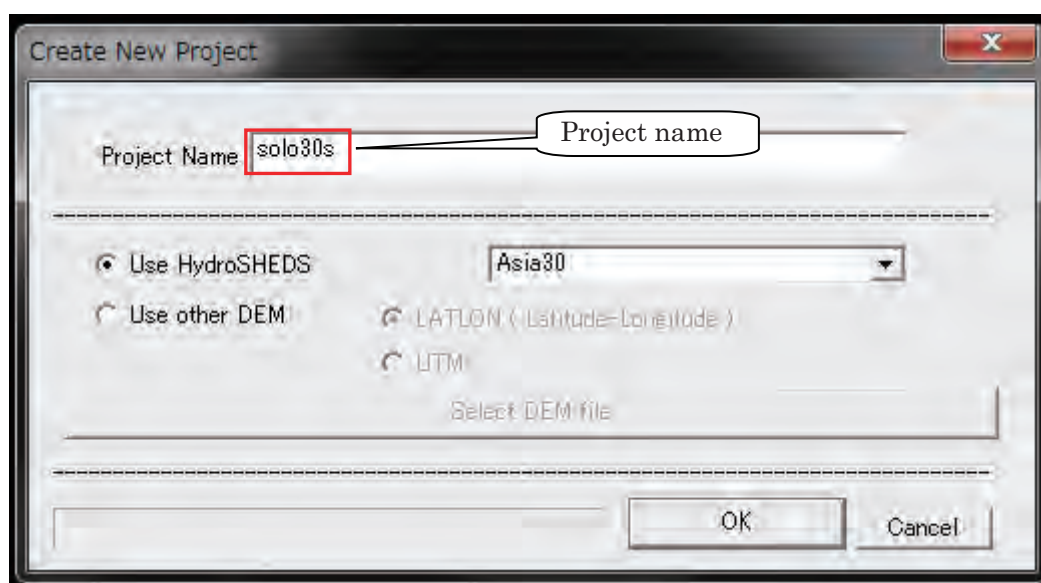
9.2.1 Preparing Input Topography Data

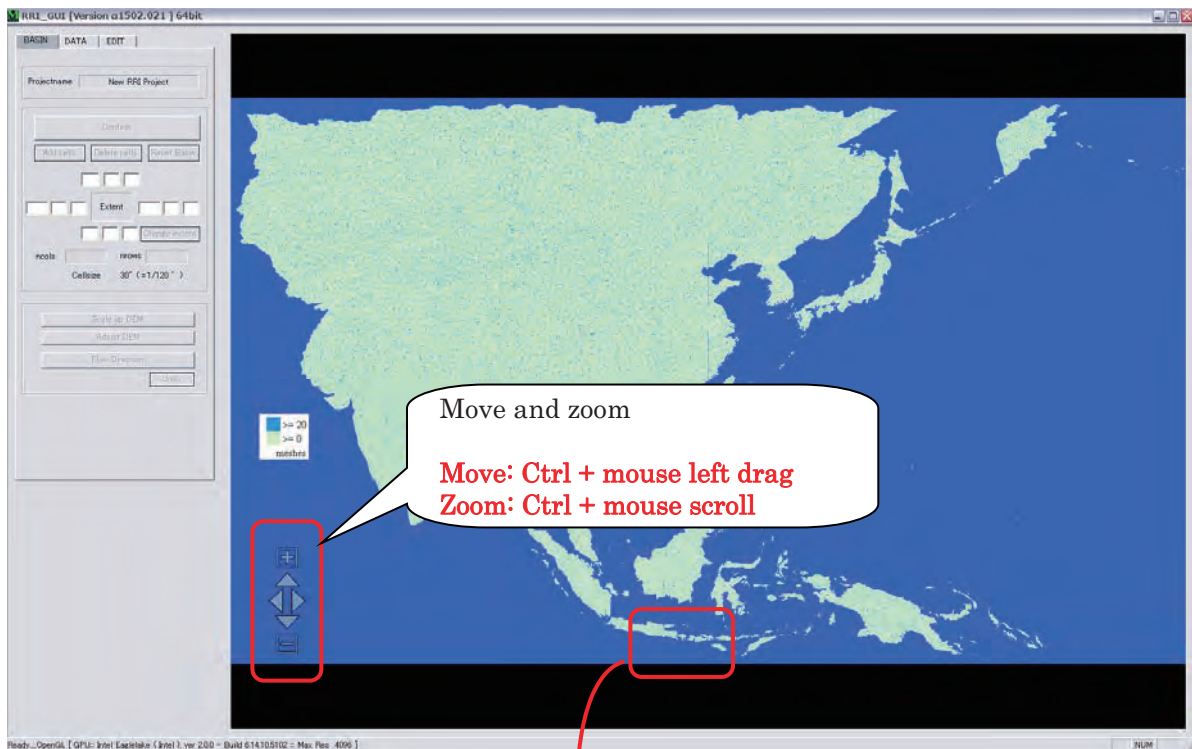
The first screen of the “RRI_BUILDER_64.exe” is to choose “New Project” or “Load Project”.



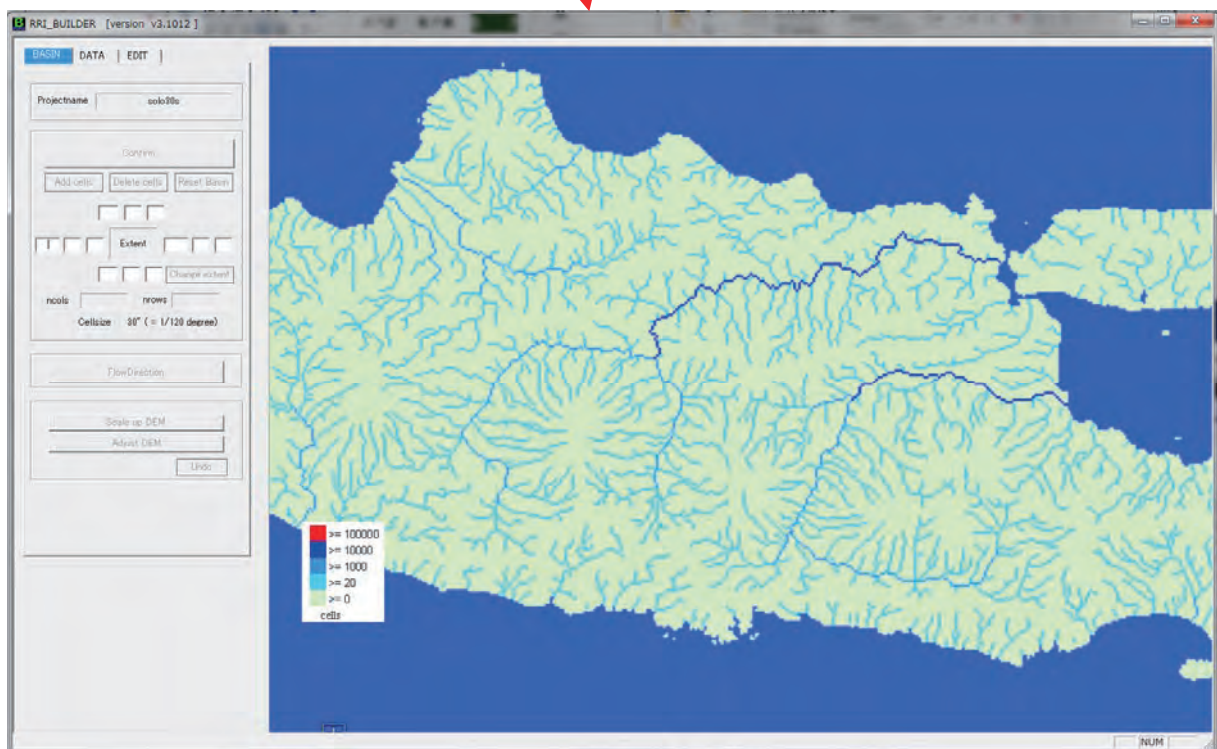
Select “New Project” in this exercise.

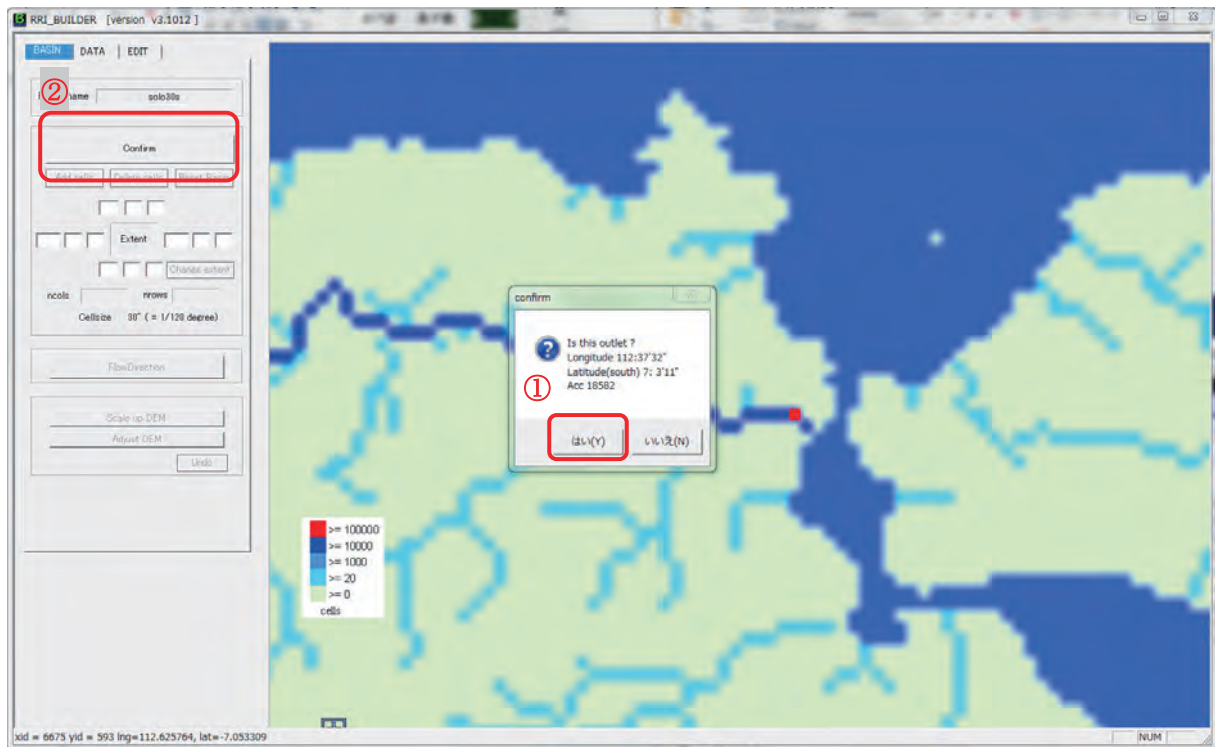
Type in a new project name (e.g. “solo30s”) with the selections of “Use HydroSHEDS” and “Asia30”, then click “OK”.





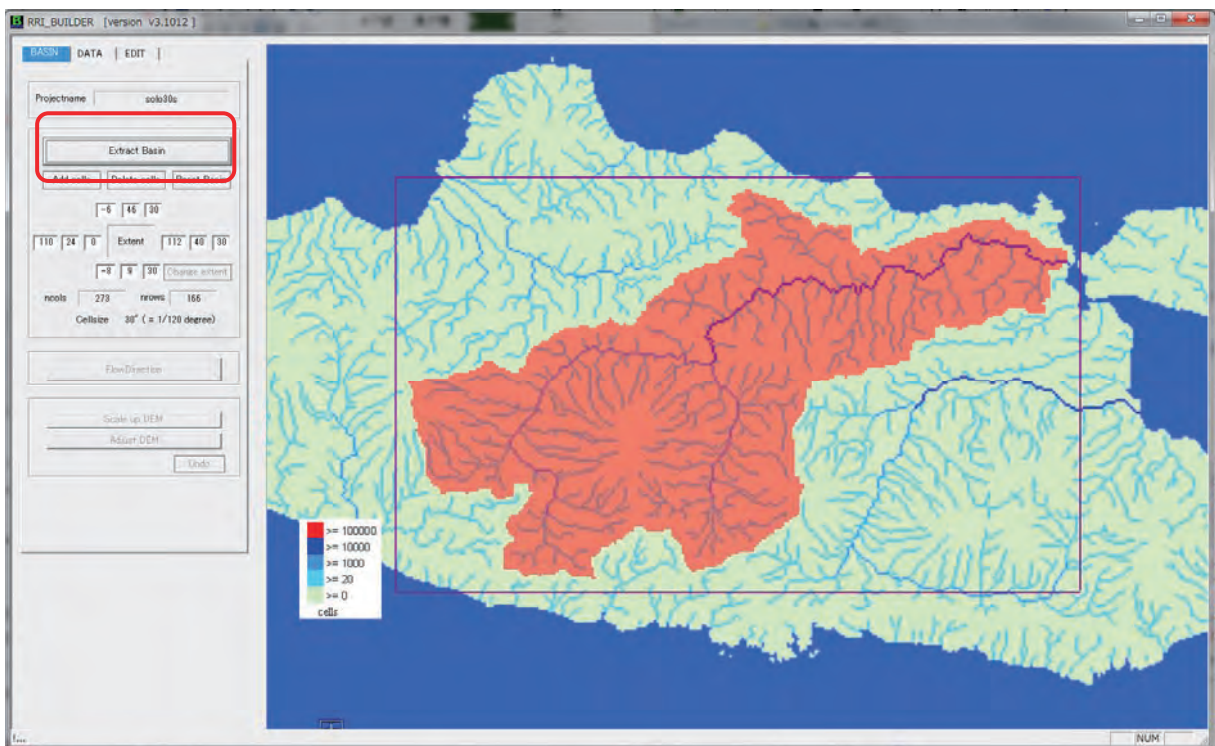
Zoom into Java Island in Indonesia





After zoom into the outlet area of the Solo River basin, **click a pixel along the main river** near the river mouth (not necessary to be exactly the same as the above example).

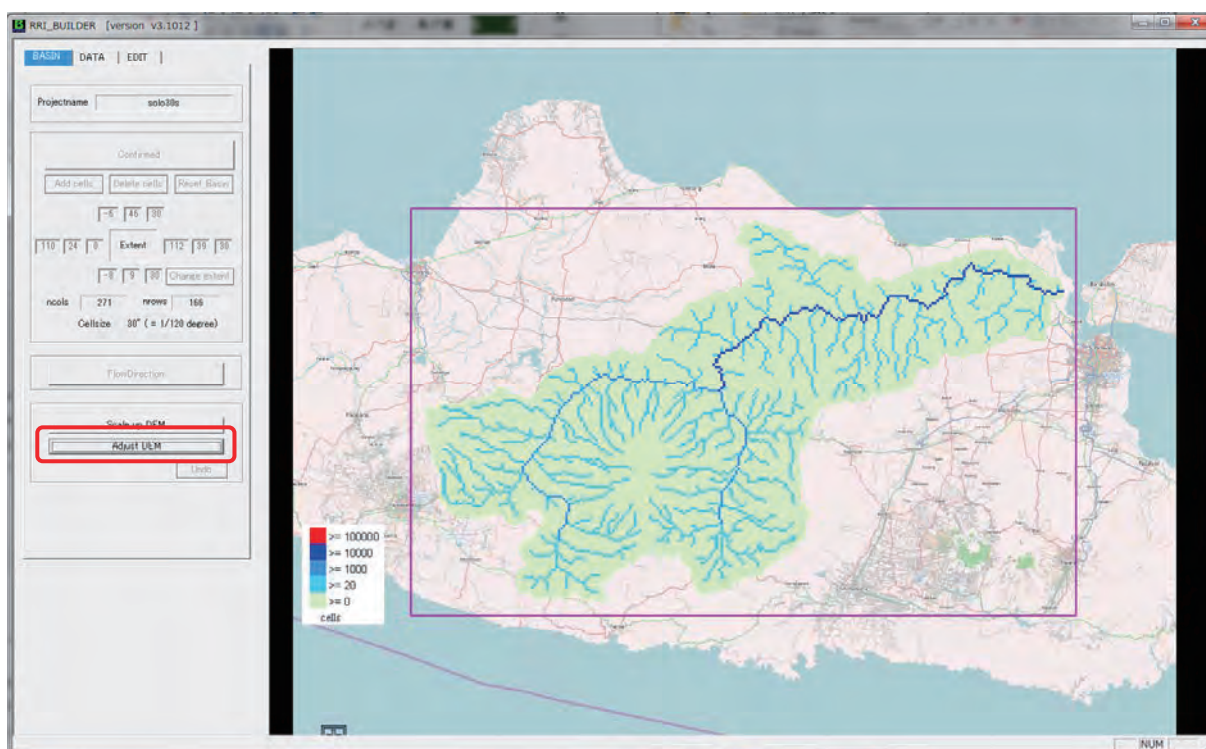
Then choose “**Yes**” on the window and “**Confirm**” on the left panel.



Click “**Extract Basin**” after you confirm the area of the basin.

(If not satisfactory, click “Reset Basin” and retry it.)

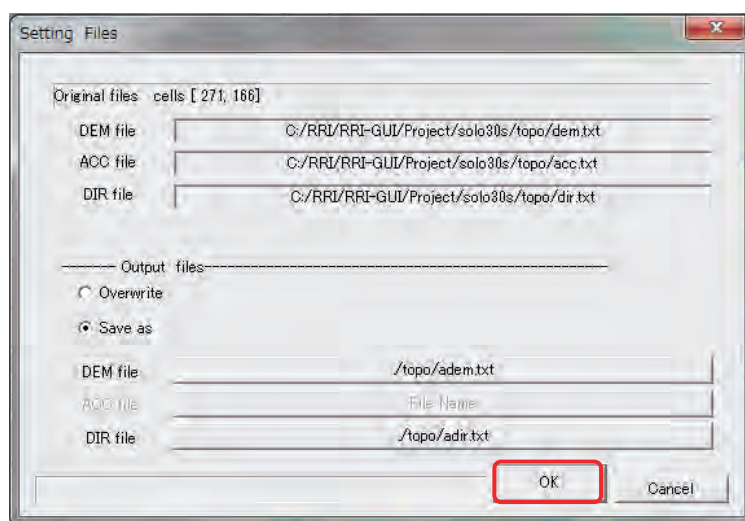
If the background map is available, the following extracted basin will be displayed.
(Even the background image is not shown for some reasons, it is essentially no problem for the following simulation).



(Optional)

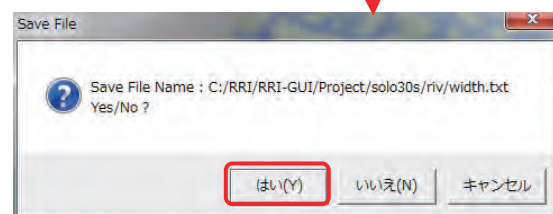
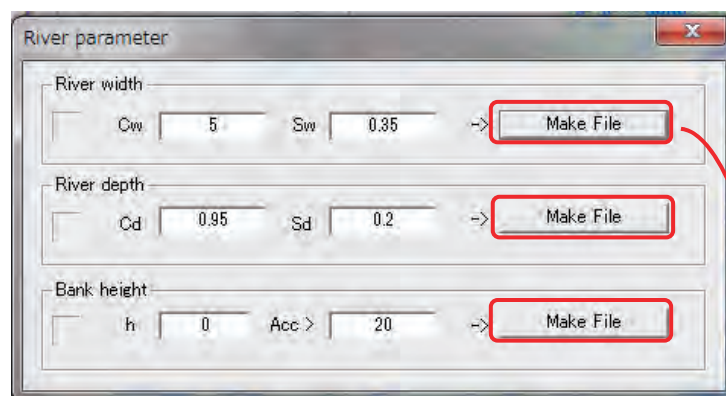
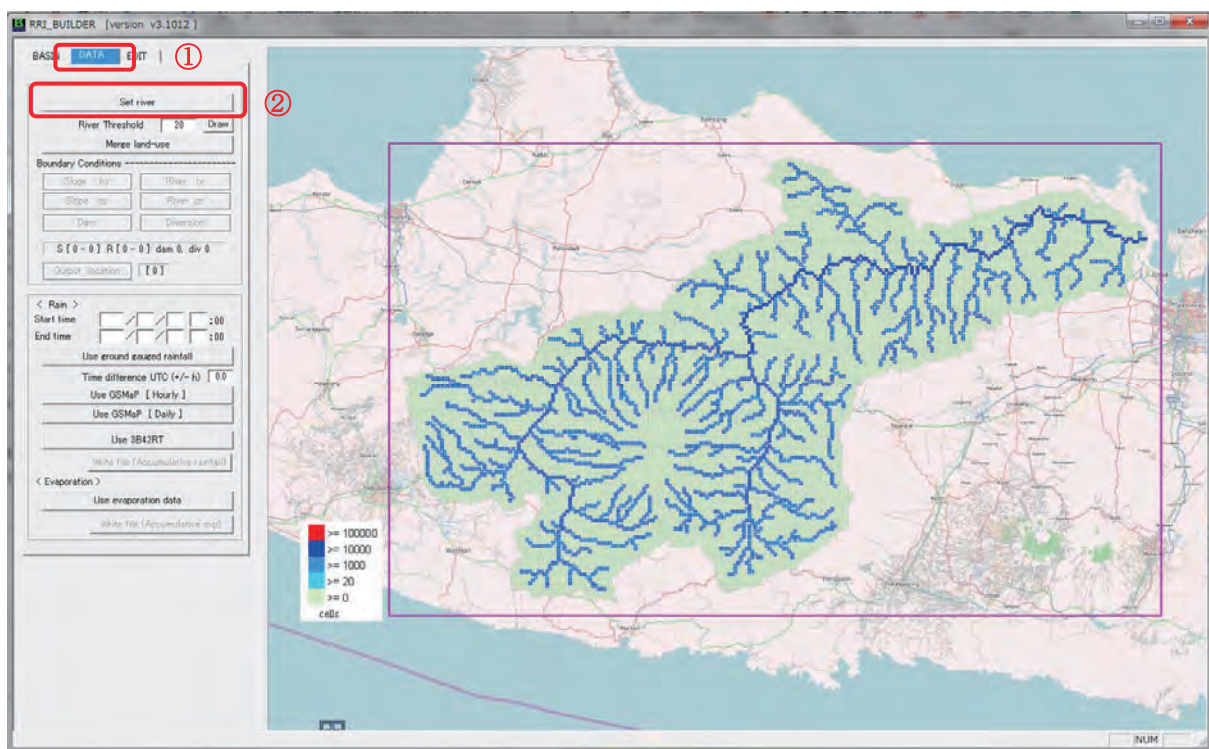
The step of “Scale up DEM” is an optional. Use this option in case you want to scale up the DEM for example changing the model resolution from 30 second to 60 seconds.

The next step is to execute “AdjustDEM”. This procedure is always necessary for the stable simulation.



Choose OK with the default setting. (you will see a command screen running AdjustDEM program).

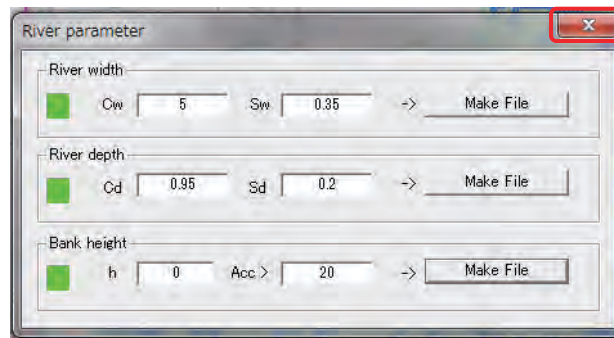
Now select “DATA” Tab on the left top and click “Set river”.



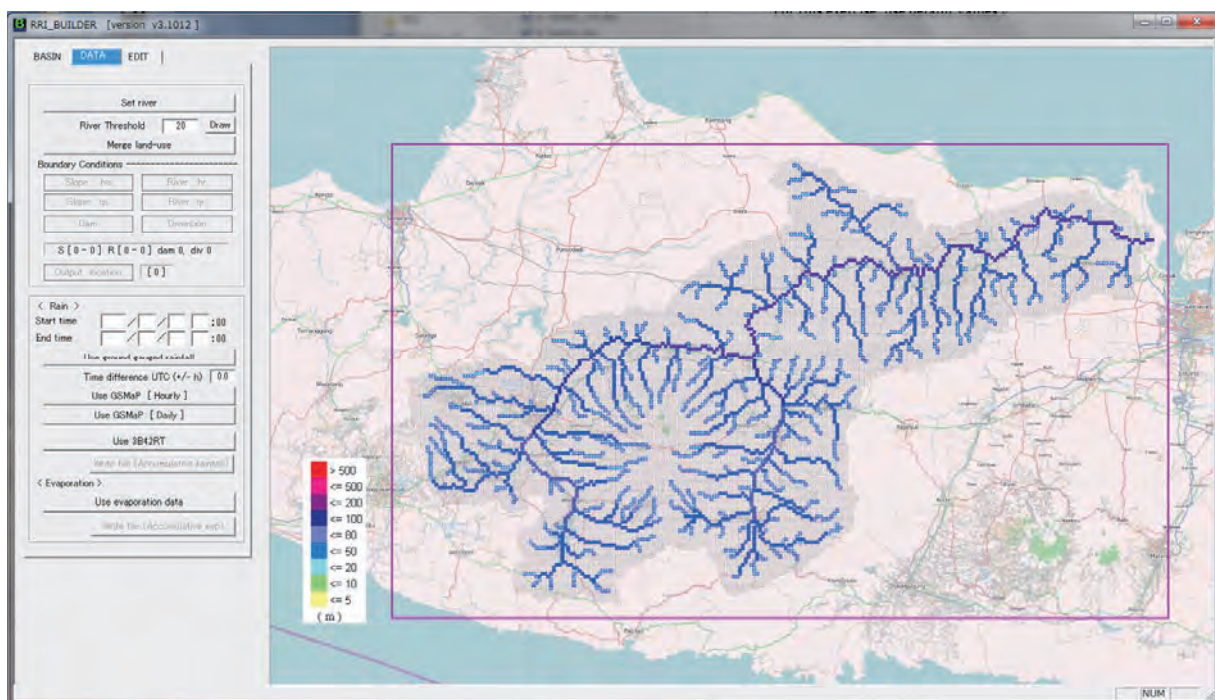
Click all the three “Make File” on River parameter setting.

These values are the parameters to determine the cross sections based on the equations.

For this exercise, use default values.



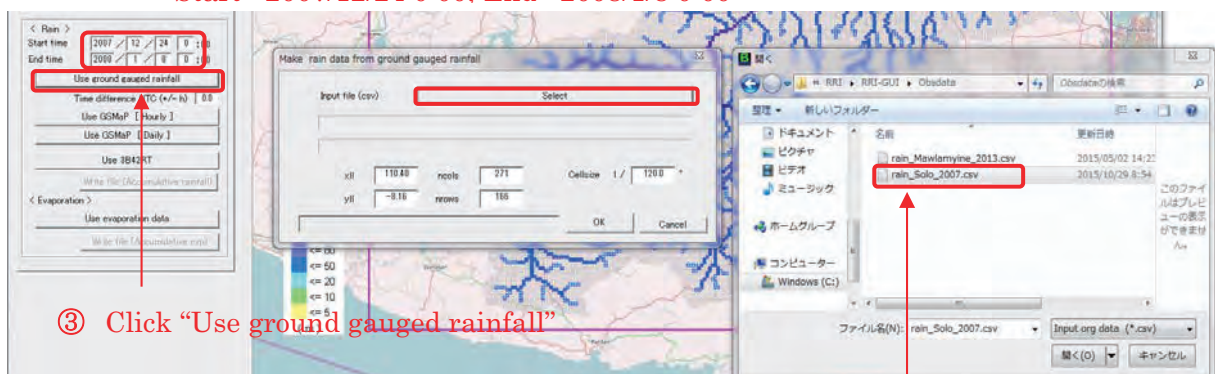
After confirming the three green signs, close this window.



9.2.2 Preparing Input Rainfall Data

① Set “Start time” and “End time” under <Rain>

Start : 2007/12/24 0:00, End : 2008/1/8 0:00



③ Click “Use ground gauged rainfall”

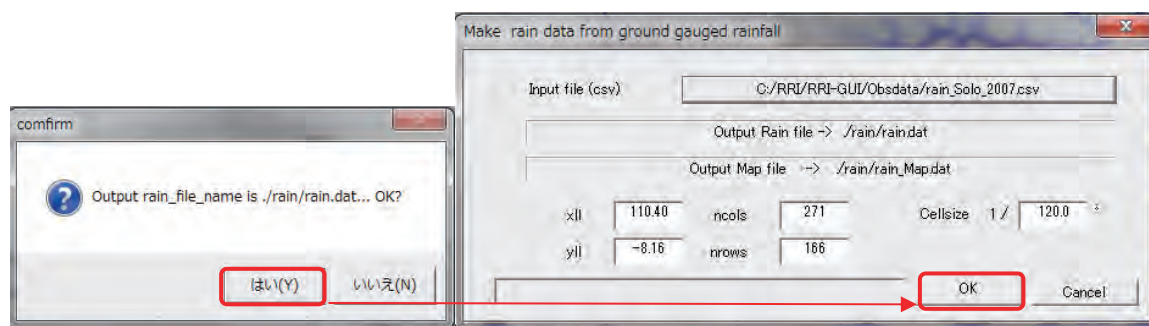
② Click “Select” to find a input rainfall file

(In this exercise, “RRI-GUI/Obsdata/rain_Solo_2007.csv”)

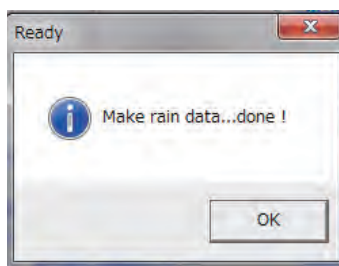
An input rainfall file must be the following format saved as csv. The file can be prepared by a text editor or Excel (saved as csv).

	A	B	C	D	E	F	G	H	I	J	K	L	M	N	O	P
1	125															
2	lat	-7.1945	-7.12661	-7.08353	-7.22057	-7.2496	-9999	-7.23782	-7.24462	-7.19858	-7.19815	-7.25191	-9999	-7.17517	-7.19885	-7.25725
3	lon	111.954	112.1116	111.5484	111.1092	111.8431	-9999	111.5095	111.8725	112.0301	111.9285	111.4876	-9999	112.0516	112.086	111.9287
4	2007/12/24 0:00	0	0	0	0	0	0	0	0	0	0	0	0	0	0	0
5	2007/12/25 0:00	15	5	14	0	2	2	6	0	0	0	0	0	2	3	9
6	2007/12/26 0:00	46	40	52	42	85	61	30	65	68	58	70	48	4	40	61
7	2007/12/27 0:00	0	0	0	0	0	0	0	0	0	0	16	0	0	0	0
8	2007/12/28 0:00	14	5	15	0	5	8	0	3	0	0	11	5	0	11	5
9	2007/12/29 0:00	0	3	3	3	7	0	0	7	8	0	0	0	0	0	8
10	2007/12/30 0:00	9	0	0	0	0	0	0	0	0	0	0	2	0	0	0
11	2007/12/31 0:00	16	2	9	0	8	2	0	4	0	15	0	1	5	0	2
12	2008/1/1 0:00	0	0	0	0	0	0	0	0	0	0	0	0	8.5	0	0
13	2008/1/2 0:00	4	7	8	0	0	0	0	0	4	3	0	3	0	2	0
14	2008/1/3 0:00	6	0	7	0	0	0	3	0	0	0	0	0	6	0	4
15	2008/1/4 0:00	8	0	25	15	20	22	0	25	2	20	0	5	3	10	16
16	2008/1/5 0:00	8	13	0	2	15	0	20	0	0	0	0	7	0	0	0
17	2008/1/6 0:00	0	0	0	0	0	0	0	0	0	0	0	0	34	0	8
18	2008/1/7 0:00	42	0	2	0	0	0	10	0	0	0	0	0	2	0	0
19	2008/1/8 0:00	8	8	37	3	5	22	0	6	12	30	0	40	7.5	0	31

Please note that the format is slightly different from the one used by the Thiessen Polygon program explained for RRI-CUI (Command User Interface). The first column of the file (L4-) is date and time. Currently the date and time must be in the form of “yyyy/mm/dd h:mm”.



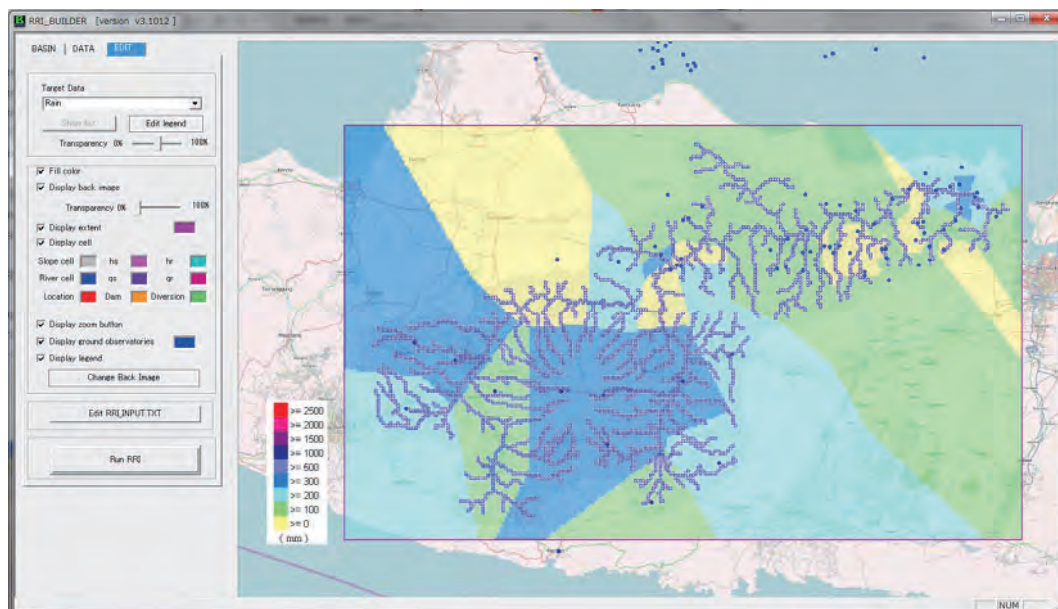
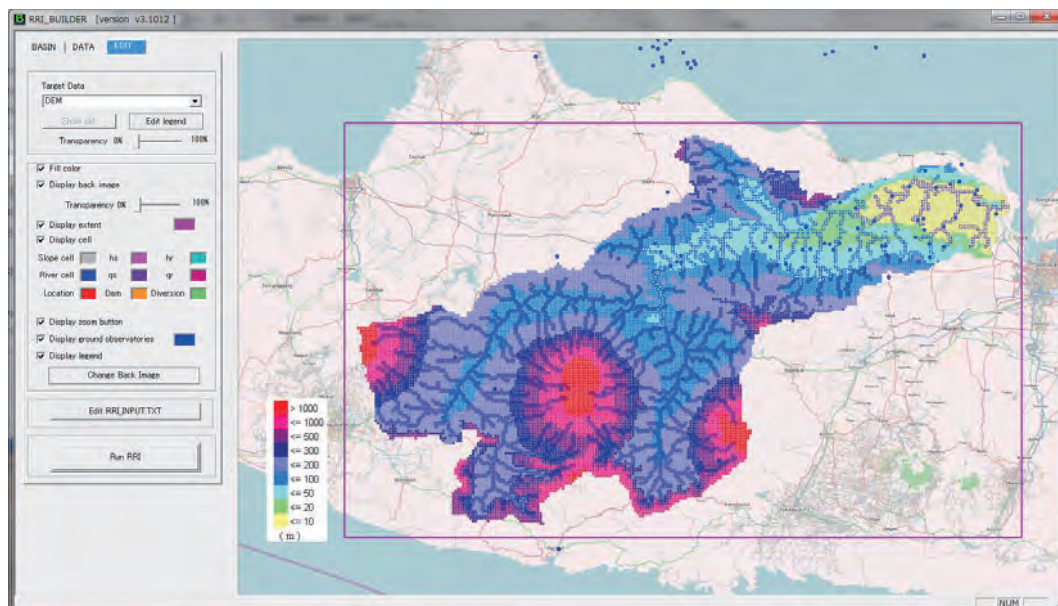
After selecting the input csv file, please choose “Yes” on the confirmation window then click “OK” with the default setting of the creating rainfall distribution file.



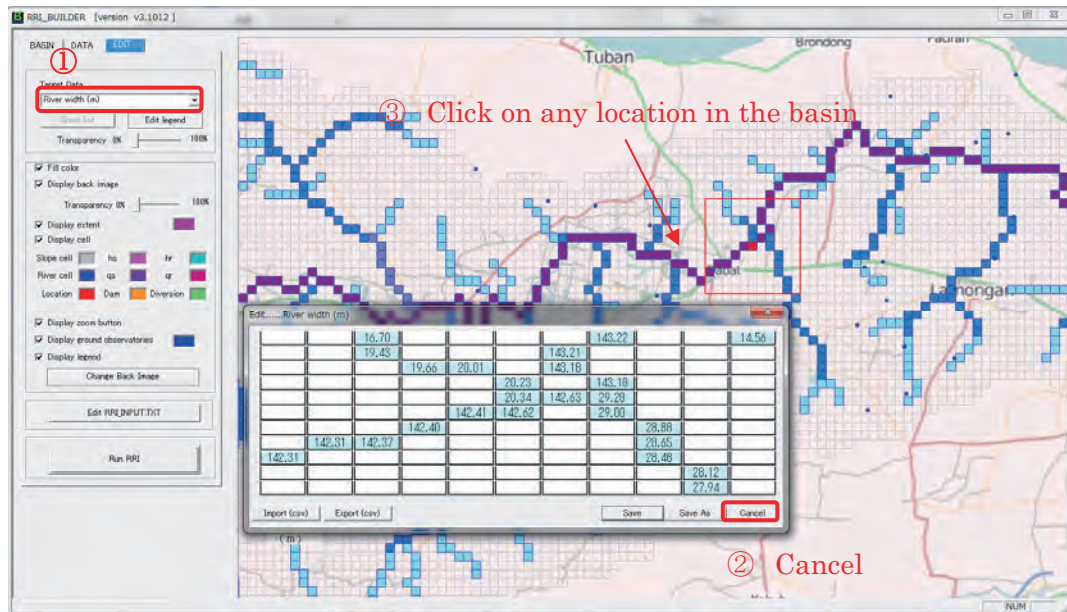
9.2.3 Running RRI Model

Select “**Edit**” tab after the topographic and rainfall data is ready.

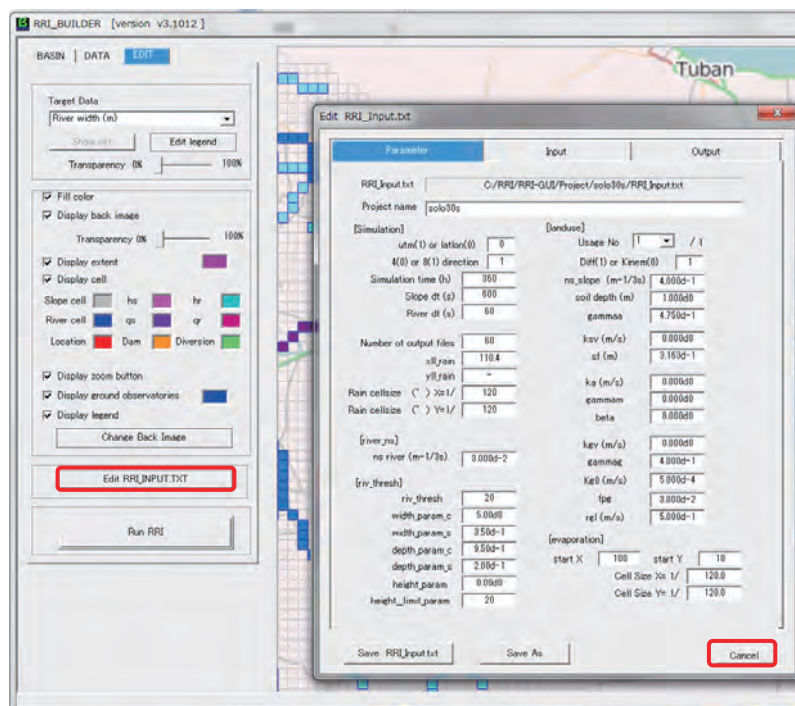
You can confirm different distributions including DEM, ACC, DIR, River Width, River Depth, Bank height as well as cumulative Rain.



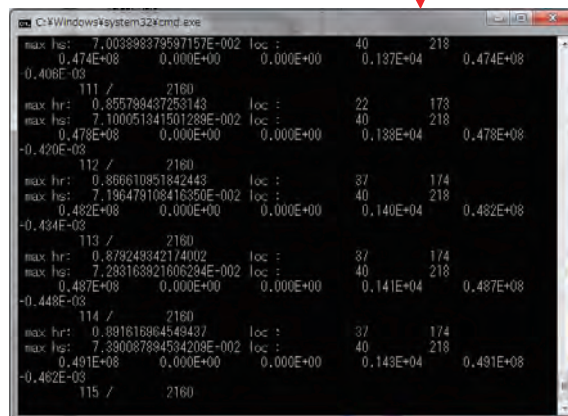
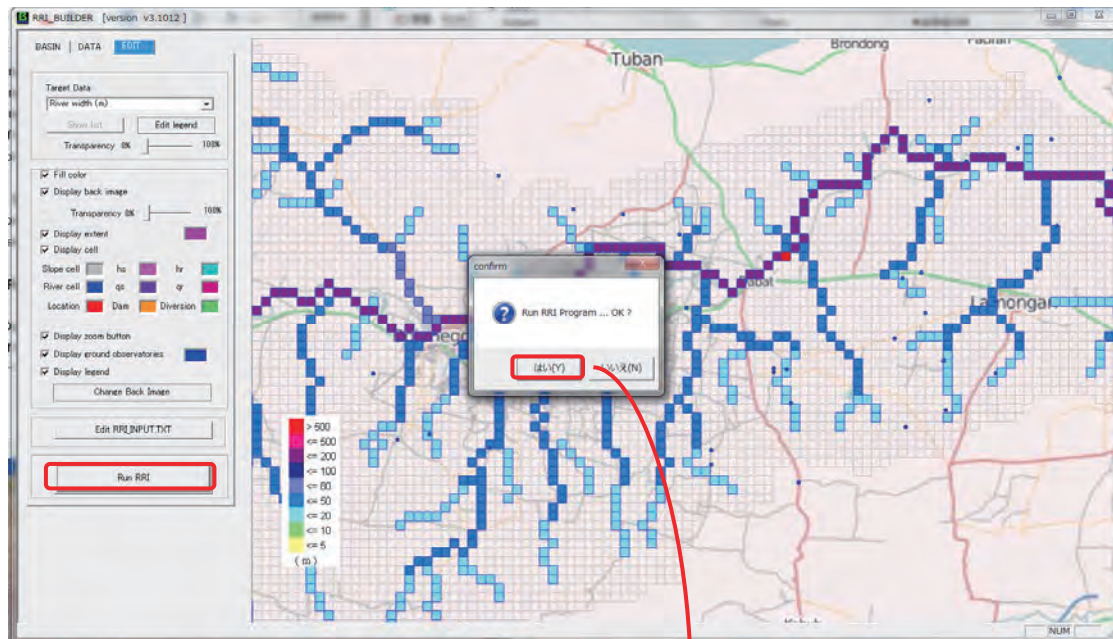
These distribution files except for the cumulative rainfall, can be edited on the window. For example you can choose river width and select any area inside the basin to display the following image. (For this exercise, no need to change the values.)



In addition, you find parameter and other input file settings if you click “Edit RRI_INPUT.TXT”. The editing the values will be reflected to the RRI_Input.txt file, which is the control file of the RRI model. (For this exercise, no need to change the values.)

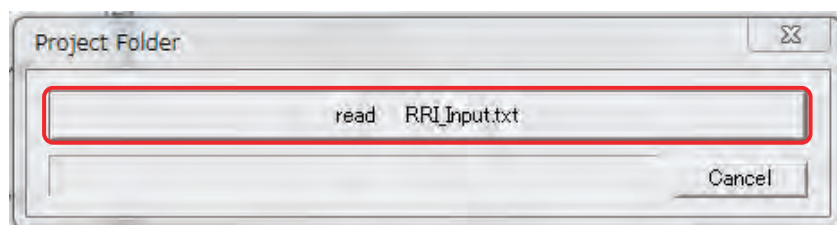


Finally, click “Run RRI” and “OK” to start the simulation.

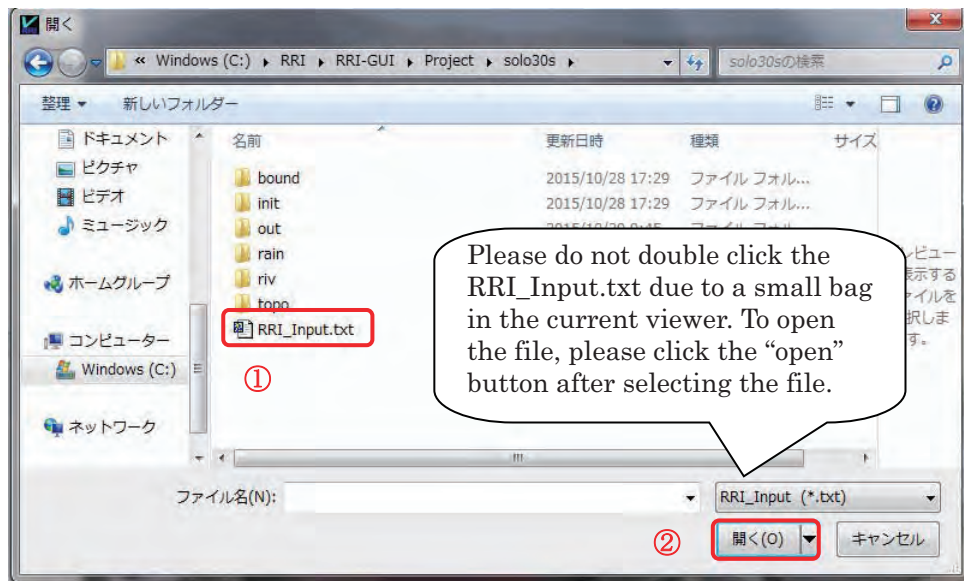


9.3 Visualizing results with RRI_VIEWER

Execute “RRI_VIEWER_64.exe” (or _32.exe for a 32 bit machine).

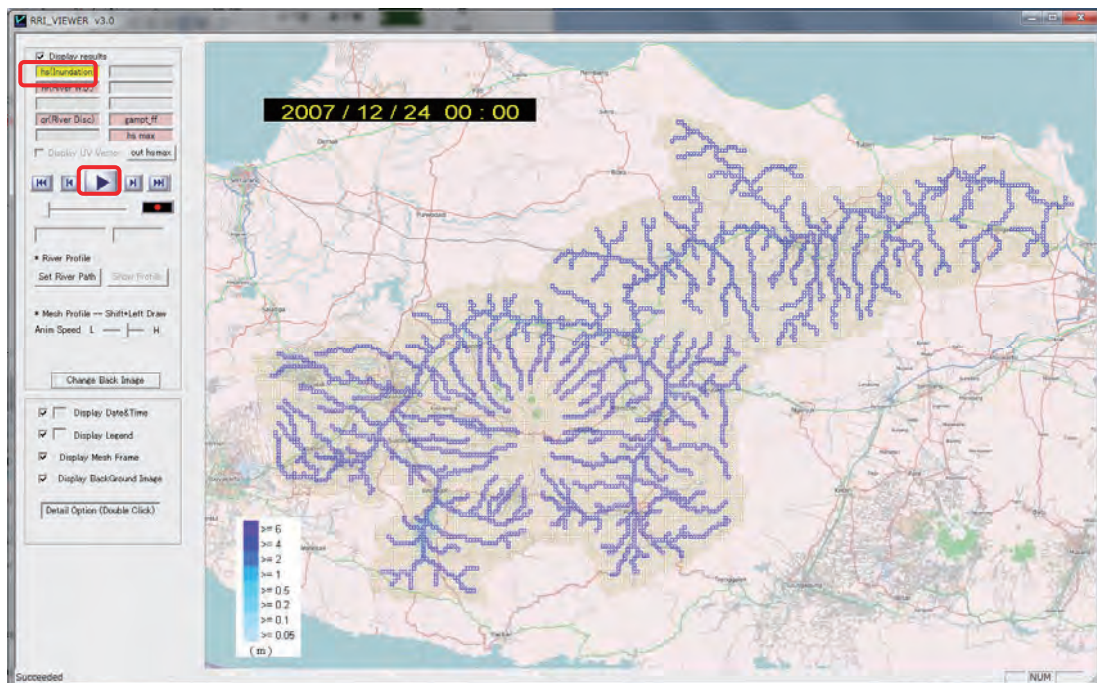


Read RRI_Input.txt file prepared in the previous subsection. In this exercise, find **RRI-GUI/Project/solo30s**

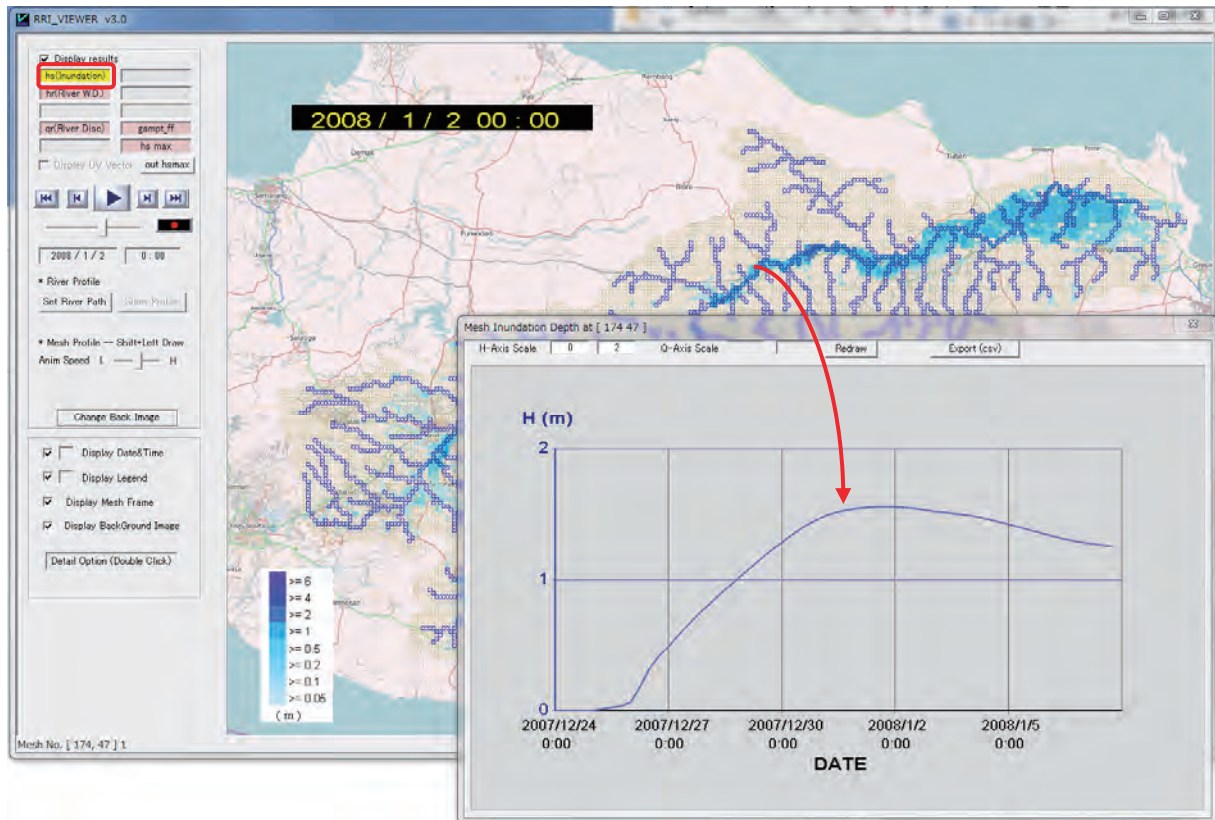


9.3.1 Visualize flood inundation

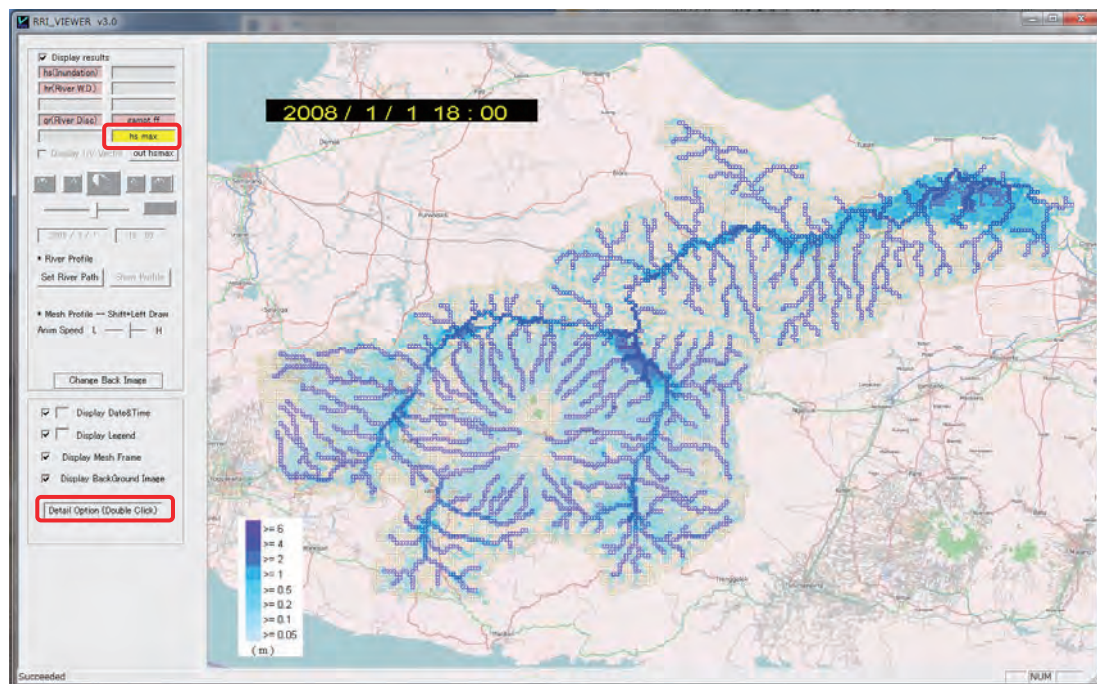
On the displayed map image, one can use CTRL and left drag to move the map and also CTRL and mouse scroll to zoom in and out. This operation is the same as RRI_BUILDER_64.exe



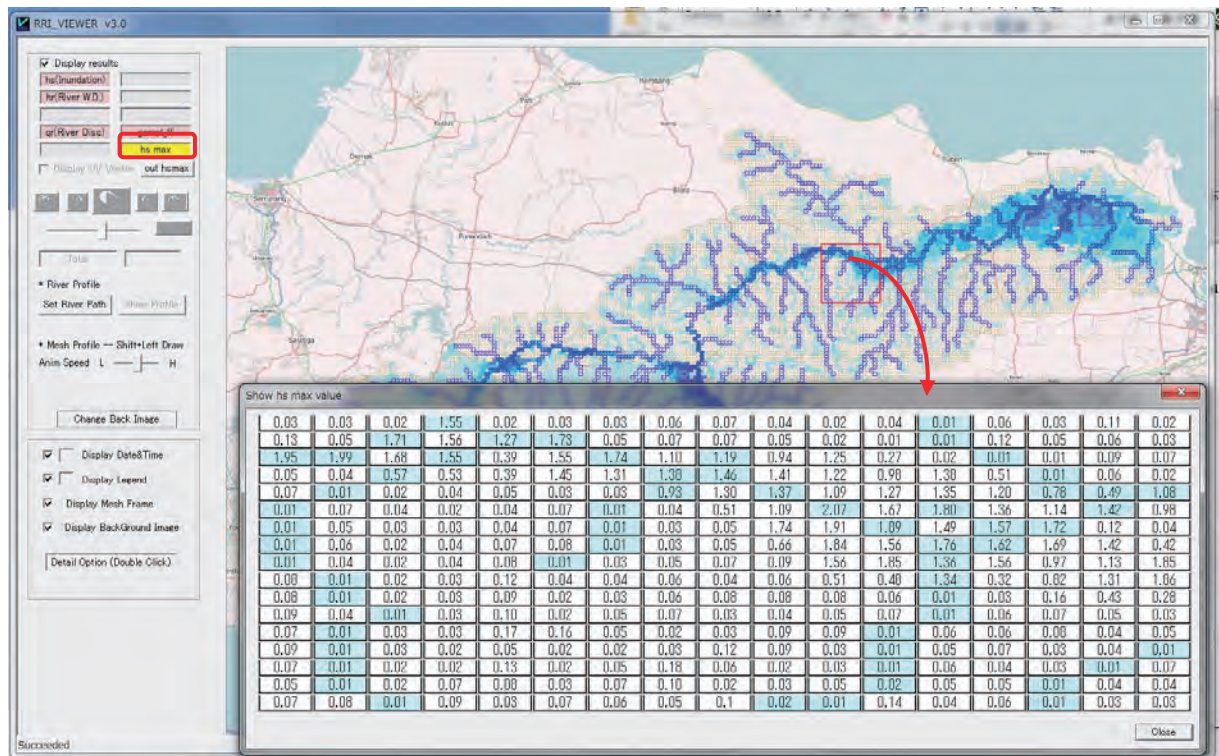
To display the animation of flood inundation depth distribution, please select inundation on the top left panel and click the start button.



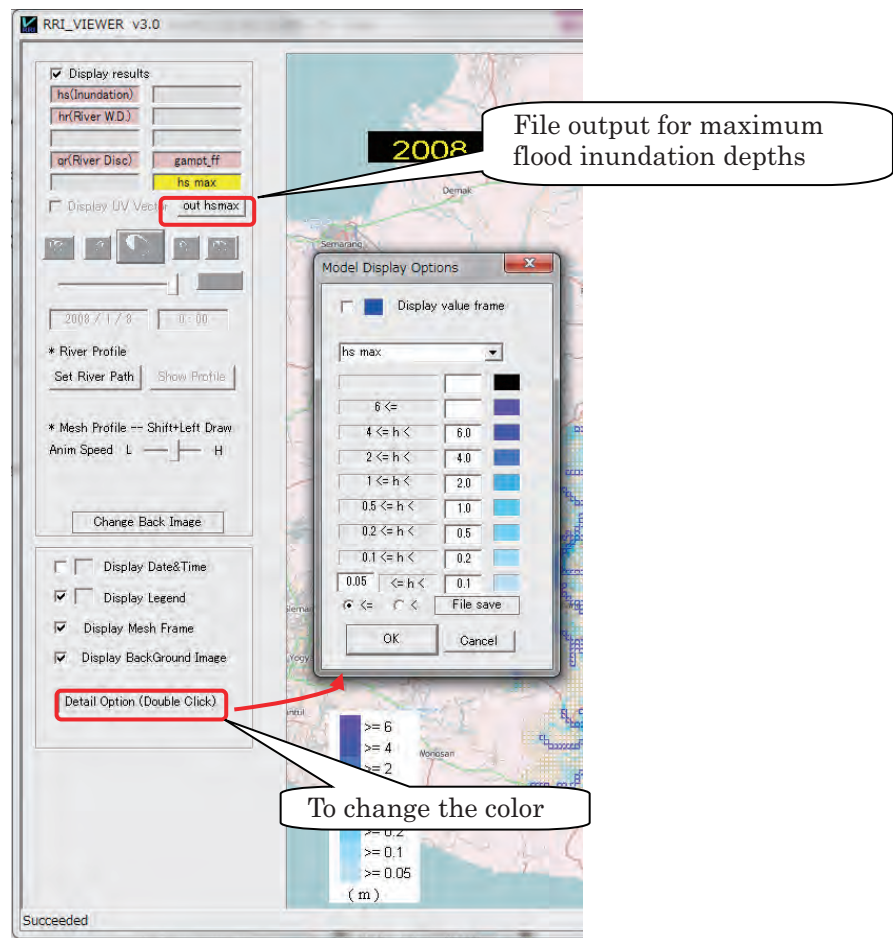
After stopping the animation, try to click any grid cell inside a basin to visualize the time series of flood inundation depths.



Then display the maximum inundation depth distribution by choosing **hs max**.
For the maximum inundation depths, one can check values by selecting a area on the map.

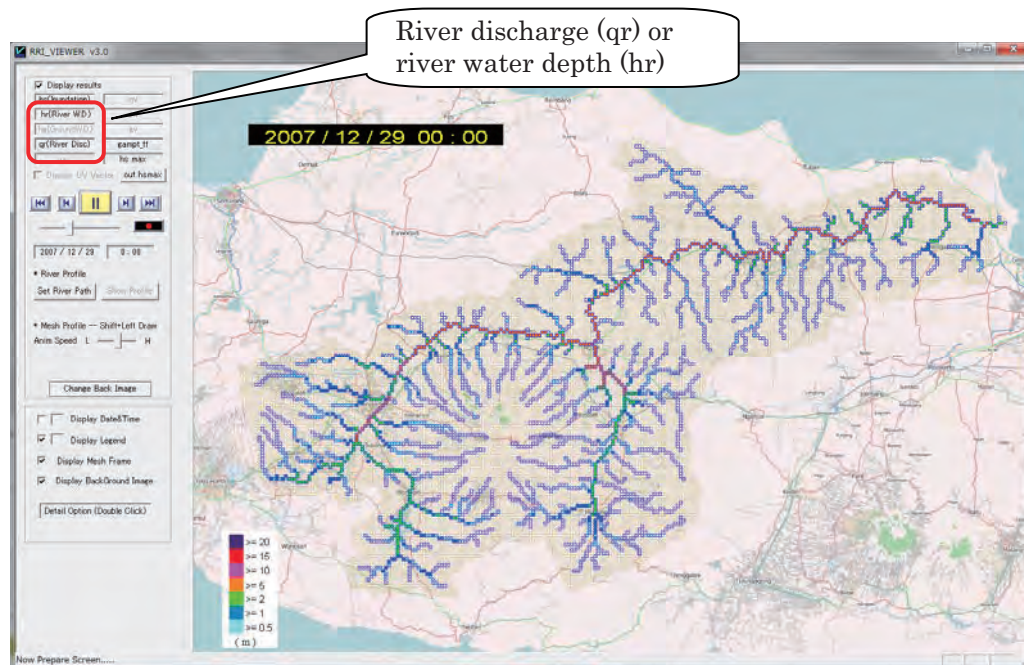


(Optional)

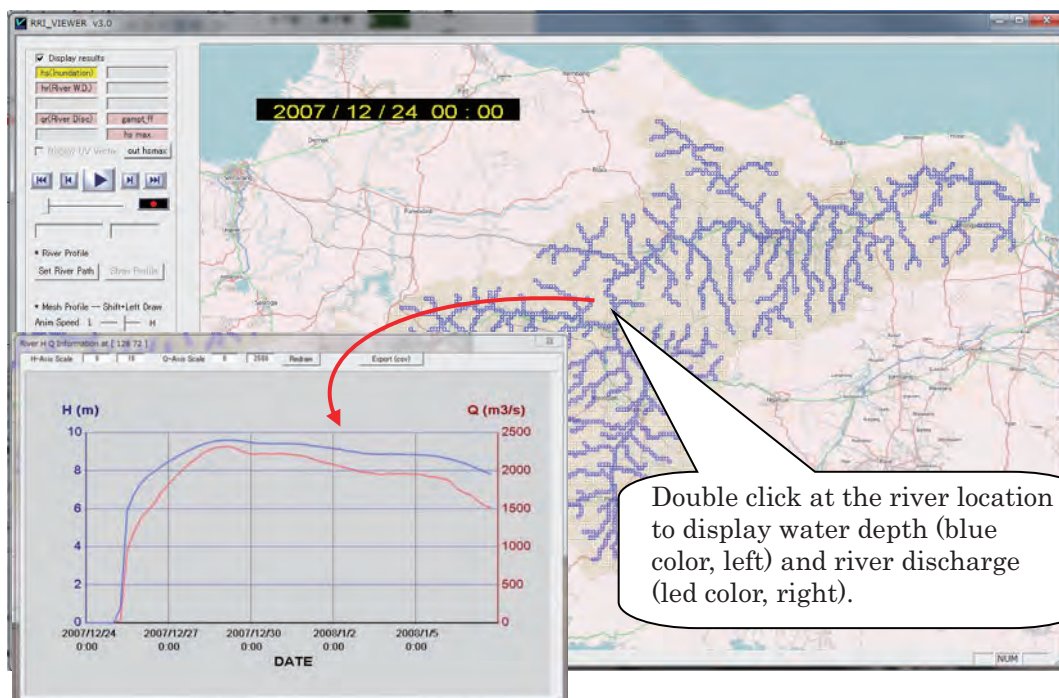


9.3.2 Visualize river discharge and water depth

To display the animation of river discharge or river water depth distribution, please select **qr** (River Disc.) or **hr** (River WD) on the top left panel and click the start button.

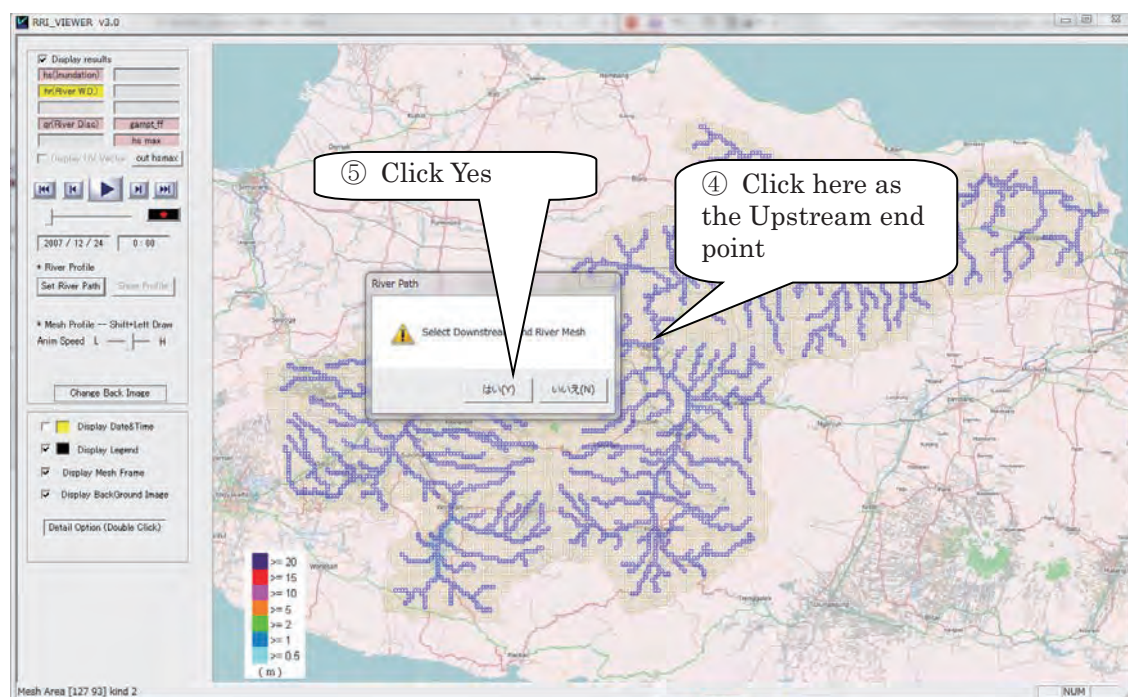
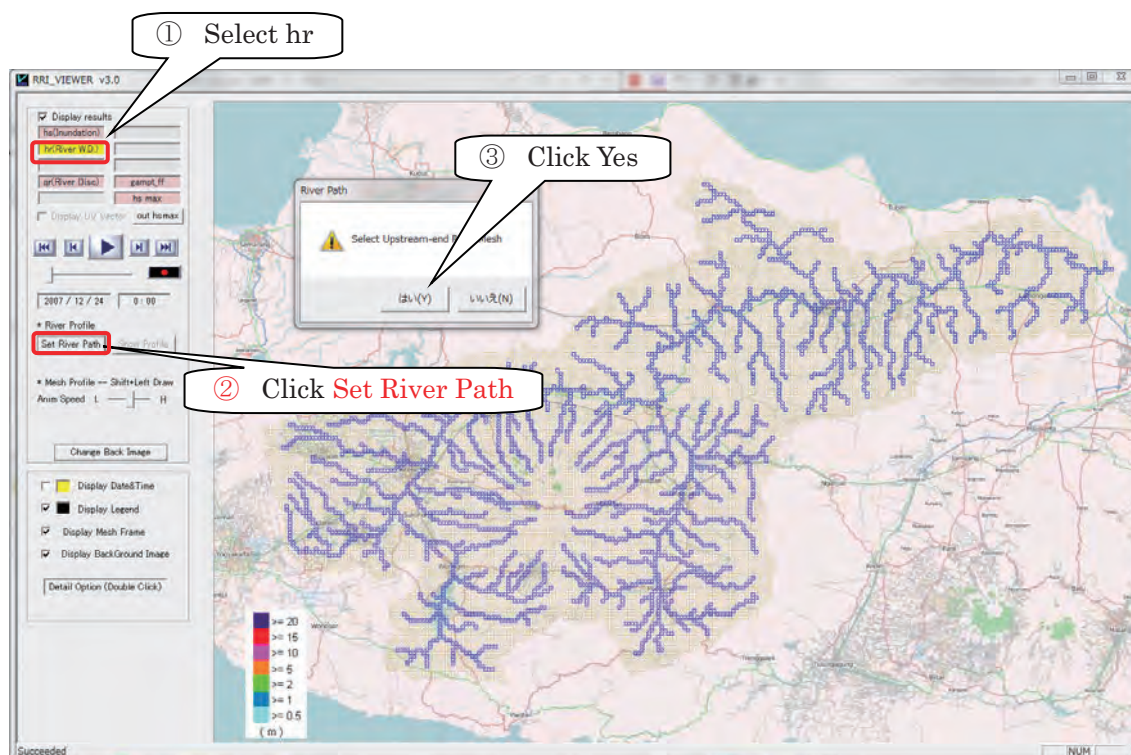


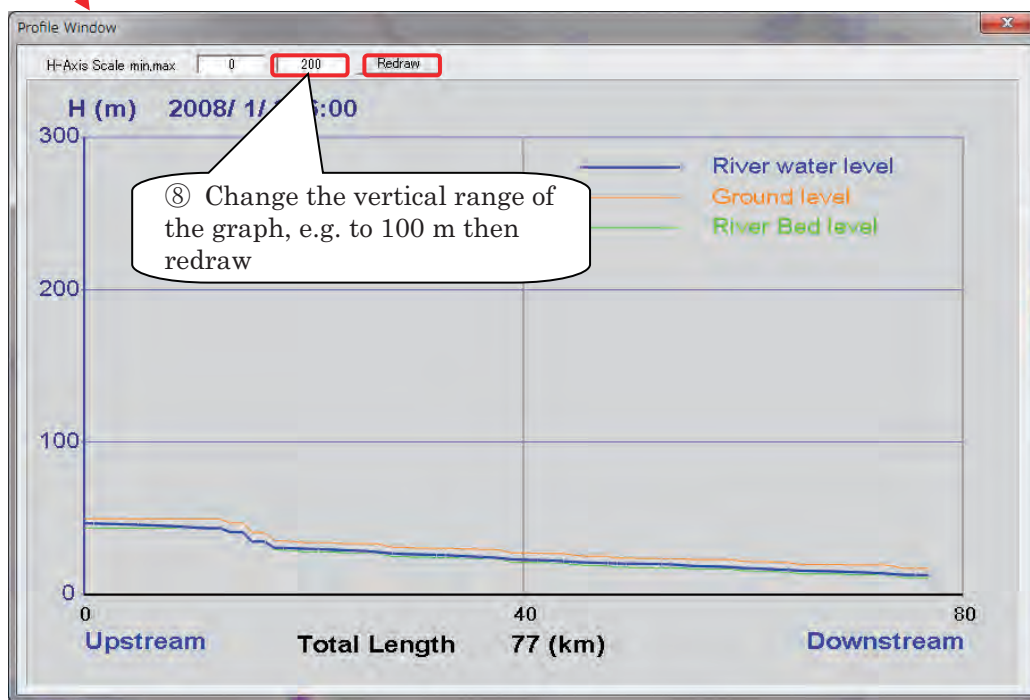
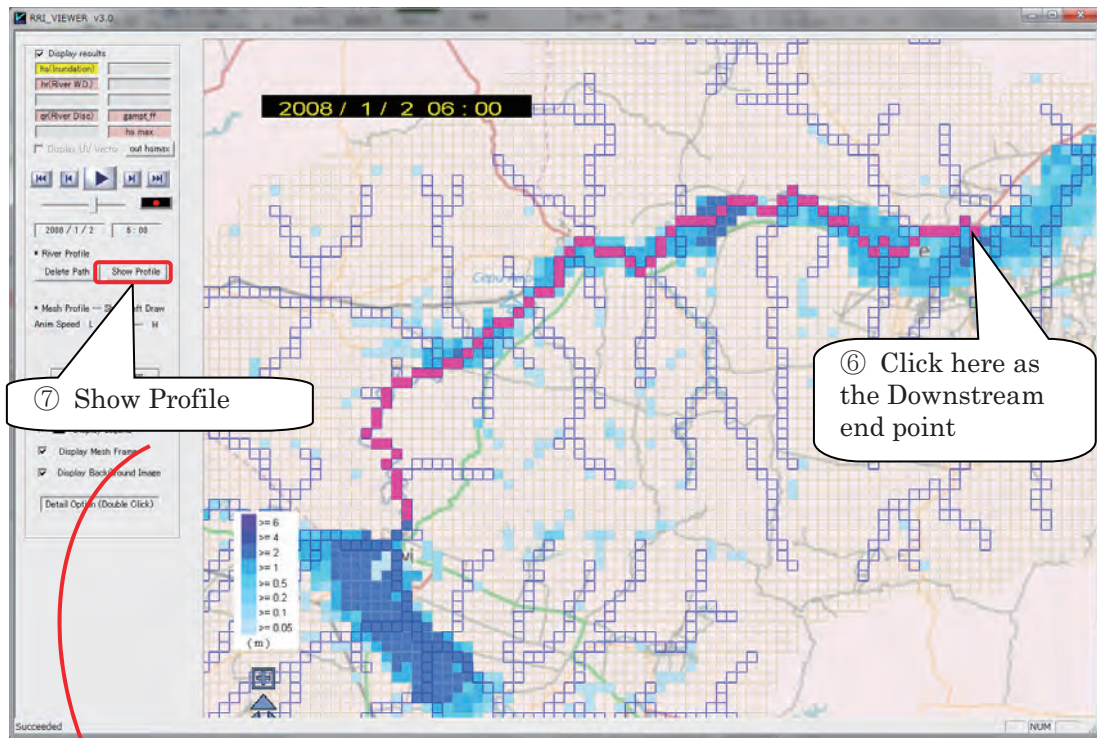
After stopping the animation, try to click any **river grid-cell** to visualize the time series of river discharge (i.e. hydrograph) and river water depth.

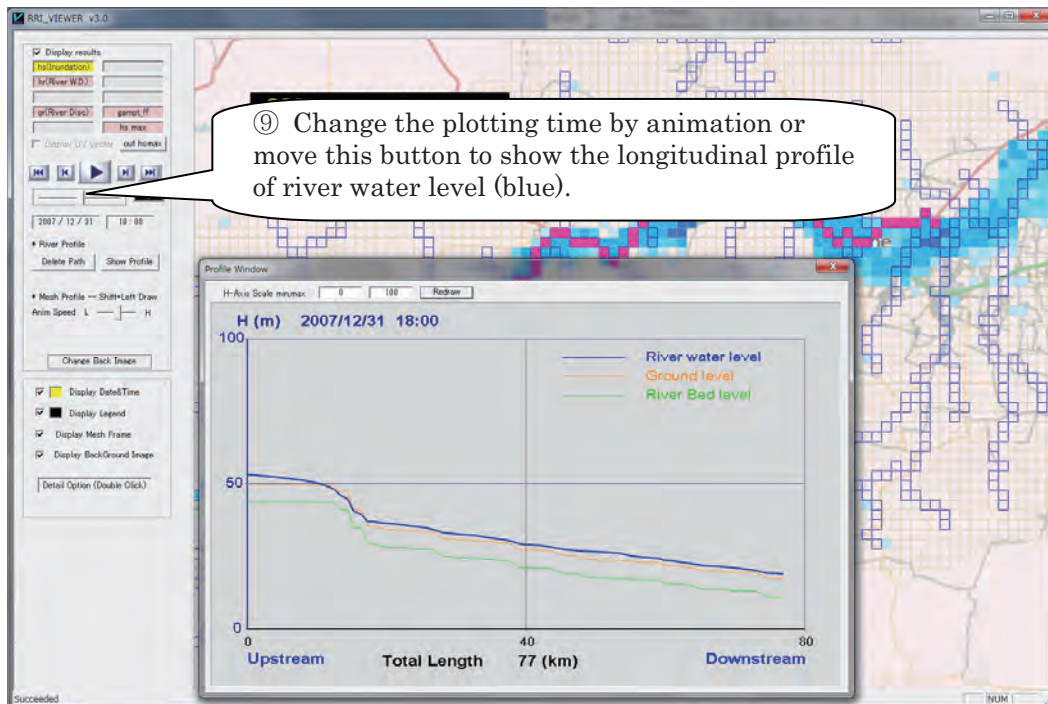


9.3.3 Visualize the longitudinal profile of river water level

To visualize the longitudinal profile of river water level, first select **hr (River WD)** and click “**Set River Path**” on the left pannel.



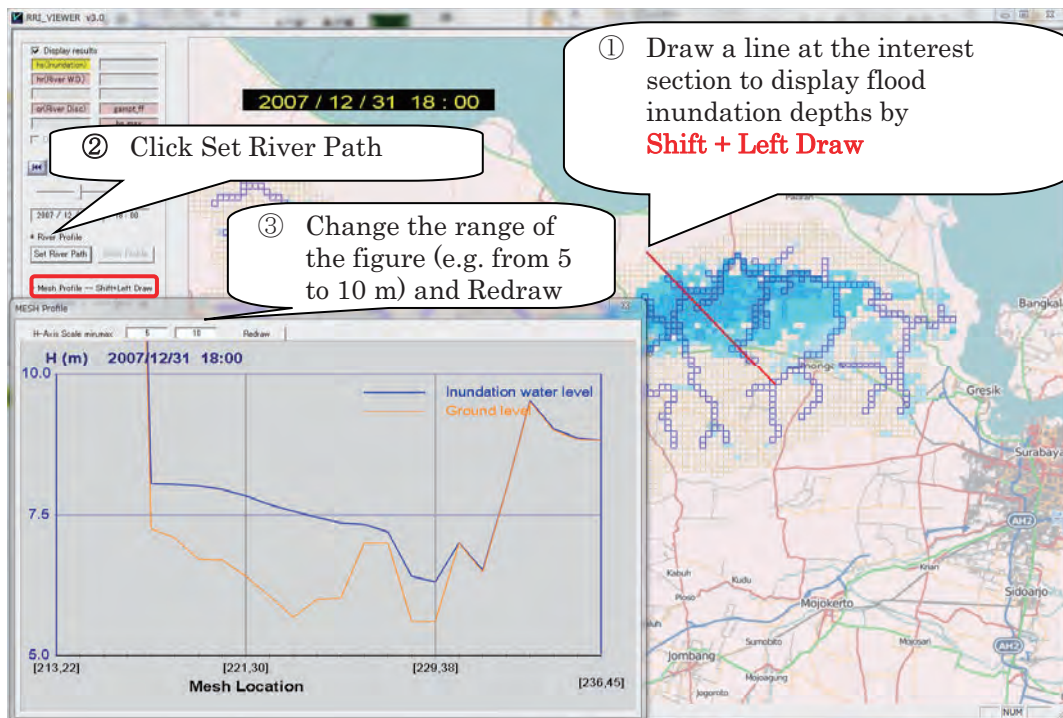




Click “Delete Path” to delete the selected longitudinal path.

9.3.1 Visualize the profile of flood inundation depth

To visualize the profile of flood inundation depth, one can draw a profile line (e.g. red line below) as “Shift + Left Draw”.

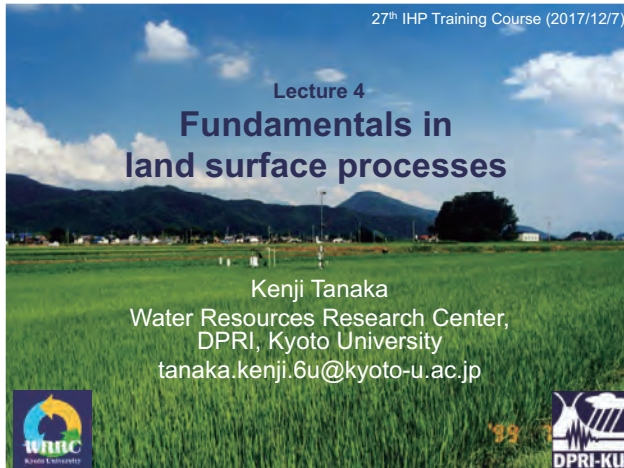


Lecture 4: Fundamentals in land surface processes

Kenji TANAKA (*Associate Professor, Disaster Prevention Research Institute, Kyoto University*)

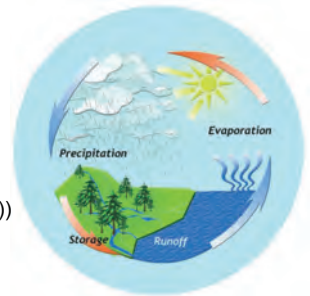
Abstract:

In this lecture, fundamental and important features of land surface processes are briefly introduced. Water is exchanged between atmosphere and land surface through processes of precipitation, evaporation, and transpiration. Water is exchanged between land surface and ocean/lake through runoff (river process). Driving force of global hydrological cycle is energy supplied from the sun. The energy absorbed by land surface is returned to atmosphere in the form of sensible and latent heat. This partitioning of energy is strongly dependent on both land cover characteristics and its hydrological state (wet/dry). As the ways of heating by sensible and latent heat are different, this partitioning is very important for global hydrological cycle. Some example of the field experiments to understand the physical processes of the land surface are shown. Then, some aspects of the land surface model are introduced to see how these processes are expressed. Land surface model is formulated by prognostic equations of land surface states such as soil moisture, soil temperature, and snow describing the change of states through energy and water balance components. Finally, some applications of land surface model are introduced such as energy and water balance analysis of the lake Biwa basin, near real-time monitoring of land surface states in Japan, global distribution of aridity index and evaporation ratio, sensitivity of rainfall data to river discharge.



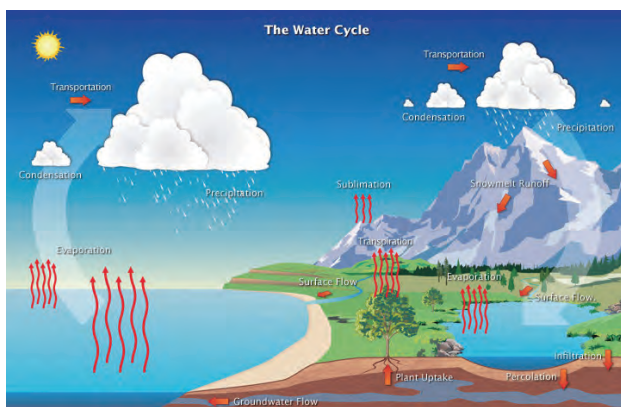
Land Surface Process

"Land surface processes are those associated with the **exchange** of water and energy between the land surface and the atmosphere and are, therefore, **integral components** of hydrologic and atmospheric sciences."
(by Bill Crosson (NASA MSFC))

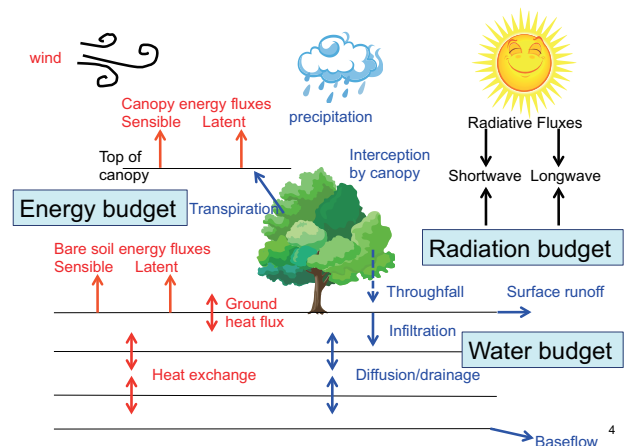


Hydrological Cycle
from GEWEX home page

2



3



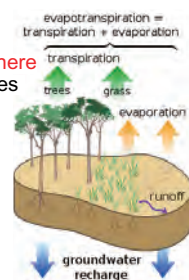
4

Water budget

- Water is exchanged **between the atmosphere and the land surface** through the processes of precipitation, evaporation, and transpiration.
- Water is exchanged **between the land surface and ocean/lake** through runoff.

$$\Delta S = P - E - R$$

P : precipitation(rain/snow) input from atmosphere
E : water vapor flux by evaporation and transpiration
R : runoff flux by river system and ground water system
 ΔS : change in the surface water and soil moisture



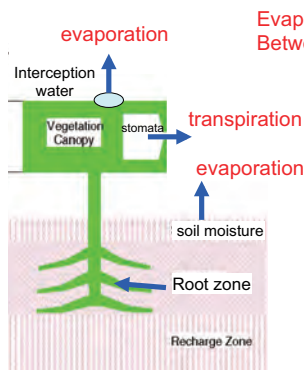
Energy budget

- Rn is partitioned into fluxes of sensible, latent, and ground heat.
- This partitioning is strongly dependent on both the **land cover characteristics (landuse)** and its **hydrological state (wet/dry)**.

Why energy partitioning is important?

$R_n = H + \lambda E + G$
H → heating lower atmosphere
 λE → heating middle atmosphere
G → surface (time lag between RB & EB)

Evapotranspiration = Evaporation + Transpiration



Evapotranspiration is an interface
Between water cycle and energy cycle

Water cycle:
Rainfall reached to surface go back to atmosphere as water vapor.
Evaporation is a loss term in terms of water resources.

Energy cycle:
Transfer the energy of vaporization to atmosphere. Energy absorbed by surface is redistributed to atmosphere.

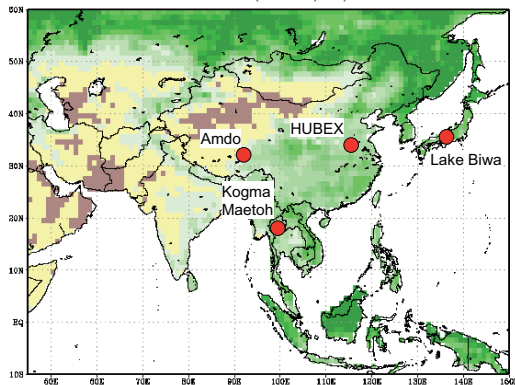
Water vapor from surface will condense (latent heat release) and fall down

GEWEX Continental Scale Experiments

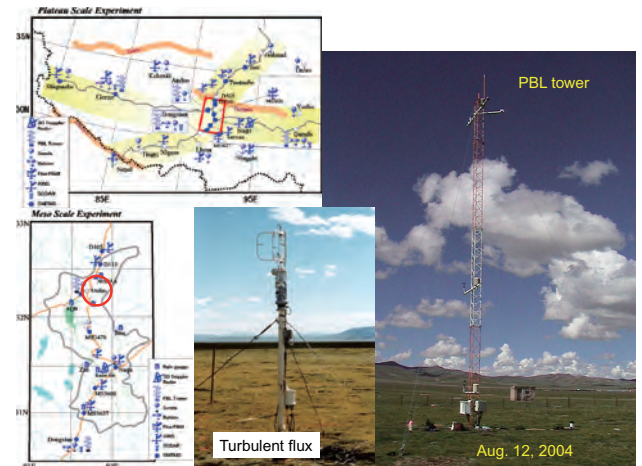


8

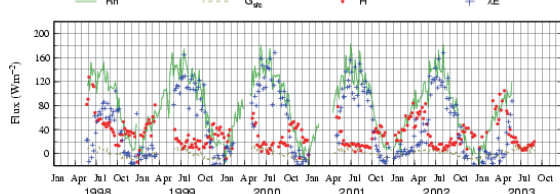
Leaf Area Index (1995/7)



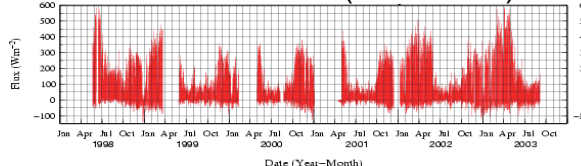
9



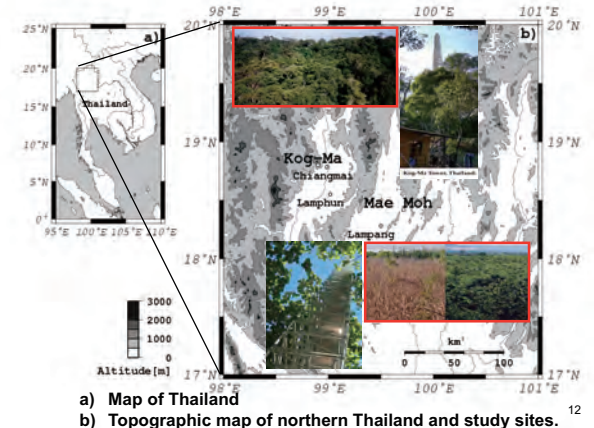
Surface energy fluxes (5day average)



Sensible heat flux (30 minutes)



11

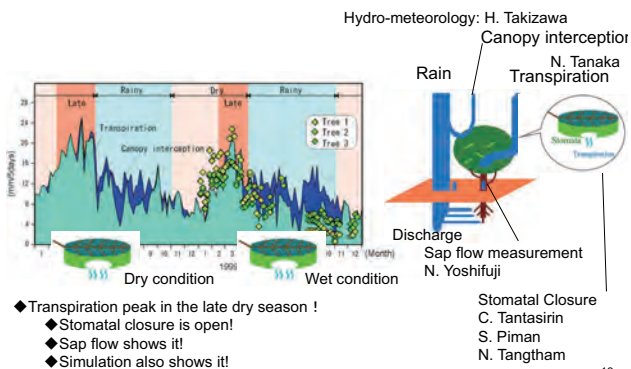


a) Map of Thailand

b) Topographic map of northern Thailand and study sites.

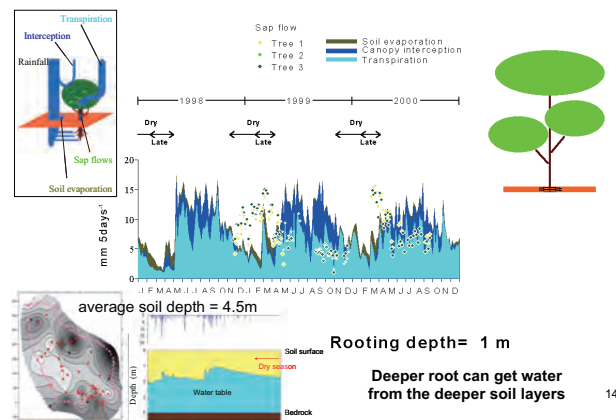
12

Result of Observation



13

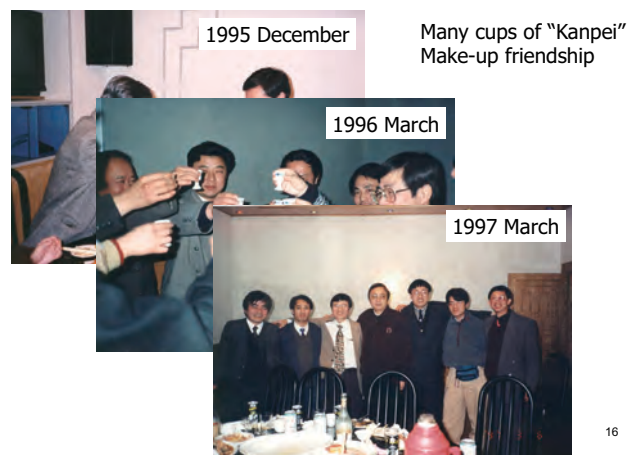
Numerical Simulation (by 田中克典さん)



14

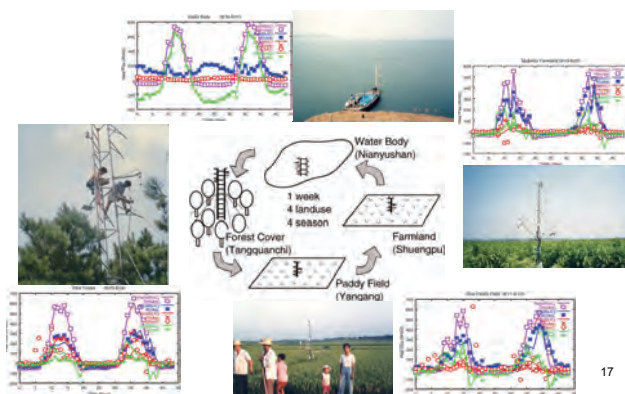
Huaihe River Basin Field Experiment (GEWEX/GAME/HUBEX)

- meso γ scale
Shouxian area (140km \times 150km)
Intensive observation area
- meso β scale
Huaihe River basin area (700km \times 500km) surrounded by upper air sounding station
- Surface weather station (146)
- Upper air sounding station (21)
- Radar network
Fuyang (operational)
3 doppler radar from Japan (Shouxian, Funtai, Huainan)
- Shouxian
Radiation, Bowen Ratio EB
Microwave radiometer, ABL tower
- Hydrological observation at Shi-Guan Basin
hourly rainfall (48), evaporation(3), water level, river discharge(3), dam outflow(2), soil moisture (3)



16

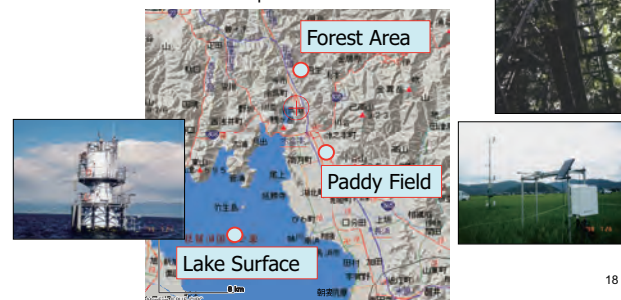
GAME-HUBEX flux measurement at 4 landuse



17

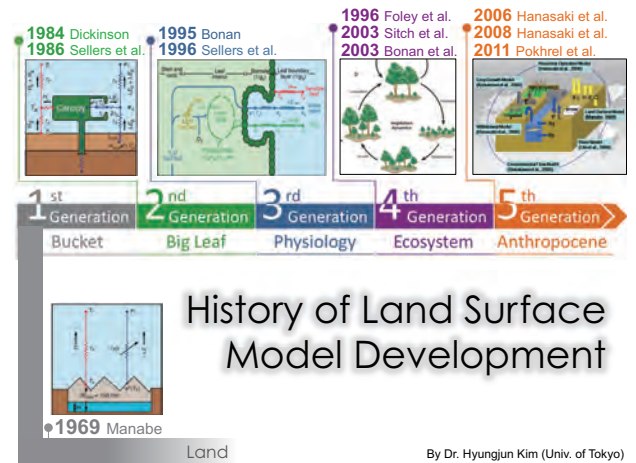
In-situ Flux station (Lake Biwa Project)

- Three sites from the Lake Biwa Project
Fluxes of radiation budget and heat budget component and related meteorological and hydrological variables can be used from these datasets.
- Two sites from the snow depth observation station



18

Flux measurement in the Paddy Field



LSS (Land Surface Scheme)

Input

Surface meteorological variables
(Prec, SWdown, LWdown, Tair, Eair, Wind, Psfc, etc.)
Surface parameters
(Vegetation type, Soil type, LAI, reflectance, etc.)

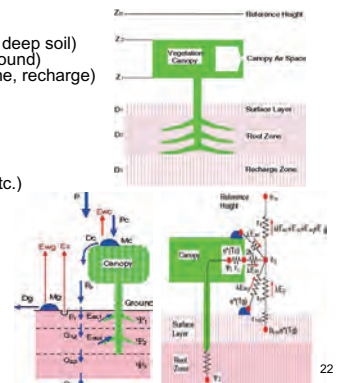
Output

Surface energy balance components (H, λE , G, etc.)
Surface water balance components (Evap, Qs, Qsb, etc.)
Surface state variables (Tsoil, SoilMois, SWE, etc.)

21

Green area model (SiB)

- Prognostic variables**
temperature (canopy, ground, deep soil)
interception water (canopy, ground)
soil wetness (surface, root zone, recharge)
- Time invariant parameter**
geometrical parameter
optical parameter
physiological parameter
soil physical properties
- Time varying parameter** (LAI etc.)
estimate from satellite data
- Physical processes**
radiative transfer
interception loss
soil hydrology
canopy resistance
transpiration
turbulent transfer,
snow, freezing/melting, ... etc.



22

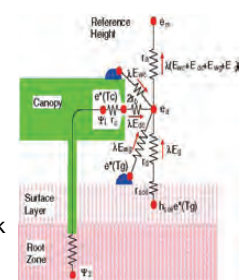
Physical Processes expressed in SiB

- the reflection, transmission, absorption and emission of direct and diffuse radiation in the visible, near infrared and thermal wavelength intervals (**radiative transfer**)
- the interception of rainfall and its evaporation from the leaf surfaces (**interception loss**)
- the infiltration, drainage, and storage of the residual rainfall in the soil (**soil hydrology**)
- the control by the photosynthetically active radiation (PAR) and the soil moisture potential over the stomatal functioning (**canopy resistance**)
- transfer of the soil moisture to the atmosphere through the root-stem-leaf system of the vegetation (**transpiration**)
- the aerodynamic transfer of water vapor, sensible heat and momentum from the vegetation and soil to a reference level within the ABL (**turbulent transfer**)

23

Surface resistances (r_c , r_{soil})

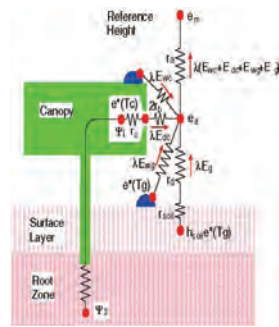
- Soil surface resistance (r_{soil}) is a function of surface soil wetness (dry \rightarrow large)
- Stomatal resistance of single leaf is a function of PAR flux, leaf temperature, water vapor deficit, leaf water potential.
- Single leaf stomatal resistances are integrated using leaf angle distribution function to produce bulk canopy resistance (r_c).



24

Sensible and latent heat fluxes

- Flux is proportional to potential difference and inversely proportional to (a series of) resistance.
- Total of evaporation from soil, evaporation of surface water, transpiration from canopy, evaporation of intercepted water is equal to the water vapor flux from canopy air space to reference height.



25

Prognostic equation of green area model

Temperature

Rn: net radiation
H : sensible heat
λE : latent heat

$$C_c \frac{\partial T_c}{\partial t} = R_{nc} - H_c - \lambda E_c$$

$$C_g \frac{\partial T_g}{\partial t} = R_{ng} - H_g - \lambda E_g - \omega C_g (T_g - T_d)$$

$$C_d \frac{\partial T_d}{\partial t} = R_{ng} - H_g - \lambda E_g$$

Soil Wetness

P1: infiltration
Qi,j : water exchange
Es : soil evaporation
Edc : transpiration
Q3 : drainage

$$\frac{\partial W_1}{\partial t} = \frac{1}{\theta_s D_1} \left[P_1 - Q_{1,2} - \frac{E_s}{\rho_w} - E_{dc,1} \right]$$

$$\frac{\partial W_2}{\partial t} = \frac{1}{\theta_s D_2} \left[Q_{1,2} - Q_{2,3} - E_{dc,2} \right]$$

$$\frac{\partial W_3}{\partial t} = \frac{1}{\theta_s D_3} \left[Q_{2,3} - Q_3 \right]$$

26

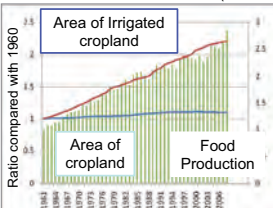
Increasing water use

- Rapid growth of world population
→ major increase in **food** and **water** demand.
- Key word: Irrigation
 - Good : Producing much food (about 2.5 times)
 - Bad : Requiring much water

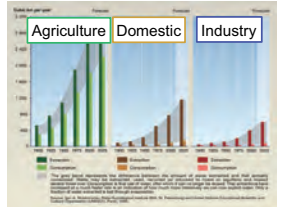


irrigation

Food Production of The World (FAOSTAT)



World Water Use (Shiklomanov, 2000)



27

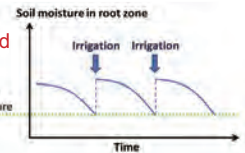
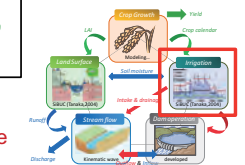


Irrigation

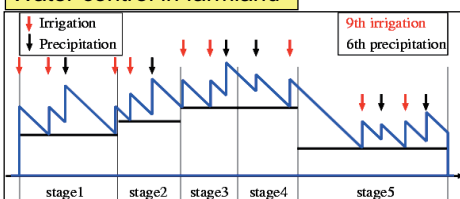
Basic concept is to maintain soil moisture/water depth within **appropriate ranges for optimal crop growth**.

Application to wheat, corn, soy bean, cotton etc...

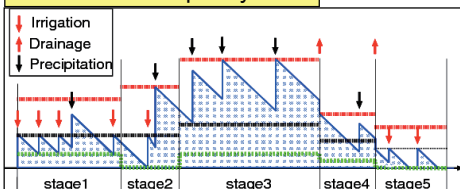
Water layer is added to treat **paddy field** more accurately.



Water control in farmland



Water control in paddy field



Paddy field model

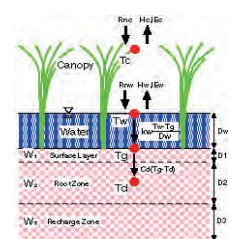
- Water depth and water temperature are added

$$C_c \frac{\partial T_c}{\partial t} = R_{nc} - H_c - \lambda E_c$$

$$C_w D_w \frac{\partial T_w}{\partial t} = R_{nw} - H_w - \lambda E_w - k_w \frac{T_w - T_g}{D_w}$$

$$C_g \frac{\partial T_g}{\partial t} = k_w \frac{T_w - T_g}{D_w} - \omega C_g (T_g - T_d)$$

$$C_d \frac{\partial T_d}{\partial t} = \omega C_d (T_g - T_d)$$



30

Applied condition

Crop type	Growing stage	1st	2nd	3rd	4th	5th
Spring wheat	Periods(%)	23	14	14	14	35
	Soil wetness	0.70	0.60	0.80	0.80	0.55
Winter wheat	Periods(%)	25	20	22	13	20
	Soil wetness	0.70	0.70	0.80	0.80	0.55
Corn	Periods(%)	8	48	6	14	24
	Soil wetness	0.75	0.65	0.70	0.75	0.65
Rice	Periods(%)	25	13	33	13	16
	Water depth (mm)	20-50	none	20-60	moistening	intermittent
soy bean	Periods(%)	3	26	16	28	27
	Soil wetness	0.75	0.65	0.65	0.70	0.65
cotton	Periods(%)	4	21	13	26	36
	Soil wetness	none	0.5	0.55	0.55	0.5

Chart by required water for cultivation in China

31

Investigation

TYPICAL IRRIGATION IN UZBEKISTAN



Water canal



Canal for drainage water



Furrow irrigation



Drip irrigation

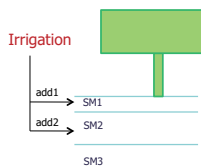


Irrigation efficiency

IRRIGATION SCHEME

⇒ Application efficiency is considered.

Perfect irrigation
(Drip irrigation)
(Application efficiency is 100%.)

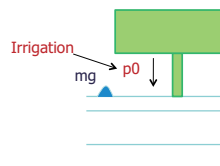


$$\Delta SM1 = \text{waterin} * \frac{d1}{d1 + d2}$$

$$\Delta SM2 = \text{waterin} * \frac{d2}{d1 + d2}$$

- Water is directly supplied to the root zone.
- Small amount of water is frequently supplied.

Realistic irrigation
(Furrow irrigation)
(Application efficiency is considered.)



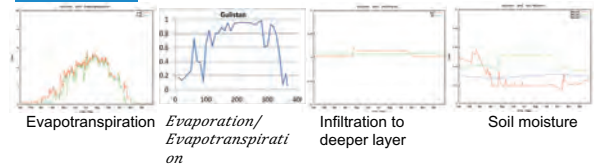
$$p0 = \text{waterin}$$

- Water is supplied from ground.
- Huge amount of water is supplied around once a week.

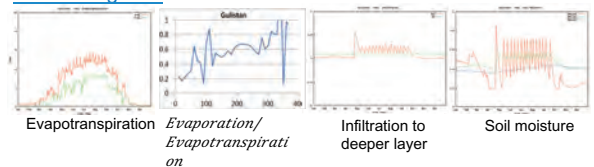
Irrigation efficiency

WATER BALANCE IN IRRIGATED FARM

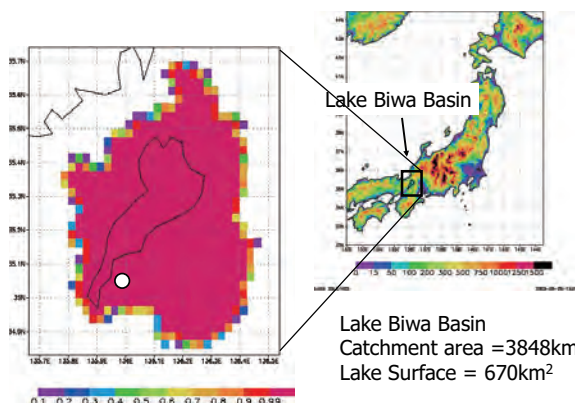
Drip irrigation



Furrow irrigation



Application to the Lake Biwa Basin (Japan)

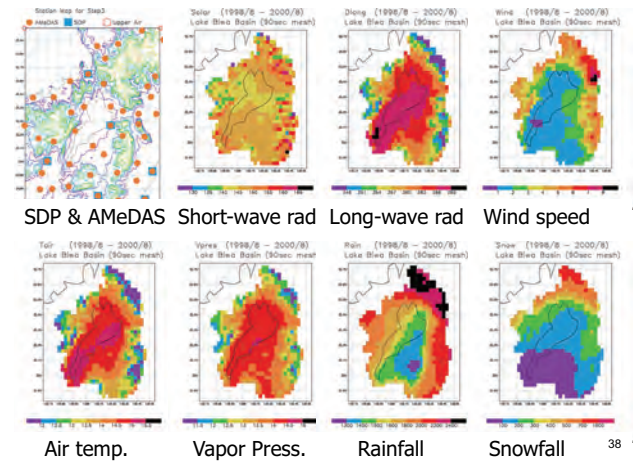
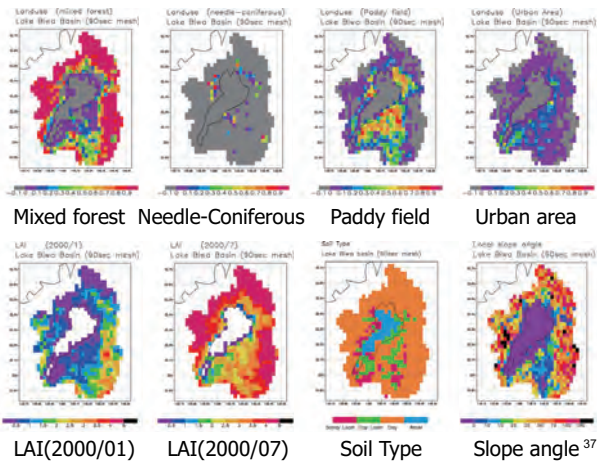


35

The Lake Biwa Basin

- The basin has a great variety of geographical features, such as high mountains, large water surface, urban area, and **paddy field**.
- This basin shows different climatic condition.
South: warm and humid in summer (dry in winter)
North&West: **much snow** in winter
East: relatively dry
- The Lake Biwa is the **largest (670km²) freshwater body in Japan**. It is also one of the ancient lakes (4million years old!!) in the world.
- The water of Lake Biwa is utilized for **drinking by 14 million people** in the Kyoto-Osaka-Kobe metropolitan area.

36



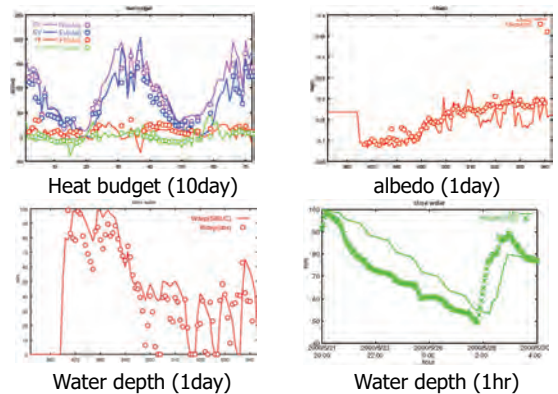
Validation at single grid

- Three sites from the Lake Biwa Project
Fluxes of radiation budget and heat budget component and related meteorological and hydrological variables can be used from these datasets.
- Two sites from the snow depth observation station

Site	Lon (E)	Lat (N)	alt (m)	note
Grid P	136.23	35.49	107	Rice paddy field
Grid L	136.15	35.38	80	Lake surface
Grid F	136.21	35.56	430	Deciduous forest
Grid W	136.21	35.62	217	Snow depth (Washimi)
Grid H	136.25	35.27	87	Snow depth (Hikone)

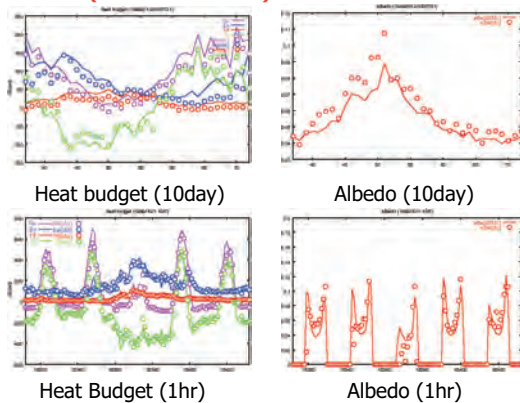
39

Grid P (paddy field)



40

Grid L (lake surface)

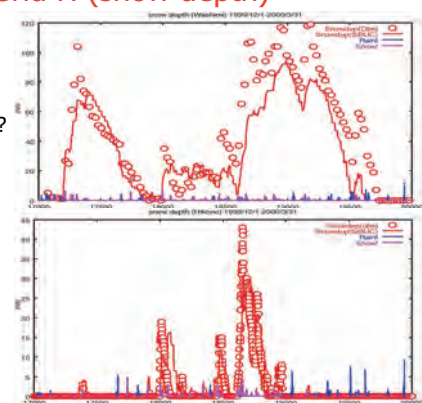


41

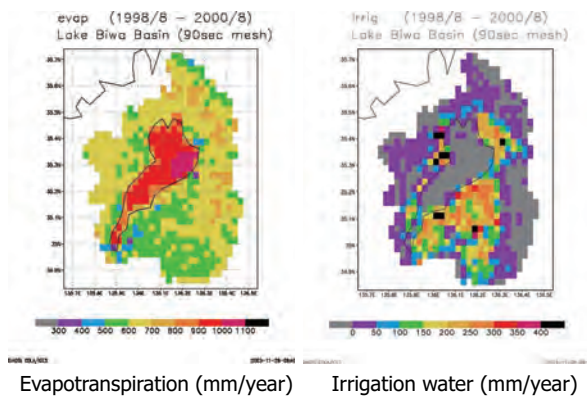
Grid W & Grid H (snow depth)

Grid W
Snowfall is underestimated?

Grid H



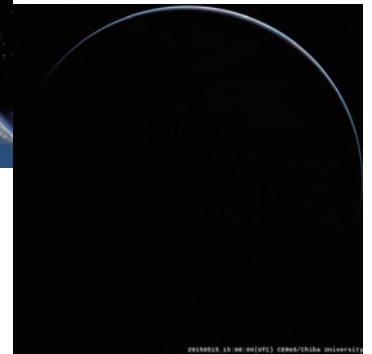
42



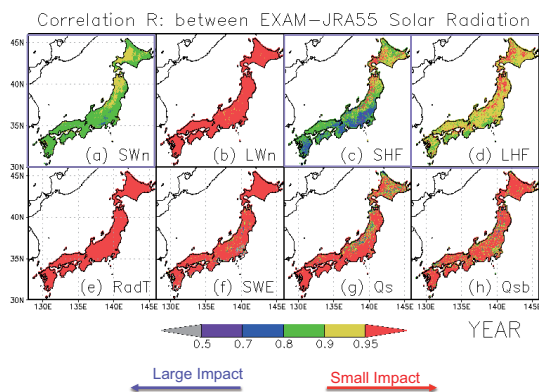
43



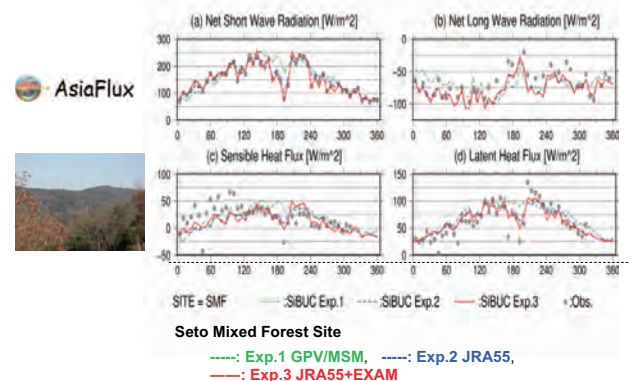
The 1st 3rd generation
Geostationary
Meteorological
Satellite
HIMAWARI-8



Impact of EXAM short-wave radiation



Impact of EXAM short-wave radiation



Sensitivity experiments to forcing data

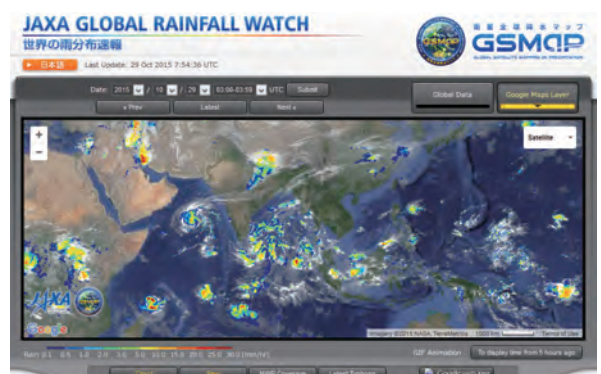
Comparison of SIBUC output relative to flux observation
@ four sites in Japan

Sites / Function	w GPV/MSM				w JRA55				w JRA55 + Satellite			
	SWn	LWn	SHF	LHF	SWn	LWn	SHF	LHF	SWn	LWn	SHF	LHF
FHK	R	0.413	0.790	0.478	0.779				0.689	0.767		
	RMSE		39.4	37.9	32.3	27.1			28.0	24.5		
SMF	R	0.720	0.483	0.233	0.528	0.899	0.837	0.434	0.653	0.953	0.879	0.566
	RMSE	52.9	28.6	36.6	42.3	32.9	21.6	31.7	37.2	22.8	19.5	29.4
TKC	R	0.740	0.386		0.833	0.724			0.922	0.783		
	RMSE	58.0	35.0		46.2	23.9			33.9	21.0		
TKY	R	0.676	0.396	0.486	0.762	0.856	0.726	0.532	0.828	0.945	0.781	0.663
	RMSE	65.0	40.6	30.5	36.9	46.5	30.6	27.2	25.8	28.4	28.4	23.2

SWn: net short wave rad., LWn: net long wave rad., SHF: sensible heat flux LHF: latent heat flux **Best experiment !**

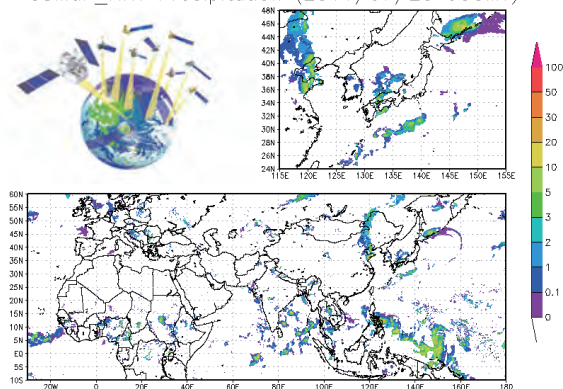
Thanks to ASIA-FLUX AsiaFlux

Kotsuki et al. (2015, HRL)

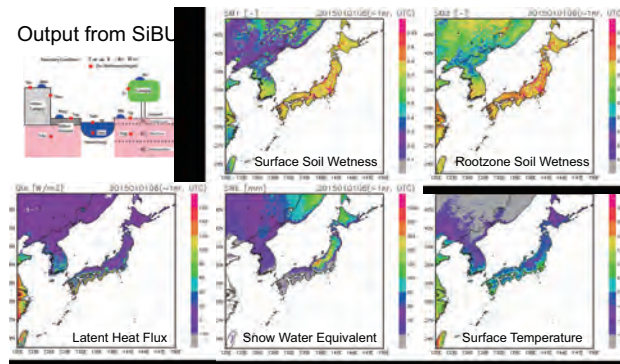


(<http://sharaku.eorc.jaxa.jp/GSMaP/>)

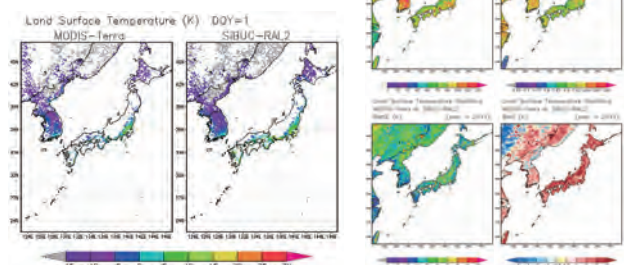
GSMaP_NRT Precipitation (2011/07/25 00GMT)



Output from SiBU



Validation of Land Surface Temperature by MODIS-Terra (10:30)



Data sets for global application

Land surface parameter

- Land cover
GLCC version2
- Soil physical parameter
Ecoclimap
- Crop type
FAO (crop type fraction)
- Remote Sensing (NDVI)
SPOT vegetation
- Crop Calendar
Analysis of NDVI

Meteorological data sets

- Precipitation [kg/s m²]
GPCC,APHRODITE,GSMaP
- Short wave radiation [W/m²]
Long wave radiation [W/m²]
Temperature [K]
Specific humidity [kg/kg]
Hirabayashi *et al.*(2008)
- Atmosphere pressure [Pa]
Wind speed [m/s]
JRA25

52

Applied condition

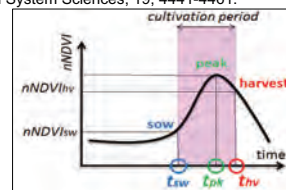
Crop type	Growing stage	1st	2nd	3rd	4th	5th
Spring wheat	Periods(%)	23	14	14	14	35
	Soil wetness	0.70	0.60	0.80	0.80	0.55
Winter wheat	Periods(%)	25	20	22	13	20
	Soil wetness	0.70	0.70	0.80	0.80	0.55
Corn	Periods(%)	8	48	6	14	24
	Soil wetness	0.75	0.65	0.70	0.75	0.65
Rice	Periods(%)	25	13	33	13	16
	Water depth (mm)	20-50	none	20-60	moistening	intermittent
soy bean	Periods(%)	3	26	16	28	27
	Soil wetness	0.75	0.65	0.65	0.70	0.65
cotton	Periods(%)	4	21	13	26	36
	Soil wetness	none	0.5	0.55	0.55	0.5

Chart by required water for cultivation in China

53

Satellite-derived crop calendar (SACRA)

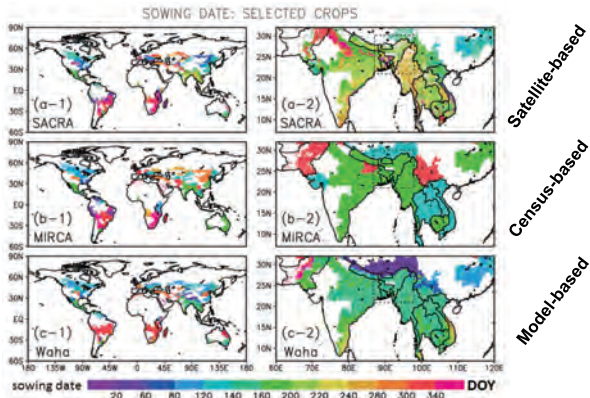
Kotsuki S. and K. Tanaka (2015):
SACRA - a method for the estimation of global high-resolution crop calendars from a satellite-sensed NDVI. Hydrology and Earth System Sciences, 19, 4441-4461.



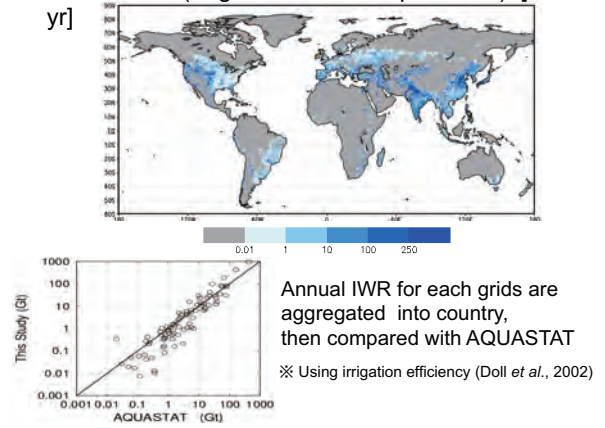
http://data-assimilation.riken.jp/opendata/sacra/sacra_des.html

Description	Sample Image	Binary (w/GRADS ctrl)
Global Map of Planting and Harvesting Dates (day of year)	click	download (13Mb)
Global Map of Cropping Intensity (yr ⁻¹)	click	download (03Mb)
Global Map of Dominant Crop (crop species)	click	download (03Mb)
Global Map of Time Series of NDVI (10-days composite)	click	download (191Mb)
ALL	click	download (219Mb)

Comparison with other products



Annual IWR (Irrigation Water Requirement) [mm/yr]



68

Climate Indicator (Aridity Index & Evaporation Ratio)

Annual evapotranspiration approaches annual precipitation in arid and semi-arid regions where the available energy greatly exceeds the amount required to evaporate annual precipitation.

Evapotranspiration is a key information for water management in the region where available water resources are limited.

Aridity Index

$$\text{Energy balance} = \frac{R_{net}}{L P}$$

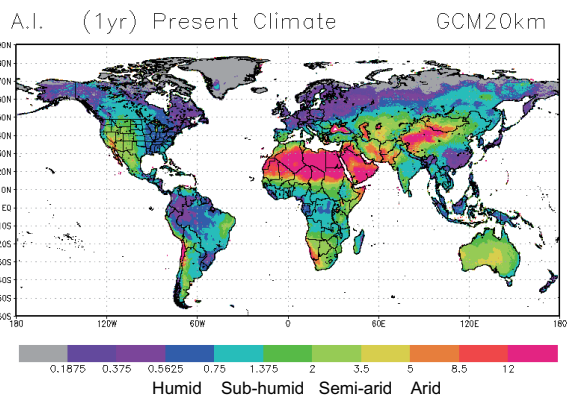
5 < AI < 12 Arid
2 < AI < 5 Semi Arid
0.75 < AI < 2 Sub Humid
0.375 < AI < 0.75 Humid
(Ponce et al. 2000)

Evaporation Ratio

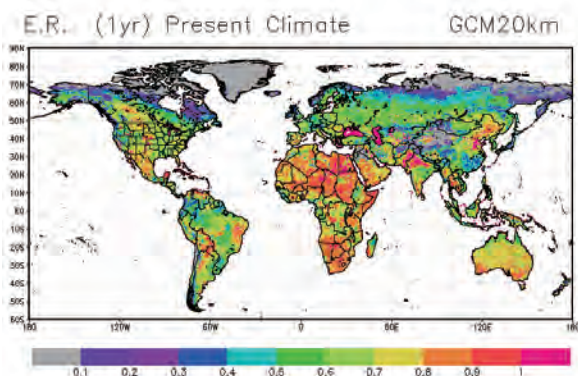
$$\text{Water balance} = \frac{E}{P}$$

R_{net}: annual mean net radiation
P: annual precipitation
L: latent heat of vaporization
E: annual evapotranspiration

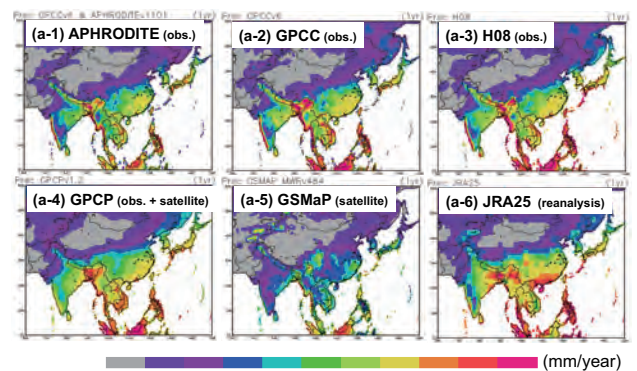
Global Distribution of Aridity Index (AI)



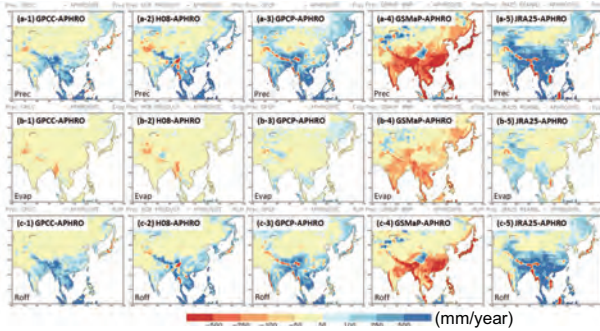
Global Distribution of Evaporation Ratio (ER)



Precipitation products over Eastern Asia

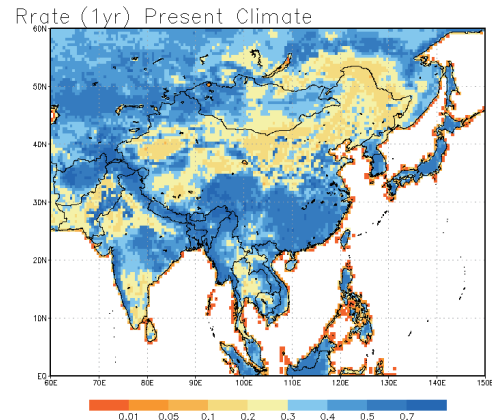


Precipitation products over Eastern Asia

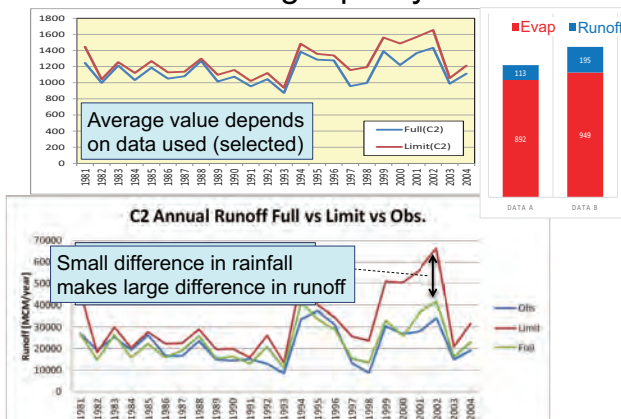


While precipitation has large difference between products, simulated evapotranspiration using products has small difference. Most of difference in precipitation translates to difference in runoff. Any error in the precipitation translates to approximately the same absolute error in runoff over the Eastern Asia.

Runoff Ratio



Need for high quality data



Summary

- **General aspects of land surface processes are introduced.**
Water is exchanged **between atmosphere and land surface** through processes of precipitation, evaporation, and transpiration. Water is exchanged **between land surface and ocean/lake** through runoff (river process). The partitioning of available energy is strongly dependent on both **land cover characteristics** and its **hydrological state (wet/dry)**.
- **Observation and modelling of physical processes of land surface are introduced.**
Field experiments in different vegetation and climate conditions. Land surface model is formulated by prognostic equations of land surface states (soil moisture, temperature, snow) describing the change of states through energy and water balance components.
- **Some applications of land surface model are introduced.**
Energy and water balance of the lake Biwa basin
Near real-time monitoring of land surface states in Japan
Global distribution of aridity index and evaporation ratio

- If you want to know the detail formulation, document of SiBUC is available on the web

<http://rwes.dpri.kyoto-u.ac.jp/~tanaka/sibuc/sibuc-web.pdf>

- Simple Biosphere including Urban Canopy

Exercise 2&3: Processing method of geographical and meteorological data

Kenji TANAKA (*Associate Professor, Disaster Prevention Research Institute, Kyoto University*)

Abstract:

This exercise aims to introduce the method to analyze the geographical and meteorological data for use in hydrological analysis. The basic geographical information for hydrological analysis are topography, landuse, and soil type. The basic meteorological information for hydrological analysis are precipitation and air temperature. In this training course, some example to analyze those information is examined. Select and cut the region, change the resolution, or aggregating the information depending on the target grid. Some statistical analyses such as annual maximum value, monthly mean value are also examined. As the participants of the training course are from different countries, global datasets are selected for analysis. Depending on your interest area, you can select any region of the world for your analysis.

Exercise 2&3 Processing method of geographical and meteorological data

Kenji Tanaka

Water Resources Research Center,
DPRI, Kyoto University
tanaka.kenji.6u@kyoto-u.ac.jp



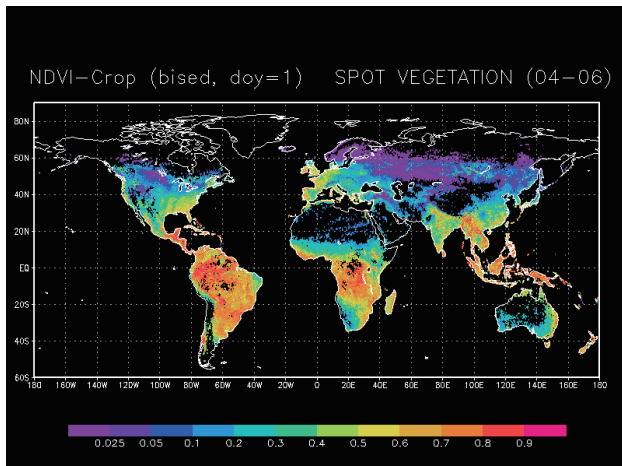
Geographical data for hydrological analysis

- Land use/Land cover
- Topography
- River basin
- Soil Type
- Vegetation index (NDVI)

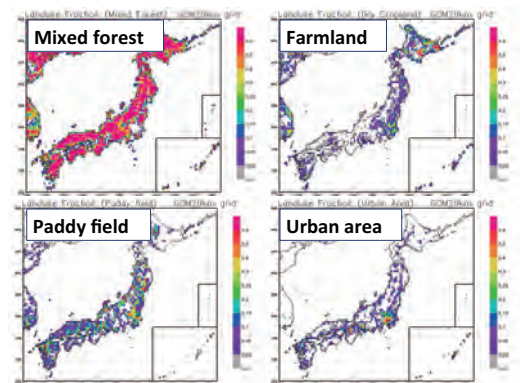
Many research institute and
Operational agencies are
Producing many products.

It is strongly recommended to download several
products and make comparison.

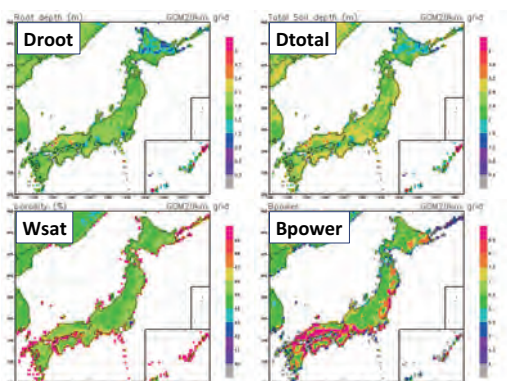
According to your knowledge and local information,
please select suitable product for your target basin.



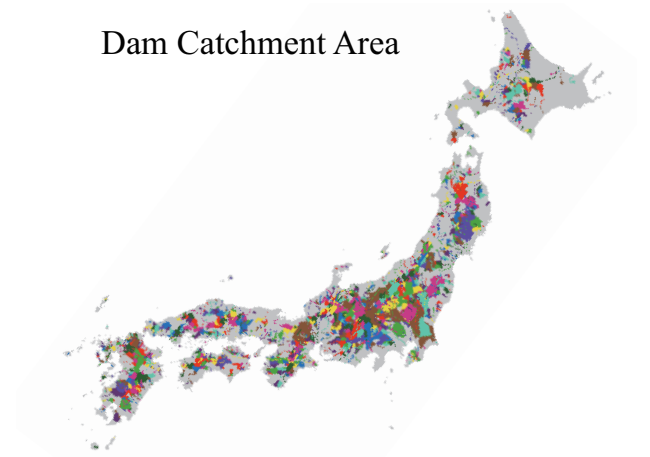
Landuse fraction (ClassFrac)



Soil parameter (from ECOCLIMAP)



Dam Catchment Area



Meteorological data for hydrological analysis

- Precipitation
 - Gauge based (accuracy depends on observation density)
 - GPCC Long history (monthly, 0.5deg 1degree)
 - APHRODITE Long history (daily, 0.25degree)
 - Satellite based (need bias correction)
 - GSMaP Real time (hourly, 0.1degree)
- Air Temperature
 - CRU
 - APHRODITE

Depending on your purpose suitable product is selected or several products are merged

GPCC (Global Precipitation Climatology Center)

ftp://ftp.dwd.de/pub/data/gpcc/html/Gate_to_the_GPCC_Products.html

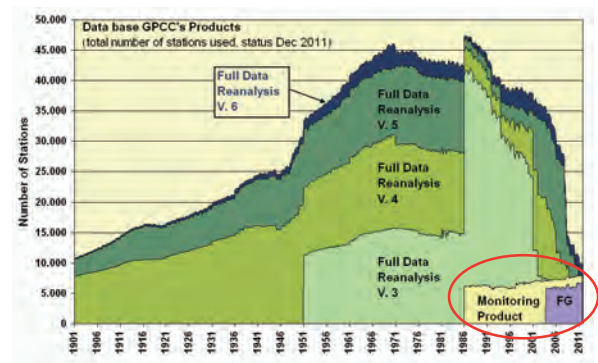
The screenshot shows the GPCC website interface with the title 'Visualize and Download GPCC Products'. It features several sections: 'Monitoring Product' (with a red box around the title), 'Full Data Reanalysis' (with a red box around the title), 'Precipitation Climatology', 'FASCIAT Dataset', 'Visualizer', and 'GPCC at DWD'. Each section includes a brief description of the data and a 'download' link.

Download page for Monitoring Product

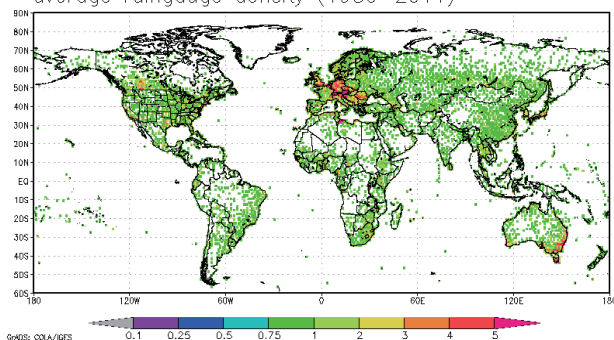
Monitoring Product for Month/Year	1.0 ° (.zip)	2.5 ° (.zip)
01-12 1986 (archive)	download	download
01-12 1987 (archive)	download	download
01-12 1988 (archive)	download	download
01-12 1989 (archive)	download	download
01-12 1990 (archive)	download	download
01-12 1991 (archive)	download	download
01-12 1992 (archive)	download	download
01-12 1993 (archive)	download	download
01-12 1994 (archive)	download	download
01-12 1995 (archive)	download	download
01-12 1996 (archive)	download	download

Download page for Full Data Reanalysis

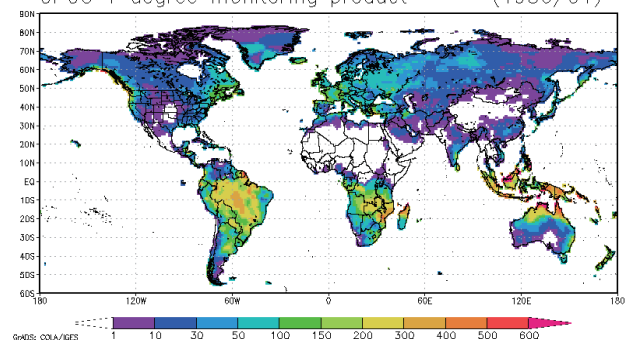
Full Data Reanalysis for 10 years	0.5 ° (.zip ~ 55 MByte)	1.0 ° (.zip ~ 15 MByte)	2.5 ° (.zip ~ 3 MByte)
01.1901 - 12.1910 (archive)	download	download	download
01.1911 - 12.1920 (archive)	download	download	download
01.1921 - 12.1930 (archive)	download	download	download
01.1931 - 12.1940 (archive)	download	download	download
01.1941 - 12.1950 (archive)	download	download	download
01.1951 - 12.1960 (archive)	download	download	download
01.1961 - 12.1970 (archive)	download	download	download
01.1971 - 12.1980 (archive)	download	download	download
01.1981 - 12.1990 (archive)	download	download	download
01.1991 - 12.2000 (archive)	download	download	download
01.2001 - 12.2009 (archive)	download	download	download

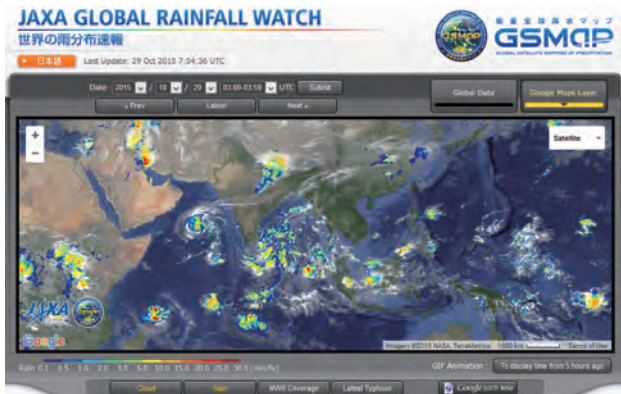


average raingauge density (1986–2011)



GPCC 1 degree monitoring product (1986/01)





(<http://sharaku.eorc.jaxa.jp/GSMaP/>)

We offer hourly global rainfall maps in near real time (about four hours after observation) using the combined MW-IR algorithm with **GPM-Core GMI**, **TRMM TMI**, **GCOM-W AMSR2**, DMSP series SSMIS, NOAA series AMSU, MetOp series AMSU and Geostationary IR data. Background cloud images are globally merged IR data produced by NOAA Climate Prediction Center (CPC), using IR data observed by JMA's MTSAT satellite, NOAA's GOES satellites and EUMETSAT's Meteosat satellites.

User Registration for Near-Real-Time Data

To use data, user registration is needed. Since September 3, 2014, near-real-time products and images will be replaced by reanalysis version about 3 days later. Reanalysis data in latest version (GSMaP_MVK Ver.6.000) currently available period after September 1, 2014, but past period data will be released sequentially after processing. Reanalysis data in old version (GSMaP_MVK ver.5.222) are available for the period from Mar. 2000 to Nov. 2010, and will be removed from the server when new version data is available.

[User Registration](#)

You can access to the GSMaP products after registration.

Procedure of data analysis

- Step0: unpack the data (gzipped file)
- Step1: select the region for analysis (GSMaP)
(GSMaP/daily/cutgsmmap.f)
- Step2: select the region for analysis (GPCC)
(GSMaP/daily/cutgpcc.f)
- Step3: calculate climatological value and correction factor
(GSMaP/daily/climanal.f)
- Step4: select the region for analysis (gsmmap hourly)
(GSMaP/hourly/cutgsmmap.f)
- Step5: change resolution to fit to the model grid
(GSMaP/hourly/chgres.f)
- Step6: bias correction of GSMaP by GPCC climatology
(GSMaP/hourly/bcgsmmap.f)

Step1: select the region for analysis (GSMaP) (GSMaP/daily/cutgsmmap.f)

```

parameter(IDIM=3600, JDIM=1200)
parameter(latN=35., latS=-5., lonW=20., lonE=45.)

```

Set the analysis region

```

do ii=2000,2010
  write(cy,'(i4.4)') ii
  open(22,file='NILE/GSMaP-Nile-1mon'//cy//'.gad',
    ,form='unformatted',access='direct',recl=mx*my*4)

```

loop for year
write the year information in cy
Use cy (year information) in file name automatically

Step2: select the region for analysis (GPCC) (GSMaP/daily/cutgpcc.f)

```

parameter(IDIM=360, JDIM=180)
parameter(latN=35., latS=-5., lonW=20., lonE=45.)

```

Set the analysis region

```

do ii=1986,2011
  write(cy,'(i4.4)') ii
  open(22,file='NILE/GPCC-Nile-1mon'//cy//'.gad',
    ,form='unformatted',access='direct',recl=mx*my*4)

```

loop for year
write the year information in cy
Use cy (year information) in file name automatically

Step3: calculate climatological value and correction factor (GSMaP/daily/climanal.f)

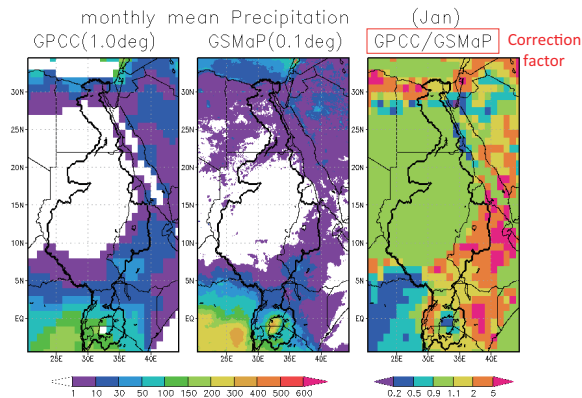
```

do ii=1,mx
  do jj=1,my
    i1=(ii-1)*10+1
    i2=ii*10
    j1=(jj-1)*10+1
    j2=jj*10
    bias(ii,jj,imon)=1.
    avevar(ii,jj)=0.
    icon2=0
    do i=i1,i2
      do j=j1,j2
        if(clim2(i,j,imon).ge.0.) then
          avevar(ii,jj)=avevar(ii,jj)+clim2(i,j,imon)
          icon2=icon2+1
        endif
      enddo
    enddo
    avevar(ii,jj)=avevar(ii,jj)/real(icon2)
    if(avevar(ii,jj).ge.1. and clim1(ii,jj,imon).ge.1.)
      bias(ii,jj,imon)=clim1(ii,jj,imon)/avevar(ii,jj)
    endif
  enddo
enddo

```

loop for 1 degree data
Initialization for averaging
loop for 0.1 degree data
calculate 1 degree average value
Correction factor (GPCC/GSMaP)

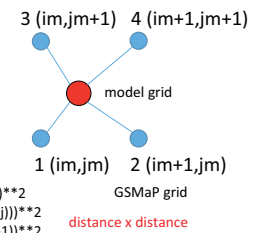
Comparison of monthly mean precipitation



Step5: change resolution to fit to the model grid (GSMaP/hourly/chgres.f)

parameter(mx1=250, my1=400) GSMaP grid
parameter(mx2=150, my2=240) model grid

do ii=1,mx2 data matching
im(ii)=nint((xlon2(ii)-lonW-0.5*res1)/res1)+1
enddo
do jj=1,my2
jm(jj)=nint((xlat2(jj)-latS-0.5*res1)/res1)+1
enddo



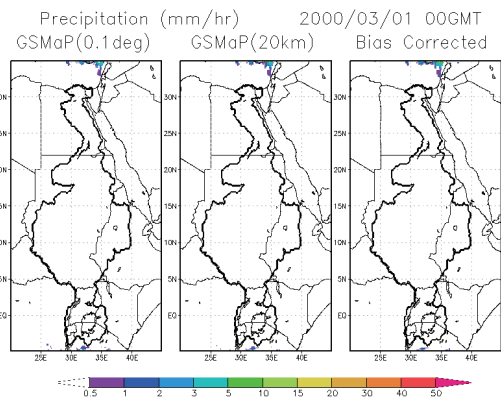
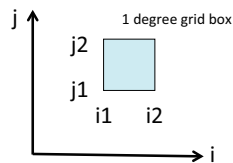
dis1=(xlon2(ii)-xlon1(im(ii)))*2+(xlat2(jj)-xlat1(jm(jj)))*2
dis2=(xlon2(ii)-xlon1(im(ii)+1))*2+(xlat2(jj)-xlat1(jm(jj)))*2
dis3=(xlon2(ii)-xlon1(im(ii))*2+(xlat2(jj)-xlat1(jm(jj)+1))*2
dis4=(xlon2(ii)-xlon1(im(ii)+1))*2+(xlat2(jj)-xlat1(jm(jj)+1))*2
www=1./dis1+1./dis2+1./dis3+1./dis4
weight(ii,jj,1)=1./(dis1*www)
weight(ii,jj,2)=1./(dis2*www)
weight(ii,jj,3)=1./(dis3*www)
weight(ii,jj,4)=1./(dis4*www)

weight for interpolation
Total weight should be 1

Step6: bias correction of GSMaP by GPCC climatology (GSMaP/hourly/bcgsmmap.f)

parameter(mx1=25, my1=40) correction factor (1 degree)
parameter(mx2=150, my2=240) model grid (1/6 degree)

do imon=1,12
read(11,rec=imon) ((bias(i,j,imon),i=1,mx1),j=1,my1) reading correction factor
do i=1,mx1
do j=1,my1 loop for 1 degree data
i1=(i-1)*iave+1
i2=i*iave
j1=(j-1)*jave+1
j2=j*jave
do ii=i1,i2 loop for model grid
do jj=j1,j2 (1/6 degree data)
bias2(ii,jj,imon)=bias(i,j,imon)
if(bias2(ii,jj,imon).gt.5.0) bias2(ii,jj,imon)=5.0
if(bias2(ii,jj,imon).lt.0.2) bias2(ii,jj,imon)=0.2



GrADS

❑ The Grid Analysis and Display System (GrADS)

❑ Free Software to display 2 Dimensional data

❑ Install

❑ **Activate** : grads-2.0.2.oga.2-win32_superpack.exe

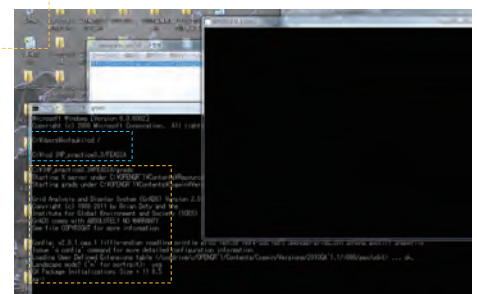
Source : <http://sourceforge.net/projects/opengrads/files/>

grads2: OpenGrADS Bundle Distribution (Windows/Mac/Linux/Unix)

How to use "Grads" ?

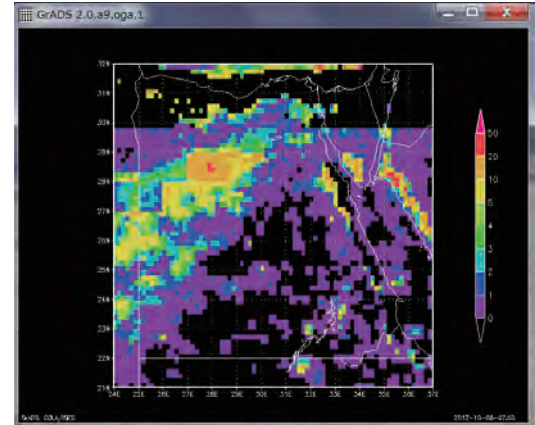
1. **Activate**: Command Prompt
- All programs/accessory/command_prompt.exe
2. **Change Directory** to C:\GSMaP\hourly/NILE/
3. **Activate**: Grads

Grads
yes



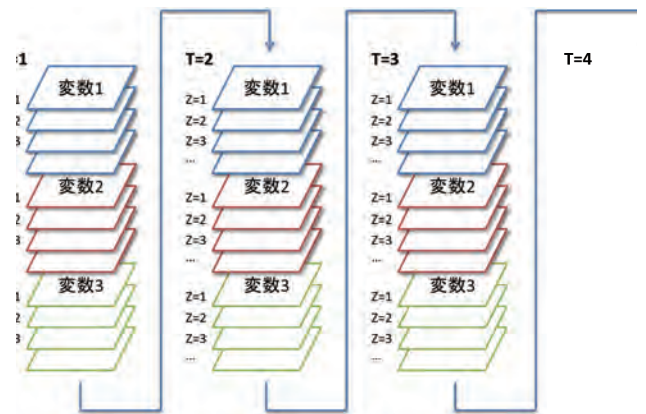
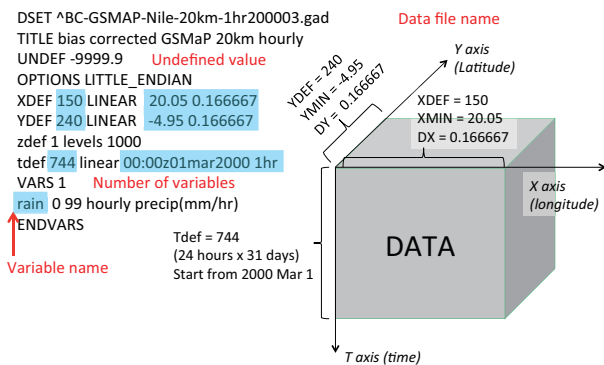
Please test grads by following command

```
ga-> open BC-GSMAP-Nile-20km-1hr200003.cti
Scanning description file: BC-GSMAP-Nile-20km-1hr200003.cti
Data file BC-GSMAP-Nile-20km-1hr200003.gad is open as file 1
LON set to 20.05 44.8834
LAT set to -4.95 34.8834
LEV set to 1000 1000
Time values set: 2000:3:1:0 2000:3:1:0
E set to 1 1
ga-> set clevs 0 1 2 3 4 5 10 20 50
Number of clevs = 9
ga-> set cools 0 9 4 5 3 10 7 12 2 6
Number of cools = 10
ga-> set lon 24 37
LON set to 24 37
ga-> set lat 21 32
LAT set to 21 32
ga-> set mpdset hires
MPDSET File name = hires
ga-> set gxout grfill
ga-> d sum(rain,1=1,1=744)
SUMming, dim = 3, start = 1, end = 744
Contouring at clevs = 0 1 2 3 4 5 10 20 50
ga-> cbarm.gs
```



Data description file (ctl file)

Ex. BC-GSMAP-Nile-20km-1hr200003.ctl

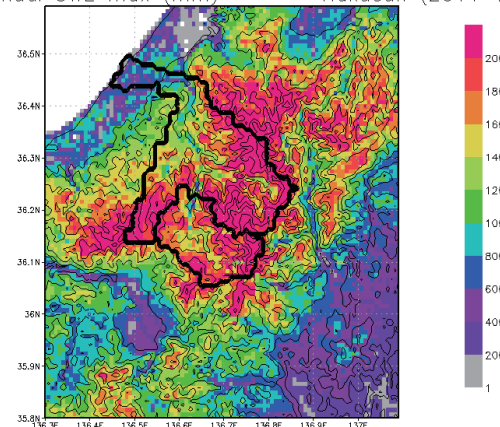


You can easily make the similar figures using grads script

```
'set display color white'
'open SIBUC_JLDAS1km_Haku_SWE.ctl'
'open Soil_JLDAS1km_Haku.ctl'
'open basmaskTedorictl'
yyy=1
while(yyy<=7)
'reset'
'set string 1'
'set strsz 0.23 0.25'
'draw string 6.5 8.1 Hakusan ("yyy+2004"-yyy+2005')
'draw string 0.4 8.1 annual SWE max (mm)'
'set mpdset hires'
'set gxout grfill'
'set grads off'
'set dfile 1'
'set t 'yyy'
'set pare 0.5 9 0.5 8'
'set clevs 1 200 400 600 800 1000 1200 1400 1600 1800 2000'
'set ccols 0 15 14 9 4 5 3 10 7 8 2 6'
'd swe'
'cbarm.gs'

'set dfile 2'
'set t 1'
'set gxout contour'
'set clab off'
'set clevs 50 100 250 500 750 1000 12'
'd elev'
'set dfile 3'
'set ccolor 1'
'set cint 0.1'
'd mask'
'q pos'
'printim GIFfile/SWE/yyy+2005.gif'
yyy=yyy+1
endwhile
return
```

annual SWE max (mm) Hakusan (2011-2012)

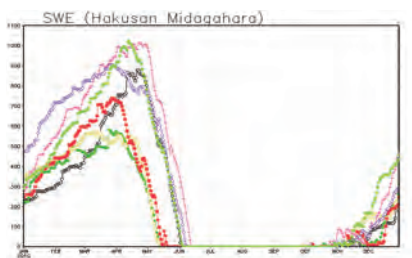


```

'open SIBUCJLDAS1km_Haku2006.cti'
'open SIBUCJLDAS1km_Haku2007.cti'
(省略)
'open SIBUCJLDAS1km_Haku2012.cti'
'set display color white'
'reset'
'set strsiz 0.27 0.3'
'draw string 1 8.1 SWE (Hakusan Midagahara)'
'set grads off'
yyy=1
while(yyy<=7)
'set dfile 'yyy''
'set lon 136.76'
'set lat 36.15'
'set t 1 365'
'set vrange 0 1100'
'set parex 0.5 10.5 1.0 8.0'
'd swe'
yyy=yyy+1
endwhile
'printim GIFFile/SWetime.gif'
return

```

You can draw line graph
by GrADS



Creating gif animation of GrADS figures

```

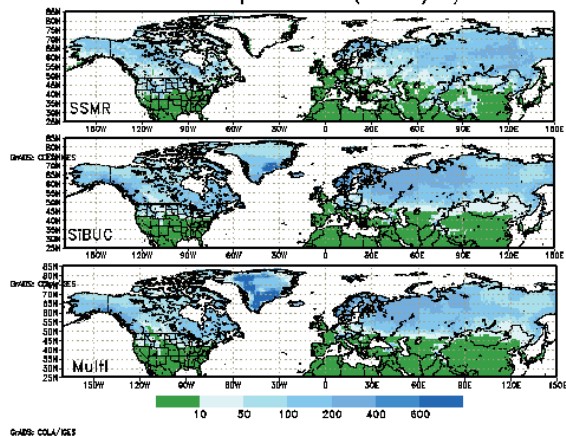
if(month<10) ; 'printim TEMPfile/im'varnum"yyy'0'month'.gif' ; endif
if(month> 9) ; 'printim TEMPfile/im'varnum"yyy'month'.gif' ; endif
month=month+1
endwhile
yyy=yyy+1
endwhile
Repeat number
time interval of each file (mil sec)
'! convert -loop 1 -delay 30 TEMPfile/im* ANIMfile/anim'varnum'.gif'
'mv TEMPfile/im* GIFFile/'
return

```

ImageMagick download site

<http://www.imagemagick.org/script/binary-releases.php>

Snow Water Equivalent (1986/1)



color

番号	名前	色
0	background	黒
1	foreground	白
2	red	赤
3	green	緑
4	dark blue	濃青
5	light blue	淡青
6	magenta	紫
7	yellow	黄
8	orange	橙
9	purple	紫
10	yellow/green	黄緑
11	medium blue	中青
12	dark yellow	濃黄
13	aqua	水色
14	dark purple	濃紫
15	gray	灰

mark

番号	マーク
0	(なし)
1	+
2	○
3	●
4	□
5	■
6	×
7	◇
8	△
9	▲
10	□
11	●

line

線種番号	線種
0	(なし)
1	実線
2	長破線
3	短破線
4	長破線+短破線
5	点線
6	一点鎖線
7	二点鎖線

Lecture 5: Fundamentals in Optimum Operation of Reservoir Systems

Tomoharu HORI (*Professor, Water Resources Research Center, DPRI, Kyoto University*)

Abstract:

A reservoir system is one of the most powerful and commonly used tools for water resources management. It regulates the river discharge in order to increase the availability of water resources and also to prevent flood disasters. Because the temporal distribution of river discharge, especially the extreme value, brings water-related disasters, the operation of reservoirs have been of great concern in the field of operational hydrology. It has been pointed out recently that the distribution of precipitation will change according to the impact of climate change. This implies that the design flood with the return period of one hundred years, for example, will come to be the one with shorter return period in future. It is not easy, however, to construct new facilities to cope with the situation and then the non-facility-based countermeasures such as higher degree application of dam reservoirs are getting more important.

From these points of view, a lot of research works have been done so far about reservoir operation. Many techniques and algorithms have been proposed and huge amount of case studies have been reported in research journals. When trying to study about reservoir operation, beginners may find some difficulty to know where to start. This course will introduce the fundamentals in optimum reservoir operation theory, which may be of great help for class participants to do more detailed study. The lecture comprises of three parts; the introduction of reservoir operation, optimization framework of reservoir operation and measures to cope with uncertainty.

In the first part, basic concept related to reservoir operation is introduced. Various purposes of dam reservoirs are summarized and how the operation policy can differ according to the purposes. The difference of on-line real time control and off-line control is also discussed. Some examples of actual reservoir operation will be shown before going into theoretical approach.

In the second part, the typical reservoir control problem is formulated in mathematical expression. Types of objective function and constraints peculiar to reservoir control problems are shown. Then it is discussed how the sequence of release discharge which gives the best value of objective function can be obtained. Dynamic programming (DP) for deterministic treatment of inflow discharge is introduced as the most fundamental optimum operation scheme. Recurrence function formula of DP application is derived for the optimum release sequence. The computational burden to obtain optimum solution is also discussed to understand the effectiveness and limitations DP approach.

In the third part, coping with uncertainty in reservoir operation is the main concern. In order to consider the uncertainty of inflow to the reservoir, first-order Markov chain is introduced and formulation of operation is modified. Then the algorithm to derive the optimum release policy is discussed and the solution search process, which is called Stochastic Dynamic Programming (SDP), is introduced. It is also shown that introduction of stochastic information requires a lot of memory area in the solution search process (curse of dimensionality). Some techniques to avoid this problem are briefly explained at the end of the class.

Fundamentals in Optimum Reservoir Operation

T. Hori
Water Resources Research Center
Disaster Prevention Research Institute
Kyoto University



Modeling of the Interaction between Water Resources and Socio-economic systems

Tomoharu HORI, Professor
Water Resources Research Center,
Disaster Prevention Research Institute,
Kyoto University

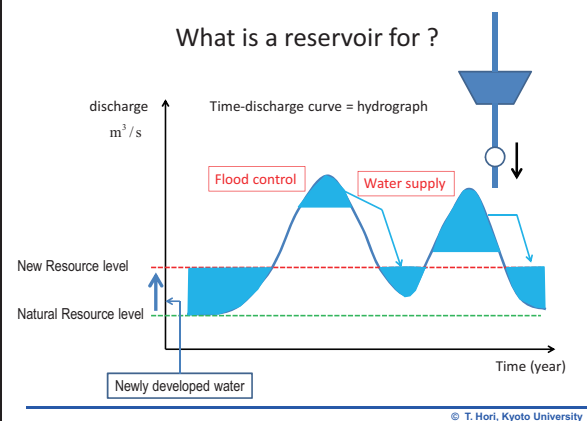
Recent Research Interest

- Modeling of the Interaction Between Water Resources and Socio-economic Systems
- Optimal Reservoir Operation scheme using Global Information
- Modeling of Human Response to Flood Emergency and Quantitative Performance Evaluation of Non-facility-based Countermeasures
- Optimal Design Framework of a Flood Control System Including In-floodplain Countermeasures Based on Distributed Risk Assessment

contents

1. Functions of Reservoirs
2. Multi-purpose reservoir - an example –
3. Mathematical expression of reservoir operation
4. Optimal operation by deterministic dynamic programming
5. Optimal operation by stochastic dynamic programming

What is a reservoir for ?



What is a reservoir for ?

1. to protect flood disasters
Keep reservoir **empty** during non-flood period
2. to supply water, to generate power
Keep reservoir **full** during non-drought period

© T. Hori, Kyoto University

A sample of multi-purpose dam reservoir - Hiyoshi dam – (1)



(Japan water agency)

© T. Hori, Kyoto University

A sample of multi-purpose dam reservoir - Hiyooshi dam – (2)

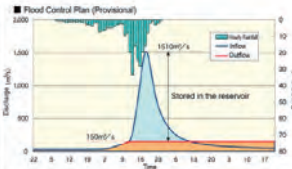
Purpose (1): Flood Control

By temporarily storing water in the dam reservoir during floods and by discharging water at a safe rate for the downstream areas, Hiyooshi Dam can reduce the damage caused by floods.

Hiyooshi Dam was constructed under a plan to control the 100-year floods. However, since river improvements in the lower reaches of the Katsura River are still in progress, flood-control operation with discharges of up to 150 m³/s has been provisionally carried out for controlling the 20-year floods. This operation is designed to maximize the effectiveness of flood control by the dam.



(Japan water agency)

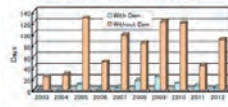


© T. Hori, Kyoto University

A sample of multi-purpose dam reservoir - Hiyooshi dam – (3)

Purpose (2): Maintenance of Normal Function of River

Days when flow rate at 14km downstream fell below the value to be secured



Hiyooshi Dam can discharge supplemental water for the vested water rights along the Katsura River and environmental preservation to maintain the normal functions of the river water. This supply has greatly reduced downstream water shortages.

However, the capacity of the dam is limited. If the dam were to continue discharging supplemental water for a long time without rainfall, the water level of the reservoir would decrease and the desirable flow rate downstream could not be secured. Therefore, the amount of supply is coordinated among the related members.

(Japan water agency)

© T. Hori, Kyoto University

A sample of multi-purpose dam reservoir - Hiyooshi dam – (3)

Purpose (3): Development of Water Use

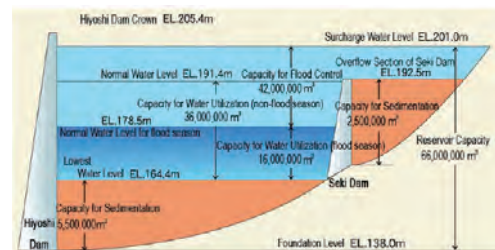
Hiyooshi Dam has created additional water use of 3.7 m³/s (sufficient for approx. 1 million people). It can supply domestic water to Kyoto Prefecture (Otokuni District, Muko City, Nagaokakyo City, and Oyamazaki Town), Osaka Prefecture (Osaka Water Supply Authority), and Hyogo Prefecture (Itami City, and Hanshin Water Supply Authority, Amagasaki City, Nishinomiya City, Ashiya City, and Kobe City). *Osaka Water Supply Authority supplies domestic water to the whole of Osaka Prefecture except Osaka City.



(Japan water agency)

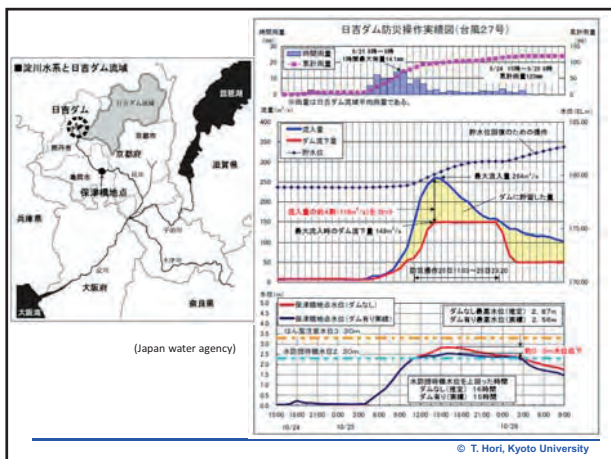
© T. Hori, Kyoto University

Capacity allocation of multi-purpose dam reservoir



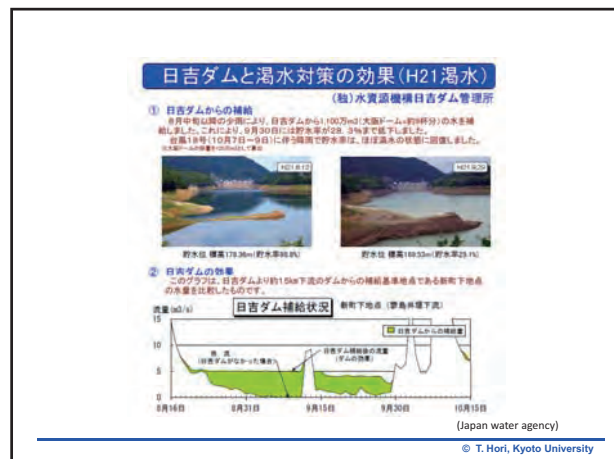
(Japan water agency)

© T. Hori, Kyoto University



(Japan water agency)

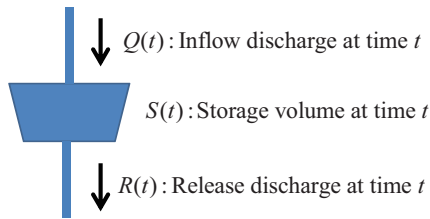
© T. Hori, Kyoto University



(Japan water agency)

© T. Hori, Kyoto University

Key variables to describe state of a reservoir



Continuity equation of a reservoir $\frac{dS(t)}{dt} = Q(t) - R(t)$

© T. Hori, Kyoto University

Objective Function (1)

Evaluation function

Damage or Loss in case of flood control

➡ Minimization problem

Benefit or Income in case of water supply and power generation

➡ Maximization problem

Conceptually can be expressed as an function of release discharge and storage

$$J(R(t), S(t))$$

© T. Hori, Kyoto University

Objective Function (2)

Evaluation of the performance of operation

Analytically expressed when the assessment can be done directly in terms of reservoir variables:

$$J(R(t), S(t)) = \{R(t) - R_{\text{target}}\}^2 + \{S(t) - S_{\text{target}}\}^2$$

In many cases, some simulation process such as flood routing and runoff is included :

$$J(R(t), S(t)) = \left(\frac{Q_{\text{ref}}(t) - D(t)}{D(t)} \times 100 \right)^2$$

where $D(t)$ denotes the demand at intake (reference) point

$J(R(t), S(t)) = f(\text{maximum inundation depth})$

$R(t) \rightarrow \text{flood flow} \rightarrow \text{inundation}$

© T. Hori, Kyoto University

Formulation

$$\max_{\substack{R(t) \\ 0 \leq t \leq T}} \left[\int_0^T J(R(t), S(t)) dt \right]$$

subject to

$$\frac{dS(t)}{dt} = Q(t) - R(t)$$

$$0 \leq R(t) \leq R_{\text{max}}$$

$$S_{\text{min}} \leq S(t) \leq S_{\text{max}}$$

$$(0 \leq t \leq T)$$

© T. Hori, Kyoto University

Design operation and Real time operation

Inflow discharge sequence $Q(t) : 0 \leq t \leq T$

Known for all time horizon

Design operation (off-line operation) : to derive optimum release sequence for historical hydrographs

Unknown in future from the current time

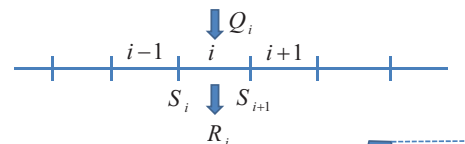
Real time operation (on-line operation) : to derive optimum release at current time in consideration with future income (current release which maximizes total benefit for the period between current time and time horizon)

© T. Hori, Kyoto University

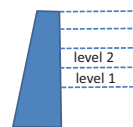
Discretization in time and volume

From actual viewpoint, release cannot be changed continuously in time

Discrete time system is introduced



Hydrologic variables such as storage, inflow, release are also discretized in level expression



© T. Hori, Kyoto University

The most fundamental case

The case where values of inflow discharge sequence Q_i ($i=1, \dots, I$) is known (given).

- Design operation
- Inflow values (levels) are explicitly given
-> Deterministic
- Single reservoir system

➡ Deterministic Dynamic Programming Operation (referred as DDP hereafter)

© T. Hori, Kyoto University

Deterministic DP operation

Problem Formulation

$$\max_{R_i} \left[\sum_{i=1}^I J(R_i, \frac{S_i + S_{i+1}}{2}) \right]$$

subject to

$$S_{i+1} = S_i + Q_i - R_i$$

$$0 \leq R_i \leq R_{\max}$$

$$S_{\min} \leq S_i \leq S_{\max}$$

$$(i = 1, \dots, I)$$

where

Q_i and R_i : inflow and release at step i , S_i : storage at the beginning of step i

$J(\bullet, \bullet)$: assessment function

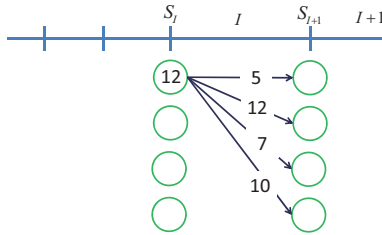
R_{\max} : upper limit of release, S_{\min} and S_{\max} : lower and upper limit of storage.

© T. Hori, Kyoto University

Deterministic DP operation

$$\max_{R_i} \left[\sum_{i=1}^I J(R_i, \frac{S_i + S_{i+1}}{2}) \right]$$

$$= \max_{R_i} \left[\sum_{i=1}^{I-1} J(R_i, \frac{S_i + S_{i+1}}{2}) + J(R_I, S_I + \frac{Q_I - R_I}{2}) \right]$$

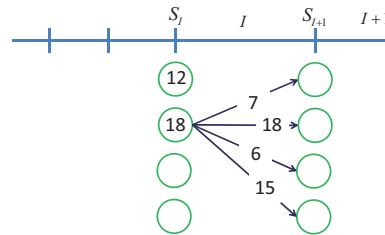


© T. Hori, Kyoto University

Deterministic DP operation

$$\max_{R_i} \left[\sum_{i=1}^I J(R_i, \frac{S_i + S_{i+1}}{2}) \right]$$

$$= \max_{R_i} \left[\sum_{i=1}^{I-1} J(R_i, \frac{S_i + S_{i+1}}{2}) + J(R_I, S_I + \frac{Q_I - R_I}{2}) \right]$$



© T. Hori, Kyoto University

Deterministic DP operation

$$\max_{R_i} \left[\sum_{i=1}^{I-1} J(R_i, \frac{S_i + S_{i+1}}{2}) + J(R_I, S_I + \frac{Q_I - R_I}{2}) \right]$$

$$= \max_{R_i} \left[\sum_{i=1}^{I-1} J(R_i, \frac{S_i + S_{i+1}}{2}) + \max_{R_I} \left[J(R_I, S_I + \frac{Q_I - R_I}{2}) \right] \right]$$

$$= \max_{R_i} \left[\sum_{i=1}^{I-1} J(R_i, \frac{S_i + S_{i+1}}{2}) + f_I(S_I) \right]$$

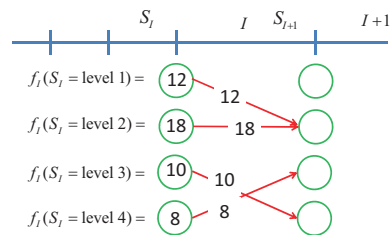
where

$$f_I(S_I) = \max_{R_I} \left[J(R_I, S_I + \frac{Q_I - R_I}{2}) \right]$$

© T. Hori, Kyoto University

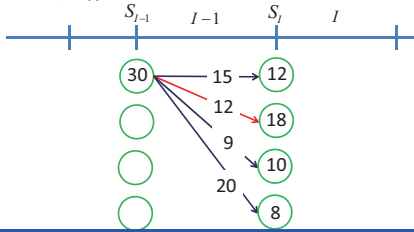
Deterministic DP operation

$$f_I(S_I) = \max_{R_I} \left[J(R_I, S_I + \frac{Q_I - R_I}{2}) \right]$$



© T. Hori, Kyoto University

$$\begin{aligned} & \max_{R_i} \left[\sum_{i=1}^I J(R_i, \frac{S_i + S_{i+1}}{2}) \right] \\ &= \max_{R_i} \left[\sum_{i=1}^{I-2} J(R_i, \frac{S_i + S_{i+1}}{2}) + \right. \\ & \quad \left. + \max_{R_{I-1}} \left\{ J(R_{I-1}, S_{I-1} + \frac{Q_{I-1} - R_{I-1}}{2}) + f_I(S_{I-1} + Q_{I-1} - R_{I-1}) \right\} \right] \end{aligned}$$



© T. Hori, Kyoto University

Defining

$$f_{I-1}(S_{I-1}) = \max_{R_{I-1}} \left\{ J(R_{I-1}, S_{I-1} + \frac{Q_{I-1} - R_{I-1}}{2}) + f_I(S_{I-1} + Q_{I-1} - R_{I-1}) \right\}$$

produces

$$\begin{aligned} & \max_{R_i} \left[\sum_{i=1}^I J(R_i, \frac{S_i + S_{i+1}}{2}) \right] \\ &= \max_{R_i} \left[\sum_{i=1}^{I-3} J(R_i, \frac{S_i + S_{i+1}}{2}) + \right. \\ & \quad \left. + \max_{R_{I-2}} \left\{ J(R_{I-2}, S_{I-2} + \frac{Q_{I-2} - R_{I-2}}{2}) + f_{I-1}(S_{I-2} + Q_{I-2} - R_{I-2}) \right\} \right] \end{aligned}$$

© T. Hori, Kyoto University

Recursive functions derived

$$f_{I-i}(S_{I-i}) = \max_{R_{I-i}} \left\{ J(R_{I-i}, S_{I-i} + \frac{Q_{I-i} - R_{I-i}}{2}) + f_{I-i+1}(S_{I-i} + Q_{I-i} - R_{I-i}) \right\}$$

for $i = 0, \dots, I-1$

$$f_{I+1}(S_{I+1}) = 0.$$

Applying the recursive function backward from the end period to the beginning one gives the optimal release as the function of storage levels at the beginning of each period.

© T. Hori, Kyoto University

Consideration of uncertainty

In the Deterministic DP model, values of inflow level are given. Actually the inflow level differs year by year even in the same day in the year.



Stochastic approach is required.



Inflow level in each period is not independent: High correlation between inflow levels at neighboring time periods is usually observed.

© T. Hori, Kyoto University

One-order Markov Chain

Conditional probability of inflow levels during time period i , Q_i , for the levels of inflow in the previous period, Q_{i-1} .

$$\begin{aligned} & \Pr[Q_i | Q_{i-1}] \\ &= \begin{pmatrix} \Pr[Q_i = 1 | Q_{i-1} = 1] & \Pr[Q_i = 2 | Q_{i-1} = 1] & \Pr[Q_i = 3 | Q_{i-1} = 1] \\ \Pr[Q_i = 1 | Q_{i-1} = 2] & \Pr[Q_i = 2 | Q_{i-1} = 2] & \Pr[Q_i = 3 | Q_{i-1} = 2] \\ \Pr[Q_i = 1 | Q_{i-1} = 3] & \Pr[Q_i = 2 | Q_{i-1} = 3] & \Pr[Q_i = 3 | Q_{i-1} = 3] \end{pmatrix} \\ &= \begin{pmatrix} 0.6 & 0.3 & 0.1 \\ 0.3 & 0.5 & 0.2 \\ 0.3 & 0.3 & 0.4 \end{pmatrix} \end{aligned}$$

© T. Hori, Kyoto University

One-order Markov Chain

$$\Pr[Q_i | Q_{i-1}] = \begin{pmatrix} 0.6 & 0.3 & 0.1 \\ 0.3 & 0.5 & 0.2 \\ 0.3 & 0.3 & 0.4 \end{pmatrix}$$

$$\text{If the probability distribution of } Q_{i-1} \text{ is given as } \Pr[Q_{i-1}] = \begin{pmatrix} 0.3 \\ 0.5 \\ 0.2 \end{pmatrix}^T$$

you can get the probability distribution of Q_i as follows

$$\Pr[Q_i] = \Pr[Q_{i-1}] \cdot \Pr[Q_i | Q_{i-1}] = (0.3 \ 0.5 \ 0.2) \cdot \begin{pmatrix} 0.6 & 0.3 & 0.1 \\ 0.3 & 0.5 & 0.2 \\ 0.3 & 0.3 & 0.4 \end{pmatrix}$$

$$= \begin{pmatrix} 0.3 \times 0.6 + 0.5 \times 0.3 + 0.2 \times 0.3 \\ 0.3 \times 0.3 + 0.5 \times 0.5 + 0.2 \times 0.3 \\ 0.3 \times 0.1 + 0.5 \times 0.2 + 0.2 \times 0.4 \end{pmatrix}^T$$

© T. Hori, Kyoto University

One-order Markov Chain

Once you have observed that the inflow discharge at the previous time period, Q_{t-1} , is level 2, then you can obtain the probability distribution of inflow at current time stage as:

$$\Pr[Q_{t-1} | Q_{t-1} = \text{level 1}] = (0.3 \quad 0.5 \quad 0.2).$$

Note that if you specify the release discharge at level 2 when the storage level at the beginning of period i is level 2, the storage level at the beginning of period $i+1$ cannot be specified uniquely. We can get instead the probability distribution of S_{i+1} as:

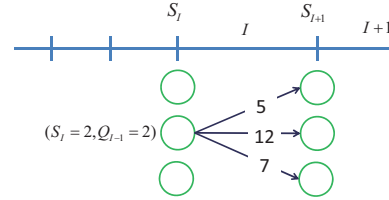
$$\Pr[S_{i+1}] = \begin{cases} 0.3 & (\text{for } S_{i+1} = 2 + 1 - 2 = 1) \\ 0.5 & (\text{for } S_{i+1} = 2 + 2 - 2 = 2) \\ 0.2 & (\text{for } S_{i+1} = 2 + 3 - 2 = 3) \end{cases}$$

© T. Hori, Kyoto University

Stochastic Dynamic Programming

Then the expected benefit when you select release discharge during period i as level 1 in case the inflow level has been observed as level 2 will be given by

$$5 \times 0.3 + 12 \times 0.5 + 7 \times 0.2 = 8.9.$$



© T. Hori, Kyoto University

Stochastic Dynamic Programming

$$f_{I-i}(S_{I-i}, Q_{I-i-1}) = \max_{\substack{R_{I-i} \\ \text{for given } S_{I-i}, Q_{I-i-1}}} \left\{ \sum_{Q_{I-i}=1}^K \Pr[Q_{I-i} | Q_{I-i-1}] \cdot \left(J(R_{I-i}, S_{I-i} + \frac{Q_{I-i} - R_{I-i}}{2}) + f_{I-i+1}(S_{I-i} + Q_{I-i} - R_{I-i}) \right) \right\}$$

for $i = 0, \dots, I-1$

© T. Hori, Kyoto University

Summary

- There are two types of operational approach: namely design operation and real time operation according to the inflow information.
- The most fundamental approach to optimal reservoir operation is optimization by deterministic dynamic programming.
- Uncertainty is inherent in reservoir operation and one of the commonly used optimum control under the uncertainty is called stochastic dynamic programming, which employs the one-order Markov chain as the model of inflow variations.

© T. Hori, Kyoto University

Lecture 6: Optimum operation of reservoir systems

Daisuke NOHARA (*Assistant Professor, Water Resources Research Center, Disaster Prevention Research Institute, Kyoto University*)

Abstract:

Optimizing reservoir operation policies considering hydrological data is crucially important for effective management of reservoir systems for both the flood control and water use purposes. In this lecture, we will learn how to optimize reservoir operation by using optimization techniques such as dynamic programming (DP). The lecture will consist of two parts.

The first part aims at learning a general procedure of calculation to optimize reservoir operation by DP techniques with a simple example problem. A simplified single multi-purpose reservoir is employed here, and reservoir operation for water supply is optimized by use of deterministic DP approach. We will learn the typical backward algorithm to estimate optimized release policies of the reservoir.

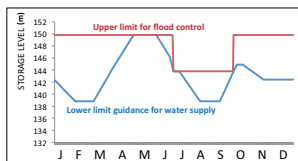
In the second part of the lecture, we will tackle to practical optimization problems considering a simplified multi-purpose reservoir, which hydrological and reservoir data are derived from an existing reservoir system in Japan. The example problems will deal with optimization of the reservoir operation for water supply by use of deterministic DP and stochastic DP models. Through tackling the problems, it will be introduced what we must prepare to set up the calculation for optimization of reservoir operation, including: choosing numbers of levels to discretize time step and states of the reservoir; setting objective functions according to the objective to optimize the reservoir; setting constraints for storage volume or release water defined by the physical constraints or regulations; preparation of hydrological data and target release of the target reservoir; and setting the time horizon to optimize the water release strategy. The optimization of operation of the target reservoir will be computed and be demonstrated with a computer program developed for DP-based optimization of reservoir operations.

Lecture 6: OPTIMUM OPERATION OF RESERVOIR SYSTEMS

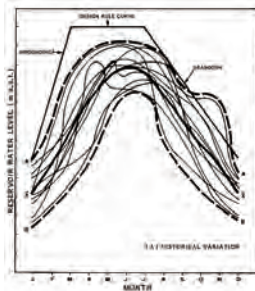
Daisuke NOHARA
Water Resources Research Center
Disaster Prevention Research Institute
Kyoto University

CONVENTIONAL RESERVOIR OPERATION METHOD

- Rule curve approaches
- Based on historical hydrological data
- Used for design of seasonal operation
- Can be categorized to offline operation



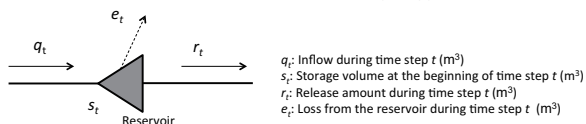
Example of rule curve (Kamafusa Reservoir)



Source: FAO (<http://www.fao.org/docrep/005/ac675e/ac675e05.htm>)

MATHEMATICAL EXPRESSION OF RESERVOIR OPERATION

State variables of a reservoir when discrete time step is applied



Continuity equation of reservoir storage

$$S_{t+1} = S_t + q_t - r_t - e_t$$

where

$$R_{\min} \leq r_t \leq R_{\max}, \quad S_{\min} \leq S_{t+1} \leq S_{\max}$$

FUNCTIONS OF A RESERVOIR

- Flood control
- Water supply (water resources development)
- Maintenance flow (including environmental flow)
- Hydropower generation
- Navigation
- Leisure

Most reservoirs are operated for more than two objectives (**multi-purpose reservoirs**), while some reservoirs are for single objective (**single purpose reservoirs**)

ALLOCATION OF RESERVOIR STORAGE

Storage capacity for each purpose is separately managed.

Advantages:

- Transparency: easy to understand for reservoir managers and public
- Designed based on hydrological statistic characteristics

Disadvantages:

- Less flexible to reflect recent conditions in the target river basin
- No consideration of real-time hydrological predictions



OBJECTIVE FUNCTION OF RESERVOIR OPERATION

Reservoir operation for disaster management

Minimization problem, where it minimizes damage or impact in the downstream due to floods or droughts

Ex) inundated area, maximal river discharge or water level, gap between water demand and supply

Reservoir operation for water supply or power generation, etc

Maximization problem, where it maximizes benefit through water supply, power generation, navigation or environmental flow

Ex) amount of supplied water, generated power, minimum level of river flow

In most cases, evaluation function can conceptually be represented as a function of **release discharge** and **storage** for both minimization or maximization problem:

$$J\left(r_t, \frac{S_t + S_{t+1}}{2}\right)$$

OBJECTIVE FUNCTION OF RESERVOIR OPERATION

When considering a maximizing problem with a single objective,

$$\max_{r_i} \sum_{t=1}^T J(r_t, \frac{S_t + S_{t+1}}{2})$$

subject to

$$S_{t+1} = S_t + q_t - r_t - e_t$$

$$R_{\min} \leq r_t \leq R_{\max}$$

$$S_{\min} \leq S_t \leq S_{\max}$$

OPTIMIZATION METHODS

- Linear programming
- Nonlinear programming
- **Dynamic programming**
- Goal programming
 - For multi-objective problems
- Heuristic approaches (e.g. genetic algorithm)
 - For multi-objective problems

DYNAMIC PROGRAMMING APPROACH

Optimization of reservoir operations based on dynamic programming (DP) approaches

- ❑ Richard Bellman's Principle of Optimality:
 - Original problem can be divided into a set of sub problems which need less computational effort to solve
- ❑ Suitable for reservoir operation simulation, which is multi-stage decision making process
- ❑ Applicable to any problem including nonlinear problems which have non-linear objective functions such as damage functions
- ❑ Compatible to computer-based solving

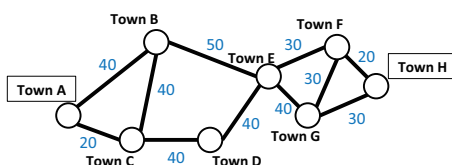
RICHARD BELLMAN'S PRINCIPLE OF OPTIMALITY

An optimal policy has the property that whatever the initial state and initial decision are, the remaining decisions must constitute an optimal policy with regard to the state resulting from the first decision.

PRINCIPLE OF OPTIMALITY - CONCEPT

Shortest path problem

Minimize time (minutes) to reach Town H from Town A

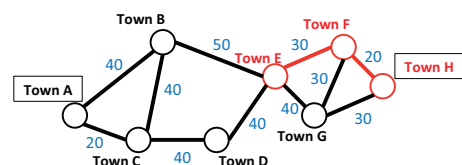


Original problem can be divided into a set of sub problems

PRINCIPLE OF OPTIMALITY - CONCEPT

Shortest path problem

Minimize time (minutes) to reach Town H from Town A



If you have already known the shortest path from Town E to Town H, then you DO NOT HAVE TO seek again the shortest path from Town E when you try to find the shortest path from Town A through Town H !

INTRODUCTION

Optimization of reservoir operations based on dynamic programming (DP) approaches

- ❑ Richard Bellman's Principle of Optimality:
 - Original problem can be divided into a set of sub problems which need less computational effort to solve
- ❑ Suitable for reservoir operation simulation, which is sequential process
- ❑ Applicable to any problem including nonlinear problems which have non-linear objective functions such as damage functions
- ❑ Compatible to computer-based solving

MATHEMATICAL DESCRIPTION

Objective function (for a maximizing problem with a single objective)

$$\max_{r_t} \sum_{t=1}^T J \left(r_t, \frac{s_t + s_{t+1}}{2} \right)$$

subject to

$$s_{t+1} = s_t + q_t - r_t - e_t$$

$$R_{\min} \leq r_t \leq R_{\max}$$

$$S_{\min} \leq s_t \leq S_{\max}$$

Recursive equation

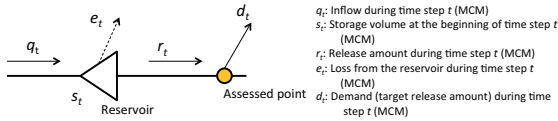
$$f_t(s_t) = \max_{r_t} \left[J \left(r_t, \frac{s_t + s_{t+1}}{2} \right) + f_{t+1}(s_{t+1}) \right] \quad (1 \leq t \leq T-1)$$

Value in the current time step Calculated backward!

Optimum value in the following time steps

SIMPLE EXAMPLE

Optimization of water supply operation of a single reservoir so as to minimize drought damage caused by deficit in water supply from the reservoir for three time steps



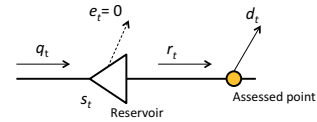
Physical constraints of the reservoir:

- $S_{\min} = 0, S_{\max} = 40$
- $R_{\min} = 0, R_{\max} = 40$

Matrix for Inflow / Target release (MCM):

	t=1	t=2	t=3
q_t	10	10	10
d_t	20	30	30

SIMPLE EXAMPLE



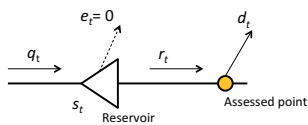
Assumptions to simplify the problem:

- No consideration of losses from the reservoir [i.e. $e_t = 0$]
- The assessed point locates just downstream the reservoir [i.e. r_t is identical to flow amount at the assessed point]

Other settings:

- Drought damage function:
 $H(r_t) = \{\max[d_t - r_t, 0]\}^2$
- Discretizing states into five levels considered for s_t , q_t and r_t with increment of 10 (MCM) from 0 to 40.

SIMPLE EXAMPLE



Objective function:

$$\min_{r_t} \sum_{t=1}^3 H(r_t)$$

subject to:

- $S_{\min} = 0, S_{\max} = 40, S_{\min} \leq s_t \leq S_{\max}$
- $R_{\min} = 0, R_{\max} = 40, R_{\min} \leq r_t \leq R_{\max}$
- $s_{t+1} = s_t + q_t - r_t - e_t$

Recursive equation:

$$f(s_t) = \min_{r(t)} [H(r_t) + f(s_{t+1})]$$

$f(\cdot)$: Future damage function

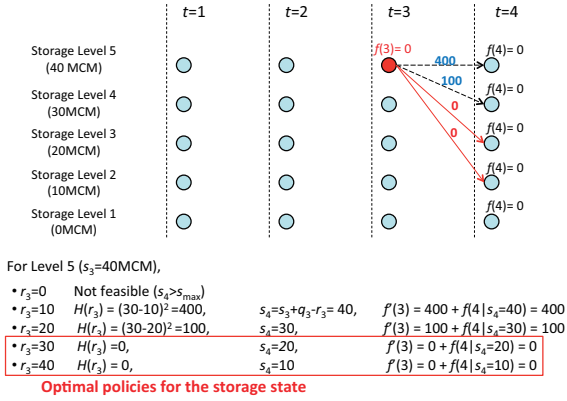
SIMPLE EXAMPLE

Calculation backward considering no damage after the last time step ($t \geq 4$)

	t=1	t=2	t=3	t=4
Storage Level 5 (40 MCM)	●	●	●	$f(4)=0$
Storage Level 4 (30 MCM)	●	●	●	$f(4)=0$
Storage Level 3 (20 MCM)	●	●	●	$f(4)=0$
Storage Level 2 (10 MCM)	●	●	●	$f(4)=0$
Storage Level 1 (0 MCM)	●	●	●	$f(4)=0$

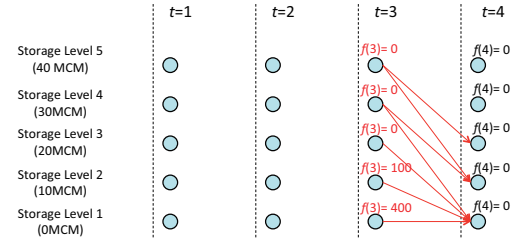
SIMPLE EXAMPLE

Calculation of $f(3)$ for each storage state s_3



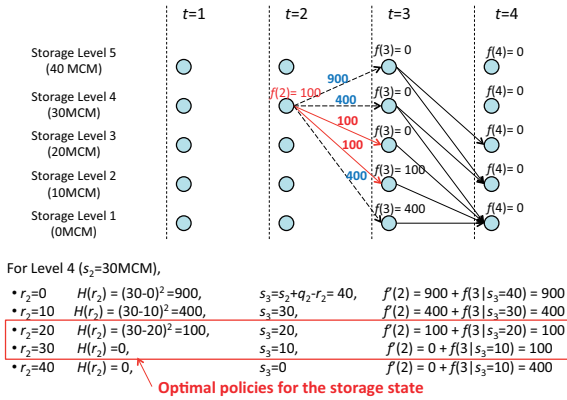
SIMPLE EXAMPLE

Calculation of $f(3)$ for each storage state s_3



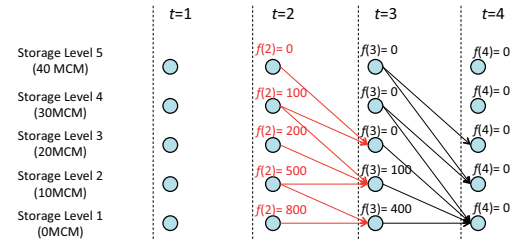
SIMPLE EXAMPLE

Calculation of $f(2)$ for each storage state s_2



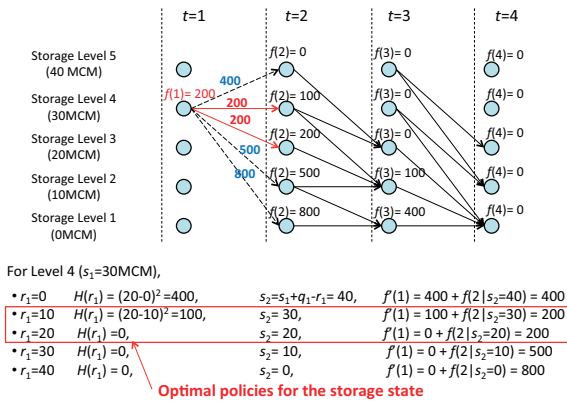
SIMPLE EXAMPLE

Calculation of $f(2)$ for each storage state s_2



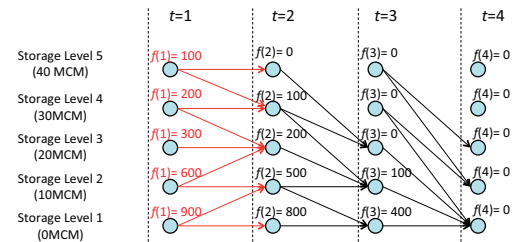
SIMPLE EXAMPLE

Calculation of $f(1)$ for each storage state s_2



SIMPLE EXAMPLE

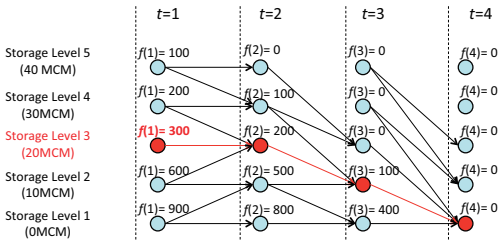
Calculation of $f(1)$ for each storage state s_2



SIMPLE EXAMPLE

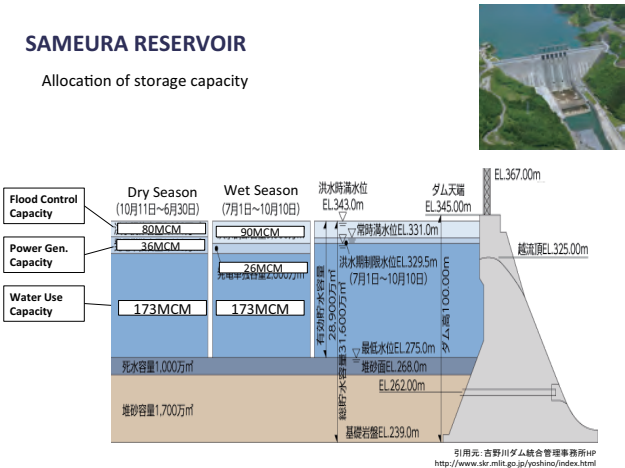
Getting optimal policies (decision and state trajectories) for each storage level at each time step

If you want to know the optimal release policy for storage level 3 at time step 1...



SAMEURA RESERVOIR

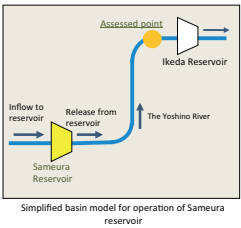
Allocation of storage capacity



EXERCISES

Exercise with the simplified Sameura Reservoir system

- Located in the Yoshino River basin, Shikoku Island, Japan
- A multipurpose reservoir for flood control, power generation and water supply
- Controlling seasonal variability in streamflow (not for inter-annual storage)

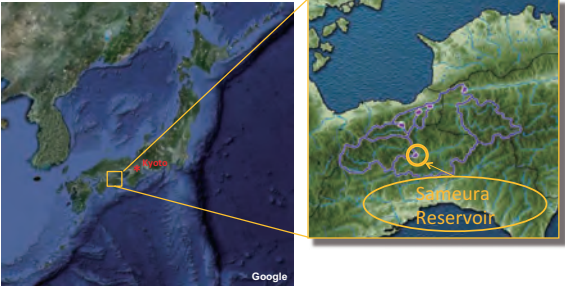


Purposes	Storage capacity	
	Dry season (Oct. 11 th - Jun. 30 th)	Wet season (Jul. 1 st - Oct. 10 th)
Water supply	173 MCM	173 MCM
Flood control	80 MCM	90 MCM
Power gen.	36 MCM	26 MCM

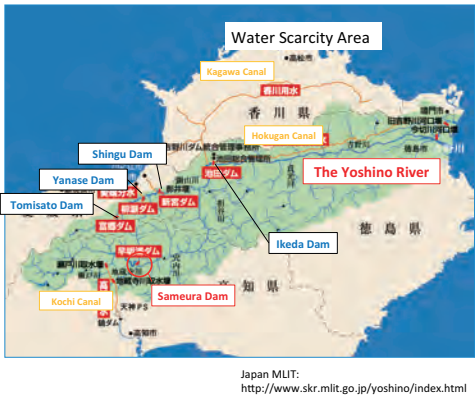
EXERCISES WITH ACTUAL RIVER BASIN

Sameura Reservoir system

- Located in the Yoshino River basin, Shikoku Island, Japan
- A multipurpose reservoir for flood control, power generation and water supply managed by Japan Water Agency
- Controlling seasonal variability in streamflow (not for inter-annual storage)



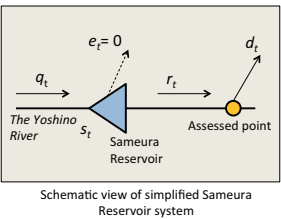
YOSHINO RIVER BASIN



EXERCISES

Exercise with the simplified Sameura Reservoir system

- Located in the Yoshino River basin, Shikoku Island, Japan
- A multipurpose reservoir for flood control, power generation and water supply
- Controlling seasonal variability in streamflow (not for inter-annual storage)



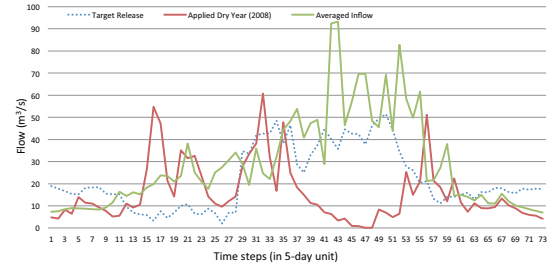
Purposes	Storage capacity	
	Dry season (Oct. 11 th - Jun. 30 th)	Wet season (Jul. 1 st - Oct. 10 th)
Water supply	173 MCM	173 MCM
Flood control	80 MCM	90 MCM
Power gen.	36 MCM	26 MCM

EXAMPLE 1: OPTIMIZATION FOR WATER SUPPLY (1)

- Optimize water release strategy from a single reservoir for each storage state at each time step **considering the historical streamflow regime in a dry year**
- Consider only water supply operation with the storage capacity for that purpose (173 MCM)
- Off-line optimization (not online optimization)
- Optimize with **deterministic DP (DDP)** for one year from January to December

FLOW REGIME AND TARGET RELEASE

Flow regime in the applied dry year (2008) and assumed water demand just downstream Sameura Reservoir (assumed target release of Sameura Reservoir)



SETTING UP OPTIMIZATION PROBLEM

Objective function

$$\min_{r_i} \sum_{t=1}^T H(r_t)$$

subject to:

- $S_{\min} \leq S_t \leq S_{\max}$
- $R_{\min} \leq r_t \leq R_{\max}$
- $S_{t+1} = S_t + Q_t - r_t - \theta_t$

Recursive equation:

$$f(s_t) = \min_{r_t} [H(r_t) + f(s_{t+1})]$$

Drought damage function:

Employing the one proposed by Ikebuchi et al. (1990):

$$H(r_t) = \begin{cases} (d_t - r_t)^2 / d_t & (r_t < d_t) \\ 0 & (r_t \geq d_t) \end{cases}$$

SETTING PARAMETERS FOR SOLVING DP

Discretization of states and time steps

The number of discretized levels of states and time steps must carefully be chosen.

- Enough many to describe reservoir and hydrological states according to the objective of optimization
- But as small as possible to secure feasibility in computation

For this exercise (drought management):

- Time Step: 5-day unit (73 time steps in a year)
- Flow (inflow and release): 100 levels (4 m³/s for each level)
- Storage: 100 levels (1.73 MCM for each level)

Constraints:

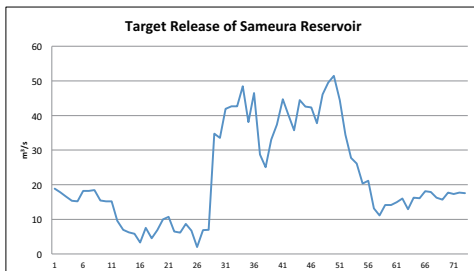
$$S_{\min} = 0, \quad S_{\max} = 173 \text{ MCM}$$

$$R_{\min} = 0, \quad R_{\max} = 400 \text{ m}^3/\text{s} (\approx 173 \text{ MCM for 5 days})$$

Other assumptions:

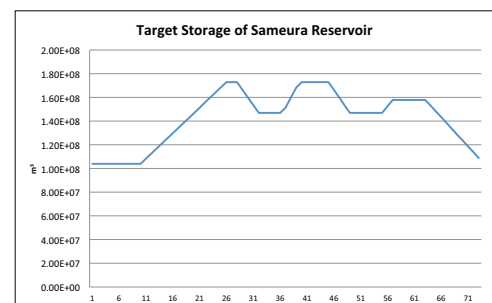
$$e_t = 0 \quad (\text{No loss from the reservoir considered})$$

ASSUMED TARGET RELEASE OF SAMEURA RESERVOIR



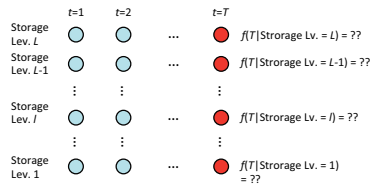
Much amount enough to secure water demand downstream in the drought event which can occur once in 5 years

TARGET STORAGE OF SAMEURA RESERVOIR



SETTING PARAMETERS FOR SOLVING DP

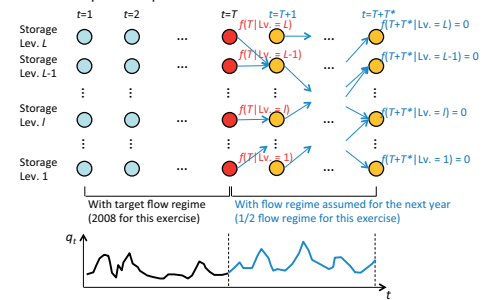
Future damage function at the last time step of optimization
Necessary to define for backward calculation of $f()$



SETTING PARAMETERS FOR SOLVING DP

Future damage function at the last time step of optimization

- Estimating by optimizing water release for a period (e.g. until end of the next year)
- Adding penalty to small storage levels which can admit drought after the final time step of the optimization



OPTIMIZATION RESULTS

Optimal release policies

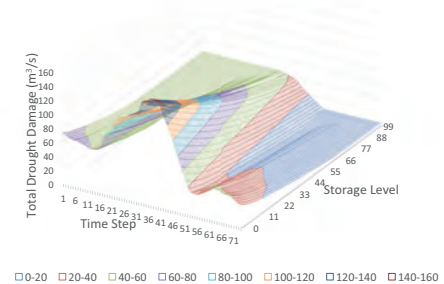
Time Step	1	2	3	4	5	6	7	8	9	10	11	12	13	14	15	16	17	18	19	20	21	22	23	24	25	26	27	28	29	30
Storage Lev.0	1	1	1	1	1	1	1	1	1	1	1	1	1	1	1	1	1	1	1	1	1	1	1	1	1	1	1	1	1	1
Storage Lev.1	1	1	1	1	1	1	1	1	1	1	1	1	1	1	1	1	1	1	1	1	1	1	1	1	1	1	1	1	1	1
Storage Lev.2	2	2	2	2	2	2	2	2	2	2	2	2	2	2	2	2	2	2	2	2	2	2	2	2	2	2	2	2	2	2
Storage Lev.3	2	2	2	2	2	2	2	2	2	2	2	2	2	2	2	2	2	2	2	2	2	2	2	2	2	2	2	2	2	2
Storage Lev.4	2	2	2	2	2	2	2	2	2	2	2	2	2	2	2	2	2	2	2	2	2	2	2	2	2	2	2	2	2	2
Storage Lev.5	2	2	2	2	2	2	2	2	2	2	2	2	2	2	2	2	2	2	2	2	2	2	2	2	2	2	2	2	2	2
Storage Lev.6	2	2	2	2	2	2	2	2	2	2	2	2	2	2	2	2	2	2	2	2	2	2	2	2	2	2	2	2	2	2
Storage Lev.7	2	2	2	2	2	2	2	2	2	2	2	2	2	2	2	2	2	2	2	2	2	2	2	2	2	2	2	2	2	2
Storage Lev.8	3	3	3	3	3	3	3	3	3	3	3	3	3	3	3	3	3	3	3	3	3	3	3	3	3	3	3	3	3	3
Storage Lev.9	2	3	3	2	2	3	3	3	2	2	2	1	1	1	1	1	1	1	1	1	1	1	1	1	1	1	1	1	1	1
Storage Lev.10	2	3	3	2	2	3	3	3	2	2	2	1	1	1	1	1	1	1	1	1	1	1	1	1	1	1	1	1	1	1
Storage Lev.11	3	3	3	2	2	3	3	3	2	2	2	1	1	1	1	1	1	1	1	1	1	1	1	1	1	1	1	1	1	1
Storage Lev.12	3	3	3	2	2	3	3	3	2	2	2	1	1	1	1	1	1	1	1	1	1	1	1	1	1	1	1	1	1	1
Storage Lev.13	3	3	3	2	2	3	3	3	2	2	2	1	1	1	1	1	1	1	1	1	1	1	1	1	1	1	1	1	1	1
Storage Lev.14	3	3	3	2	2	3	3	3	2	2	2	1	1	1	1	1	1	1	1	1	1	1	1	1	1	1	1	1	1	1
Storage Lev.15	3	3	3	2	2	3	3	3	2	2	2	1	1	1	1	1	1	1	1	1	1	1	1	1	1	1	1	1	1	1

- Matrix of optimal release levels for storage states (Levels 0 to 15 are shown in this chart) at each time step
- More release can be possible for better storage states (greater levels)
- Release must be decreased before the drought season³⁹

OPTIMIZATION RESULTS

Optimized values of reservoir operation

Minimized total drought damage expected after each time step

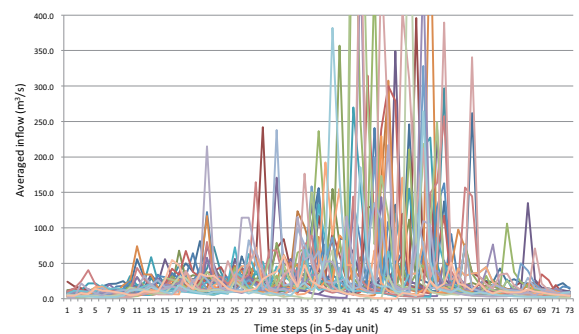


EXAMPLE 2: OPTIMIZATION FOR WATER SUPPLY (2)

- Optimize water release strategy from a single reservoir for each storage state at each time step **considering historical streamflow regimes observed for 30 years**
- Consider only water supply operation with the storage capacity for that purpose (173 MCM)
- Off-line optimization (not online optimization)
- Optimize with **stochastic DP (SDP)** for one year from January to December

HISTORICAL HYDROLOGICAL DATA

Inflow sequences observed for 30 years (1979-2008)



SETTING UP OPTIMIZATION PROBLEM FOR SDP

Objective function

$$\min_{r_i} \sum_{t=1}^T E[H(r_t, q_t)]$$

subject to:

- $S_{\min} \leq S_t \leq S_{\max}$
- $R_{\min} \leq r_t \leq R_{\max}$
- $S_{t+1} = S_t + q_t - r_t - e_t$

Recursive equation:

$$f(s_t) = \min_{r(t)} E\{H(r_t, q_t) + f_{t+1}(s_t)\}$$

(Neglecting persistence in streamflow)

Drought damage function:

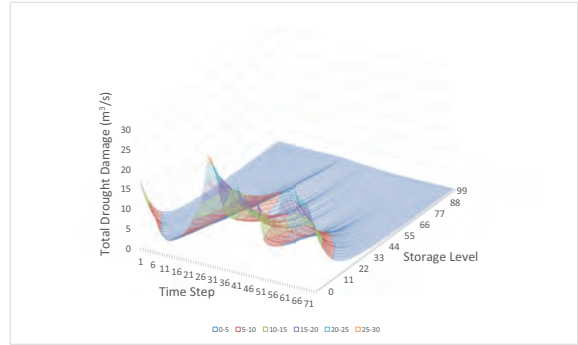
Same as the one employed in Example 1:

$$H(r_t) = \begin{cases} (d_t - r_t)^2 / d_t & (r_t < d_t) \\ 0 & (r_t \geq d_t) \end{cases}$$

OPTIMIZATION RESULTS

Optimized values of reservoir operation

Minimized total drought damage expected after each time step



FOR FURTHER DISCUSSIONS

The further discussions about DP based optimization of reservoir operation can be seen in the following references.

DP based optimization of reservoir operation

- Nandalal, K.D.W. and Bogardi, J.J. (2007): Dynamic programming based operation of reservoirs – Applicability and limits -, UNESCO, Cambridge University Press, 130pp, ISBN 978-0-521-87408-3.
- Loucks, D. and Van Beek, E. (2005): Water resources systems planning and management – An introduction to methods, models and applications, Studies and Reports in Hydrology, UNESCO Publishing, 680pp. (with contributions from J.R. Stedinger, J.P.M. Dijkman and M.T. Villars), ISBN 92-3-103998-9.

Application of DP models to optimize actual reservoir systems

- Kumar, D.N., Baliarsingh, F. and Raju, Srinivasa (2010): Optimal reservoir operation for flood control using folded dynamic programming, *Water Resources Management*, 24, 1045-1064.
- Faber, B.A. and Stedinger, J.R. (2001): Reservoir optimization using sampling SDP with ensemble streamflow prediction (ESP) forecasts. *Journal of Hydrology*, 249, 113-133.
- Turgeon, A. (1980): Optimal operation of multireservoir power systems with stochastic inflows, *Water Resources Research*, 16(2), 275-283.
- Tilmant, A. Vanclooster, M., Duckstein, L. and Persoons, E. (2002): Comparison of fuzzy and nonfuzzy optimal reservoir operation policies, *Journal of Water Resources Planning and Management*, 128(6), 390-398.

Lecture 7: Integrated sediment management for reservoir sustainability

Tetsuya SUMI (*Professor, Disaster Prevention Research Institute, Kyoto University*)

Abstract:

Reservoir sedimentation is one of the most crucial issues for reservoir sustainability in the world (ICOLD 2009). In many countries, various countermeasures have been implemented to reduce sediment accumulation and loss of storage capacity (Kondolf et al. 2014). Such measures include: (i) reducing sediment inflow, (ii) routing sediments and (iii) removing sediment. Among the latest methodologies, effective and ecofriendly sediment flushing, bypassing and replenishment techniques have been intensively developed in Japan. Even though the target volume of sediment differs greatly between these approaches, the positive effects should be examined in terms of both reservoir sustainability and downstream environmental improvement. The sediment yields of Japanese rivers are high due to the topographical, geological and hydrological conditions. This has caused sedimentation problems for many reservoirs constructed for water resource development or flood control. Accordingly, methods of estimating sediment volume and countermeasures for sedimentation have been studied for a long time. Currently, the management of reservoir sedimentation in Japan is entering a new stage from two points of view. First, in contrast to emerging and local conventional countermeasures such as dredging and excavation, sediment flushing using sediment flushing outlets and sediment bypass systems is being actively introduced with the aim of radically reducing the inflow and deposition of sediment. The Unazuki and Dashidaira dams on the Kurobe River, Miwa dam on the Tenryu River, Asahi dam on the Shingu River and the Mimikawa River are advanced examples of using sediment flushing, sediment bypassing and sluicing techniques as permanent measures for sedimentation at dams. Second, in consideration of the zones of sediment movement from mountains through to coastal areas, a comprehensive approach to restoring effective sediment transport in the sediment routing system is being initiated. However, these advanced techniques for managing sediment aimed at extending the life of dams have only been applied in a limited number of cases, and so further studies are required. It is also important to solve social issues, such as consensus-building among the people living in the basin on the need for sediment management, and the establishment of both legal and cost allocation systems. This lecture describes the latest situation of reservoir sedimentation management in Japan and the new paradigms.

ICOLD (2009) "Sedimentation and Sustainable Use of Reservoirs and River Systems," Bulletin 147, Basson, G. (ed).

Kondolf, G.M., Gao, Y., Annandale, G.W., Morris, G.L., Jiang, E., Zhang, J., Cao, Y., Carling, P., Fu, K., Guo, Q., Hotchkiss, R., Peteuil, P., Sumi, T., Wang, H-W., Wang, Z., Wei, Z., Wu, B., Wu, C., and Yang, C.T. (2014) "Sustainable sediment management in reservoirs and regulated rivers: Experiences from five continents," *Earth's Future*, 2, doi:10.1002/2013EF000184, pp. 256–280.



The 27th UNESCO - IHP Training Course on
Integrated Basin Management under Changing Climate,
Dec.4-Dec.15, 2017.



Integrated sediment management for reservoir sustainability

Tetsuya SUMI

Disaster Prevention Research Institute, Kyoto University



Flushing, Dashidaira dam



Sediment Replenishment, Nunome dam



Contents of the lecture

- **Concept of Reservoir Sustainability**
- **Japanese Regulation**
- **Methodologies of Reservoir Sedimentation Management**
- **Case Studies in Japan**



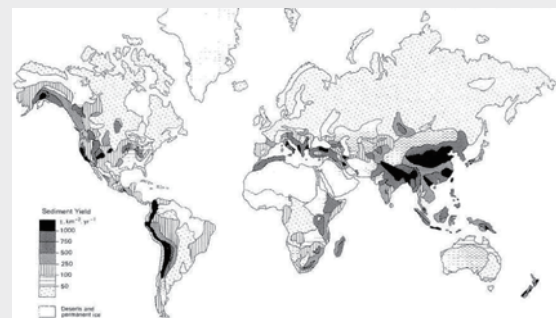
Worldwide distribution of dams



Data from the GRanD database © Global Water System Project, 2011



Sediment yield map of the world



Walling and Webb, 1983



Dam Impacts caused by reservoir sedimentation

- Dam construction dramatically influences the river basin balance for water / sediment inflow and outflow.

Dam Impacts

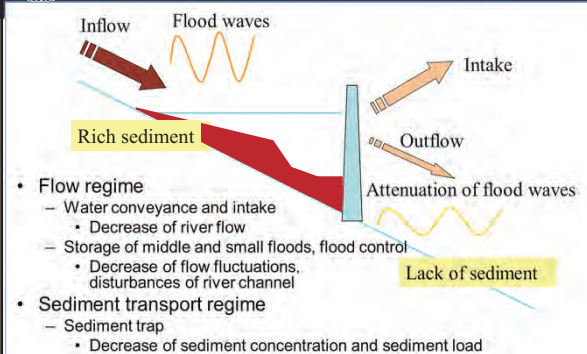
- **Discontinuity of sediment transport downstream**
- **Modification of flow regimes downstream**

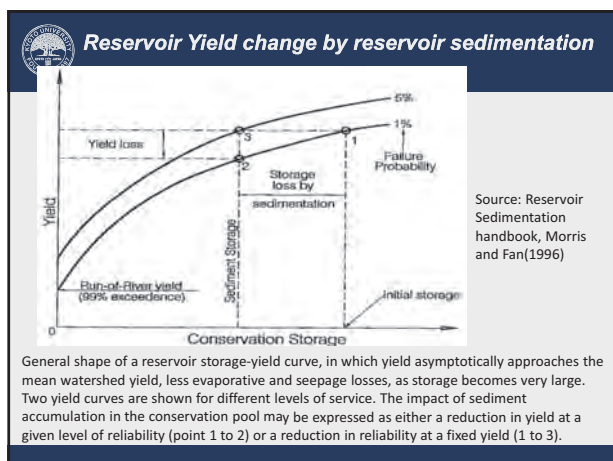
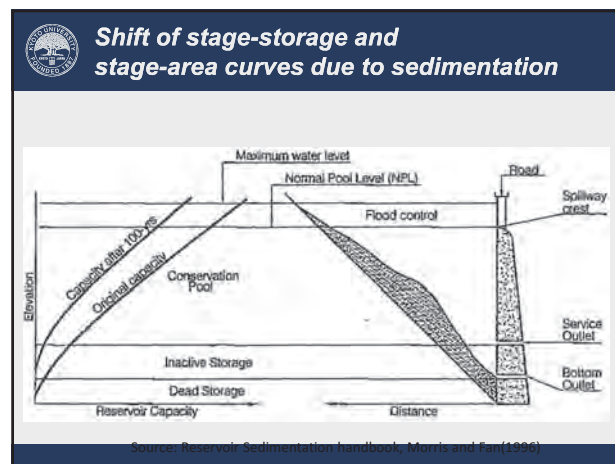
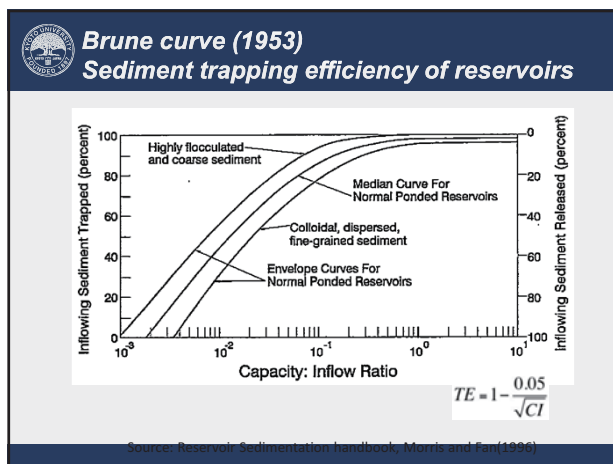
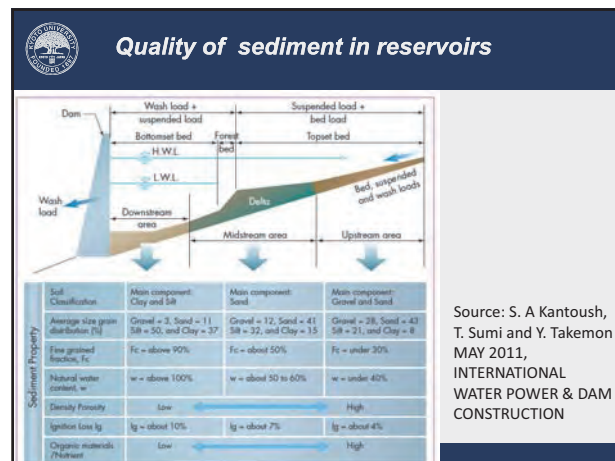
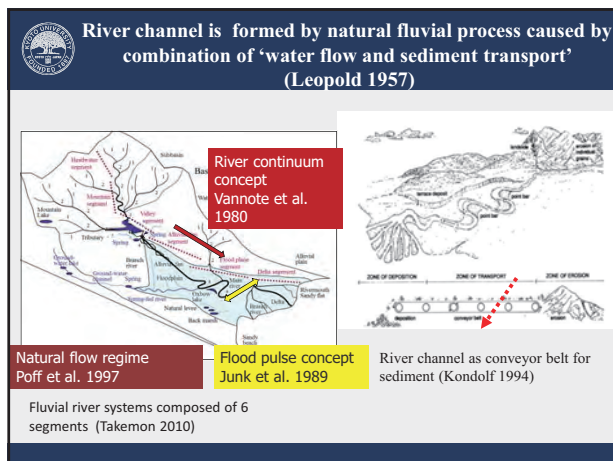
Sedimentation in reservoir

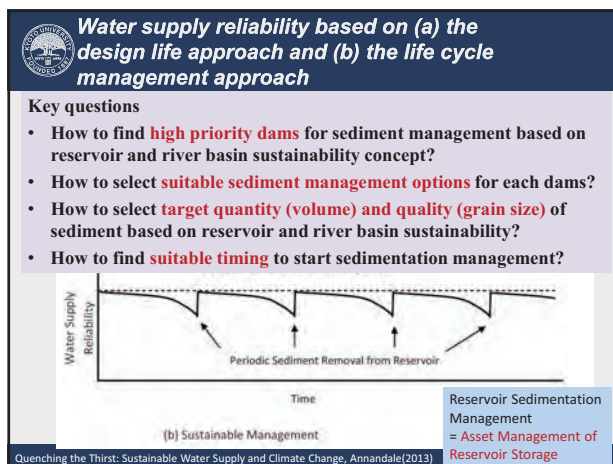
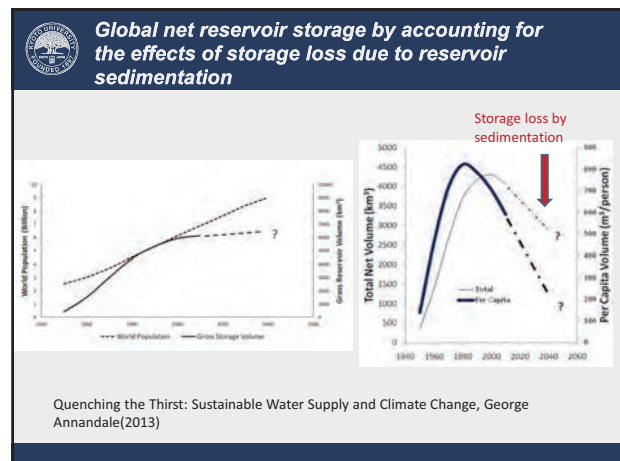
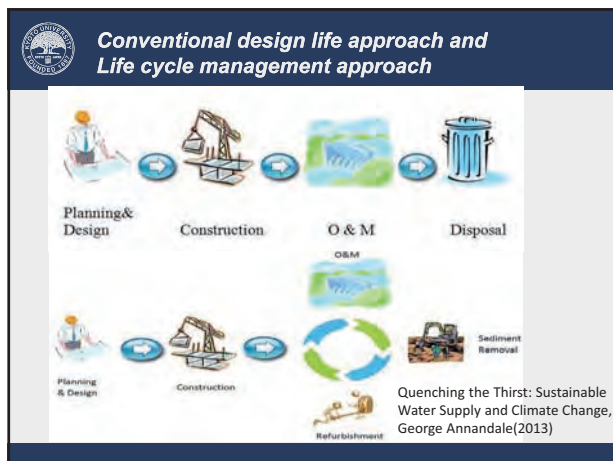
- Reduction of storage capacity
- Downstream geomorphology**
 - Bed armouring and degradation
- Downstream hydrology**
 - Water table lowering, changes in seasonal flow, flood frequency and magnitude
- Downstream ecosystem**
 - Reduced ecosystem health (Biodiversity, Quality and quantity of food resources, Water quality)



Change of flow and sediment transport regimes



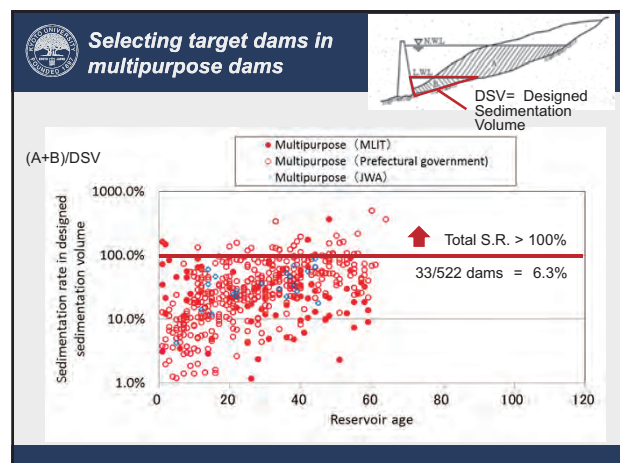
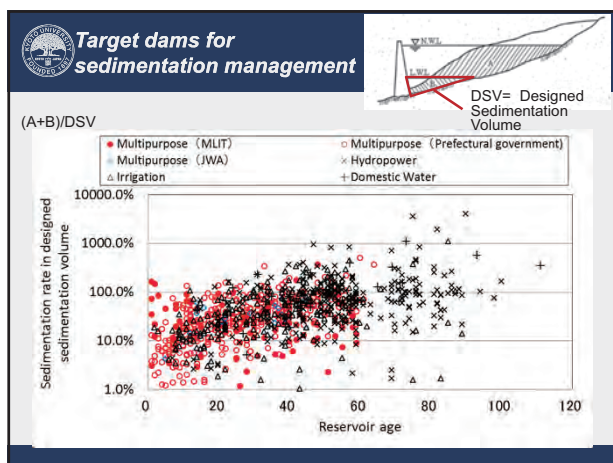
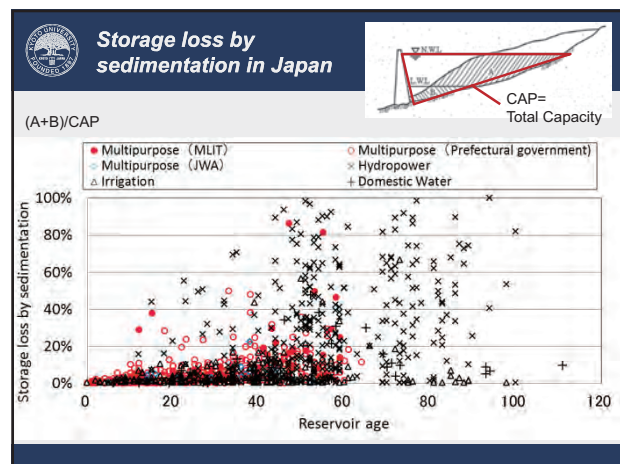
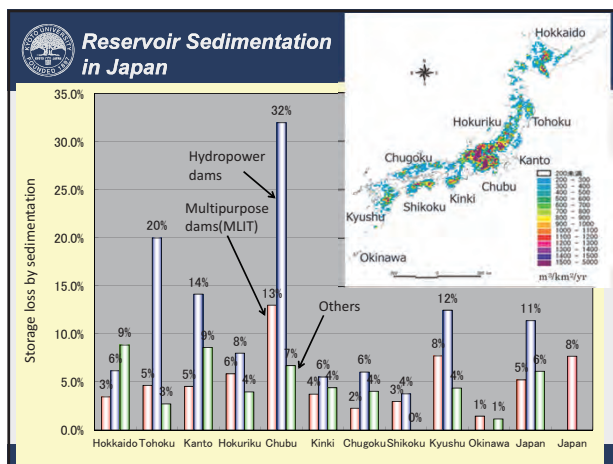
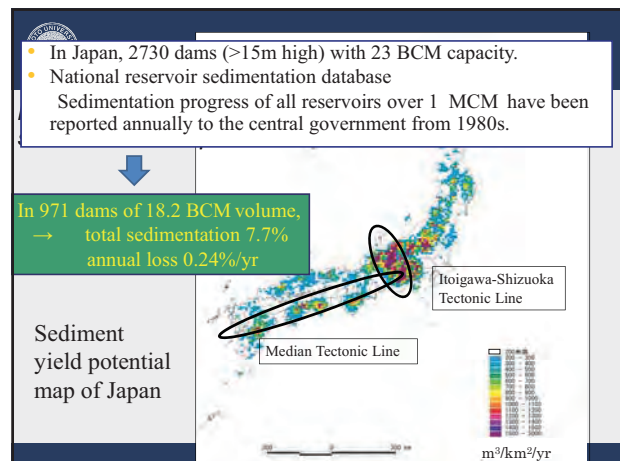
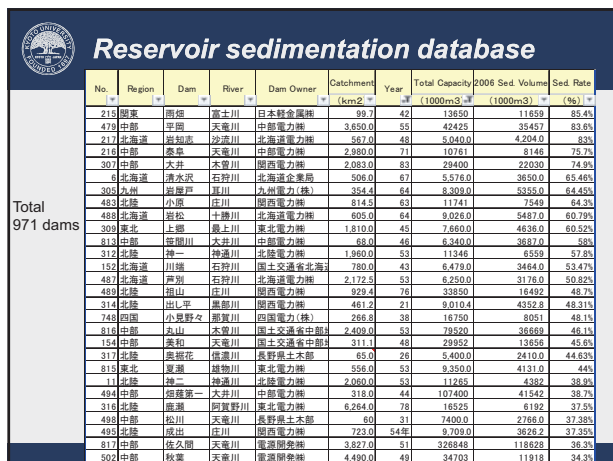


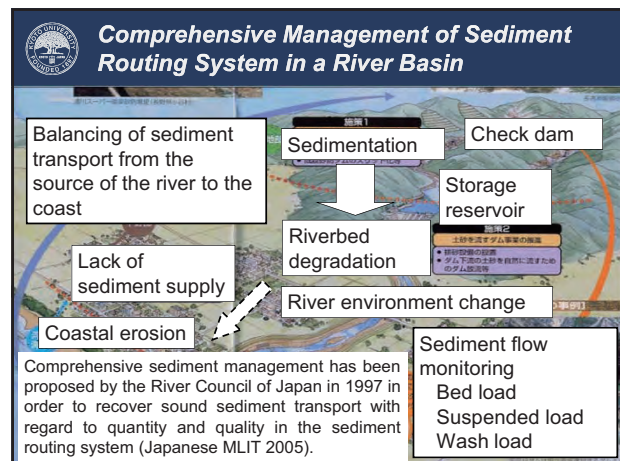
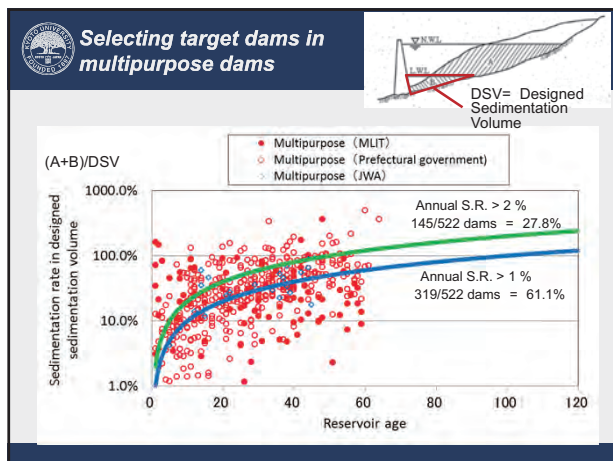


- Long term aspects for Reservoir and River Basin Sustainability**
- Storage loss by sedimentation**
 - Population growth**
 - Decrease of available storage per capita
 - Climate change impact on flow regime and sediment yield changes**
 - Accelerating storage loss
 - Modification of reservoir operation rule
 - Dam heightening or excavating sediment
 - Asset management**
 - Reservoir sedimentation management based on
 - appropriate evaluation of current conditions and future scenarios
 - technically-economically feasible, environmentally acceptable solutions
 - priority based approach
 - Integrated sediment management in sediment routing systems**
 - Deterioration of downstream river and coastal areas such as bed armoring, degradation and coastal erosions
 - Necessary sediment supply (sediment replenishment) for mitigation

- Contents of the lecture**
- Concept of Reservoir Sustainability**
 - Japanese Regulation**
 - Methodologies of Reservoir Sedimentation Management**
 - Case Studies in Japan**

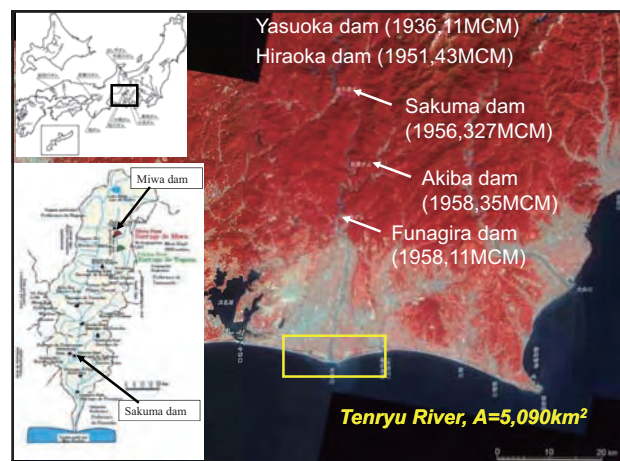
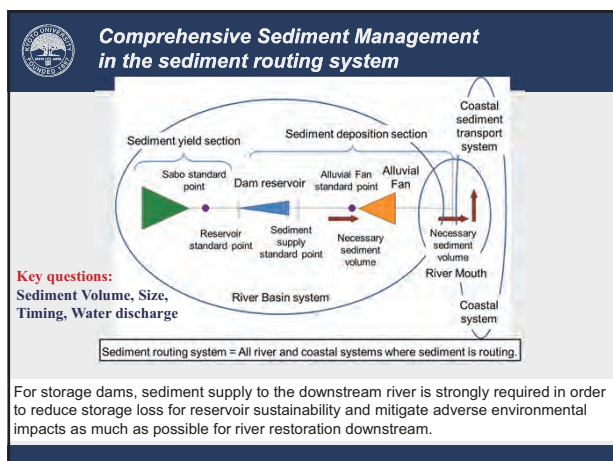
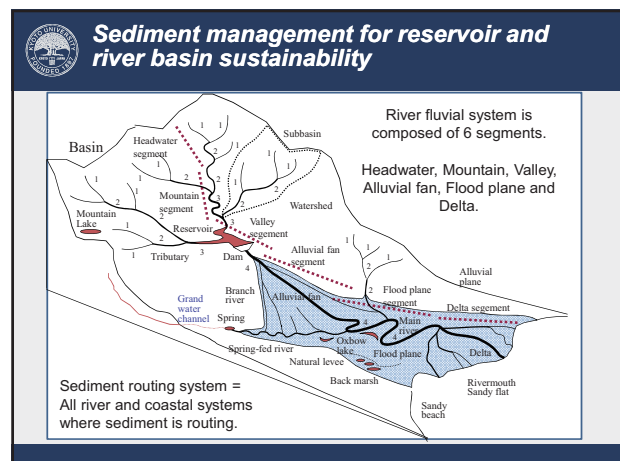
- History of guidelines on reservoir sedimentation design in Japan**
- 1958, Technical Criteria for River Works, Ministry of Construction**
 - Necessary volume for reservoir sedimentation is 100 years
 - 1966, Reservoir sedimentation database guideline, MOC**
 - To check riverbed aggradation in order to prevent flooding risks upstream of reservoirs caused by sedimentation
 - 1982, National reservoir sedimentation database, MOC**
 - All reservoirs over 1 MCM should report accumulated sedimentation volume of B, below LWL, and A, LWL to NWL, separately and sedimentation profile almost annually to MOC.
-
- In Japan, 2730 dams (>15m high) with 23 BCM capacity.
- Target dams : 971 dams of 18.2 BCM capacity

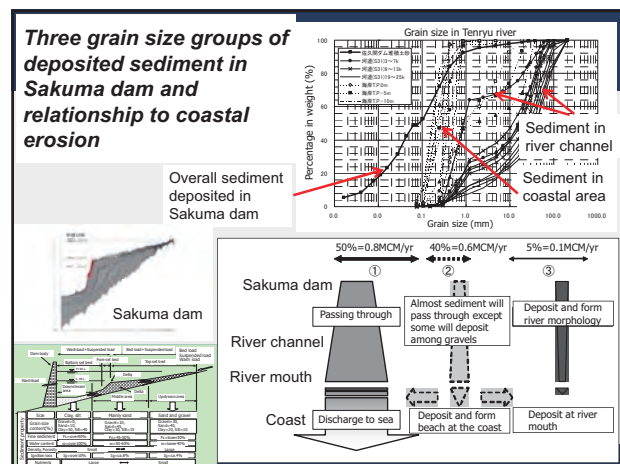
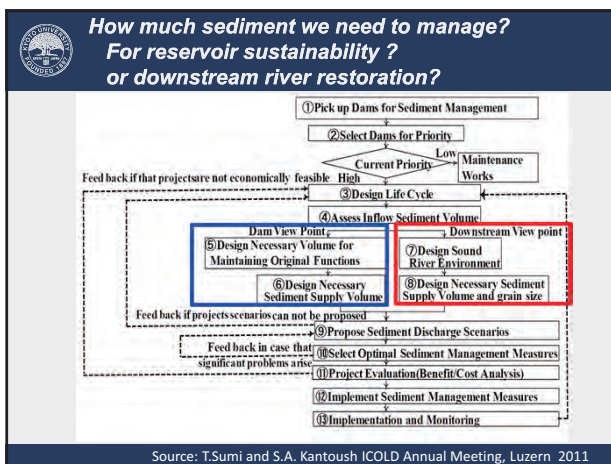
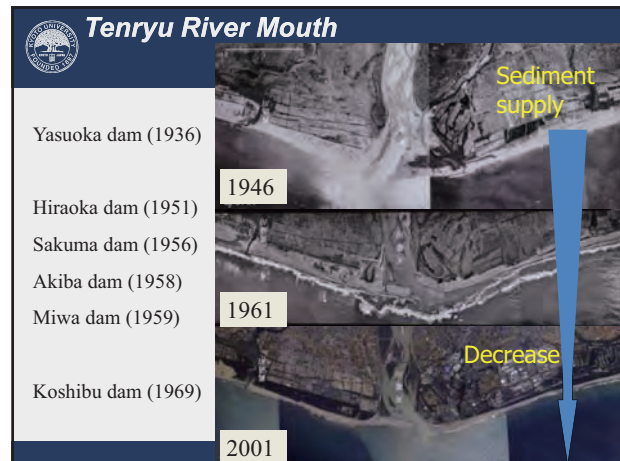
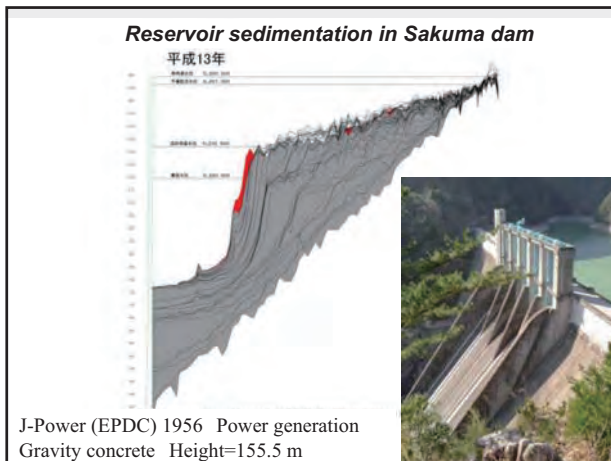




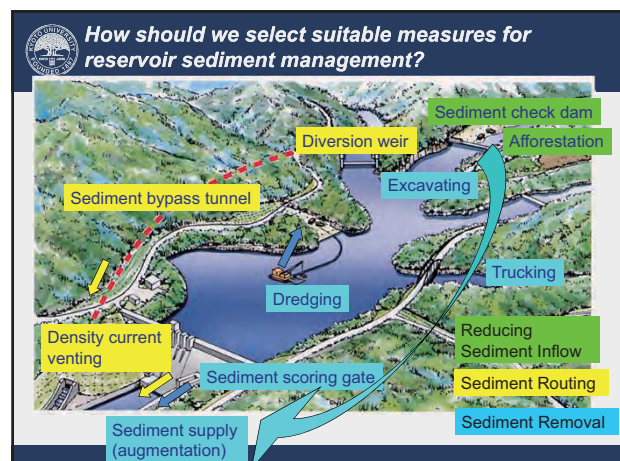
Environmental changes in downstream rivers

- River channel change
 - Fixed sand bars, degradation of water course
 - Degradation of river channel
 - Tree growth in river channels
- Riverbed material change
 - Armoring (granulation)
 - Decrease of small porosity





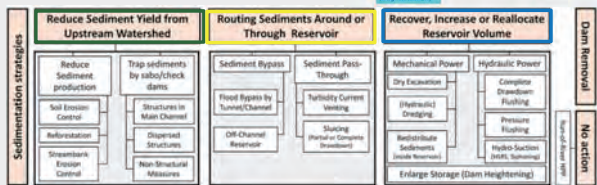
- Contents of the lecture**
- Concept of Reservoir Sustainability
 - Japanese Regulation
 - Methodologies of Reservoir Sedimentation Management
 - Case Studies in Japan





Classification of sediment management strategies (ICOLD Technical Committee)

Sediment management to minimize aggradation in reservoirs is achieved with a variety of techniques categorized in three main strategies (ICOLD 1989, 1999, 2009, Morris & Fan 1998, Kantoush & Sumi 2010, Annandale 2011, 2013, Kondolf et al. 2014, Auel et al. 2016).



Auel et al. 2016



Reduce Sediment Yield from Upstream Watershed

- The first strategy refers to a reduction in the sediment inflow into the reservoir, i.e. soil erosion control in the catchment area by reforestation and upstream sediment trapping by sabo dams (check dams).



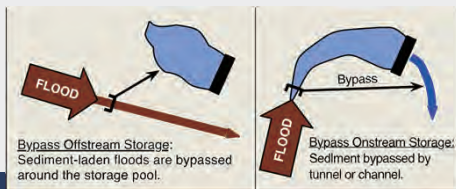
(Source: MLIT, Japan)

(Koshiu dam, Japan)



Routing Sediments around or through Reservoir

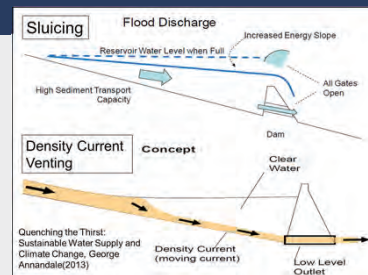
The second one deals with routing of sediments into the tailwater downstream of the dam. Within this strategy various effective techniques can be applied: direct bypassing around the dam using tunnels or channels, diverting to an off-channel reservoir, and passing sediments through the reservoir by either sluicing or turbidity current venting. Both techniques route incoming sediments to the tailwater without settling in the reservoir.



(Source: Morris)



Sluicing and Density Current Venting



- Sluicing requires a partial water level drawdown to transport incoming and to some extent accumulated sediments to the dam outlet structure, whereas venting of turbidity density currents can be performed without lowering.
- Sluicing includes both bedload and suspended sediment, whereas venting is only possible for the latter.



Recover, Increase or Reallocate Reservoir Volume

- The third strategy refer to increase the capacity by removing accumulated sediments or dam heightening to re-suspend or reallocate the deposited sediment.
- Strategies are either using mechanical or hydraulic power. The former implies dry excavation during complete water level drawdown, hydraulic dredging with pumps during high reservoir levels and redistribution of sediments inside the reservoir.
- Dry excavation and sediment flushing during complete water level drawdown have drawbacks as they result in a complete storage water loss. Furthermore, a complete drawdown is only reasonably applicable when the reservoir capacity is small compared to the annual inflow.
- One further removal technique is termed hydro-suction (siphoning) where sediments are pumped to a lower level using only the hydraulic head (HSRS). Advantages are low costs and no use of mechanical power.



Sediment Flushing

- Sediment flushing should be designed carefully. Disadvantage of flushing sediments is the high quantity of eroded material leading to immediate ecological impacts on the biota of the downstream river reach. Pools may be filled, sediment size distribution may change, and suspended sediment may clog the bed surface.
- Negative effects of flushing may be largely decreased if operated during a natural flood event. Also consecutive annual flushing is favourable as the sediments only accumulate during one year. In Japan, flushing of sediments is frequently applied in times of comparatively high reservoir inflow such as typically one-year floods.





Dam removal or change to run-of-river hydropower scheme

- Despite these strategies, a dam removal could be another option to restore the original river reach. However, all benefits provided by a reservoir as hydropower generation, water supply, and flood protection are thereby eliminated making this option literally not an adequate strategy against reservoir sedimentation as no reservoir remains.
- Finally, taking no action against reservoir sedimentation may be an option in case of reservoirs used for hydropower generation. The plant may operate as a daily reservoir or a run-of-river scheme.
- The Maigrauge dam in Switzerland, many older dams in Japan are operated as run-of-river hydropower schemes after prone to large sedimentation volumes. In these dams only dredging or local sediment flushing is implemented to clean up just upstream of the intake facilities.



Selecting a suitable sedimentation strategy

- In order to increase the number of suitable examples for reservoir sediment management, it is important to establish a guideline to select appropriate sediment management measures. ICOLD released the Bulletin 147 titled 'Sedimentation and Sustainable Use of Reservoirs and River Systems' in 2009. This Bulletin discusses the upstream and downstream fluvial morphological impacts of reservoir sedimentation, and emphasizes on the selection of sedimentation strategies.
- The two parameter reservoir life ($CAP/MAS = \text{Reservoir CAPacity} / \text{Mean Annual Sediment inflow}$) and water turnover rate ($CAP/MAR = \text{Reservoir CAPacity} / \text{Mean Annual Runoff}$) are used to classify suitable techniques (ICOLD 1999, 2009, Sumi 2008, Annandale, 2013).



Bulletin 147

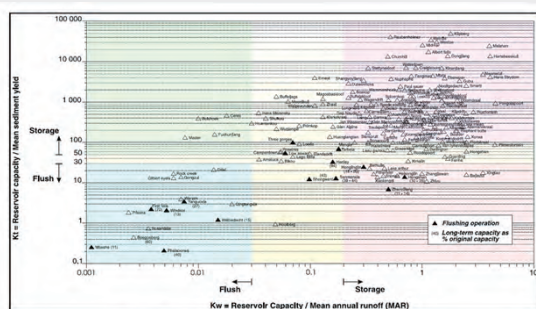


Figure 2.1-3 Dams with different modes of operation (Source: Basson)



Suitable conditions for each options

- Sluicing and flushing is recommended for low $CAP/MAR < 0.03$, and seasonal flushing (duration up to two months) for $CAP/MAR < 0.02$. For higher ratios only storage operation, and to some extent turbidity venting is supposed to be feasible due to water scarcity.
- Sumi (2008) analyzed Japanese dams based on this approach. With increasing CAP/MAR , strategies change from sediment flushing ($CAP/MAR < 0.04$), bypassing/sluicing ($0.01 < CAP/MAR < 0.3$), to check dams and excavating and dredging ($0.06 < CAP/MAR < 1$).
- Annandale (2013) has integrated these approaches with threshold for reservoir sustainability.
- The RESCON model (REservoir CONservation) which considers a life cycle approach and reservoir conservation is presented (Palmieri et al. 2003). This model by the World Bank is developed to guide suitable options based on the reservoir conditions.



Appropriate selection of reservoir sediment management strategy (Japanese Case Study)

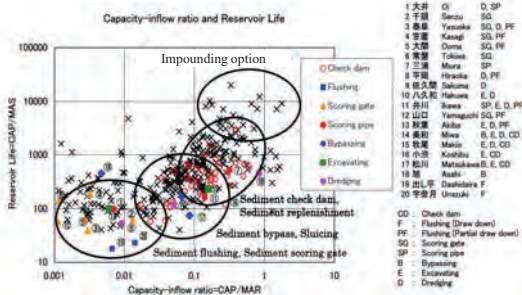
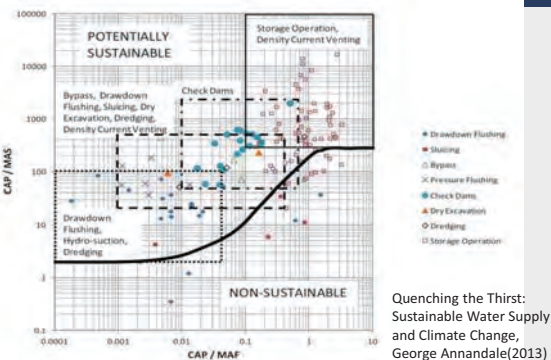


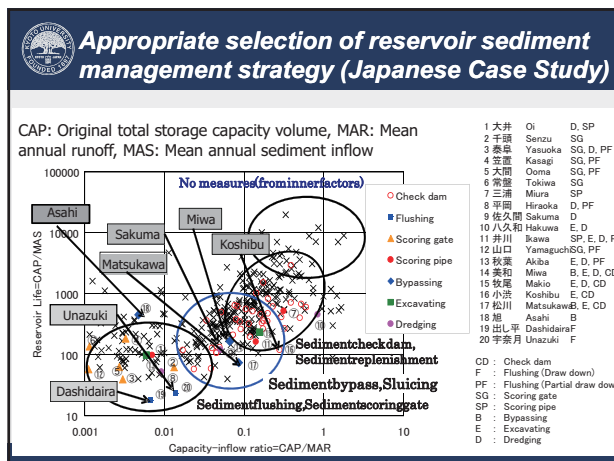
Fig. 1 Representative sediment control examples in Japan (Relationship between capacity-inflow ratio and reservoir life)



Reservoir sedimentation management approaches (Annandale 2013)



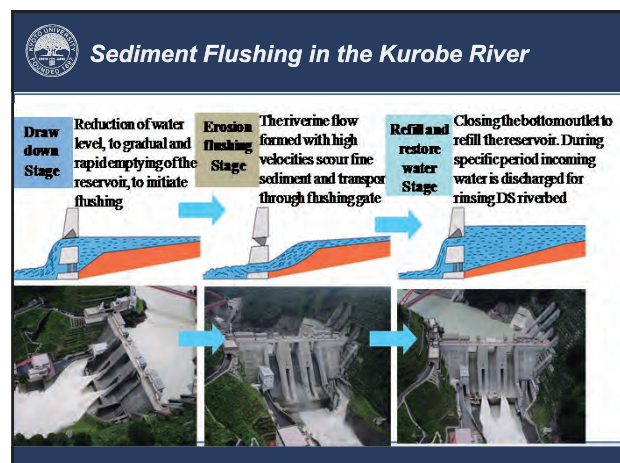
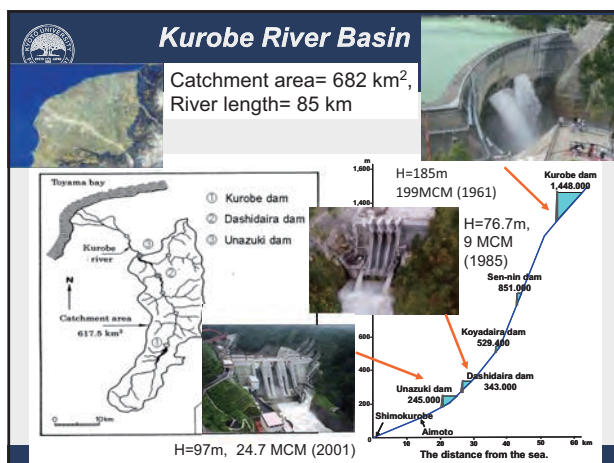
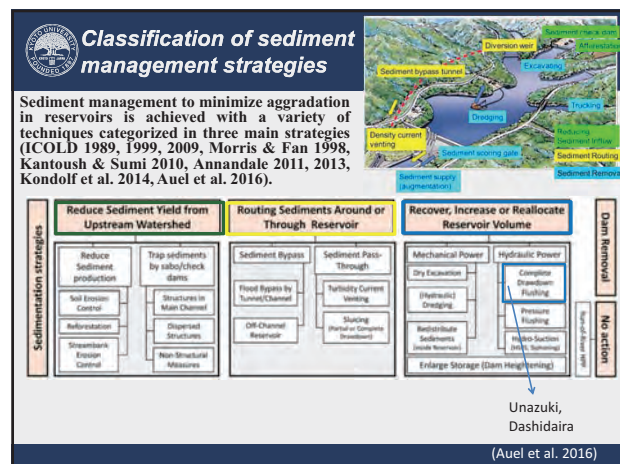
Quenching the Thirst: Sustainable Water Supply and Climate Change, George Annandale(2013)



Sediment management options and sediment passing functions

Classification of options	Normal Impoundment	Draw down level	Frequency	Sediment passing	
				Coarse	Fine
Normal Impoundment		○	None	None	Small
Sediment Replenishment		○	None	Several times/year	Partially (Concentrated)
Sediment Flushing		○	All (Empty)	Once/yr	All (Concentrated)
Sediment Sluicing		○	Half	Several times/yr	Almost all (Partially concentrated)
Sediment Bypassing		○	None	Several times/yr	Almost all (Distributed)
Dry dam		None	All (Empty)	—	Almost all (Naturally)
Decommissioning		None	—	—	All

- ### Contents of the lecture
- Concept of Reservoir Sustainability
 - Japanese Regulation
 - Methodologies of Reservoir Sedimentation Management
 - Case Studies in Japan





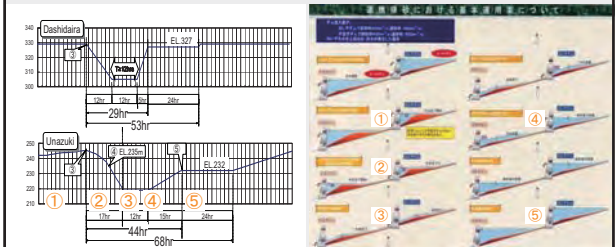
Sediment flushing dams in the World

Name of Dam	Country	Dam completed	Dam Height (m)	Initial Storage Capacity (GAP) (million m ³)	Mean Annual Sediment Inflow (MAS) (million m ³ /yr)	1/2 (Mean Annual Runoff) (=GAP/MAR)	Reservoir Life (=GAP/MAR)	Average Flushing Discharge (m ³ /s)	Flushing Duration (hrs)	Flushing Frequency (1/yr)
Dashidaira	Japan	1985	76.7	9.01	0.62	0.00674	14.5	200	12	1
Unazuki	Japan	2001	97	24.7	0.95	0.014	25.7	300	12	1
Gebdam	Switzerland	1955	113	9	0.5	0.021	18.0	15	70	1
Verbois	Switzerland	1943	32	15	0.33	0.00144	45.5	600	30	3
Barenburg	Switzerland	1960	64	1.7	0.02	0.000473	85.0	90	20	5
Innerferera	Switzerland	1961	28	0.23	0.008	0.00018	28.8	80	12	5
Genissiat	France	1948	104	53	0.73	0.00467	72.6	600	36	3
Baira	India	1981	51	9.6	0.3	0.00489	32.0	90	40	1
Gmund	Austria	1945	37	0.93	0.07	0.00465	13.3	6	168	N.A.
Hengshan	China	1966	65	13.3	1.18	0.842	11.3	2	672	2~3
Santo Domingo	Venezuela	1974	47	3	0.08	0.00667	37.5	5	72	N.A.
Jen-shan-pai	Taiwan	1936	30	7	0.23	N.A.	30.4	12.2	1272	1
Guangxi	China	1953	43	2270	60	1.5	37.8	80	120	N.A.
Guernsey	USA	1927	28.6	91	1.7	0.0433	53.5	125	120	N.A.
Heisonglin	China	1959	30	8.6	0.7	0.6	12.3	0.8	72	N.A.
Ichari	India	1975	36.8	11.6	5.7	0.00218	2.0	2.16	24	N.A.
Quchi-Kurgan	Former USSR	1981	35	56	13	0.00376	4.3	1000	2400	N.A.
Sanmenxia	China	1960	45	9640	1600	0.224	6.0	2000	2900	N.A.
Sefid-Rud	Iran	1962	82	1760	50	0.352	35.2	100	2900	N.A.
Shuicaozi	China	1958	28	9.6	0.63	0.0186	15.2	50	36	N.A.

1) Average after dam completion, 2) Sluicing dams



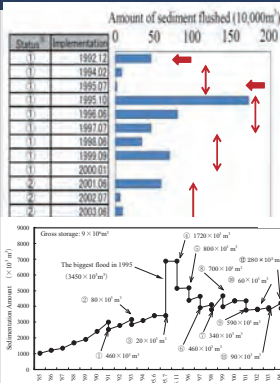
Coordinated sediment flushing in the Kurobe river



Coordinated water and sediment management is very much important. Rainy season, June-July, and natural flood timing is suitable for flushing.



History of sediment flushing in the Kurobe River



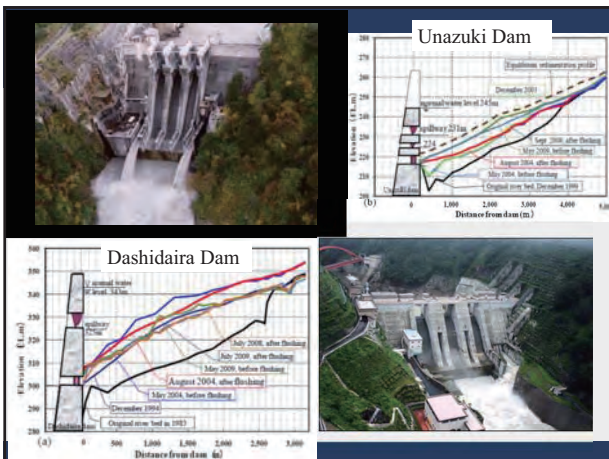
- Dashidaira dam 1985
- First flushing in Dec. 1991
Severe water quality problem
- Tentatively stopped
- Sediment Flushing Evaluation Committee 1992
- Extreme Flood 1995
- Restart of flushing 1995, 96, 97
- After 1998, general flushing operation started
- Unazuki dam 2001
- Coordinated flushing started 2001



History Operation rules of sediment flushing in the Kurobe river

- Sediment flushing operation rule from 2001.

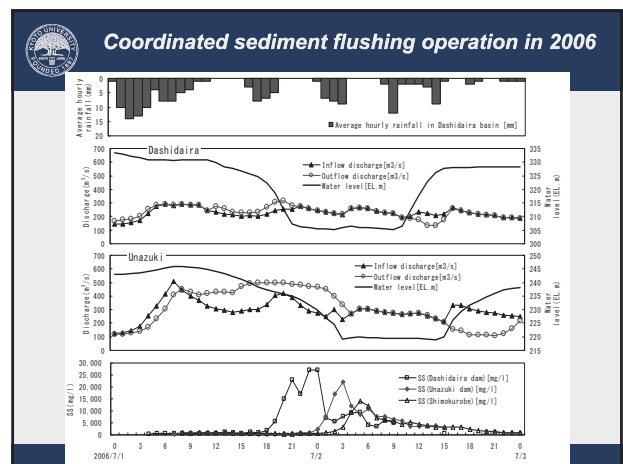
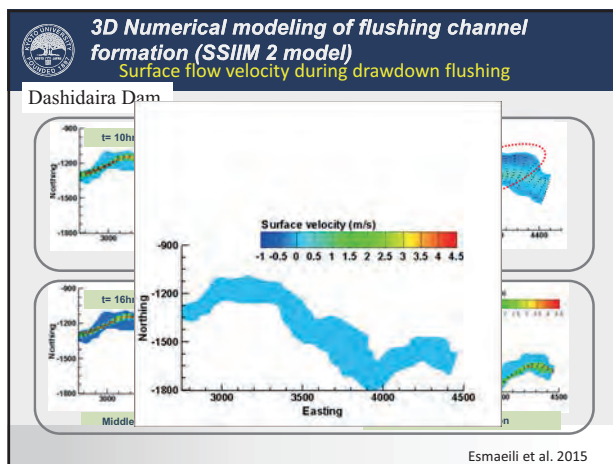
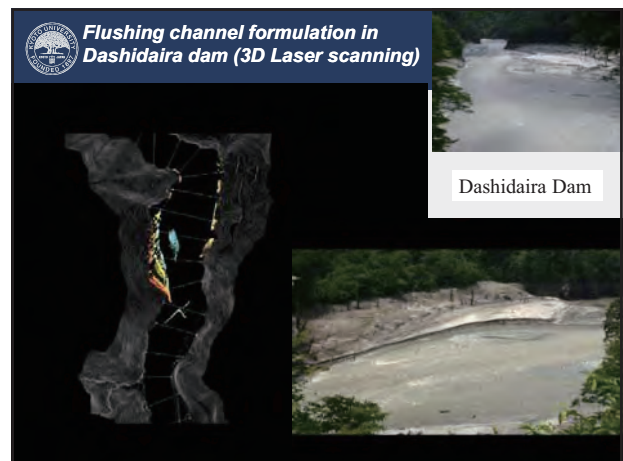
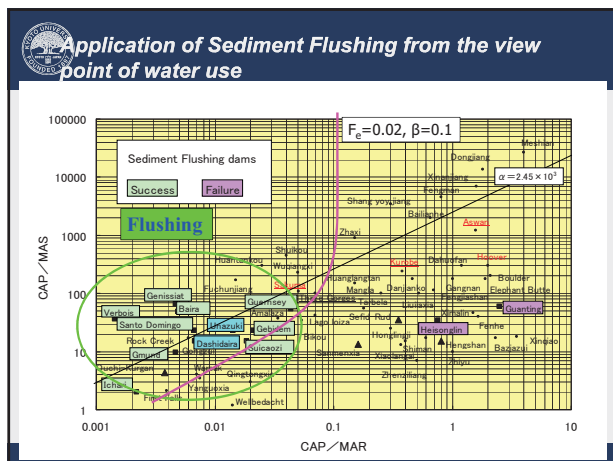
Item	Sediment flushing		Sediment sluicing	
	Dashidaira dam	Unazuki dam	Dashidaira dam	Unazuki dam
(1) Period	*The first flood whenever either of Dashidaira or Unazuki exceed the flood levels of 300m/s or 400m/s from June to August.		*Whenever either of Dashidaira or Unazuki exceed the flood levels of 400m/s or 650m/s from June to August after implementing the sediment flushing.	
(2) Amount of sediment flushed	*The exceed sediment for keeping the stable longitudinal profile.		*Transporting the incoming sediment from upstream to downstream under the flood flow.	
(3) Measure	*Gravity flow		the same as on the left	
(4) Hour	*The hour required for flushing the exceed sediment for keeping the stable longitudinal profile.		*Within implementing gravity flow at Unazuki.	*Within 12 hours after the gravity flow.
(5) Post-treatment after flushing & sluicing operation	*The withdrawal for power generation is stopped for 24 hours after sediment flushing; discharge the entire flow entering the dam downstream.		*Entire flow is discharged from the dam and Unazuki power station for 24 hours after sediment flushing.	
			*Flush at the dams and the power station located on the downstream for 12 hours after sediment sluicing.	



Challenges of sediment flushing

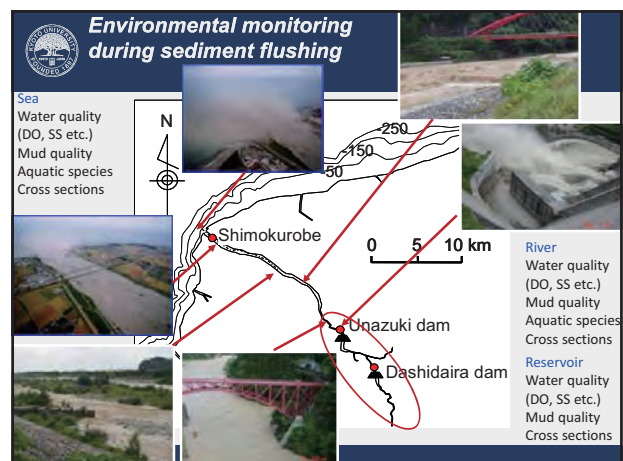
- Flushing efficiency
= scoured sediment volume / water use
- Flushing effect
= scoured sediment volume / total deposited sediment volume before flushing
- Environmental impacts
~ the influences of SS rising and DO dropping - duration time etc.
SS: Suspended solid concentration
DO: Dissolved oxygen

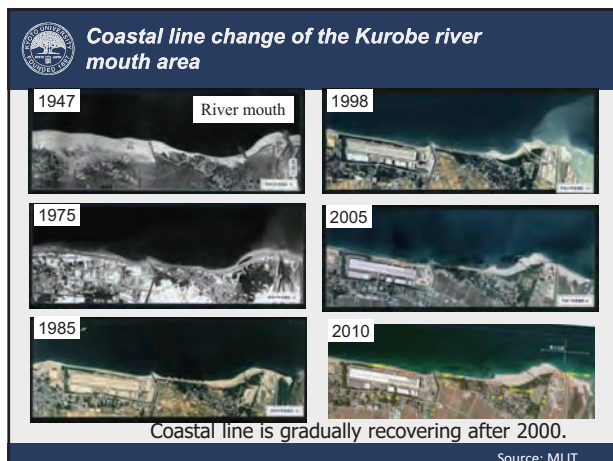
Study on sediment discharge process during flushing operations from quantity and quality point of view is very important.



Actual sediment flushing and sluicing operations at the Dashidaira Dam

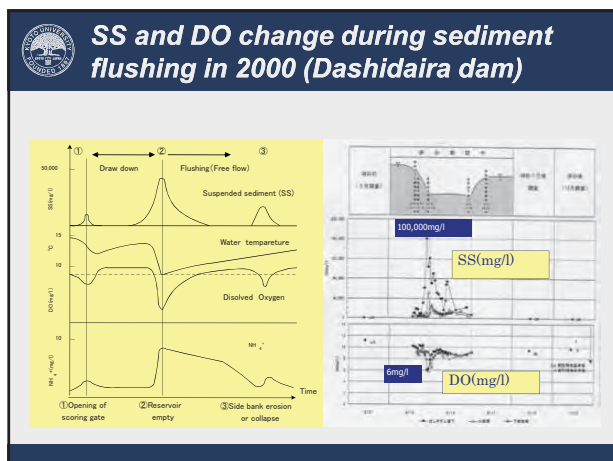
	Maximum Discharge Inflow (m³/s)	Average Discharge Inflow (m³/s)	Flushing Volume (10³ m³)	Maximum SS (mg/l)	Average SS (mg/l)
2001 Flushing	333	277	590	90,000	15,000
2001 Sluicing	491	273		29,000	6,700
2002 Flushing	362	215	60	22,000	4,500
2003 Flushing	777	217	90	69,000	7,100
2004 Flushing	356	229	280	42,000	10,000
2004 Sluicing	1,152	281		16,000	7,300
2005 Flushing	958	290	510	47,000	17,000
2005 Sluicing 1	835	275		90,000	16,000
2005 Sluicing 2	790	250		40,000	7,300
2006 Flushing	308	246	240	27,000	6,500
2006 Sluicing 1	378	203		12,000	2,500
2006 Sluicing 2	685	264		27,000	5,200
2006 Sluicing 3	529	196		7,400	1,800
2007 Flushing	418	245	120	25,000	3,500
Average of Flushing	502	246	270	46,000	9,100
Average of Sluicing	694	249		31,600	6,700
Average of All Data	598	247	270	38,800	7,900





Environmental issues relating sediment management

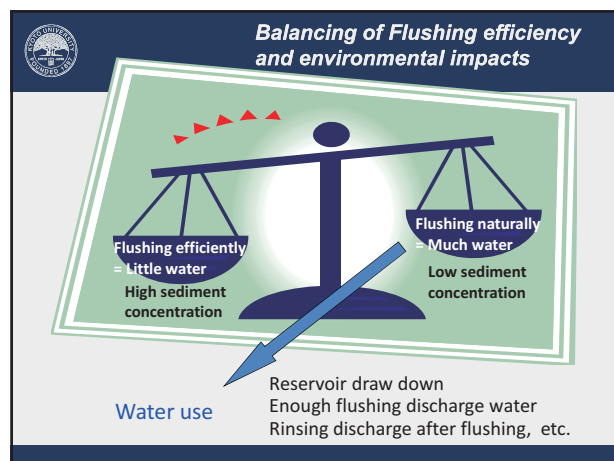
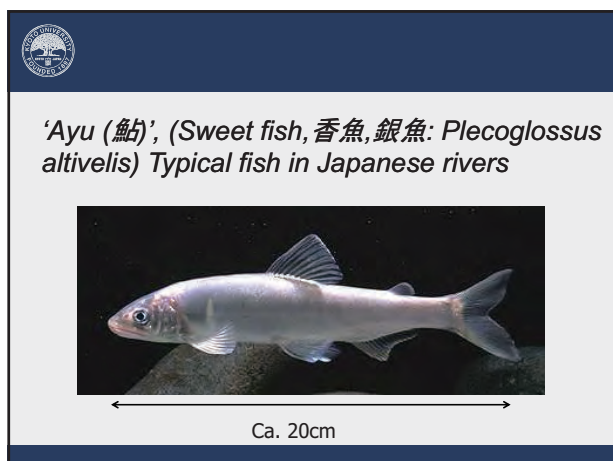
- Minimize negative environmental impacts
 - Water quality changes caused by discharging accumulated sediment containing organic matters and those impacts on the aquatic ecosystem
 - Estimate the influences of SS rising and DO dropping
 - Establish minimizing measures (ex. Sediment Discharge Rule)
 - Re-deposition of fine sediment on the river and the coastal areas and those impacts on the aquatic ecosystem
 - Estimate the influences of fine sediment on river channel, mouth and coastal areas
 - Establish minimizing measures (ex. Rinsing Flow Operation)
- Evaluate positive impacts correctly
 - Contribution to the comprehensive management of the Sediment Routing System
 - Restoration of supplying nutrients and other materials to the river channel and the sea



Measurement values of DO and SS during flushing

Sediment flushing	Amount of Dashidaira sediment flushing	DO (mg/l) (Minimum value)			SS (mg/l) (Maximum value)		
		Dashidaira	Unazuki	Shimo-kurobe	Dashidaira	Unazuki	Shimo-kurobe
Jul-95 Flood	—	—	11.3	10.5	—	3,700	1,800
Oct-95 Flushing	1.72MCM	8.8	9.7	8.9	103,500	29,400	26,000
Jun-96 Flushing	0.8MCM	10.7	10.3	9.8	56,800	9,470	6,770
Jul-97 Flushing	0.46MCM	9.5	9.2	9.3	93,200	28,900	4,330
Jun-98 Flushing	0.34MCM	8.2	7.0	7.3	44,700	9,400	6,750
Jul-98 Flood	—	—	10.5	9.5	—	6,090	5,260
Sep-99 Flushing	0.7MCM	6.0	5.8	6.5	161,000	52,100	25,700
Jun-01 Coordinated flushing	0.59MCM	7.2	11.4	10.2	90,000	2,500	1,500
Jul-01 Coordinated sluicing	—	11.1	10.6	9.6	29,000	3,700	2,200
Jul-02 Coordinated flushing	0.06MCM	9.5	10.5	9.5	22,000	5,400	2,800
Jun-03 Coordinated flushing	0.09MCM	11.8	11.3	9.6	69,000	17,000	10,000
Jul-04 Coordinated flushing	0.28MCM	9.3	10.2	9.8	42,000	6,800	11,000
Jul-04 Flood	—	10.8	11.2	10.3	30,000	12,000	14,000
Jul-04 Coordinated sluicing	—	10.6	11.2	9.6	16,000	17,000	21,000

Manual sampling in every one hour
Continuous monitoring method for DO and SS is necessary





Lessons learned in the Kurobe River

1) Periodical sediment flushing is important.

In the Kurobe River, both sediment flushing and sluicing are performed approximately once a year. It reduces flushing sediment volume in one time.

2) Selecting suitable timing can reduce is important.

Appropriate sediment flushing seasons (June to August), and times when the natural water flow rate exceeds a certain level, 300 (250 in some special case) m³/s or more for sediment flushing, and 480 m³/s or more for sediment sluicing.

3) Flushing efficiency at Dashidaira Dam is about 0.01 to 0.03.

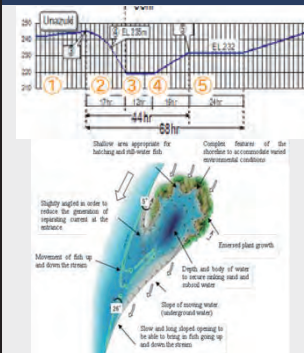
Discharged SS at the Dashidaira Dam during a sediment flushing operation was 8,000 mg/l on average and 40,000 mg/l on the peak.

5) Dashidaira Dam is currently at an equilibrium state by passing of approximately 1 MCM sediment annually.

6) By suppling sediment, downstream riverbed aggradation and bed armoring as well as coastal erosion have been recovered gradually.



Methodologies to reducing risks in downstream river channel

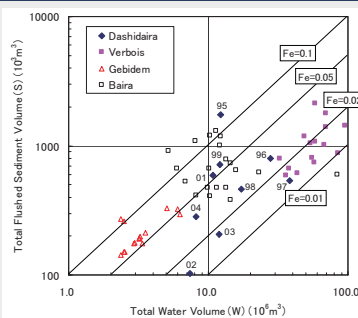


7) In order to prevent accumulation of fine sediment on the downstream gravel bars, the **rinsing discharge** from both dams is performed after recovering reservoir water level.

8) **Evacuation channels** have been prepared as shelters for many species of fish, such as Ayu, during high turbidity in the main stem due to sediment flushing.



Total water use and flushed sediment volume in sediment flushing dams



F_e : Flushing efficiency = Total flushed sediment volume / Total water volume



Efficiency of Sediment Flushing

Application of Sediment Flushing from the view point of water use

$$\frac{CAP}{MAS} > \frac{\frac{CAP}{MAR}}{F_e \left(\beta - \frac{CAP}{MAR} \right)}$$

CAP / MAR : Capacity-inflow ratio or Retention time (yr)

CAP / MAS : Reservoir life (yr)

CAP : Storage capacity

MAR : Mean annual runoff

MAS : Mean annual sediment inflow

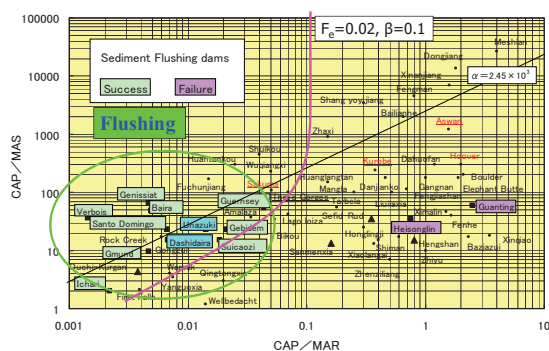
F_e : Flushing efficiency = V_s / V
 V_s : Sediment discharge volume (m³)

V : Water use (m³)

β : Ratio of water use for sediment flushing to the mean annual runoff = V / MAR

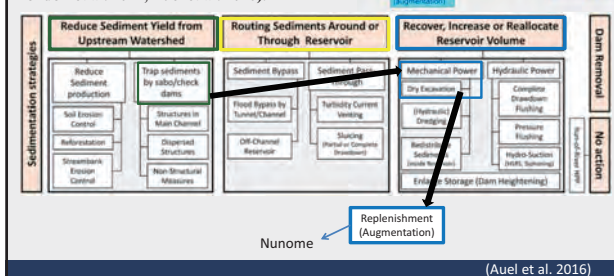


Application of Sediment Flushing from the view point of water use



Classification of sediment management strategies

Sediment management to minimize aggradation in reservoirs is achieved with a variety of techniques categorized in three main strategies (ICOLD 1989, 1999, 2009, Morris & Fan 1998, Kantoush & Sumi 2010, Annandale 2011, 2013, Kondolf et al. 2014, Auel et al. 2016).



(Auel et al. 2016)

Sediment Replenishment (Augmentation)
Ock et al. (2013)

(1) Early augmentation (1970-80s): simply to construct 'spawning riffles' mechanically
(2) Modern augmentation (after 2000s): to support **geomorphic processes** for channel complexity and substrate quality

Spawning Riffle Construction

In-channel stockpile (Trinity R.)

High-flow stockpile (Nunome R.)

High-flow injection (Trinity R.)

Sediment replenishment (augmentation) dams in Japan

Sakurai et al. (2013)

Sediment management should be designed with the combination of flow regime operations

Flow regime operation: Peak cut, flushing flow, environmental flow

Sediment supply manipulation: Sediment replenishment, Erosion control and enhancement

Geomorphic measures: Bar types, bar area, B/h, wetted perimeter, hydraulic radius, sineuosity, riffle-pool ratio, base rock area, grain size, etc.

Habitat measures: Temporary pools, backwaters, moss mats, litter packs, loose bed, hyporheic flow, DO concentration, habitat longevity, etc.

Biodiversity measures: Species diversity, life forms, functional feeding groups, trophic levels, RDB species, alien species, etc.

Material cycle measures: Retention time of POM, Filtering efficiency of POM, Trophic origin of organic matters

Management objectives

Source: Takemon

High-flow stockpile in the Nunome River, Japan
(Ock et al. 2013)

1) Source of sediment: Upstream end of reservoir

2) Frequency: 1-3 times a year depending on natural flood-runoff
Peak duration: 2-4 hours

3) Volume of sediment: depending on release flow (upto 500 m³ per event)
Size of sediment: mixed sand and gravel (0.075-19mm)

(1) Excavating
(2) Trucking
(3) Augmentation

(a) Before flood (sediment placed)
(b) During flood (Oct 8th 2009) (sediment eroded)
(c) After flood (Oct 14th 2009) (sediment transported downstream)

(a) 9:30 Q=9.46m³/s
B=30m
H=0.7m
H=5m

(b) 11:50 Q=15.36m³/s

(c) 13:00 Q=5.71m³/s
100m²

(d)

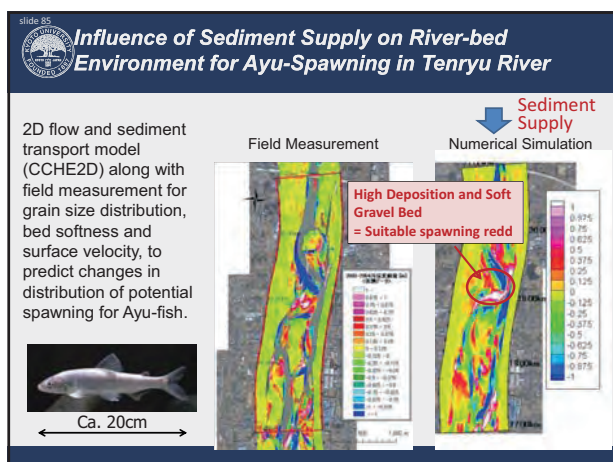
Sediment management based on bedload budget reduction from original condition (Swiss Examples)

- Adjust management of gravel traps
- Reduce excavation
- Extract and dump
- Modify weirs
- Lower water level at weirs during floods

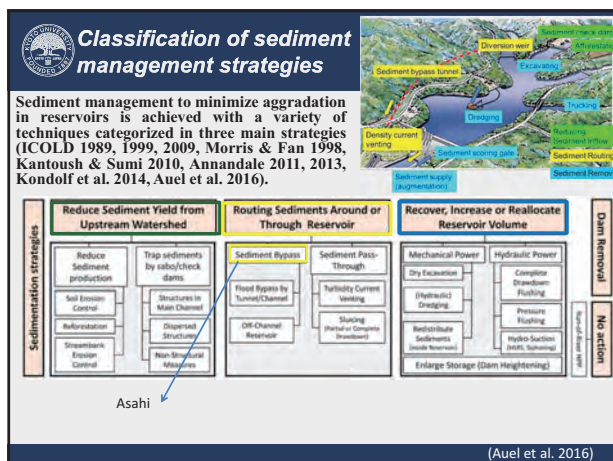
Aare River 2005

Limmat River 2011

(Source: Hunziker)



- ### Summary of sediment replenishment (or augmentation) in Japan
- 1) In order to reduce sediment inflow, mainly coarse bed load sediment is trapped by a low check dam constructed at the end of reservoir and regularly excavated mechanically. Recently, sediment replenishment has been carried out more than 20 dams in Japan.
 - 2) Percentages of sediment replenishment are very limited, ranging between 0.1 to 10 % of annual reservoir sedimentation since these projects are still in trial stage.
 - 3) Sediment replenishment volume and grain size are recognized as key factors for a successful management in the river basin to create and maintain physical habitats, aquatic and riparian ecosystems.
 - 4) Creating new habitats for spawning and other fish life stages are new challenging topics in Japan. Long riffles supplemented by high-flow stockpile could function as an important natural filter for removing reservoir plankton, subsequently contributed to macroinvertebrates' richness and functional feeding group.



2nd International Workshop on Sediment Bypass Tunnels

May 9-12 2017 Kyoto-Japan

2nd Announcement

Workshop Statement

Themes & Prices

Themes:

We kindly invite you to submit your abstract on one of the following topics:

A Upstream Aspects

A.1 Hydrology

A.2 Sediment Erosion & Inflow

B Tunnel

B.1 Hydraulics & Sediment Transport

B.2 Planning & Design

B.3 Tunnel & Inlet Works

B.4 Invert Abrasion

B.5 Maintenance

C Downstream Aspects

C.1 Morphological Changes

C.2 Ecological Effects

D Operation

D.1 Monitoring & Instrumentation

D.2 Real Time Operation

PRICES:

Workshop fee: 15,000 JPY incl. Welcome Reception & 2 x Lunch

Study Tour: 45,000 JPY incl. 2x Hotel, Dinner & Lunch

The tour is limited to 40 participants on a first come - first serve basis.

Workshop Venue and Topics

Impressions:

- Upstream Aspects
 - Hydrology
 - Sediment Erosion & Inflow
- Tunnel
 - Hydraulics & Sediment Transport
 - Planning/Design
 - Invert Abrasion
 - Maintenance
- Downstream Aspects
 - Morphological Changes
 - Ecological Effects
- Operation
 - Monitoring & Instrumentation
 - Real-time Operation

Location & Contact:

The Workshop takes place at Kyoto University, 51-8 Yamate, Gakko Hall.

Contact:

Water Resources Research Center
Dissertation Preparation Research Institute
Kyoto University
Gakko Hall, 51-8 Yamate, Gakko Hall, Japan

Web:

www.kyoto.ac.jp/workshop/2017/

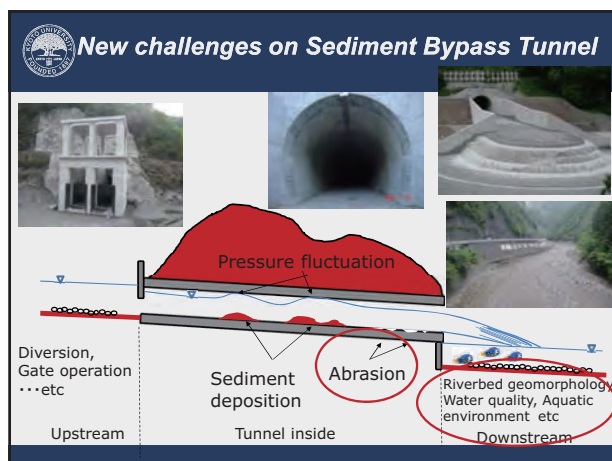
Organizing Committee:

Takafumi Saito Kyoto University
Akihiro H. Banno ETH Zurich, Switzerland
Shin-ichi Kato NRI, Tokyo
Sachiko A. Kikuchi Kyoto University
Yoshitaka Tadokoro Kyoto University
Sachiko Kikuchi Kyoto University
Chikara Arai Kyoto University
Takafumi Saito Kyoto University

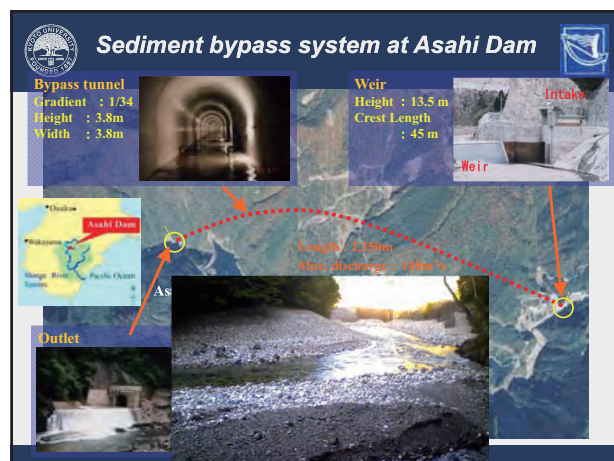
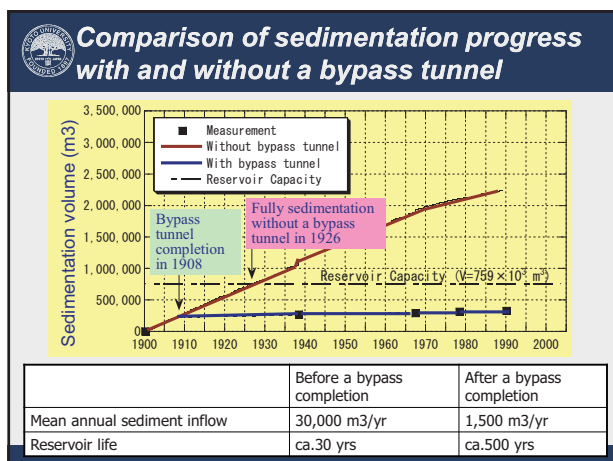
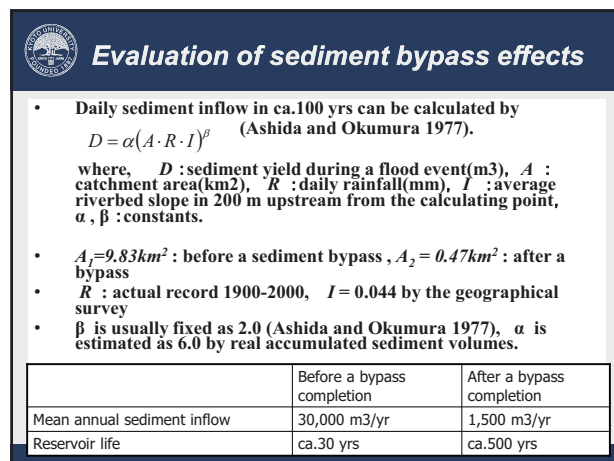
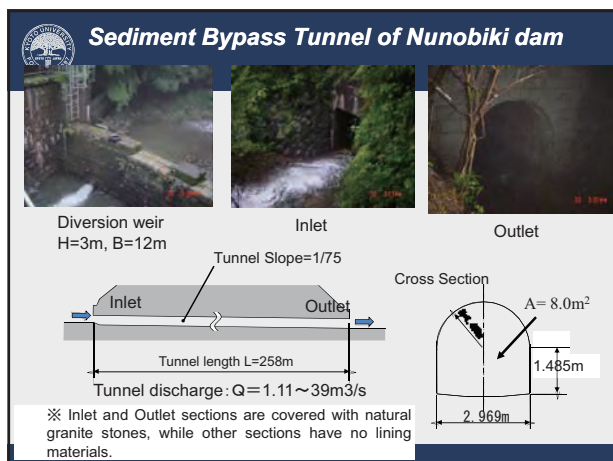
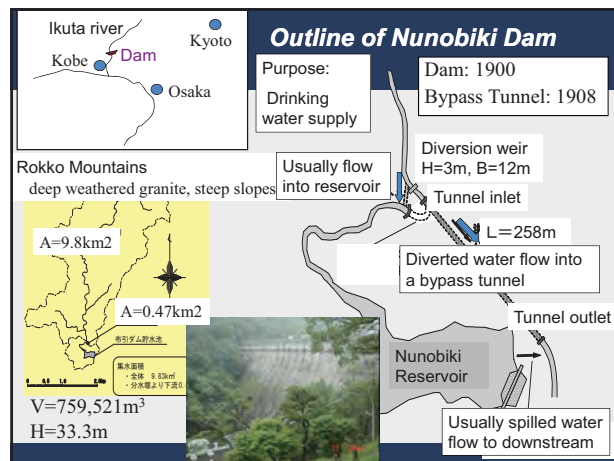
Important Dates:

Abstract submission: 15 December 2016
Full paper/Extended abstract workshop: 1-5 April 2017
Study Tour: 2 days 10-12 May 2017

Both, full papers and extended abstracts are accepted
Extended abstracts: max. 4 pages
Full paper: max. 8 pages



Characteristics of successful sediment bypass tunnels in Japan and Switzerland										
Name	Country	Completion	Cross section	Diameter B×H(m)	Length (m)	Slope (%)	Design Discharge (m³/s)	Design Flood Velocity (m/s)	Design Sediment Size (mm) d_{90}/d_{50}	Operation (Day/yr)
Nunobiki Gohonmatsu	Japan	1908	Hood	2.9×2.9	258	1.3	39	7		
Asahi	Japan	1998	Hood	3.8×3.8	2,350	2.9	140	12	50/300	13
Miwa	Japan	2004	Horse shoe	2r = 7.8	4,300	1	300	10	WL only	2~3
Matsukawa	Japan	UC	Hood	5.2×5.2	1,417	4	200	15		-
Koshibu	Japan	UC	Horse shoe	2r = 7.9	3,982	2	370	9	(5/30)	-
Pfaffensprung	Swiss	1922	Horse shoe	A = 21.0m²	280	3	220	14	250/2700	ca.200
Runcahez	Swiss	1961	Horse shoe	3.8×4.5	572	1.4	110	9	230/500	4
Palagnedra	Swiss	1974	Horse shoe	2r = 6.2	1,800	2	110	13	74/160	2~5
Egschi	Swiss	1976	Circle	r = 2.8	360	2.6	74	10	100/300	10
Rempen	Swiss	1983	Horse shoe	3.5×3.3	450	4	80	12	60/200	1~5
Solis	Swiss	2012	Horse shoe	4.4×4.68	973	1.8	170	11	60/150	1~10



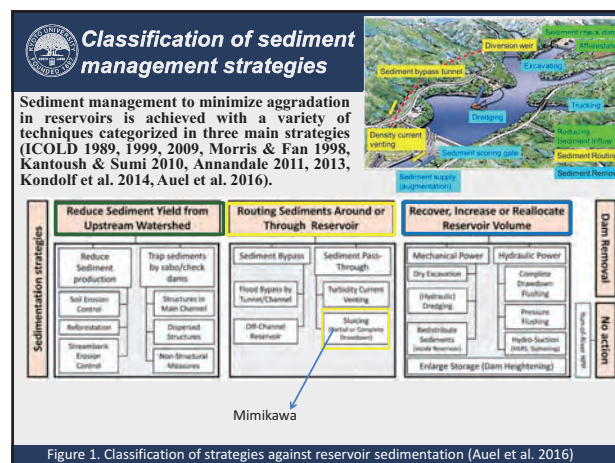
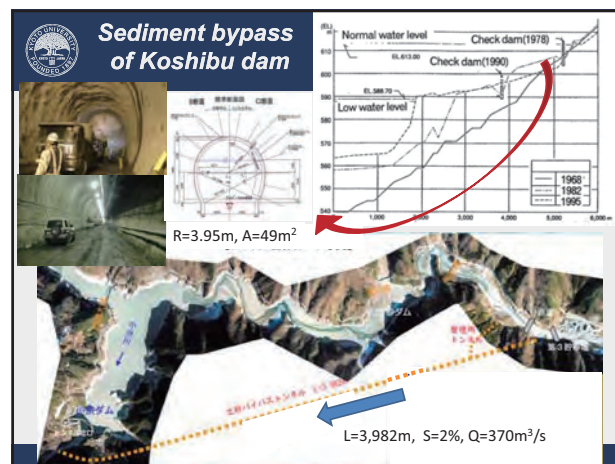
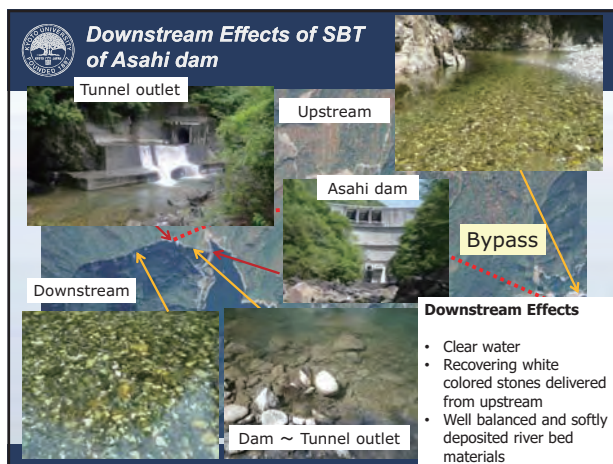
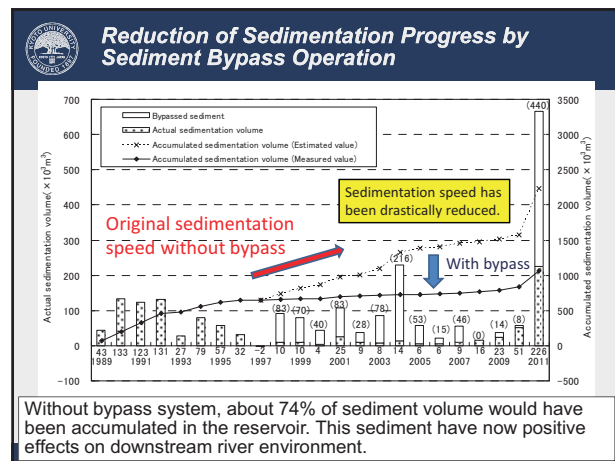
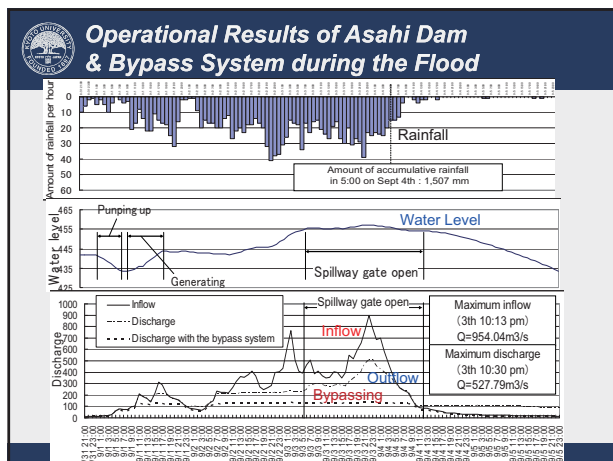
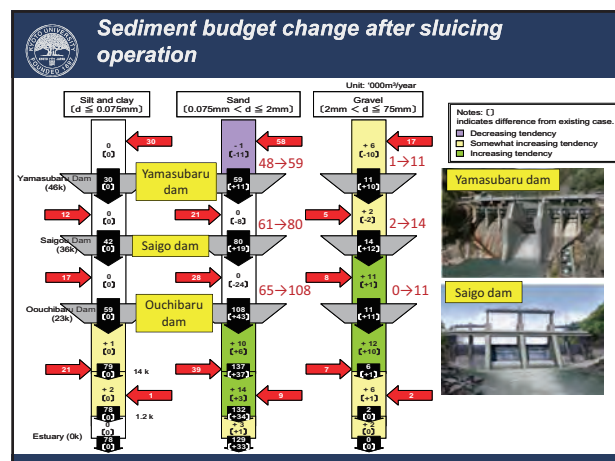
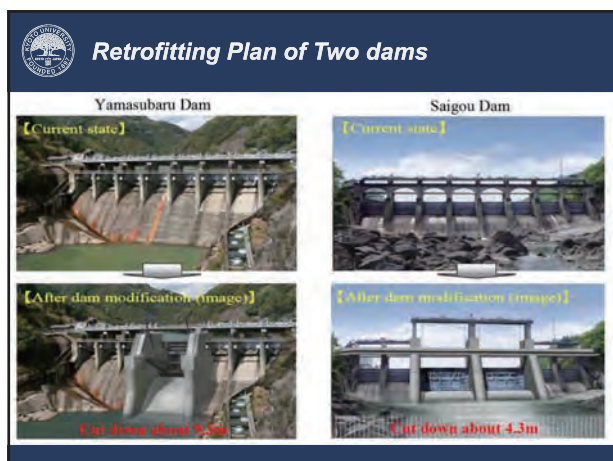
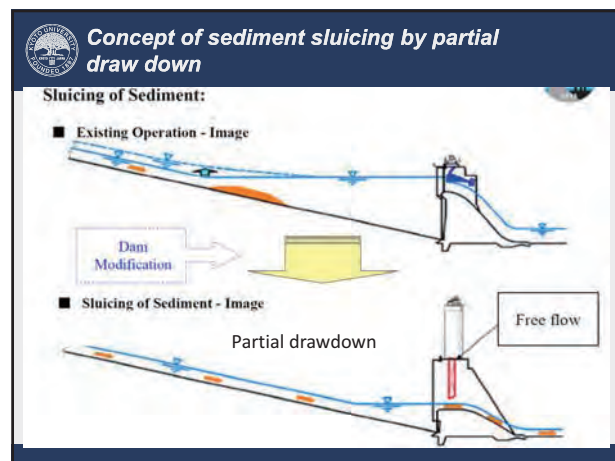
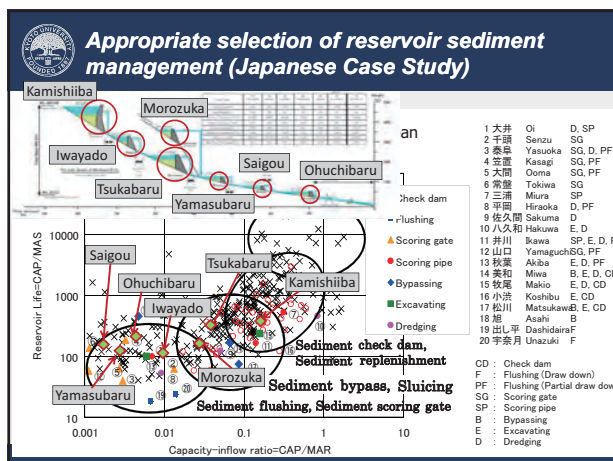
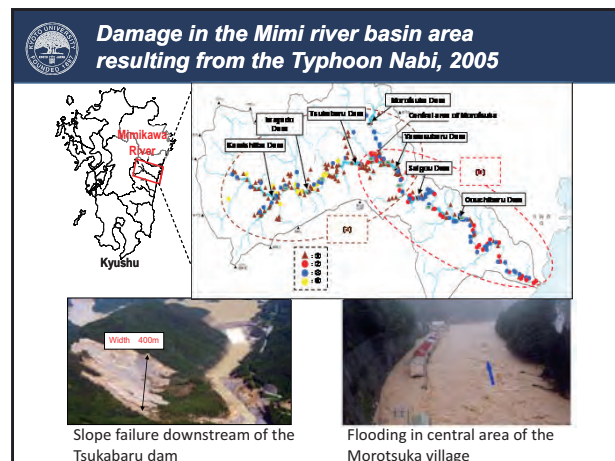
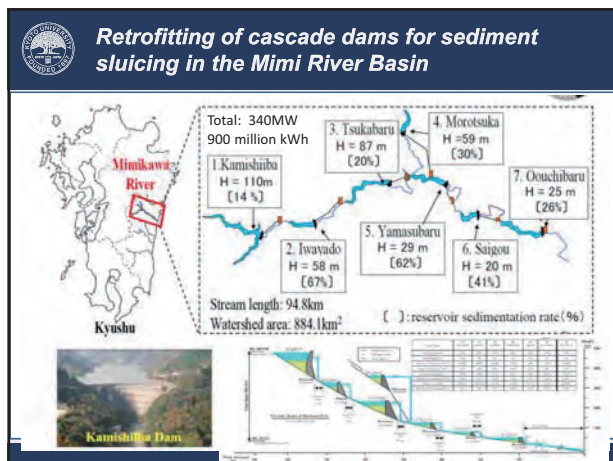


Figure 1. Classification of strategies against reservoir sedimentation (Auel et al. 2016)





Sediment recovering to downstream river



Conclusions

- Sediment management is important both for **reservoir and river basin sustainability**.
- Sediment supply downstream will be beneficial to improve river geomorphology by **creating suitable habitat**, and maintaining biodiversity and suitable material cycles.
- We should check necessary **quantity** (amount added) and **quality** (grain size and source materials) of sediment **both for reservoir and downstream river basin point of views**.
- **Flushing, bypassing and replenishment (augmentation)** are attractive options for reservoir sediment management.
- Sediment management should be appropriately selected based on **reservoir size vs annual sediment and water inflows**.

Lecture 8: Sustainable management of river basin ecosystem services

Sohei KOBAYASHI (*Assistant Professor, Disaster Prevention Research Institute, Kyoto University*)

Abstract:

Ecosystem provides various benefits to human lives, which are called ecosystem services, including production of energy resources, maintaining good water-atmosphere condition, and supporting diverse lives and landscapes for recreation. Eco-DRR is a recent hot topic attracting attention.

River ecosystem from headwater to river mouth consists of main-flow water body, underneath bed layer, lateral floodplain, and various organisms that live in these habitats. Sediment of various grain sizes as well as water and flow is a key factor maintaining aquatic biodiversity and ecosystem services in rivers. First, many species spend their lives on surface of or inside bed sediment layer. Second, a diverse flow condition, which is essential for coexistence of species adapted to different conditions, is generated by bedform (wave of sediment). Third, fluvial sediment deposition masses such as bars and fans act to naturally purify water by infiltration and also generate a mild flow condition for aquatic species to escape during floods. Fourth, a connection between main flow and floodplain or tributary is maintained by sufficient bed level of thalweg. Finally, a high biodiversity in Japanese rivers is assumed to be ultimately maintained by hazardous conditions of Japanese islands that sustain high sediment yields from mountains.

River ecosystems are facing threats caused by human resource utilization in the past and present, and by future climate change. Channel degradation by reduced sediment supply is an important issue especially for downstream rivers and coastal areas. Degraded channels are typically incised, homogenized, and dominated by immobile beds. Projects to increase sediment in downstream rivers, including sediment augmentation, construction of dam-bypassing tunnels, modification of dam gates to sluice/flash sediment, have effects on the recovery of the downstream ecosystems. Our understanding is still limited on the effect of future climate change on river ecosystem. Although an increase of the frequency and intensity of flood and drought may damage ecosystem, complex responses of ecosystem may occur due to adaptations of many species to such disturbances. Changes of flood season are likely to damage aquatic species that grow in originally non-flood seasons.

River ecosystem with certain conditions would show high resilience to disturbance (strong to hazards caused by climate change). For example, outlet rivers of natural lakes and artificial reservoirs may act as refugee for aquatic species by flow and thermal stability. Infiltration of river surface water to bed sediment layer also contributes to provide patchily distributed stable conditions. Sufficient space for rivers to diversify and a mainflow-tributary connection during floods would also increase chances for organisms to survive during floods. Because river ecosystem is structured and maintained by disturbance, sustainable management should allow the occurrence of hazards.

Lecture 8:

Sustainable Management of River Basin Ecosystem Services



Sohei KOBAYASHI (Assis Prof, DPRI, Kyoto)

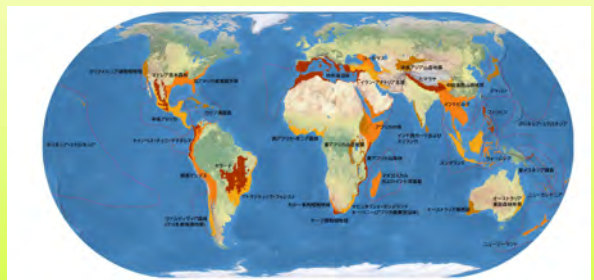
Outline

1. Biodiversity and ecosystem services
2. River ecosystem and sediment
3. Threats to river ecosystem (present and future)
4. Ecosystem resilience and sustainable managements

1. Biodiversity and ecosystem services

Biodiversity hotspots

Places on Earth that are both biologically rich and deeply threatened:
That contain >0.5% or >1,500 species of vascular plants as endemics.
That have lost at least 70% of its primary vegetaFon.



Japan is one of the 36 hotspots

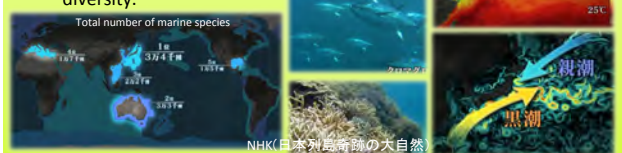
Background of biodiversity in Japan (forest)

- Forest covers 2/3 of the land.
- There are 4-5 biomes.
- Many endemic species in forests.
- PrecipitaFon and temperature difference by laFtude and elevaFon are key of biodiversity.

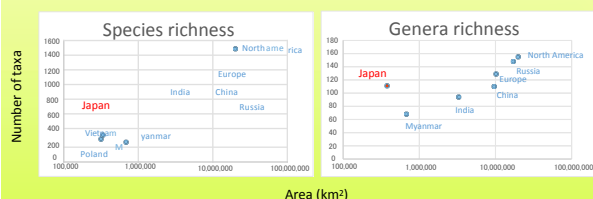


Background of biodiversity in Japan (marine)

- We are surrounded by ocean.
- One of the top of species diversity: 15% of total marine species in the world occur near Japan.
- LaFtudinal difference, mix of warm-cold currents, complex coastal geography, and deep trench support the high diversity.



Caddisfly: a major insect group in rivers



Number of species occurrence increases with the area of places.
Number of species is high in Japan despite its small area.

Ecosystem service

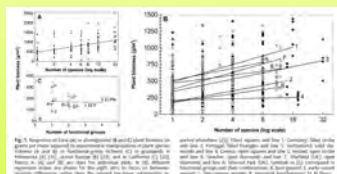
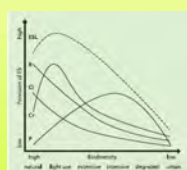
Conditions that make human life possible (food, clean water, regulating climate), or benefits that humans freely gain from the natural environment (including educational, recreational, cultural and spiritual value).



<https://freshwaterwatch.thewaterhub.org/content/ecosystem-services>

Links between biodiversity and ecosystem-service

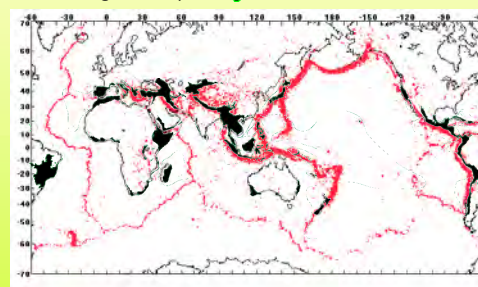
- Biodiversity is one of the ecosystem services for humans
- Biodiversity regulates rates of ecosystem processes, and a certain level of diversity is required to maintain a service.



Loreau et al. 2001

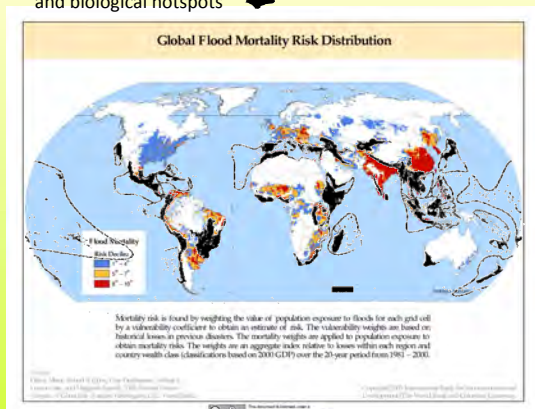
Natural hazard and biodiversity

World distribution of earthquake (seismic center) and biological hotspots

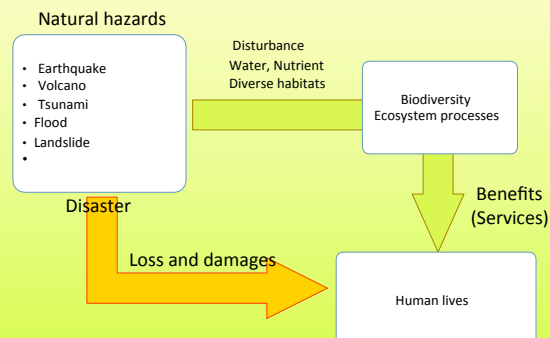


Biological hotspots largely overlaps with earthquake and also volcanic area, or

World distribution of flood mortality risk and biological hotspots



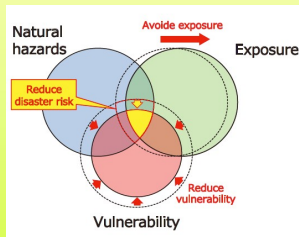
Different aspects of natural hazard for humans



We are benefited from ecosystem services, which are partially maintained by natural hazards, which also directly damages our lives as disasters.

Ecosystem-based Disaster Risk ReducFon (Eco-DRR)

It recommends use of ecosystem services to avoid exposure to natural hazards and/or reduce vulnerability as methods for realizing the disaster risk reducFon



Concept of disaster risk reducFon (Aher ADRC, 2005; Nature ConservaFon Bureau, 2016)

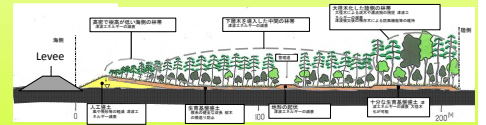
Forest as the eco-DRR measures

Tohoku Commitee for Levee construcFon
http://www.tohokucommitee.com/?page_id=62

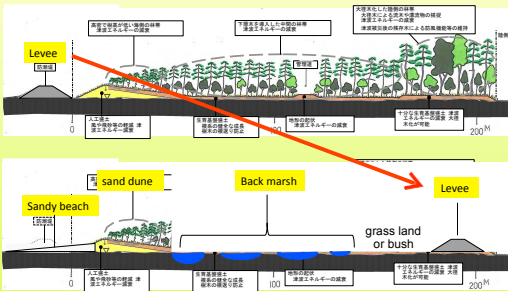


Proposed levee construcFon

Department of Forestry
<http://www.dfo.go.jp/press/2014/04/syoutu-4-4.pdf>

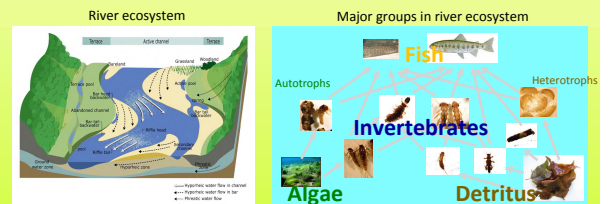


But, from a view point of sustainable management of aquaFc ecosystem

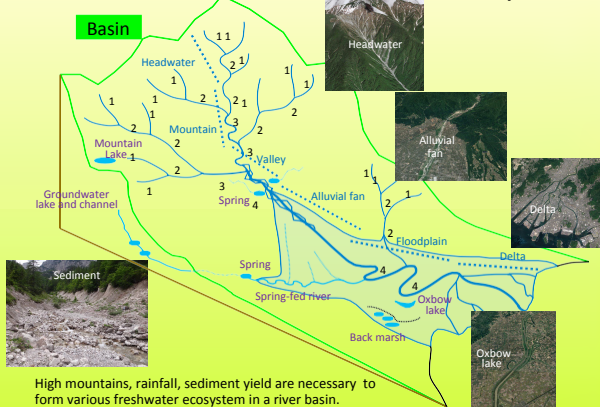


Levee should locate much inner side for sand dune to be mobile and keep the dynamism of coastal habitat structure.

2. River ecosystem and sediment

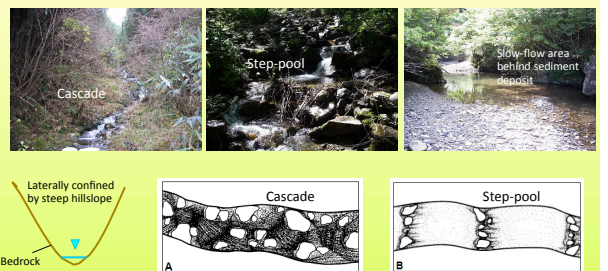


River basin and various freshwater ecosystems



High mountains, rainfall, sediment yield are necessary to form various freshwater ecosystem in a river basin.

Headwater segments



Channel characteristics: laterally confined (=narrow), longitudinally very steep, often dominated by bedrocks and boulders (>50cm), predominantly fast-flow (but, slow-flow occurs by sediment deposit)

Mountain and valley segments



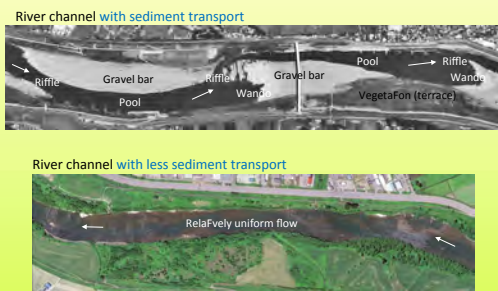
Channel characteristics: laterally confined (but flat bottom by sediment deposit), steep/mild, various sediment including sand (<2mm), gravel (<5cm), cobbles (<30cm), coexistence of fast and slow flow (by pool-riffle bed form), some multiple flow and stagnant water (by large bar formation).

Floodplain segments

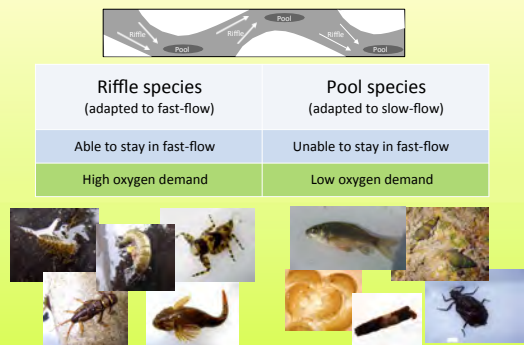


Channel characteristics: laterally unconfined, multiple flow, longitudinally mild/gentle, dominance of sand (<2mm) and gravel (<5cm) over cobbles, multiple flow channels and ponds in floodplain area.

Sediment and bar formation is the basis of diversity in terms of flow, bed material, and aquatic species

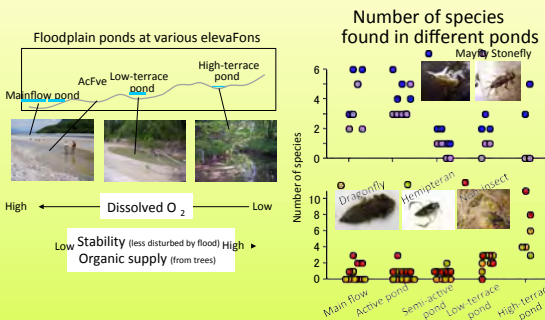


Coexistence of species with different requirements



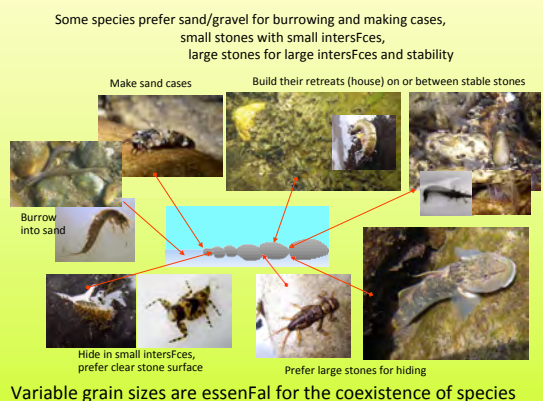
Bar formation and the existence of pool-riffle structure enables both types of species to occur in the same reaches

Coexistence of species with different requirements

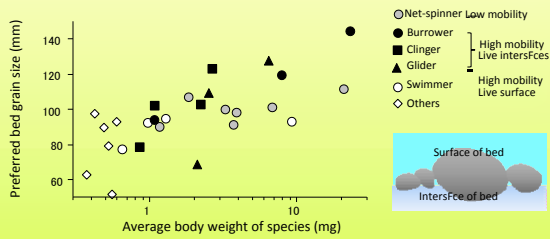


Formation of backwater and ponds with various elevations provides habitats for species with different O₂ or stability requirements.

Grain size is important for aquatic species

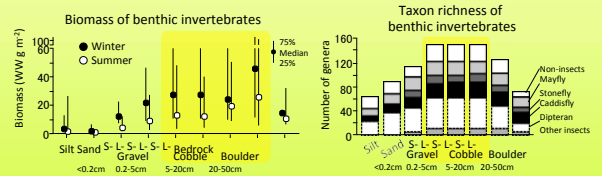
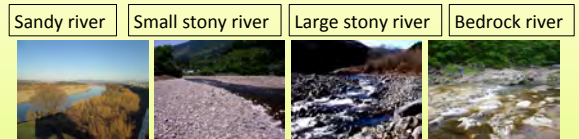


The way they live in the bed determines the suitable stone size for the species



Low mobile species prefer relaFvely large grains (for stability). High mobile and intersFce-living species prefer grain size that matches to their body size.

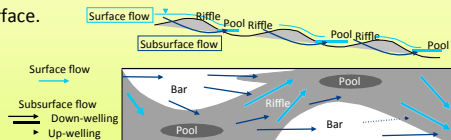
Which type of river is invertebrate rich?



In terms of the biomass and taxon richness of invertebrates, cobble rivers are richer than sandy and bedrock rivers.

Water filtraFon by riverbed and bars

If bars are developed, they infiltrate water and a significant part of surface water goes down the bed and reappears on the surface.

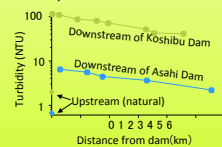


Turbid water becomes clear by filtraFon.



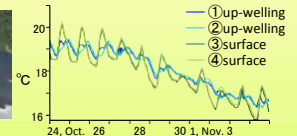
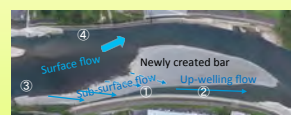
√Turbid water and very fine sediment are unfavorable for aquaFc species and ecosystem.

Turbidity decreases downstream as a consequence of the filtraFon.



Water filtraFon by riverbed and bars

Filtered water is milder than surface water in terms of water temperature, flow, and turbidity, which benefits certain species.



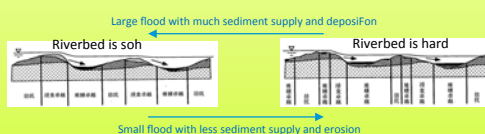
Places fed by sub-surface flow increase survival rate of fish during extreme condiFons such as high turbidity during floods, >30°C in summer.

Thus, water filtraFon by bars is an important funcFon of river ecosystem.

Floods are necessary for refreshing sediment deposiFon and restoring habitat



Ayu fish (popular for fishing and eaFng) spawn eggs on the upstream of newly created riffle, where bed is soh and high oxygen supply from surface.

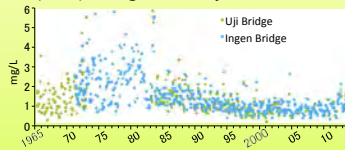


Good spawning riffles are generated after a large flood and sediment supply (=disturbance is required for habitat generaFon)

3. Threats to river ecosystem (present and future)

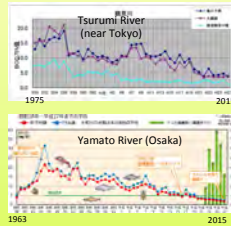
Water quality has been greatly improved in many Japanese rivers

Biological oxygen demand (BOD) change in the Uji River



The quality was worst in 1970's. The improvement in quality was due largely to a development of sewage treatment system.

BOD change in worst quality rivers

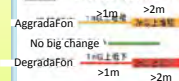


Channel degradaFon

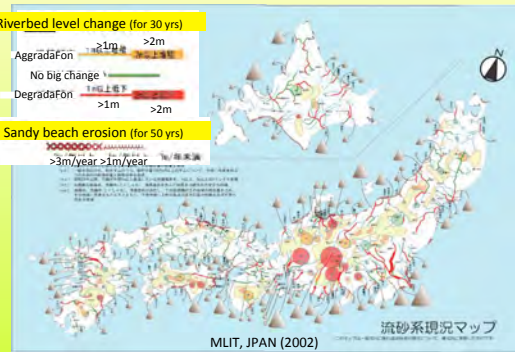
A major environmental issue in Japanese rivers.

Rivers and sandy beaches have been eroded for >30-50 years.

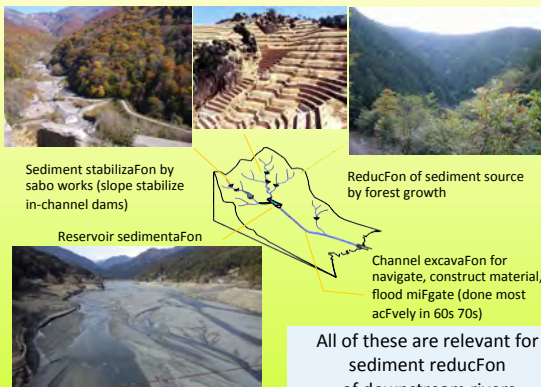
Riverbed level change (for 30 yrs)



Sandy beach erosion (for 50 yrs)



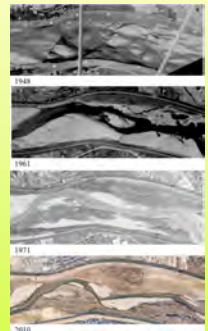
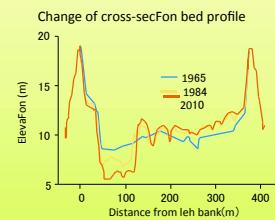
Reasons of channel degradaFon



Changes of river landscapes by degradaFon

1. Incision and main-flow stabilization

Change of plan view flow pattern

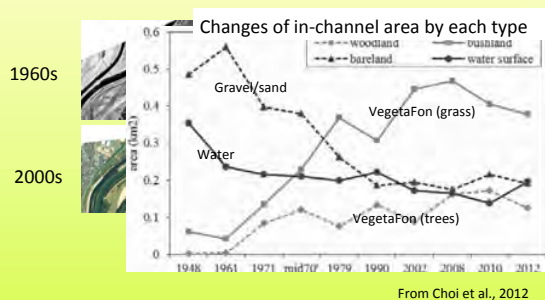


From Choi et al., 2012

Example of Kizu River, Kyoto Pref., Japan

Changes of river landscapes by degradaFon

2. In-channel vegetation (over-growth)

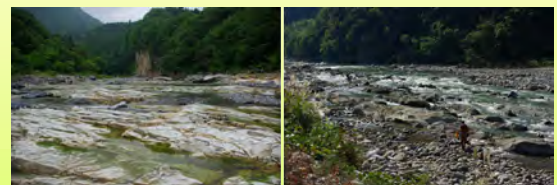


From Choi et al., 2012

Example of Kizu River, Kyoto Pref., Japan

Changes of river landscapes by degradaFon

3. Bedrock exposure (loss of sediment cover)



Kinu River, Tochigi Pref.

Todoriki River, Kanazawa Pref.

Bedrock exposure causes severe damage because many aquatic species live beneath stones and in sand.



Possible changes of river ecosystems by sediment reduction

Degradation (sediment reduction)

Incision and flow stabilization,
Over-growth of vegetation,
Bedrock exposure

Loss of habitats for many aquatic species,
Reduction of ecosystem services

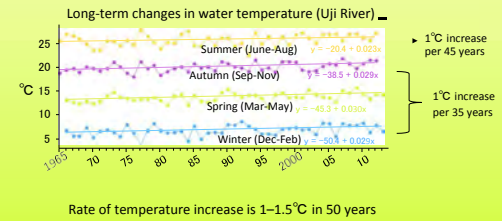
Many aquatic species live beneath stones and in sand



Effects of climate change on river ecosystems

Climate change

- Increase of water temperature
- Increase of flood frequency and intensity, and sediment supply
- Increase of drought



An expected effect of temperature increase

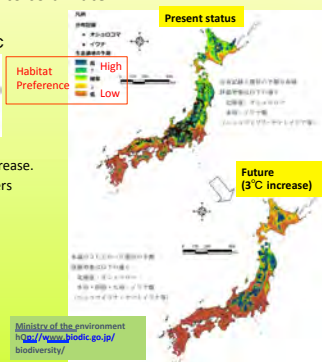
Changes in spatial distribution of aquatic species
Extinction of species adapted to cold water

White-spotted char: prefer water <17°C



Distribution largely shrinks by 3°C increase.
= extinction of population in many rivers

Species have their own upper-limit temperature to survive. Most aquatic insects cannot tolerate >30°C.

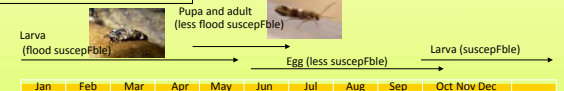


An expected effect of flood change

Increase of flood frequency, intensity, sediment supply may positively affect river ecosystem, because of the roles in habitat generation and maintenance, and the effect probably depends on detail conditions of river.

Changes in seasonality of flood may negatively affect aquatic insects, because some of them have life-cycles that are adapted to present flood regimes.

Univoltine with spring emergence

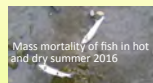


Multivoltine

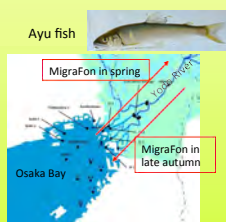


An expected effect of drought (flow reduction)

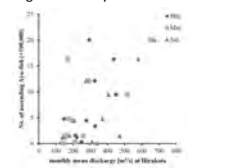
Reduced flow or drought decreases river width, flow speed, dissolved O₂, etc., thus decreases habitable area especially for species requiring flow to live.



Migration of fish and other species in rivers is likely to be discouraged by reduced flow.



Number of Ayu fish upstream migration each year



Urabe et al. 2016

4. Ecosystem resilience and sustainable managements

Sediment supply to downstream for restoring river ecosystem

Sediment management practices of reservoirs are the limited possibilities of increasing sediment in downstream degraded river. Reservoir sedimentation



Downstream of dam (degraded channel)

To maintain the function of dam, sediment in reservoirs should be removed away or transported downstream.

Sediment control measures of reservoirs



Measures for supplying sediment to downstream

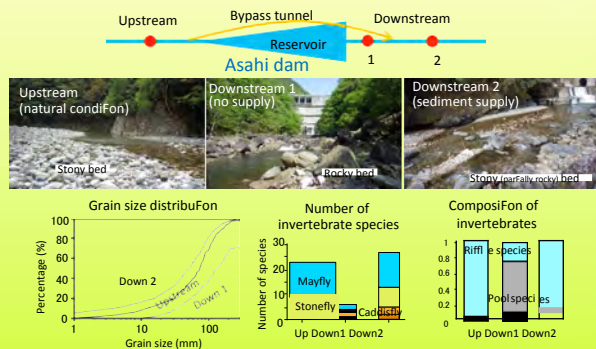
Several measures are known in Japan and other countries.

Augmentation	Bypassing	Flushing/sluicing	Dry dam	Dam removal
国多の 水機能のダム	（電、西、耳） （電、西、耳） スリスダム、台湾3ダム	（電、西、耳） （電、西、耳） スリスダム、台湾3ダム	（電、西、耳） （電、西、耳） スリスダム、台湾3ダム	（電、西、耳） （電、西、耳） スリスダム、台湾3ダム
土砂供給量：自然状態より減少 出水時濁水：やや濁水 平時濁水：ダム上流水	土砂供給量：自然状態 出水時濁水：自然状態 平時濁水：ダム上流水	土砂供給量：多し自然状態 出水時濁水：濁水 平時濁水：ダム上流水	土砂供給量：自然状態 出水時濁水：自然状態 平時濁水：ダム上流水	土砂供給量：多し自然状態 出水時濁水：濁水 平時濁水：ダム上流水
ダム機能維持	ダム機能維持	ダム機能維持	ダム機能は消失のみ	ダム機能なし

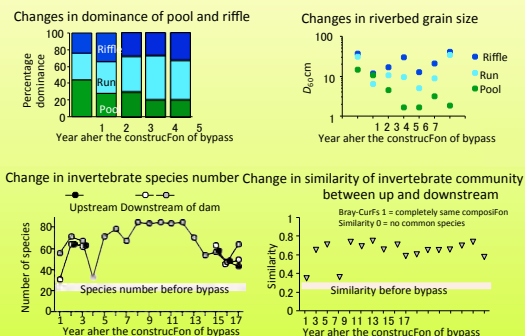
Important features for downstream river ecosystem

Amount of sediment transport	Amount of sediment transport	Amount of sediment transport	Amount of sediment transport	Amount of sediment transport
Small, middle	Middle, large	Large	Large	Large
Natural/unnatural	Natural	Unnatural→natural	Natural	Unnatural→natural
Source of water during normal-flow	Source of water during normal-flow	Source of water during normal-flow	Source of water during normal-flow	Source of water during normal-flow
Reservoir	Reservoir/upstream river	Reservoir	Upstream river	Upstream river

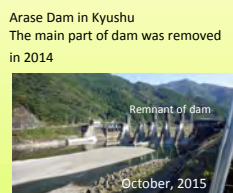
Downstream of dam becomes more like upstream if sediment is supplied by bypass tunnel



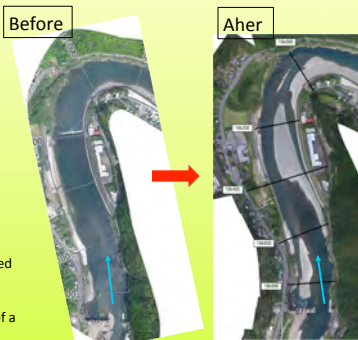
Ecosystem greatly changes within 3-5 years after the start of sediment bypass



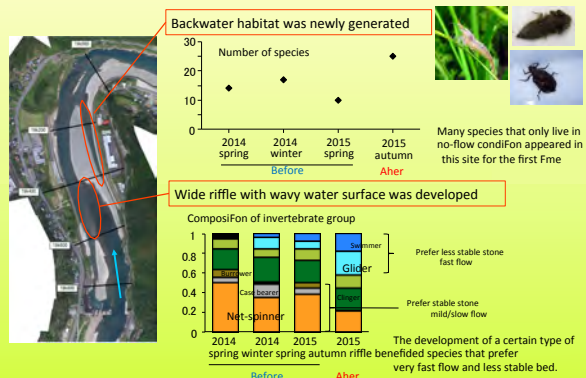
Downstream greatly changes by the first flood event after dam removal



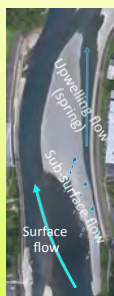
Floods in June 2015 released a large amount of sediment, which was deposited in the reservoir, to the downstream. Bedform and flow of the downstream completely changed by a development of a large bar.



Habitats were diversified by bar development



Infiltration of surface water by bar development



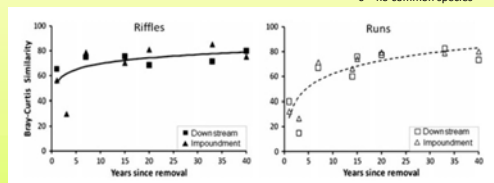
3.2% of river discharge (38 m³/s) was filtered by the bar based on the measurement of surface and upwelling flow.



Contribute to reduce turbidity and mild temperature for fish.

Dam removal and ecosystem recovery (a case of North America, Hansen et al. 2012)

Similarity between upstream and downstream
100 = completely same composition
0 = no common species



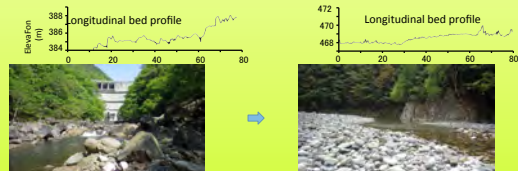
Invertebrate community of downstream as well as pre-reservoir reaches became more like upstream within 10 years after dam removal.

Changes in downstream river by sediment supply (frequently reported changes)

Bed materials become smaller and mobile during flood

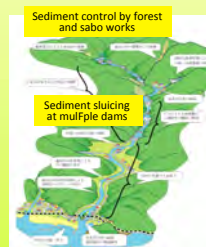


Riverbed becomes smooth, and flow becomes shallow and fast

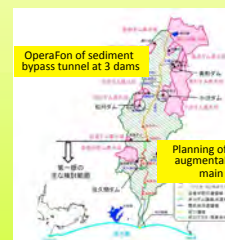


Integrated management of sediment is required for the sustainability of river basin ecosystem

There are usually multiple dams in a river basin. Sediment supplied from one dam may just deposit in another dam in the downstream, and have limited effect on the restoration of ecosystem in overall. An integrated management system is needed to achieve meaningful sediment control that connect headwaters and coastal area.



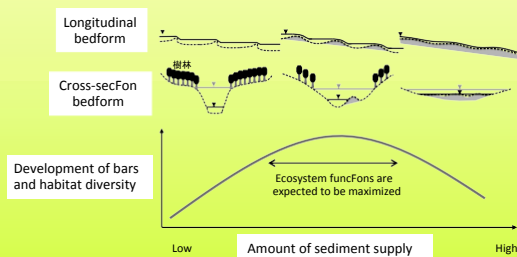
Ongoing project of "Integrated Sediment Flow Management" in Mimikawa River Basin, Kyushu



Partially ongoing project of "Comprehensive Sediment Management Plan" in Tenryu River Basin

Suitable sediment supply for maximizing ecosystem function

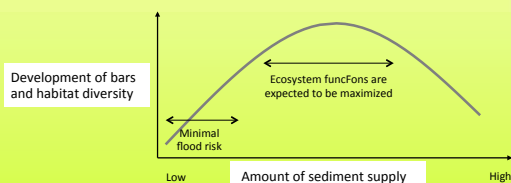
Certain amount of sediment supply is needed to maintain diverse river habitats (e.g., pool and riffle, various floodplain ponds), but over-supply of sediment would in turn act to reduce the diversity



Sediment requirements of flood control and ecosystem


Flood control measures often degrade the channel or modify channel that lowers habitat heterogeneity. Sediment supply for restoring river ecosystem is often not welcome by river manager and river side residents because it increases the risk of inundation.

Comprehensive concept that allows meaningful amount of sediment supply for restoring river ecosystem is required.



Dam as a countermeasure of the impact of climate change on river ecosystem

ReducFons of flood peak and seasonal temperature fluctuaFon by dams are usually unfavorable for river ecosystem. However, in an extreme hydrologic condifon (e.g., catastrophic flood, drought, extremely high summer temperature) in future, some of these controls by dams may be advantageous for ecosystem.



Mass mortality of fish in hot and dry summer

Downstream of dam supports greater species number than upstream and unregulated rivers in regions of harsh environment (e.g., high sediment transport, frequent flood).

Discharge

Time

Inflow of dam

Outflow of dam

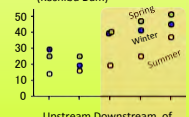
Water temperature

Season

Inflow of dam

Outflow of dam

Invertebrate species richness (Koshibu Dam)



Upstream of dam



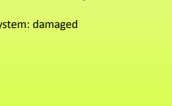

Downstream of dam

Spring

Winter

Summer

Future different scenarios from the aspect of ecosystem restoration

Present	Future
	A. Removing dams  <p>Flow: uncontrolled Sediment transport: high Downstream river: aggraded Ecosystem: fully restored Impact of extreme hydro-event: large</p>
	B. Maintaining dams with sediment transport measure  <p>Flow: controlled Sediment transport: increased Downstream river: mid-graded Ecosystem: partially restored Impact of extreme hydro-event: possibly small</p>

Summary

Biological diversity and ecosystem function are potentially high in Japan due to its geomorphic and hydrological conditions associated with occurrence of natural hazards. Many ecological services are supported by biological diversity.

Sediment as well as water are the basic resource for habitat structure of river ecosystem. Biological diversity is largely affected by available amount and size of sediment, and by the form of deposited bars.

Sediment shortage and channel degradation are the main issues of river ecosystems. Biological diversity would be also damaged by temperature increase and flood-regime change in future.

Several projects of sediment supply to downstream are ongoing, and evidence of ecosystem recovery is accumulating. For ecosystem to be sustainable, managements that span whole basin and solve flood risk-ecosystem issues are required.

Thank you for listening

Resource for river habitats

Riverside sediment augmentation

Typical animals in stony rivers

Evidence of water infiltration

A benefit from biologically rich river ecosystem

Exercise 5-6: Evaluation procedure of riverbed geomorphology and habitat

Yasuhiro TAKEMON (*Associate Professor, DPRI, Kyoto University*)

Sohei KOBAYASHI (*Assistant Professor, DPRI, Kyoto University*)

1. INTRODUCTION

Reservoir dams often show ecological impacts on downstream ecosystems through increasing amount of particulate organic matter mainly composed of planktons produced in the reservoir. As a result, the interstices of the riverbed will be clogged up and DO concentration in the hyporheic zone is expected to decrease. The similar situation will occur in case of “sediment pollution” caused by increasing fine sediments of silt and/or clay in the river.

In filed exercise of this training course, we will visit two Japanese gravel/sandy rivers and observe their riverbed habitat structure. A set of measurement of environmental factors related to hyporheic habitat conditions will be conducted in the Kizu River and the Uji River.

2. HYPORRHEIC HABITATS OF GRAVEL BAR

Figure 1 shows the two- and three-dimensional view of typical gravel river geomorphology. Several important habitat categories have been classified in relation to the geomorphology as in Figure 1a (Takemon, 2010). Each habitat category corresponds to specific inhabitants and thereby takes a role for creating and maintaining biodiversity in river ecosystems.

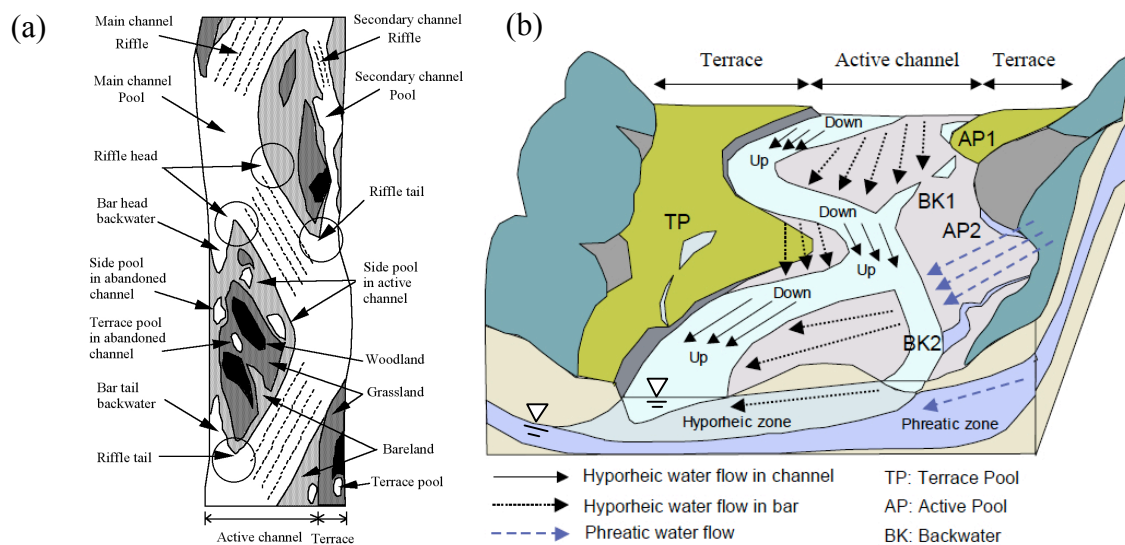


Figure 1 Classification of riverbed geomorphology for aquatic habitat in case of a gravel bed river with moderate sediment supply. (a) Two dimensional figure with head-tail classification of riffle and bar. (b) Three dimensional figure with hyporheic flow and phreatic flow. Down and Up represents downwelling zone and upwelling zone of the hyporheic flow, respectively. AP1 and BK1 are fed by river water, AP2 and BK2 by groundwater, and TP by rainwater. (after Takemon , 2010).

Figure 1 also shows that the habitat categories correspond to units of hyporheic water flow: i.e., riffle head and riffle tail, as well as bar head and bar tail, corresponds to downwelling and upwelling area of the hyporheic water flow, respectively. Most of the aquatic animals depending on these habitats require high DO concentration and/or more DO supply by faster hyporheic water flow.

Hyporheic zones are important not only for interstitial dwellers, so called “hyporheos”, but also for a lot of stream dwelling animals such as fishes and aquatic insects because their spawning redds and oviposition sites are corresponding to downwelling zone of the hyporheic water (Takemon, 1997). At the same time, the hyporheic water flow function as a place for transformation of nitrogen and phosphorus (Anbutsu et al., 2006).

3. FACTORS FOR HYPORRHEIC HABITAT CONDITIONS

As mentioned above, DO concentration is a key factor for the hyporheic habitat quality. However, DO concentration is affected by several environmental factors such as water temperature, organic matter concentration, current velocity of interstitial water, hydraulic gradient, porosity of substrates and riverbed softness (Table 1). Thus, it is required to measure these environmental factors in order to understand problems to be solved. In this Chapter, importance of each factor for habitat conditions and methods for measurement are described.

Table 1 Factors for hyporheic habitat condition of the gravel bar in river ecosystems.

Factor	Process of influence
Water temperature (WT)	oxygen solubility, metabolism of organisms
Dissolved oxygen concentration (DO)	metabolism of organisms
Particulate organic matter concentration (POM)	clogging of interstices, metabolism of organisms
Dissolved organic matter concentration (DOM)	metabolism of organisms, DO consumption
Current velocity of interstitial water (V)	speed of DO supply
Hydraulic gradient (i)	current velocity determinant
Substrate grain size distribution (D)	porosity determinant
Porosity (n)	space volume determinant
Permeability (k)	current speed determinant
Riverbed softness (RS)	porosity determinant

3.1. Water temperature

Water temperature is one of the most basic environmental conditions for aquatic organisms. Thanks for the higher values of specific heat of water body, thermal conditions of aquatic habitats are much more moderate and stable than terrestrial habitats in the air. The characteristics of such moderate thermal conditions in aquatic ecosystem let organisms evolve their metabolic regimes adjusted to the seasonal fluctuation patterns in water temperature. In particular for poikilothermic organisms being highly subject to habitat thermal conditions in their metabolism, thermal conditions of their habitats are more critical than for homoiothermal organisms. In addition, increasing water temperature results in decrease in oxygen solubility.

Daily thermal fluctuation is more moderate in the hyporheic zone in river channels than in the surface water. However, the hyporheic zone in the bar shows a wider fluctuation reaching severe high water temperature in daytime by solar energy absorbed in the bar ground (Yamada et al, 2004).

The water temperature of the hyporheic zone will be able to be monitored by the temperature sensor and logger deposited underground in the hyporheic zone. When the standpipe is installed, the temperature can be measured directly by inserting the thermal sensor into the standpipe. In this training course, we will use the YSI Proplus sensor for the measurement.

3.2. Dissolved oxygen concentration

The oxygen is more soluble in cold water than in hot water. The decrease in oxygen solubility with increased temperature has serious consequences for aquatic life. The solubility of oxygen is affected by temperature and by the partial pressure of oxygen over the water. Oxygen in water obeys Henry's law: i.e., solubility is roughly proportional to the partial pressure of oxygen in the air:

$$P_{O_2} = K_{O_2} X_{O_2}$$

where P_{O_2} is the partial pressure of oxygen in Torr, X_{O_2} is the mole fraction of oxygen in oxygen-saturated water, and K_{O_2} is the Henry's law constant for oxygen in water (ca. 3.30×10^7 K/Torr for at 298 K)(Atkins,

1998). Higher air pressure means higher partial pressure of oxygen, so waters at sea level can contain dissolve slightly more oxygen than mountain streams at the same temperature.

For measurement of DO concentration, the Azide-Winkler Method is the most reliable method. Refer the Washington State University's website, entitled "How to Measure Dissolved Oxygen" for further information (<http://www.ecy.wa.gov/programs/wq/plants/management/joymanual/4oxygen.html>). However, the Azide-Winkler Method requires troublesome jobs, and sometimes the DO probe meters are used instead. In this case, we should remember that the DO probes are easily ruined through deterioration of the membrane. It often is difficult to assess whether or not a probe is functioning properly. Because of this, the meter must be calibrated before and after each series of measurements. In this training course, we will use the YSI Proplus sensor for the measurement.

Hyporheic water along the bar shoreline will be sucked up through a tube buried underground at a depth of 20cm from the ground surface. In order to bury a tube a standpipe will be installed previously (Figure 2a) and the interstitial water will be sucked up using a cylinder (Figure 2b).

(a)



(b)



Figure 2 Method for sampling hyporheic water for testing water quality. (a) Penetration of standpipe for installation of water suction tube. (b) Collection of sample water by sucking up using a cylinder of 100cc in inner volume.

3.3. Organic matter concentration

The particulate organic matter (POM) becomes food resources for benthic animals including microorganisms and thus facilitates consumption of DO in the water. In addition, the POM causes clogging of the interstitial water flow resulting in the decrease in current speed of the water flow leading to reduction of DO concentration. The POM concentration can be measured by filtering water to collect POM using a sieve of 63 μ m mesh size, measuring dry weight and then ash-free dry weight (AFDW). In this training course, POM measurement will be neglected for time saving.

Dissolved organic matter (DOM) becomes food resources for microorganisms and thus facilitates DO consumption as same as POM. The DOM concentration is usually measured by BOD (biological oxygen demand) or by COD (chemical oxygen demand) test as an indicator instead of absolute concentration value. In this training course, the COD test will be conducted using the Oxidation with Potassium Permanganate in Alkalinity and Color Comparison Method, by a package test produced by Kyoritsu Chemical Check Lab., Corp. Water sample will be taken from the hyporheic zone in the same way shown in Figure 2.

3.4. Hydraulic gradient

The hydraulic gradient is a vector gradient between two hydraulic head measurements over the length of the flow path. It is also called the Darcy slope, which can be calculated between two piezometers as:

$$i = dh / dl = (h_2 - h_1) / L$$

where

i : the hydraulic gradient (dimensionless),

dh : the difference between two hydraulic heads (Length, usually in m or ft),

dl : the flow path length between the two piezometers (Length, usually in m or ft).

The hydraulic gradient indicates the direction of the groundwater flow, where negative values indicate flow along the dimension, and zero indicates no flow. This vector can be used in conjunction with Darcy's law and a tensor of hydraulic conductivity to determine the flux of water in three dimensions. Hydraulic head in the bar area can be measured from the distance between the entrance of a piezometer and the water surface elevation. Hydraulic head in a column of water will be measured using a standpipe piezometer by measuring the height of the water surface in the tube relative to a common surface.

In the present training course, the hydraulic head of the bar head and bar tail will be measured using a power level and an average value of the hydraulic gradient will be obtained by measuring the distance between the bar head and bar tail.

3.5. Substrate grain size distribution

Substrate grain size affects porosity and permeability. Characteristics of the grain size distribution are often expressed as the median particle size (d₅₀) but porosity and permeability are usually more influenced by the amount of fine sediments such as silt and clay. In the present training course, substrate grain size distribution of the bar surface will be measured using the grid sampling method within one square meter. Spatial distribution patterns of substrate grain size distribution will be analyzed based on the data. The grain size analysis on the matrix sediment (fine grained sediments filling between stones and rocks) will be omitted this time.

3.6. Porosity

Porosity is a measure of how much open space included in the sediment. The space can be among grains or within cracks or cavities of the grain. The amount of porosity does not always represent permeability because water flow will be limited if inter-spatial connectivity is low even when there are big rooms. Porosity is of importance as a habitat for meiobenthos and microorganisms. Exact measurement of porosity is not easy since the sediment structure will be broken when we collect sediment samples. In this sense, sampling by freeze-core methods (Bretschko and Klemens, 1986) will result in more plausible values. In this training course, however, riverbed softness will be measured as the indicator of porosity.

3.7. Permeability

Permeability refers to how well water flows within the sediment. Thus, the value is the essential for conditioning current velocity and DO supply to organisms living in the hyporheic zone.

Darcy's Law explains the relationships between mean current speed and hydraulic gradient by

$$V = ki$$

where V is mean current speed, i is hydraulic gradient and k is hydraulic conductivity. In order to measure the hydraulic conductivity in the field, the Packer Method and the Piezometer Method have been used according to the field conditions (Yamada and Nakamura, 2009). The Packer Methods can be expressed as,

$$k = \frac{Q}{2\pi hl} \sinh^{-1} \left(\frac{l}{2r} \right)$$

where Q : flow volume, l : length of sediment column, and h : height of water column under equilibrium condition. And the Piezometer Method,

$$k = \frac{r^2}{2l(t_2 - t_1)} \ln \left(\frac{h_1}{h_2} \right) \sinh^{-1} \left(\frac{l}{2r} \right)$$

where t_i : initial time of water injection, t_f : completion time of penetration condition.

Application of the Darcy's Law assumes the saturated flow (Darcy flow). Thus, both the Packer and Piezometer Method are applicable to the riverbed with the sediment grain size condition less than 9.5mm in D10, since the interstitial flow of larger interstices than 9.5mm becomes turbulent flow under usual hydraulic gradient of the rivers. Figure 3 shows a scene of measurement of hydraulic conductivity by the Packer Method in the Kamo River, Kyoto.



Figure 3 Measurement of hydraulic conductivity by the Packer Method in the field. Constant water flow is installed by an electric pump measuring the water level in the standpipe.

3.8. Riverbed softness

Riverbed softness or hardness can be measured by the cone penetration test using the special device composed of penetration cone, falling weight and scale (Figure 4). Riverbed softness is a good indicator for porosity and permeability of the riverbed materials (Samoto, 2010). We can detect hyporheic habitat conditions using the riverbed softness although theoretical relationships to porosity and permeability have never been established yet for the riverbed with a wide range of mixed grain size.

From an aspect of habitat conditions for aquatic animals, the riverbed softness is important not only as a determinant of interstitial flow and efficiency for DO supply, but also as an indicator of easiness for the animals to dig out the substrate to make nests and/or spawning redds.

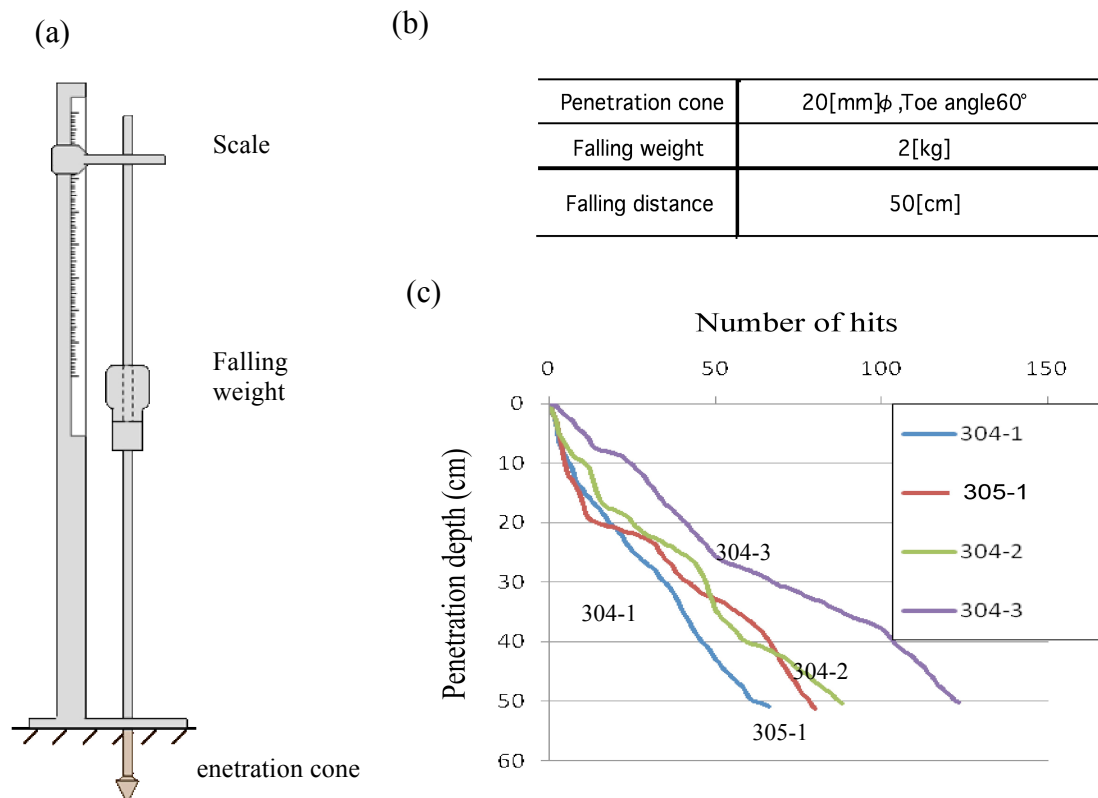


Figure 4 Method for measurement of riverbed softness and an example of measured data. (a) Schematic figure of the penetration test device. (b) Cone size, falling weight and falling distance of the device. (c) Example data of the penetration depth in relation to the number of hits measured in the Tenryu River (after Sumi et al, 2011).

4. PRACTICE OF MEASUREMENT OF HABITAT CONDITIONS

In the course of exercises for ecological field surveys, we will visit two river sites different in sediment dynamism of the riverbed. One site locates in the Uji River below the Amagase Dam with less sediment supply because of only small basins remaining for sediment supply. The other site is in the Kizu River where the sediment movement is comparatively preserved because the main river has no high dams and sand supply has been continues to occur in spite of several high dams constructed in tributaries.

4.1. Study sites

The first study site will be established in the Uji River at 43.0km from the river mouth of the Yodo River (Figure 1 and 2). The Yodo River and the Uji River has the basin area of 8,240 km² and that of 4,354 km², respectively. The study site locates 10km below the Amagase Dam constructed in 1964. There is a point bar with a length of ca. 200m and a width of ca. 80m at the site. Since there are only a few remain basins below the Dam, the sediment supply from the upper basin to the Uji River has been stopped for more than 46 years and distinctive riverbed degeneration can be observed in the reaches (Figure 3a).

The second study site will be established in the Kizu River at 44.0km from the river mouth of the Yodo River (Figure 1 and 2). The Kizu River has the basin area of 1,596 km². There is a very wide sandy bar with a length of ca. 1,100m and a width of ca. 300m at the site (Figure 3b). The site locates 40km below the Takayama Dam constructed in 1969. Since there are no high dams in the main river and there are a lot of tributaries producing sediment, the sediment dynamism of the Kizu River has been fairly active comparing with other tributaries of the Yodo River.



Figure 5 Map of the two study sites in Western Japan. The open square indicates the area of the map in Figure 6 and the circle a and b corresponds to the Uji River site and the Kizu River site, respectively.

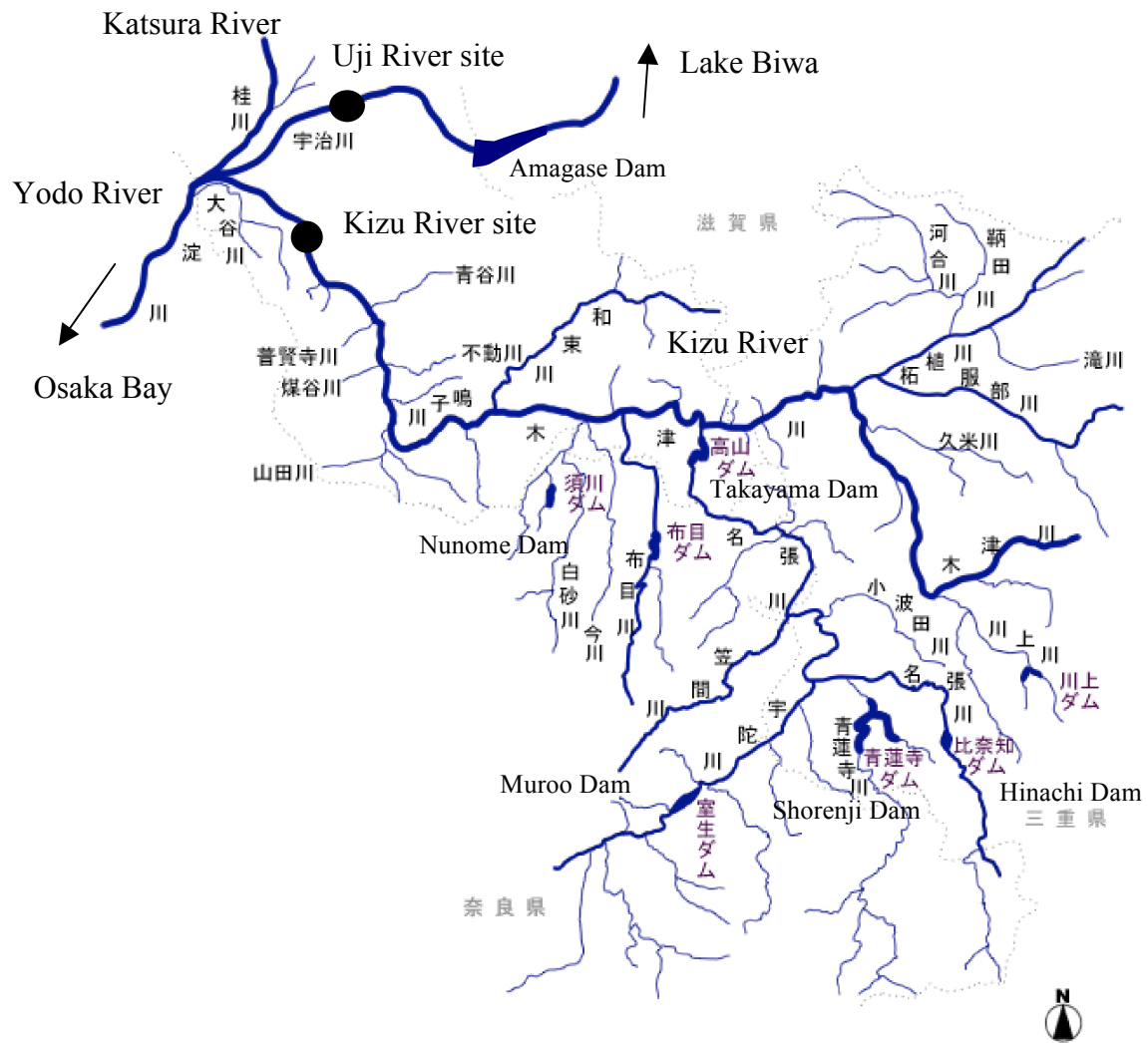


Figure 6 Map of two study sites for the exercise of field surveys. One in the Uji River and the other in the Kizu River, indicated by black circles.

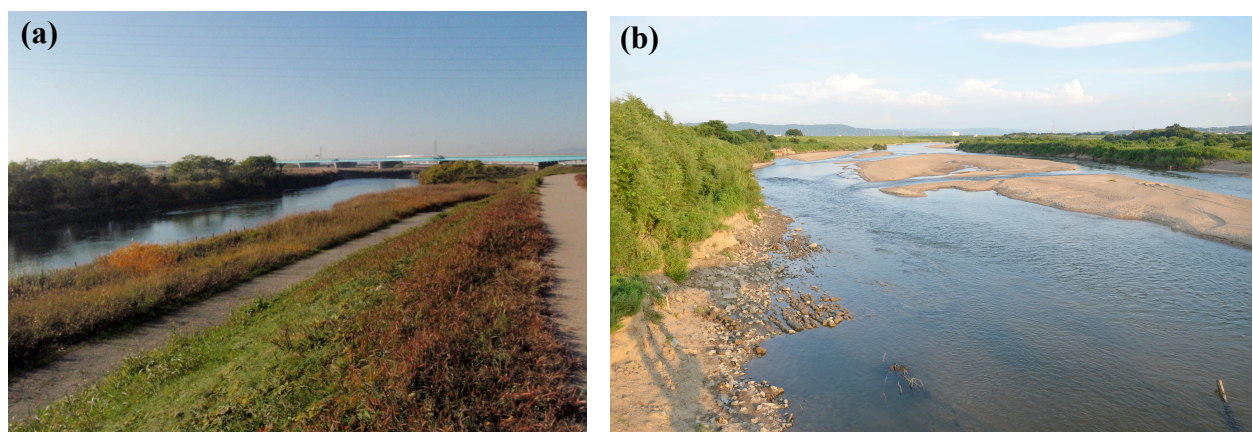


Figure 7 Picture of the two study sites for the exercise of field surveys. (a) the Uji River at 43.0 km from the river mouth and (b) the Kizu River at 44.0 km from the river mouth.

4.2. Schedule for practice

On 13th Dec 2017 in the IHP training course, the practice on the measurement of riverbed environmental conditions will be carried out according to the following schedule.

9:00 Assemble at the Bus stop in front of DPRI
9:10 Leave for the Uji River by bus
9:50 Arrive at the Open Laboratory of DPRI
 Measurement of current velocity and DO concentration of the hyporheic zone in the Uji River
11:30 Move to the Kizu River
12:20 Arrive at Tamamizu Bridge in the Kizu River
 Lunch at the river side
13:00 Measurement of current velocity and DO concentration of the hyporheic zone in the Kizu River
16:00 Leave for DPRI
17:00 Arrive at the Bus stop in front of DPRI
 Bring the survey tools, apparatus and wearing to lab
17:10 Break up

4.3. Report subjects

Participants of this ecological field surveys are required to make a short report on the results of measurement of environmental factors related to hyporheic habitat conditions at two river sites. Calculation of hydraulic conductivity k of the two sites and discussions on possible reasons for the site differences are recommended to be included in the report.

5. REFERENCES

- Anbutsu, K., Makajima, T., Takemon, Y., Tanida, K., Goto, N. and Mitamura, O. (2006), *Distribution of biogeochemical compounds in interstitial and surface standing water bodies in the gravel bar of the kizu River, Japan*. Archiv fur Hydrobiologie, 166, 145-167.
- Atkins, P. W. (1998), *Physical Chemistry, 6th ed.*, Oxford University Press, page 174.
- Bretschko, G. and Klemens, W. (1986) *Quantitative methods and aspects in the study of the interstitial fauna of running waters*. Stygologia, 2, 297-316.
- Sumi, T., Nakajima, K., Takemon, Y. and Suzuki, T. (2011), *Evaluation of suitable river morphology for spawning of Ayu-fish*, Annuals of Disas. Prev. Res. Inst., Kyoto Univ., No. 54 B, 719-725. In Japanese with English Abstract.
- Takemon, Y. (1997), *Management of biodiversity in aquatic ecosystems: dynamic aspects of habitat complexity in stream ecosystems*, in Abe, T., Levin, S. and Higashi, M. (Eds) *Biodiversity: An Ecological Perspective*, Springer, pp. 259-275.
- Takemon, Y. (2010), *Habitatology for linking sediment dynamism and ecology*. International Symposium on Sediment Disasters and River Environment in Mountain Area. JSPS Asia-Africa Science Platform Program pp.25-32.
- Takemon, Y., Tanaka, T., Yamada, H. and Ikebuchi, S. (2005), *An experimental study on hyporheic environmental conditions required for mayfly reproduction in a mountain stream*. Annuals of Disas. Prev. Res. Inst., Kyoto Univ., No. 47 C, 263-272.
- Yamada, H., Tanaka, T., Takemon, Y. and Ikebuchi, S. (2004), *Changing Patterns of Water Quality Associated with Hyporheic Flow of a Gravel Bar in the Kamo River*. Annuals of Disas. Prev. Res. Inst., Kyoto Univ., No. 47 C, 263-272.
- Yamada, H. and Nakamura, F. (2009), *Effects of fine sediment accumulation on the redd environment and the survival rate of masu salmon (Oncorhynchus masou) embryos*. Landscape and Ecological Engineering, 5 (2), 169-181.

The 27th IHP-TC Exercise 5-6

Field Guide

Evaluation procedure of
riverbed geomorphology and habitat



Yasuhiro TAKEMON (Associate Professor, DPRI, Kyoto University)
Sohei KOBAYASHI (Assistant Professor, DPRI, Kyoto University)

Difference in geomorphology between Rivers

Uji River



Flat and active
riverbed

Degraded and inactive
riverbed

Kizu River



At Uji River on 9th Dec 2017

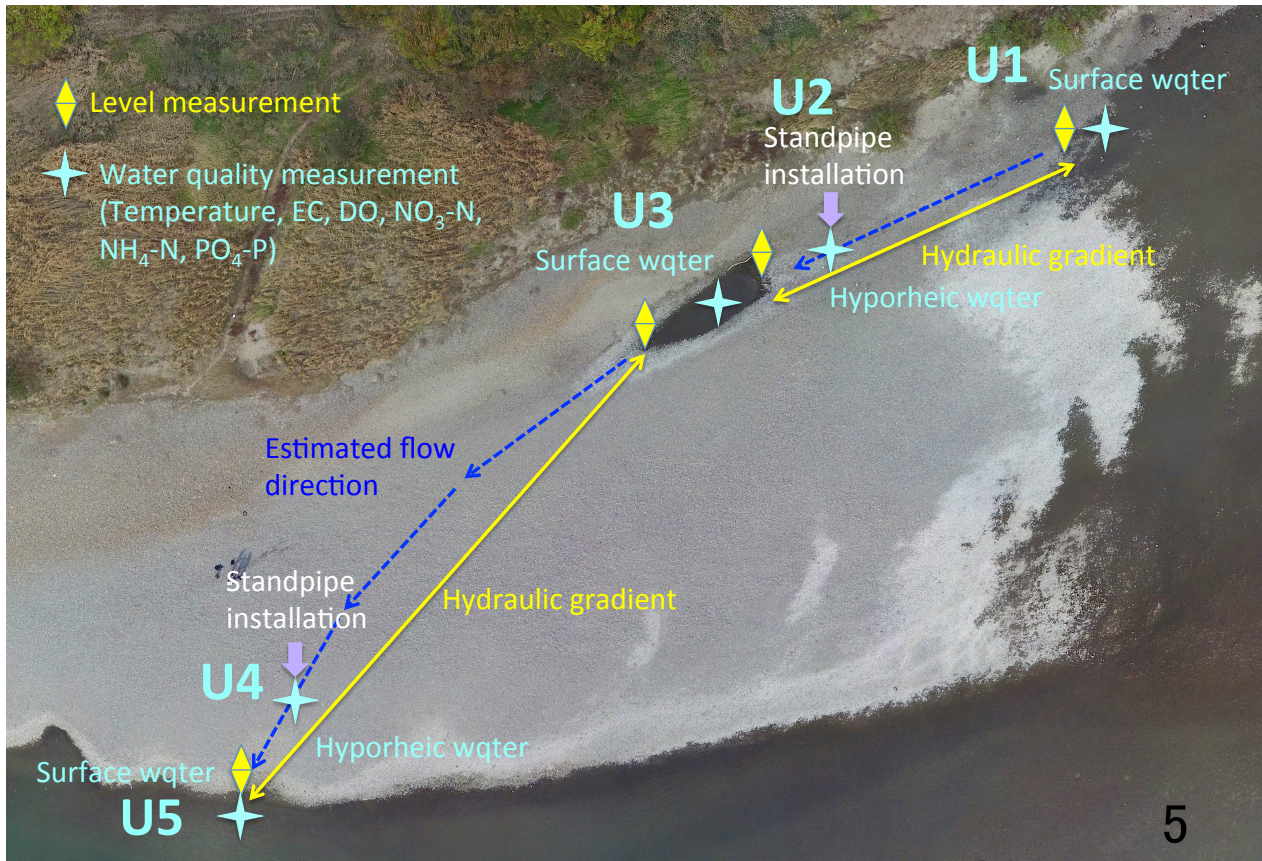


3

Uji River Survey Site



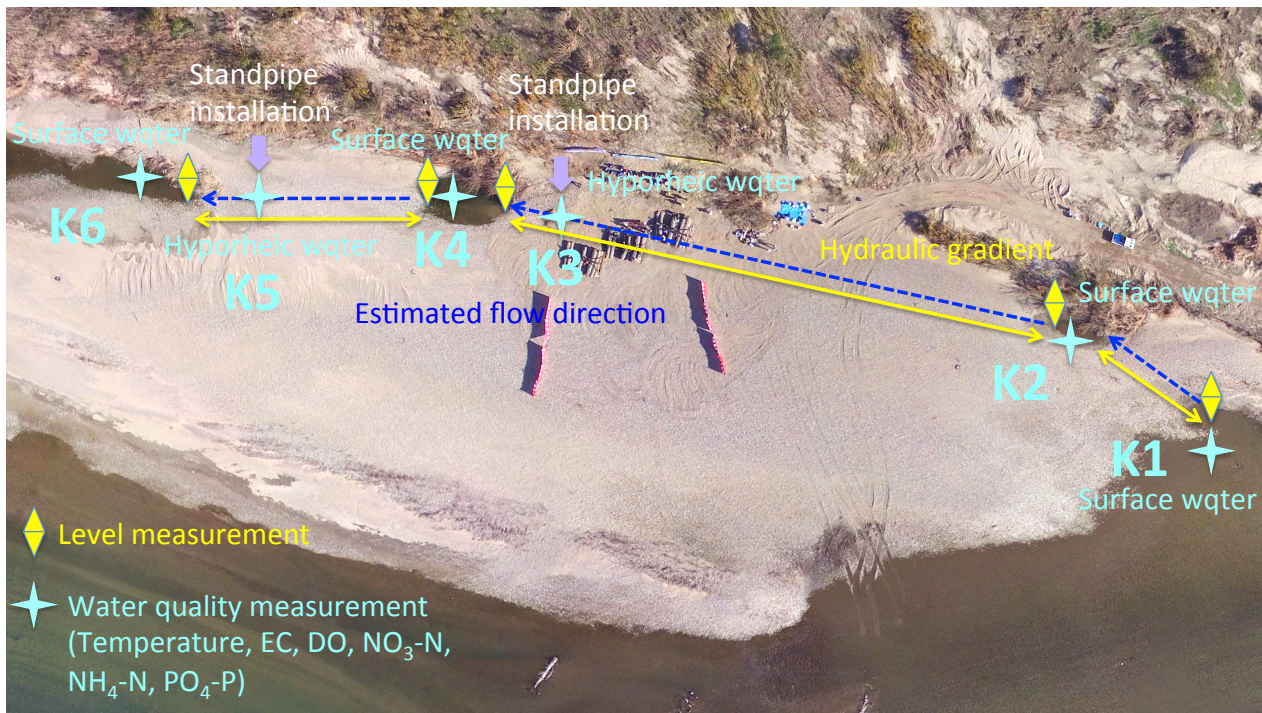
Measurement of hyporheic water in the bar



Kizu River Survey Site



Measurement of hyporheic water in the bar



7

1953年 南山城村大河原駅付近の木津川にあった聖牛

2017年 12月 12日 福井作成



1953年 9月撮影



聖牛
左写真がアップ
したもの

沈下橋？

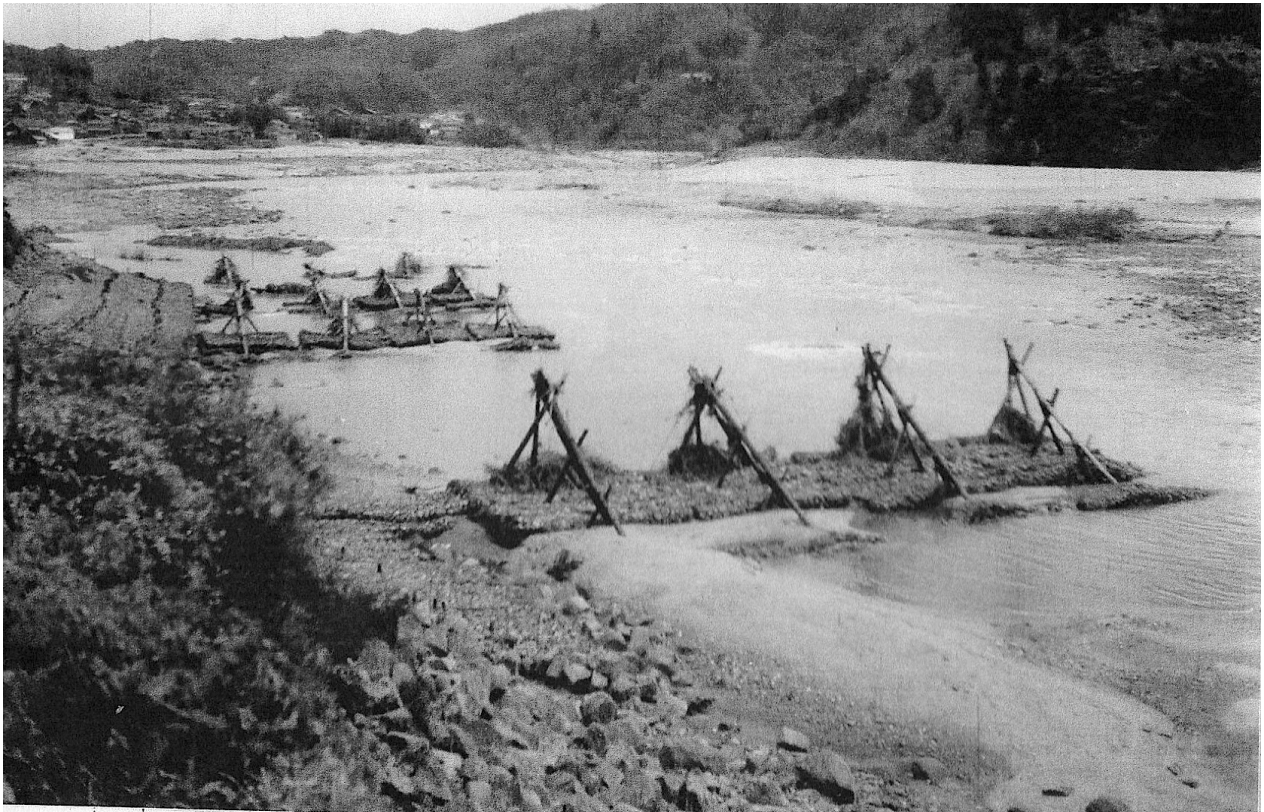
坂南郷土史研究会の中津川
敬朗先生から「福井さん、
堀井先生から頂いた資料を
整理していたら南山城村大
河原の聖牛の様な写真があ
ったよ。福井さんからもら
った資料とおなじだと思
うけど見てくれるか」と連
絡を戴きました。
左の写真を見ると 4 列に並
べてあるように見えます。
木津川が右岸に曲がってい
て、流れを変えるために作
ってあったのではとおっし
やっていました。
木津川にもあったなんて感
動してしまいました。

南山城水宮(1953.8.15)の5枚
木津川右岸(大河原駅南側)

立命館大学地学教室 — の5枚立命館大学地学教室
地学研究会 会長は
堀井篤士さん撮影
(1953年 9月)

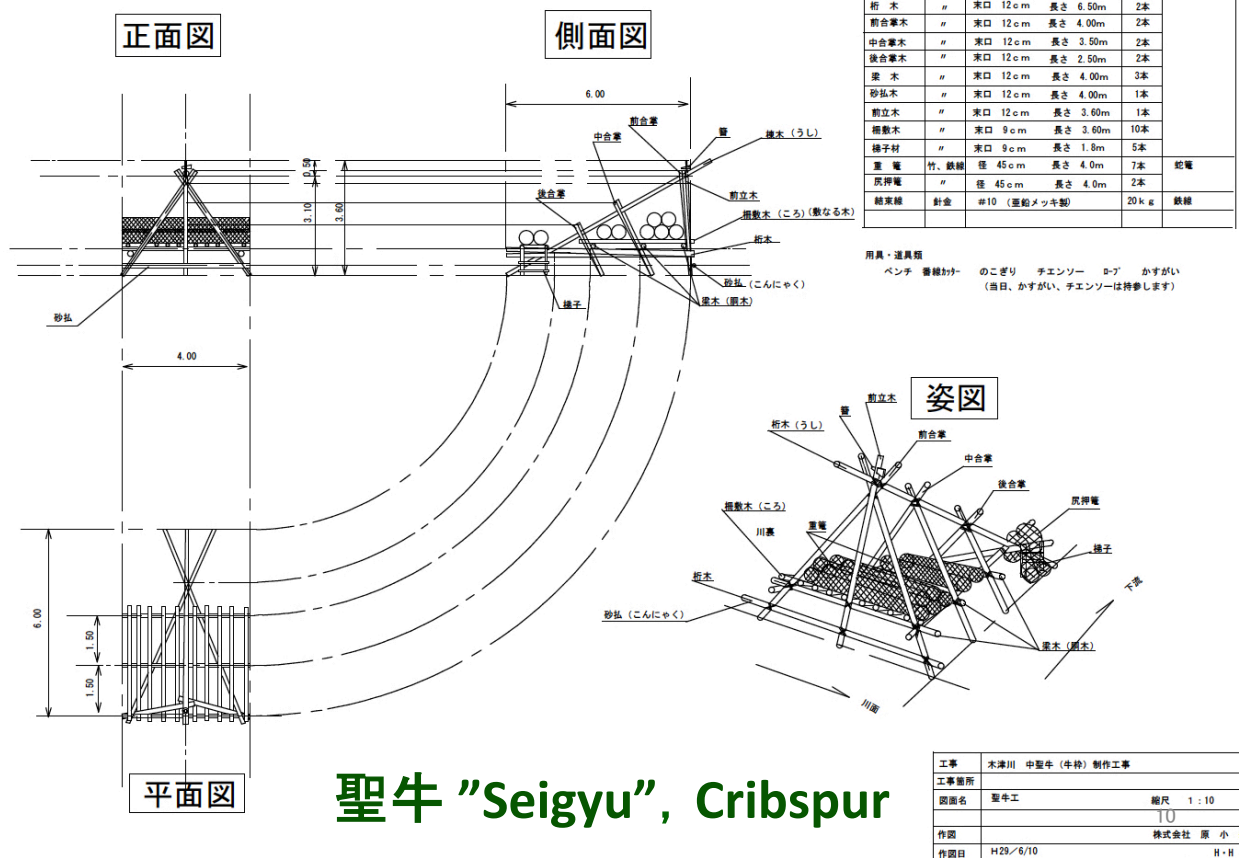
木津川
大河原駅
南側
写真
1.
2.
3.

・地学団体研究会 2016年 8月 29日 死去 90才



9

Japanese traditional river work "Seigyū", Cribspur



2017年 12月2日(土) 10:00集合-16:00解散

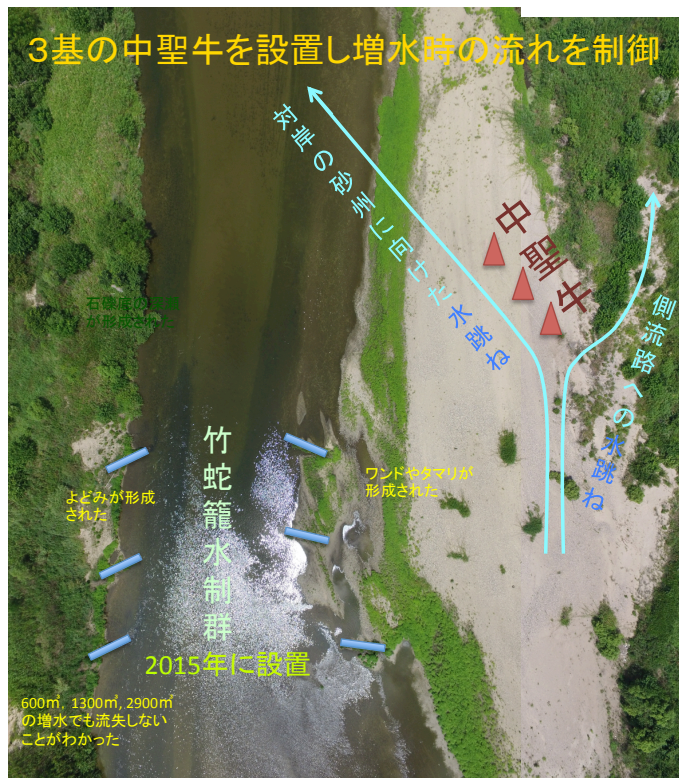
中聖牛設置講習会会場および集合場所

共催: やましろ里山の会・京の川の恵みを活かす会・淀川管内河川レンジャー



集合場所は、玉水橋右岸の橋たもとです。堤防上に駐車していただきます。電車でお越しの方は、JR玉水駅から集合場所まで徒歩をお願いします。参加希望の方は、裏面要領でお申し込みください。

Japanese traditional river work "Seigyū", Cribspur



聖牛 "Seigyū"
Cribspur

竹蛇籠 "Take Jakago"
Bamboo gabion

Exercise 7 Dam operation experiment using a laboratory model

Tetsuya SUMI (*Professor, Disaster Prevention Research Institute, Kyoto University*)

Abstract:

Flood management is conducted by the combination of river channel improvement and dam construction. Because of limited possibility for channel enlargement and/or levee heightening, many flood control dams have been planned and constructed in major rivers in Japan. Generally, these dams are multi-purpose including flood control, water supply for domestic, irrigation and industrial water use and hydropower objectives. In order to effectively utilize limited storage volume, flood control is designed to reduce the peak flow discharge to the acceptable maximum design discharge for the downstream river channel by cutting and storing excess inflow water volume in the reservoir.

In this experiment, the following three parts of flood control processes can be demonstrated.

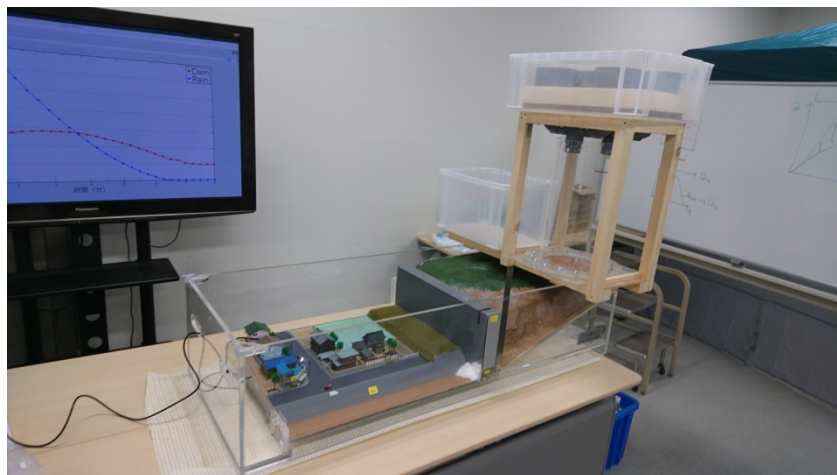
- 1) Rainfall and runoff by a simple tank model with two different size of outlets
- 2) Flood control by a dam model with an ungated bottom outlet and a spillway
- 3) Flood passage and inundation by a downstream channel model with a partial cutting section in the levee

In the experiment, the following three scenarios can be compared by the combination of these three parts of the model

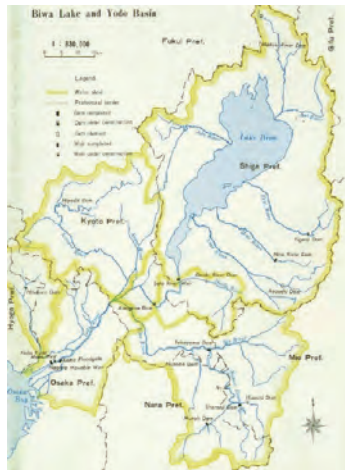
- A) Designed flood without dam
- B) Designed flood with dam
- C) Excess flood with dam

In the exercise, these data will be checked by simple measurements.

- 1) Discharge from a tank model with measurement of water level change
- 2) Water budget of a dam model with measurement of reservoir water level change
- 3) Starting time of inundation from the levee



Edited by
Yasuhiro TAKEMON
(DPRI, Kyoto Univ)



History of lakes in the area

- Lake Katata (1–0.4 million years ago)
- Lake Biwa (Recent)
- Gamo Lakotanda (2.5–1.8 million years ago)
- Lake Koka (2.7–2.5 million years ago)
- Lake Ayama (3–2.7 million years ago)
- Lake Oyamada (4–3.2 million years ago)

Lake Biwa Facts

- Size: 674 square km
- Volume: Total 27.5 cubic km
 - North Basin 27.3 cubic km
 - South Basin 0.2 cubic km
- Max depth:
 - North Basin 104 m
 - South Basin 8 m
- Mean depth:
 - North Basin 44 m
 - South Basin 3.5 m
- Length of shoreline: 235 km
- Catchment area: 3,174 square km
- No. of inflowing rivers: 120
- No. of outflowing rivers: 1 (the Seta River)
- Trophic status:
 - North basin mesotrophic
 - South basin eutrophic
- Conservation Status:
 - Lake Biwa was designated a quasi-national park in 1950
 - The entire Lake Biwa region was designated as a wildlife sanctuary in 1971
 - Lake Biwa was registered with the Ramsar Convention on Wetlands in 1993 as a wetland of international importance
- No. of endemic species/subspecies: 59, including:
 - 11 species/subspecies of fish (19% of total)
 - 9 species of bivalves (56% of total)
 - 11 species of gastropods (39% of total)

Hazard Map of Lake Biwa Area

[illegible]

1. Restaurant
2. Library
3. Shop

2F

Human History

Geological History

Research zone

Aquarium

1F

Special Exhibitions

Discovery Room

Atrium

Meeting place for lunch 11:30

Meeting place for departure 13:30

Main Entrance

Natural Resources Exploitation in Lake Biwa

Fishing in Lake Biwa
Fishing has played a central role in the culture of the area, and many different techniques have been employed. One ancient technique that is still used today is the 'eri' fish trap. These are permanent, anchor-shaped fish traps built near the shore, that concentrate fish into two traps. The fishermen scoop the fish from the trap using long-handled nets. The placement of these traps requires detailed knowledge of fish behaviour and water currents, and their use was strictly controlled. A village that could obtain permission to build an 'eri' usually became very prosperous and powerful.

Mastering Water: Modern Period
Rice farming requires a very careful control of the water system for irrigation purposes. As a result, the natural streams and rivers in Japan have been extensively modified. Several devices, such as human-powered irrigation wheels and versions of Archimedes' screw, were developed for drawing water from a river or the lake and directing it to the fields.

Model of an 'eri' fish trap

Archimedes' screw

An irrigation wheel

HUMAN

Fisherman's life in Lake Biwa

A fisherman emptying an 'eri' fish trap

Lake Biwa; Cold-Water Biwa Salmon
The Biwa salmon is a land-locked subspecies endemic to the lake. They live in the deep pelagic zone of the lake where the water is around 15°C. Spawning takes place in the middle reaches of rivers during October to November when the fish reach 3 to 5 years old. Due to the destruction of the natural river systems around the lake, the population of Biwa salmon is now maintained through artificial propagation in hatcheries.

Okishima
Okishima Island is the only inhabited island in Lake Biwa and supports a fishing village.

Produce of the lake

History of flood control in Lake Biwa

Regulating Water Levels
Although they have long enjoyed the benefits of Lake Biwa's water supply, the lakeside residents until recently also had to endure its floods. With 120 inflowing rivers, but only one outflowing river, the Seto River, coupled with deforestation of the areas around the lake, flooding has been a major problem in the area. In 1896 a devastating flood occurred, with water levels rising 3.7 m above normal, and some areas remained under water for over eight months. Today, floodgates on the outflowing Seto River allow careful control of the water levels in Lake Biwa so that lake flooding is no longer a problem for the residents in the region.

Physical Characteristics of the Lake
The waters of the lake can be classified into two types according to light availability and the potential for photosynthesis. The upper zone where light can penetrate sufficiently for photosynthesis is called the euphotic zone, and below that is the decomposition zone. During the summer Lake Biwa is stratified thermally. The sun heats up the top layer of the lake and this warm water rests on top of the colder water below. During the winter the top layer of water gets colder than the underlying water and because cold water is denser than warmer water, it sinks causing vertical mixing of the water column.

Topography of the lake

ENVIRONMENT

Environmental problems in Lake Biwa

A Countryside House
Opposite the 'kawaya' is a countryside house that was built between 1880 and 1890. It was occupied until 1933, after which it was donated to the Museum. The house is set out as it would have looked in 1964. Items from that time include a barrel-shaped bath. Using only 10 buckets of water, this type of bath was very efficient. In the traditional living room is a television set, another item that dramatically changed the Japanese way of life.

Life with Tapwater
With the development of modern water supply systems, even the average household has access to unlimited quantities of cold and hot water for washing dishes and for bathing. Toilets and sinks now collect wastewater loaded with a great variety of chemicals, detergents and food items, which get flushed together down the drain.

The living room

A barrel bath

Household waste

You can see a lot of freshwater fishes of Lake Biwa in the aquarium

Lake Biwa; The Biwa Catfish
Known as the guardian spirit of Lake Biwa, the endemic Biwa catfish is one of the largest fish in the lake. It can grow up to 1.2 m in length and weigh over 10 kg. It is a nocturnal predator, spending the day at over 40 m depth and coming up into shallower water at night to prey on smaller fish.

Lake Biwa; Ko-Ayu
Although small in size, the ko-ayu is one of the most abundant fish in Lake Biwa, and also comprises the highest-value fishery in the lake. The ko-ayu spawns either in rivers or on wave-washed pebble beaches along the lake shore.

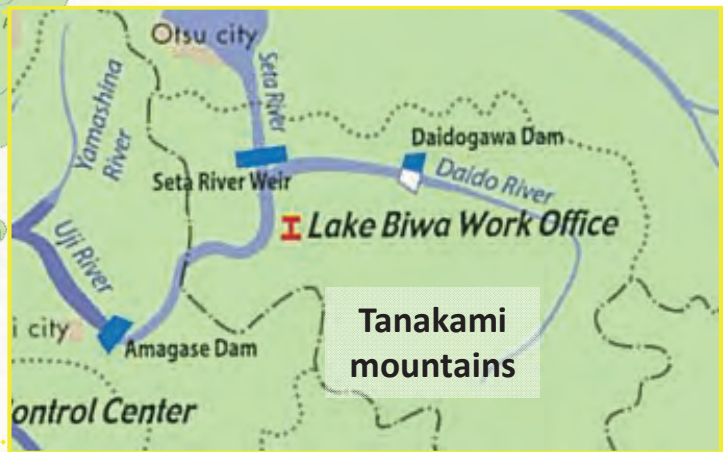


Sedimentation of Amagase-dam

1. Upstream watershed and sediment yield

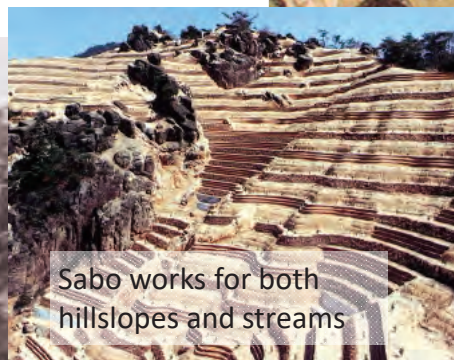


Seta River is the outlet of **Lake Biwa**. The name changes to **Uji River** from the border of Kyoto Prefecture. **Amagase dam** is located in the upstream reach of Uji River. **Daido River** is the largest tributary of Seta/Uji River and **the largest source of sediment** because little sediment supply from Lake Biwa outlet.

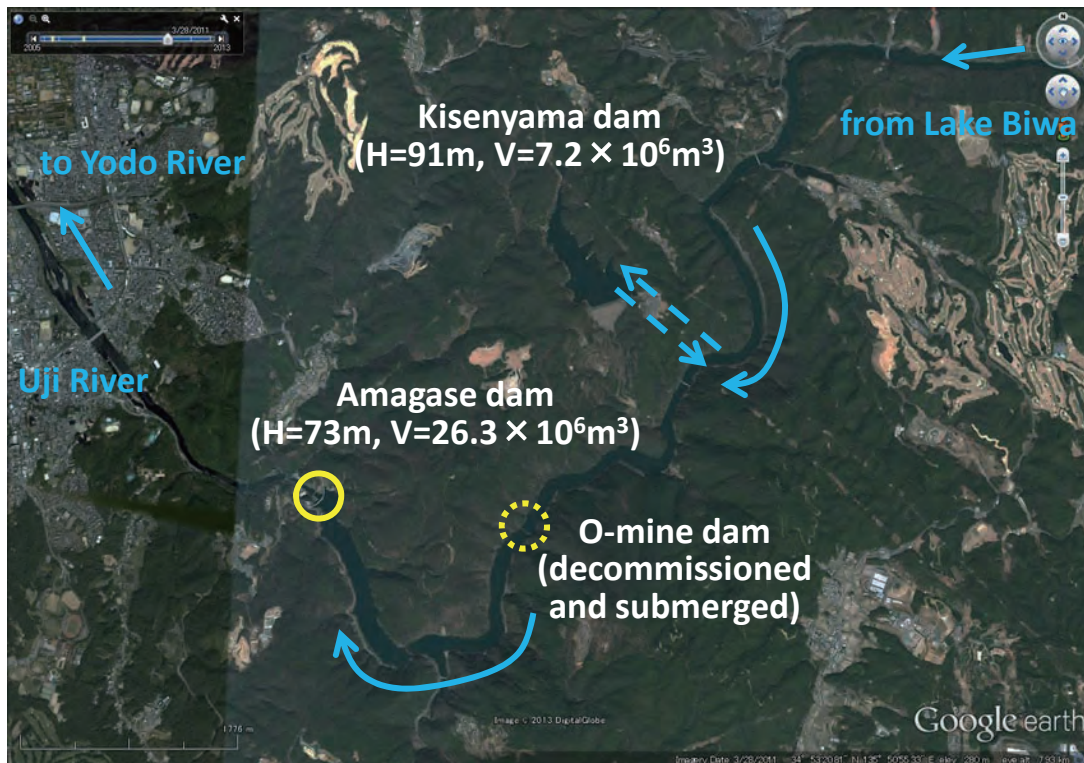


Tanakami, upstream basin of Daido river, has yield substantial amount of sediment **since >1200 year ago** due to heavy logging (for temple construction) and **deforestation of granite hillslopes**.

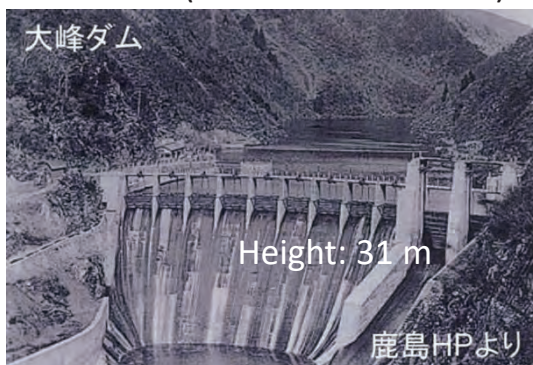
Vegetation has been recovered after **Sabo works**, which started in early 20th century. Sediment yield has been reduced, though Daido River still contributes to increasing sedimentation of Amagase-dam.



2. Construction and operation of dams in Uji River



O-mine dam (constructed in 1923)



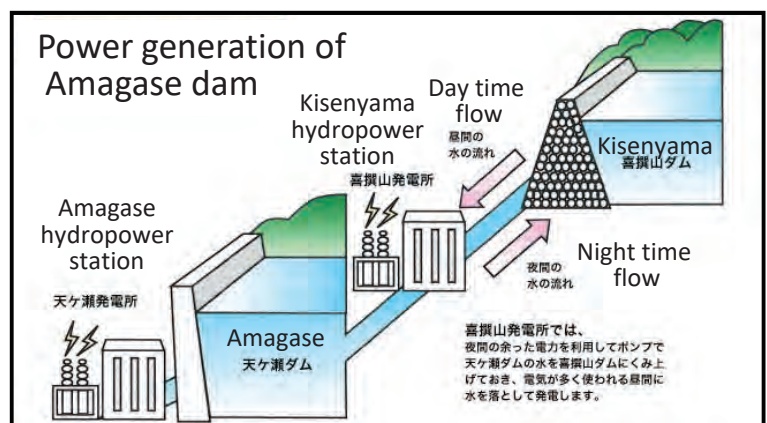
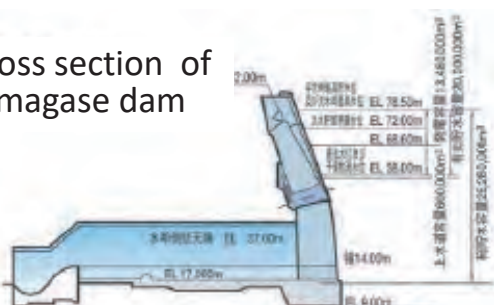
O-mine dam was constructed for hydro-power after an increase of energy demand of Kansai area. It was **the first concrete-gravity dam** in Japan. The **dam was decommissioned** (submerged) by the Amagase dam construction.

Amagase dam (constructed in 1964)

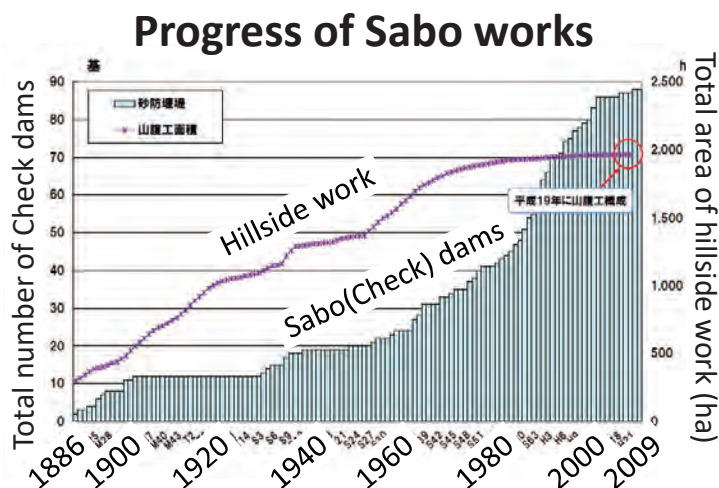
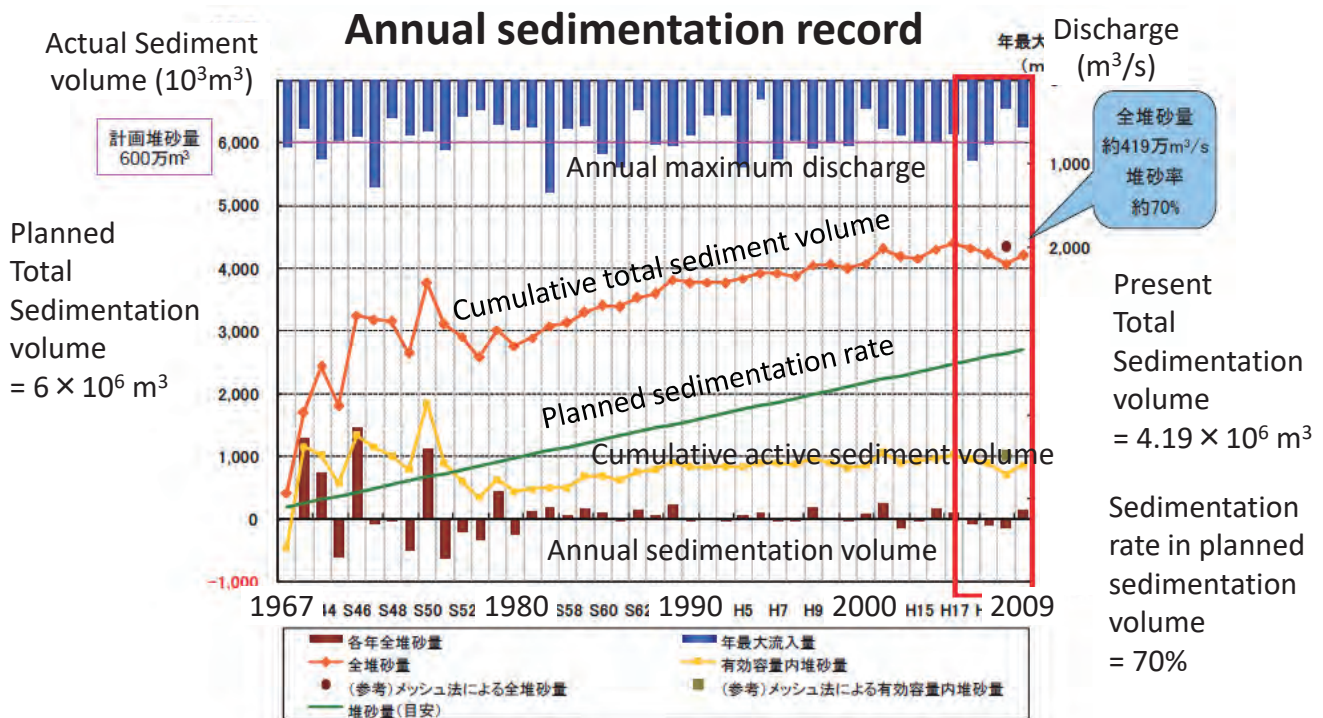


The construction of **Amagase dam** was initiated by **a big typhoon in 1953** that caused heavy damage in the downstream Yodo River and Osaka. It is **a multipurpose dam** (hydro-power, flood mitigation, drinking water supply) supporting Kansai area. **Pumped storage hydro-power station** is also installed between Amagase and Kisenyama dams.

Cross section of Amagase dam



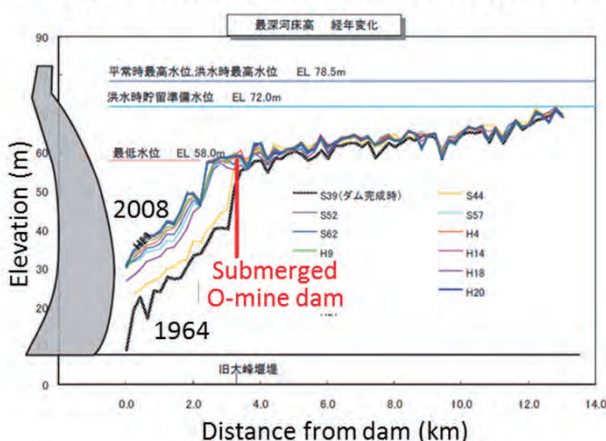
3. Reservoir sedimentation in Amagase dam



Sedimentation rate was greater in 1960s and 70s. Hillside work and check dam construction have been intensively implemented in 1890-1970 and 1950-2000 respectively. **These Sabo works have drastically reduced sediment yield** from Daido River to Amagase dam.

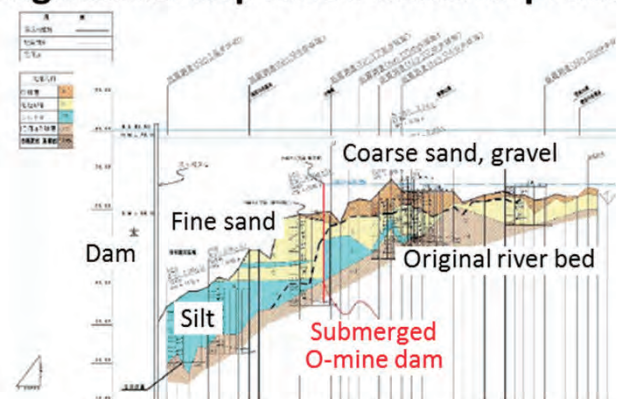
Almost 70% of planned sedimentation volume has been already filled. Capacity loss of total storage is 16%.

Longitudinal sedimentation profile



Most sediment deposit can be observed in the downstream of submerged O-mine dam, where deposit depth is almost 20 m.

Longitudinal deposited material profile



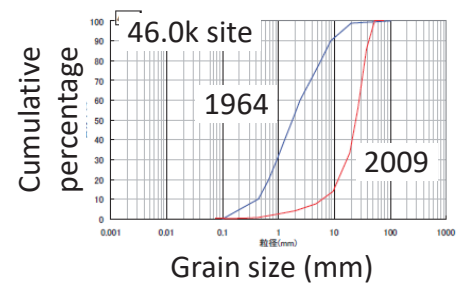
Deposited materials change at submerged O-mine dam, coarse sediment in the upstream, while fine one in the downstream.

4. Dam and environmental issues in Uji River

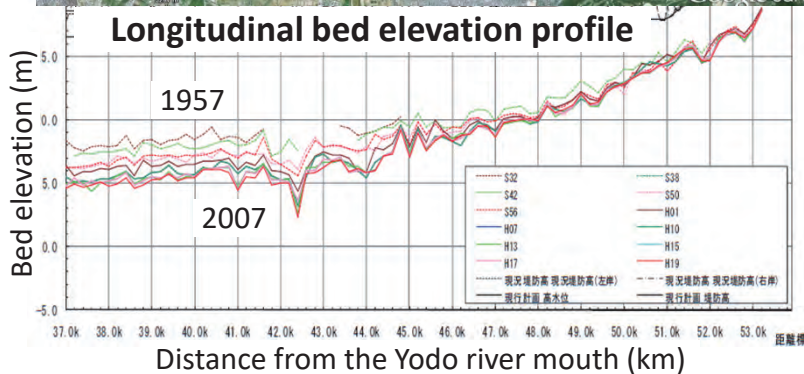
Downstream area of Amagase dam



Bed grain size distribution



In the downstream of Amagase dam, the **channel was degraded** (bed lowered for >3 m in the downstream part) due to **reduced sediment supply from upstream** and channel excavation. Bed materials have been coarsened.



Environmental issues and future works



Sandy bars and river-floodplain ecotones have decreased in area, which negatively impacted habitats of various aquatic plants and animals, while encouraged increase of particular organisms including exotic species. Supply of sediment, especially coarse sand and gravel, is essential for the recovery of biodiversity and ecosystem function of Uji River. The issues should be solved together with sedimentation of Amagase dam.